Identification and functional characterisation of glycoside hydrolases from the kauri dieback pathogen, *Phytophthora agathidicida*

A thesis presented in partial fulfilment of the requirements for the degree of

Doctor of Philosophy (PhD)

in

Plant Science

at Massey University, Manawatū

New Zealand

Ellie L. Bradley

2022

MASSEY UNIVERSITY
TE KUNENGA KI PŪREHUROA
UNIVERSITY OF NEW ZEALAND

GRADUATE RESEARCH SCHOOL

Note for Examiners of Doctoral Theses
Explanation of COVID-19 Impacts

The Doctoral Research Committee recognises the impacts of Covid-19 on research, particularly for doctoral candidates, and we appreciate the efforts made by supervisors and candidates to ensure timely completion of the doctoral thesis. We know that in some cases this has meant the project has needed to be changed in some way, including its final presentation. For students whose work has been impacted, we invite supervisors to provide a note for examiners explaining the circumstances.

Instructions for Supervisors:

The note is designed to enable you to communicate to examiners your desire for them to take account of certain factors in their assessment of a thesis to address delays and disruptions experienced by a thesis student as a result of the Covid-19 pandemic.

The attached form should be used to provide an explanation to the examiners on what to consider in their evaluation. It should detail how the project was altered or how the final product of the thesis has been affected as a result of the disruption. Statements should be clear and succinct for the benefit of the examiners and in fairness to the student and others in the student cohort.

The form should be signed by the student, the supervisor and the Head of Academic Unit, or nominee, and included in the information that is sent out with the thesis.

For doctoral candidates, the completed form should be inserted into the front of the thesis before the abstract by the candidate when submitting their digital thesis for examination in the Student Portal. At the completion of the examination, the amended form which excludes any confidential comments to the examiners, should be included in the appendices.

Please be sure to indicate whether a student has received a suspension of studies due to Covid-19 and/or an extension, as it is important to note if students have already had some special consideration.

Approved by DRC 10/Feb/2021
DRC 21/02/03

MASSEY UNIVERSITY
TE KUNENGA KI PŪREHUROA
UNIVERSITY OF NEW ZEALAND

GRADUATE RESEARCH SCHOOL

Note for Examiners
Explanation of COVID-19 Impacts

Thank you for taking the time to examine this thesis, which has been undertaken during the Covid-19 pandemic. The New Zealand Government's response to Covid-19 includes a system of Alert Levels which have impacted upon researchers. Our University's pandemic plan applied the Government's expectations to our research environment to ensure the health and safety of our researchers, however, research was impacted by restrictions and disruptions, as outlined below.

For a six-week period from March 26 to April 27 2020, New Zealand was placed under very strict lockdown conditions (Level 4 – Lockdown), with students and staff unable to physically access University facilities, unless they were involved in essential research related to Covid-19. All field work ceased and data collection with humans was restricted to online methods, if appropriate. The restrictions were partially lifted on April 27, but students and staff were not generally allowed back into University facilities until May 13.

Ongoing disruptions have also been encountered for some students due to uncertainties over the potential for future Covid-19-related restrictions on activities, and a Covid-19 cluster outbreak based in Auckland in New Zealand on 12 August 2020 led to the imposition of rolling Level 2 (Reduce) and Level 3 (Restrict) conditions until 23 September 2020. Auckland campus based students remained on Level 2 until 7 October 2020. This Alert Level system continues to be utilised throughout 2021.

These changing Alert Levels have meant that some research students had experimental, clinical, laboratory, field work, and/or data collection or analysis interrupted, and consequently may have had to adjust their research plans. For some students, the impacts of Covid-19 stretched far beyond the lockdown period in April/May 2020, as they may have had to significantly revise their research plans.

Overseas travel is not permitted by the University and restrictions have been placed on the New Zealand borders which are closed to non-New Zealand citizens and permanent residents. This meant that international students who were based offshore at the time of lockdown, were unable to return to New Zealand. A small number of offshore students were provided permission to return to New Zealand in early 2021. Many students have also suffered from anxiety and stress-related issues, and have had financial impacts, meaning their research progress has been significantly delayed.

This form, as completed by the supervisor and student, outlines the extent that the research has been affected by Covid-19 conditions.

Approved by DRC 10/Feb/2021
DRC 21/02/03

Please consider the factors listed below in your assessment of the work.

This statement has been prepared by the candidate's supervisor in consultation with the student and has been endorsed by the relevant Head of Academic Unit.

Student Name:	Ellie Lynn Bradley	ID Number:	[redacted]
Supervisor Name:	Carl Mesarich	Date:	31-Jul-22
Thesis title:	Identification and functional characterisation of glycoside hydrolases from the kauri die		

Considerations to be taken into account. Note: This statement will remain in the final copy of the thesis which will be available from the Massey University Library following the examination process.
[*Enter key considerations here for the examiners. This can include but is not limited to change of scope, scale, topic, focus; limitations in relation to data collection, access to necessary literature or archival materials, laboratories, field sites; disruptions as a result of lockdown and various alert levels, medical or health considerations etc*]

Chapter 3: As a consequence of the first and second nation-wide Covid-19 lockdowns, all Nicotiana benthamiana and Nicotiana tabacum used by the student in Agrobacterium tumefaciens-mediated transient expression assays involving candidate effectors Phytophthora agathidicida (GH and RxLR proteins) could not be watered, and therefore died. The plants that were lost were ready for experimental work, and it took at least six weeks for new Nicotiana plants to be ready for research (i.e. from seed germination).

Chapters 4 and 5: Also as a consequence of the first nation-wide Covid-19 lockdown, many of the kauri saplings provided by Scion that were to be used for isolating leaf apoplastic wash fluid for NMR and LC-MS experiments were lost. Initially, these saplings were being grown in a climate-controlled growth room at Massey University. However, given that the kauri saplings could not be watered during the lockdown period, the student was forced to take these plants home to Pahiatua, where the saplings unfortunately experienced cold-shock and either defoliated or died (i.e. through a loss of climate control). Those that survived were in poor condition. Thankfully, the student was able to secure replacement saplings from Scion. However, these saplings were considerably smaller than the original plants. A period of approximately 6 months was then spent waiting for the surviving plants to regain sufficient health and needle biomass to be used in experiments in conjunction with the smaller saplings. In addition to this delay, delivery issues with essential reagents due to the COVID-19 pandemic (particularly Trypsin, which took 19 weeks to arrive), meant that the LC-MS experiment was further delayed.

Approved by DRC 10/Feb/2021
DRC 21/02/03

Confidential for Examiners Only: *[Please enter any other considerations which are confidential for examiners only and should not be placed in the final thesis version submitted to Library following the examination process]*

Signed, confirming this is a fair reflection of the impact of Covid-19 on this research.

Student	Ellie Bradley	Digitally signed by Ellie Bradley Date: 2022.08.01 11:10:29 +12'00'
Supervisor	Carl Mesarich	Digitally signed by Carl Mesarich Date: 2022.08.01 10:53:47 +12'00'
Head of Academic Unit (or nominee)	Peter Tozer	Digitally signed by Peter Tozer DN: cn=Peter Tozer, o=NZ, email=p.tozer@massey.ac.nz Date: 2022.08.01 11:37:07 +12'00'

Approved by DRC 10/Feb/2021
DRC 21/02/03

Abstract

The survival of kauri, an ancient conifer species endemic to New Zealand, is currently threatened by kauri dieback disease, caused by the oomycete plant pathogen *Phytophthora agathidicida*. As *P. agathidicida* continues to spread throughout kauri forests in the northern North Island of New Zealand, encouraging research has indicated there may be natural tolerance to the disease within the kauri population. This resistance is likely governed, in part, by the plant immune system, which is activated upon recognition of pathogen invasion patterns such as microbe-associated molecular patterns (MAMPs), damage-associated molecular patterns (DAMPs), and effectors (virulence factors required for host colonisation), which are recognised at the plant cell surface by plant immune receptors. To better understand how *P. agathidicida* interacts with its plant host on a molecular level, pathogen-produced proteinaceous invasion patterns need to be identified and characterized to aid in the identification of cognate immune receptors in the plant host, which may be involved in activation of the plant immune system. As the role of glycoside hydrolase (GH) proteins in virulence and pathogenicity of fungal and oomycete plant pathogens is well established (**Chapter two**), an effectoromics approach was used to identify six *P. agathidicida* GH12 proteins that appear to act as MAMPs in both *Nicotiana benthamiana* and *Nicotiana tabacum* (**Chapter three**). Furthermore, nuclear magnetic resonance was used to identify considerable changes in kauri leaf apoplastic wash fluid of approximately 17 metabolites, including sucrose and glucose, in response to *P. agathidicida* inoculation (**Chapter four**), thus suggesting a role for GH proteins in the hydrolysis of some of these metabolites. Finally, proteomic analysis of *P. agathidicida* culture filtrates via liquid chromatography-mass spectrometry (LC–MS) was used to validate the expression of predicted *P. agathidicida* proteins and to investigate the capacity of this method to identify candidate invasion patterns for future analysis. **Chapter five** established that LC–MS analysis of *Phytophthora* culture filtrate was an effective method for the identification of putative apoplastic invasion pattern candidates and confirmed the production of all six *P. agathidicida* GH12 cell death elicitors in culture. Collectively, this thesis has advanced our understanding of the molecular mechanisms underpinning the interaction of *P. agathidicida* with its host and has contributed to the identification of candidate apoplastic effectors.

Acknowledgements

The last few years have been some of the most challenging. However, they have also been packed with research, experiments, successes, failures, friends, and family. While this thesis shows the results of my research and experiments, none of that would have been possible without guidance and support from those around me.

I am extremely grateful to Carl. As only your second PhD student, I can honestly say you have been a wonderful supervisor. You have been extremely patient and approachable, no matter what is going on, and you invest huge amounts of time and energy into all your students and their projects. You have been a big part of the lab; Not many supervisors would join us on late-night trips to Kmart!

Thank you to Prof. Rosie Bradshaw for all your input, guidance and suggestions. This is the second time you have been a part of my supervisory team, and I am so appreciative of your support. I am grateful to Dr Preeti Panda for your patience and support during the early stages of my PhD, and to Dr Rebecca McDougal for your guidance and suggestions over the last few years.

A huge thank you to Dr Laura Raymond, for generously carrying out the NMR analysis on my samples, and for your patience in answering all my questions, while on maternity leave no less! I wish you and your family all the best for the future. Thank you also to Trevor Loo for your guidance in the lab on all things LC-MS. You provide an invaluable resource, and it was much appreciated.

This project was completed with cultural authority from Te Roroa, the mana whenua from the Waipoua region, and from Ngāti Rehua, the mana whenua from Aotea | Great Barrier Island, from where samples were obtained for this work. I am grateful to Taoho Patuawa and Te Roroa for provision of kauri seedlings from your rohe via Scion and your permission and support for us to work with these at Massey University. Thank you also to Ngāti Rehua for your support that enabled me to use *Phytophthora agathidicida* NZFS 3770 isolated from your rohe Aotea (Great Barrier Island).

My research was funded by the BioProtection Research Centre, to whom I am very grateful. The conferences and meetings based in Lincoln were well-run and great opportunities to meet other scientists and PhD students working on related projects. My gratitude also to Dr Garrick Latch, from whom I was awarded a travel grant to attend the IUFRO conference, *Phytophthora* in Forests and Native Ecosystems in Sardinia, Italy. The Garrick Latch scholarship also provided additional funding which allowed me to finish my thesis. These were opportunities which would not be available were it not for his generosity.

To my colleagues, friends and lab-mates; Mel, Silvia, Merce, Mariana, Hannah, Ashleigh, and Berit, I am so grateful for your friendship. For the laughter at lunchtimes, for the songs and dances in the lab, for celebrating the wins, and for your support when things got tough. It was a privilege to share the lab with such a brilliant group of strong talented women, I wish you all success in everything you do.

To my family who back me 100%, thank you for all your support over the last 10 years. A special thank you to Grandad for supporting me during my undergraduate studies. To Nan, thank you for being the person to bring me up to speed on all the family whenever I called. I only wish you were here to see me complete my studies. Mum and Dad, without your love and support I would not be who I am today. You both go above and beyond to help me in any way you can, and I cannot begin to describe how grateful I am. Thank you for your honesty, for lending an ear, and for always supporting me. I love you both.

Ben, we have accomplished so much together over the course of my PhD. Thank you for always supporting me and my studies, for celebrating the wins, and being there when I had a bad day. Thank you for taking over cooking AND cleaning this last month. Tui and Evee, you have brought us so much happiness in the last couple of years, and I could not imagine life without you. You both make me laugh every day and your cuddles are second to none.

Table of contents

List of figures

List of tables

List of abbreviations

°C	Degrees Celcius
µL	Microlitre
µM	Micrometre
^{1}H NMR	Proton nuclear magnetic resonance
AA	Auxilary activity
aa	Amino acid
At	Arabidopsis thaliana
ATTA	*Agrobacterium tumefaciens*-mediated transient transformation Assay
Avr	Avirulence
AWF	Apoplastic wash fluid
BAK1	BRI1-associated kinase 1
BGTETB	Tetrasaccharide 3^{1}-β-D-cellotriosyl-glucose
BGTETC	3^{3}-β-D-glucosyl-cellotriose
BGTRIB	Trisaccharide 3^{1}-β-D-cellobiosyl-glucose
BLASTp	Basic local alignment search tool (protein)
BMGY	Buffered complex methanol medium
BMMG	Buffered complex glycerol medium
BSA	Bovine serum albumin
CATAStrophy	CAZyme-assisted training and sorting of trophy
CAZymes	Carbohydrate-active enzymes
CBEL	Carbohydrate-binding elicitor lectin
CBM	Carbohydrate-binding module
CC	Coiled-coil
CE	Carbohydrate esterases
CIR	Cytoplasmic immune receptor
cm	Centimetres
CM	Cellophane membrane
CRISPR	Clustered regularly interspaced short palindromic repeats
CRN	Crinkler
CTAB	Cetyltrimethylammonium bromide
cum	Cumulative
DAMPs	Damage-associated molecular patterns
df	Degrees of freedom

DNA	Deoxyribonucleic acid
dpi	Days post-inoculation
DTT	Dithiothreitol
E.B.	Ellie Bradley
EC	Enzyme commission number
EDTA	Ethylenediaminetetraacetic acid
EIX	Ethylene-inducing xylanase
ER	Endoplasmic reticulum
ETI	Effector-triggered immunity
ETS	Effector-triggered susceptibility
EV	Extracellular vesicles
EWCA	Effectors with chitinase activity
ExIPs	Extracellular immunogenic patterns
FAME	Fatty acid methyl ester
FAO	Food and Agricultural Organisation of the United Nations
FDR	False discovery rate
FPKM	Fragments per kilobase million
g	Gravity
GFP	Green fluorescent protein
GH	Glycoside hydrolase
GlcNac	β-1,4-N-acetylglucosamine
GmGIP1	*Glycine max* glucanase inhibitor protein 1
GOI	Gene of interest
GPI	Glycophosphatidylinositol
GT	Glycosyltransferases
h	Hour
H_2O_2	Hydrogen peroxide
HAMPs	Herbivorous-associated molecular patterns
HCD	Higher energy collisional dissociation
hpi	Hours post-inoculation
HR	Hypersensitive response
ID	Identity
IIR	Intracellular immune receptor
InIPs	Intracellular immunogenic patterns
IP	Invasion pattern

IPPC	International plant protection convention
IPR	Invasion pattern receptor
IPTR	Invasion pattern-triggered response
L.R.	Laura Raymond
LAMP	Loop-mediated isothermal amplification
LB	Lysogeny broth
LC-MS	Liquid chromotography mass spectrometry
LPMOs	Lytic polysaccharide monooxygenases
LRR	Leucine-rich repeat
LysM	Lysin motif
M	Molar
MA	Massachussets
MAMPs	Microbe-associated molecular patterns
MD	Minimal dextrose
min	Minute
mL	Millilitre
mm	Millimetre
mM	Millimolar
MPI	Ministry for Primary Industries
mRFP	Messenger red fluorescent protein
mRNA	Messenger ribonucleic acid
MS	Mass spectrometry
MTI	MAMP-triggered immunity
N	Amino
NAMPs	Nematode-associated molecular patterns
NB	Nucleotide-binding
NCBI	National Center for Biotechnology Information
NEB	New England Biolabs
NESI	New Zealand eScience Infrastructure
ng	Nanogram
NLPs	Necrosis- and ethylene-inducing peptide 1-like proteins
NLR	Nucleotide-binding domain leucine-rich repeat protein
nm	Nanometre
NMR	Nuclear magnetic resonance
NO	Nitric oxide

NOS	Nopaline synthase
NPP1	Necrosis-inducing *Phytophthora* protein 1
nr	Non-redundant
NZ	New Zealand
O_2^-	Superoxide
OD	Optical density
Pa	*Phytophthora agathidicida* 3770 PacBio genome
Pa3772	*Phytophthora agathidicida* 3772 Illumina genome
Pag	*Phytophthora agathidicida* 3770 latest PacBio genome
PAGE	Polyacrylamide gel electrophoresis
PaI	*Phytophthora agathidicida* 3770 Illumina genome
PAMPs	Pathogen-associated molecular patterns
parAMPs	Parasitic-associated molecular patterns
PC	Principal component
PCA	Principal component analysis
PCNB	Pentachloronitrobenzene
PCR	Polymerase chain reaction
PD	Potato dextrose
PGIPs	Polygalacturonase-inhibiting proteins
PGs	Endopolygalacturonases
PL	Pectate lyase
POIs	Proteins of interest
ppm	Parts per million
PR	Pathogenesis-related
PRR	Pattern recognition receptors
PsXLP1	*Phytophthora sojae* XEG1-like protein 1
PTA	*Phytophthora* taxon Agathis
PVDF	Polyvinylidene fluoride
PVPP	Polyvinylpolypyrrolidone
qRT-PCR	Quantitative reverse transcriptase polymerase chain reaction
R	Resistance protein
R	Resistance gene
RBPG1	Responsiveness to *Botrytis* PolyGalacturonases receptor
RLK	Receptor-like kinase
RLP	Receptor-like protein

RNA	Ribonucleic acid
ROS	Reactive oxygen species
rpm	Revolutions per minute
RXEG1	Receptor of XEG1
SAR	Systemic acquired resistance
SDS	Sodium dodecyl sulfate
SOBIR1	Suppression of BIR1
SP	Signal peptide
SSP	Small-secreted protein
T0	Time zero sample
T10d	Samples taken 10 days post-inoculation
T24h	Samples taken 24 hours post-inoculation
TAE	Tris/Acetic acid/Ethylenediamenetetraacetic acid
tBLASTn	Basic local alighnment search tool (protein-translated nucleotide)
TBST	Tris-buffered saline with Tween
TE	Tris/ethylenediamenetetraacetic acid buffer
TEMED	Tetramethylethylenediamine
TIR	Toll-interleukin-1
USA	United states of America
UV	Ultraviolet
v/v	Volume/volume
VIGs	Virus-induced gene silencing
w/v	Weight/volume
WT	Wild-type
YNB	Yeast nitrogen base
YPD	Yeast/peptone/dextrose

Chapter one: Overview

1.1 Important plant diseases

Plants, and thus plant health, will always be tightly intertwined with society. According to the International Plant Protection Convention (IPPC) and the Food and Agricultural Organisation (FAO) of the United Nations, 80% of the human diet is made up of plants (2017). However, this does not consider plants required to sustain other parts of our diet, such as meat and fish, or plants that are used in other areas of society (e.g. the timber industry). Up to 40% of food production globally is lost due to the impact of plant pests and diseases (IPPC & FAO, 2017), resulting in loss of income, famine, and in some cases, death.

In 2012, two studies were published describing the importance of both fungal (Dean et al., 2012) and bacterial (Mansfield et al., 2012) plant pathogens. *Magnaporthe oryzae*, the causal agent of rice blast disease, took out the top spot in the fungal pathogens (Dean et al., 2012). It is estimated that the loss in rice production due to the impacts of rice blast disease, on average about 30% of the crop, could feed 60 million people (Nalley et al., 2016). Like *M. oryzae*, several other fungal species which made it into the 'Top 10' list, affect staple plants such as cereals (*Puccinia* spp., *Blumeria graminis*, *Fusarium graminearum*, *Zymoseptoria tritici*) (Dean et al., 2012). Though *Pseudomonas syringae* pathovars were voted as the most important plant-pathogenic bacteria it is the second on the list, *Ralstonia solanacearum* with its global distribution and extremely wide host range, which is likely the most destructive (Mansfield et al., 2012).

It was not until several years later that a similar publication on the most important oomycete plant pathogens was published (Kamoun et al., 2015). Unsurprisingly, it was *Phytophthora infestans* which came in first place (Kamoun et al., 2015), likely due its wealth of historical, scientific, and economic impacts. The causal agent of potato blight, *P. infestans*, was responsible for the 1845–1847 Irish famine, but also contributed to the less well-known continental famine (1845–1846), resulting in approximately 700,000 and 600,000 excess deaths, respectively (Kamoun et al., 2015, Zadoks, 2008). Though potato is only the world's fourth most important food crop (Zhang et al., 2017a), it is an environmentally friendly crop with higher nutritional benefits compared to other staples (Liu et al., 2021a, Zhang et al., 2017a). Of all the oomycete species that were given a place in the 'Top 10', six of them belonged to the *Phytophthora* genus, and four of those (*Phytophthora infestans*, *Phytophthora ramorum*, *Phytophthora sojae* and *Phytophthora capsici*) were in the top five (Kamoun et al., 2015), demonstrating just how important this genus is to plant health.

1.2 Important *Phytophthora* species in New Zealand

Approximately 30 *Phytophthora* species have been identified in New Zealand so far, over half associated with diseases of agricultural plants, and the remainder with diseases of exotic forests and natural ecosystems (Scott & Williams, 2014). Among the forest *Phytophthoras* are *Phytophthora kernoviae* and *Phytophthora pluvialis*, which were isolated from *Pinus* species with red needle cast symptoms, although *P. pluvialis* is considered the primary cause (Dick et al., 2014). New Zealand *P. pluvialis* isolates were similar to those from the only other known population in Oregon, USA, from where the New Zealand isolates are thought to have originated, where they were isolated from stem cankers in tanoak (Dick et al., 2014, Brar et al., 2018, Reeser et al., 2013). However, the recent discovery of *P. pluvialis* in two neighbouring counties (Cornwall and Devon) in the United Kingdom indicates this pathogen has now spread to Europe (https://www.gov.uk/government/news/forestry-commission-act-on-new-tree-disease-found-in-cornwall). In contrast, *P. kernoviae*, based on genome analysis, phylogenetic position, and the lack of serious disease symptoms in New Zealand compared to those on plants species from other parts of the world, is thought to originate from the Southern hemisphere (Brasier et al., 2005, Studholme et al., 2019, Gardner et al., 2015, Ramsfield et al., 2007). Interestingly, disease caused on New Zealand native species by *P. cinnamomi*, considered one of the worst invasive alien species (Lowe et al., 2000), pales in comparison to its effect in other parts of the world where it devastates a variety of crop, horticultural, and forest plant species (Hardham, 2005, Podger & Newhook, 1971, Robin et al., 2012). It is suggested that *P. cinnamomi* arrived in New Zealand with the first human settlers (Beever et al., 2009, Johnston et al., 2001) and is thought to have originated in eastern Asia or Papua New Guinea (reviewed in Arentz (2017)). Currently, the *Phytophthora* species which causes the most concern in New Zealand is *Phytophthora agathidicida*, a pathogen responsible for a dieback disease, which affects one of New Zealand's most iconic and treasured tree species, New Zealand kauri, or *Agathis australis*.

1.3 *Agathis australis*/kauri

The *Agathis* genus is comprised of 13 species found in tropical and temperate regions ranging from the Northern Philippines (10˚30'N) to Northern New Zealand (38˚S) (Bellgard et al., 2016b, Whitmore, 1980), with only one species, *A. australis*, found in New Zealand (Steward & Beveridge, 2010, Whitmore, 1980). Commonly known as kauri, *A. australis* is an ancient tree species with a natural lifespan in excess of 1,500 years (Steward & Beveridge, 2010), a height of up to 50 m, and a diameter of up to 7 m in exceptional circumstances (Ecroyd, 1982). Kauri are endemic to New Zealand and have special significance to indigenous people, where the largest trees are often identified by name and afforded special standing in Māori culture (Steward & Beveridge, 2010). In Waipoua forest, a kauri tree

of approximately 47 m in height and estimated to be between 1,250–2,500 years old, is named after Tāne Mahuta, the Māori God of the forest (Bellgard et al., 2016b).

Kauri are ecologically important, a cornerstone species forming associations with many rare plants, including endemic epiphytes (Dawson, 1986, Verkaik & Braakhekke, 2007, Wyse & Burns, 2013, MPI, 2014, Orwin, 2007b). Historically, kauri were sought after for their high quality timber and had significant economic value (Bergin & Steward, 2004). Arguably, this economic value remains; as kauri are an important part of the local tourism industry (Cropp, 2019), they have potential as a silvicultural species (Steward et al., 2014a, Steward et al., 2014b), and sequester carbon faster than any other native NZ conifer (Kimberley et al., 2014) which may provide financial benefits in the form of carbon credits. Prior to European settlement, kauri-containing forests covered upwards of one million hectares (ha) in the northern half of the North Island. However, primarily through logging, less than 1% (7,500 ha) of this forest remains (Steward & Beveridge, 2010). Despite this, secondary forests containing kauri were estimated to cover approximately 60,000 ha as of 2007, and many of these areas are protected by community and conservation organisations (Orwin, 2007a). Current threats to the survival and preservation of kauri forests include introduced pests and weeds, although the most dangerous is *P. agathidicida* (Orwin, 2007a, Beever et al., 2010, Bellgard et al., 2016b, Hill & Waipara, 2017, Steward & Beveridge, 2010). In recognition of the threat posed by *P. agathidicida*, kauri have for the first time been placed on the list of threatened, nationally vulnerable, species (de Lange et al., 2018).

1.4 Kauri dieback disease

1.4.1 Oomycetes – an overview

Oomycetes are eukaryotic organisms that, although they are related and have several common traits, are not considered true fungi but instead share a common ancestor with brown algae and diatoms (Rossman & Palm, 2006, Jiang & Tyler, 2012). While fungi and oomycetes may have similar morphological features and lifestyles (Latijnhouwers et al., 2003), there are several distinguishable differences. Cell wall composition is a key difference between fungi and oomycetes, as while both fungal and oomycete cell walls contain β-1,3/1,6-glucans, fungi have high levels of chitin and chitosan whereas oomycete cell walls are primarily cellulose (Wanke et al., 2020a). In addition, unlike fungi, oomycetes lack sterols in their membrane and many are considered sterol auxotrophs, unable to synthesise the sterols they need for growth and reproduction (Latijnhouwers et al., 2003, Steel & Drysdale, 1988, Wang et al., 2021). These differences in cell wall composition have repercussions for the control of oomycete phytopathogens. Oomycetes are resistant to both plant-produced saponins which interact with 3β-hydroxyl sterols in fungal plasma membranes to compromise integrity (Wang et al., 2021), and to fungicidal chitin synthase inhibitors (Latijnhouwers et al., 2003). Other distinguishing

features include septate (fungi) and non-septate (oomycete) hyphae, primarily haploid (fungi) vs diploid (oomycete) lifecycles, and the presence of two (oomycete) flagella on their zoospores while fungi may have none or one (AccessScience, 2015, Latijnhouwers et al., 2003, Thines, 2014).

Plant- and animal-pathogenic oomycetes have evolved separately from each other. Therefore while most oomycete plant pathogens belong in the class Peronosporomycetidae, oomycete animal pathogens are found in Saprolegniomycetidae (Tyler, 2009, Jiang et al., 2013), though there are exceptions (Diéguez-Uribeondo et al., 2009). The aptly named *Phytophthora* (plant destroyer) species are the causal agents of disease in many plants, so much so that a majority of the more than 90 species are plant pathogens (Hansen, 2015, Tyler, 2009, Kamoun et al., 2015). In the past, *Phytophthora* species were classified based on morphology using the Waterhouse key (Waterhouse, 1963), as well as growth under different conditions (Kroon et al., 2012). However, due to the development of DNA sequencing technologies, a phylogenetic approach to classification is now standard, resulting in 12 phylogenetically distinct clades (Kroon et al., 2012, Jung et al., 2017, Rahman et al., 2015, Blair et al., 2008, Martin et al., 2014, McCarthy & Fitzpatrick, 2017, Yang et al., 2017). Interestingly, the various species within each clade share few common features in terms of morphology and reproductive lifecycle (McCarthy & Fitzpatrick, 2017, Kroon et al., 2012, Yang et al., 2017). Kroon et al. (2012) provide an excellent review on what was known about the species within each clade at the time of publication.

1.4.2 *Phytophthora agathidicida*

1.4.2.1 Identification

P. agathidicida, the causal agent of kauri dieback, is a species that was described after the publication by Kroon et al. (2012) (Weir et al., 2015). The recognition of this disease on mainland New Zealand did not come until 2006 when it was given the name *Phytophthora* taxon Agathis (PTA) (Beever et al., 2009), 34 years after it was first discovered on Great Barrier Island, where it was associated with an unhealthy kauri stand and described as *Phytophthora heveae* (Gadgil, 1973). Analysis of eight additional gene sequences subsequently revealed that *P. agathidicida* is a separate species belonging to *Phytophthora* clade 5, along with *P. heveae*, *Phytophthora castanae*, and *Phytophthora cocois* (Weir et al., 2015).

1.4.2.2 Infection and symptoms

Though much remains to be discovered about *P. agathidicida,* a lifecycle has been established based on observations of *P. agathidicida* and similarities to other *Phytophthora* species (**Figure 1.1**). Asexual sporangia germinate to release short-lived, unicellular zoospores which chemotactically 'swim' (using

flagella) through soil and water towards kauri roots (Beever et al., 2010, Bradshaw et al., 2020, Fawke et al., 2015, Osswald et al., 2014). Upon reaching fine roots, the zoospores develop into a cyst from which a germ tube emerges to grow along the root surface before invading the root epidermis through naifu invasion (Bronkhorst et al., 2021). Naifu invasion describes a mechanism by which the *Phytophthora* species uses a combination of polar force and an oblique angle in order to exert pressure on the cell surface which fractures, allowing hyphal entry (Bronkhorst et al., 2021). Once inside the root, there is a period of intercellular growth prior to entering cells (Osswald et al., 2014). Haustoria, specialized infection structures that differentiate from hyphae in the plant cell and allow the pathogen to both absorb nutrients and deliver effectors (see below), have been detected in *P. agathidicida*, although they are not common to all *Phytophthora* species (Osswald et al., 2014, Padamsee et al., 2015). Hyphal growth may result in the formation of lignitubers as they try to enter the plant cells (Bellgard et al., 2016a), which are thought to act as a reservoir for pathogen persistence (Jung et al., 2013). Thick-walled oospores that are formed in the plant tissue are a particular concern in the effort to contain kauri dieback disease as they remain viable for long periods of time (e.g. in soil or root fragments). Human activity, movement of local fauna, as well as land contours and movement are all thought to be factors in disease spread (Bassett et al., 2017, Hill & Waipara, 2017, Beever et al., 2010, Bellgard et al., 2016b).

P. agathidicida is highly pathogenic to kauri (Beever et al., 2010, Beever et al., 2009). Outward symptoms of infection include canker or resin exudate above the base of the tree (collar), chlorosis or yellowing of leaves, and crown decline where the upper branches lose their leaves (Beever et al., 2010, Beever et al., 2009, Bellgard et al., 2016a, Bellgard et al., 2016b, Hill & Waipara, 2017). Less visible symptoms may also include lesions on structural peg roots, rotting roots, and wilting seedlings (Hill & Waipara, 2017). Later stages of the disease often take years to manifest, presenting a challenge when trying to ascertain the range and infection rate of the disease (Hill & Waipara, 2017, Bellgard et al., 2016b). While other plant species have been found to host *P. agathidicida*, where a host is defined as any plant *P. agathidicida* can live on or in (Bellgard et al., 2013, Ryder, 2016), further work is needed in this area. Perhaps surprisingly, Queensland kauri (*Agathis robusta*) was not found to be a host species (Bellgard et al., 2013), and while the focus is on potential host plants that are known to associate with kauri (Bellgard et al., 2013), it may also be of interest to identify whether other *Agathis* species are susceptible to *P. agathidicida*.

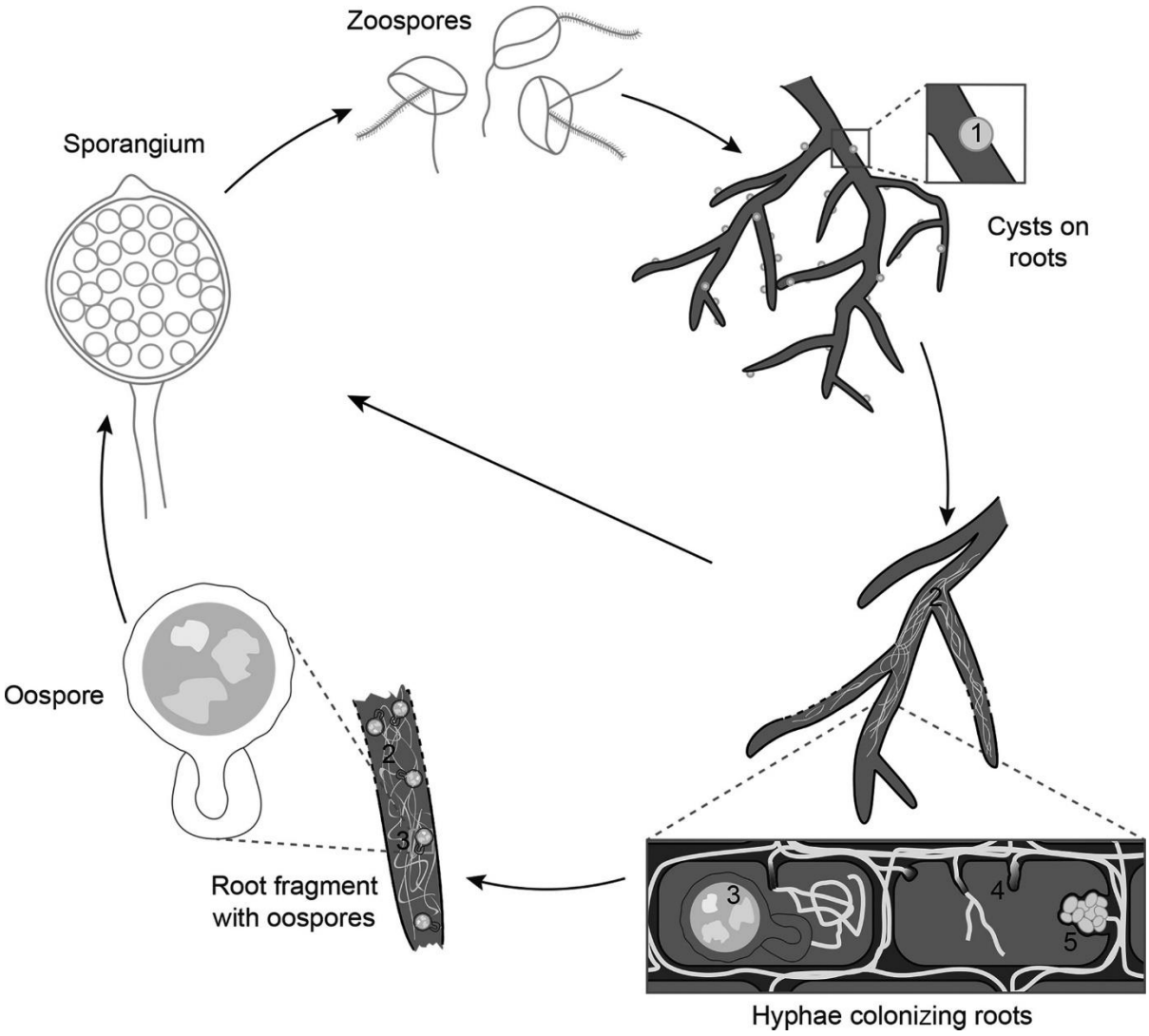

Figure 1.1. Lifecycle of *Phytophthora agathidicida* adopted from Bradshaw et al. (2020) with permission.

Phytophthora agathidicida life cycle. Zoospores are unicellular, short-lived and motile, and move through wet soil along chemotactic gradients towards kauri roots, where they encyst and form a penetration structure, allowing infection of the fine root epidermis and colonization of the cortex. Lignituber formation, a result of hyphae attempting to enter plant cells, and stromata-like structures, are often observed. Thick-walled and durable oospores are produced via sexual reproduction and germinate to produce sporangia. Sporangia can also be produced directly on colonized roots. Sporangia then release zoospores to complete the life cycle. 1, cyst; 2, hypha; 3, oospore; 4, lignituber; 5, stromata-like structures. Figure not drawn to scale. Figure legend taken from Bradshaw et al. (2020).

1.4.2.3 Distribution of *P. agathidicida* in New Zealand

The devastating nature of kauri dieback, and unpublished data showing there is little genetic variation between *P. agathidicida* isolates, has led to the assumption that the species is a recent arrival in New Zealand, and suggests a 'founder effect' where a small subset of the population from an as yet unknown origin has established (Beever et al., 2009, Bellgard et al., 2016b). As such, *P. agathidicida* was classified as an unwanted organism under the NZ Biosecurity Act (1993). However, recent research has suggested a much earlier arrival, possibly several hundred to several thousand years ago (Winkworth et al., 2021). If this pathogen has indeed been here for a long time, it is likely that there has been a recent change in at least one aspect of the disease triangle which considers both biotic (host and pathogen) and abiotic (environmental) factors (Scholthof, 2007).

Regardless of the origins of *P. agathidicida*, the pathogen is now widespread throughout the natural range of kauri forests (**Figure 1.2**) (Bradshaw et al., 2020). Encouragingly however, recent research suggests that *P. agathidicida* is currently confined to the periphery of the forest, at least within the Waitakere ranges (Ashby et al., 2022). It should be noted that *P. agathidicida* is not the only pathogen of kauri, and indeed not the only *Phytophthora* pathogen of kauri. *Phytophthora cinnamomi*, *Phytophthora multivora*, and *Phytophthora cryptogea* are all species that are commonly isolated on kauri seedlings and were found to cause minor growth suppression and small lesions, though they were not able to kill the plants in a nursery setting (Beever et al., 2009, Horner & Hough, 2014). While the pathogenicity of *P. agathidicida* on kauri is unquestionable, further research is needed to understand the sudden appearance and increase in prevalence of this disease, and the effects the biotic and abiotic environments may have. Furthermore, while determining the origin of *P. agathidicida* would be useful to better understand the biology of the pathogen in its native environment, it may also provide insight into potential biocontrol agents (Brasier, 2007).

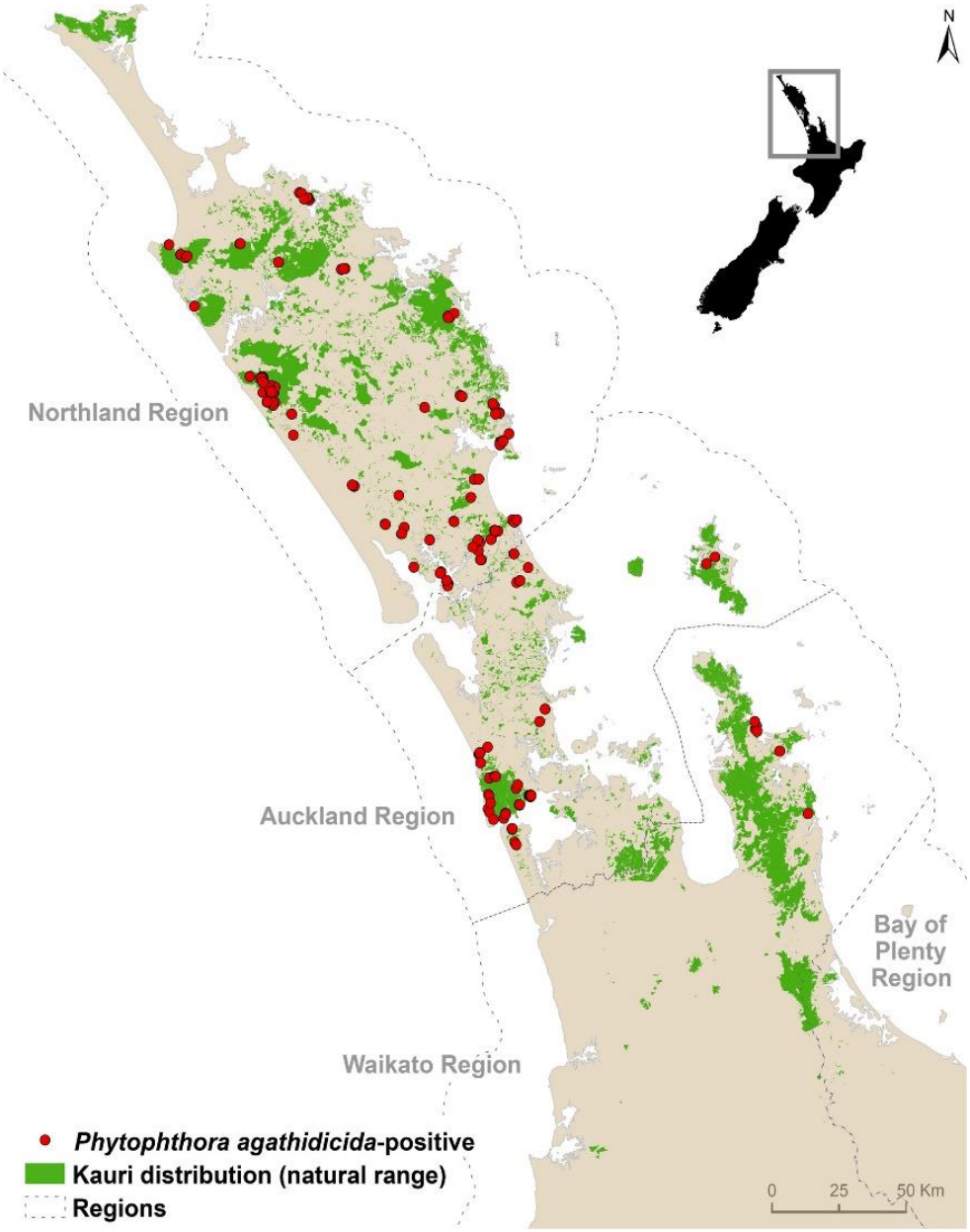

Figure 1.2. Distribution of *Phytophthora agathidicida* in New Zealand. Figure adopted from Bradshaw et al. (2020) with permission.

Distribution of *P. agathidicida* across the natural range of kauri. Red dots indicate locations where the *P. agathidicida* pathogen has been confirmed within the native range of kauri in the northern part of New Zealand. The distribution map (Crown copyright) was created by Biosecurity New Zealand (Ministry for Primary Industries; MPI) on 14 August 2019 based on data obtained from various sources available at that time. While all reasonable measures have been taken to ensure accuracy, MPI gives no warranty in relation to the accuracy, completeness, reliability or fitness for purpose of the map and accepts no liability whatsoever in relation to any loss, damage or other costs relating to any person's use of the map. The small New Zealand map is from Wikimedia (Creative Commons CC0 1.0 Universal Public Domain). Legend adapted from Bradshaw et al. (2020).

1.4.2.4 Management

With the classification of *P. agathidicida* as an unwanted organism, a disease management programme 'Keep Kauri Standing', similar to management of *P. cinnamomi* in Western Australia (Hansen, 2015), was initiated in an effort to contain the pathogen (MPI, 2016). This multifaceted programme works to educate the public, place measures to limit the spread of the disease (access restrictions to walking tracks, elevated boardwalks, and boot washing stations), provide funding for research and development of alternative control measures (Bellgard et al., 2016b, Hill et al., 2021, MPI, 2016), and is reviewed in Bradshaw et al. (2020). Some of the research in this space includes:

- Improved methods of pathogen identification, specifically aimed at improving knowledge on pathogen distribution. The development of a loop-mediated isothermal amplification (LAMP) assay targeting the coding sequence from *P. agathidicida mitochondrial apocytochrome b* is a promising step, providing a quicker, more sensitive, and cost-efficient method compared to soil baiting and culture techniques (Winkworth et al., 2020). However, as the LAMP assay used baited plant tissue material, the initial part of the soil baiting process, which takes up to two weeks, is still required (Winkworth et al., 2020). Researchers have since characterised the fatty acid methyl ester (FAME) profile of *P. agathidicida* as a step towards developing FAME analysis as a way to quantitatively detect *P. agathidicida* in soil samples in less than a day (Lacey et al., 2021b). However, further investigation is required to determine whether FAME analysis can distinguish between different *Phytophthora* species, as none of the 12 fatty acids identified were unique to *P. agathidicida* (Lacey et al., 2021b).
- Identifying potential chemical controls. The application of phosphite (phosphorous acid) is known to provide protection against various *Phytophthora* spp. in a range of different plants, acting to directly inhibit oomycete growth as well as to trigger the plant immune system (Smillie et al., 1989). Despite minor issues with phototoxicity during initial trials in which kauri rickers were injected with various concentrations of phosphite, particularly at higher phosphite concentrations, evidence suggested phosphite was effective against *P. agathidicida* (Horner et al., 2015). A subsequent study on larger kauri used substantially less phosphite but, while no phytotoxicity symptoms were observed, the lower rate was unable to suppress *P. agathidicida* lesion growth sufficiently (Horner & Arnet, 2020). While phosphite is clearly an important tool in *P. agathidicida* management, the injection method is unsuitable for covering large, forested areas. While trials to determine the best concentration, number of doses, and application method of phosphite are still ongoing (Horner & Arnet, 2020), additional research is identifying other compounds which have potential to be used in the control of *P. agathidicida* (Lacey et al.,

2021a, Lawrence et al., 2017), including some isolated from the native New Zealand kānuka (*Kunzea robusta*) (Lawrence et al., 2019).

- Developing a greater understanding of ecosystem interactions surrounding *P. agathidicida*. Research suggests that exotic pine forest soils may act as a reservoir for this pathogen, although the properties of the soil that support this activity are still unknown (Lewis et al., 2019). In addition, recent research has uncovered significant differences in microbial soil communities between symptomatic and asymptomatic kauri stands (Byers et al., 2020). This includes an increase in the presence of *Penicillium* and *Trichoderma* spp. in asymptomatic kauri soil, both of which have previously been found to exhibit antagonistic activities towards other microbes (Chen et al., 2021, Jiang et al., 2016, La Spada et al., 2020, Ma et al., 2008, Nicoletti et al., 2004) and may have roles in suppressing *P. agathidicida*, though further investigation is required to determine the biocontrol capabilities of these taxa against *P. agathidicida* (Byers et al., 2020).
- Determining whether natural genetic tolerance or resistance in kauri could allow survival even in an environment where *P. agathidicida* was present (Williams & Faulds, 2018).

1.5 The plant immune system

Much like our own ability to recognise and fight off infection, plants have an immune system that recognises self from non-self. Aside from the physical barrier of the plant cell wall and cuticle (Newman et al., 2013), there are two layers of plant immunity: non-specific and specific. Over the years, several models have been used to describe the complexity of the plant immune system, detailed below.

1.5.1 Non-specific immunity

Non-specific immunity involves the recognition of molecular patterns associated with infecting microbes, known as **m**icrobe/**p**athogen-**a**ssociated **m**olecular **p**atterns (MAMPs/PAMPs), such as cell wall components, e.g., bacterial peptidoglycan, fungal chitin, or oomycete ß-glucan, by extracellular plant **p**attern **r**ecognition **r**eceptors (PRRs) (Newman et al., 2013). MAMPs are often essential structures for microbes (Newman et al., 2013) and, for this reason, are generally conserved, creating ideal markers for the plant to recognise invaders. Due to the need for conservation, it was previously thought that MAMP-triggered immunity evolves slowly, although several examples have since shown that MAMP evolution is faster than expected (Cai et al., 2011, Clarke et al., 2013). In addition to MAMPs, the plant defence system may recognise **d**amage-**a**ssociated **m**olecular **p**atterns (DAMPs), such as cutin monomers which are released as the plant cuticle is degraded by microbial cutinases (Boller & Felix, 2009).

1.5.2 Specific immunity

Specific immunity is commonly known as **e**ffector-**t**riggered **i**mmunity (ETI) and is based on the recognition of pathogen effector proteins (virulence factors required for host colonisation) by corresponding plant immune receptors (recognized effectors are often termed **av**i**r**ulence (Avr) effectors, as their recognition renders the pathogen avirulent). Typically, effectors function to promote host colonisation by suppressing or interfering with activation of the plant immune system (e.g. following the recognition of MAMPs or DAMPs) (Abramovitch & Martin, 2004, Nürnberger & Lipka, 2005). The receptors that have evolved to recognize effector proteins are either extracellular **p**attern **r**ecognition **r**eceptors PRRs or intracellular **r**esistance (R) proteins, both encoded by **r**esistance (*R*) genes (Aguilera-Galvez et al., 2018), reviewed in Petit-Houdenot and Fudal (2017). Over time, several models have been suggested to describe the complex process of plant immunity. While all models have both merits and limitations, it should be recognised that not all complex natural systems can be easily labelled and, the more specific the model, the more exceptions to the rule there are likely to be.

1.5.2.1 The gene-for-gene model

The first and the oldest model to describe plant immunity is the 'gene-for-gene' model described by Flor (1942) (**Figure 1.3**). As this model suggests, the pathogen Avr factor (encoded by an *Avr* gene) is recognised by a matching plant R factor (encoded by an *R* gene) thereby preventing infection, while non-matching gene pairs result in disease of the plant host (Flor, 1942, Nürnberger & Lipka, 2005). However, as noted in Cook et al. (2015), this model fails to consider the immune response triggered by MAMPs or DAMPs. Furthermore, there are a number of exceptions to the gene-for-gene rule with some R factors capable of recognising several Avr factors, and vice-versa (Petit-Houdenot & Fudal, 2017).

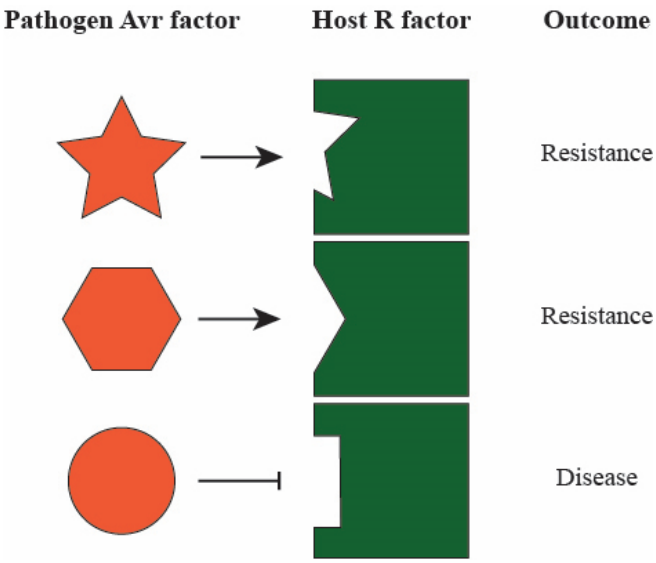

Figure 1.3. A representation of potential outcomes based on the gene-for-gene model.

When pathogen Avr factors (encoded by *Avr* genes) are recognised by corresponding host R factor (encoded by *R* genes), the hosts immune response is triggered to resist pathogen invasion. However, when pathogen Avr factors are not recognised by a corresponding host R factor, the host immune system is not activated, thereby allowing pathogen infection.

1.5.2.2 The Zigzag model

The Zigzag model (**Figure 1.4**) (Jones & Dangl, 2006) describes the ongoing battle between pathogens and their plant hosts to evolve and adapt new strategies for infection and resistance, but perhaps most importantly, brings together observations of both **M**AMP-**t**riggered **i**mmunity (MTI) and ETI (Cook et al., 2015). Jones and Dangl (2006) outline four phases. In the first phase, MAMPs are recognised by PRRs leading to MTI, then effectors are released by the pathogen to overcome MTI in phase two. Phase three demonstrates ETI, as a plant R protein specifically recognises an effector (Avr), and finally phase four represents the selection pressure on the pathogen as it evolves to avoid ETI (Jones & Dangl, 2006). This may include deletion or mutation of existing effector genes to avoid recognition, or the addition and/or adaptation of effector genes to suppress the plant immune response. Successful pathogens are expected to continue to evolve new methods of avoidance, as the host evolves new resistance mechanisms to recognise the changes in pathogen effectors. However, this model assumes PTI/MTI evolves slowly in comparison with ETI, an assumption which has since been disputed (Cook et al., 2015, Michelmore et al., 2013). Moreover, certain features are not represented in this model, including DAMPs, and both necrotrophic and symbiotic interactions (Pritchard & Birch, 2014). In addition, the classification of molecules as either effectors or MAMPs has been somewhat muddied, with certain effectors found to be more widespread than initially thought, suggesting a continuum between MTI and

ETI rather than two discrete responses (Bohm et al., 2014, Thomma et al., 2011, Cook et al., 2015, Gijzen & Nurnberger, 2006, Qutob et al., 2006).

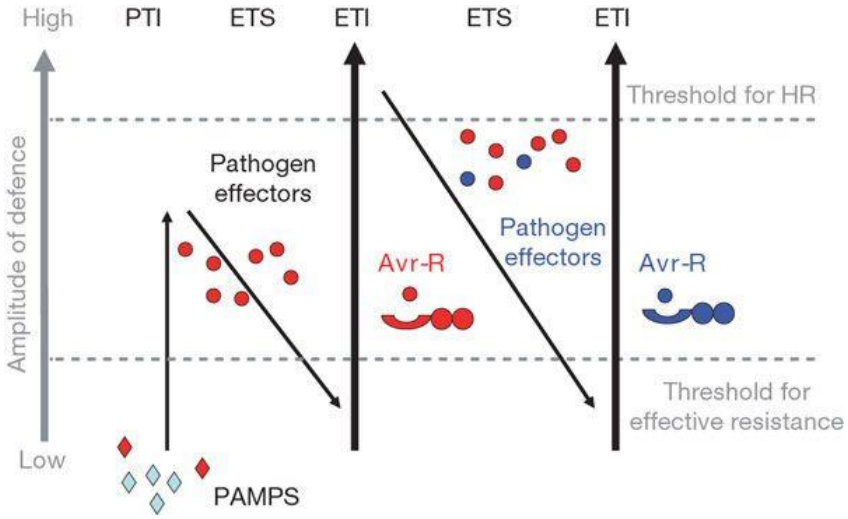

Figure 1.4. The Zigzag model of plant immunity as described by Jones and Dangl (2006), adopted with permission.

In this model, pathogen-associated molecular patterns (PAMPs) activate **P**AMP-**t**riggered **i**mmunity (PTI) (phase 1). However, the release of pathogen effectors by successful pathogens results in **e**ffector-**t**riggered **s**usceptibility (ETS) (phase 2). The recognition of a particular pathogen Avr effector by a host R-protein results in **e**ffector-**t**riggered **i**mmunity (ETI) (phase 3). Consequently, evolution of pathogen effectors that are capable of avoiding/suppressing ETI (phase 4) results once again in ETS. ETI responses are seen as stronger than PTI responses, and therefore often pass the threshold for a **h**ypersensitive **r**esponse (HR).

1.5.2.3 The invasion model

Perhaps the simplest model of plant immunity was proposed by Cook et al. (2015) (**Figure 1.5**). The invasion model suggests plant **i**nvasion **p**attern **r**eceptors (IPRs), either extracellular or intracellular, detect **i**nvasion **p**atterns (IPs), be they MAMPs, DAMPs or effectors, resulting in an **i**nvasion **p**attern-**t**riggered **r**esponse (IPTR), ultimately leading to one of two outcomes, continued symbiosis, or the end of symbiosis (Cook et al., 2015). This model works because of its broad generalisation, removing assumptions made by previous models as well as distinctions made between the two 'layers' of plant immunity and the type of pattern or receptor, while also providing only one point of view (that of the host plant). Furthermore, it represents a range of different lifestyles by recognising that while some interactions are terminated by the IPTR, others (such as necrotrophic pathogens) use the IPTR to support plant infection.

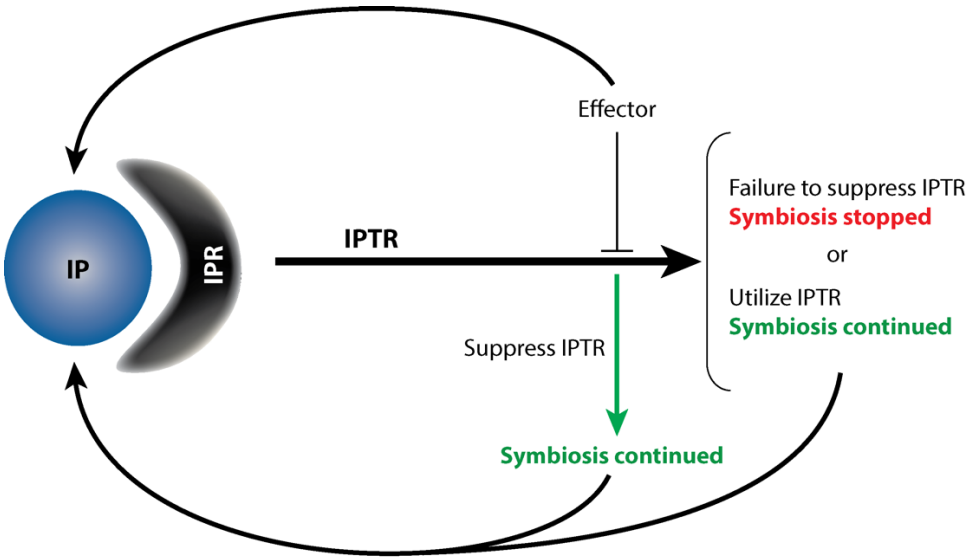

Figure 1.5. The invasion model as described by Cook et al. (2015), adopted with permission.

Recognition of **i**nvasion **p**atterns (Ips) by plant **i**nvasion **p**attern **r**eceptors (IPRs) generates an **i**nvasion **p**attern **t**riggered **r**esponse (IPTR). For some interactions (e.g. biotrophs) failure to suppress this IPTR prevents symbiosis from occurring, while other interactions (e.g. necrotrophs) use this IPTR to continue symbiosis (invasion). Effector proteins may serve to either suppress the IPTR or may themselves be recognized, thereby triggering an IPTR.

1.5.2.4 The spatial invasion model and the spatial immunity model

The spatial invasion model is the most recent attempt to describe the complexities of the plant immune system (Kanyuka & Rudd, 2019). Building on the aforementioned invasion model (Cook et al., 2015), it introduces an additional spatial dimension to account for recognition of the 'invasion molecule' occurring in the apoplast or cytoplasm (Kanyuka & Rudd, 2019). This is for the simple reason that effective resistance is more likely to come from '**i**ntracellular **i**mmune **r**eceptors' (IIRs) for pathogens which colonise the plant cell, and from '**c**ell **s**urface **i**mmune **r**eceptors' (CIRs) for those which are restricted to the apoplast. The authors, Kanyuka and Rudd (2019), further differentiate from the invasion model by only considering interactions between host plants with their adaptive pathogens. Similarly, van der Burgh and Joosten (2019) also suggest the addition of a spatial dimension. However, rather than the invasion model (Cook et al., 2015) which does not recognise IPTR that may be triggered by abiotic factors (e.g., DAMPs that are released due to mechanical damage), they suggest an adaption of the danger model (Gust et al., 2017) (**Figure 1.6**). Thus, differentiating danger signals further into **ex**tracellular **i**mmunogenic **p**atterns (ExIPs), which act outside the cell, and **in**tracellular **i**mmunogenic **p**atterns (InIPs), which are detected by cytoplasmic receptors (van der Burgh & Joosten, 2019).

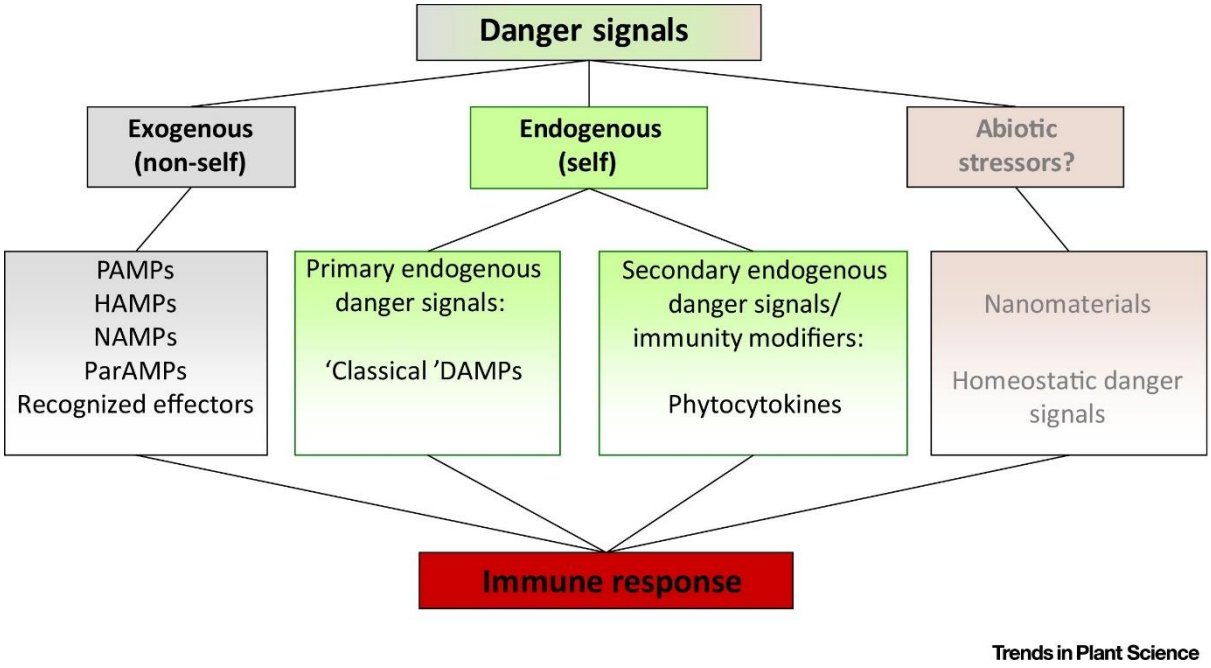

Figure 1.6. The danger model as described by Gust et al. (2017), adopted with permission.

Danger signals recognised by the plant immune system that may lead to an immune response include **p**athogen/**m**icrobe-**a**ssociated **m**olecular **p**atterns (P/MAMPs), as well as associated molecular patterns from **h**erbivores (HAMPs), **n**ematodes (NAMPs), **par**asitic plants (parAMPs) and endogenous **d**amage-**a**ssociated **m**olecular **p**atterns (DAMPs). Recognised microbial effectors and abiotic stresses may also trigger an immune response.

1.5.3 Response to invasion

The plant immune system is quickly activated upon recognition of IPs. A **h**ypersensitive **r**esponse (HR), characterised by localised cell death, is often generated to limit pathogen growth (Lamb & Dixon, 1997, Staskawicz et al., 1995). Fast acting, the HR typically occurs within 24 h of infection, and involves the accumulation of superoxide (O_2^-) and hydrogen peroxide (H_2O_2) at the site of infection (Kombrink & Schmelzer, 2001, Lamb & Dixon, 1997). Other responses include the deposition of callose (Brown et al., 1998), accumulation of lignin (Bhuiyan et al., 2009, C P Vance et al., 1980), production of secondary metabolites (Erb & Kliebenstein, 2020) and extracellular alkalinisation (Moroz et al., 2017). In addition, the **s**ystemic **a**cquired **r**esistance (SAR) pathway is gradually activated throughout the plant to prevent subsequent pathogen invasion, evidenced by increased expression of **p**athogenesis-**r**elated (PR) genes (Durrant & Dong, 2004, Ali et al., 2018, Lamb & Dixon, 1997, Ryals et al., 1996). SAR provides longer-term resistance (weeks/months) to a range of pathogens, although there are fitness consequences to the plant for long-term activation (Durrant & Dong, 2004, Sticher et al., 1997).

1.6 Effectors

1.6.1 Characteristics and application

Effectors are molecules produced by the microbe to aid host colonisation (Lo Presti et al., 2015). The term 'effector' describes an incredibly diverse group of non-enzymatic proteins, secondary metabolites (Collemare & Lebrun, Pusztahelyi et al., 2015), small RNAs (Huang et al., 2016, Weiberg & Jin, 2015), and enzymes (Ma et al., 2015b). These molecules are particularly important in biotrophic or hemi-biotrophic micro-organisms, which require live plant tissue, at least initially. Therefore, it follows that effector gene expression is highest during the early stages of infection (Vleeshouwers & Oliver, 2014). Two waves of effector gene expression have been detected during infection, immediate-early expression targeting ETI, and early expression targeting MTI (Wang et al., 2011a, Jiang & Tyler, 2012). In many cases, effectors are proteins that are small (<300 aa in length), cysteine-rich (four or more cysteine residues) and possess an amino (N)-terminal **s**ignal **p**eptide (SP) for secretion to the host environment (reviewed in Lo Presti et al. (2015)).

The study of effectors has greatly improved knowledge about a variety of plant development processes (Win et al., 2012) and provided scientists with tools to help manage plant diseases. Effector profiles of pathogen populations can be monitored to allow specific and appropriate mitigation responses (Vleeshouwers & Oliver, 2014). As is the aim with this study, scientists are able to use effectors to screen for resistance in plants (e.g. Mesarich et al. (2018)), identify the *IPR*/*R* gene responsible for resistance (Matthiesen et al., 2016), and consequently develop a plant line containing the *R* gene. To improve durability of resistance, *R* genes are often stacked or deployed over space and time to match the life expectancy of the cultivar (Michelmore et al., 2013, Rietman et al., 2012).

1.6.2 Evolution

Unlike MAMPs, effectors (and plant R proteins) are often thought of as dispensable molecules, a feature which has supported their antagonistic co-evolution (Lo Presti et al., 2015). Fungal and oomycete effector-encoding genes are often found in gene-poor AT-rich regions of the genome and on accessory chromosomes, encouraging effector evolution (Lo Presti et al., 2015, Vleeshouwers & Oliver, 2014). All of these factors contribute to effectors being some of the fastest evolving genes in plant-associated organisms (Win et al., 2012). Several studies have highlighted the functional redundancy in effectors targeting the same plant processes, which may provide means for the pathogen to escape detection by losing certain effectors with no cost to fitness (Anderson et al., 2015, Birch et al., 2008). For example, both Avr4 and Ecp6 effectors produced by *Cladosporium fulvum* target chitin perception in the host tomato plant (de Jonge et al., 2010, van den Burg et al., 2006), albeit using different methods; while

Avr4 prevents the release of chitin, Ecp6 sequesters any released fragments to prevent detection by immune receptors. This strategy may further aid pathogens by positively selecting for isolates with a different effector arsenal when the environment changes (Win et al., 2012).

1.6.3 Apoplastic effectors

The apoplast, which includes both the intercellular space between plant cells and the plant cell wall (Farvardin et al., 2020), is an inhospitable environment. Not only with regard to the slew of plant-produced secondary metabolites, proteases and hydrolytic enzymes, but also due to the presence of other competing microbes with their own complex mix of secretions (Carrión et al., 2019). Despite this, the apoplast is a key interface between host plant and pathogen, with the latter secreting effectors. Apoplastic effectors common to both fungi and oomycetes include **n**ecrosis- and ethylene-inducing peptide 1-**l**ike **p**roteins (NLPs), as well as **g**lycoside **h**ydrolases (GHs) and **p**ectate **l**yases (PLs) (Li et al., 2020) which are both **c**arbohydrate-**a**ctive en**zymes** (CAZymes), reviewed in **Chapter two**. Extensive research over the last few decades has contributed greatly to our understanding of how some of these effectors function, whether it be sequestering chitin fragments to prevent activation of the plant immune response (*C. fulvum* Ecp6 (de Jonge et al., 2010, Sánchez-Vallet et al., 2013), *Moniliophthora pernicosa* MpChi (Fiorin et al., 2018)), inhibiting host enzyme activity (*C. fulvum* Avr2 (Rooney et al., 2005, Shabab et al., 2008, van Esse et al., 2008), *P. infestans* EPI1 (Tian et al., 2004), EPI10 (Tian et al., 2005), and EPIC2B (Tian et al., 2007)), or detoxifying host-produced fungitoxic compounds (*C. fulvum* CfTom1 (Ökmen et al., 2013), *Fusarium oxysporum* FoTom1 (Lairini & Ruiz-Rubio, 1997, Pareja-Jaime et al., 2008)). Progress made in the identification and characterisation of apoplastic effectors has been highlighted in recent reviews (Li et al., 2020, Rocafort et al., 2020).

1.6.4 Cytoplasmic effectors

Not all effectors secreted into the apoplast are destined to function there; a subset are instead translocated into the plant cell cytoplasm to perform their virulence function (Rocafort et al., 2020). In oomycetes, there are two main classes of intracellular effectors: RxLRs and Crinklers (CRNs).

1.6.4.1 RxLRs

RxLRs are one of the major classes of effectors produced by *Phytophthora* species, so named due to the conserved amino (N)-terminal amino acid motif Arg-X(any amino acid)-Leu-Arg (RxLR) (Jiang & Tyler, 2012). While RxLRs are known to activate plant defence responses as IPs, they have also been shown to suppress both ETI and MTI elicited by other IPs (Bos et al., 2006, Murphy et al., 2018, Oh et al., 2009). In addition to the RxLR motif, these effectors all have an N-terminal SP for secretion from

the pathogen, while many also contain an EER motif that is carboxyl (C)-terminal to RxLR motif, and some contain WY-repeat motifs (Anderson et al., 2015, Birch et al., 2008, Jiang & Tyler, 2012). Though the extra-haustorial matrix between the pathogen's haustorium and the plant cell wall is thought to be the primary site of interaction (Whisson et al., 2007, Win et al., 2012), it remains to be determined how RxLRs are translocated into host cells. Interestingly, despite their abundance in *Phytophthora* genomes, only 10–15% of RxLR effectors are positively selected for or are moderately expressed during infection, again highlighting the functional redundancy within effectors, with pathogens only relying on a subset of those potentially available (Jiang & Tyler, 2012). In keeping with this, none of the 78 RxLR effectors identified in *P. agathidicida* (Guo et al., 2020b) were found to be undergoing diversifying selection.

1.6.4.2 Crinklers

Crinklers (CRN), reviewed in Amaro et al. (2017), are so named for the **cr**inkling and **n**ecrosis phenotype by which they were first identified (Torto et al., 2003), and have been found in all sequenced oomycete plant pathogens (Amaro et al., 2017), though the numbers of these effectors in the genome vary greatly between different species (Stam et al., 2013). Like RxLRs, CRNs are translocated into the plant host cell, where some act inside the host nucleus (Schornack et al., 2010). Also, like RxLRs, they have a conserved N-terminal domain, though it contains the LxLFLAK motif, and a C-terminal domain with variation that appears to be driven by recombination (Haas et al., 2009). Despite their name, it is not particularly common for CRNs to trigger a cell death response in a host plant; in fact of 15 CRNs randomly selected in *P. sojae*, only one triggered a plant cell death response, while thirteen instead functioned to suppress the cell death response elicited by the *P. sojae* necrosis-inducing protein (PsojNIP (Qutob et al., 2002)) (Shen et al., 2013). Of these 15 *P. sojae* CRNs, two had previously been identified as required for full virulence in *P. sojae* (Liu et al., 2011): PsCRN63 as a cell death elicitor, and PsCRN115 as a suppressor of both PsojNIP- and PsCRN63-induced cell death. Subsequent studies found that expression of PsCRN63 in *A. thaliana* suppressed *FRK1*, a MTI marker gene, and resulted in increased susceptibility to *P. capsici* (Li et al., 2016), while expression of PsCRN115 in *Nicotiana benthamiana* increased resistance to infection by *Phytophthora* species, and improved tolerance to certain abiotic stresses (Zhang et al., 2015), highlighting the varied role these effectors have in pathogen virulence. Interestingly, while perhaps most studied for their role as intracellular effectors of plant pathogens, CRNs have been identified in a huge range of different species, including members of Viridiplantae (*A. thaliana*, *Solanum lycopersicum* (tomato)), and the beetle *Tribolium castaneum* (Zhang et al., 2016), where they are suggested to play a role in the resolution of inter-organism conflict (Amaro et al., 2017, Zhang et al., 2016).

1.7 Plant immune receptors

Plant immune receptors or IPRs, traditionally known as PRRs or R proteins, can be either cell surface receptors or intracellular receptors (Wu et al., 2018). In the simplest form, immune receptors are responsible for recognising IPs and subsequently triggering a plant defence response which may result in plant cell death or an HR. PRRs are cell surface receptors responsible for recognising conserved molecular patterns, and are consequently conserved in a number of plant species (Zipfel, 2014), where they provide broad spectrum resistance to pathogens (e.g. FLS2 responsible for recognition of bacterial flagellin (Gomez-Gomez & Boller, 2000), *Arabidopsis* PepR1 and PepR2, which recognise DAMPs in the form of AtPep peptides (Krol et al., 2010, Yamaguchi et al., 2010, Yamaguchi et al., 2006), and CEBiP which recognises fungal chitin (Kaku et al., 2006, Miya et al., 2007, Wan et al., 2008)). In contrast, R proteins are intracellular receptors and are lineage-specific (Dangl & Jones, 2001, Tyler, 2009), such that the *R* gene encoding the R protein may be present in one cultivar, but not another of the same species. The distinction between PRRs and R proteins has become somewhat blurred over the years as it becomes clear that there is considerable crosstalk between both classes of plant immune receptors (Cook et al., 2015, Ngou et al., 2021). The term 'immune receptor' describes both PRRs and R proteins and will be used henceforth.

1.7.1 Cell surface receptors

Cell surface receptors are commonly either **r**eceptor-**l**ike **k**inases (RLKs), which consist of an extracellular ligand-binding domain (which often contains **l**eucine-**r**ich **r**epeats (LRRs) for the recognition of proteinaceous ligands (Gust & Felix, 2014, Shiu & Bleecker, 2003)), a single pass transmembrane domain and an intracellular kinase domain, or receptor-like proteins (RLPs), which contain a shorter cytoplasmic domain rather than the kinase domain (Jeong et al., 1999, Ma et al., 2016, Zipfel, 2014). Both RLKs and RLPs are known to dimerize with other RLKs (Ma et al., 2016) such as **B**RI1-**a**ssociated receptor **k**inase **1** (BAK1) (Li et al., 2002) and **s**uppressor **o**f **BIR1** (SOBIR1), though SOBIR1 interacts specifically with LRR-RLPs (Liebrand et al., 2013a). Upon perception of an IP, the immune receptor heterodimerizes with BAK1 and subsequent phosphorylation events mediated by the BAK1 kinase domain play a key role in signal transduction (Schulze et al., 2010). Because RLPs do not contain intracellular signaling domains, they must interact with other proteins, such as RLKs, in order to direct a cellular response (Gust & Felix, 2014, Liebrand et al., 2013b, Liebrand et al., 2014, Tor et al., 2009). For example, Liebrand et al. (2013b) found that Cf-4, an RLP in tomato that provides resistance to *C. fulvum* upon recognition of the Avr effector protein Avr4, interacts with the SOBIR1 in a way which is required for HR and resistance to *C. fulvum* invasion.

1.7.2 Intracellular receptors

Intracellular receptors can be classified into one of eight different groups based on their amino acid domains, the most common being proteins with a variable N-terminus (often containing a **t**oll-**i**nterleukin-1 **r**eceptor (TIR) or **c**oiled-**c**oil (CC) domain (Meyers et al., 1999, Pan et al., 2000, Zhang et al., 2017b), a central **n**ucleotide-**b**inding domain, and a LRR domain at the C terminus (NB-LRRs/NLRs) (Cesari, 2018, Takken & Goverse, 2012). NLRs recognise the IP either directly or indirectly, resulting in a conformational change that culminates in the activation of plant defences (DeYoung & Innes, 2006, Tor et al., 2009, Zhang et al., 2017b). While NLRs can (and do) function individually (Dodds et al., 2006, Jia et al., 2000), as described in the gene-for-gene model (Flor, 1942), many NLRs function in pairs with one member containing a domain targeted by the pathogen effector of interest (receptor) and the other member activating the plant defence response upon recognition (signal transducer) (Cesari et al., 2014, Sarris et al., 2015, Zhang et al., 2017b). Wu et al. (2018) noted that some signal transducer NLRs associate with several receptor NLRs, forming a network and creating functional redundancy while also uncoupling pathogen recognition from activation of plant defence responses. This may act to increase resilience of immune receptors to environmental perturbations, allowing rapid evolution with few constraints (Wu et al., 2018).

1.7.2.1 Mode of recognition

Due to the propensity for NLRs to work in pairs/complexes (Cesari et al., 2014, Dangl & Jones, 2001, Sarris et al., 2015, Zhang et al., 2017b), several hypotheses have been introduced to describe the modes by which they recognise IPs/effectors.

Direct recognition, or the **gene-for-gene** model (discussed in **section 1.5.2.1**, **Figure 1.3**) whereby the invasion pattern is directly recognised by the cognate plant immune receptor, described by (Flor, 1942).

The **guard hypothesis** was first used to explain the perception and subsequent initiation of plant defence mechanisms brought about from *P. syringae* infection of tomato (Dangl & Jones, 2001, Oldroyd & Staskawicz, 1998, van der Biezen & Jones, 1998) and is described by Jones and Dangl (2006) as the indirect recognition of an effector by an immune receptor. In this case, they suggest that the host immune receptor monitors cellular targets and recognises "pathogen-induced modified self" (Jones & Dangl, 2006). The *P. syringae* effector, AvrPto, aims to suppress the activity of the plant host immune receptor Pto, this interference is detected by the 'guard' Prf, which subsequently activates plant defence responses (Dangl & Jones, 2001, Oldroyd & Staskawicz, 1998, van der Biezen & Jones, 1998) (**Figure 1.7**).

Interestingly, the mechanism of AvrPto perception was also used as the basis for the **decoy model**, first described by van der Hoorn and Kamoun (2008), to explain research findings that fit neither the gene-for-gene hypothesis (Flor, 1942), nor the guard model (Dangl & Jones, 2001). The decoy is a host-derived protein that mimics the effectors target (van der Hoorn & Kamoun, 2008). The primary difference between the decoy model and the guard model is that the decoy is not assumed to benefit the pathogen should the real immune receptor not be present, but simply acts to recognise the target (van der Hoorn & Kamoun, 2008). van der Hoorn and Kamoun (2008) also suggest the decoy may compete with the target for effector binding, potentially contributing to limit pathogen invasion should the real immune receptor not be present (**Figure 1.7**).

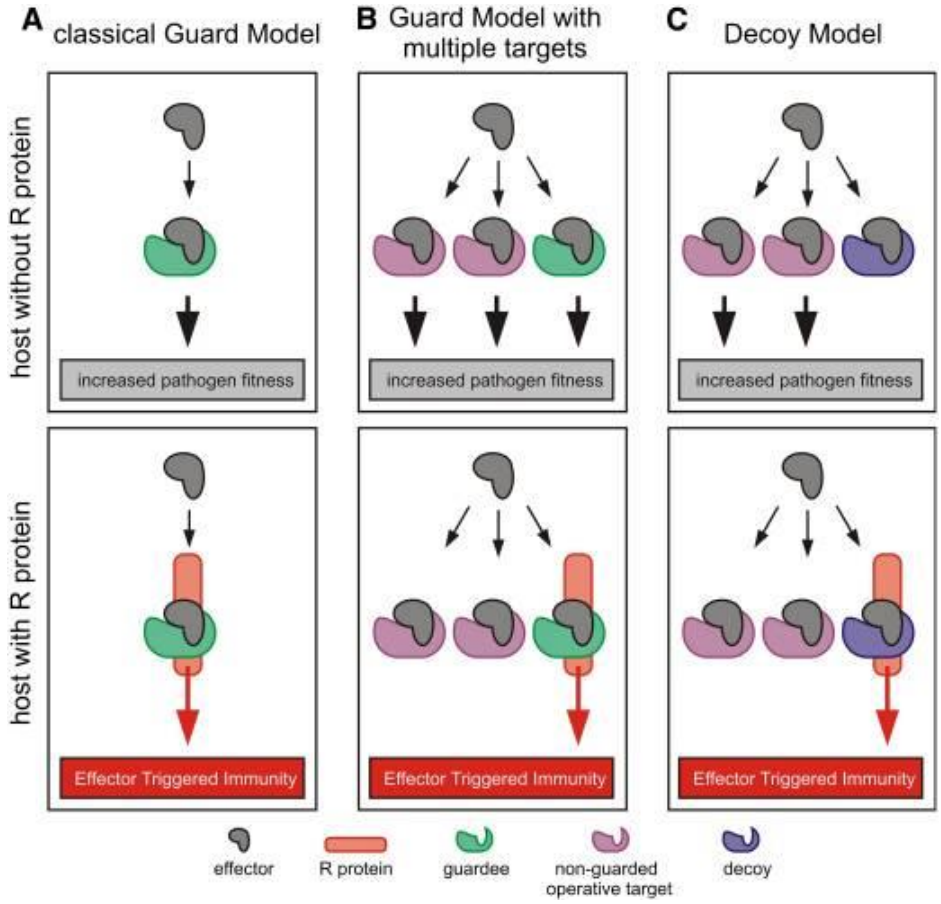

Figure 1.7. Comparison of the guard and decoy models as described by van der Hoorn and Kamoun (2008), adopted with permission.

Grey = Effectors, Purple = Effector target, Green = Guardee, Blue = Decoy, Orange = Resistance (R) protein. Taken from van der Hoorn and Kamoun (2008).

More recently, Cesari et al. (2014) described the **integrated decoy model** to encompass the mode of action detected in NLR pairs after noticing that at least one partner in the pair contained an additional non-conserved domain. Rather than two separate proteins, immune receptor and decoy, the integrated

decoy model suggests the decoy is 'integrated' into, or part of, the structure of the immune receptor, allowing direct recognition of pathogen effectors (Cesari et al., 2014). For example, in *Arabidopsis* the *rps*4 and *rrs*1 genes encode NLR proteins required for the recognition of the PopP2 effector from plant pathogenic bacterium *R. solanacearum* (Tasset et al., 2010) and *Ps. syringae* AvrRPS4 (Gassmann et al., 1999). However, recognition is race-specific, with different alleles from different *Arabidopsis* accessions (RRS1-R and RRS1-S) conferring resistance to different effectors (Sarris et al., 2015). Citing unpublished work, Cesari et al. (2014) suggested "AvrRPS4 and PopP2 interact with the WRKY domain of RRS1". This has since been confirmed (Le Roux et al., 2015) and suggests the WRKY domain is an integrated decoy for both PopP2 and AvrRPS4 (Zhang et al., 2017b).

1.8 Plant resistance (gymnosperms)

As reviewed in Fraser et al. (2016), plant defence mechanisms in gymnosperms may be pre- or post-penetration. Pre-penetration defence mechanisms include the physical and chemical properties of the leaves which may prevent or hinder pathogen entry into the plant (Franich et al., 1977, Fraser et al., 2016, Smith et al., 2006). Post-penetration defences include induced responses such as antimicrobial peptides, PR proteins, and HR, as well as lignification of plant tissues to prevent pathogen movement through the plant, and the presence of certain metabolic compounds (Kinloch & Dupper, 2002, Liu et al., 2013, Smith et al., 2006, Wallis et al., 2010). However, the review by Fraser et al. (2016) is limited only to Pinaceae species and *P. agathidicida* is known to be attracted to and colonise kauri via the fine roots rather than the leaves (Beever et al., 2010, Bellgard et al., 2016b, Fawke et al., 2015, Osswald et al., 2014). Nevertheless, differences in the physical and chemical properties of fine root systems in kauri could be examined as a first layer of defence. Other factors that may contribute to resistance could include tree age (Bassett, 1972, Bulman et al., 2004) and endophyte community (Ganley et al., 2008, Rodriguez et al., 2009). While *P. agathidicida* has been shown to infect all life stages of kauri, the importance of endophytes in infection and disease progression is currently under investigation (Padamsee et al., 2016).

1.8.1 Qualitative vs quantitative resistance

Resistance can be either qualitative or quantitative. Qualitative resistance is often controlled by a major single gene, while quantitative resistance is controlled by several genes and does not follow typical Mendelian segregation ratios, making it more difficult to understand (St Clair, 2010). Given the longevity of the host of interest (kauri), resistance needs to be durable. Interestingly, this is perhaps the most difficult aspect to investigate, as Johnson (2000) observes that there is no single resistance phenotype or genetic basis for durable resistance, only the act of durability that allows identification.

1.8.2 Resistance of kauri

Long term survival of kauri in New Zealand is likely determined by whether the trees will be able to resist infection by *P. agathidicida* and subsequent disease onset. For that reason, scientists are already investigating whether there is natural resistance within kauri populations (Williams & Faulds, 2018). Identifying the IPs responsible for eliciting a defence response in kauri may help identify the corresponding immune receptors that are involved in plant defence. This information will contribute towards forming a breeding scheme, allowing scientists and plant breeders to decide how to best produce and/or select plants with resistance to the pathogen.

A collaborative effort by the government, researchers, Māori iwi, and the community is needed to have any chance of preventing the decline of kauri. Urgent research is currently taking place to further understand *P. agathidicida*, its range, and how to manage or prevent further spread and infection (Bassett et al., 2017, Beever et al., 2010, Bellgard et al., 2016a, Bellgard & Probst, 2018, Bellgard et al., 2013, Auckland-Council, 2017, Horner & Hough, 2013, Horner et al., 2015, Padamsee et al., 2015, Smith, 2017, Williams & Faulds, 2018). This essential work not only buys time for further research but will help maintain existing genetic diversity in kauri.

1.8.3 Importance of genetic diversity

Genetic diversity is a factor that must be considered in both the perspective of the pathogen and the host. A pathogen with very little genetic diversity may increase chances of a successful resistance breeding approach by making it harder to adapt to plant resistance mechanisms (Hirst et al., 1999, Hoffmann & Hercus, 2000). For this reason, it is important to establish what genetic diversity exists in *P. agathidicida* and, if possible, determine both the origin and current geographical range. Should *P. agathidicida* be found to be native to New Zealand, it is likely to be genetically diverse and consequently harder to find resistance to all genotypes. Whereas if recently introduced (Bellgard et al., 2016b), the population is likely to be recovering from a bottleneck caused by founder effect and therefore be less genetically diverse than the native population, wherever that may be (Futuyma, 2009).

Genetic diversity in kauri and, indeed, any organism, is important for a population to maintain resistance and adapt to pathogens and environmental perturbations (Futuyma, 2009). In contrast, low genetic diversity in kauri could decrease the chances of successfully identifying durable resistance. Not only would there be less natural genetic variation to work with, but a plant breeding approach may result in kauri that are susceptible to other diseases or less able to adapt should the initial *R* genes be overcome. History has clearly demonstrated the value of diversity as a defence against disease, as reliance on the

‘lumper’ potato monoculture was partially responsible for the Irish potato famine caused by *P. infestans* in the 1800’s (Fraser, 2003, Gopal & Oyama, 2005, Lohr, 2013).

1.9 Summary

Mentioned above are gaps in the research that need to be filled in order to help contain and limit the spread of *P. agathidicida*. While closing those knowledge gaps is of urgent priority, it should be noted that no country has yet been successful in eradicating a *Phytophthora* species (Hansen, 2015). Thus, it is likely that, regardless of origin and status, *P. agathidicida* is here to stay. Therefore, long-term management of both the pathogen and host must be considered to ensure survival of kauri for generations to come.

Although *P. agathidicida* is highly pathogenic to kauri, suggesting the pathogen has not encountered this host before, it is possible that some kauri already have varying levels of natural resistance (Beever et al., 2010, Beever et al., 2009, Bellgard et al., 2016b, Williams & Faulds, 2018). Identifying IPs which are important to *P. agathidicida* pathogenicity and virulence during infection of kauri, and their subsequent immune receptors, may assist in creating a database which could be used to selectively breed kauri for durable resistance to *P. agathidicida*.

1.10 Aim

The aim of this work is to better understand the molecular basis of kauri infection by *P. agathidicida*. This will be done by identifying and characterising molecular IPs of *P. agathidicida*, with a focus on CAZymes that are recognised by immune receptors in kauri and/or model host/non-host plants and are important for pathogen virulence. Understanding *P. agathidicida* IPs and their corresponding immune receptors will aid our understanding of how the pathogen interacts with its host on a molecular level. The findings of this study are expected to not only inform about the interaction between *P. agathidicida* and kauri, but also other pathosystems, particularly those involving *Phytophthora* species and gymnosperm hosts.

1.11 Objectives

Objective one

Review the roles that GH proteins from plant-associated fungi and oomycetes play in plant–microbe interactions.

The specific tasks associated with this review were to:

- Gather literature pertaining to GH proteins involved in interactions between fungal or oomycete species and their plant hosts (to be carried out in conjunction with other parties).
- Discuss the role of GH proteins in the interaction between fungi and oomycetes and their plant hosts with detailed examples and illustrations (to be carried out in conjunction with other parties).

Objective two

Identify and characterise effector/MAMP/DAMP candidates from *P. agathidicida*, focusing on known or highly expressed GH proteins.

Genes encoding GH proteins have been found to be particularly abundant in the genomes of *Phytophthora* species (Jiang & Tyler, 2012, Yang et al., 2018a, Zerillo et al., 2013), and are well-known in fungi to have functions in virulence and pathogenicity (Lai & Liou, 2018, Pareja-Jaime et al., 2008, Quidde et al., 1998, Sella et al., 2013, Zhu et al., 2017). For this objective the specific tasks were to:

- Identify candidate *P. agathidicida* GH proteins using the annotated genomes of two *P. agathidicida* strains (3770 and 3772), together with well-established and freely available prediction tools.

- Select candidate *P. agathidicida* GH proteins for further investigation using the transcriptomic data of *P. agathidicida* (NZFS 3813) during infection of kauri roots and leaves to determine the most highly expressed GH-encoding genes.

- Clone the selected GH-encoding gene candidates into the *Agrobacterium tumefaciens* expression vector, pICH86988.

- Express the GH-encoding genes of interest in model host species *N. benthamiana* (and *N. tabacum*) using the well-established method of an *A. tumefaciens*-mediated transient transformation assay (ATTA) to identify those GH proteins which trigger plant cell death.

- Assess whether secretion to the apoplast or enzymatic activity are required for any observed plant cell death response by performing ATTAs in *N. benthamiana* or *N. tabacum* after removing N-terminal signal peptides or mutating predicted catalytic residues in the GH-encoding gene of interest.

- Determine whether previously identified *P. agathidicida* RxLR proteins (Guo, Unpublished-a, Guo et al., 2020a) are capable of suppressing the cell death response induced by the GH protein(s) of interest in *N. benthamiana*.

- Investigate whether prior expression of the GH-encoding gene of interest in *N. benthamiana* (via ATTAs) impacts the lesion size of *P. agathidicida*.

Objective three

Determine whether the composition of kauri leaf apoplastic wash fluid (AWF) is altered by the presence of *P. agathidicida*.

The specific tasks associated with understanding whether there are metabolite changes in kauri leaf AWF following inoculation with *P. agathidicida* were to:

- Develop a method to harvest AWF from kauri leaves using the available resources.

- Harvest kauri leaf AWF from five different family lines and inoculate with *P. agathidicida* NZFS 3770 mycelia or cellophane membranes (negative control).

- Harvest the resulting culture filtrate and send for analysis by nuclear magnetic resonance (NMR) (to be carried out by a third party).

- Assess the resulting data to establish whether any changes in metabolites are observed in kauri leaf AWF following inoculation with *P. agathidicida* (to be carried out in conjunction with a third party).

Objective four

Profile the in culture secretome of *P. agathidicida*

To better understand what proteins are being secreted by *P. agathidicida* under different conditions, the specific tasks associated with this objective were to:

- Grow *P. agathidicida* in a variety of nutrient-poor and nutrient-rich liquid media.

- Harvest the resulting *P. agathidicida* culture filtrates.

- Prepare *P. agathidicida* culture filtrates for analysis via liquid chromatography-mass spectrometry using the well-established method of trypsin digestion (LC–MS).

- Perform LC–MS analysis (to be carried out by a third party).

- Identify and evaluate the *P. agathidicida* proteins present in culture filtrates using the data obtained from LC–MS analysis and a curated list of *P. agathidicida* NZFS 3770 predicted proteins, together with various freely available web-based prediction tools to gain insights into the extracellular secretome of *P. agathidicida* during growth in liquid culture.

Chapter two: Secreted glycoside hydrolase (GH) proteins as effectors and invasion patterns of plant-associated fungi and oomycetes

Ellie L. Bradley[1], Bilal Ökmen[2,3], Gunther Doehlemann[2], Bernard Henrissat[4,5,6], Rosie E. Bradshaw[7] and Carl H. Mesarich[1,*]

[1]Bioprotection Aotearoa, School of Agriculture and Environment, Massey University, Palmerston North, New Zealand.
[2]Institute for Plant Sciences and Cluster of Excellence on Plant Sciences (CEPLAS), University of Cologne, Cologne, Germany.
[3]Department of Microbial Interactions, IMIT/ZMBP, University of Tübingen, Tübingen, Germany.
[4]DTU Bioengineering, Technical University of Denmark, Kongens Lyngby, Denmark.
[5]Architecture et Fonction des Macromolécules Biologiques (AFMB), UMR 7257 Centre National de la Recherche Scientifique (CNRS), Université Aix-Marseille, Marseille, France.
[6]Department of Biological Sciences, King Abdulaziz University, Jeddah, Saudi Arabia.
[7]Bioprotection Aotearoa, School of Natural Sciences, Massey University, Palmerston North, New Zealand.

Chapter two has been published as a paper in *Frontiers in Plant Science* as part of the research topic "Secretomics: More secrets to unravel of plant-fungus interactions, Volume II".

Abstract

During host colonization, plant-associated microbes, including fungi and oomycetes, deliver a collection of glycoside hydrolases (GHs) to their cell surfaces and surrounding extracellular environments. The number and type of GHs secreted by each organism is typically associated with their lifestyle or mode of nutrient acquisition. Secreted GHs of plant-associated fungi and oomycetes serve a number of different functions, with many of them acting as virulence factors (effectors) to promote microbial host colonization. Specific functions involve, for example, nutrient acquisition, the detoxification of antimicrobial compounds, the manipulation of plant microbiota, and the suppression or prevention of plant immune responses. In contrast, secreted GHs of plant-associated fungi and oomycetes can also activate the plant immune system, either by acting as microbe-associated molecular patterns (MAMPs), or through the release of damage-associated molecular patterns (DAMPs) as a consequence of their enzymatic activity. In this review, we highlight the critical roles that secreted GHs

from plant-associated fungi and oomycetes play in plant–microbe interactions, provide an overview of existing knowledge gaps and summarise future directions.

2.1 Introduction

Plant–microbe and microbe–microbe interactions

Filamentous fungi and oomycetes have evolved as efficient colonizers of plants, utilizing multiple strategies to interact with their hosts. Many of these organisms primarily reside in the plant apoplast during at least the first stages of colonization (Rocafort et al., 2020). The apoplast comprises all extracellular matrices and compartments outside the plasma membrane of plant cells (Sattelmacher, 2001) and contains toxic compounds and hydrolytic enzymes that disrupt fungal and oomycete growth (Doehlemann & Hemetsberger, 2013). Cell surface-localized immune receptor proteins, termed pattern recognition receptors (PRRs), also monitor the extracellular space for molecular invasion patterns to activate the plant immune system (Cook et al., 2015, van der Burgh & Joosten, 2019). Here, PRRs recognize microbe- or damage-associated molecular patterns (MAMPs or DAMPs, respectively) to activate immune responses that further slow or halt fungal and oomycete growth. These responses include the production of defensive compounds and reactive oxygen species (ROS), the deposition of polysaccharides and proteins (e.g. lignin, callose and hydroxyproline-rich glycoproteins that reinforce or strengthen plant cell walls and infection sites) (Kuć, 1997) and, in some cases, a localised cell death response (Dickman & Fluhr, 2013). Of the invasion patterns, MAMPs typically comprise broadly conserved molecules, such as proteins, lipids and polysaccharides of invading fungi or oomycetes, whereas DAMPs are made up of endogenous molecules, such as cytosolic proteins, peptides, nucleotides, amino acids and polysaccharides that are released from the plant upon fungal or oomycete attack (Hou et al., 2019, Newman et al., 2013, Tanaka & Heil, 2021, Raaymakers & Van den Ackerveken, 2016).

Outside of the apoplast, plant-associated fungi and oomycetes are exposed to exudates that may contain a cocktail of plant-derived antimicrobial compounds (Jacoby et al., 2020). Furthermore, at all locations of colonization, secondary metabolite compounds, hydrolytic enzymes and other proteins may be produced by other co-inhabiting microbes with roles in microbial antagonism (e.g. Carrión et al. (2019), Snelders et al. (2020), Snelders et al. (2021)). It is no surprise then that plant-associated fungi and oomycetes must neutralize or suppress plant defences, whether constitutive or induced, as well as the antimicrobial activities of co-inhabiting microbes, in order to colonize their hosts. For this purpose, plant-associated fungi and oomycetes deploy a collection of virulence factors, termed effectors. These effectors, many of which are proteinaceous, function outside the plant cell in locations such as the apoplast, or inside the plant cell, where they are translocated into various cell compartments (He et al.,

2020, Rocafort et al., 2020, Okmen & Doehlemann, 2014). In some cases, these effectors can also act as MAMPs (Thomma et al., 2011) or generate DAMPs that are recognized by PRRs to activate the plant immune system.

Plant and microbial cell walls

Immediately outside the plant plasma membrane is the plant cell wall, which forms part of the apoplast. The plant cell wall is a complex structure that fulfils diverse cellular functions ranging from maintenance of structural integrity to regulation of plant development (Zhang et al., 2021a). In terms of composition, more than 90% of the plant cell wall is made up of carbohydrates, with cellulose, hemicelluloses and pectic polysaccharides the main carbohydrate components (Kumar & Turner, 2015, Popper et al., 2011). Crucially, the plant cell wall also provides a protective barrier against abiotic stresses and invading microbes (Rui & Dinneny, 2020, Vaahtera et al., 2019). Indeed, many plant-associated fungi and oomycetes must first breach the plant cell wall in order to colonize their hosts (Bellincampi et al., 2014). Breakdown or hydrolysis of the plant cell wall does, however, risk the release of DAMPs (such as oligogalacturonides, mixed-linked glucans, xyloglucans and cellulose-derived oligomers) that can then be recognized by plant PRRs to activate the plant immune system (Aziz et al., 2007, Benedetti et al., 2015, Brutus et al., 2010, Claverie et al., 2018, Souza et al., 2017, Ferrari et al., 2013, Mélida et al., 2018, Mélida et al., 2020, Rebaque et al., 2021).

Like in plants, the cell walls of plant-associated fungi and oomycetes play a vital role in maintaining the structural integrity of the cell, as well as in regulating development. Although types, distributions and linkages of cell wall carbohydrates vary from species to species (e.g.Gow et al. (2017)), the main ones in fungi are chitin (β-1,4-N-acetylglucosamine [GlcNAc]; inner layer) and β-1,3/1,6-glucans (outer layer), while the most abundant carbohydrates in oomycetes are cross-linked cellulose, β-1,4- and β-1,3/1,6-glucans (Wanke et al., 2020a). Research on fungi, in particular, has shown that the cell wall is dynamic, with ongoing remodelling required for the morphological differentiation of specialized infection structures *in planta*. Such remodelling is necessary to protect fungal cell wall carbohydrates against hydrolysis by plant-derived enzymes, as well as to prevent their detection by PRRs (Becker et al., 2016, El Gueddari et al., 2002, Fujikawa et al., 2009, Fujikawa et al., 2012, Noorifar et al., 2021, Oliveira-Garcia & Deising, 2013, Oliveira-Garcia & Deising, 2016). As might be expected, however, this remodelling also runs the risk of releasing MAMPs (e.g. chitin and β-glucan fragments) that activate the plant immune system (Cao et al., 2014, Fesel & Zuccaro, 2016, Miya et al., 2007, Rovenich et al., 2016, Sánchez-Vallet et al., 2015, Shimizu et al., 2010, Wanke et al., 2020a, Wanke et al., 2020b).

Glycoside hydrolases (GHs) of plant-associated fungi and oomycetes

Many plant- and microbe-derived hydrolytic enzymes are carbohydrate-active enzymes (CAZymes). CAZymes are involved in the breakdown, biosynthesis or modification of glycosidic bonds present in carbohydrates and glycoconjugates. Based on sequence and structural similarity of their functional domains, CAZymes can be classified into six main classes: glycoside hydrolases (GHs), carbohydrate esterases (CEs), polysaccharide lyases (PLs), glycosyltransferases (GTs), auxiliary activity enzymes (AAs) and carbohydrate-binding modules (CBMs) (http://www.cazy.org/; Lombard et al. (2014); Drula et al. (2022)).

GH proteins represent the largest class of CAZymes, and are involved in the hydrolysis and/or rearrangement of glycosidic bonds in glycoconjugates, oligo- and polysaccharides (Henrissat, 1991, Henrissat & Davies, 1997). The CAZy database describes 172 GH families, which are grouped into 18 different GH clans (GH-A to -R) based on sequence similarity (Henrissat & Davies, 1997). Although a classification system based on sequence similarity is a very powerful way to predict the enzymatic activity of a novel GH enzyme, many GH families are polyspecific, meaning that one GH family can comprise enzymes with different substrate specificities (Henrissat, 1991).

The number and type of secreted GH proteins produced by plant-associated fungi and oomycetes with different lifestyles is highly variable. In biotrophic pathogens, as well as plant-associated endophytic microorganisms, a relatively low number of GHs targeting the plant cell wall are produced during host penetration and colonization, which minimizes host damage (Hane et al., 2020). On the other hand, necrotrophs and hemibiotrophs display more aggressive strategies during host colonization. At the necrotrophic stage of colonization, these pathogens secrete a wide range and number of GHs to directly or indirectly break down plant cell walls, and thus host cells, to feed on dead tissue (Hane et al., 2020). This is reflected in the genomes of these organisms, where it is generally accepted that biotrophs contain relatively few genes encoding plant cell wall-degrading GHs compared to necrotrophs and hemibiotrophs (Hane et al., 2020). Comparative genome analyses have revealed that, regardless of phylogenetic distance, the number and diversity of GH-encoding genes present in fungal and oomycete genomes is associated with their lifestyle. Although there are exceptions, many necrotrophic and hemibiotrophic fungi and oomycetes have around 300 GH-encoding genes (Zerillo et al., 2013, Zhao et al., 2013), while biotrophic and endophytic (symbiotic) fungi and oomycetes often contain only around 100 GH-encoding genes (Zerillo et al., 2013, Zhao et al., 2013, Hane et al., 2020). In contrast to necrotrophs and hemibiotrophs, biotrophs and symbiotic fungi lack GH6 family members, which display endoglucanase and cellobiohydrolase activities that target cellulose in the plant cell wall (Martin et al., 2010, Couturier et al., 2012, Zhao et al., 2013). Although saprophytes are not associated with plant diseases, they have a similar number of GH-encoding genes to hemibiotrophs and necrotrophs,

supporting their well-known capacity for biomass decomposition (Zerillo et al., 2013, Zhao et al., 2013). On the other hand, saprophytic yeasts (such as those in the Class *Saccharomycetes*) lack many GH families including GH1, GH6, GH10, GH11, GH30 and GH79, and possess even fewer GH-encoding genes than biotrophs (Zhao et al., 2013).

In addition to lifestyle, the diversity of GH families is also correlated with cell wall composition of the host plants. For example, dicot plants encode more pectin in their cell wall compared to monocot plants. Thus, dicot-specific pathogens tend to have more pectinases, including GH28, GH88 and GH105 families, than monocot-specific pathogens (Zhao et al., 2013). Since the plant cell wall-degrading GH repertoire of plant-associated fungi and oomycetes is strongly associated with infection strategy or lifestyle, Hane et al. (2020) developed a CAZyme-Assisted Training And Sorting of -trophy (CATAStrophy) pipeline to predict the lifestyle of a microorganism.

Over recent years, it has become increasingly clear that secreted GH proteins of plant-associated fungi and oomycetes (i.e. those that are targeted extracellularly, but that lack a transmembrane domain or a glycophosphatidylinositol lipid modification site) play diverse roles in promoting host colonization and/or activating host immune responses (e.g. as effectors, MAMPs, or proteins that generate DAMPs) (Kubicek et al., 2014, Rafiei et al., 2021) (**Figure 2.1** and **Appendix 2.1**). In this review, we highlight these roles, provide an overview of existing knowledge gaps and summarise future directions.

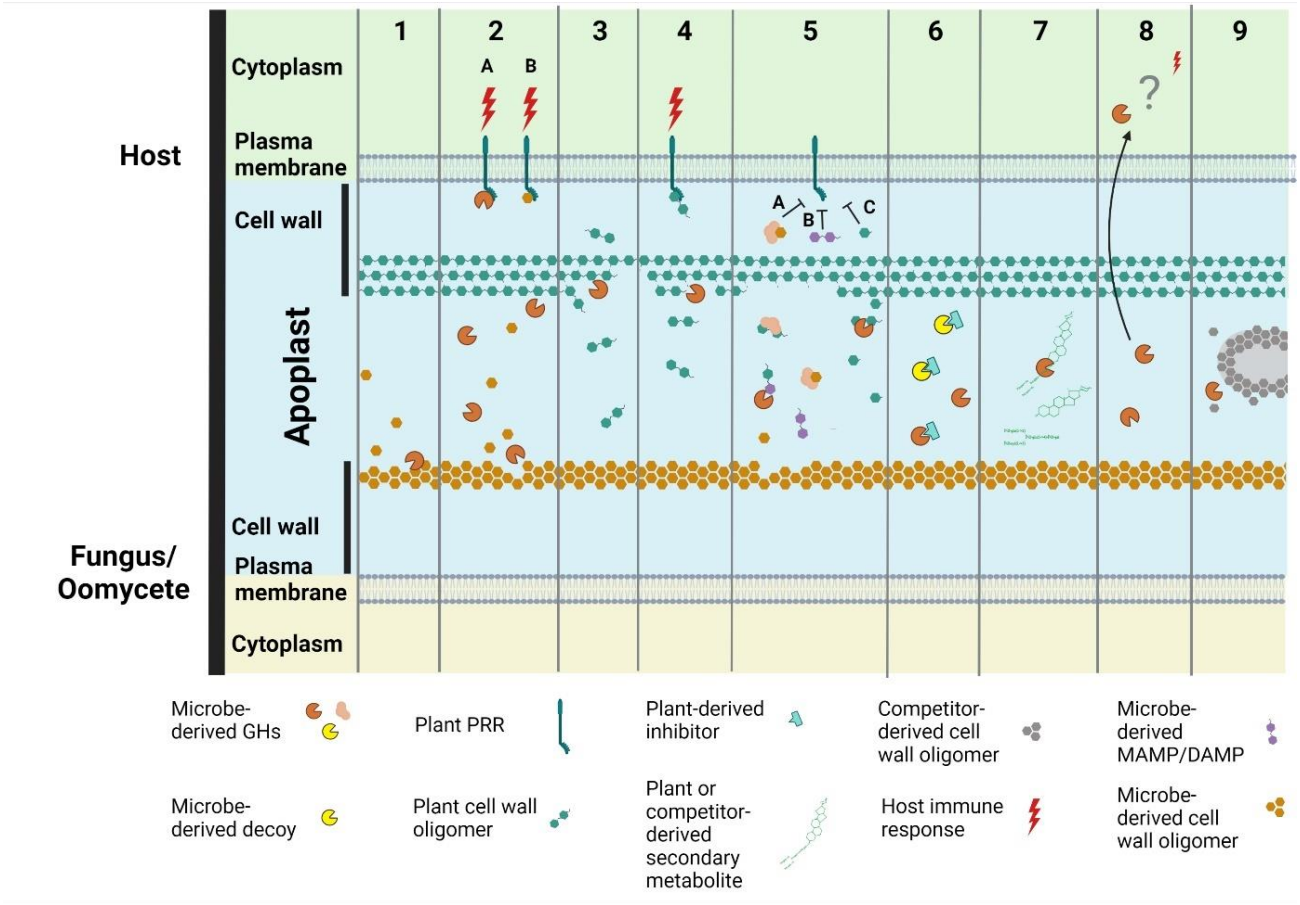

Figure 2.1. Potential roles of glycoside hydrolase proteins in virulence and pathogenicity of plant-associated fungi and oomycetes.

Secreted glycoside hydrolase (GH) proteins from plant-associated fungi and oomycetes play diverse roles in promoting plant colonization and/or activating plant immune responses. These roles include: **(1)** the modification of surface-associated carbohydrates present in their own cell walls to enable the remodeling of hyphal surfaces or infection structures produced during plant colonization; **(2)** the induction of plant immune responses, such as plant cell death, following their recognition as microbe-associated molecular patterns (MAMPs; **2A**), or the recognition of cell wall carbohydrate fragments (e.g., chitin or β-glucan oligomers) released from their own cell walls as a consequence of their activity [e.g. in **(1)**; **2B**], by pattern recognition receptors (PRRs) at the plant cell surface to provide plant resistance or susceptibility. Regarding the latter, plant cell death could, for example, result in a release of nutrients to support the growth of fungal or oomycete pathogens with a necrotrophic lifestyle, or drive a switch from biotrophy to necrotrophy for fungal or oomycete pathogens with a hemibiotrophic lifestyle; **(3)** nutrient acquisition through the release of carbohydrate fragments from plant cell walls or the breakdown of entire plant cells; **(4)** the induction of plant immune responses, such as cell death, following the recognition of plant cell wall carbohydrate fragments, generated as a consequence of their activity [e.g., in **(3)**] by PRRs at the plant cell surface to provide plant resistance or susceptibility. Again, plant cell death could support necrotrophy (as in **2B**); **(5)** the sequestration **(5A)**, modification **(5B)** or degradation **(5C)** of MAMPs or DAMPs to prevent their recognition by PRRs at the plant cell surface to prevent activation of plant immune responses; **(6)** acting as a decoy to bind host-produced proteins that would otherwise inhibit GH proteins produced by plant-associated fungi or oomycetes; (7) the detoxification of antimicrobial compounds produced by plants or microbial competitors (e.g., through the removal of a sugar group from enzymatic or non-enzymatic proteins or secondary metabolites); (8) functions that promote host colonization upon uptake into plant cells (currently uncharacterized); (9) manipulation of the host microbiome through, for example, breaking down the cell walls of microbial competitors. Figure created with BioRender.com.

2.2 Secreted GH proteins from plant-associated fungi and oomycetes with roles in promoting plant colonization and/or activating plant immune responses

Secreted glycoside hydrolase family 3 (GH3) and 10 (GH10) proteins

Saponins are fungi-toxic plant-derived secondary metabolites that play a role in plant defence, such as α-tomatine of tomato (*Solanum lycopersicum*) and avenacin of oat (*Avena sativa*) (Bowyer et al., 1995). These saponins form a complex with sterols in the plasma membrane of fungi, but not oomycetes, resulting in a loss of membrane integrity (Bangham et al., 1962, Bowyer et al., 1995, Steel & Drysdale, 1988). Several fungal species, however, produce GH family 3 (GH3 tomatinase or avenacinase) or 10 (GH10 tomatinase) enzymes that break down or detoxify these saponins into non-toxic or less toxic compounds. For GH3 tomatinases, this is achieved through the removal of a terminal glucose from α-tomatine to give β_2-tomatine, while for GH10 tomatinases, the entire lycotetraose moiety is removed to give tomatidine and β-lycotetraose (Osbourn, 1996, Turner, 1961).

Research on these enzymes was initially performed on a GH3 avenacinase from *Gaeumannomyces graminis* var. *avenae*, the necrotrophic fungal pathogen responsible for take-all disease in grasses. Similar to GH3 tomatinases, this avenacinase removes the terminal glucose molecules from avenacin A1 to give less toxic compounds (Crombie et al., 1986). Disruption of the avenacinase-encoding gene in *G. graminis* var. *avenae* resulted in an inability of the pathogen to cause disease on oat, suggesting an important role in pathogenicity (Bowyer et al., 1995).

Unlike the avenacinase-encoding gene from *G. graminis* var. *avenae*, targeted disruption of the GH3 tomatinase-encoding gene from *Septoria lycopersici*, a necrotrophic fungal pathogen responsible for leaf spot disease on tomato and other solanaceous plants, did not affect the ability of this pathogen to cause disease symptoms on currant tomato (*Solanum pimpinellifolium*) (Martin-Hernandez et al., 2000). Instead, disruption only led to the increased expression of plant defence-related genes (Martin-Hernandez et al., 2000). Interestingly, while infection of *Nicotiana benthamiana* by wild type (WT) *S. lycopersici* resulted in clear disease lesions, no disease symptoms were observed upon infection with the tomatinase-deficient mutant (Bouarab et al., 2002). Disease symptoms were, however, observed when *N. benthamiana* leaves were pre-treated with either the GH3 tomatinase, or the resulting product (β_2-tomatine), prior to infection with the tomatinase-deficient mutant (Bouarab et al., 2002). This suggested that the tomatinase enzyme of *S. lycopersici* is required for infection of *N. benthamiana* and, furthermore, that β_2-tomatine is key to disease establishment by this pathogen (Bouarab et al., 2002).

Another tomatinase enzyme that has been studied in detail is FoTom1, a GH10 protein from *Fusarium oxysporum* f. sp. *lycopersici*, a hemibiotrophic fungal pathogen responsible for vascular wilt disease of tomato (Pareja-Jaime et al., 2008). In line with a role in virulence, Δ*fotom1* deletion mutants were significantly delayed in their ability to cause death of tomato plants, when compared to plants infected with WT *F. oxysporum* f. sp. *lycopersici* or a strain overexpressing *FoTom1* (Pareja-Jaime et al., 2008). It should be pointed out, however, that although a role in virulence was shown, Δ*fotom1* deletion mutants only showed a 25% reduction in tomatinase activity in culture (Pareja-Jaime et al., 2008). Thus, it was anticipated that *F. oxysporum* f. sp. *lycopersici* produces other GH3 enzymes that also function as tomatinases (Pareja-Jaime et al., 2008).

In another example, *Cladosporium fulvum*, a biotrophic fungal pathogen responsible for tomato leaf mould disease, was shown to produce a functional GH10 tomatinase enzyme, CfTom1 (Ökmen et al., 2013). As with *FoTom1* (Pareja-Jaime et al., 2008), *CfTom1* expression was induced in culture in the presence of α-tomatine (Ökmen et al., 2013). During the early stages of tomato infection (3, 6 and 9 d post-inoculation [dpi]), the expression of *CfTom1* was low, but was significantly induced at 12 dpi and peaked at 15 dpi (Ökmen et al., 2013). While both WT *C. fulvum* and Δ*cftom1* deletion mutants displayed similar levels of biomass during the initial penetration stages of infection, Δ*cftom1* biomass was significantly reduced from 10 dpi and, unlike WT infection, no accumulation of tomatidine was observed (Ökmen et al., 2013). Taken together, these results demonstrated that CfTom1 is required for the full virulence of *C. fulvum* on tomato (Ökmen et al., 2013).

Secreted glycoside hydrolase family 11 (GH11) proteins

A large number of GH proteins from several GH families trigger cell death in host and/or non-host plants (Table 1). In many cases, the ability of these proteins to trigger cell death is independent of enzymatic activity, suggesting that they are recognized as MAMPs by PRRs localized on the plant cell surface (Table 1). One such example is ethylene-inducing xylanase (EIX), a GH family 11 (GH11) protein with β-1-4-endoglucanase activity from *Trichoderma viride*, the symbiotic biocontrol fungus associated with plant roots and soil (Dean & Anderson, 1991, Dean et al., 1989, Fuchs & Anderson, 1987, Fuchs et al., 1989). EIX (hereafter referred to as TvEIX) triggers a wide range of plant immune responses (mostly in *N. benthamiana* cv. Xanthi), including the induction of ethylene biosynthesis, electrolyte leakage, pathogenesis-related (PR) protein expression, phytoalexin and ROS production, as well as cell death (Avni et al., 1994, Bailey et al., 1990, Bailey et al., 1992, Fluhr et al., 1991, Laxalt et al., 2007, Lotan & Fluhr, 1990, Ron et al., 2000, Yano et al., 1998). Consistent with the recognition of TvEIX as a MAMP, mutation of the active site residues in this protein revealed that the xylanase activity of TvEIX is not required for cell death elicitation (Furman-Matarasso et al., 1999). This is in line with a previous study which concluded, based on protoplast assays, that the enzymatic activity of TvEIX is

also not required for induction of ethylene biosynthesis (Sharon et al., 1993). It has since been shown that a five-amino acid surface-exposed pentapeptide motif, TKLGE, which is not required for enzymatic activity, is the epitope recognized by *N. benthamiana* cv. Xanthi (Rotblat et al., 2002).

The cell death responses triggered by TvEIX in *N. benthamiana* cv. Xanthi and tomato are governed by a single dominant locus (Bailey et al., 1993, Ron et al., 2000). In tomato, this locus is made up of two genes, *SlEIX1* and *SlEIX2*, which both encode leucine-rich repeat receptor-like protein (LRR-RLP) PRRs capable of binding TvEIX (Ron & Avni, 2004). Of these two PRRs, however, only SlEIX2 is capable of initiating immune responses upon recognition of TvEIX, whilst SlEIX1 instead acts as a decoy immune receptor to attenuate TvEIX-induced immune signalling by SlEIX2 (Bar et al., 2010, Ron & Avni, 2004). It is known that LRR-RLPs often dimerise with receptor-like kinases (RLKs), such as suppressor of BIR1 (SOBIR1) and/or BRI1-associated kinase-1 (BAK1), in order to initiate signal transduction (Li et al., 2002, Liebrand et al., 2013a, Liebrand et al., 2014). Interestingly, while SlEIX2 associates with the co-receptor SOBIR1 (Liebrand et al., 2013a), the co-receptor BAK1 has been shown to interact with SlEIX1 only, indicating that the recognition of TvEIX by SlEIX2 is BAK1-independent (Bar et al., 2010). Based on these and other experiments, a model was put forward in which SlEIX1, in the presence of BAK1, binds to TvEIX, and heterodimerizes with SlEIX2 to prevent SlEIX2 endocytosis and resultant plant immune responses (Bar & Avni, 2009, Bar et al., 2011, Bar et al., 2010). Because longer TvEIX exposure leads to a stronger immune response, including cell death (Bar et al., 2010), it is anticipated that the function of SlEIX1 is to prevent immune responses over the short term which, in turn, enables symbiotic *T. viride* to enter host plants. Importantly, this function is not expected to prevent immune responses from occurring against pathogenic microbes when necessary (Bar et al., 2011, Bar et al., 2010).

Following on from the research on TvEIX and SlEIX1/SlEIX2, an LRR-RLP PRR named NbEIX2, which is orthologous to SlEIX2 from tomato, was identified in *N. benthamiana* (Yin et al., 2021). NbEIX2 recognizes VdEIX3, a TvEIX-like protein from *Verticillium dahliae*, a broad host-range, hemibiotrophic fungal pathogen responsible for vascular wilt disease (Yin et al., 2021). While NbEIX2 constitutively associates with both BAK1 and SOBIR1, co-immunoprecipitation assays revealed that NbEIX2 dissociates from BAK1 after treatment with VdEIX3, indicating that the cell death and other immune responses elicited by VdEIX3 (i.e. ROS production and the induction of *PR* and MAMP-triggered defence genes) are BAK1-independent (Yin et al., 2021). This result was corroborated by gene silencing experiments in which VdEIX3 triggered cell death and other immune responses, including ROS production, in *N. benthamiana* plants silenced for the *BAK1* gene (Yin et al., 2021). The same was observed in *N. benthamiana* plants silenced for *SOBIR1*, indicating that the immune responses triggered by VdEIX3 are also SOBIR1-independent (Yin et al., 2021).

Another well characterized fungal GH11 is BcXyn11A, a protein with β-1,4-endoxylanase activity from *Botrytis cinerea*, the broad host-range necrotrophic pathogen responsible for grey mould disease (Brito et al., 2006). During invasion of tomato, the *BcXyn11A* gene is expressed from the beginning of the infection process, increasing from 24 to 48 hours post-inoculation (hpi), with Δ*bcxyn11a* deletion mutants showing significantly reduced virulence (Brito et al., 2006). BcXyn11A hydrolyses the linear backbone of xylan, which is the main hemicellulose component of plant cell walls. The BcXyn11A protein was shown to induce immune responses including the upregulation of defence-related genes, ROS production, electrolyte leakage and cell death, when infiltrated into leaves of tomato and *Nicotiana tabacum* cvs. Havana, Alcalá and Paraíso (Brito et al., 2006, Frías et al., 2019, Noda et al., 2010). Like TvEIX, enzymatic activity is not required for cell death induction, suggesting that BcXyn11A is recognized as a MAMP by host plants (Noda et al., 2010). Remarkably, although Δ*bcxyn11a* deletion mutants had reduced virulence on both tomato leaves and grape berries (Brito et al., 2006), when Δ*bcxyn11a* mutants were complemented with copies of the *BcXyn11A* gene that encode enzymatically inactive versions of the protein, virulence was restored, suggesting that BcXyn11A contributes to the virulence of *B. cinerea* through cell death induction (i.e. necrosis), rather than by enzymatic activity (Noda et al., 2010).

A 25-amino acid peptide, Xyn25, has since been identified as the component of BcXyn11A that is sufficient for elicitation of cell death, as well as other immune responses, in *N. tabacum* cv. Havana and *S. lycopersicum* cv. Moneymaker (Frías et al., 2019). From this peptide, two regions consisting of four consecutive amino acid residues (YGWT and YYIV, respectively) are required for the induction of defence responses (Frías et al., 2019). These amino acids are partially exposed on the predicted tertiary structure of BcXyn11A and are conserved across other xylanases like TvEIX (Frías et al., 2019). Interestingly, a xylanase inhibitor protein, TAXI-I, has been identified from wheat (*Triticum aestivum*) that can prevent the necrotizing activity of BcXyn11A when expressed in the host plant *Arabidopsis thaliana* (Brutus et al., 2005, Tundo et al., 2020). As the 25-amino acid cell death elicitation region is located next to the catalytic site in the predicted tertiary structure of BcXyn11A, it is hypothesized that binding of TAXI-I to the catalytic site hides the necrotizing region from recognition by a putative PRR (Tundo et al., 2020).

Secreted glycoside hydrolase family 12 (GH12) proteins

Like the GH11 proteins described above, a diverse range of GH family 12 (GH12) proteins belonging to both plant-associated oomycetes and fungi are capable of triggering cell death when transiently expressed in, or infiltrated into, plants (Table 1). One of the best studied is PsXEG1, a GH12 protein with hydrolytic activity towards both β-glucan and xyloglucan that was identified from *Phytophthora sojae*, a hemibiotrophic oomycete pathogen (Ma et al., 2015b). PsXEG1 triggers cell death in some

solanaceous plant species, including the model host *N. benthamiana*, as well as the native fabaceous host, soybean (*Glycine max*) (Ma et al., 2015b). While either silencing of *PsXEG1*, or mutation of the catalytic residues present in the protein it encodes, significantly reduced *P. sojae* virulence on soybean, PsXEG1 catalytic mutants were still capable of eliciting cell death. This suggested that not only is PsXEG1 an important virulence factor of *P. sojae*, but also that its contribution to virulence on soybean is dependent on enzyme activity. Furthermore, given that enzymatic activity is not required for cell death induction by PsXEG1, these results suggested that PsXEG1 is recognized as a MAMP (Ma et al., 2015b, Ma et al., 2017).

PsXEG1 is secreted into the apoplast as two isoforms. The larger isoform is N-glycosylated at positions N174 and N190, protecting it from degradation by the apoplastic aspartic protease of soybean, GmAP5. However, the smaller, non-glycosylated isoform of PsXEG1 is bound by GmAP5 and quickly degraded (Ma et al., 2015b, Xia et al., 2020). In the apoplast, non-glycosylated PsXEG1 is also bound by the soybean glucanase inhibitor protein, GmGIP1, which not only prevents xyloglucan hydrolysis by this isoform of PsXEG1, but also inhibits the contribution of this isoform to *P. sojae* virulence (Ma et al., 2015b, Xia et al., 2020). Interestingly, only one other GH12 protein of *P. sojae*, PsXLP1, which shares 67% amino acid identity and a similar expression profile with PsXEG1 (i.e. highly expressed from 20 min to 2 hours during *P. sojae* infection of soybean (Ma et al., 2015b, Ma et al., 2017)), was found to bind to GmGIP1 (Ma et al., 2017). PsXLP1 harbours a C-terminal deletion that results in the loss of E222, one of the residues essential for enzyme activity (Ma et al., 2015b), rendering it catalytically inactive (Ma et al., 2017). Despite this C-terminal deletion, PsXLP1 was found to bind GmGIP1 with five times higher affinity than PsXEG1 (Ma et al., 2017). In doing so, PsXLP1 acts as a decoy, preventing GmGIP1 inhibition of PsXEG1 (Ma et al., 2017).

Using a virus-induced-gene silencing (VIGS) approach, Wang et al. (2018) showed that the recognition of PsXEG1 as a MAMP in the apoplast of *N. benthamiana* is mediated by the LRR-RLP PRR RXEG1, which is an ortholog of the SlEIX2 and NbEIX2 PRRs described above. Notably, RXEG1 recognises not only PsXEG1, but also a broad range of GH12 cell death elicitors from both fungal and oomycete species (Wang et al., 2018). This recognition is achieved through the LRR domain of the PRR, with co-operation of both BAK1 and SOBIR1 (Ma et al., 2015b, Wang et al., 2018). Here, both co-receptors interact with RXEG1 even in the absence of PsXEG1, although interaction between RXEG1 and BAK1 is enhanced in the presence of PsXEG1 (Wang et al., 2018).

GH12 proteins have also been characterized in *V. dahliae*. Of the six GH12 proteins identified in this species by Gui et al. (2017), only two (VdEG1 and VdEG3) triggered plant immune responses (ROS accumulation, callose deposition, and cell death) in *N. benthamiana*. These responses were independent of their cellulolytic activity (Gui et al., 2017). Similar to PsXEG1, VdEG1-triggered cell death was

dependent on both BAK1 and SOBIR1, while only BAK1 was required for VdEG3-triggered cell death (Gui et al., 2017). A deletion analysis demonstrated that while full length VdEG1 was required for induction of cell death, only a 63-amino acid peptide from VdEG3 was necessary (Gui et al., 2017). Interestingly, VdEG3 is composed of both a GH12 domain and a carbohydrate-binding module family 1 (CBM1) domain, but expression of the VdEG3 GH12 domain alone triggered stronger cell death than full length VdEG3. This suggested that the CBM1 domain suppresses VdEG3-GH12-triggered cell death (Gui et al., 2017). The addition of more CBM1 domains appeared to have an additive effect, suppressing both VdEG3-triggered cell death and ROS accumulation (Gui et al., 2017). Furthermore, the VdEG3-CBM domain also suppressed cell death triggered by GH12 proteins from other fungal species (Gui et al., 2017). Of note, several other microbial GH proteins have been found to contain CBM domains (Tundo et al., 2021, Takeda et al., 2022). These include MoCel10A and MoCel6A, a GH10 xylanase and GH6 cellobiohydrolase, respectively, from *Magnaporthe oryzae*, the hemibiotrophic fungal pathogen responsible for blast disease of rice (*Oryza sativa*). Recently it has been shown that both of these proteins interact through their CBM domains with the rice protein OsCBMIP, which subsequently inhibits their plant cell wall degrading activity (Takeda et al., 2022).

Infection of *N. benthamiana* with *V. dahliae* strains harbouring a deletion of either the *VdEG1* or *VdEG3* gene resulted in increased virulence and significantly increased fungal biomass compared to infection by WT *V. dahliae* (Gui et al., 2017). However, the opposite was true during infection of cotton (*Gossypium hirsutum*). In this case, there was a reduction in both *Verticillium* wilt symptoms and fungal biomass. During infection of cotton with *V. dahliae VdEG1* or *VdEG3* complementation strains, fungal biomass was restored to WT levels as expected; however, complementation with catalytic mutant versions of these genes did not restore biomass, suggesting that enzyme activity is required for the virulence function of VdEG1 and VdEG3 in this plant host. In addition, VdEG1 and VdEG3 were unable to trigger plant cell death or ROS accumulation, suggesting they are not recognised as MAMPs by cotton (Gui et al., 2017).

Another example of a secreted GH12 protein that is recognized as a MAMP by plants is FoEG1 from *F. oxysporum* (Zhang et al., 2021c). During infection of cotton and tomato roots, *FoEG1* is most highly expressed during the early stages of infection, from 24 to 48 hpi (Zhang et al., 2021c). Deletion mutants (Δ*foeg1*) demonstrated reduced virulence on cotton plants (Zhang et al., 2021c). This reduction in virulence was also observed for Δ*foeg1* mutants complemented with a catalytically-inactivated version of the gene, indicating that the enzymatic activity of FoEG1 is required for full virulence of the pathogen (Zhang et al., 2021c). In line with the protein being recognized as a MAMP, FoEG1 triggered cell death, independent of enzymatic activity, upon infiltration into *N. benthamiana, N. tabacum*, tomato and cotton and, in *N. benthamiana*, was dependent on both BAK1 and SOBIR1 (Zhang et al., 2021c). Other defence responses reported in *N. benthamiana* included ROS accumulation, callose deposition and the

induction of defence-related genes (Zhang et al., 2021c). Notably, an internal 86-amino acid fragment from amino acid positions 144 to 229 of FoEG1 was found to be sufficient for cell death induction and ROS accumulation in *N. benthamiana* (Zhang et al., 2021c).

Secreted GH12 proteins from plant-associated fungi and oomycetes also play an active role in DAMP release. Examples include MoCel12A and MoCel12B, two secreted GH12 proteins with β-glucanase (endoglucanase) activity from *M. oryzae* (Takeda et al., 2010, Yang et al., 2021). The expression of both *MoCel12A* and *MoCel12B* is upregulated during the early stages of infection when the fungus is undergoing biotrophic growth. Here, expression is initiated at 8 hours post-inoculation (hpi), around the time of primary infection hyphae formation, then peaks at 24 and 12 hpi, respectively (Yang et al., 2021). While Δ*mocel12a* deletion mutants did not display reduced virulence on rice, Δ*mocel12a/b* double-mutants exhibited enhanced virulence, as measured by more severe disease symptoms and increased fungal biomass (Yang et al., 2021). Furthermore, strains overexpressing *MoCel12A* had reduced biomass during host infection (Yang et al., 2021). Taken together, these results suggested that MoCel12A and/or MoCel12B negatively contribute to the virulence of *M. oryzae*. This is supported by the finding that the ectopic expression of *MoCel12A* in rice leads to enhanced resistance against this fungus, associated with the significant upregulation of immune-responsive genes, a dwarf phenotype, and the formation of spontaneous lesions on leaves of transgenic plants (Yang et al., 2021).

Notably, ectopic expression of an enzymatically inactive variant of MoCel12A, with mutations in both active site residues, failed to provide resistance to *M. oryzae*, suggesting that MoCel12A activates the plant immune system through the production of DAMPs (Yang et al., 2021). In line with this, only extracts from rice cell walls pre-incubated with active MoCel12A or MoCel12B enzymes triggered a ROS burst and induction of immunity-related genes in rice suspension cells (Yang et al., 2021). It was subsequently established that MoCel12A and MoCel12B release two major Poaceae-specific oligosaccharides from the hemicellulose component of rice cell walls, namely the trisaccharide 3^1-β-D-cellobiosyl-glucose (BGTRIB) and the tetrasaccharide 3^1-β-D-cellotriosyl-glucose (BGTETB), which are detectable along with MoCel12A in the apoplastic wash fluid of *M. oryzae*-infected rice plants, and that activate the rice immune system (Yang et al., 2021). Consistent with this finding, BGTRIB, as well as another immune system-activating oligosaccharide identified in the study, 3^3-β-D-glucosyl-cellotriose (BGTETC), can prime the immune system of rice, with BGTRIB and BGTETC pre-treatment providing enhanced resistance against rice blast disease (Yang et al., 2021). Yang et al. (2021) also showed that the abovementioned oligosaccharides are perceived by the PRR OsCERK1, a lysin motif (LysM) RLK, but not the LysM-RLP PRR OsCEBiP (Yang et al., 2021). This recognition induces OsCERK1 homodimerization, as well as heterodimerization with OsCEBiP, which Yang et al. (2021) suggest likely form OsCERK1-OsCEBiP tetramers to transduce immune signalling.

In the case of MoCel12A and MoCel12B, it remains unclear what their primary role is in promoting host colonization. However, it has been shown that the virulence of *M. oryzae* is enhanced when *MoCel12A* is overexpressed in an *oscerk1* mutant background, suggesting that the endoglucanase activity of this protein is important for infection when released oligosaccharides cannot be perceived (Yang et al., 2021). As such, MoCel12A and MoCel12B may play a vital role in nutrient acquisition but, through this activity, can produce DAMPs that are inadvertently recognized by OsCERK1 (Yang et al., 2021). It should be noted, though, that roles in the modification of MAMPs or other DAMPs, or in the switch from biotrophy to necrotrophy, have not yet been ruled out.

Secreted glycoside hydrolase family 16 (GH16) proteins

Although nothing has yet been shown for plant-associated oomycetes, research is emerging that selected secreted GH proteins from plant-associated fungi can be translocated into host cells. One such example is BcCrh1, a GH family 16 (GH16) transglycosylase from *B. cinerea* that requires dimerization for enzymatic activity (Bi et al., 2021). BcCrh1 was originally identified in the secretome of *B. cinerea*-infected bean (*Phaseolus vulgaris*) leaves (Zhu et al., 2017) and triggers cell death and other defence responses (e.g. ROS accumulation, callose deposition and the upregulation of defence-related genes) in *N. benthamiana* and tomato (Bi et al., 2021). During host infection, the expression of *BcCrh1* is induced following first contact of the fungus with the plant, and peaks at 12 hpi, while at the protein level, BcCrh1 is initially released into the apoplast from structures called infection cushions (Bi et al., 2021). Mutation of catalytic site residues (E120Q/D122H/E124Q) demonstrated that the ability of BcCrh1 to trigger cell death was independent of enzymatic activity (Bi et al., 2021). However, this cell death could still be triggered by a mutant version of the protein incapable of forming dimers (Bi et al., 2021).

Notably, following secretion into the apoplast of *N. benthamiana*, BcCrh1 was shown to be targeted to the cell cytoplasm, with a version of the protein lacking a signal peptide (i.e. confined to the plant cytoplasm) retaining its ability to trigger cell death (Bi et al., 2021). A 35-amino acid region of BcCrh1 (position 93–127) was determined to be sufficient for this cell death-inducing activity, while a 53-amino acid region (position 21–74, directly after the native signal peptide) was found to mediate the uptake into plant cell cytoplasm (Bi et al., 2021). Interestingly, deletion or overexpression of *BcCrh1* had no effect on *B. cinerea* virulence (Bi et al., 2021). However, overexpression of the enzyme-inactive version of BcCrh1 in a Δ*BcCrh1* mutant background significantly reduced *B. cinerea* virulence (Bi et al., 2021). This reduction is thought to be due, in part, to impaired infection cushion formation, as a result of accumulating enzyme-inactive dimers (Bi et al., 2021). Taken together, it has been proposed that BcCrh1 may have a role in the formation of infection cushions, and that excessive BcCrh1 is released from these structures to induce plant cell death (i.e. as an effector) upon translocation into host cells from the apoplast (Bi et al., 2021).

Secreted glycoside hydrolase family 17 (GH17) proteins

Another example of a secreted GH protein that releases a DAMP through its enzymatic activity is CfGH17-1, an apoplastic GH family 17 (GH17) protein with 1,3-β-glucanase activity from *C. fulvum* (Ökmen et al., 2019). *CfGH17-1* expression is down-regulated during the biotrophic phase of *C. fulvum* growth, but upregulated during later stages of infection when tomato leaves are necrotic and the fungus is saprophytic (Ökmen et al., 2019). CfGH17-1 was shown to trigger cell death in three out of four lines of Moneymaker tomato tested, but not in the non-host plants *N. benthamiana* and *N. tabacum* (Ökmen et al., 2019). Through targeted mutation of the enzymatic active site residues present in CfGH17-1, cell death activity could be prevented, indicating that the protein is not recognized as a MAMP (Ökmen et al., 2019). Instead, it is anticipated that CfGH17-1 releases a sugar molecule from the plant cell wall that is subsequently recognized as a DAMP by an uncharacterized PRR present in specific tomato lines, but not in *N. benthamiana* or *N. tabacum* (Ökmen et al., 2019). Based on this observation, it was proposed that CfGH17-1 likely plays a role in nutrient acquisition by acquiring sugar molecules from the host cell wall to support the growth and reproduction of *C. fulvum* during the late stages of infection when the host is no longer able to recognize and respond to DAMPs (Ökmen et al., 2019). Consistent with this, symptom development remained unchanged in tomato plants infected with Δ*cfgh17-1* deletion mutants of *C. fulvum*, when compared to plants infected with WT fungus, whereas fewer disease symptoms were observed in tomato plants infected with strains constitutively overexpressing the *CfGH17-1* gene (Ökmen et al., 2019).

Secreted glycoside hydrolase family 18 (GH18) proteins

Although the manipulation of chitin-triggered immunity in plants by pathogen effectors is not new, the involvement of GH proteins in this process has only recently been shown. A notable example is MpChi, an enzymatically inactive, secreted chitinase-like GH18 protein from *Moniliophthora pernicosa*, the hemibiotrophic fungal pathogen responsible for witches' broom disease of cacao (*Theobroma cacao*) (Fiorin et al., 2018). MpChi, which is encoded by a gene that is highly expressed during biotrophic infection of cacao, is able to bind chitin oligomers (Fiorin et al., 2018). However, it was determined that MpChi harbours an amino acid substitution in the catalytic motif conserved in GH18 chitinases (E167Q), as well as substitution of a residue that forms part of the catalytic pocket in these enzymes (M238L); together these substitutions abolish chitinolytic activity (Fiorin et al., 2018). Strikingly, in line with a role in manipulating chitin-triggered immunity, treatment of *N. tabacum* cell suspensions with MpChi prevented defence gene expression and medium alkalinisation that would otherwise be triggered by chitin oligomers (Fiorin et al., 2018). As this role was dependent on the chitin binding

capacity of MpChi, it was determined that MpChi prevents chitin-triggered immunity through the sequestration of immunogenic chitin fragments (Fiorin et al., 2018).

Interestingly, the orthologue of MpChi from *Moniliophthora roreri*, a related hemibiotrophic pathogen of cacao responsible for frosty pod rot disease, has canonical catalytic residues and is enzymatically active (Fiorin et al., 2018). However, a paralogous secreted GH18 protein from this pathogen, MrChi, was identified that has a different amino acid substitution in its GH18 chitinase catalytic motif (D135N) (Fiorin et al., 2018). This substitution resulted in reduced, but not abolished, enzymatic activity (Fiorin et al., 2018). Like MpChi, MrChi is encoded by a gene that is highly expressed during biotrophic infection and can suppress the chitin-triggered immune response in *N. tabacum* cell suspensions (Fiorin et al., 2018). Taken together, this study highlighted that GH18 proteins from two cacao pathogens of the same genus have independently evolved to prevent chitin-triggered immunity through the sequestration of immunogenic chitin fragments (Fiorin et al., 2018).

Investigations have also been led into the roles of enzymatically active GH18 chitinases from fungal pathogens in modulating chitin-triggered immunity. In 2019, two separate studies focussed on the same extracellularly-targeted GH18 chitinase from *M. oryzae*, named MoChia1 by Yang et al. (2019) and MoChi by Han et al. (2019). *MoChia1*/*MoChi* (hereafter referred to as *MoChia1*) is highly expressed at 48 hpi in rice (Yang et al., 2019). Like many other GH proteins described above, MoChia1 is recognized as a MAMP and can induce a ROS burst and callose deposition in rice cell suspensions independent of enzymatic activity (Yang et al., 2019). In line with the recognition of MoChia1 as a MAMP, overexpression of *MoChia1* in rice resulted in reduced virulence (Yang et al., 2019). Interestingly, deletion of *MoChia1* in *M. oryzae* gave delayed appressorium and germ-tube formation on glass coverslips (Yang et al., 2019), as well as a slower post-penetration growth-rate, fewer lesions, and reduced biomass in rice leaves (Han et al., 2019, Yang et al., 2019). Further analyses revealed that these *in planta* phenotypes were at least partially mediated by an enhanced immune response, as measured by the increased expression of defence-related genes in rice, suggesting that MoChia1 also plays a role in the suppression of MAMP-triggered immunity (Han et al., 2019, Yang et al., 2019).

Both studies also identified an interacting partner of MoChia1 in rice. More specifically, Yang et al. (2019) identified an interaction between the carbohydrate-binding domain of MoChia1 and the plasma membrane-localized tetratricopeptide-repeat protein OsTPR1, while Han et al. (2019) identified an interaction between MoChia1 and the plasma membrane-localized, chitin-binding, jacalin-related lectin OsMBL1. In both cases, the genes that encode these proteins were induced by *M. oryzae* infection, suggesting a role in plant defence (Han et al., 2019, Yang et al., 2019). In support of this, overexpression of *OsTPR1* or *OsMBL1* in rice resulted in fewer lesions by *M. oryzae* and was concomitant with a

significant reduction in fungal biomass, as well as the activation of defence-related genes (Han et al., 2019, Yang et al., 2019).

More in-depth analyses determined that MoChia1 suppresses the chitin-triggered ROS burst in rice (Han et al., 2019, Yang et al., 2019), but that this suppression can be prevented by OsTPR1 (Yang et al., 2019). Coincident with this, MoChia1 suppressed the chitin-induced ROS burst in rice plants overexpressing *OsTPR1* (Yang et al., 2019). The immune response following the recognition of MoChia1 as a MAMP, however, was not suppressed upon *OsTPR1* overexpression (Yang et al., 2019). Yang et al. (2019) discovered that, although OsTPR1 was unable to bind chitin, the interaction between OsTPR1 and MoChia1 was stronger than the interaction between MoChia1 and chitin. Based on these and other results, it was proposed that, through its interaction with MoChia1, OsTPR1 allows free chitin that would otherwise be bound or degraded by MoChia1 to activate chitin-triggered immune responses (Yang et al., 2019)

Unlike OsTPR1, Han et al. (2019) demonstrated that OsMBL1 interacts with chitin and observed a negative correlation between the amount of MoChi1 present and the amount of chitin bound by OsMBL1. Thus, it was proposed that OsMBL1 is a cell surface-localized PRR required for the recognition of chitin oligomers in rice, and that MoChia1 and OsMBL1 compete with each other for the binding of these chitin oligomers (Han et al., 2019). As MoChia1 has a higher affinity for chitin oligomers than OsMBL1, MoChia1 can then degrade or sequester the chitin oligomers to prevent their recognition by OsMBL1, and in doing so, prevent the activation of chitin-triggered immune responses (Han et al., 2019).

In addition to the functions described above, it is also expected that a subset of GH18 proteins secreted by plant-associated fungi and oomycetes during host colonization function as effectors with roles in manipulating plant microbiota. Mycoparasite-produced chitinases have been found to inhibit a number of competitor species (reviewed in Patil et al. (2000)) and play an important role in antagonistic fungal interactions. Recently, a chitinase from the biocontrol fungus *T. asperellum* PQ34 was observed to have a strong inhibitory effect on the growth of fungal pathogens on their plant hosts (*Sclerotium rolfsii* on peanut and *Colletotrichum* species on mango or chilli) (Loc et al., 2020). Similar findings have also been made in *Trichoderma* sp. SANA20 (Aoki et al., 2020). Furthermore, deletion and/or disruption of genes encoding GH18 chitinases from the mycoparasitic biocontrol fungus *Clonostachys rosea* (*CrChiC2* (Tzelepis et al., 2015), *CrEch37*, *CrEch42*, and *CrEch58* (Mamarabadi et al., 2008)) were found to reduce the inhibition of *B. cinerea* and *Fusarium culmorum*, respectively, in culture. While no such inhibition was observed *in planta*, this could be explained by the high degree of functional redundancy within GH18 chitinases (Langner & Göhre, 2016). However, further research is required to determine whether this is the case.

Secreted glycoside hydrolase family 25 (GH25) proteins

Similar to the GH18 proteins described above, other secreted GH proteins of plant-associated fungi and oomycetes function as effectors with roles in manipulating plant microbiota during host colonization (Rovenich et al., 2014, Snelders et al., 2018). An example is MbA_GH25, a GH family 25 (GH25) protein with lysozyme activity of the epiphytic, basidiomycete yeast *Moesziomyces bullatus* ex *Albugo* (*MbA*) (Eitzen et al., 2021). While *M. bullatus* is a smut pathogen of millet, *MbA* has been identified in the microbial phyllosphere of *A. thaliana*, where it showed antagonistic interactions with several bacteria (Eitzen et al., 2021). *MbA* was originally co-isolated with the oomycete white rust pathogen *Albugo laibachii*, which is the primary hub microbe of the *A. thaliana* phyllosphere (Agler et al., 2016). Interestingly, MbA strongly inhibited virulence of *A. laibachii* when co-inoculated onto *A. thaliana* leaves. RNA-sequencing of *MbA* identified the transcriptional induction of several GH-encoding genes upon contact with *A. laibachii* on the leaf surface (Eitzen et al., 2021). Strikingly, deletion of an *Albugo*-induced *GH25* gene, *MbA-GH25*, largely abolished the antagonistic activity of *MbA* towards *A. laibachii* (Eitzen et al., 2021). Similarly, enzymatically active, recombinant MbA-GH25 protein could significantly block *A. laibachii* infection of *A. thaliana*, demonstrating the biological function of this fungal lysozyme in microbial antagonism (Eitzen et al., 2021). Beyond this recent example, the biological functions of GH25 enzymes are poorly understood. Some of these hydrolases had been reported to be associated with microbial hyperparasitism in both fungal and oomycete species (Horner et al., 2012, Hyde et al., 2019). Since GH25 hydrolases can be found in many plant-associated fungi, future research will be necessary to elucidate the functions of these enzymes in the microbial leaf phyllosphere.

Secreted glycoside hydrolase family 28 (GH28) proteins

Secreted GH family 28 (GH28) endopolygalacturonases (PGs) (Table 1), which hydrolyse the homogalacturonan domain of pectic polysaccharides present in plant cell walls, can also be recognized as MAMPs by plant PRRs. To date, PGs have been most extensively studied in *B. cinerea*, which carries six PG-encoding genes (*BcPG1–6*) (Wubben et al., 1999). The expression of these genes *in planta* is dependent on both the infection stage and the host that is being colonized (ten Have et al., 2001). Early research highlighted a role for the PGs of *B. cinerea* in promoting host colonization, with mutants deleted for either the *BcPG1* or *BcPG2* gene displaying a strong reduction in virulence on tomato and broad bean (*Vicia faba*) leaves (Kars et al., 2005, ten Have et al., 1998). Subsequent research revealed that four PGs from *B. cinerea* (BcPG2, BcPG3, BcPG4 and BcPG6), as well as one PG from the fungal saprotroph *Aspergillus niger* (AnPGB), trigger cell death upon infiltration into leaves of *A. thaliana* accession Colombia (Zhang et al., 2014a). This recognition was mediated by RLP42/RBPG1, an LRR-

RLP PRR, with cell death elicitation dependent on SOBIR1 (Zhang et al., 2014a). Consistent with these proteins being recognized as MAMPs, the cell death response was also triggered by a catalytically-inactivated form of BcPG3 (Zhang et al., 2014a). Furthermore, RLP42 and BcPG3 were found to physically interact (Zhang et al., 2014a). This recognition of *B. cinerea* PGs as MAMPs is not restricted to *A. thaliana*; BcPG1 is also able to induce defence responses such as ROS production in cell suspensions of grape (*Vitis vinifera*), independent of enzymatic activity (Poinssot et al., 2003).

More recently, it has been shown that a nine-amino acid fragment from BcPG6, pg9(At), which is conserved across fungal PGs and is a derivative of a slightly larger but equally active 13-amino acid fragment, pg13(At), is sufficient to activate RLP42-dependent immunity in *A. thaliana* (Zhang et al., 2021b). Indeed, in immune system activation experiments involving ethylene production, synthetic pg9(At) or pg13(At) peptides derived from BcPG6 (and BcPG2), as well as the other fungal PGs AnPGI, AnPGB and AnPGD from *A. niger*, CluPG1 from *Colletotrichum lupine* (hemibiotrophic fungal pathogen of lupin) and FmPGA from *Fusarium verticillioides* (hemibiotrophic fungal pathogen of maize), were active upon infiltration into leaves from *A. thaliana* accession Colombia (Zhang et al., 2021b). Pg9(At) derived from PGs of *Phytophthora* species, however, induced only residual ethylene production, suggesting that whilst PGs from this class of pathogens can be recognized, it is with lower efficiency (Zhang et al., 2021b). Consistent with the findings of (Zhang et al., 2014a), RLP42 bound the pg13(At) peptide, leading to the recruitment of SERK family members, including BAK1, for activation of plant immune responses (Zhang et al., 2021b). A structure-function analysis based on domain-swap experiments between recombinant proteins RLP42 and RLP40 (a paralogue of RLP42 that is insensitive to PGs; (Zhang et al., 2014a), as well as domain deletion and amino acid substitution experiments, subsequently revealed that LRRs 3, 5, 7 and 10, as well as a region containing a 49-amino acid island domain, are required for pg9(At) recognition by RLP42 (Zhang et al., 2021b).

Interestingly, in an assessment of recognition across a range of plant species and accessions, only 16 of 52 *A. thaliana* accessions tested responded to pg13(At), while all 16 other plant species tested were unresponsive. This indicated that pg13(At) recognition is, so far, restricted to *A. thaliana*, albeit with notable within-species diversity (Zhang et al., 2021b). Strikingly, *Arabidopsis arenosa* and *Brassica rapa*, two Brassicaceae species closely related to *A. thaliana* that are unresponsive to pg13(At), but responsive to BcPG6, instead perceived the overlapping PG peptides pg20(Aa) (20-amino acid fragment) and pg36(Bra) (36-amino acid fragment), respectively (Zhang et al., 2021b). As these two peptides are structurally distinct from pg9(At), it was concluded that there are distinct recognition specificities for PGs within the Brassicaceae family (Zhang et al., 2021b).

In contrast to that described for the PGs of *B. cinerea* in *A. thaliana*, *A. arenosa* and *B. rapa*, the BcPG2 protein was found to trigger necrosis when infiltrated into broad bean leaves or transiently expressed in

N. benthamiana. However, this activity could be abolished upon mutation of the enzymatic active site (Joubert et al., 2007, Kars et al., 2005). This suggested that, in some host species, the PGs of *B. cinerea* may release oligogalacturonides from plant cell wall pectin that are subsequently recognized as DAMPs by plant PRRs to activate the plant immune system.

It should be noted that plants produce extracellular LRR-containing polygalacturonase-inhibiting proteins (PGIPs), which specifically inhibit pathogen-secreted PGs (Liu et al., 2017). Examples include PvPGIP2 from bean, which inhibits BcPG1 from *B. cinerea*, and is associated with reduced colonisation by this fungus in transgenic *A. thaliana* and *N. tabacum* plants overexpressing PvPGIP2 (Manfredini et al., 2005), as well as GhPGIP1 from cotton (*Gossypium hirsutum*), which interacts with VdPG1 and FovPG1 (albeit weakly) from *V. dahliae* and *F. oxysporum* f. sp. *vasinfectum* respectively, and provides enhanced susceptibility to these pathogens in cotton when transcriptionally silenced (Liu et al., 2017). Along these lines, silencing of *AcPGIP* from kiwifruit (*Actinidia chinensis*) has also recently been shown to result in increased susceptibility to *B. cinerea* (Li et al., 2021).

GH28 proteins have also been found to play important roles in the establishment of symbiotic interactions. One such example is a GH28-encoding gene from the ectomycorrhizal fungus *Laccaria bicolor*, *LbGH28A*, which was found to be induced during the formation of ectomycorrhiza in *Populus trichocarpa* (Veneault-Fourrey et al., 2014) and *P. tremula* x *alba* (Zhang et al., 2022). Immunocytolocalisation of LbGH28A demonstrated that the protein was present at hyphal tips within the Hartig net (Zhang et al., 2022), which is formed by a network of hyphae growing between the rhizodermal cells of the plant to create a symbiotic interface through which nutrients are exchanged (Becquer et al., 2019). Remarkably, *LbGH28* knockdown mutants of *L. bicolor* were found to be deficient in their ability to form Haritg nets (Zhang et al., 2022). As LbGH28A was shown to be an active endopolygalacturonase with pectinase activity, (Zhang et al., 2022) suggest that LbGH28 may be involved in remodelling the middle lamella through pectin hydrolysis, thus playing an essential role in plant-fungal symbiosis.

Secreted glycoside hydrolase family 45 (GH45) proteins

Outside of the GH11, GH12 and GH28 proteins, other GH family members are also recognized as MAMPs by plants. An example is EG1, a GH family 45 (GH45) endoglucanohydrolase from *Rhizoctonia solani*, a broad host-range, soil-borne, necrotrophic fungal pathogen (Ma et al., 2015a). The *EG1* gene is most highly expressed during the early stages of infection on maize (*Zea mays*), peaking at 2–3 days post-inoculation (dpi), with expression also detected at 4–7 dpi (Ma et al., 2015a). This expression coincided with cell death induction during infection of maize by *R. solani* (Ma et al., 2015a). Protein infiltration experiments showed that EG1, as well as a catalytically inactive form of this

protein, can trigger cell death in leaves of maize, *N. tabacum* cv. NC89 and *A. thaliana*, indicating that EG1 is recognized as a MAMP, with defence-related genes shown to be upregulated in both maize and *N. tabacum* cv. NC89 (Ma et al., 2015a). Other defence responses, such as ROS accumulation and ethylene biosynthesis, were also observed when these proteins were applied to suspension-cultured cells of *N. tabacum* cv. NC89 (Ma et al., 2015a). It has since been shown that three amino acid residues in a seven-amino acid sequence within EG1 (S**PW**AVN**D**), as well as two amino acid residues in a five-amino acid sequence (G**C**S**R**K), are required for cell death induction in *N. benthamiana* (Guo et al., 2022). Structural modelling suggests that these regions of EG1 are surface-exposed, but structurally independent (Guo et al., 2022).

2.3 Conclusions and future perspectives

A large body of research over many years has focussed on understanding the role of small, mostly non-enzymatic, secreted proteins from plant-associated fungi and oomycetes in plant–microbe interactions. However, it is clear from this review that a role for secreted GH proteins in these interactions cannot be overlooked. Indeed, like a lot of the small secreted proteins described to date from plant-associated fungi and oomycetes, many secreted GH proteins from these microbial organisms also function as effectors to promote host colonization. Likewise, GH proteins can also act as (or produce) invasion patterns that activate the plant immune system to hinder host infection. Consequently, the identification and functional characterization of secreted GH proteins will be pivotal to our future understanding of how plant-associated fungi and oomycetes interact with their hosts at the molecular level to cause disease or trigger host resistance. Such an understanding is important, as it may inform disease control strategies. This could be mediated through, for example, the use of *PRR* genes active against secreted GH proteins. In the case of the PRR RXEG1, for instance, which recognizes GH12 proteins from various fungal and oomycete species, a contribution to plant immunity against the broad host-range oomycete pathogen *Phytophthora parasitica* was observed in *N. benthamiana* (Wang et al., 2018), suggesting it may be an interesting candidate for transfer to other plant species.

Much is still left to be learnt, however, about the full diversity of virulence functions performed by secreted GH proteins. In particular, it is not yet clear to what extent these proteins are involved in the remodelling of surface-associated carbohydrates present in fungal or oomycete cell walls, for example to enable modification of hyphal surfaces or infection structures required during plant colonization. Fujikawa et al. (2012), for instance, identified MoAGS1, a transmembrane α-1,3-glucan synthase from *M. oryzae* that carries an extracellular GH family 13 (GH13) domain. While MoAGS1 is essential for the pathogenicity of *M. oryzae* on rice, and is responsible for the accumulation of α-1,3-glucan on the cell wall surface of infection structures (likely to prevent the hydrolysis of fungal chitin and β-1,3-glucan by plant-derived hydrolytic enzymes, as well as the detection of these carbohydrates by the plant

immune system) (Fujikawa et al., 2012), the precise role of the GH13 domain in this protein remains uncertain. In any case, a better understanding of substrate specificity will provide further information on the virulence functions that secreted GH proteins from plant-associated fungi and oomycetes play in plant–microbe interactions.

More research is also required to better understand to what extent secreted GH proteins of plant-associated fungi and oomycetes interact synergistically with each other or other CAZymes to perform their roles, as has been shown for FgXyr1 (GH10) and FgPg1 (GH28) of *F. graminearum*, which function synergistically to promote virulence in soybean and wheat (Paccanaro et al., 2017). Indeed, several other CAZymes have now been shown to be important virulence factors of plant-associated fungi and oomycetes, including CEs (Gui et al., 2018), chitin deacetylases (Cord-Landwehr et al., 2016, Gao et al., 2019, Noorifar et al., 2021, Rizzi et al., 2021), PLs (Fu et al., 2015, Yang et al., 2018b), and lytic polysaccharide monooxygenases (LPMOs) (Sabbadin et al., 2021). Another class of proteins not yet classified as CAZymes, but that have a DUF3129 domain (called effectors with chitinase activity; EWCA), have also been recently implicated in fungal virulence (Martínez-Cruz et al., 2021). As an example of synergism outside of the GHs, a CE family 5 (CE5) cutinase from *V. dahliae*, VdCUT11, was found to trigger cell death and other defence responses in *N. benthamiana* only in the absence of VdCBM1, a carbohydrate-binding module family 1 (CBM1) protein from this fungus (Gui et al., 2017). It has been suggested that the defence responses triggered by VdCUT11 are the result of DAMP recognition, following the degradation of suberin in the roots of *N. benthamiana* by this enzyme, and that VdCBM1 suppresses these defence responses to promote host colonization (Gui et al., 2017).

The synergistic interaction between VdCUT11 and VdCBM1 raises an important issue. Many of the secreted GH proteins from plant-associated fungi and oomycetes that have been shown to trigger cell death or other defence responses in plants have been studied in isolation from the microorganisms from which they are derived, for example by using *Agrobacterium tumefaciens*-mediated transient expression assays (ATTAs) or protein infiltration experiments. As a consequence, these responses have been studied in the absence of other effectors that make up the microorganism's full effector repertoire. This is important, because under natural infection conditions, other effectors in the repertoire may function to suppress or prevent the plant defence responses elicited by the secreted GH protein. An excellent example of this is the RXLR effector repertoire of *P. sojae*, from which 23 RXLR effectors were found to suppress XEG1-mediated cell death in *N. benthamiana* upon co-expression with XEG1 in ATTA experiments, including several known to be expressed within 30 minutes of host infection by *P. sojae* (Ma et al., 2015b).

In cases where *A. tumefaciens*-mediated transient expression assays or protein infiltration experiments have been used exclusively to determine whether a secreted GH triggers plant defence responses, care

also needs to be taken as to whether the observed responses are biologically relevant or an artefact of over-production or excessive protein concentration. Under natural infection conditions, the secreted GH protein may never be produced in sufficient quantities to elicit plant defence responses. Moreover, responses that are observed in non-host plants might not be representative of responses observed in host plants; for example, secreted GH proteins may release a DAMP in the non-host plant that is not present in the host plant. Thus, ideally, secreted GH proteins should be functionally characterized in the context of the microorganism from which they are derived, and the natural host plant.

Another area of research that requires more attention involves understanding why some secreted GH proteins from the same GH family trigger strong plant defence responses (i.e. cell death), while others trigger only weak defence responses (e.g. ethylene production or ROS accumulation) or no response at all. This has been shown for several GH12 proteins of fungal and oomycete species (Ma et al., 2015b), as well as GH17 proteins from *C. fulvum* (Ökmen et al., 2019). In such cases, differences in the amino acid sequence of the family members might influence their tertiary structure, surface charge, glycosylation status, or stability in the plant environment, for example; these differences could translate into variations in substrate specificity (e.g. affecting DAMP release) or the affinity for cognate immune receptors and/or other host targets involved in plant defence. Certainly, using experiments based on ATTAs or protein infiltration, secreted GH proteins that only trigger weak plant defence responses have largely been overlooked to date, with preference tending to be given to those that instead trigger cell death. Experiments that focus on the identification of secreted GH proteins that do not trigger cell death, but instead induce responses such as ethylene production, ROS accumulation or the expression of defence-related genes, would provide a starting point for addressing this knowledge gap.

Finally, more research is required to better understand how secreted GH proteins, such as the BcCrh1 GH16 protein from *B. cinerea* (Bi et al., 2021), enter plant cells. Here, one line of enquiry could involve the delivery of these proteins by extracellular vesicles (EVs), given that fungal EV cargo often contains CAZymes, such as GHs with a signal peptide (e.g. Garcia-Ceron et al. (2021)).

In recent years, huge leaps have been made in our understanding of the roles that secreted GH proteins from plant-associated fungi and oomycetes play in promoting host colonization or in activating the plant immune system. However, much is still to be learnt about the full diversity of roles played by this intriguing class of proteins, as well as the molecular mechanisms that underpin them. With more and more secreted GH proteins being identified, facilitated through the ever-increasing number and availability of new fungal and oomycete genomes, we anticipate that GH proteins will in future gain the same level of recognition as small secreted non-enzymatic proteins as critical effectors in plant-microbe interactions.

Conflict of Interest

The authors declare that the research was conducted in the absence of any commercial or financial relationships that could be construed as a potential conflict of interest.

Author Contributions

All authors made a substantial, direct and intellectual contribution to the work, and approved it for publication.

Funding

ELB, REB and CHM are supported by the Tertiary Education Commission through the Centres of Research Excellence Program http://www.tec.govt.nz/funding/funding-and-performance/funding/fund-finder/centres-of-research-excellence/current-cores/.

MASSEY UNIVERSITY
GRADUATE RESEARCH SCHOOL

STATEMENT OF CONTRIBUTION
DOCTORATE WITH PUBLICATIONS/MANUSCRIPTS

We, the candidate and the candidate's Primary Supervisor, certify that all co-authors have consented to their work being included in the thesis and they have accepted the candidate's contribution as indicated below in the *Statement of Originality*.

Name of candidate:	Ellie L. Bradley
Name/title of Primary Supervisor:	Dr Carl Mesarich
Name of Research Output and full reference:	
Bradley, E. L., Oliver, R., Daehlemann, G., Hensbast, R., Bradshaw, R. E., & Mesarich, C. H. (2022). Secreted glycoside hydrolase proteins as effectors and invasion patterns of plant-associated fungi and oomycetes. Frontiers in Plant Science, 13	
In which Chapter is the Manuscript /Published work:	Chapter 2
Please indicate:	
• The percentage of the manuscript/Published Work that was contributed by the candidate:	60%
and	
• Describe the contribution that the candidate has made to the Manuscript/Published Work:	
Literature research and compiling a draft manuscript together with the associated table and figure	
For manuscripts intended for publication please indicate target journal:	
Candidate's Signature:	Ellie Bradley Digitally signed by Ellie Bradley Date: 2022.08.03 11:21:30 +12'00'
Date:	03.08.2022
Primary Supervisor's Signature:	Carl Mesarich Digitally signed by Carl Mesarich Date: 2022.08.03 11:43:02 +12'00'
Date:	03.08.2022

(This form should appear at the end of each thesis chapter/section/appendix submitted as a manuscript/ publication or collected as an appendix at the end of the thesis)

Chapter three: Identification and characterization of secreted glycoside hydrolase proteins from *Phytophthora agathidicida*.

3.1 Introduction

Glycoside hydrolase (GH) proteins represent the largest class of carbohydrate-active enzymes (CAZymes) and are made up of 172 families that can be further divided into 18 different clans (GH-A to -R) based on sequence similarity (Henrissat & Davies, 1997). Regardless of the families or clans to which they belong, the purpose of these GH proteins is to hydrolyse and/or rearrange glycosidic bonds in glycoconjugates, oligo- and polysaccharides (Henrissat, 1991, Henrissat & Davies, 1997).

It has been well established that many of the secreted GH proteins produced by fungal and oomycete plant pathogens function as virulence or pathogenicity factors, termed effectors, to promote or enable host colonization (see **Chapter two** (Bradley et al., 2022)). Given that plant cell walls, the primary physical barrier to pathogen infection, are primarily composed of carbohydrates (e.g. cellulose, hemicellulose and pectin) (Keegstra, 2010), and that carbohydrates are necessary for pathogen nutrition (reviewed in Fatima and Senthil-Kumar (2015)), a subset of these secreted GH proteins likely function in facilitating host cell entry or nutrient acquisition (Bradley et al., 2022). However, it is important to note that other roles including the detoxification of plant-produced antimicrobial compounds (Bowyer et al., 1995, Crombie et al., 1986, Ökmen et al., 2013, Pareja-Jaime et al., 2008), or the sequestration/degradation of microbe- or damage-associated molecular patterns (MAMPs and DAMPs, respectively) to avoid pathogen recognition by the plant immune system (Fiorin et al., 2018, Han et al., 2019), have also been shown.

As part of an arms race of co-evolution between fungal or oomycete pathogens and their hosts, an effector protein that contributes to virulence, or is required for pathogenicity, may also become a recognised elicitor of the plant immune system. Indeed, in some cases, plants can perceive pathogen GH proteins as MAMPs, or can recognize the products of their hydrolytic activity as DAMPs, with this recognition mediated by specific cell surface-localized immune receptors to activate plant defence responses that halt further pathogen ingress (Bradley et al., 2022). Another possibility is that the host somehow interferes with the core function of the GH protein in a way that prevents infection. In any case, to successfully cause disease, the pathogen in question must then evolve or acquire new effectors that can prevent these processes, or any ensuant defence responses, from happening (Jones & Dangl, 2006).

A well-characterized example of the complex interactions that take place between a pathogen and a host is provided by the interaction between the oomycete *Phytophthora sojae* and both soybean (native host) and *Nicotiana benthamiana* (model host). In this example, PsXEG1, a GH12 enzyme from *P. sojae*, was found to be important for the virulence of the pathogen, but also acts as a MAMP, eliciting a defence response in soybean (Ma et al., 2015b). In soybean, PsXEG1 interacts with glucanase inhibitor protein 1 (GmGIP1), which subsequently inhibits the virulence activity of PsXEG1 (Ma et al., 2017). Intriguingly, PsXLP1, a GH12 protein paralogous to PsXEG1, which lacks enzyme activity, can bind to GmGIP1 more tightly than the enzymatically active PsXEG1, acting as a decoy and leaving PsXEG1 free to carry out its virulence function (Ma et al., 2017).

Identifying effector proteins which contribute to pathogen virulence or are required for pathogenicity and/or are recognised as elicitors of plant defence is crucial to understanding pathogen–plant interactions at a molecular level. The identification of key pathogen effector proteins can then inform selective breeding and/or genetic engineering strategies to aid in disease control and prevention. Effectoromics is a high-throughput, functional genomics, approach where pathogen effectors, such as GH proteins, can be screened across plant species to identify individuals carrying cognate immune receptors (Vleeshouwers & Oliver, 2014). This identification is typically mediated through the visualization of a chlorotic or necrotic cell death response following expression/infiltration of the effector protein in/into the plant (Du & Vleeshouwers, 2014). Notably, several studies have identified an apparent expansion of CAZyme-encoding genes in plant-pathogenic *Phytophthora* species, of which the majority encode GH proteins (Ma et al., 2015b, Zerillo et al., 2013). With this in mind, it is likely that a subset of GH proteins produced by *Phytophthora agathidicida* contribute to the interaction of this pathogen with its host, kauri (*Agathis australis*). This chapter therefore aims to identify *P. agathidicida* proteins which may have an important role in virulence or cell death elicitation using an effectoromics approach, with a particular focus on GH proteins. Genomic information from two different *P. agathidicida* type strains, together with transcriptomic information from an *in-planta* RNA-sequencing time-course experiment during *P. agathidicida* infection of kauri leaves and roots was used to select a number of candidate proteins for analysis. The genes encoding candidate proteins of interest (POI) of *P. agathidicida* were cloned, then expressed in the model plant species *N. benthamiana* and *Nicotiana tabacum*, using an *Agrobacterium tumefaciens*-mediated transient transformation assay (ATTA). The ATTA is a well-established method allowing expression of genes encoding POIs in the chosen host plant and is often used to identify whether a POI is recognised by the plant immune system. This method has aided characterisation of many plant defence elicitors, including PsXEG1 from *P. sojae* (Ma et al., 2015b) and nine RxLR effectors from *P. agathidicida* (Guo et al., 2020a).

While *P. agathidicida* is known to infect kauri, and likely a number of other native and introduced plant species in the wild (Bradshaw et al., 2020, Ryder, 2016), unpublished data suggest that *N. benthamiana*

is susceptible to *P. agathidicida* infection (Guo, Unpublished-b). Due to time and space requirements for kauri growth, and out of respect for the cultural importance of this taonga species, characterisation of *P. agathidicida* POIs, via ATTAs, was instead carried out in *N. benthamiana* and *N. tabacum*.

3.2 Methods

3.2.1 *In silica* analysis

3.2.1.1 Identification of *P. agathidicida* carbohydrate-active enzymes of interest

The CAZyme prediction programme dbCAN2 (Zhang et al., 2018) was used to identify CAZyme families from available protein predictions based on the annotated genomes of two different *P. agathidicida* strains (NZFS 3770 and NZFS 3772). Here, all proteins with a GH domain predicted by any two of the three tools used by dbCAN2 (Zhang et al., 2018) were retained and manually curated, with exon/intron boundaries and structure, appropriate start and stop codons. This was collated in a spreadsheet together with level of expression (i.e. based on previously generated RNA-sequencing data from *P. agathidicida* grown in kauri leaves and roots (Guo & Panda, Unpublished)). Only genes encoding GH proteins expressed higher than 50 FPKM at any point during *P. agathidicida* infection of kauri roots or leaves (6 hours post-inoculation (hpi), 24 hpi, 48 hpi, 72 hpi) were considered for further analysis. As no single genome annotation yielded a list of reliably annotated CAZyme proteins, the *P. agathidicida* 3770 PacBio genome (Pa3770) was used as the primary genome, with support from both the *P. agathidicida* 3770 Illumina genome (PaI3770) and the *P. agathidicida* 3772 Illumina genome (Pa3772) (Studholme et al., 2016).

Amino (N)-terminal signal peptides present in GH proteins were predicted using SignalP (version 3.0 (Bendtsen et al., 2004) and 4.1 (Petersen et al., 2011)), transmembrane domains were predicted using TMHMM version 2.0 (Krogh et al., 2001), while glycosylphosphatidylinositol (GPI) anchors were predicted using PredGPI (Pierleoni et al., 2008) and big-PI-fungal predictor (Eisenhaber et al., 2004). Prediction of N-glycosylation was performed using NetNGlyc (version 1.0) (Gupta & Brunak, 2002). Python™ (2.7.15) was used to extract sequence lists from the genome and protein sequence data. Microsoft© excel (16.16.3) was used to filter and group genes and proteins as required. Geneious® version 9.1.8 was used to view and interact with nucleotide (nt) and amino acid (aa) sequences, align sequences using Geneious alignment or MUSCLE (Edgar, 2004), and construct phylogenetic trees (PhyML 3.0 plugin (Guindon et al., 2010)). Homology to proteins from other species was identified using the non-redundant (nr) protein database (Pruitt et al., 2005) at the National Center for Biotechnology Information (NCBI) in conjunction with tBLASTn and BLASTp (version 2.8.1) using an E-value cut-off of 0.05 (Altschul et al., 1997).

3.2.1.2 Selecting *P. agathidicida* hypothetical proteins of interest

Hypothetical proteins were identified based on the previously generated RNA-sequencing data (Guo & Panda, Unpublished) in conjunction with bioinformatic tools. More specifically, the top 10 most highly expressed *P. agathidicida* genes *in planta* that encoded proteins where the amino acid sequences were predicted to contain an N-terminal signal peptide, lack both a transmembrane domain and a GPI anchor, and have no homology with proteins of characterised function, based on the abovementioned bioinformatic tools described in **section 3.2.1.1**, were selected for further analysis.

3.2.1.3 Selecting *P. agathidicida* RxLR proteins of interest

A total of 110 proteins from *P. agathidicida* that contain an RxLR motif were previously characterised by another member of our lab (Guo, Unpublished-a, Guo et al., 2020a). From this list of proteins, a selection of RxLRs that were highly expressed *in planta* based on the previously generated RNA-sequencing data (Guo & Shiller, Unpublished)) were selected to examine whether RxLR expression could suppress the cell death response triggered by *P. agathidicida* GH12 proteins.

3.2.2 Biological materials

A summary of bacterial and oomycete strains, as well as the plant material used in this chapter, are listed in **Table 3.1**. A full list of bacterial strains and plasmids used in this chapter are listed in **Appendix 3.1** and **3.2** respectively.

Table 3.1. Bacterial strains, oomycetes strains and plant material used in Chapter three.

Organism	Characteristics	Reference
Bacteria		
Escherichia coli DH5α	F^-, φ80*lac*ZΔM15, Δ(*lac*ZYA-*argF*), U169, *rec*A1, *end*A1, *hsd*R17 (r_k^-, m_k^-), *pho*A , *sup*E44, λ^-, *thi*-1, *gyr*A96, *rel*A1	Dr. K. Sohn[a]; Invitrogen
Agrobacterium tumefaciens GV3101::pMP90	pMP90 (pTiC58); C58C1; Rif^R, $Gent^R$	Hellens et al. (2000)
Oomycete		
Phytophthora agathidicida NZFS 3770	*P. agathidicida* type strain NZFS 3770	Studholme et al. (2016)
Yeast		
Pichia pastoris GS115	His4, Mut+, His-, Aox1, Aox2	Assoc. Prof. P. Dijkwel[b]
Plants		
Nicotiana benthamiana	Wild type	Dr. K. Sohn[a]
Nicotiana tabacum	Wisconsin 38	Dr. K. Sohn[a]

[a] Previously School of Agriculture and Environment (SAE), Massey University.

[b] School of Natural Science (SNS), Massey University.

3.2.3 Media

All media used in this study are described in **Appendix 3.3**.

3.2.4 Growth conditions

3.2.4.1 *Agrobacterium tumefaciens*

A. tumefaciens GV3101::pMP90 cells were grown on LB agar for 2 days at 28°C, or in LB medium overnight with shaking at 180 rpm (Ecotron, INFORS-HT, Switzerland). For use in ATTAs, *A. tumefaciens* was grown in LB broth for 16 h. For short-term storage, *A. tumefaciens* cells were kept up to 1 month at 4°C. For long-term storage, actively growing *A. tumefaciens* cells were used for storage in 30% (v/v) glycerol (Ajax lab chemicals, New South Wales, Australia) at –80°C.

3.2.4.2 *Escherichia coli*

E. coli DH5α cells were grown overnight at 37°C on LB agar, or in LB broth with shaking at 180 rpm (Classic series C10 platform shaker (New Brunswick Scientific, Edison, New Jersey, USA)). *E. coli* cells were stored for up to a month at 4°C, but long-term were stored in 30% (v/v) glycerol at –80°C.

3.2.4.3 *Nicotiana* species

N. benthamiana and *N. tabacum* were germinated from seed in soil (Daltons premium seed mix, Fruitfed, New Zealand) sterilised by heating to 60°C for no less than 72 h. Two weeks after sowing, seedlings were transplanted into individual pots. Seedlings and plants were watered on an as-needed basis (two-to-three times per week). Germination and growth were carried out in a light-and temperature-controlled room at 22°C on a 12 h:12 h light:dark cycle with 80–85 µmol/m^2/s light intensity.

3.2.4.4 *Phytophthora agathidicida*

For sub-culturing and use in *N. benthamiana* virulence assays, *P. agathidicida* strain 3770 was grown on clarified V8 agar for 3–5 days at 22°C in the dark. For long-term storage*, P. agathidicida* 3770, grown on V8 agar as above, was diced into small pieces and inoculated into 1.5 mL tubes containing sterile water and incubated at 22°C in the dark for several months. When retrieving *P. agathidicida* 3770 from water storage, the small agar pieces were first sub-cultured onto cornmeal agar containing PARP (Pimaricin 10 µg/mL (w/v), Ampicillin 250 µg/mL (w/v), Rifampicin 10 µg/mL (w/v), Pentachloronitrobenzene (PCNB) 100 µg/mL (w/v)) as selective agents and grown for approximately 5 days at 22°C in the dark. Subsequent sub-culturing was carried out on clarified V8 agar as above.

3.2.4.5 *Pichia pastoris*

Wild type *Pichia pastoris*, strain GS115, was sub-cultured onto YPD agar and grown at 28°C for 2–3 days. Genetically modified yeast was grown on MD agar at 28°C for approximately 2–3 days. Short-term, *P. pastoris* colonies were stored at 4°C on either YPD or MD agar plates. For long-term storage, actively growing *P. pastoris* in either YPD or BMGY broth was mixed with an equal volume of 60% (v/v) glycerol (Ajax lab chemicals) and stored at –80°C. Growth for transformation and expression is described in **sections 3.2.7.3** and **3.2.9.1-2** respectively.

3.2.5 DNA isolation and manipulation

3.2.5.1 *P. agathidicida* genomic DNA extraction

Genomic DNA extraction was performed using a variation of the CTAB (**c**etyl**t**rimethyl**a**mmonium **b**romide) method (Moller et al., 1992). For this purpose, 0.1 g of freeze-dried *P. agathidicida* mycelia was ground to a fine powder with liquid nitrogen in a microcentrifuge tube and resuspended in 750 µL 2% CTAB (Sigma-Aldrich, Missouri, USA), 1.4 M NaCl (Panreac, Barcelona, Spain), 20 mM EDTA (Sigma-Aldrich), 100 mM Tris-HCl (Gold Biotechnology) (pH8), then incubated at 65°C for 30 min. Next, 750 µL of 25:24:1 phenol:chloroform:isoamylalcohol (Sigma-Aldrich) was added at room temperature and the microtube inverted to mix before centrifugation at 6.2 x *g* for 10 min. The supernatant was decanted into a clean microtube and one volume of 24:1 chloroform:isoamylalcohol (Sigma-Aldrich) added prior to a second centrifugation at 6.2 x *g* for 10 min. The supernatant was transferred to a clean microtube, and two volumes of chilled 100% ethanol added prior to incubation at –20°C for 20 min. After a further centrifugation step at 6.2 x *g* for 10 min, the supernatant was removed, and the pellet washed with one volume of 70% ethanol. After one last centrifugation step at 6.2 x *g* for 10 min, the supernatant was removed and the pellet left to dry at room temperature before resuspension in 60 µL 1 x TE (10 mM **T**ris-HCl (pH8), 1 mM **E**DTA (pH 8)). Finally, 80 ng RNAse A (Invitrogen, California, USA) was added and the sample incubated at 37°C for 30 min, then heated to 65°C to inactivate the RNAse A. The integrity of the genomic DNA was checked via agarose gel electrophoresis (**section 3.2.5.4**).

3.2.5.2 Plasmid DNA extraction

A single *E. coli* colony carrying the plasmid of interest was inoculated into 5 mL of LB medium together with the appropriate selective agent and grown as described in **section 3.2.4.2**. Plasmid DNA was isolated using the E.Z.N.A.® Plasmid Mini Kit I (Omega Bio-tek, Norcross, USA) according to the manufacturer's instructions.

3.2.5.3 **P**olymerase **c**hain **r**eaction (PCR)

All PCRs were carried out in a Mastercycler® nexus (Eppendorf, Hamburg, Germany) machine. PCR conditions were carried out according to the manufacturers' instructions, dependent on the Taq polymerase that was used, for 30 cycles.

PCR primer design

PCR primers were designed using Geneious® version 9.1.8 (https://www.geneious.com) software.

Primers to amplify the selected *P. agathidicida* genes, for cloning into the pICH86988 expression vector via golden gate assembly (**section 3.2.5.10**), were designed after the native signal peptide sequence, with the appropriate overlap, BsaI restriction site, and spacer sequences added at the 5′ end (**Figure 3.1 A**).

Primers for the mutation of DNA bases were approximately 20 bp long and designed to overlap each other, either partially (**Figure 3.1 B**) or completely (**Figure 3.1 C**), in a head-to-tail configuration using Geneious® version 9.1.8) software. To mutate BsaI sites, the last base in a codon was changed to a base that would not result in any aa change, while to mutate catalytic sites, a single nt was mutated in a way that would result in change of aa to one with similar physiochemical properties.

Primers used to remove introns from *P. agathidicida* genomic DNA were designed to match the mRNA sequence of the target gene across the intron site (**Figure 3.1 D**). PCRs were carried out to amplify one exon at a time, and the correct fragments were gel extracted (**section 3.2.5.6**). Both exon fragments were then pooled in a single PCR using primers for the 5′ and 3′ end of the mRNA sequence.

Primers used to split genes in two (necessary because the golden gate reaction was unsuccessful for genes larger than 1.5 kb) prior to re-ligation during the golden gate reaction were designed using Geneious® version 9.1.8 software with BsaI sites added to the 5′ end. To ensure the genes were amplified and then re-ligated without altering the DNA sequence, the primers were designed in a head-to-tail configuration with exactly 6 bp of overlap (**Figure 3.1 E**).

A table of primers used in this research are in **Appendix 3.4**.

High quality PCR amplification for downstream manipulation

Amplification of DNA for gel purification was carried out in 50 µL reactions performed using Phusion Flash High-Fidelity PCR Master Mix (Thermo Scientific™, Auckland, New Zealand) according to the manufacturer's instructions. Template concentrations ranged between 0.2-2 ng/µL.

Standard PCR

Standard PCRs, primarily used to screen for the correct sized gene fragment, were performed using Taq DNA polymerase (New England Biolabs Inc., Massachusetts, USA) in combination with dNTPs (Takara Bio Inc., Shiga Prefecture, Japan) as per the manufacturer's instructions. Either <100 ng of plasmid or a small number of cells obtained from a single bacterial colony using a sterile tip were used as a template. To analyse several different colonies in a pooled PCR, up to 10 colonies were inoculated into a 50 µL aliquot of sterile water, incubated at 99°C for 10 min, and 1 µL of the resultant solution was added to the PCR.

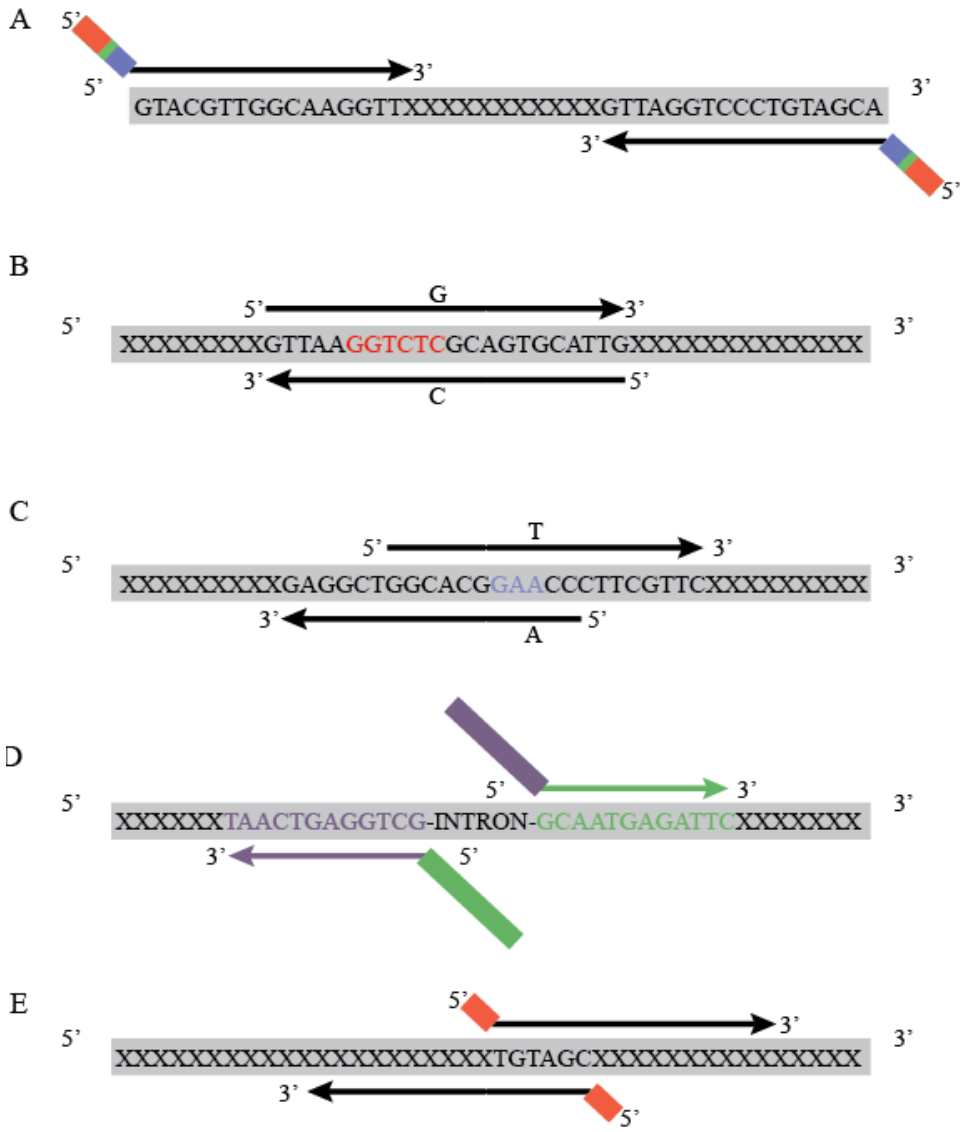

Figure 3.1. Primer design schematic.

Schematic to illustrate the design of primers as described (**section 3.2.5.3.1**). **(A)** Primers designed to amplify the gene of interest by PCR in preparation for golden gate cloning. **(B–C)** Two different methods of primer design to mutate a single nucleotide. **(B)** Example of primers designed to mutate a BsaI recognition site (shown in red text). **(C)** Primers designed to mutate (Glu>Asp) one of the predicted catalytic residues in GH12 Pa|009244 (codon in blue text). **(D)** Primers designed to amplify an intron-containing gene from genomic DNA. Half of the primer matched the sequence on one side of the intron and the other half matched the nucleotide sequence on the other side of the intron. The reverse primer (with the green tail) was used in conjunction with the forward primer at the 5' end of the gene (not shown), while the forward primer was used in conjunction with the reverse primer at the 3' end of the gene (not shown). These two exon fragments were later used in a second PCR with only the 5' forward and 3' reverse primers to amplify the entire gene as one fragment. **(E)** Primers designed to split, and then re-ligate, genes which were too long to use intact in a golden gate reaction. 'X's' in the grey box indicate nucleotide sequence. Primer colour coding: Red = BsaI recognition site, Green = Spacer, Blue = 5' overhang.

3.2.5.4 Agarose gel electrophoresis

DNA was resolved on a 1% (w/v) agarose (HyAgarose™, HydraGene) gel at 100–110 volts in 1x **T**ris/**a**cetic acid/**E**DTA (TAE) buffer (190 mM Tris, 342 mM acetic acid (Emsure ®, Merck, New Jersey, USA), 2.5 mM EDTA). DNA was loaded with a 1:4 dilution of SDS loading dye (BDH Ltd., Poole, England) (0.2% (w/v) bromophenol blue (Avantor Sciences Inc., Pennsylvania, USA), 20% (w/v) sucrose, 1% (w/v) SDS, 5 mM EDTA, pH 6.8). DNA was stained with ethidium bromide (1 µg/mL) for 15 min. DNA was visualised and imaged with the UV Transilluminator Gel Documentation system (Bio-Rad, California, USA). A 1 kb plus DNA ladder (Invitrogen) was used to estimate DNA fragment size.

3.2.5.5 Gene synthesis

Genes that were difficult to clone, due to harboring several internal *Bsa*I sites, several introns, or simply being difficult to amplify by PCR, were instead synthesised in the pICH86988 expression vector by Twist Bioscience (San Francisco, California, USA).

3.2.5.6 Purification of DNA from agarose gels

Following agarose gel electrophoresis (**section 3.2.5.4**), DNA bands of interest were identified on a DarkReader™ transilluminator (Clare Chemical, Colorado, USA) and sliced out with a sterile scalpel. DNA was purified from gel slices using the E.Z.N.A.® Gel Extraction Kit (Omega Bio-tek, Norcross, USA) according to the manufacturer's instructions, and resuspended in 30 µL of sterile water. Purified DNA products were stored at 4°C for use within a week, or at –20°C for long-term storage.

3.2.5.7 DNA digestion

Approximately 1 µg of plasmid was digested with selected NEB (NEB Inc., Ipswich, MA, USA) restriction enzymes according to the manufacturer's instructions.

3.2.5.8 DNA phosphorylation and de-phosphorylation

Gel-purified PCR products were phosphorylated with T4 polynucleotide kinase (NEB Inc., Ipswich, MA, USA) in 20 µL reactions according to the manufacturer's instructions. Plasmids which had been digested to produce blunt ends (e.g., pUC19 entry vector) were de-phosphorylated with Shrimp alkaline phosphatase (NEB Inc., Ipswich, MA, USA) according to the manufacturer's instructions.

3.2.5.9 DNA ligation

DNA ligations were performed in 20 µL reactions using T4 DNA ligase (NEB Inc., Ipswich, MA, USA) and mixed, according to the manufacturer's instructions, in a 3:1 molar ratio (insert:vector). Ligation reactions were incubated at 4°C overnight.

3.2.5.10 Golden gate assembly

Golden gate assembly (**Figure 3.2**) was performed using a master mix containing 10% (v/v) 1 x T4 ligase buffer (Invitrogen), 5% (v/v) T4 ligase (Invitrogen), 10% (v/v) 10 x BSA buffer (New England Biolabs), 1% (v/v) BsaI restriction enzyme (New England Biolabs). In addition, 10 fmol of each fragment required to make the construct of interest were added (PR1α-3xFLAG, GOI, pICH86988 backbone). Golden gate conditions were as described by Engler et al. (2008).

3.2.5.11 Sepharose filtration

Sepharose® 4B beads (45–165 µm bead diameter (Sigma-Aldrich®)) were gently resuspended, and 150 µL added to a 600 µL microtube with a small needle hole in the bottom. The 600 µL microtube was inserted into a second, larger, 1.5 mL microtube, and centrifuged at 2,000 *g* for at least 5 min, or until the Sepharose beads appeared dry. The 600 µL microtube containing the dry beads was then inserted into a clean 1.5 mL microtube, and the contents of the DNA ligation reaction, or golden gate assembly, added. A second centrifugation at 2,000 *g* for 1 min filtered the reaction mix through the beads and into the 1.5 mL collection tube, removing salt and purifying the reaction in preparation for transformation by electroporation.

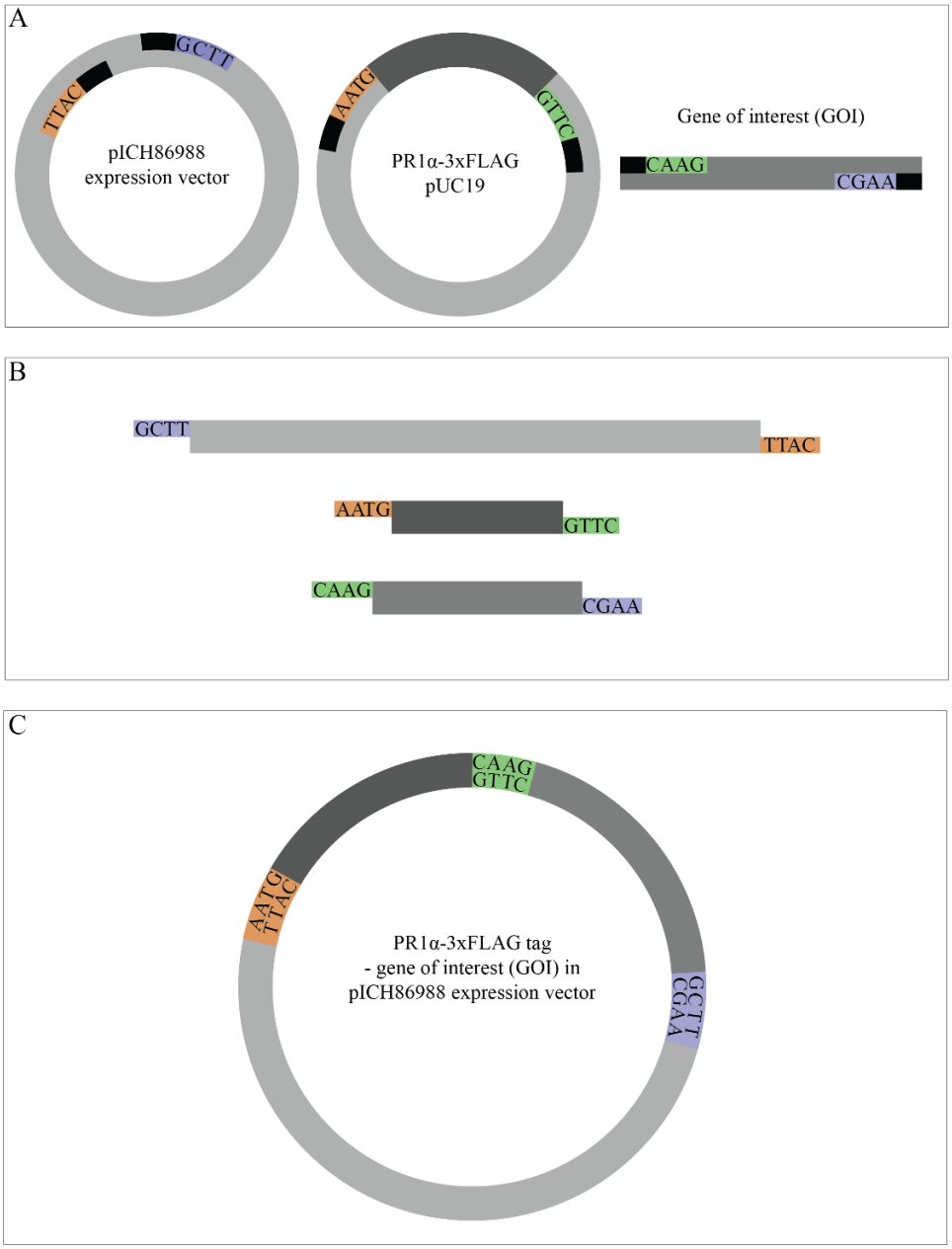

Figure 3.2. Schematic illustrating golden gate assembly of DNA fragments.

(A) All nucleotide components of the reaction contain *Bsa*I sites for restriction enzyme digest. The pICH86988 expression vector contains two *Bsa*I restriction sites, indicated by black boxes. The *Nicotiana tabacum* PR1α signal peptide, for protein secretion to the apoplast, is fused to a 3xFLAG tag for detection by Western blot (PR1α-3xFLAG; dark blue) and is flanked by two *Bsa*I restriction sites in the pUC19 vector. In addition, the gene of interest (GOI; light blue) is amplified by PCR with primers containing *Bsa*I restriction sites at the 5′ ends. **(B)** Digestion with *Bsa*I during the golden gate reaction results in the formation of overlapping ends, colour-coded to demonstrate how they match. **(C)** During ligation, the overlapping ends join, resulting in a pICH86988 expression vector containing both the PR1α-3xFLAG tag and the GOI. The original *Bsa*I restriction sites are lost during the digestion and ligation process.

3.2.5.12 DNA sequencing

DNA sequencing reactions were performed by the Massey Genome Service sequencing facility at Massey University, Palmerston North, using 3.2 pmol of primer and 300 ng of plasmid DNA or 17.5 ng of purified PCR amplicon as template.

3.2.6 Preparation of electrocompetent cells

3.2.6.1 *E. coli*

A 10 mL aliquot of *E. coli* DH5α cells grown as described in **section 3.2.4.2** was inoculated into 500 mL of LB medium and cultured at 37°C and 180 rpm (classic series C10 platform shaker, New Brunswick Scientific (Edison, New Jersey, USA)), until an OD_{600} of between 0.6 and 0.8 was reached (approximately 3 h). The culture was then poured into 50 mL Falcon tubes (Fisher Scientific, Waltham, Massachusetts, United States of America) and cooled on ice before cells were collected by centrifugation at 5,000 rpm (Heraeus Megafuge 16R Centrifuge (ThermoFisher Scientific)) for 20 min. The supernatant was discarded, and pelleted cells resuspended in one volume of 10% (v/v) glycerol.

The centrifugation step was repeated, the supernatant discarded, and the cells resuspended in 0.5 volumes of 10% (v/v) glycerol. Centrifugation and resuspension were continued until cells were collected into a single Falcon tube. Finally, the pelleted cells were resuspended in 2 mL 10% (v/v) glycerol and 50 µL aliquots were dispensed into sterile 0.6 µL tubes and stored at –80°C until required.

3.2.6.2 *A. tumefaciens*

A 10 mL aliquot of *A. tumefaciens* GV3101::pMP90 cells grown as described in **section 3.2.4.1** was inoculated into 500 mL of LB medium and cultured at 37°C and 180 rpm (Ecotron (INFORS-HT)), until an OD_{600} of between 0.6 and 0.8 was reached. Preparation of electrochemically competent *A. tumefaciens* cells was carried out as for *E. coli* in **section 3.2.6.1**. Resuspended cells were dispensed into microcentrifuge tubes in 50 µL aliquots and stored at –80°C.

3.2.6.3 *P. pastoris*

P. pastoris (**section 3.2.4.5**) was grown in 5 mL YPD broth at 28°C overnight with shaking at 225 rpm (Innova 42 biological shaker, John Morris Scientific, Sydney, NSW, Australia). The resulting culture was added to 75 mL of YPD in a 300 ml baffled flask and incubated, with shaking at 225 rpm, at 28°C overnight or until an OD_{600} of between 1.3–1.5 was achieved. The culture was centrifuged at 4°C at 1,500 x g for 5 min and the pellet resuspended in 50 mL ice-cold sterile water. Two more centrifugation

steps were carried out with the pellet resuspended in 25 mL ice-cold sterile water and 10 mL ice-cold 1 M sorbitol respectively. After a final centrifugation, the pelleted cells were resuspended in 1 mL ice-cold 1 M sorbitol and ready for same-day transformation by electroporation (**section 3.2.7.3**).

3.2.7 Transformation by electroporation

3.2.7.1 *E. coli*

Electrocompetent *E. coli* cells (50 µL) were thawed on ice and 5 ng of the plasmid of interest added. Cells were incubated for 10 min on ice prior to electroporation in a 0.2 mm electroporation cuvette with a MicroPulser™ (BioRad) electroporator using pre-set *E. coli* settings. Electroporated cells were mixed with 1 mL LB medium and incubated at 180 rpm (classic series C10 platform shaker (New Brunswick Scientific)), 37°C for 1 h. Cells were collected by centrifugation at 2,000 x *g* for 2 min, after which 950 µL of supernatant was discarded. The remaining supernatant was used to resuspend the pelleted cells, all of which were subsequently spread on LB agar containing the appropriate selective agents and incubated at 37°C overnight.

3.2.7.2 *A. tumefaciens*

Electrocompetent *A. tumefaciens* cells (50 µL) were left to thaw on ice before 5 ng of uncut plasmid was added. Cells were incubated for a further 10 min on ice prior to electroporation in a 0.2 mm electroporation cuvette with a MicroPulser™ (BioRad) electroporator, using the pre-set *Agrobacterium* settings. Electroporated cells were mixed with 1 mL LB medium and incubated at 180 rpm (Ecotron (INFORS-HT)), 28°C for 1 h. Approximately 50 µL of cells were spread on LB agar containing the appropriate selective agents which were subsequently incubated at 28°C for 2 days.

3.2.7.3 *P. pastoris*

Electrocompetent *P. pastoris* cells (80 µL) were mixed with the linearised DNA of interest and incubated in a 0.2 cm chilled electroporation cuvette for 5 min. Using the pre-set *Pichia* settings (Voltage 1,500 V, Resistance 200 ohms; MicroPulser™ (BioRad) electroporator), cells were electroporated and immediately mixed with 1 mL ice-cold 1 M sorbitol before spreading on MD agar. MD plates were then incubated at 28°C for 2–4 days.

3.2.8 *A. tumefaciens* transient transformation assays (ATTAs)

3.2.8.1 Identification of proteins triggering a plant cell death response

A. tumefaciens cells harboring the pICH86988 expression vector with the gene of interest were grown overnight as described (**section 3.2.4.1**) until an OD_{600} of between 0.4 and 2 was reached. Cells were collected by centrifugation at 2,500 *g* for 5 min and resuspended in 0.5 mL of infiltration buffer (10 mM $MgCl_2$:$6H_2O$ (BDH Ltd), 10 mM MES-KOH (Sigma, St. Louis, USA), 100 µM acetosyringone (Sigma, St. Louis, USA)). The OD_{600} was measured using a Ultrospec 3100 pro UV/visible spectrophotometer (Amersham Biosciences (Amersham, United Kingdom)) and infiltration buffer added to reach a final OD_{600} of 0.6. Cells were incubated at room temperature for 3 h. The second, third, and/or fourth leaves of 5 to 6-week-old *N. benthamiana* and *N. tabacum* plants were marked (with large circles on *N. benthamiana* or small points on *N. tabacum*), to indicate the sites of infiltration, and infiltrated with the appropriate *A. tumefaciens* cell solution using a 1 mL Terumo syringe without needle (Terumo Corporation, Binan, Laguna, Philippines). Plants were maintained for 7 days post-infiltration, after which photos of the infiltrated leaves were taken using a Canon EOS 600D camera with an 18–55 mm lens (Canon, Ota City, Tokyo, Japan). At least two biological replicates were performed for each protein that was studied, in both *N. benthamiana* and *N. tabacum*; in this case each biological replicate started with an independent collection of *A. tumefaciens* cells (taken from either sub-culture or glycerol stock) and taking those cells through to perform the ATTA. For each of the biological replicates a minimum of ten technical replicates were performed, a technical replicate being an ATTA performed on a single leaf. A maximum of three leaves could be infiltrated on any one plant, although in most cases only two leaves were infiltrated due to size constraints.

3.2.8.2 RxLR cell death suppression assays

A. tumefaciens cells harbouring the pICH86988 expression vector with the gene of interest were grown (**section 3.2.4.1**) and prepared (**section 3.2.8.1**) as described, but to a final OD_{600} of 0.5. The second, third, and/or fourth leaves of 5-week-old *N. benthamiana* plants were marked with large circles. On the first day of infiltration *A. tumefaciens* strains carrying plasmids encoding either: the known cell death suppressor, *Phytophthora infestans Avr3a*; the negative control, a *P. agathidicida* GH19 gene which was shown not to elicit a cell death response (*Pa|001110*); or the *P. agathidicida* RxLR genes of interest were infiltrated using a 1 mL Terumo syringe without needle (Terumo Corporation). After 24 h, *A. tumefaciens* strains carrying plasmids encoding the cell death elicitors*, P. agathidicida INF1* or *P. agathidicida* genes encoding GH12 proteins identified as able to trigger a cell death response, were infiltrated. Plants were maintained for 7 days post-infiltration, after which photos of the infiltrated leaves were taken using a Canon EOS 600D camera with an 18–55 mm lens. Images were also taken

under UV light with a UV Transilluminator Gel Documentation system (Bio-Rad). A minimum of ten technical replicates were performed.

3.2.8.3 *P. agathidicida* virulence assays

A. tumefaciens strains harbouring the pICH86988 expression vector with the gene of interest were grown and prepared as described (**section 3.2.8.2**). The entire underside of the second, third and/or fourth leaves of 5-week-old *N. benthamiana* plants were infiltrated with the *A. tumefaciens* strains using a 1 mL Terumo syringe without needle (Terumo Corporation). After 24 h, the leaves were removed from the plant. The leaf surface was sterilised by spraying with 70% ethanol, and the stems were wrapped in strips of paper towel soaked with milliQ water. Leaves were placed, underside up, in a square petri dish which had been sterilised under UV light. A 2 mm tissue wound was inflicted at the site on infiltration and a 6 mm mycelial plug from the leading edge of a *P. agathidicida* 3770 colony grown on V8 agar (**Appendix 3.3**) was cut out with a cork borer and placed, mycelia side down, atop the wound. The petri dishes containing the infected leaves were wrapped in tinfoil and placed at 22°C for 48 h, after which time the mycelial plugs were gently removed and the *P. agathidicida* infection lesions measured using 150 mm digital callipers with 0.01 mm resolution (Jobmate®, Mitre10, Auckland, New Zealand). Leaves were photographed using a Canon EOS 600D camera with an 18–55 mm lens on a Huion (Shenzhen, China) A3 LED light pad.

3.2.9 Protein analysis

3.2.9.1 Protein production in the *P. pastoris* expression system

The presence of the gene of interest in *P. pastoris* colonies that grew on MD agar was assessed via colony PCR. Colonies that contained the gene of interest were inoculated into 5 mL BMGY media and incubated overnight at 28°C, 225 rpm (Innova® 42, New Brunswick Scientific, Edison, New Jersey, USA) until an OD_{600} between 2–6 was achieved. The cells were collected by centrifugation at 3,000 x g for 5 min at room temperature and the cell pellet resuspended in 4 mL BMMY. The cells were once again collected by centrifugation at 3,000 x g for 5 min, and the cell pellet resuspended in 10 mL BMMY. The resulting culture was transferred to a 150 mL flask, covered in two layers of miracloth (Merck, New Jersey, USA) and incubated at 28°C, 225 rpm (Innova® 42, New Brunswick Scientific), for 72 h. The *P. pastoris* cultures were fed sterilised 100% methanol (Emsure®) to a final concentration of 0.5% every 24 h. To identify colonies that were producing the construct of interest, samples were taken every 24 h and centrifuged at 1,300 x g for 3 min. Pellet and supernatant were stored separately and analysed via Western blot.

Once it had been ascertained that a particular *P. pastoris* colony was producing protein, the cells in all 10 ml of culture filtrate were removed by centrifugation at 1,300 x g for 3 min and the supernatant transferred to a 15 mL Falcon tube. The supernatant, containing the protein of interest, was then stored at -20°C until required.

3.2.9.2 Enzyme activity assays

In order to test for xyloglucanase activity of selected GH12 proteins, *P. pastoris* supernatant containing the protein of interest and azo-xyloglucan substrate solution (0.1M sodium acetate trihydrate (Sigma-Aldrich) (v/v), 2% Azo-xyloglucan (w/v) (Megazyme, Wicklow, Ireland), pH4.5) were pre-equilibrated to 40°C in a water-bath. Exactly 500 µL of *P. pastoris* supernatant was added to 1000 µL of azo-xyloglucan substrate solution. The resulting mixture was vortexed for 10 s and incubated at 40°C for 10 min, at which time 2.5 mL precipitation solution (0.3M (w/v) sodium acetate tri-hydrate (Sigma-Aldrich), 0.02M (w/v) zinc acetate dihydrate (Sigma-Aldrich), 80% (v/v) ethanol (VWR, Radnor, Pennsylvania, USA), pH5) was added. The mixture was vortexed again for 10 s and left at room temperature for 10 min. The mixture was vortexed once more, and then centrifuged at 1000 x *g* for 10 min at 20°C. The resulting supernatant was decanted into a plastic cuvette and the absorbance read at 590 nm on a Ultrospec 3100 pro UV/visible spectrophotometer (Amersham Biosciences). The blank reaction used to zero the spectrophotometer was made by adding the precipitation solution directly to azo-xyloglucan substrate solution prior to the addition of the *P. pastoris* supernatant. This blank reaction was then subjected to the same conditions as the test reactions. Reactions were photographed using a Canon EOS 600D camera with an 18–55 mm lens on a Huion (Shenzhen, China) A3 LED light pad.

3.2.10 Western blots

3.2.10.1 Preparation of plant material

N. benthamiana plants were grown as previously described (**section 3.2.4.3**) and half a leaf was infiltrated with an ATTA carrying the gene of interest. After 48 h the infiltrated leaves were cut off and the mid-vein removed. Each half-leaf was rolled, wrapped, and labelled in aluminium foil, then flash-frozen in liquid nitrogen. Samples were stored at –80°C until required.

3.2.10.2 Crude protein extraction

Frozen plant samples were ground to a fine powder in liquid nitrogen using a mortar and pestle. An equal volume of extraction buffer was added (GTEN buffer (10% v/v glycerol, 0.1 M (v/v) Tris-HCl (pH 7.5), 1 mM (v/v) EDTA, 150 mM (w/v) NaCl) plus 10 mM (v/v) dithiothreitol (DTT) (Sigma), 0.1% (v/v) Tween20 (Ajax Fine Chemicals, Auckland, New Zealand), one anti-protease tablet

(cOmplete mini protease inhibitor cocktail tablets, Roche, Basel, Switzerland), and 2% (w/v) **p**oly**v**inyl**p**oly**p**yrrolidone (PVPP) (Sigma)) and the samples were incubated at 4°C on a Heidolph rotator (John Morris Scientific) at 60 rpm for 30 min. To remove cell debris, samples were spun at 4°C, 5,000 x *g*, for 20 min and the supernatant was transferred to a fresh 1.5 mL microcentrifuge tube through a small square of miracloth (Merck, New Jersey, USA). The crude protein solution was concentrated to half the original volume using a SpeedVac (Savant SPD131DDA SpeedVac Concentrator, Thermo Scientific, USA). The concentrated protein extract was mixed with 3 x SDS loading dye (30% v/v glycerol, 3% w/v SDS, 94 mM v/v Tris (pH7.5), 0.05% w/v bromophenol blue, 24 mM v/v DTT, in sterile water) in a 2:1 ratio in preparation for gel loading.

3.2.10.3 **S**odium **d**odecyl **s**ulfate-**p**oly**a**crylamide **g**el **e**lectrophoresis (SDS-PAGE)

Proteins were resolved by sodium dodecyl sulfate-polyacrylamide gel electrophoresis (SDS-PAGE). The Tris-glycine gel was prepared in two stages; firstly the 10% resolution gel (10.2% (v/v) acrylamide (Bio-Rad, California, USA), 390 mM Tris (v/v) (pH8.8), 0.1% SDS (v/v), 0.1% (v/v) ammonium persulfate, 0.04% (v/v) **te**tra**m**ethyl**e**thylene**d**iamine TEMED (Sigma), with a layer of 50% (v/v) ethanol for levelling which was later tipped off; secondly the 5% stacking gel (5.1% (v/v) acrylamide, 130 mM (v/v) Tris (pH6.8), 0.1% (v/v) SDS, 0.1% (v/v) ammonium persulfate, 0.001% (v/v) TEMED). In both gels, the final two components (ammonium persulfate and TEMED) were added last, immediately before casting the gel. The pre-stained PAGE ladder and protein samples were added to the wells in 15 µL aliquots. A Mini-Protean II Electrophoresis Cell system (Bio-Rad) was assembled according to the manufacturers' instructions. Gels were immersed in SDS running buffer (25 mM (w/v) Tris, 192 (w/v) mM glycine, 0.1% (w/v) SDS, pH 8.3), and proteins resolved at 80 V for the first 20 min (stacking gel) and 100 V thereafter (resolution gel).

3.2.10.4 Western blotting

After SDS-PAGE, proteins were transferred to an immune-blot® **p**oly**v**inyli**d**ene **f**luoride (PVDF) membrane (Bio-Rad), previously activated in 100% (v/v) methanol (Emsure®), submerged in transfer buffer (25 mM (v/v) Tris, 190 mM (v/v) glycine, 20% (v/v) methanol (pH 8.3)) and sandwiched between four sheets of Whatman 3MM paper (pre-soaked in transfer buffer) at 30 V and 4°C, overnight. The membrane was then placed in a blocking solution (20 mM (v/v) Tris, 136 mM (v/v) NaCl, 10% (v/v) Tween, 5% (w/v) skim milk) for 1 h at room temperature with gentle shaking (20 rpm) on a Heidolph rotator (John Morris Scientific). The blocking solution was decanted off and replaced with more blocking solution containing a 1:5,000 dilution of the (primary) monoclonal anti-FLAG® M antibody (Sigma-Aldrich) produced in mouse. After a 1.5 h incubation with the primary antibody, the solution was decanted off and three washes were performed with the membrane submerged in TBST buffer (20

mM (v/v) Tris, 136 mM (v/v) NaCl, 10% (v/v) Tween, pH 7.6) with rotation at 20 rpm (Polymax 1040, Heidolph (Schwabach, Germany)), room temperature, for 10 min per wash. The secondary antibody (chicken anti-mouse, produced by Santa Cruz Biotechnology, Texas, USA) was added to the membrane in blocking solution at a 1:20,000 ratio and incubated for 1 h at room temperature with shaking (20 rpm), followed by three washes with TBST for 10 min. The membrane was incubated with 0.5 mL of SuperSignal® West Dura Extended Duration substrate (Thermofisher, Massachusetts, USA) for 5 min and visualised with an Azure Biosystems c600 Bioanalytical Imaging system (Azure Biosystems, CA, USA). After visualisation, the membrane was incubated with Ponceau S stain to develop the protein bands, thoroughly washed with sterile water, and left to dry.

3.3 Results

3.3.1 Prediction of carbohydrate-active enzymes (CAZymes) in *P. agathidicida*.

The online CAZyme prediction tool dbCAN2 (Zhang et al., 2018) was used to predict CAZymes in the *P. agathidicida* predicted proteome. The predicted proteome lists used came from annotations of three different *P. agathidicida* genome assemblies; NZFS 3770 Illumina (PaI) and PacBio (Pa) genomes (2018) annotated by Preeti Panda (Scion), as well as the *P. agathidicida* NZFS 3772 Illumina (Pa3772) genome annotated by McGowan and Fitzpatrick (2017). At the time of analysis, the dbCAN2 server used three different tools, HMMER (Eddy, 2011), Diamond (Buchfink et al., 2021), and Hotpep (Busk et al., 2017), though Hotpep has since been exchanged for eCAMI (Xu et al., 2019) to improve performance (Hobbs et al., 2021). There is some variation in the numbers of CAZymes predicted by dbCAN2 between the three predicted proteome lists (**Figure 3.3**), which is more representative of differences in genome quality, length/number of contigs, and annotation as opposed to real differences between type strains. In support of this, a closer inspection revealed that several proteins had been misannotated. For example, the 759 aa protein PaI|007507 was predicted to contain three GH12 domains from the Illumina PaI3770 genome data; however, comparison to predicted GH12 proteins in the Pa3770 PacBio and Pa3772 Illumina proteome annotations instead revealed three individual GH12 proteins (identified as Pa|009588/Pa3772|09073 (244 aa), Pa|009589/Pa3772|09072 (241 aa), and Pa|009590/Pa3772|09071 (279 aa)) (**Figure 3.4**). As no single predicted proteome annotation yielded a list of reliably annotated CAZyme-encoding proteins, Pa3770 was used as the primary database, with any other proteins of interest predicted by the other two predicted protein lists (Pa3772 and PaI3770) included as additions. A table of cross-matched protein identification between the Pa3770 and Pa3772 protein lists as well as the predicted proteome list from a recently available *P. agathidicida* chromosome-level resolution PacBio genome (Pag3770) is available in **Appendix 3.5**.

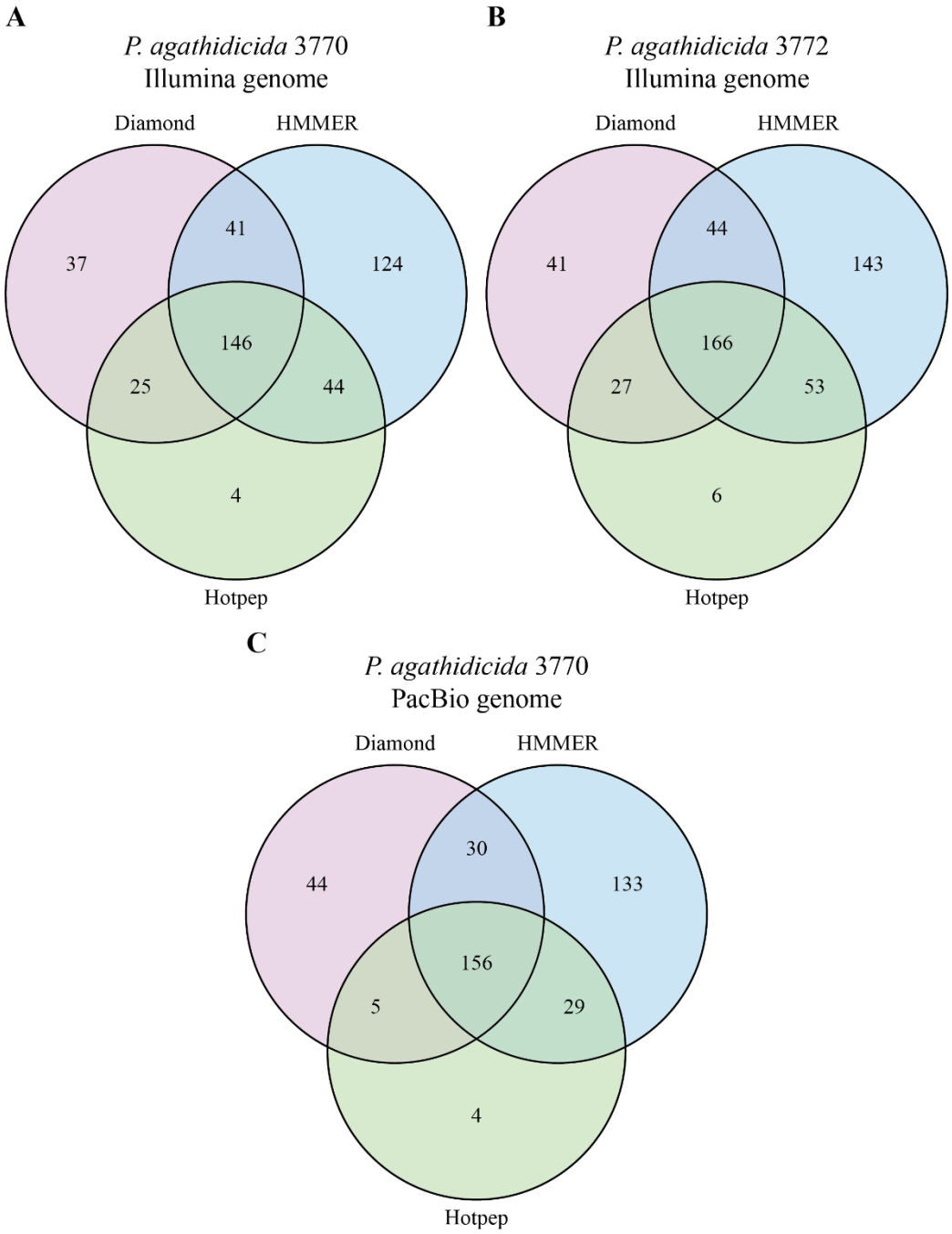

Figure 3.3. Number of carbohydrate-active enzymes (CAZymes) predicted by dbCAN2 from the available *Phytophthora agathidicida* genomes.

Venn diagrams illustrating variation in the number of CAZymes predicted by each of the dbCAN2 tools (HMMER, Diamond, Hotpep) for each of the genome annotations. Only those predicted by two or more dbCAN2 tools were retained for further analysis. (**A)** *P. agathidicida* 3770 Illumina genome. (**B)** *P. agathidicida* 3772 Illumina genome. (**C)** *P. agathidicida* 3770 PacBio genome. Venn diagrams adapted from dbCAN2.

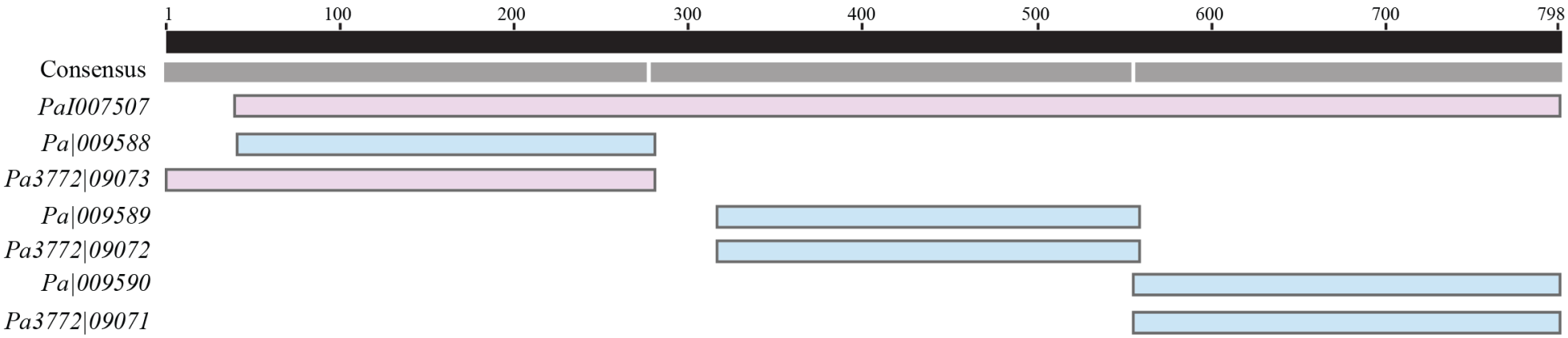

Figure 3.4. Comparison between the three available genomes enabled correction of mis-annotated genes.

Alignment illustrating the differences in genome annotations between *Phytophthora agathidicida* type strain 3770 Illumina (PaI) and PacBio (Pa) genomes and the *P. agathidicida* type strain 3772 Illumina (Pa3772) genome. Lilac, incorrect annotation; blue, correct annotation.

3.3.2 Identification of GH family proteins of interest in *P. agathidicida*

The CAZymes identified in **Figure 3.3** were then classified into six different superfamilies (**Table 3.2**). GH proteins represented over 45% of the total number of CAZymes predicted for each *P. agathidicida* predicted proteome annotation and were the focus of this research going forward.

Table 3.2. Number of *Phytophthora agathidicida* proteins encoded by the three available genome assemblies belonging to each of the carbohydrate-active enzyme (CAZyme) superfamilies.

	Auxiliary activity (AA) proteins	Carbohydrate esterase (CE) proteins	Glycoside hydrolases (GH) proteins	Glycosyl transferases (GT) proteins	Polysaccharide lyase (PL) proteins	Carbohydrate binding module (CBM) proteins
PaI3770[a]	34	38	197	123	23	6
Pa3770[a]	32	29	196	127	11	6
Pa3772|[b]	35	43	228	140	27	7

***** Number of *P. agathidicida* proteins belonging to each group as predicted by at least one of the three tools used by dbCAN2.

[a] Protein sequences used to obtain the information relevant to this strain were predicted by Scion (Rotorua, New Zealand). PaI (*P. agathidicida* illumina genome), Pa (*P. agathidicida* PacBio genome)

[b] Protein sequences used to obtain information relevant to this strain were predicted by J. McGowan (McGowan & Fitzpatrick, 2017).

As expected, there was considerable overlap between the GH predictions in the *P. agathidicida* Pa3770 and Pa3772 predicted proteomes, with 196 and 228 GH proteins predicted respectively. A total of 242 distinct GH proteins were predicted between the two predicted proteomes. The genes encoding these proteins were manually investigated for intron-exon structure, coding sequence (cds) boundaries and presence of a stop codon (**Figure 3.5**). The gene was then translated *in silico*, and the resulting protein sequence assessed for the presence of a signal peptide and the absence of either a GPI anchor or transmembrane domain (**Figure 3.5**). This part of the analysis was designed to identify any predicted genes that were likely mis-annotated, while also selecting for proteins that were predicted to be secreted and not retained in the cell membrane or wall. A 'core set' of 141 GH proteins was established that fit all criteria, representing 27 different GH families. Prior to the commencement of my PhD, an RNA sequencing time-course experiment was carried out on the leaves and roots of kauri seedlings inoculated with *P. agathidicida* type strain 3813 (Guo & Panda, Unpublished). As very few differences have been identified between the 3770 and 3772 *P. agathidicida* genome sequences (Guo et al., 2020a), it is likely that the *P. agathidicida* 3813 genome will also be highly similar. The resulting expression data were used to further narrow down the core set of genes encoding the 141 *P. agathidicida* GH proteins to enrich for those which were highly expressed *in planta*. Of the 141 core genes, four were not detected in the Pa|3770 genome and thus no expression information was available, while 38 did not align well

with the region that was predicted to be expressed and were subsequently removed from further analysis. An arbitrary cut-off of 50 **f**ragments **p**er **k**ilobase of **t**ranscript (FPKM), at any time point (excluding zero) in the RNA sequencing experiment, was imposed on the remaining *P. agathidicida* GH-encoding genes. As a result, a total of 48 *P. agathidicida* GH-encoding genes, belonging to 18 different GH families were selected for further analysis (**Table 3.3**). However, simply belonging to a particular GH family does not specify a single enzymatic function, with many families harbouring enzymes with a number of different substrate specificities and modes of action. As such, there are many overlaps in enzyme activities between different families (**Table 3.4**); for example, GH3, GH5 and GH30 family enzymes are all predicted to have β-glucosidase (EC 3.2.1.21) activities. Thus, while in some cases family affiliation may give an idea as to gene function, this could be misleading.

Among the GH12 family, a particular effort was made to identify proteins from *P. agathidicida* that are possible orthologues of the functionally characterised PsXEG1 and PsXLP1 proteins from *P. sojae* (Ma et al., 2015b, Ma et al., 2017). Unsurprisingly, an orthologue of PsXEG1, which acts as a virulence factor and PAMP during *P. sojae* infection of soybean, had already been identified as part of the 48 proteins selected for further analysis (Pa|009244) (**Figure 3.6**). However, no orthologue of PsXLP1, the paralogous decoy for PsXEG1, was identified in the *P. agathidicida* genome. Research carried out by Ma et al. (2015b) identified GH12 proteins in both oomycetes and fungi which were capable of triggering a plant cell death response in the model host plant *N. benthamiana*, while several other studies have since further characterised/identified GH12 proteins involved in a plant cell death response and/or pathogen virulence (Gui et al., 2017, Yang et al., 2021, Zhang et al., 2021c, Zhu et al., 2017). Curiously, a phylogenetic tree of fungal and oomycete GH12 proteins illustrates that while several proteins on a branch may trigger a plant cell death response in *N. benthamiana*, not all proteins on that branch elicit such a response (**Figure 3.6**).

Mapping of the *P. agathidicida* GH-encoding genes of interest (as well as other genes of interest identified later in this chapter (**Section 3.3.5**)) to the *P. agathidicida* chromosome-level genome (Pag3770, mentioned above and discussed in **Chapter 5**) (**Figure 3.7**) illustrates that the genes of interest appear to be randomly distributed throughout the genome. While some families of genes are clustered together (e.g. those encoding proteins belonging to the GH28 family on chromosome 1, CBEL and CBEL-like proteins on chromosome 2, and GH17 family proteins on chromosome 5), suggesting they have arisen through duplication events, others are spread across several chromosomes (e.g. GH10 encoding genes are found on chromosomes 1 and 5).

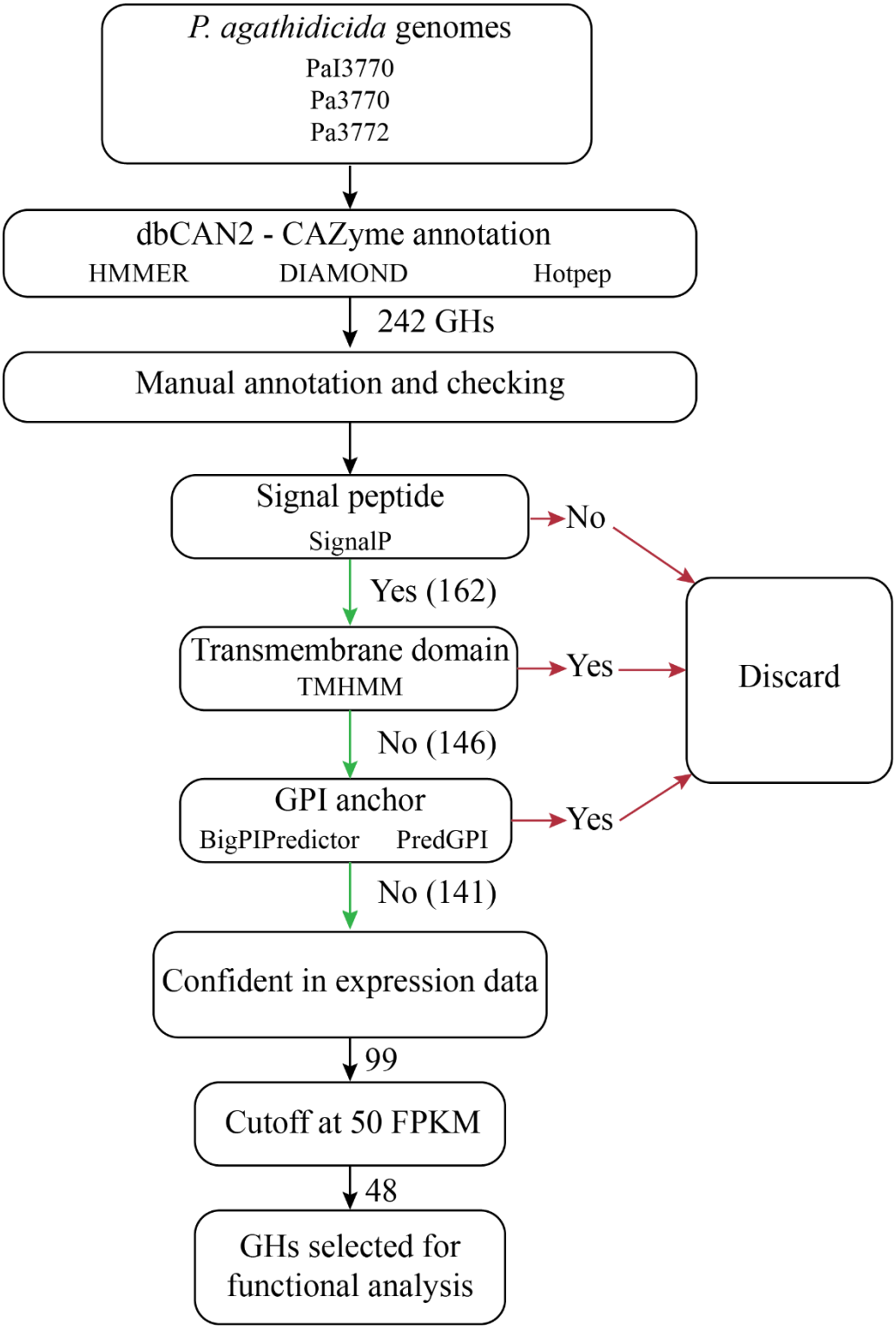

Figure 3.5. Schematic of the selection criteria used to predict *Phytophthora agathidicida* glycoside hydrolase (GH) proteins of interest for further study.

Prediction pipeline used to identify and select proteins of interest from the available *P. agathidicida* predicted protein lists.

Table 3.3. Summary of the glycoside hydrolase (GH)-encoding genes from *Phytophthora agathidicida* selected for further analysis.

Pa3770[1] gene ID	Pa3772[2] gene ID	GH[3] family	Peak expression[4] (Leaf)	Peak expression[4] (Root)
-	*Pa3772|10819*	GH3	11	126
-	*Pa3772|01058*	GH3	5	62
Pa|008620	*Pa3772|12459*	GH3	34	50
Pa|007147	*Pa3772|13973*	GH5	147	111
Pa|000587	*Pa3772|05440*	GH5	44	100
Pa|006408	-	GH6	45	103
Pa|005790	-	GH7	1637	825
Pa|005788	*Pa3772|13959*	GH7	972	747
Pa|004761	*Pa3772|09270*	GH7	493	333
Pa|011130	*Pa3772|10261*	GH10	433	466
Pa|009529	*Pa3772|11202*	GH10	32	58
Pa|009588	*Pa3772|09073*	GH12	1560	1325
Pa|009589	*Pa3772|09072*	GH12	815	909
Pa|009244	*Pa3772|09148*	GH12	137	506
Pa|004637	*Pa3772|02502*	GH12	150	228
Pa|004638	*Pa3772|02503*	GH12	114	36
Pa|009590	*Pa3772|09071*	GH12	58	72
Pa|002158	*Pa3772|08236*	GH17	1223	1730
Pa|002159	*Pa3772|08237*	GH17	534	495
Pa|002164	*Pa3772|08545*	GH17	274	171
Pa|006097	*Pa3772|03703*	GH17	139	117
Pa|001510	*Pa3772|02546*	GH17	29	112
Pa|002171	*Pa3772|06548*	GH17	76	35
Pa|005713	*Pa3772|11227*	GH17	28	58
Pa|002157	*Pa3772|08235*	GH17	32	52
Pa|001110	*Pa3772|04013*	GH19	101	70
Pa|010669	*Pa3772|09413*	GH28	319	111
Pa|010672	*Pa3772|13875*	GH28	317	277
Pa|010670	*Pa3772|09412*	GH28	186	189
Pa|002064	*Pa3772|08005*	GH28	106	111
Pa|010677	*Pa3772|13283*	GH28	106	9
Pa|010678	*Pa3772|12772*	GH28	18	105
Pa|010664	*Pa3772|11553*	GH28	97	0
Pa|010674 and Pa|010675	*Pa3772|12892*	GH28	24	94
Pa|010663	*Pa3772|11552*	GH28	55	0
Pa|003417	*Pa3772|11624*	GH30	53	132
Pa|003416	*Pa3772|11623*	GH30	9	131
Pa|000923	*Pa3772|10344*	GH30	71	35
Pa|003420	*Pa3772|11269*	GH30	63	63
Pa|008512	*Pa3772|00722*	GH31	113	116
Pa|010041	*Pa3772|01768*	GH43	15	77
Pa|004285	*Pa3772|10526*	GH54	256	52

Pa|004319	*Pa3772|11040*	GH78	5	120
Pa|000751	*Pa3772|09856*	GH81	62	25
Pa|008554	*Pa3772|11435*	GH105	200	129
Pa|006336	*Pa3772|11298*	GH131	987	1026
Pa|006337	*Pa3772|04128*	GH131	338	355
Pa|004184	*Pa3772|12992 and Pa3772|14066*	GH140	14	99

[1] *P. agathidicida* strain type 3770 PacBio genome annotated by Preeti Panda (Scion, Rotorua, New Zealand).

[2] *P. agathidicida* type strain 3772 Illumina genome annotated by McGowan and Fitzpatrick (2017).

[3] Glycoside hydrolase.

[4] Expression values are from an RNA-sequencing time-course experiment involving kauri infected with *P. agathidicida* type strain 3813 and are measured in fragments per kilo base of transcript per million mapped fragements (FPKM) (Guo & Panda, Unpublished). Samples were harvested from root or leaf tissue at 6, 24, 48, and 72 hours post-inoculation.. Peak gene expression levels are taken from any time point during the experiment except Time 0.

Table 3.4. Enzyme activities present in the selected glycoside hydrolase (GH) families as described by the CAZY website (Drula et al., 2022).

GH family	Enzyme activities
GH3	β-glucosidase (EC 3.2.1.21); xylan 1,4-β-xylosidase (EC 3.2.1.37); β-glucosylceramidase (EC 3.2.1.45); β-N-acetylhexosaminidase (EC 3.2.1.52); α-L-arabinofuranosidase (EC 3.2.1.55); glucan 1,4-β-glucosidase (EC 3.2.1.74); isoprimeverose-producing oligoxyloglucan hydrolase (EC 3.2.1.120); coniferin β-glucosidase (EC 3.2.1.126); exo-1,3-1,4-glucanase (EC 3.2.1.-); β-N-acetylglucosaminide phosphorylases (EC 2.4.1.-); β-1,2-glucosidase (EC 3.2.1.-); β-1,3-glucosidase (EC 3.2.1.-); xyloglucan-specific exo-β-1,4-glucanase / exo-xyloglucanase (EC 3.2.1.155); stevioside-β-1,2-glucosidase (EC 3.2.1.-); lichenase / endo-β-1,3-1,4-glucanase (EC 3.2.1.73); protodioscin 26-O-β-D-glucosidase (EC 3.2.1.186)
GH5	endo-β-1,4-glucanase / cellulase (EC 3.2.1.4); endo-β-1,4-xylanase (EC 3.2.1.8); β-glucosidase (EC 3.2.1.21); β-mannosidase (EC 3.2.1.25); β-glucosylceramidase (EC 3.2.1.45); glucan β-1,3-glucosidase (EC 3.2.1.58); exo-β-1,4-glucanase / cellodextrinase (EC 3.2.1.74); glucan endo-1,6-β-glucosidase (EC 3.2.1.75); mannan endo-β-1,4-mannosidase (EC 3.2.1.78); cellulose β-1,4-cellobiosidase (EC 3.2.1.91); steryl β-glucosidase (EC 3.2.1.104); endoglycoceramidase (EC 3.2.1.123); β-primeverosidase (EC 3.2.1.149); xyloglucan-specific endo-β-1,4-glucanase (EC 3.2.1.151); endo-β-1,6-galactanase (EC 3.2.1.164); β-1,3-mannanase (EC 3.2.1.-); arabinoxylan-specific endo-β-1,4-xylanase (EC 3.2.1.-); mannan transglycosylase (EC 2.4.1.-); lichenase / endo-β-1,3-1,4-glucanase (EC 3.2.1.73); β-glycosidase (EC 3.2.1.-); endo-β-1,3-glucanase / laminarinase (EC 3.2.1.39); β-N-acetylhexosaminidase (EC 3.2.1.52); chitosanase (EC 3.2.1.132); β-D-galactofuranosidase (EC 3.2.1.146); β-galactosylceramidase (EC 3.2.1.46); ; β-rutinosidase /α-L-rhamnose-(1,6)-β-D-glucosidase (EC 3.2.1.-); α-L-arabinofuranosidase (EC 3.2.1.55); glucomannan-specific endo-β-1,4-glucanase (EC 3.2.1.-); hesperidin 6-O-α-L-rhamnosyl-β-glucosidase (EC 3.2.1.168)
GH6	endoglucanase (EC 3.2.1.4); cellobiohydrolase (EC 3.2.1.91); lichenase / endo-β-1,3-1,4-glucanase (EC 3.2.1.73)
GH7	endo-β-1,4-glucanase (EC 3.2.1.4); reducing end-acting cellobiohydrolase (EC 3.2.1.176); chitosanase (EC 3.2.1.132); endo-β-1,3-1,4-glucanase (EC 3.2.1.73)
GH10	endo-1,4-β-xylanase (EC 3.2.1.8); endo-1,3-β-xylanase (EC 3.2.1.32); tomatinase (EC 3.2.1.-); xylan endotransglycosylase (EC 2.4.2.-); endo-β-1,4-glucanase (EC 3.2.1.4); [retaining] arabinoxylan-specific endo-β-1,4-xylanase (EC 3.2.1.-)
GH12	endoglucanase (EC 3.2.1.4); xyloglucan hydrolase (EC 3.2.1.151); β-1,3-1,4-glucanase (EC 3.2.1.73); xyloglucan endotransglycosylase (EC 2.4.1.207)
GH17	glucan endo-1,3-β-glucosidase (EC 3.2.1.39); licheninase (EC 3.2.1.73); ABA-specific β-glucosidase (EC 3.2.1.175); β-1,3-glucanosyltransglycosylase (EC 2.4.1.-); β-1,3-glucosidase (EC 3.2.1.-)
GH19	chitinase (EC 3.2.1.14); lysozyme (EC 3.2.1.17)
GH28	polygalacturonase (EC 3.2.1.15); exo-polygalacturonase (EC 3.2.1.67); exo-polygalacturonosidase (EC 3.2.1.82); rhamnogalacturonase (EC 3.2.1.171); rhamnogalacturonan α-1,2-galacturonohydrolase (EC 3.2.1.173); xylogalacturonan hydrolase (EC 3.2.1.-)
GH30	endo-β-1,4-xylanase (EC 3.2.1.8); β-glucosidase (3.2.1.21); β-glucuronidase (EC 3.2.1.31); β-xylosidase (EC 3.2.1.37); β-fucosidase (EC 3.2.1.38); glucosylceramidase (EC 3.2.1.45); β-1,6-glucanase (EC 3.2.1.75); glucuronoarabinoxylan endo-β-1,4-xylanase (EC 3.2.1.136); endo-β-1,6-galactanase (EC:3.2.1.164); [reducing end] β-xylosidase (EC 3.2.1.-)

GH31	α-glucosidase (EC 3.2.1.20); α-galactosidase (EC 3.2.1.22); α-mannosidase (EC 3.2.1.24); α-1,3-glucosidase (EC 3.2.1.84); sucrase-isomaltase (EC 3.2.1.48) (EC 3.2.1.10); α-xylosidase (EC 3.2.1.177); α-glucan lyase (EC 4.2.2.13); isomaltosyltransferase (EC 2.4.1.-); oligosaccharide α-1,4-glucosyltransferase (EC 2.4.1.161); α-N-acetylgalactosaminidase (EC 3.2.1.49); sulfoquinovosidase (EC 3.2.1.199); α-6-glucosyltransferase (EC 2.4.1.24)
GH43	β-xylosidase (EC 3.2.1.37); α-L-arabinofuranosidase (EC 3.2.1.55); xylanase (EC 3.2.1.8); α-1,2-L-arabinofuranosidase (EC 3.2.1.-); exo-α-1,5-L-arabinofuranosidase (EC 3.2.1.-); [inverting] exo-α-1,5-L-arabinanase (EC 3.2.1.-); β-1,3-xylosidase (EC 3.2.1.-); [inverting] exo-α-1,5-L-arabinanase (EC 3.2.1.-); [inverting] endo-α-1,5-L-arabinanase (EC 3.2.1.99); exo-β-1,3-galactanase (EC 3.2.1.145); β-D-galactofuranosidase (EC 3.2.1.146)
GH54	α-L-arabinofuranosidase (EC 3.2.1.55); β-xylosidase (EC 3.2.1.37).
GH78	α-L-rhamnosidase (EC 3.2.1.40); rhamnogalacturonan α-L-rhamnohydrolase (EC 3.2.1.174); L-Rhap-α-1,3-D-Apif -specific α-1,3-L-rhamnosidase (EC 3.2.1.-)
GH81	endo-β-1,3-glucanase (EC 3.2.1.39)
GH105	unsaturated rhamnogalacturonyl hydrolase (EC 3.2.1.172); d-4,5-unsaturated β-glucuronyl hydrolase (EC 3.2.1.-); d-4,5-unsaturated α-galacturonidase (EC 3.2.1.-)
GH131	broad specificity exo-β-1,3/1,6-glucanase with endo-β-1,4-glucanase activity (EC 3.2.1.-);
GH140	β-1,2-apiosidase (EC 3.2.1.-)

[1] Glycoside hydrolase.

[2] EC number = enzyme commission number associated with that enzymatic activity.

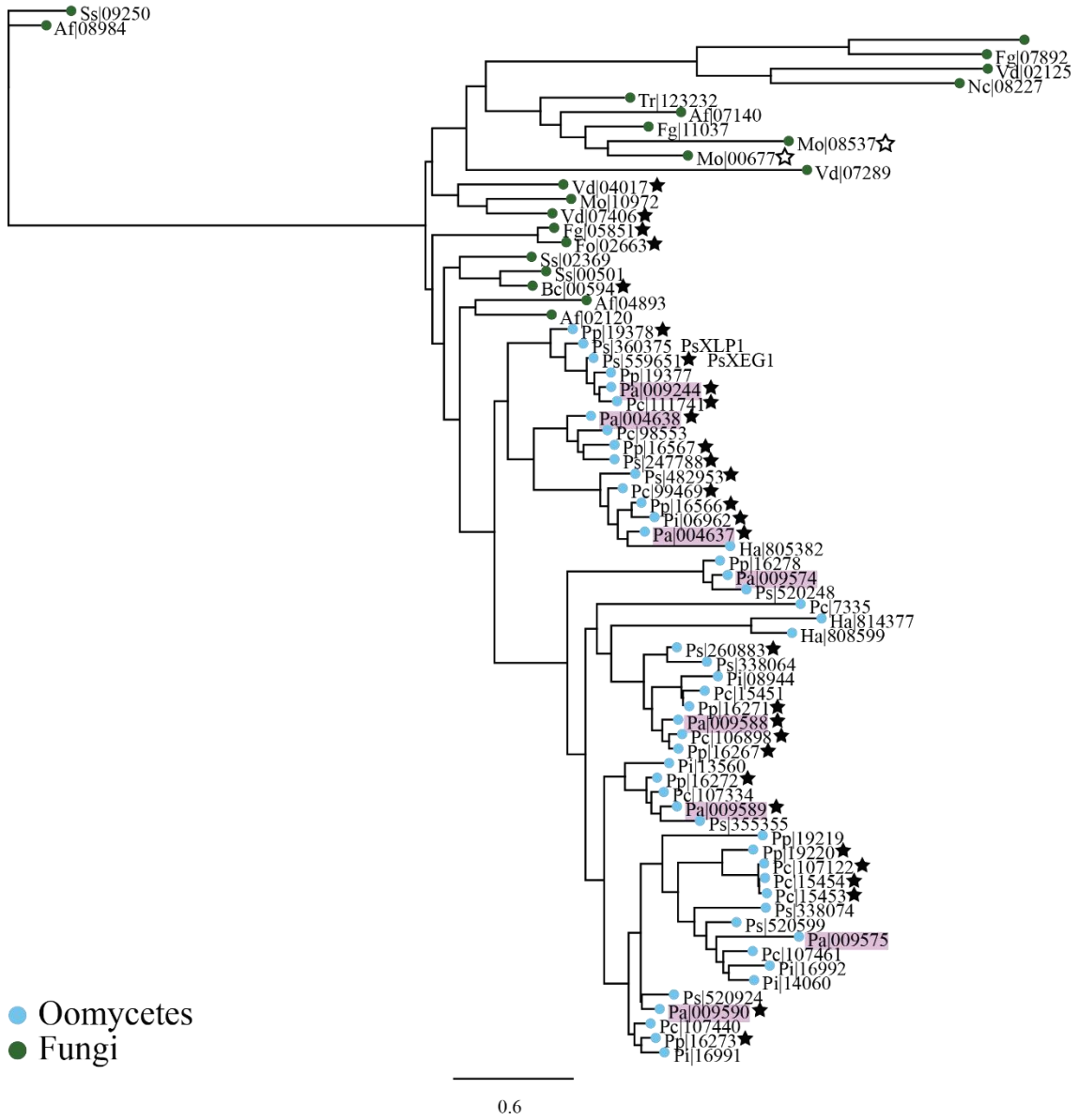

Figure 3.6. Phylogenetic tree of GH12 proteins from *Phytophthora agathidicida* and other oomycetes and fungi.

An adaptation of the phylogenetic tree found in Ma et al. (2015b). Alignments were performed using Geneious with the MAFFT-EINSI set of parameters and the tree built using the PHYML (Le Gascuel) method. Green circles represent proteins identified in fungal species (Af = *Aspergillus flavus*, Bc = *Botrytis cinerea*, Fg = *Fusarium graminearum*, Fo = *Fusarium oxysporum*, Mo = *Magnaporthe oryzae*, Nc = *Neurospora crassa*, Ss = *Sclerotinia sclerotiorum*, Tr = *Trichoderma reesei*, Vd = *Verticillium dahliae*), blue circles represent proteins found in oomycete species (*Hyaloperonospora arabidopsis*, Pa = *Phytophthora agathidicida*, Pc = *Phytophthora capsici,* Pi = *Phytophthora infestans*, Pp = *Phytophthora parasitica*, Ps = *Phytophthora sojae*). Filled in stars indicate proteins identified to trigger a plant cell death response in *Nicotiana benthamiana* (Ma et al., 2015b). Empty stars indicate proteins which did not trigger a cell death response in *N. benthamiana* but did in the native host (Yang et al., 2021). *P. agathidicida* proteins are highlighted in lilac. PsXEG1 and PsXLP1 are indicated. Scale bar represents a phylogenetic distance of 0.6 substitutions per site.

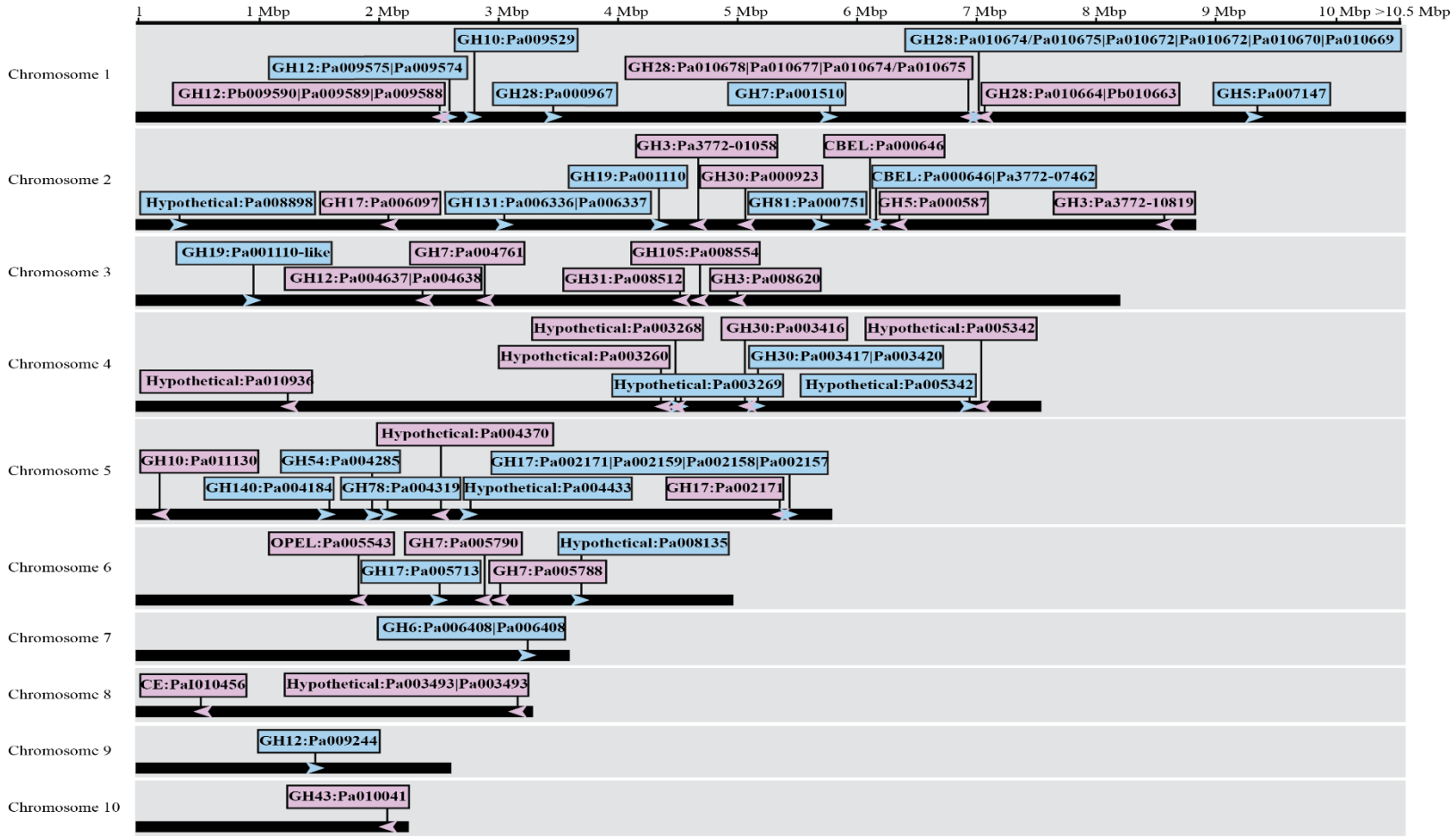

Figure 3.7. *Phytophthora agathidicida* genes of interest mapped to a chromosome-level assembly of the Pa3770 genome.

P. agathidicida genes encoding for the proteins of interest were mapped to the latest PacBio strain 3770 genome using Geneious (version 9.1.8). While the 10 *P. agathidicida* chromosomes are to scale, genes indicated by the arrows are not. In some cases, arrows are indicative of more than one gene, where this is so genes are separated by '|'. Intron/exon structure not shown. A '/' indicates two genes that were found to be the same in this genome. Light blue indicates genes in the forward direction. Pink indicates genes in the reverse direction.

3.3.3 Cloning of selected genes from *P. agathidicida*

Selected GH-encoding genes (**Table 3.5**) were cloned into the pICH86988 expression vector (**Appendix 3.6**) together with an N-terminal PR1α *N. benthamiana* signal peptide, for secretion into the apoplast, which was fused to a 3xFLAG-tag, for future Western blot analysis. In some cases, financial and time constraints dictated that efforts to clone or synthesise certain genes were abandoned (**Table 3.5**), particularly when other *P. agathidicida* genes encoding GH proteins of the same family had already been cloned; these included GH7: Pa|005788; GH28: Pa|002064, Pa|010663, Pa|010678; GH30: Pa|000923 that were all dropped from further analysis).

Interestingly, sequencing to confirm gene authenticity identified a gene (designated *Pa|001110-like*) which was similar, but not identical to the gene encoding GH19 Pa|001110. *Pa|001110-like* had 39 nucleotide differences from *Pa|001110*, which translated to five differences predicted at the amino acid (aa) level, one of which was an aa insertion. A nucleotide match to *Pa|001110-like* was identified in the Pa3770 genome; however, a predicted protein match was not. Instead, a 100% amino acid identity match was found in Pa3772|10247, though this protein appeared to be misannotated with the N-terminus 68 amino acids longer and the C-terminus 45 amino acids shorter than expected when compared to the translated nucleotide match from the Pa3770 genome. As this *Pa|001110-like* gene had already been cloned, it was carried through for further analysis.

Table 3.5. List of *Phytophthora agathidicida* glycoside hydrolase (GH)-encoding genes selected for cloning into the pICH86988 expression vector.

P. agathidicida gene ID	GH family	Notes
Pa|008620	GH3	Synthesised.
Pa3772|01058	GH3	Synthesised.
Pa3772|10819	GH3	Synthesised.
Pa|000587	GH5	Cloned via golden gate.
Pa|007147	GH5	Dropped from analysis.
Pa|006408	GH6	Dropped from analysis.
Pa|004761	GH7	Cloned via golden gate.
Pa|005788	GH7	Dropped from analysis.
Pa|005790	GH7	Cloned via golden gate.
Pa|009529	GH10	Synthesised.
Pa|011130	GH10	Synthesised.
Pa|004637	GH12	Cloned via golden gate.
Pa|004638	GH12	Cloned via golden gate.
Pa|009244	GH12	Cloned via golden gate.
Pa|009588	GH12	Cloned via golden gate.
Pa|009589	GH12	Cloned via golden gate.
Pa|009590	GH12	Cloned via golden gate.
Pa|001510	GH17	Synthesised.
Pa|002157	GH17	Cloned via golden gate.
Pa|002158	GH17	Synthesised.
Pa|002159	GH17	Cloned via golden gate.
Pa|002164	GH17	Synthesised.
Pa|002171	GH17	Cloned via golden gate.
Pa|005713	GH17	Cloned via golden gate.
Pa|006097	GH17	Cloned via golden gate.
Pa|001110	GH19	Cloned via golden gate.
Pa|001110-like	GH19	Cloned via golden gate.
Pa|002064	GH28	Dropped from analysis.
Pa|010663	GH28	Dropped from analysis.
Pa|010664	GH28	Dropped from analysis.
Pa|010669	GH28	Cloned via golden gate.
Pa|010670	GH28	Cloned via golden gate.
Pa|010672	GH28	Synthesised.
Pa|010674	GH28	Synthesised.

Pa|010677	GH28	Cloned via golden gate.
Pa|010678	GH28	Dropped from analysis.
Pa|000923	GH30	Dropped from analysis.
Pa|003416	GH30	Cloned via golden gate.
Pa|003417	GH30	Dropped from analysis.
Pa|003420	GH30	Cloned via golden gate.
Pa|008512	GH31	Synthesised.
Pa|010041	GH43	Cloned via golden gate.
Pa|004285	GH54	Cloned via golden gate.
Pa|004319	GH78	Synthesised.
Pa|000751	GH81	Dropped from analysis.
Pa|008554	GH105	Cloned via golden gate.
Pa|006336	GH131	Synthesised.
Pa|006337	GH131	Cloned via golden gate.
Pa|004184	GH140	Dropped from analysis.

3.3.4 Cell death elicitation by *P. agathidicida* GH proteins of interest in model *Nicotiana* species

The proteins encoded by cloned *P. agathidicida* GH genes were expressed in both *N. benthamiana* and *N. tabacum* at approximately five weeks post-germination via ATTAs, to assess whether they or their enzymatic activity could trigger a cell death response, suggesting that they or a product of their enzymatic activity are recognized by the plant immune system. Seven days after infiltration, photos were taken to record any symptoms that had developed (**Figures 3.8–10**). Plant host responses to the GH proteins of interest ranged from no response to a strong localised necrotic cell death response at the site of agroinfiltration. A positive (PaINF1, known to trigger a plant cell death response (Guo et al., 2020a)) and negative (GFP, known not to elicit a plant cell death response (Guo et al., 2020a)) control were also expressed in each leaf by ATTAs. Data for the *P. agathidicida* proteins being tested were only accepted if the expected results were observed for both positive and negative controls. A Western blot with anti-FLAG antibody was performed to determine the presence of each *P. agathidicida* GH protein of interest in *N. benthamiana* leaves (**Appendix 3.7**).

As expected, the positive control PaINF1 elicited a cell death response in both *N. benthamiana* and *N. tabacum*, while no cell death was observed in response to GFP expression (**Figure 3.8**). Of all the 38 tested proteins of interest (POI), only six members of the GH12 family consistently elicited a strong cell death response in *Nicotiana* plants. More specifically, the GH12 proteins Pa|004637, Pa|004638, Pa|009244, Pa|009589, and Pa|009590 triggered a strong cell death response (with more than half of the infection zone showing cell death symptoms) 100% of the time in both *N. benthamiana* and *N. tabacum*, while the GH12 protein Pa|009588 triggered a strong cell death response 100% of the time in *N. tabacum*, and over 94% of the time in *N. benthamiana* (**Figure 3.8**). On one occasion (~6%), a weaker cell death response, characterised by lesions that appeared more chlorotic than necrotic, was observed in response to infiltration with Pa|009588 via ATTAs. RNA sequencing data, recently re-mapped to the new *P. agathidicida* PacBio chromosome-level genome (Guo & Shiller, Unpublished), showed that the genes encoding these GH12 proteins were more highly expressed during *P. agathidicida* infection of kauri compared to *in vitro* controls (**Figure 3.11 A**), albeit at different time points. Expression of *Pa|009244* peaked 6 hours post-inoculation (hpi) in kauri leaves and roots, while expression of *Pa|009588* and *Pa|009589* peaked 48 hpi in both kauri leaves and roots (**Figure 3.11 A**). Expression of *Pa|004638* fluctuated in kauri leaves, finally peaking 72 hpi, while in kauri roots, a slight peak was observed at 6 hpi, followed by a decrease in expression compared to the *in vitro* controls (**Figure 3.11 A**). Expression of *Pa|004637* and *Pa|009590* also fluctuated in kauri leaves, after an initial peak 6 hpi and a peak at 48 hpi respectively (**Figure 3.11 A**). In roots, a peak expression was observed at 24 hpi for *Pa|004637*, while *Pa|009590* slowly increased expression to peak at 72 hpi (**Figure 3.11 A**).

In addition to the six GH12 proteins, two proteins belonging to the GH28 family (Pa|010674 and Pa|010677) triggered a weak cell death or chlorotic response in 57.7% and 64% of the leaf infiltrations in *N. benthamiana*, respectively (**Figure 3.9**). Furthermore, Pa|010677 sometimes triggered a strong cell death response (in 20% of the ATTAs in *N. benthamiana*). The observations in *N. benthamiana* in response to Pa|010674 and Pa|010677 were statistically significant when compared to *N. benthamiana* ATTAs with other *P. agathidicida* GH28 proteins (Pa|010669 and Pa|010670) (**Table 3.8**). Different results were observed in the ATTAs with Pa|010674 and Pa|010677 in *N. tabacum*; with a weak cell death/chlorotic response only observed once for the Pa|010674 protein, and twice for the Pa|010677 protein (**Figure 3.9**). RNA sequencing data showed that *Pa|010674* was most highly expressed at 6 hpi during *P. agathidicida* infection of kauri roots and leaves, after which expression decreased considerably (**Figure 3.11 B**). In contrast, *Pa|010677* expression fluctuated in kauri leaves, but peaked at 72 hpi, while in kauri roots expression it remained low (**Figure 3.11 B**). Interestingly, it was the expression of two other GH28-encoding genes that was most noticeable. Neither Pa|010669 nor Pa|010672 were associated with a cell death response in *Nicotiana* species, but expression of the genes encoding these proteins increased dramatically 6 hpi in both kauri roots and leaves (*Pa|010672*) or primarily in leaves (*Pa|010669*) (**Figure 3.11 B**).

Several other *P. agathidicida* proteins belonging to different GH families also triggered a cell death response in either *N. benthamiana*, *N. tabacum*, or both (e.g. GH54, Pa|004285) (**Figure 3.10**). The paucity of these observations suggest further investigation is needed to confirm these results.

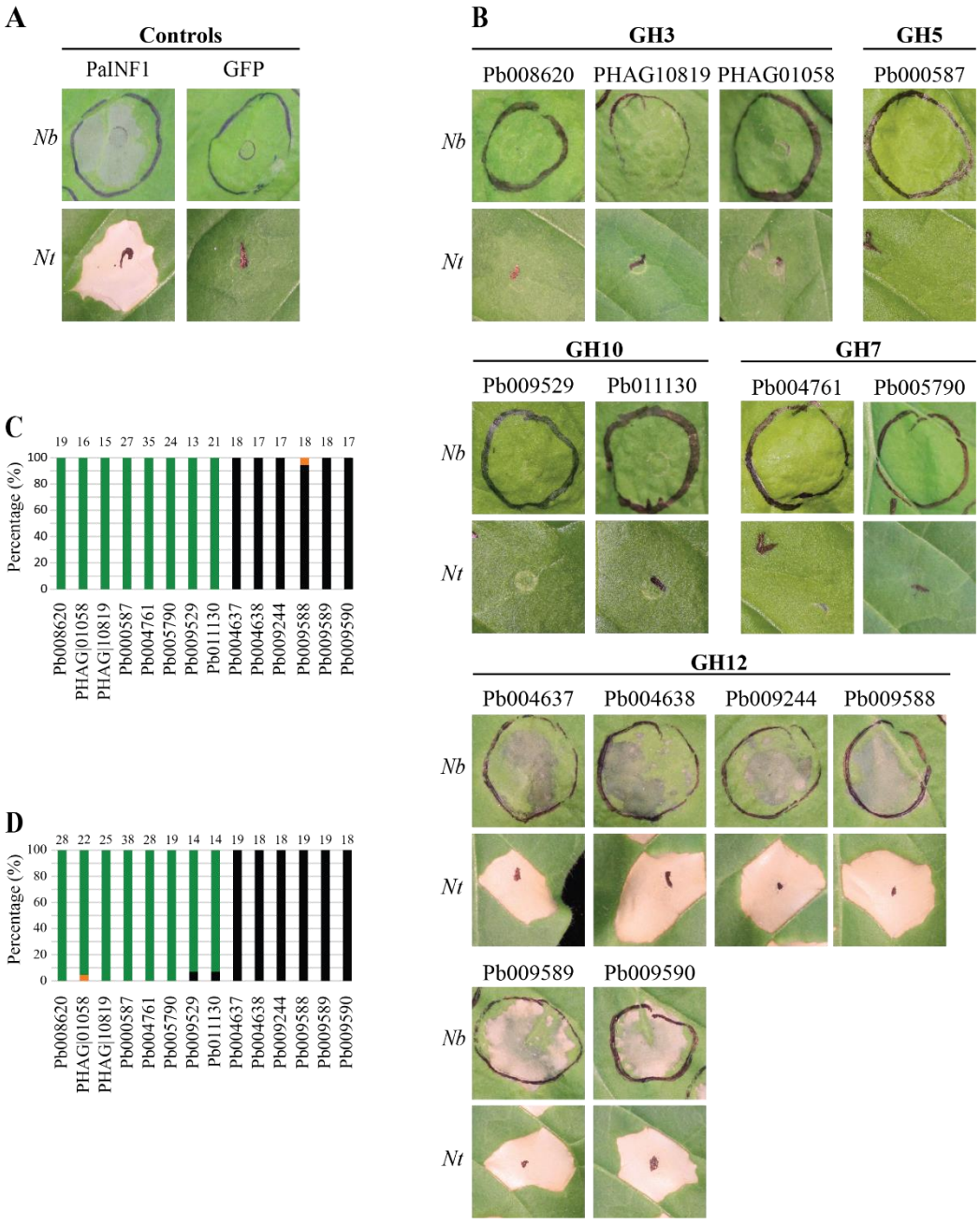

Figure 3.8. Only CAZymes of glycoside hydrolase family 12 (GH12) from *Phytophthora agathidicida* consistently triggered a cell death response in in *Nicotiana benthamiana* or *Nicotiana tabacum*.

(A–B) CAZymes belonging to families GH3, GH5, GH10, GH7 and GH12 from *P. agathidicida* were produced in *N. benthamiana* (N.b.) (top layer of photographs) or *N. tabacum* (N.t.) (bottom layer of photographs) using an *Agrobacterium tumefaciens*-mediated transient expression assay (ATTA); their ability to trigger a cell death response was recorded at 7 days post-agroinfiltration. Images are representative of what was observed. All proteins had an N-terminal PR1α signal peptide from *N. tabacum* for secretion to the apoplast fused to a 3xFLAG tag for detection by Western blotting. **(A)** A *P. agathidicida* homolog of the cell death elicitor INF1 from Phytophthora infestans was used as a positive control, while green fluorescent protein (GFP) was used as a negative control. **(B)** Six GH12 proteins from *P. agathidicida* consistently triggered a cell death response in both *N. benthamiana* and *N. tabacum*. **(C–D)** Bar graphs depicting the frequency of responses observed in *N. benthamiana* **(C)** and *N. tabacum* **(D)**. Green indicates no response; orange, chlorosis or weak cell death; black, cell death. Numbers above each bar indicate the total number of observations for each listed protein. Observations were over a minimum of two independent biological experiments.

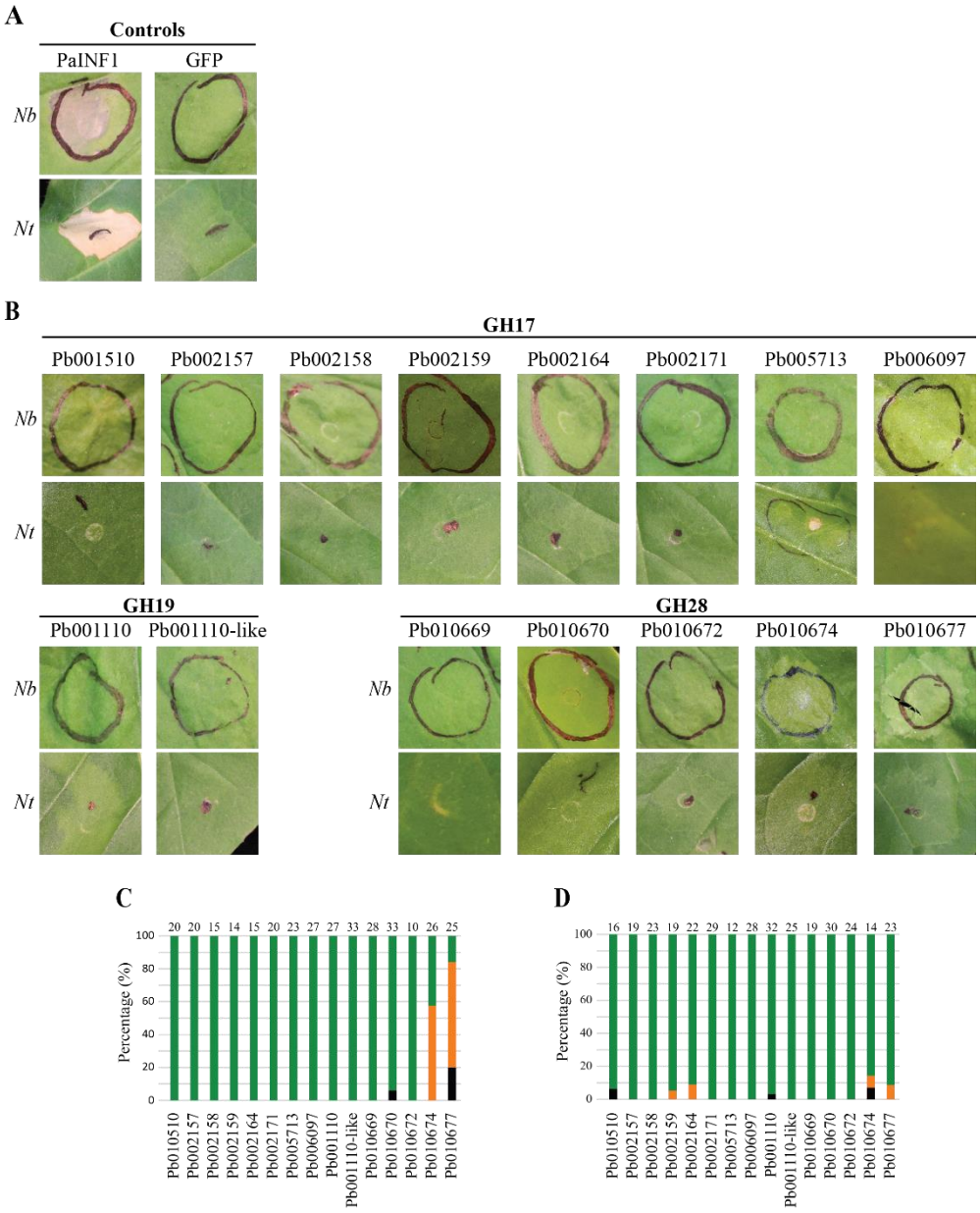

Figure 3.9. CAZymes of glycoside hydrolase family 28 (GH28) family from *Phytophthora agathidicida* triggered a chlorotic response in *Nicotiana benthamiana* but not *Nicotiana tabacum*.

(A–B) CAZymes belonging to families GH17, GH19, and GH28 from *P. agathidicida* were produced in *N. benthamiana* (N.b.) (top row of photographs) or *N. tabacum* (N.t.) (bottom row of photographs) using an *Agrobacterium tumefaciens*-mediated transient expression assay (ATTA); their ability to trigger a cell death response was recorded at 7 days post-agroinfiltration. Images are representative of what was observed. All proteins had a N-terminal PR1α signal peptide from *N. tabacum* for secretion to the apoplast fused to a 3xFLAG tag for detection by Western blotting. **(A)** A *P. agathidicida* homolog of the cell death elicitor INF1 from *Phytophthora infestans* was used as a positive control, while green fluorescent protein (GFP) was used as a negative control. **(B)** Only two proteins (Pa|010674 and Pa|010677) belonging to the GH28 family of enzymes from *P. agathidicida* were able to elicit a chlorotic response in *N. benthamiana*, while a similar response was not observed in *N. tabacum*. **(C–D)** Bar graphs depicting the frequency of the responses observed in *N. benthamiana* **(C)** and *N. tabacum* **(D).** Green indicates no response; orange, chlorosis or weak cell death; black, cell death. Numbers above each bar indicate the total number of observations for each listed protein. Observations were over a minimum of two independent biological experiments.

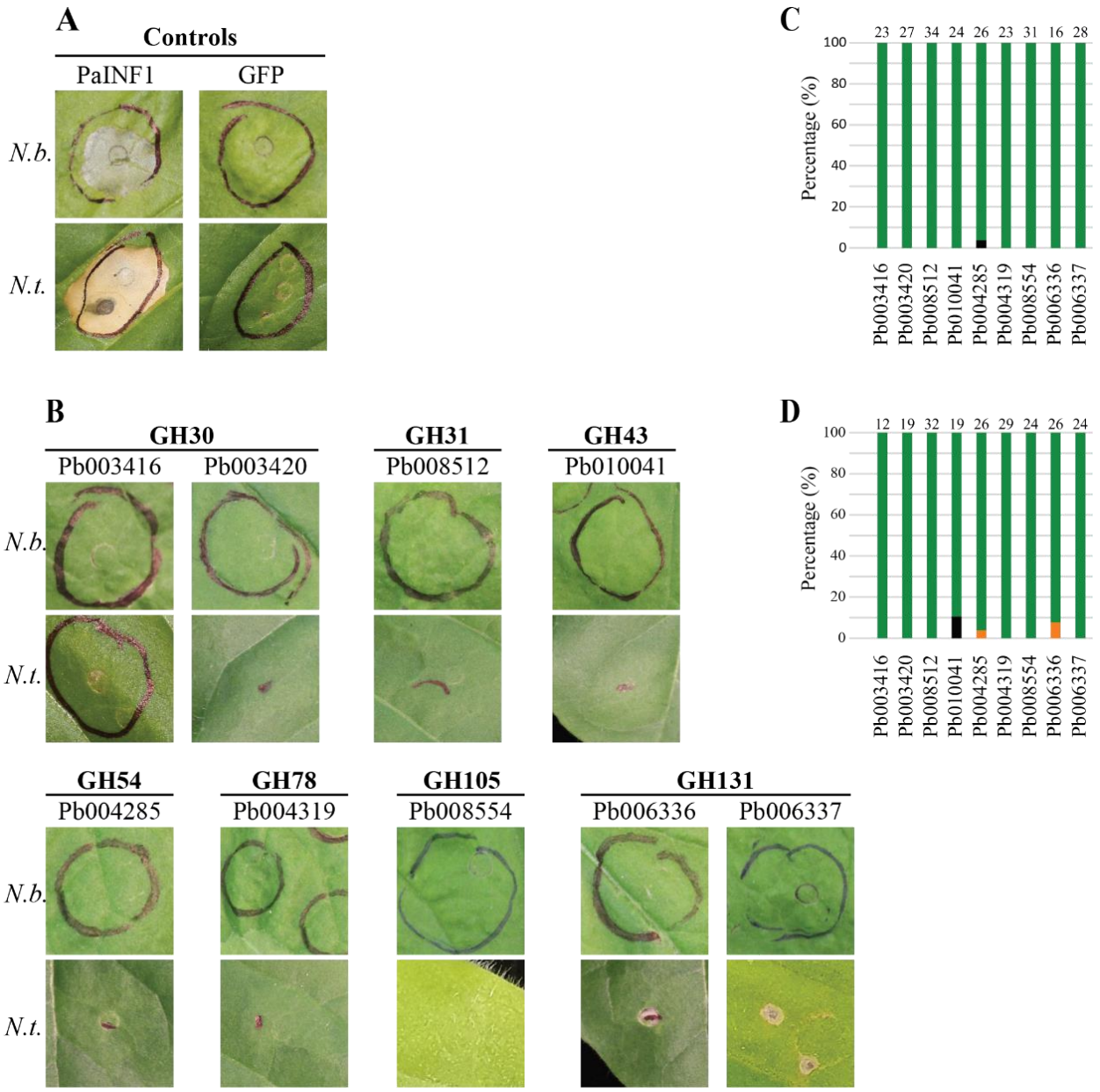

Figure 3.10. No other glycoside hydrolases from *Phytophthora agathidicida* triggered a consistent chlorotic or cell death response in *Nicotiana benthamiana* or *Nicotiana tabacum*.

(A–B) CAZymes belonging to families GH30, GH31, GH43, GH54, GH78, GH105, and GH131 from *P. agathidicida* were produced in *N. benthamiana* (*N.b.*) (top row of photographs) or *N. tabacum* (*N.t.*) (bottom row of photographs) using an *Agrobacterium tumefaciens*-mediated transient expression assay (ATTA); their ability to trigger a cell death response was recorded at 7 days post-agroinfiltration. Images are representative of what was observed. All proteins had a N-terminal PR1α signal peptide from *N. tabacum* for secretion to the apoplast fused to a 3xFLAG tag for detection by Western blotting. **(A)** A *P. agathidicida* homolog of the cell death elicitor INF1 from *Phytophthora infestans* was used as a positive control, while green fluorescent protein (GFP) was used as a negative control. **(B)** None of the *P. agathidicida* proteins belonging to the above GH families were able to elicit a chlorotic response in *N. benthamiana* or *N. tabacum.* **(C–D)** Bar graphs depicting the frequency of the responses observed in *N. benthamiana* (**C**) and *N. tabacum* (**D**). Green indicates no response; orange, chlorosis or weak cell death; black, cell death. Numbers above each bar indicate the total number of observations for each listed protein. Observations were over a minimum of two independent biological experiments.

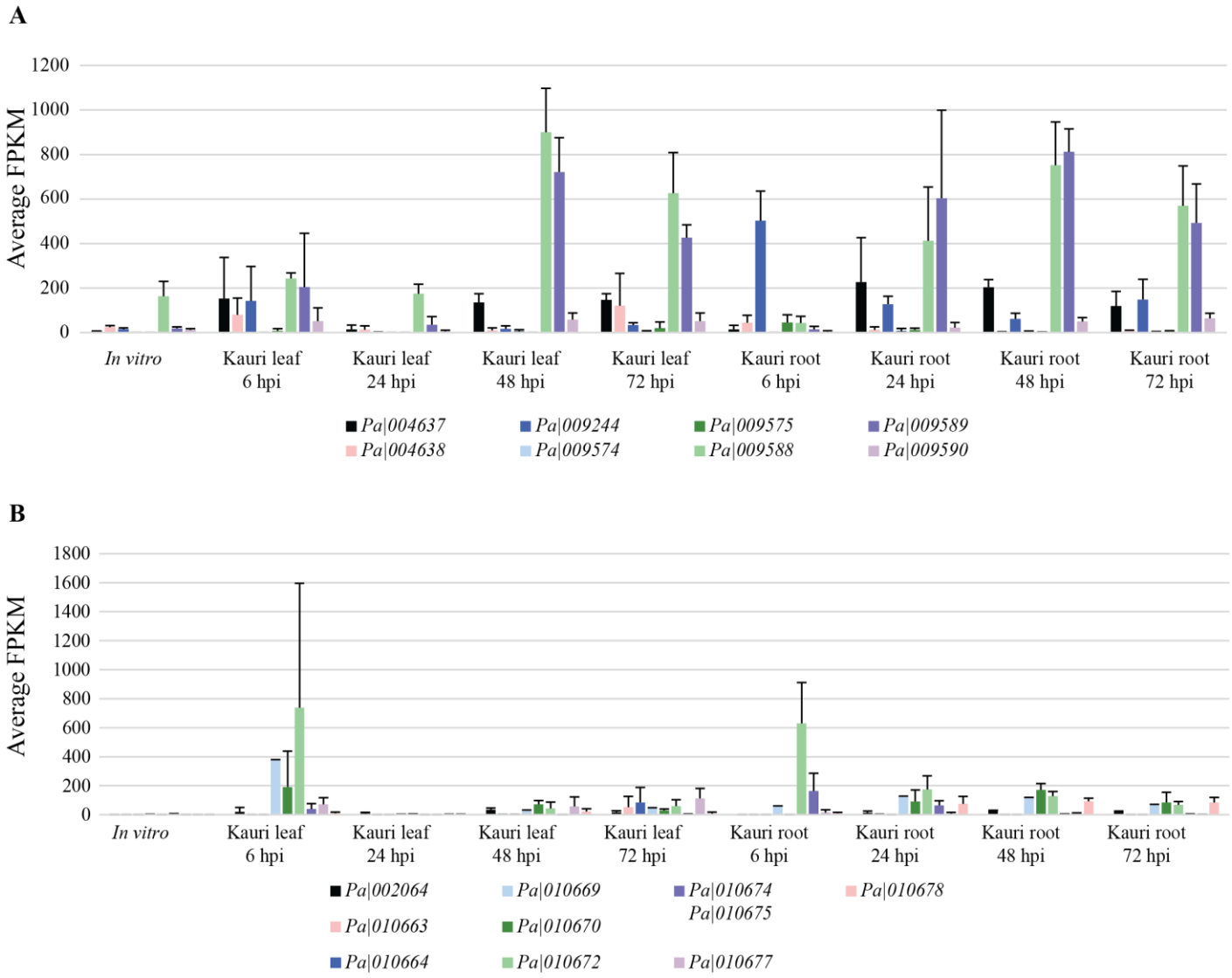

Figure 3.11. Bar graph showing average expression of *Phytophthora agathidicida* GH12- and GH28-encoding genes of interest over time during infection of kauri leaves and roots.

An RNA-sequencing time course experiment was performed by Guo and Shiller (Unpublished). *P. agathidicida* was inoculated onto kauri roots or leaves and samples taken at 6-, 24-, 48-, and 72-hours post-inoculation (hpi). These data were compared to RNA-sequencing data of *P. agathidicida* grown in culture in clarified V8 liquid medium. Three biological replicates were performed and averaged. **(A)** *P. agathidicida* GH12-encoding genes of interest. **(B)** *P. agathidicida* GH28-encoding genes of interest. Unit = fragments per kilo base of transcript per million mapped fragments (FPKM). Error bars represent the standard deviation across three biological replicates.

Table 3.6. Results of an X^2 analysis to investigate cell death/chlorotic responses in *Nicotiana benthamiana* and *Nicotiana tabacum* to expression of *Phytophthora agathidicida* genes encoding GH28 proteins via *Agrobacterium tumefaciens* transient transformation assays.

N. benthamiana						
Protein	**No response**	**Response[a]**	**X^2**	**df[b]**	***P* value**	***P* value (FDR)[c]**
Pa|010674*	11	15	19.584	1	9.63E-06	2.57E-05
Pa|010669	28	0				
Pa|010674*	11	15	16.467	1	4.95E-05	9.90E-05
Pa|010670	31	2				
Pa|010677*	4	21	35.523	1	2.52E-09	2.02E-08
Pa|010669	28	0				
Pa|010677*	4	21	32.924	1	9.58E-09	3.83E-08
Pa|010670	31	2				

N. tabacum						
Protein	**No response**	**Response[a]**	**X^2**	**Df[b]**	***P* value**	***P* value (FDR)[c]**
Pa|010674*	12	2	0.92495	1	3.36E-01	4.09E-01
Pa|010669	19	0				
Pa|010674*	12	2	1.8009	1	1.80E-01	2.88E-01
Pa|010670	30	0				
Pa|010677*	21	2	0.3472	1	5.56E-01	5.56E-01
Pa|010669	19	0				
Pa|010677*	21	2	0.84512	1	3.58E-01	4.09E-01
Pa|010670	30	0				

[a] Both chlorotic/weak cell death and strong cell death were combined into the 'Response' variable for the purposes of the X^2 test.

[b] degrees of freedom.

[c] *P* values for ATTAs carried out in *N. benthamiana* and *N. tabacum* were adjusted to account for the false discovery rate (FDR).

*GH28 proteins which appeared to elicit a cell death response (*) in *N. benthamiana* were compared to GH28 proteins which elicited a cell death response less frequently in *N. benthamiana* to determine whether the observations of cell death were significant.

**Data from a minimum of two independent trials.

3.3.5 Identification and screening of additional *P. agathidicida* carbohydrate-related proteins of interest

Due to the localised necrosis observed as a response to the *P. agathidicida* GH12 proteins, an effort was made to identify any additional GH12-encoding genes in the *P. agathidicida* genome. Three further GH12-encoding genes were identified by BLASTp analysis of cell death eliciting GH12 proteins against the *P. agathidicida* predicted proteome (**Table 3.7**). One of these three genes was eventually dropped from the analysis due to a lack of confidence in the gene prediction (*Pa|009650*), while the remaining two genes (*Pa|009575* and *Pa|009574*) were cloned into the pICH86988 expression vector. Both *Pa|009574* and *Pa|009575* were originally excluded from the subset of GH-encoding genes selected for further analysis because they did not meet the 50 FPKM expression cut-off. The original RNA sequencing experiment was recently re-mapped to a new chromosome-level *P. agathidicida* 3770 PacBio genome (Pag3770) (Guo & Shiller, Unpublished), with growth of *P. agathidicida* in clarified V8 liquid medium used as an in-culture control. In the new RNA sequencing data (Guo & Shiller, Unpublished), these genes were also not highly expressed (**Appendix 3.8**); *Pa|009574* peaked at 24 hpi in kauri roots at approximately 10 FPKM, while *Pa|009575* peaked at 6 hpi in kauri roots with almost 45 FPKM. Expression of these genes was lower in kauri leaves than was observed in roots (**Appendix 3.8, Figure 3.11 A**). Interestingly, at least four different versions of *Pa|009575* were identified during cloning. Both *Pa|009574* and all four identified *Pa|009575* alleles were screened in *N. benthamiana* and *N. tabacum* via ATTAs. However, unlike the six previously screened *P. agathidicida* GH12 proteins, no cell death response was observed (**Figure 3.12**).

In addition to GH-encoding genes, several other CAZyme-related genes, encoding carbohydrate-binding elicitor lectins (CBELs) and a pectin esterase (belonging to the carbohydrate esterase (CE) superfamily), as well as a number of highly expressed hypothetical proteins, were selected for analysis from the *P. agathidicida* genome (**Table 3.7**). Hypothetical proteins were selected for further analysis if they were predicted to contain an N-terminal signal peptide, lack a transmembrane domain and GPI anchor, had not previously been characterised (based on a BLASTp analysis of the NCBI nr protein database), and the genes encoding the described proteins were highly expressed during infection of kauri roots or leaves as illustrated by the RNA-sequencing database mapped to the early *P. agathidicida* PacBio (Pa3770) genome (Guo & Panda, Unpublished). Like the selected *P. agathidicida* GH-encoding genes of interest, these genes were also cloned into the pICH86988 expression vector and the proteins they encode investigated for their ability to trigger a chlorotic/cell death response in *Nicotiana* species using ATTAs (**Figures 3.13 A–B** and **3.14 A–B)**. Following the ATTAs, the CBEL protein, Pa3772|07462, triggered a weak cell death response in just over 10% of assays in *N. benthamiana* (**Figure 3.13 C**). In *N. tabacum,* however, a cell death response was observed in more than 20% of trials

for the Pa3772|07462 CBEL, and in less than 10% of assays for Pa|000646 and PaI|010457 (**Figure 3.13 D**). Among the hypothetical proteins tested, Pa|003260 triggered a weak cell death/chlorotic response in 45.4% of experiments carried out in *N. benthamiana* (**Figure 3.14 C**). However, no cell death response was observed in *N. tabacum* (**Figure 3.14 D**). No other *P. agathidicida* hypothetical proteins were found to trigger any cell death response in either *N. benthamiana* or *N. tabacum*.

Table 3.7. Characterizing additional genes of interest identified in the *Phytophthora agathidicida* genome.

P. agathidicida gene ID	Glycoside Hydrolase (GH) family	Notes
Glycoside hydrolases		
Pa|009574	GH12	Cloned via golden gate.
Pa|009575	GH12	Allele 2. Cloned via golden gate.
Pa|009575	GH12	Allele 3. Cloned via golden gate.
Pa|009575	GH12	Allele 4. Cloned via golden gate.
Pa|009575	GH12	Allele 1. Cloned via golden gate.
Pa|009650	GH12	Unlikely to be real. Dropped from analysis.
Carbohydrate-related genes		
Pa3772|07462	CBEL	Cloned via golden gate.
Pa|-000646	CBEL	Cloned via golden gate.
Pa|-005543	OPEL	Gave unspecific PCR products. Dropped from analysis.
Pa-010456	Pectinesterase (carbohydrate esterase; CE)	Cloned via golden gate.
Hypothetical genes		
Pa|-003260	Hypothetical gene	Cloned via golden gate.
Pa|-003268	Hypothetical gene	Similar to *Pa|003260*. Dropped from analysis.
Pa|-003269	Hypothetical gene	Identical to *Pa|003269*. Dropped from analysis.
Pa|-004370	Hypothetical gene	Cloned via golden gate.
Pa|-004433	Hypothetical gene	Gave unspecific PCR products. Dropped from analysis.
Pa|-003493	Hypothetical gene	Cloned via golden gate.
Pa|-005342	Hypothetical gene	Cloned via golden gate.
Pa|-008135	Hypothetical gene	Gave unspecific PCR products. Dropped from analysis.
Pa|-008898	Hypothetical gene	Gave unspecific PCR products. Dropped from analysis.
Pa|-010936	Hypothetical gene	Cloned via golden gate.

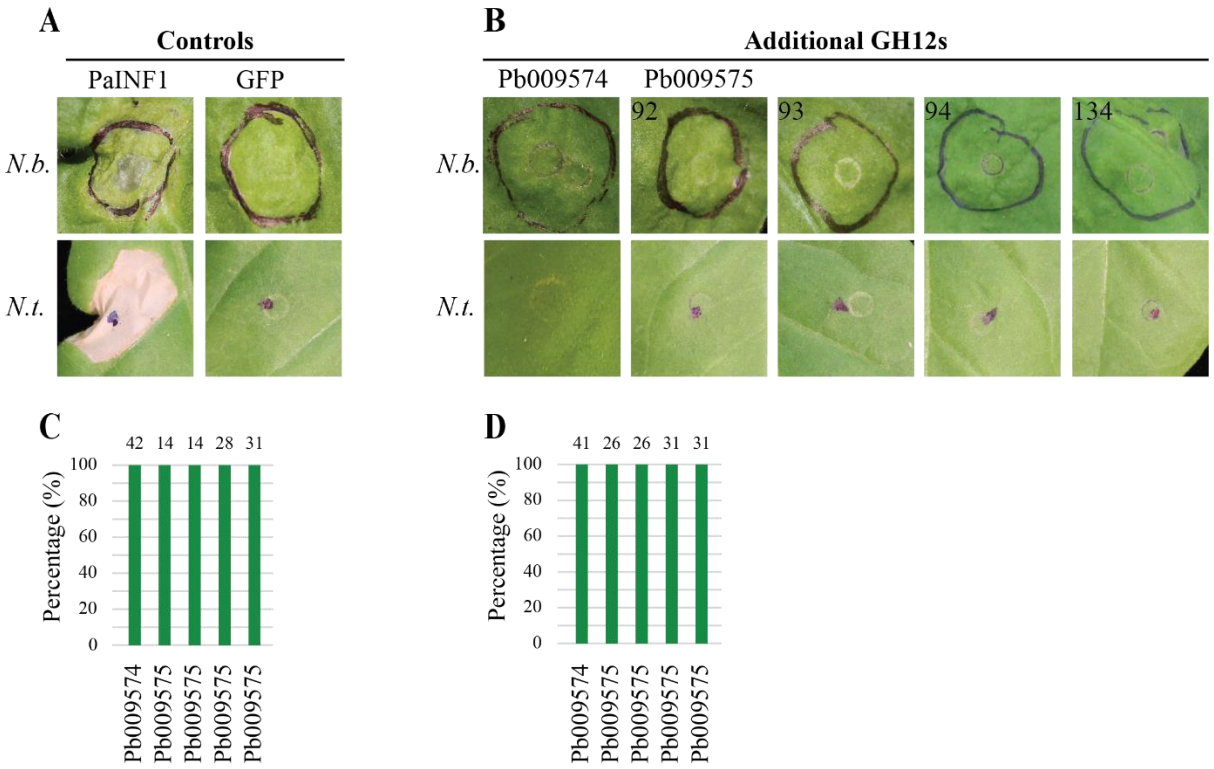

Figure 3.12. *Phytophthora agathidicida* GH12-encoding genes not expressed above 50 FPKM do not trigger cell death in *Nicotiana* species.

(A–B) *P. agathidicida* GH12-encoding genes which did not meet the initial selection criteria were later analysed for their ability to trigger an immune response in *Nicotiana* species. These additional GH12 proteins from *P. agathidicida* were produced in *Nicotiana benthamiana* (*N.b.*) or *Nicotiana tabacum* (*N.t.*) plants using an *Agrobacterium tumefaciens*-mediated transient expression assay (ATTA), and their ability to trigger a cell death response recorded at 7 days post-agroinfiltration. Images are representative of what was observed. All proteins had a N-terminal PR1α signal peptide from *N. tabacum* for secretion to the apoplast fused to a 3xFLAG tag for detection by Western blotting. **(A)** A *P. agathidicida* homolog of the known cell death elicitor INF1 from *Phytophthora infestans* was used as a positive control, while green fluorescent protein (GFP) was used as a negative control. **(B)** No response was observed in either *N. benthamiana* or *N. tabacum.* **(C–-D)** Bar graphs depicting the frequency of responses observed in *N. benthamiana* (**C**) and *N. tabacum* (**D**). Green indicates no response. Numbers above each bar indicate the total number of observations for each listed protein. Observations were over a minimum of two independent biological replicates.

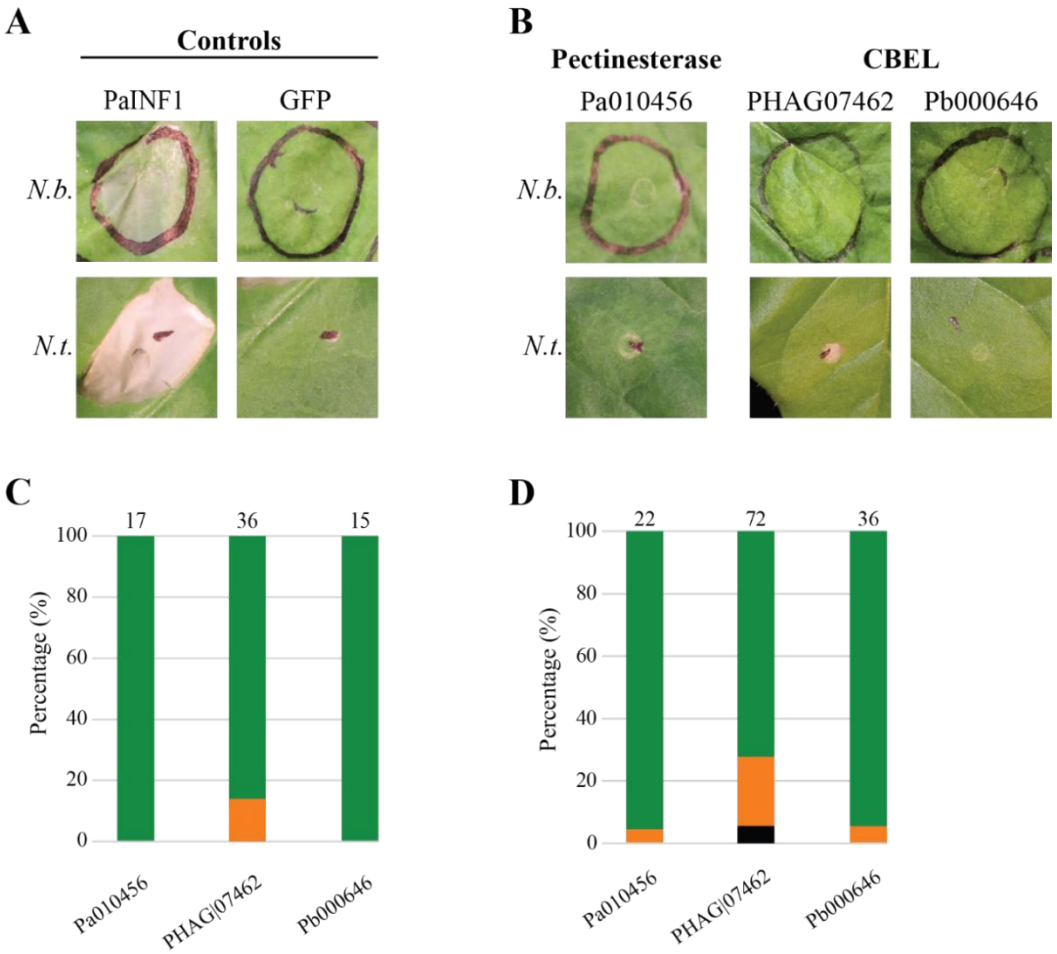

Figure 3.13. Neither selected CBEL nor pectinesterase proteins from *Phytophthora agathidicida* triggered a consistent cell death response in either *Nicotiana benthamiana* or *Nicotiana tabacum*.

(A–B) Pectinesterase and cellulose binding elicitor lectin (CBEL) proteins from *Phytophthora agathidicida* were produced in *Nicotiana benthamiana* (*N.b.*) or *N. tabacum* (*N.t.*) plants using an *Agrobacterium tumefaciens*-mediated transient transformation assay (ATTA), and their ability to trigger a cell death response (chlorosis or cell death) recorded at 7 days post-agroinfiltration. Images are representative of what was observed. All proteins had a N-terminal PR1α signal peptide from *N. benthamiana* for secretion to the apoplast fused to a 3xFLAG tag for detection by Western blotting. **(A)** A *P. agathidicida* homolog of the known cell death elicitor INF1 from *Phytophthora infestans* was used as a positive control, while green fluorescent protein (GFP) was used as a negative control. **(B)** The pectinesterase PaI|010456, and CBEL Pa3772|07462 and Pa|000646 proteins from *P. agathidicida* were unable to consistently produce a cell death response in either *N. benthamiana* or *N. tabacum*. **(C–D)** Bar graphs depicting the percentage of responses observed in *N. benthamiana* **(C)** and *N. tabacum* **(D)**. Green indicates no response; orange, chlorosis or weak cell death; black, cell death. Numbers above each bar indicate the total number of observations for each listed protein. Observations were over a minimum of two independent biological experiments.

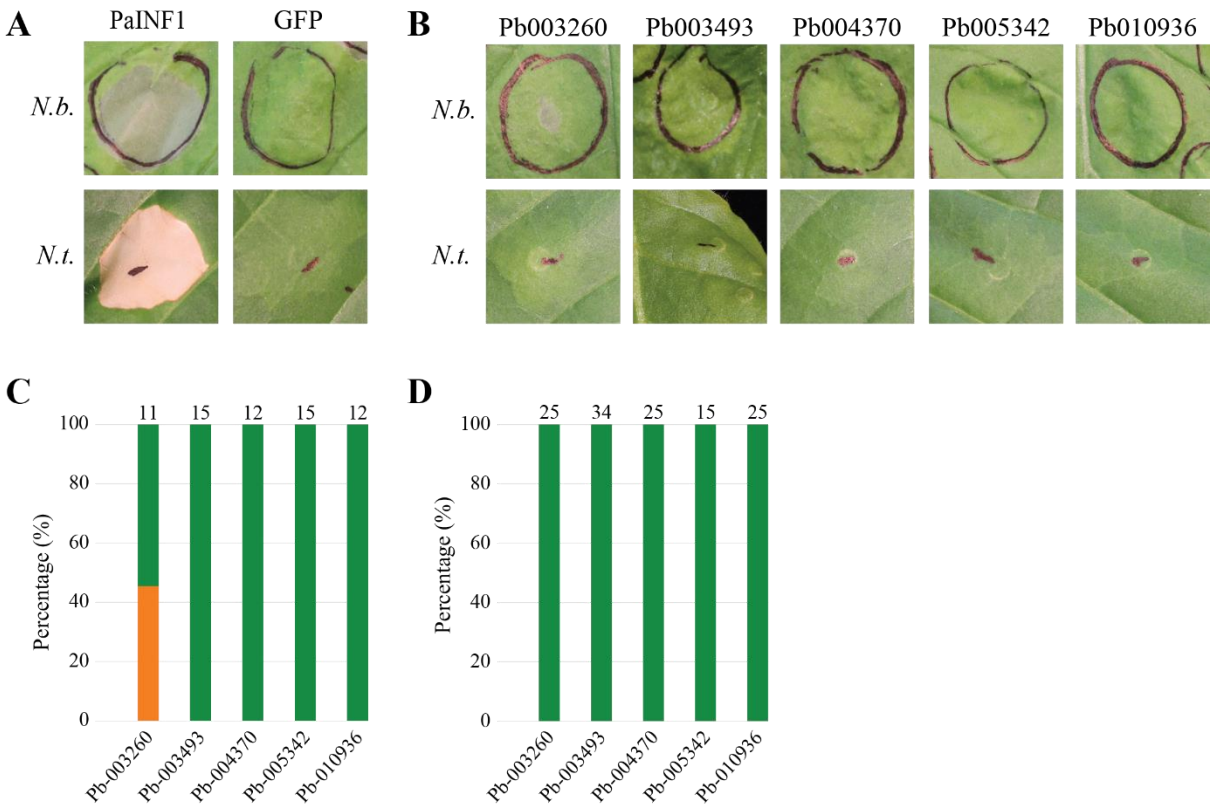

Figure 3.14. None of the selected hypothetical proteins identified from *Phytophthora agathidicida* were sufficient to trigger a strong cell death response in *Nicotiana benthamiana* or *Nicotiana tabacum*.

(A–B) Hypothetical proteins from *Phytophthora agathidicida* were produced in *Nicotiana benthamiana* (*N.b.*) or *N. tabacum* (*N.t.*) plants using *Agrobacterium tumefaciens*-mediated transient transformation assays (ATTAs), and their ability to trigger a plant immune response (chlorosis or cell death) recorded at 7 days post-agroinfiltration. Images are representative of what was observed. All proteins had a N-terminal PR1α signal peptide from *N. benthamiana* for secretion to the apoplast fused to a 3xFLAG tag for detection by Western blotting. **(A)** A *P. agathidicida* homolog of the known cell death elicitor INF1 from *Phytophthora infestans* was used as a positive control, while green fluorescent protein (GFP) was used as a negative control. **(B)** Hypothetical proteins from *P. agathidicida* were unable to consistently produce a cell death response in either *N. benthamiana* or *N. tabacum*. **(C–D)** Bar graphs depicting the percentage of time each response was observed in *N. benthamiana* **(C)** and *N. tabacum* **(D)**. Green indicates no response; orange, chlorosis or weak cell death; black, cell death. Numbers above each bar indicate the total number of observations for each listed protein. Observations were over a minimum of two independent biological experiments.

3.3.6 Secretion to the apoplast, but not enzyme activity, is required for GH12 proteins to trigger a cell death response in *Nicotiana* species

To further investigate the mechanism by which some of the *P. agathidicida* GH12 proteins were able to trigger cell death in *Nicotiana* species, one of the key catalytic residues for each of the proteins' genes was mutated. It was previously shown that Glu-136 and Glu-222 are both required for catalytic activity in the PsXEG1 GH12 from *P. sojae* (Ma et al., 2015b). These essential catalytic residues are also conserved in all six of the *P. agathidicida* GH12 proteins which trigger cell death in *N. benthamiana* (**Figure 3.15**).

A single nucleotide change was made to the codon encoding the first conserved catalytic residue in all six genes, resulting in a glutamine (Glu) to aspartic acid (Asp) substitution. The resulting Pa|004637-E135D, Pa|004638-E134D, Pa|009244-E136D, Pa|009588-E135D, Pa|009589-E134D, and Pa|009590-E137D catalytic mutants were evaluated for their ability to trigger a cell death response in *Nicotiana* species via ATTAs (**Figure 3.16 C**). All six catalytic mutants retained their ability to trigger a cell death response in both *N. benthamiana* and *N. tabacum* in 100% of experiments (**Figure 3.16 E–F**), indicating that catalytic activity is not required for cell death eliciting activity in the *Nicotiana* species tested.

To confirm that the mutants generated were, in fact, deficient in xyloglucanase enzymatic activity, two of the native GH12 proteins (Pa|009244 and Pa|009588) and their catalytic mutant counterparts (Pa|009244-E136D and Pa|009588-E135D) were heterologously produced using the *P. pastoris* expression system. *P. pastoris* supernatant containing the protein of interest, was subsequently used in an enzyme activity assay. The empty pPic9 vector construct was used as a negative control, to ensure that the *P. pastoris* supernatant did not itself contain enzymes with xyloglucanase activity. The results (**Figure 3.17 A**, **Table 3.8**) demonstrate that *P. pastoris* supernatant containing wild-type Pa|009244 or Pa|009588 were able to hydrolyse xyloglucan, while *P. pastoris* supernatant containing the pPic9 empty vector, Pa|009244-E136D and Pa|009588-E135D could not. Western blot analysis was used to determine that the protein was indeed produced by the catalytic mutants (**Figure 3.17 B**).

One of the criteria during the initial search for *P. agathidicida* CAZymes of interest was the presence of a signal peptide (SP), which would suggest that the protein was secreted into the apoplastic space of the host plant via the endoplasmic reticulum (ER)-Golgi secretory pathway. To confirm that the six *P. agathidicida* GH12 proteins which triggered a cell death response in *N. benthamiana* and *N. tabacum* were acting in the apoplastic space, the PR1α SP was removed. The six no-SP mutants (Pa|004637-NoSP, Pa|004638-NoSP, Pa|009244-NoSP, Pa|009588-NoSP, Pa|009589-NoSP, and Pa|009590-NoSP) were analysed for their capacity to trigger a cell death response in *Nicotiana* species via ATTAs (**Figure**

3.16 D). In both *N. benthamiana and N. tabacum*, ATTAs performed with Pa|004637-NoSP and Pa|004638-NoSP resulted in no response observed (**Figure 3.16 E–F**), a result significantly different from the WT proteins with the PR1α signal peptide (**Table 3.9**). Varied responses were observed in the ATTAs carried out in *N. benthamiana* with the remaining four proteins. Cell death or chlorotic responses were observed approximately 50% of the time in ATTAs performed in *N. benthamiana* with Pa|009244-NoSP (**Figure 3.16 E**); and approximately 70% of the time for ATTAs with Pa|009588-NoSP in *N. benthamiana* (**Figure 3.16 E**); while in ATTAs performed in *N. benthamiana* with Pa|009589-NoSP and Pa|009590-NoSP, cell death/chlorotic responses were observed less than 30% of the time (**Figure 3.16 E**). However, all these results were significantly different from the results observed for their WT counterparts which contained the PR1α SP (**Table 3.9**). This was not the case in *N. tabacum*, where the Pa|009244-NoSP, Pa|009588-NoSP, Pa|009589-NoSP, and Pa|009590-NoSP proteins triggered a plant cell death response over 60% of the time (**Figure 3.16 F**). These results were not significantly different from their WT counterparts with the PR1α signal peptide after adjusting for the false discovery rate (**Table 3.9**).

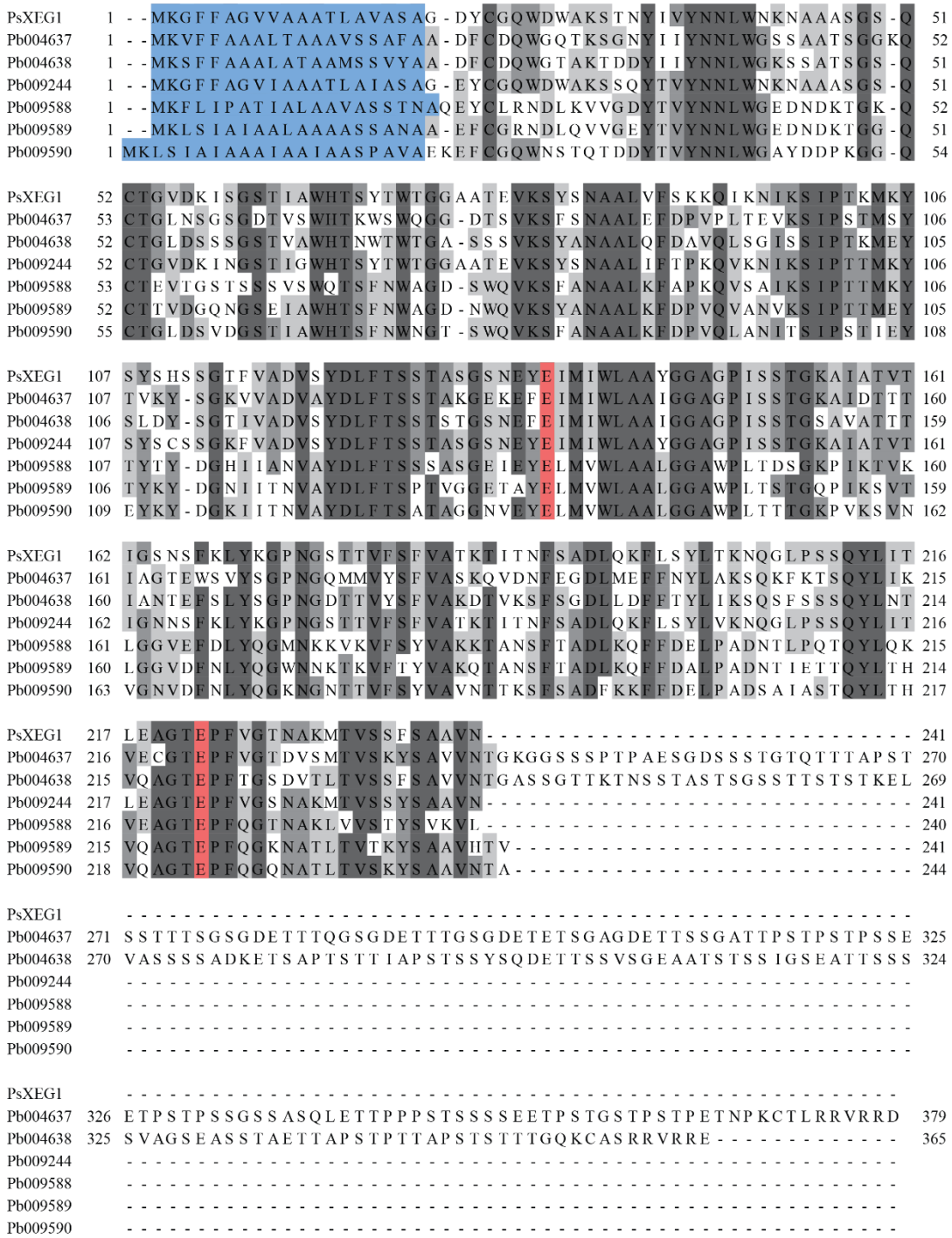

Figure 3.15. Catalytic sites are conserved between *Phytophthora sojae* PsXEG1 and *Phytophthora agathidicida* glycoside hydrolase family 12 (GH12) proteins which trigger an immune response in the model host plants *Nicotiana benthamiana* and *Nicotiana tabacum*.

Amino acid sequence alignment of PsXEG1 from *P. sojae* with the six *P. agathidicida* GH12 proteins that triggered cell death in *Nicotiana* species. The native signal peptide, which was replaced with the PR1α signal peptide from *N. tabacum* for use in the *Agrobacterium tumefaciens*-mediated transient transformation assays (ATTAs), is highlighted in blue. Catalytic sites identified in PsXEG1 and conserved in *P. agathidicida* GH12 proteins are highlighted in red.

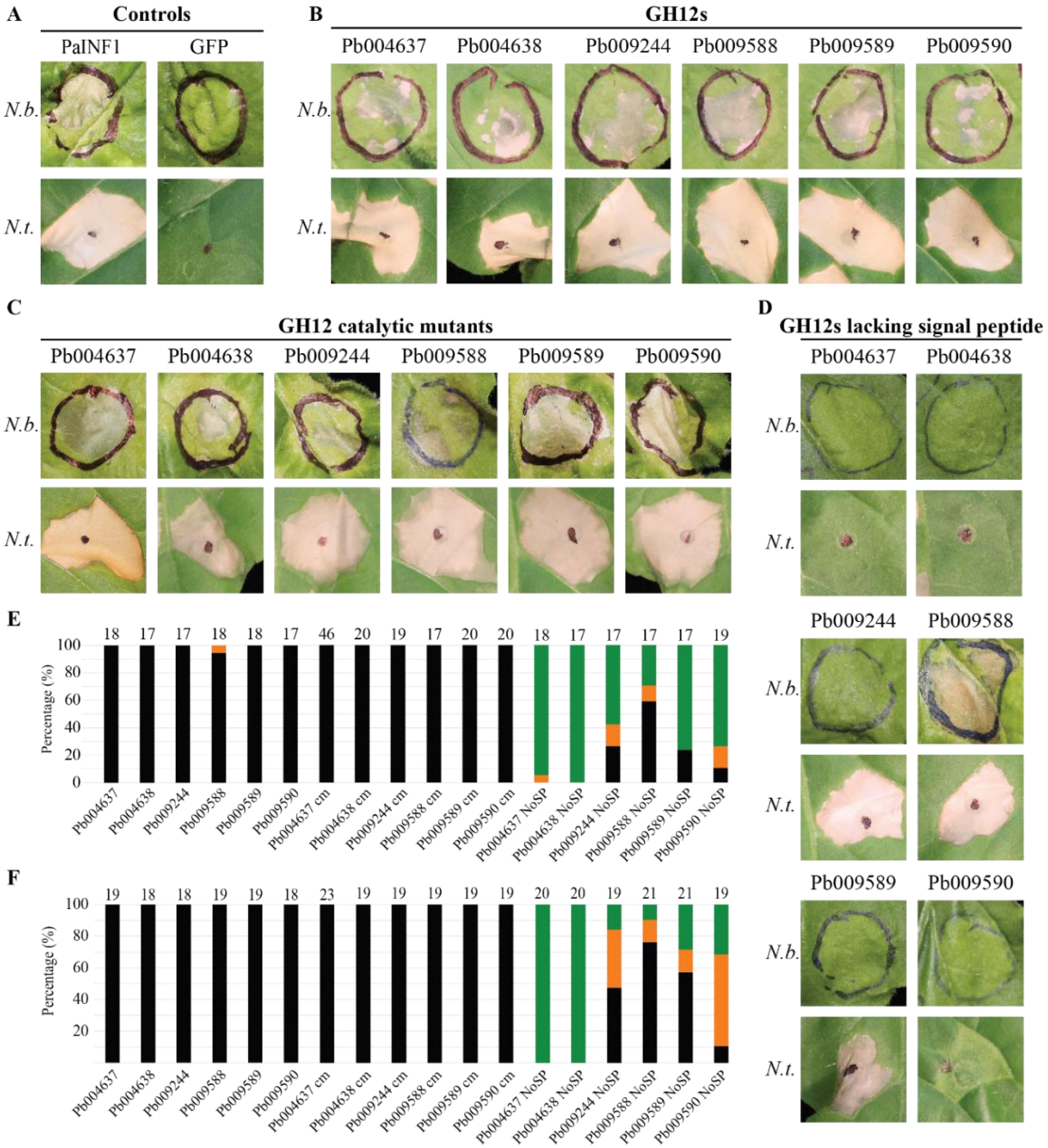

Figure 3.16. A signal peptide, but not enzymatic activity, is required for glycoside hydrolase family 12 (GH12) proteins of *Phytophthora agathidicida* to trigger a cell death response in *Nicotiana benthamiana* and *Nicotiana tabacum*.

(A–D) GH12 proteins of *P. agathidicida* were produced in *N. benthamiana* (*N.b.*; top row of photographs) or *N. tabacum* (*N.t.* bottom row of photographs) using *Agrobacterium tumefaciens*-mediated transient transformation assays (ATTAs), and their ability to trigger a plant immune response recorded at 7 days post-agroinfiltration. Images are representative of what was observed. In **(A)**, a *P. agathidicida* homolog of the known cell death elicitor INF1 from *Phytophthora infestans* was used as a positive control, while green fluorescent protein (GFP) was used as a negative control. Both controls had an N-terminal PR1α signal peptide from *N. benthamiana* fused to a 3xFLAG tag for detection by Western blotting. **(B)** shows the GH12 proteins which were found to trigger cell death response in both *N. benthamiana* and *N. tabacum,* also with N-terminal PR1α-3xFLAG tag fusion. In **(C)**, GH12 proteins had an Glu>Asp mutation in the first of their two predicted catalytic site residues, as well as an N-terminal PR1α signal peptide fused to a 3xFLAG tag. In **(D)**, GH12 proteins had an N-terminal 3xFLAG tag but lacked a PR1α signal peptide. **(E)** Bar graphs illustrating the percentage (%) of times the expressed protein elicited a cell death response (black), a chlorotic or weak cell death response (orange), or no response (green) in either *N. benthamiana* **(E)** or *N. tabacum* **(F)**. Numbers above the bar correspond to the total number of observations. Observations were over a minimum of two independent biological experiments.

Table 3.8. Hydrolysis activity of wild-type and mutant forms of selected *Phytophthora agathidicida* GH12 proteins towards xyloglucan.

Protein ID	Absorbance at 590 nm (#1)	Absorbance at 590 nm (#2)
pPic9 empty vector (EV)	-0.02[a] ± 0.04[b]	0.00 ± 0.04
Pa|009244	1.11 ± 0.10	1.92 ± 0.35
Pa|009244-E136D	-0.03 ± 0.04	0.01 ± 0.01
Pa|009588	1.07 ± 0.09	2.00 ± 0.33
Pa|009588-E135D	-0.03 ± 0.04	-0.01 ± 0.04

[a] Values are compared to blank.

[b] Standard deviation is shown.

#1 = The first independent experiment with three technical replicates.

#2 = The second independent experiment with two technical replicates.

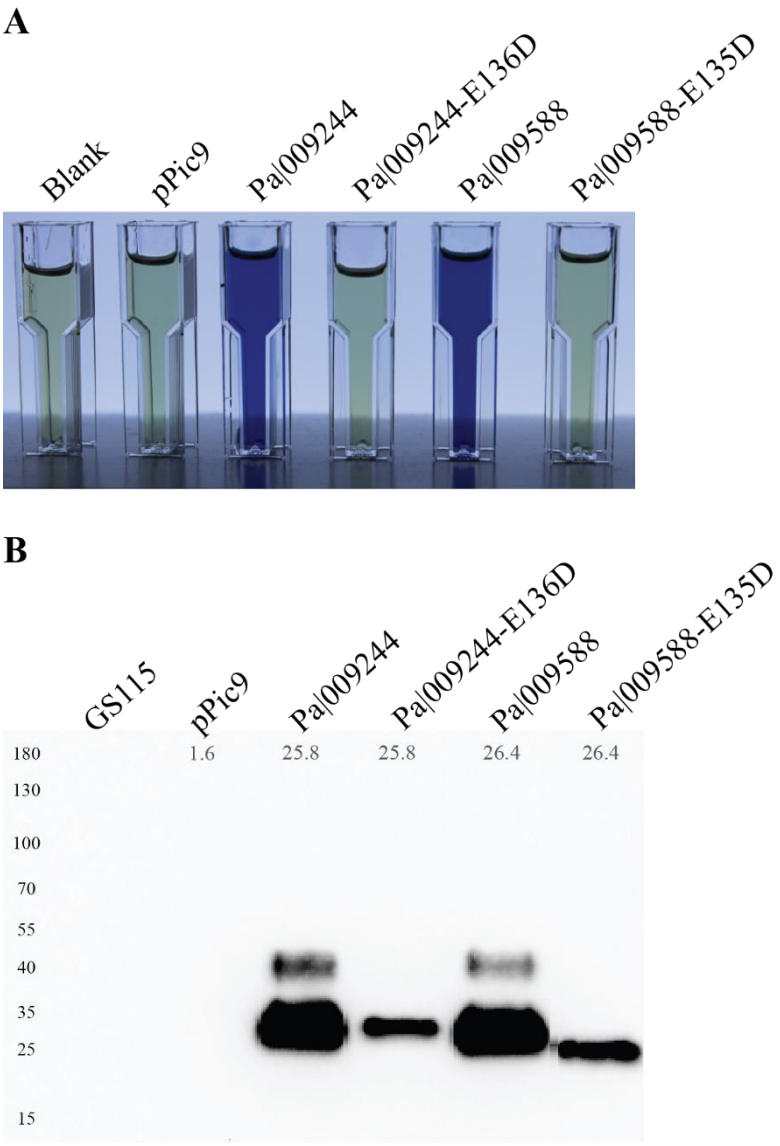

Figure 3.17. Selected *Phytophthora agathidicida* GH12 proteins can hydrolyse xyloglucan, while their corresponding catalytic mutants are not.

Selected *P. agathidicida* GH12 proteins were heterologously produced in the *Pichia pastoris* expression system and the resulting supernatant used to perform an enzyme activity assay on azo-xyloglucan (Megazyme, Wicklow, Ireland). **(A)** *P. pastoris* supernatant containing the protein of interest was incubated with the xyloglucan substrate for 10 mins at 40°C prior to measuring the absorbance of the resultant solution at 590 nm. The blue colour observed is a result of the hydrolysis activity of the enzyme releasing dye molecules. **(B)** Western blot analysis of *P. pastoris* supernatant was used to confirm presence of the protein of interest. Smaller dark grey numbers detail the expected protein size (kDa).

Table 3.9. Results of a chi-squared test comparing responses of six glycoside hydrolase family 12 (GH12) proteins and their respective no-signal peptide (NoSP) mutants from *Phytophthora agathidicida* in *Nicotiana* species.

N. benthamiana						
Protein	**No response**	**Response[a]**	**X^2**	**df[b]**	***P* value**	***P* value (FDR)[c]**
Pa|004637	0	18	29.524	1	5.52E-08	1.66E-07
Pa|004637-NoSP	18	1				
Pa|004638	0	17	32.099	1	1.47E-08	8.79E-08
Pa|004638-NoSP	19	0				
Pa|009244	0	17	11.576	1	6.68E-04	8.02E-04
Pa|009244-NoSP	11	8				
Pa|009588	0	18	4.008	1	4.53E-02	4.53E-02
Pa|009588-NoSP	5	12				
Pa|009589	0	18	18.745	1	1.49E-05	2.99E-05
Pa|009589-NoSP	13	4				
Pa|009590	0	17	17.514	1	2.85E-05	4.28E-05
Pa|009590-NoSP	14	5				

N. tabacum						
Protein	**No response**	**Response[a]**	**X^2**	**df[b]**	***P* value**	***P* value (FDR)[c]**
Pa|004637	0	19	35.1	1	3.13E-09	1.57E-08
Pa|004637-NoSP	20	0				
Pa|004638	0	18	34.095	1	5.25E-09	1.57E-08
Pa|004638-NoSP	20	0				
Pa|009244	0	18	1.052	1	3.05E-01	0.366
Pa|009244-NoSP	3	16				
Pa|009588	0	19	0.042738	1	5.13E-01	0.513
Pa|009588-NoSP	2	19				
Pa|009589	0	19	4.3422	1	3.72E-02	5.58E-02
Pa|009589-NoSP	6	15				
Pa|009590	0	18	4.6592	1	3.09E-02	5.58E-02
Pa|009590-NoSP	6	13				

[a] Both chlorotic/weak cell death and strong cell death were combined into the 'Response' variable for the purposes of the chi-squared test.

[b] Degrees of freedom.

[c] *P* values for *Agrobacterium tumefaciens*-mediated transient expression assays (ATTAs) carried out in *Nicotiana benthamiana* and *Nicotiana tabacum* were adjusted to account for the false discovery rate (FDR).

Data from a minimum of two independent trials.

3.3.7 The *N. benthamiana* cell death response triggered by *P. agathidicida* Pa|009244 is suppressed by *P. agathidicida* RxLR40

It has been shown that some *P. sojae* RxLR effectors are capable of suppressing plant cell death responses elicited by *P. sojae* GH12 proteins (Ma et al., 2015b). Like *P. sojae*, *P. agathidicida* also has an RxLR effector arsenal (Guo et al., 2020a), and thus it was investigated whether selected *P. agathidicida* RxLR proteins could suppress the cell death response elicited by the cell death-inducing GH12 proteins. A selection of nine *P. agathidicida RxLR* genes, highly expressed *in planta* (**Table 3.10**), which had been previously cloned into the pICH86988 expression vector and transformed into *A. tumefaciens* (Guo et al., 2020a), were assessed for their ability to suppress *P. agathidicida* GH12-triggered cell death in *N. benthamiana*.

During the initial phase of the experiment, each of the nine *P. agathidicida* RxLR proteins were investigated for their ability to suppress the cell death response triggered by Pa|009244, the GH12 protein orthologous to *P. sojae* XEG1 (*Ps*XEG1). A positive suppression control (ATTAs with Avr3a followed by ATTAs with PaINF1 24 h later) is shown in the first infiltration site (**Figure 3.15 A1**), as Avr3a has previously been shown to suppress the cell death response elicited by PaINF1 in *N. benthamiana* (Guo et al., 2020a, Kanzaki et al., 2008). The second and third infiltration sites are also controls to illustrate that while no response is triggered by Avr3a alone (**Figure 3.15 A2**), ATTAs with only PaINF1 trigger a strong cell death response (**Figure 3.15 A3**). The fourth infiltration site (**Figure 3.15 A4**) was used as a dilution control (ATTAs performed with Pa|001110, a GH19 shown not to trigger cell death (**section 3.3.4**) infiltrated 24 h prior to infiltration with Pa|009244, a GH12 cell death elicitor (**section 3.3.4**)) to ensure that any apparent suppression of cell death was not occurring simply due to the cell death elicitor being diluted by prior ATTAs performed with a non-cell death elicitor. The fifth (**Figure 3.15 A5**), sixth (**Figure 3.15 A6**), and seventh (**Figure 3.15 A7**) infiltration sites were used as controls for Pa|001110 (should not trigger cell death), Pa|009244 (GH12 cell death elicitor), and the RxLR of interest (should not trigger cell death) respectively. Finally, the eighth infiltration site (**Figure 3.15 A8**) was used to determine whether the RxLR of interest could suppress the Pa|009244 GH12 cell death elicitor.

The results of the experiment were only considered if each of the seven controls had worked as expected. Of the nine RxLR proteins studied, only one, RxLR40, could suppress the Pa|009244-triggered cell death response (**Figure 3.15**). Subsequent experiments focused on whether RxLR40 was also capable of suppressing cell death responses elicited by any of the six cell death-inducing *P. agathidicida* GH12 proteins (**Figure 3.16 A**). Surprisingly, only the cell death response elicited by the *Ps*XEG1 orthologue, *P. agathidicida* Pa|009244, was consistently suppressed by *Pa*RxLR40 (in over

80% of experiments) (Figure **3.16 B**). *N. benthamiana* cell death elicited by any of the other five GH12 proteins was suppressed in less than half of the experiments. As all *P. agathidicida* GH12 cell death elicitors (Pa|004637, Pa|004638, Pa|009244, Pa|009588, Pa|009589, Pa|009590) triggered cell death in *N. benthamiana* 100% of the time (**see section 3.3.4**), any suppression observed in response to prior ATTAs with PaRxLR40 is significant. However, the variable responses observed make it difficult to draw conclusions with certainty. Western blots are now needed to confirm expression of GH12 cell death elicitors, RxLR proteins, and controls.

Table 3.10. Nine highly expressed *Phytophthora agathidicida* RxLR proteins were screened for their ability to suppress *P. agathidicida* GH12-triggered cell death in *Nicotiana benthamiana*.

Pa|3770 gene[1]	Pa3772|3772 gene[2]	Pag|3770 gene[3]	RxLR protein name	*In vitro*[4]	[5]Kauri leaf 6 hpi[6]	Kauri leaf 24 hpi	Kauri leaf 48 hpi	Kauri leaf 72 hpi	[7]Kauri root 6 hpi	Kauri root 24 hpi	Kauri root 48 hpi	Kauri root 72 hpi
Pa|005613	*Pa3772||05917*	*Pag|014600*	Pa-RxLR6	0	47	67	721	722	13	235	477	233
Pa|007201	*Pa3772||12698*	*Pag|017832*	Pa-RxLR26	9	455	522	3295	2459	76	1719	2110	1360
Pa|009546	*Pa3772||13789*	*Pag|014603*	Pa-RxLR38	7	154	34	418	317	60	281	497	378
Pa|006882	*Pa3772||12136*	*Pag|002383*	Pa-RxLR39	6	81	114	1444	1148	99	158	667	387
*	*Pa3772||12021*	*Pag|001184*	Pa-RxLR40	0	0	71	160	160	3	91	89	42
*	*	*Pag|016631*	Pa-RxLR53[8]	133	373	207	2146	1482	97	1284	2696	1762
*	*Pa3772||12809*	*Pag|002731*	Pa-RxLR99	1	1	64	916	559	0	215	563	298
*	*Pa3772||13731*	*Pag|001920*	Pa-RxLR106	2	103	275	3189	2275	38	1771	4341	2430
*	*Pa3772||13754*	*Pag|016610*	Pa-RxLR107	229	853	195	4222	3270	57	2297	5805	3863

[1] Identification code given in the *P. agathidicida* type strain 3770 PacBio genome.

[2] Identification code given in the *P. agathidicida* type strain 3772 Illumina genome.

[3] Identification code given in the recent chromosome-level *P. agathidicida* type strain 3770 PacBio genome.

[4] RNA sequencing results of *P. agathidicida* grown in clarified V8 liquid medium.

[5] Results of an RNA sequencing time-course experiment infecting kauri leaves with *P. agathidicida*.

[6] Hours post-inoculation.

[7]Results of an RNA sequencing time-course experiment infecting kauri roots with *P. agathidicida*.

[8] Pa-RxLR53 was identified in the *P. agathidicida* 3770 Illumina genome as MSTRG.12955.1.

* Not identified in this genome annotation.

** All expression data given in FPKM (Fragments per kilobase million).

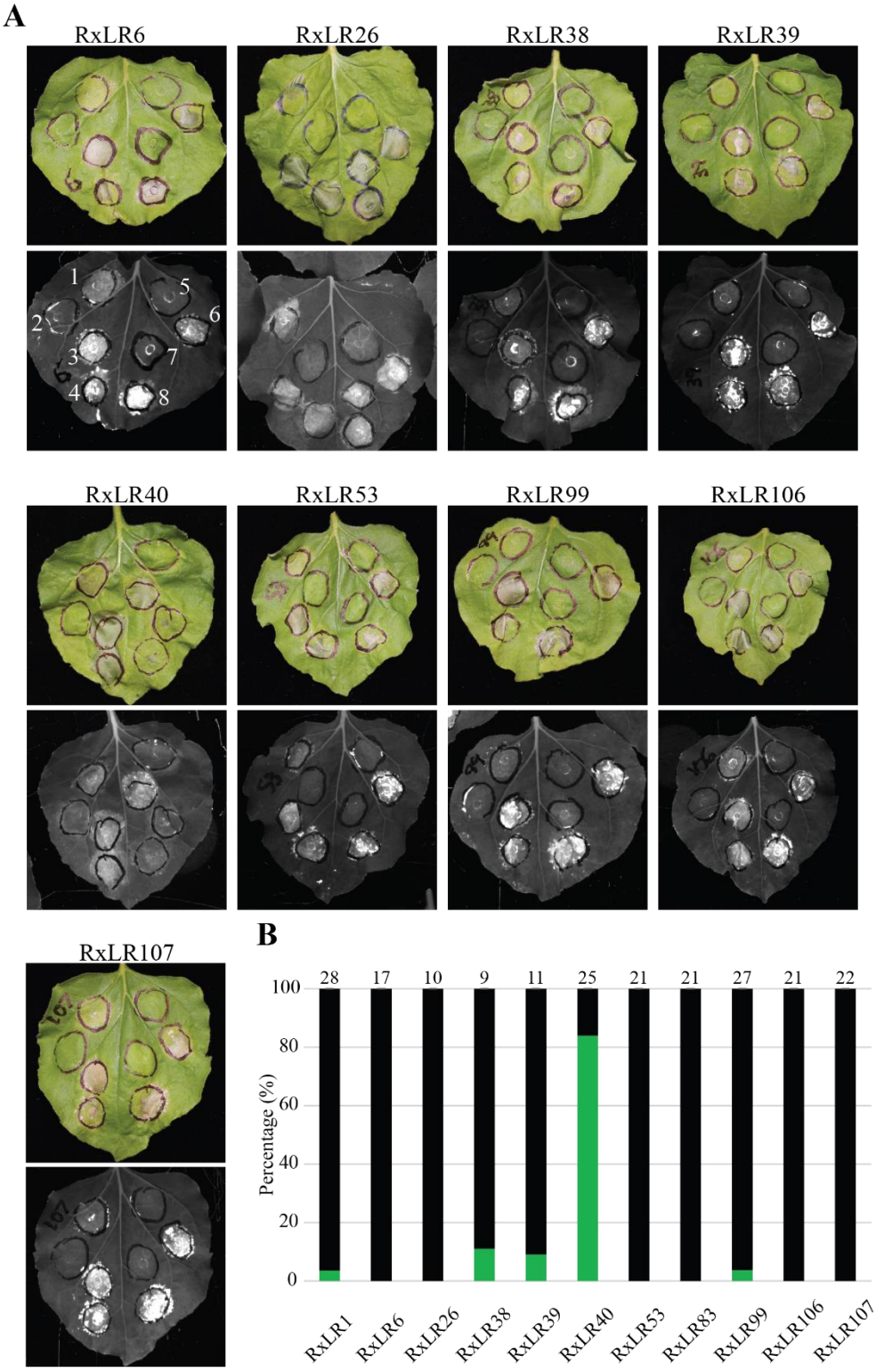

Figure 3.18. *Phytophthora agathidicida* RxLR40 suppresses *P. agathidicida* Pa|009244-triggered cell death in *Nicotiana benthamiana*.

(A) *P. agathidicida* RxLR proteins and the GH12 protein Pa|009244 were produced in *N. benthamiana* plants using *Agrobacterium tumefaciens*-mediated transient transformation assays (ATTAs). *A tumefaciens* carrying the *RxLR* gene of interest, *Avr3a* or *EB091* was infiltrated 24 hours prior to infiltration with *A. tumefaciens* carrying *Pa|009244* or known cell death elicitor gene *PaINF1*. Seven days post-infiltration of strains carrying cell death elicitor genes, photographs were taken under both natural light and UV light to record any response. Images are representative of what was observed. **1:** positive suppression control (Avr3a/INF1), as Avr3a is known to suppress INF1; **2:** Avr3a-only control; **3:** PaINF1-only positive cell death control; **4:** dilution effect control (EB091/Pa|009244); EB091 has been shown not to trigger plant cell death (**Figure 3.9**); **5:** EB091-only control; **6:** Pa|009244 cell death control; **7:** RxLR-only control (selected RxLR); **8:** test to determine whether the selected RxLR could suppress Pa|009244-triggered cell death (selected RxLR/Pa|009244). PaINF1, EB091, Pa|009244 and RxLRs had an N-terminal PR1α signal peptide from *Nicotiana tabacum* fused to a 3xFLAG tag for detection by Western blotting. Avr3a had an N-terminal PR1α signal peptide from *N. tabacum* fused to a GFP (green fluorescent protein) tag for detection via Western blot. **(B)** Bar graphs illustrating the percentage (%) of times the Pa|009244 elicited a cell death response (black) or no response (green) in *N. benthamiana* when pre-infiltrated with the selected RxLR. Numbers above the bar correspond to the total number of observations. Observations were over a minimum of two independent experiments (except RxLR26 which was only tested once).

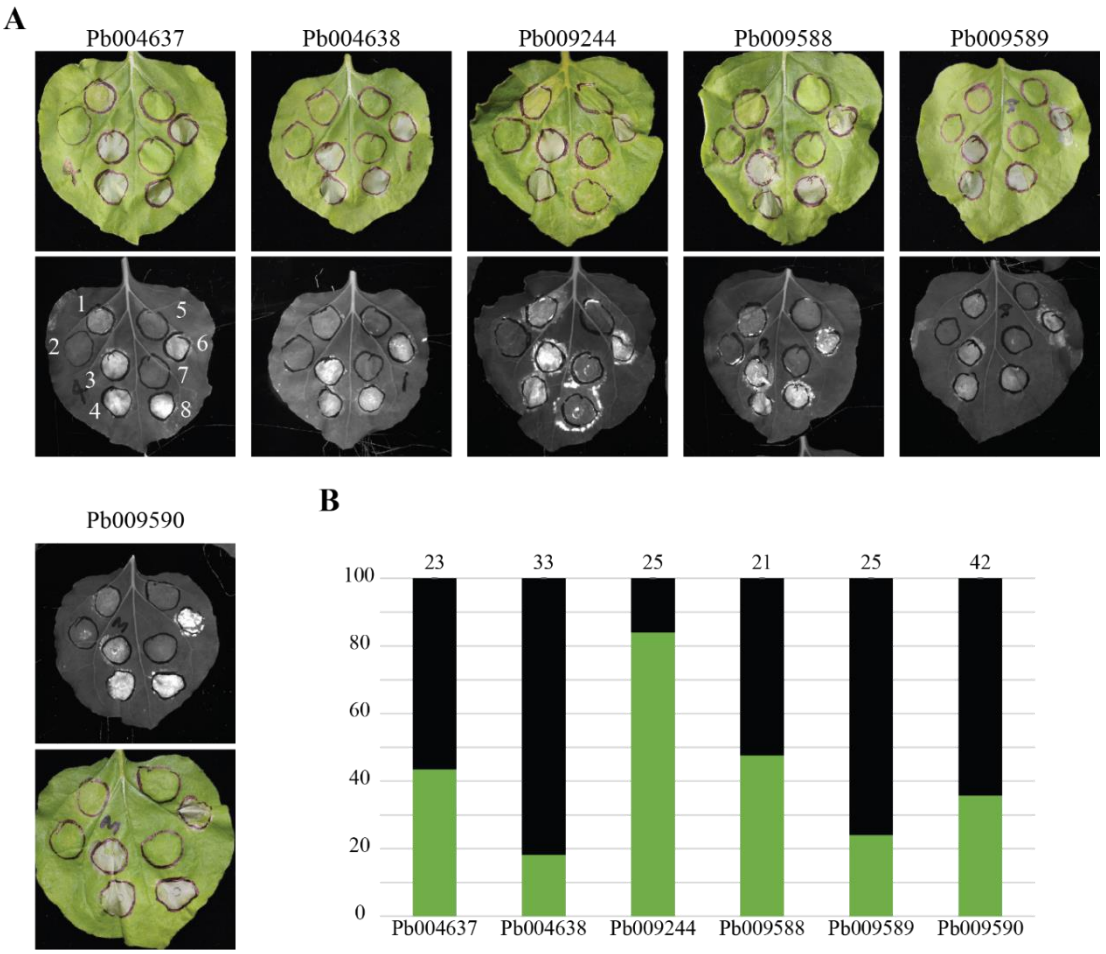

Figure 3.19. *Phytophthora agathidicida* RxLR40 could only consistently suppress the cell death response triggered by *P. agathidicida* GH12 Pa|009244 in *Nicotiana benthamiana*.

(A) *P. agathidicida* RxLR40 and the six GH12 proteins were produced in *N. benthamiana* plants using *Agrobacterium tumefaciens*-mediated transient transformation assays (ATTAs). *A tumefaciens* carrying the *RxLR40*, *Avr3a* or *EB091* gene was infiltrated 24 hours prior to infiltration with *A. tumefaciens* carrying any of the *GH12* cell death elicitor genes or known cell death elicitor gene *PaINF1*. Seven days post-infiltration of strains carrying cell death elicitor genes, photographs were taken under both natural light and UV light to record any response. Images are representative of what was observed. **1:** positive suppression control (Avr3a/PaINF1), as Avr3a is known to suppress PaINF1 (Guo et al., 2020a); **2:** Avr3a-only control; **3:** PaINF1- only cell death control; **4:** dilution effect control (EB091/selected GH12); EB091 has been shown not to trigger plant cell death (**Figure 3.9**); **5:** EB091- only control; **6:** selected GH12 cell death control; **7:** RxLR40-only control (RxLR40); **8:** test to determine whether RxLR40 could suppress GH12-triggered cell death (RxLR40/selected GH12). PaINF1, EB091, RxLR40 and the six GH12s had N-terminal PR1α signal peptide from *N. tabacum* fused to a 3xFLAG tag for detection by Western blotting. Avr3a had an N-terminal PR1α signal peptide from *N. tabacum* fused to a GFP (green fluorescent protein) tag for detection via Western blot. **(B)** Bar graphs illustrating the percentage (%) of times the selected *P. agathidicida* GH12 elicited a cell death response (black) or no response (green) in *N. benthamiana* when pre-infiltrated with RxLR40. Numbers above the bar correspond to the total number of observations. Observations were over a minimum of two independent biological experiments.

3.3.8 The cell death response triggered by GH12 proteins negatively affects *P. agathidicida* lesion size during infection of *N. benthamiana*

Of all the *P. agathidicida* GH-encoding, carbohydrate-related, and hypothetical proteins studied as part of this research, only a selection of *P. agathidicida* GH12-encoding proteins were found to consistently elicit a cell death response (**section 3.3.4**) in *N. benthamiana* and *N. tabacum*. Thus, the next step was to understand whether any of the aforementioned proteins also contributed to *P. agathidicida* virulence. To this effect, ATTAs were performed to express the POI 24 hours prior to inoculation with *P. agathidicida* mycelia. The lesion size on the infected leaf was then measured after approximately 48 h (**Appendix 3.9**).

Two of the three negative controls included ATTAs performed with GFP or an empty pICH86988 vector. The third negative control was no leaf infiltration. As seen in **Figure 3.20**, there was considerable variation in lesion size of the three negative controls, particularly in the un-infiltrated control. This was a similar finding for most of the *P. agathidicida* proteins in this study (**Figure 3.20**). None of the proteins analysed appeared to increase *P. agathidicida* lesion size when agroinfiltration was performed prior to inoculation, which would have been observed as an increase in lesion diameter (compared to controls). Interestingly, all six *P. agathidicida* GH12 cell death elicitors resulted in a decrease in lesion diameter, as did five of the corresponding catalytic mutants (except Pa|004637-E135D), and two of the proteins lacking a signal peptide (Pa|009588-NoSP and Pa|009589-NoSP) (**Figure 3.20**). This decrease is evidenced by the lack of overlap between the notches of the above-mentioned proteins and the notches of the controls (shown by the shaded band in **Figure 3.20**).

In some cases, *P. agathidicida* did not appear to infect the leaf. So as not to skew the data, these non-infections were recorded and analysed separately from the box and whisker plots (**Figure 3.21**). While instances on non-infection occurred only once for a number of proteins, most of the instances of non-infection occurred when *N. benthamiana* was infiltrated with *A. tumefaciens* carrying *P. agathidicida* GH12-encoding genes prior to inoculation. Other examples of non-infection occurring more than once were in ATTAs with a GH3, GH7, two GH17s, a GH28 (Pa|010677 which was shown to trigger chlorosis when infiltrated into *N. benthamiana* (**Figure 3.9**)), a GH54, a CBEL, and a hypothetical protein. The GH12 cell death inducing proteins, and their various associated constructs (catalytic mutants and No-SP) account for approximately 34% of the proteins studied in this experiment. However, the percentage of non-infection due to expression of these genes (via ATTAs) prior to *P. agathidicida* inoculation is more than 65%, almost double what would be expected. Thus, it appears the presence of selected *P. agathidicida* GH12 proteins in *N. benthamiana* (via ATTAs) prior to inoculation with *P. agathidicida* reduces *P. agathidicida* lesion size in this model system.

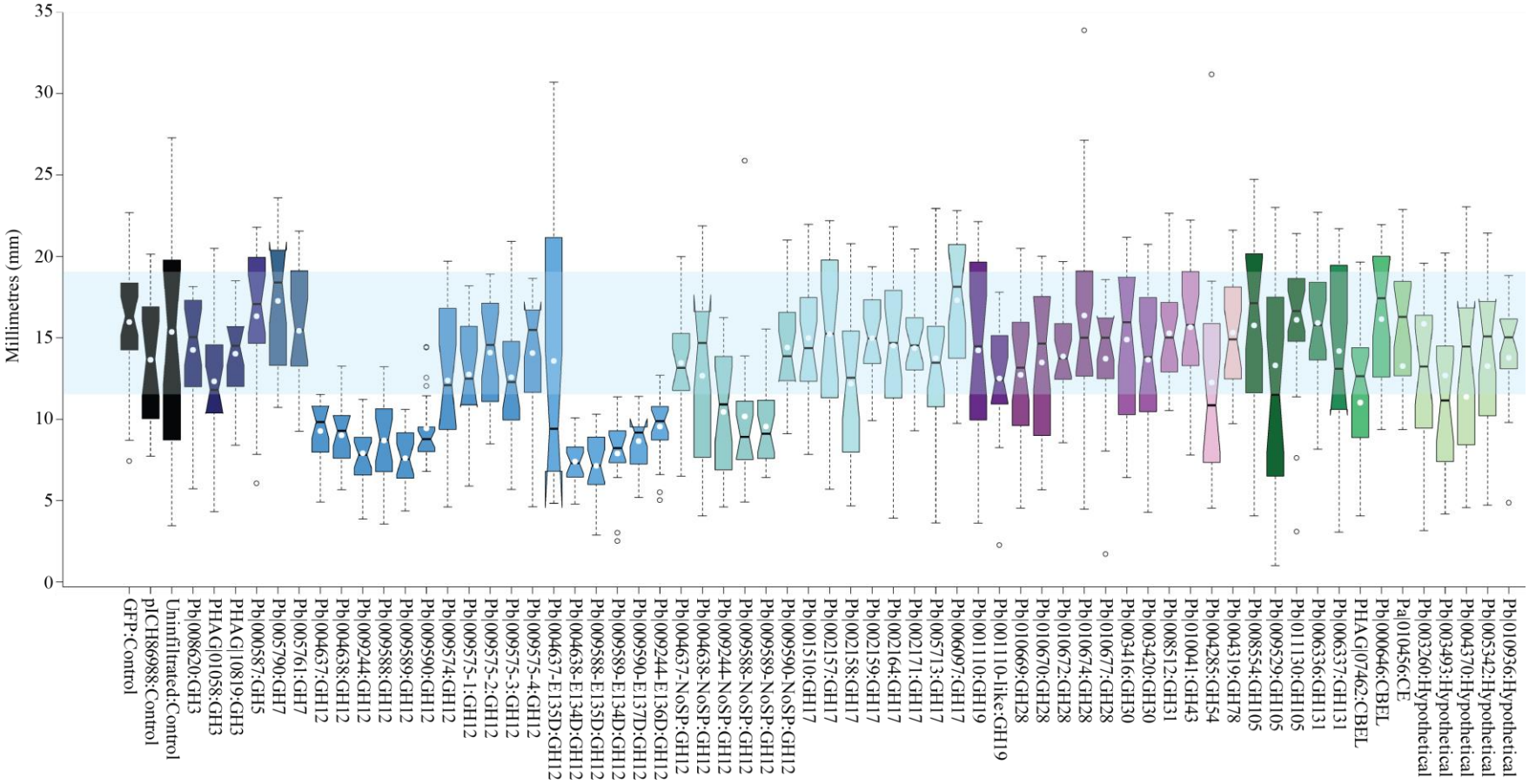

Figure 3.20. Boxplot of the effect of selected *Phytophthora agathidicida* glycoside hydrolase, carbohydrate-related, and hypothetical proteins on *P. agathidicida* lesion diameter during infection of *Nicotiana benthamiana* leaves.

P. agathidicida proteins of interest were produced in *N. benthamiana* plants using *Agrobacterium tumefaciens*-mediated transient transformation assays (ATTAs), followed by inoculation with plugs of *P. agathidicida* mycelia grown on V8 agar 24 hours later. The diameters of *P. agathidicida* lesions were measured 48 hours post-inoculation. ATTAs with green fluorescent protein (GFP), the pICH86988 empty vector, or no infiltration were used as negative controls. White dots indicate the mean or average lesion diameter. Light blue shading indicates the area spanned by the notches in the negative controls. Any individual boxplots with notches that do not overlap with the shaded area are considered different to the controls. Three biological replicates, each with eight technical replicates, were performed for each selected *P. agathidicida* protein.

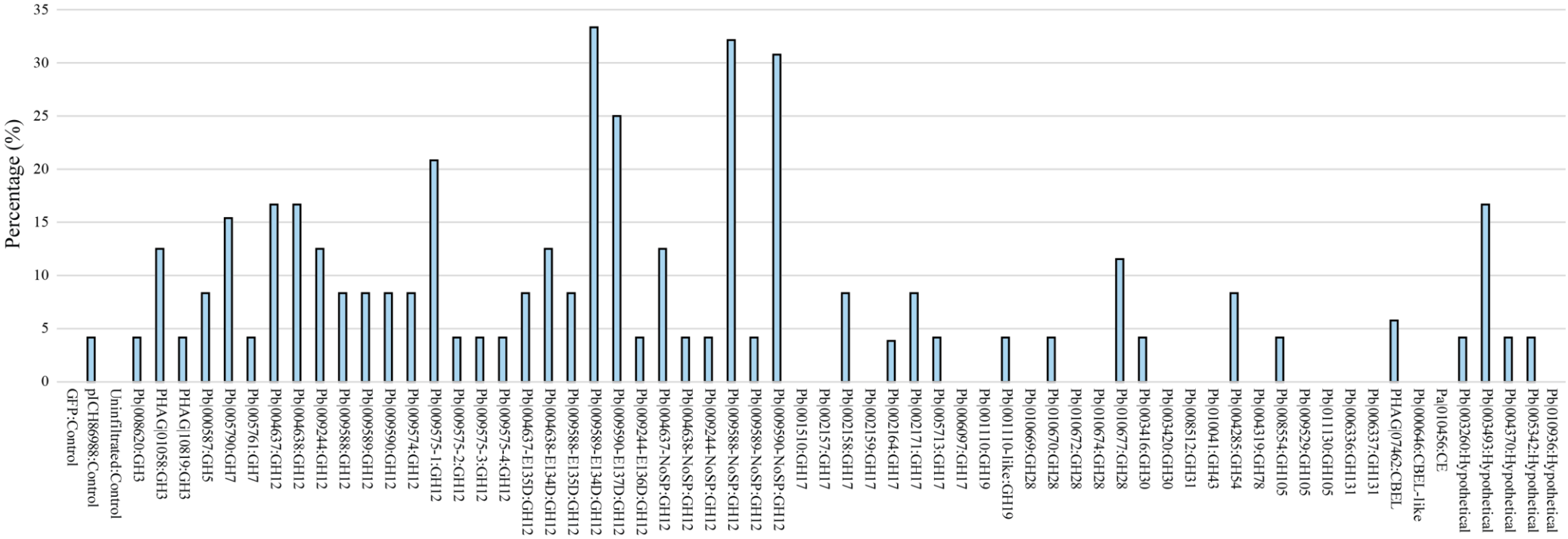

Figure 3.21. Bar graph illustrating the percentage of times inoculation with *Phytophthora agathidicida* did not result in infection 24 hours after *Nicotiana benthamiana Agrobacterium tumefaciens*-mediated transient transformation assays (ATTAs) involving selected *P. agathidicida* proteins of interest.

P. agathidicida proteins of interest were produced in *N. benthamiana* plants using *Agrobacterium tumefaciens*-mediated transient transformation assays (ATTAs), followed by inoculation with plugs of *P. agathidicida* mycelia grown on V8 agar 24 hours later. The presence of *P. agathidicida* lesions was determined 48 hours post-inoculation. ATTAs with green fluorescent protein (GFP), the pICH86988 empty vector, or no infiltration were used as negative controls.

3.4 Discussion

Investigation into the highly expressed, secreted, CAZyme repertoire of *P. agathidicida* revealed a subset of GH12 family proteins which trigger cell death in in *N. benthamiana* and *N. tabacum*. As these proteins are able to trigger cell death independently of their enzymatic activity, it is anticipated that they are recognised as MAMPs by an immune receptor in these plant species. Such a response may act to reduce pathogen virulence; observed as the smaller lesion size following *P. agathidicida* inoculation onto *N. benthamiana* leaves expressing the cell death eliciting GH12 proteins. Interestingly, prior expression of the *P. agathidicida* RxLR40 protein was able to suppress the GH12-triggered cell death response, further highlighting that the outcome of the interaction between pathogen and host is the result of a complex network of interactions.

While the observed plant cell death response could be the result of the plant immune system mounting a response upon recognition of the GH12 protein of interest, it could also be possible that the GH12 protein of interest is directly toxic to the plant, perhaps by interacting with and perturbing the host plant membrane. Cell death assays were always carried out with a positive control, using a *P. agathidicida* homolog of the *P. infestans* INF1 cell death elicitor, PaINF1, which is known to trigger necrotic cell death in response to recognition by the NbLRK1 immune receptor in *N. benthamiana* (Kanzaki et al., 2008), and a negative control, using either green fluorescent protein or *P. agathidicida* Pa|001110, which does not trigger plant cell death. The negative control served as both a control for the plasmid/bacterial system/infiltration buffer used, and a control for physical damage caused by the infiltration itself. It has previously been identified that the production of reactive oxygen species (ROS) and nitric oxide (NO) (Mittler et al., 2004, Torres et al., 2002), as well as the upregulation of various plant defence response genes are markers of the initiation of a plant immune response. Thus, to further confirm that the plant cell death response observed in response to ATTAs with selected *P. agathidicida* GH12s was due to the plant host mounting a defence response, additional experiments, such as quantitative reverse transcriptase polymerase chain reaction (RT-qPCR) of plant defence-related genes (pathogenesis related (*PR*) genes or *ACO* (involved in ethylene synthesis (Khatib et al., 2004, Yao et al., 2011)), or measuring ROS or NO production, (Kulye et al., 2012) could be carried out.

That the *P. agathidicida* GH12 proteins triggered a cell death response in *N. benthamiana* and *N. tabacum* was unsurprising. A study by Ma et al. (2015b), identified a number of GH12 proteins from several *Phytophthora* species including *P. sojae*, *Phytophthora parasitica*, *Phytophthora capsici* and *P. infestans* which triggered plant immune responses in *N. benthamiana*. In addition, a number of fungal plant pathogens (*Verticillium dahliae* (Gui et al., 2017), *Botrytis cinerea* (Zhu et al., 2017), *Fusarium oxysporum* (Zhang et al., 2021c) and *Magnaporthe oryzae* (Yang et al., 2021) have also been found to produce GH12 proteins which induce plant defence responses. Interestingly, not all GH12 proteins are

alike. While eliciting plant defence responses was in most cases independent of GH12 enzymatic activity, suggesting that the GH12 proteins were recognised as MAMPs, *M. oryzae* MoCel12A and MoCel12B were instead found to function as DAMPs, releasing oligosaccharides from rice cell walls which subsequently activate the rice immune system (Yang et al., 2021). The study by Yang et al. (2021) also illustrates the importance of studying native pathogen/host associations, as the oligosaccharides released are Poaceae-specific, and thus the plant immune responses would likely not have been observed using a different host. In fact, when screened by Ma et al. (2015b) in *N. benthamiana*, no immune response was observed. That the catalytic mutants of the six *P agathidicida* GH12 cell death elicitors triggered a cell death response equivalent to the wild-type proteins indicates that, like *P. sojae* PsXEG1 (Ma et al., 2015b), the cell death activity of these proteins is independent of enzymatic activity.

Surprisingly, cell death-triggering *P. agathidicida* GH12 proteins that lacked a SP were variable in their ability to trigger cell death. Given the presence of a SP in the native protein sequence, and that GH12 effectors identified in other pathogens are secreted (Gui et al., 2017, Ma et al., 2015b, Yang et al., 2021, Zhang et al., 2021c, Zhu et al., 2017), it was expected that secretion would be required to elicit a cell death response. Consequently, removing the SP should prevent a cell death response if recognition occurred in the apoplast. In most cases, GH12 proteins lacking a SP were unable to trigger a cell death response in *N. benthamiana*, with the exception of Pa|009588, which suggests secretion is a key factor in GH12 cell death activity. A caveat to this experiment is that it is not known whether the proteins that failed to trigger a response were folded correctly or were appropriately post-translationally modified (e.g. through glycosylation or removal of a pro-domain), as they did not enter the ER-Golgi secretory pathway. However, while Pa|004637 and Pa|004638 did not elicit a response in *N. tabacum*, the remaining four GH12 proteins triggered a weak chlorotic or strong cell death response in more than 60% of experiments. Despite this, it is important to note that considerably more observations of 'no response' were made upon infiltration of any of the six *P. agathidicida* GH12 cell death elicitors without a SP, than were observed during ATTAs carrying the GH12 cell death elicitors with an N-terminal PR1α SP. Furthermore, evidence suggests that some proteins may be secreted in extracellular vesicles, despite containing a signal peptide (Rosa-Fernandes et al., 2017). As such, it is possible that a proportion of *P. agathidicida* cell death triggering GH12 proteins are secreted to the apoplast regardless of whether they contain a SP. Thus, while it is likely that apoplastic localisation is important for *P. agathidicida* GH12-triggered cell death activity, it remains experimentally unclear. Repeating this experiment with access to optimal growing conditions, or additional localisation experiments (e.g. fluorophore fusions) may help to clarify this quandary.

While there is considerable variation in the number of *GH12* genes in the genomes of *Phytophthora* species (Ma et al., 2015b), it is of particular interest that *P. agathidicida* lacks a homolog to *P. sojae*

PsXLP1. In the interaction between *P. sojae* and soybean (*Glycine max*), PsXEG1 is inhibited by the soybean glucanase inhibitor protein GmGIP1 (Ma et al., 2017). However, PsXLP1 can bind GmGIP1 more tightly than PsXEG1, freeing PsXEG1 to carry out its virulence function. *PsXLP1* is highly similar to *PsXEG1*, despite a truncated C-terminus due to a frameshift mutation resulting in a premature stop codon. Consequently, while the first predicted catalytic residue is retained, PsXLP1 lacks the second catalytic site and lacks the glycohydrolase activity of PsXEG1. Moreover, Ma et al. (2017) identified PsXEG1 and PsXLP1 homologs in the same head-to-head arrangement as was found in *P. sojae* in the genomes of eight of the nine different *Phytophthora* species analysed. It should then be asked, what differentiates those *Phytophthora* species that have XLP1 versus those that have not? Does it simply relate to the evolutionary history of *Phytophthora*, or could it be correlated to the natural hosts? That is, is it that the *P. agathidicida* host does not contain an equivalent glucanase inhibitor protein, and thus there is no need for a decoy? Or is there another effector that can perform the same role of PsXLP1 in *P. agathidicida*? Again, this is an area which requires further investigation.

The *P. sojae* PsXEG1 protein is recognised in *N. benthamiana* by the pattern recognition receptor, RXEG1, a leucine-rich repeat receptor-like protein. However, NbRXEG1 also recognises a number of other GH12 proteins from other *Phytophthora* species (Ps138787, Ps119627, Pp16272 and Pi06962) (Wang et al., 2018) which have homologs in *P. agathidicida*. Thus, it is likely that the *P. agathidicida* GH12 proteins are also recognised by NbRXEG1. A loss of the cell death response observed when silencing *NbRXEG1* in *N. benthamiana* using the virus-induced gene silencing (VIGS) method (Wang et al., 2018), followed by infiltration of the GH12 cell death elicitors via ATTAs would confirm this. That *N. tabacum* is a relative of *N. benthamiana* and as the *P. agathidicida* GH12 proteins that triggered a plant cell death response in *N. benthamiana* triggered the same response in *N. tabacum*, suggests that *N. tabacum* is also likely to have a homologous *RXEG1* gene. While the potential recognition of *P. agathidicida* GH12 cell death elicitors by NbRXEG1 is a topic for future investigation, it also raises additional questions. Namely, does kauri have an NbRXEG1 homolog that would allow recognition of *P. agathidicida* GH12 proteins; and why do two other secreted *P. agathidicida* GH12 proteins (Pa|009574 and Pa|009575) not trigger a cell death response in *Nicotiana* species? It could be that amino acid differences have affected key features of these GH12 proteins relating to tertiary structure, surface charge or even substrate specificity (Bradley et al., 2022) have affected their ability to be recognised by NbRXEG1. Interestingly, the only *P. agathidicida* GH12 proteins which did not elicit a defence response, were also those which were shown to not be highly expressed in the transcriptome data and therefore were not initially selected for analysis, suggesting perhaps that these genes are not required for host infection.

One of the GH12 proteins that did not trigger cell death, Pa|009575, is considerably shorter than all other secreted *P. agathidicida* GH12 proteins, and thus could have lost binding residues important for

interaction with a cognate immune receptor. In addition, it does not have one of the two predicted catalytic sites, which could suggest that it may also lack enzymatic activity, though this enzymatic activity has been shown to be dispensable for induction of cell death in *N. benthamiana* and *N. tabacum*. In contrast, Pa|009574 has retained both predicted catalytic sites. Determining whether Pa|009574 has xyloglucanase activity, and indeed whether any of the *P. agathidicida* GH12 proteins have the β-glucanase activity observed with PsXEG1 (Ma et al., 2015b), would be avenues for further investigation. In addition, an alignment of GH12 proteins from various fungal and oomycete species known to act as MAMPs and elicit a cell death response, together with GH12 proteins, such as *P. agathidicida* Pa|009574 and Pa|009575, which fail to elicit a cell death response, may help identify residues important in recognition by the cognate immune receptor. Mutating these sites and expressing the mutant GH12 proteins in *N. benthamiana* via ATTAs should help identify key residues bound by the LRR region of NbRXEG1 and may shed light on why some GH12 proteins are not recognized.

It has previously been demonstrated that RxLR proteins are capable of both eliciting plant cell death responses (Wang et al., 2011a), and suppressing plant cell death responses elicited by other pathogen effectors (Bos et al., 2010). Indeed, the cell death activity elicited by *P. agathidicida* RxLR24 was suppressed by *P. agathidicida* RxLR40 (Guo et al., 2020a). Time and space requirements meant there was not the capacity to test all identified *P. agathidicida* RxLR proteins against the *P. agathidicida* GH12 cell death elicitors. Thus, it was decided to select only those that were highly expressed, once again using the *P. agathidicida* RNA sequencing data (Guo & Panda, Unpublished), for further analysis. In addition, the selected RxLR proteins were initially only screened for the ability to suppress *P. agathidicida* Pa|009244-triggered *N. benthamiana* cell death. Only one of the nine RxLR proteins, PaRxLR40, was found to suppress cell death elicited by Pa|009244 in *N. benthamiana* and was subsequently investigated for its ability to suppress the cell death response elicited by the remaining five GH12 cell death-eliciting proteins. Surprisingly, the results of the ATTAs were extremely variable. However, it could be argued that even when suppression was observed less than 20% of the time (Pa|004638), this was considerably more than the 100% cell death observed upon ATTAs with only the GH12 cell death elicitors. While it would be particularly interesting if PaRxLR40 could only suppress cell death triggered by some but not all *P. agathidicida* GH12 cell death elicitors, this is unlikely. More likely is that again the conditions were not optimal for this kind of experiment, and it would have benefited from access to natural light. Indeed, similar ATTAs carried out by members of our lab have demonstrated stronger, more consistent results when plants were exposed to natural light as opposed to artificial light in plant growth rooms, and it is well established that some pathogen effector proteins require light to trigger a plant cell death response (Kettles et al., 2017). Further experiments in better conditions would aid in establishing whether this is the case.

As is often the case, with answers come more questions. In this study, the selected *P. agathidicida* proteins were studied in isolation, without any other *P. agathidicida* proteins present, except when carrying out the suppression assay using *P. agathidicida* RxLR proteins. In the natural host-pathogen interaction, there is a complex mix of proteins, enzymes, and other small molecules. It is possible, likely even, that *P. agathidicida* produces proteins other than PaRxLR40 that suppress GH12-triggered cell death that have not yet been characterised. For example, carbohydrate-binding module (CBM)-containing proteins have been shown to suppress cell death in *N. benthamiana* triggered by GH12 and CE5 proteins from *V. dahliae* (Gui et al., 2017, Gui et al., 2018). Identifying proteins which follow a similar expression pattern to the cell death eliciting GH12s may help to narrow down this list of potential candidates.

P. agathidicida GH12s were the only proteins, when expressed in *N. benthamiana* via ATTAs prior to *P. agathidicida* inoculation, which appeared to influence pathogen lesion size; resulting in smaller lesions, and in several cases no lesions, compared to the negative controls and indeed any of the other *P. agathidicida* proteins studied. Furthermore, GH12 enzymatic activity was not required for this reduction in lesion size, analogous to findings with *P. sojae* PsXEG1 (Ma et al., 2015b). *P. agathidicida* is a hemibiotroph, meaning it infects a living host and establishes itself prior to a necrotrophic switch. That *P. agathidicida* has been shown to infect *N. benthamiana,* may suggest that the cell death inducing GH12 proteins are expressed at a level below the threshold for detection during infection of *N. benthamiana* or that the cell death response is suppressed early in the interaction. Thus, the cell death triggered in *N. benthamiana* by these proteins may inhibit/slow *P. agathidicida* infection because the tissue has already started to degrade before the pathogen had a chance to suppress the response or because the cell death observed in response to expression of the *P. agathidicida* GH12 genes is a representation of the activation of a plant immune response on a molecular level due to recognition of these GH12 proteins as MAMPs. Therefore, it would be of interest to **a)** use a lower concentration of *A. tumefaciens* during the experiment, **b)** reduce the time between ATTAs and *P. agathidicida* inoculation or **c)** perform ATTAs and *P. agathidicida* inoculation simultaneously, to observe whether expression of these genes affects *P. agathidicida* lesion size when cell death is minimised.

As described above, many studies have shown that expression of a cell death elicitor prior to challenge with a pathogen results in the inhibition of pathogenicity or a reduction in virulence (Guo et al., 2019, Liu et al., 2021b, Ma et al., 2015b). To truly understand the effect of *P. agathidicida* GH12 proteins on virulence, the pathosystem needs to be studied in the absence of the genes encoding these proteins. CRISPR (**c**lustered **r**egularly **i**nterspaced **s**hort **p**alindromic **r**epeats) is a gene editing technology that has shown promise in a swathe of different systems, including fungi and oomycetes (Fang & Tyler, 2016, McCarthy et al., 2022, Rocafort et al., 2022). Identified in prokaryotes where it was used as a viral defence mechanism (Barrangou et al., 2007), CRISPR has been adapted as a genome editing

technology that works at the DNA level, using a Cas nuclease protein attached to a guide RNA which specifically targets the DNA region of interest and creates double stranded breaks in the DNA (Sander & Joung, 2014). These breaks are subsequently repaired by a typically error prone non-homologous end joining mechanism (Sander & Joung, 2014). CRISPR has been used to functionally disrupt or knockout genes (McCarthy et al., 2022) and also to replace genes with selective markers, such as antibiotic resistance (Kariyawasam et al., 2022).

The identification of resistance mechanisms in related species would help to identify potential sources of resistance in the New Zealand kauri population, which could then be used in a selective breeding programme. Thus, it would be of particular interest to investigate the mechanisms by which other related gymnosperms are able to escape infection by *P. agathidicida*. For example, *Agathis robusta* (Queensland kauri) does not appear susceptible to *P. agathidicida*, as three months after inoculation, no *P. agathidicida* was recovered from *A. robusta* roots (Bellgard et al., 2013). This suggests the possibility that *A. robusta* may harbor immune receptors capable of recognising and mounting a plant defence response against *P. agathidicida* effectors which prevent pathogenicity. While it is of interest that *N. benthamiana* produces an immune receptor, RXEG1 (Wang et al., 2018), that is capable of eliciting plant cell death in response to *P. agathidicida* GH12 proteins (Wang et al., 2018), current evidence does not suggest that this alone would contribute to *P. agathidicida* resistance in kauri. *P. agathidicida* has been shown capable of infecting *N. benthamiana*, thus there are likely other effectors capable of suppressing the *N. benthamiana* GH12-induced defence response.

To my knowledge, few studies have investigated the role of a collection of different GH families as broadly, instead focusing on one or two families of interest. Therefore, it was a little surprising that of the more than 40 different proteins investigated, belonging to 15 different GH families (as well as the other carbohydrate-related and hypothetical proteins), only one family, the GH12 proteins, triggered a reliable cell death response. Multiple families of GH proteins which are involved in pathogen virulence or elicit a necrotic cell death response have been identified in several fungal phytopathogens, including proteins belonging to the GH10 and GH17 families of *Cladosporium fulvum* (Ökmen et al., 2019, Ökmen et al., 2013), the GH10 and GH12 families of *Fusarium oxysporum* (Pareja-Jaime et al., 2008, Roldan-Arjona et al., 1999, Zhang et al., 2021c) and GH10, GH11, GH12, GH28 and GH93 families in the related *Fusarium graminearum* (Hao et al., 2019, Ma et al., 2015b, Moscetti et al., 2015, Paccanaro et al., 2017, Sella et al., 2013, Tundo et al., 2015, Tundo et al., 2021). A similar story is told in oomycete pathogens with GH10, GH12, and GH16 families in *P. parasitica* (Chang et al., 2015, Lai & Liou, 2018, Ma et al., 2015b, Ma et al., 2017) and GH7 and GH12 families in *P. sojae* (Ma et al., 2015b, Ma et al., 2017, Tan et al., 2020). That more *P. agathidicida* proteins were not identified that consistently elicited a cell death response may suggest that other *P. agathidicida* GH proteins do not elicit a cell death response, or that the appropriate recognition receptors or substrates are not present in *N.*

benthamiana or *N. tabacum.* It could also be that the GH proteins selected for analysis were studied in isolation, and that in fact two or more proteins work synergistically to elicit a cell death response. For many phytopathogens, it is likely only a matter of time before other GH proteins are identified which elicit plant cell death.

Several *P. agathidicida* GH28 family members (Pa|010674 and Pa|010677), primarily predicted to act as polygalacturonases, elicited weaker and less consistent cell death responses in *N. benthamiana* (**Figure 3.4**). So far, the Responsiveness to *Botrytis* PolyGalacturonases (RBPG1) receptor has only been identified in some *Arabidopsis* accessions and has not been identified in *N. benthamiana* (Zhang et al., 2014a). In line with this, while the *Botrytis cinerea* BcPG2 protein was found to trigger cell death in *N. benthamiana*, this was dependent upon enzymatic activity (Joubert et al., 2007, Kars et al., 2005). These results suggested that, in the *N. benthamiana* system, BcPG2 releases oligogalacturonides that act as DAMPs rather than the BcPG2 protein being directly recognised, once again illustrating the importance of investigating putative effectors in the context of the native pathosystem. Due to the lack of consistency observed in response to expression of Pa|010674 and Pa|010677 *in planta*, the potential cell death and enzyme activity of these GH28 proteins was not investigated further. It is important to note that a weak cell death/chlorotic response is still a response. While weak cell death or chlorotic responses are often overlooked, as is the case here, because they are difficult to distinguish and may present as inconsistencies. Perhaps it should then be asked whether the expression of these proteins result in biochemical/gene expression changes in the host that are not observed as cell death. Thus, it would be of interest to investigate whether **a)** plant cell death is observed in response to ATTAs with these proteins (and others such as the pectinesterase, CBELs, and Pa|003260 hypothetical protein) under natural light conditions, **b)** whether there are changes in host gene expression, particularly with a focus on known plant defence genes, in response to protein expression, and **c)** whether any biochemical changes, such as production of ROS, ethylene, or NO occur in response to expression of these proteins *in planta*.

During this study, Western blots were used as a relatively cheap and efficient method to determine whether ATTAs had been successful in expressing the protein of interest. However, many of the bands observed differed from the expected size of the protein. In many cases this is likely due to post-translational modifications such as N-glycosylation or phosphorylation in the ER-Golgi pathway, but it could also be due to the formation of protein multimers (e.g., if doublets are observed). In some cases, proteins were not able to be identified via Western blot, either because no bands, or non-specific bands, were observed. Where this was the case for a protein that triggered a cell death response, the cell death itself was evidence the protein of interest was being produced. Because infiltrated leaf material for Western blots was harvested from leaves 48 hours after ATTAs were performed, leaves infiltrated with cell death elicitors were beginning to show signs of decay. Therefore, it could be that the dying cells

were unable to produce protein anymore or that the protein was being degraded. To remedy this, some leaves containing cell death elicitors were harvested at 24 hpi, which may have been too early for sufficient protein production to occur. For several proteins, non-specific banding patterns were observed, i.e., they did not correspond to the expected protein size. This could be caused by an antibody concentration that is too high, or insufficient blocking. Given time, Westerns blots that resulted in non-specific banding could be repeated with longer washing steps, and a decrease in antibody concentration. Alternatively, liquid chromatography-mass spectrometry analysis on apoplastic wash fluid of *N. benthamiana* leaves expressing the protein of interest would also serve to demonstrate that the protein of interest was being produced and secreted to the apoplast.

To conclude, of the *P. agathidicida* genes selected in this study, only those encoding proteins belonging to the GH12 family were found to trigger a cell death response in the model plant species *N. benthamiana* and *N. tabacum*. Cell death responses were capable of being supressed, at least in part, by the *P. agathidicida* cytoplasmic RxLR40 effector protein. It is also likely that in addition to the observed cell death response, recognition of the cell death-eliciting GH12 proteins results in a plant immune response at a molecular level, including the upregulation of plant defence genes, which would serve to prevent subsequent pathogen infection. RNA sequencing data has shown that expression of genes encoding GH12 cell death elicitors peaked at different points during *P. agathidicida* infection of kauri, suggesting that they may have different roles during host colonisation. Despite these findings, there are still many unknowns when it comes to the molecular basis of the interaction between *P. agathidicida* and kauri. The next chapters explore this interaction further, investigating changes in the composition of kauri apoplastic wash fluid to identify resources utilised by *P. agathidicida* and the proteins involved in their harvest, asking what *P. agathidicida* proteins are being produced and whether liquid media are suitable for the production and identification of pathogen effector proteins.

Chapter four: Analysis of metabolite changes in kauri leaf apoplastic wash fluid in response to inoculation with *Phytophthora agathidicida*.

4.1 Introduction

It is currently unknown what metabolites of kauri or *Phytophthora agathidicida* are produced, utilized or depleted during the interaction between these organisms. Such information would provide a greater understanding of how these organisms interact on a molecular level. As a starting point to investigate this knowledge gap, the work described in this chapter set out to ask whether *P. agathidicida* alters the composition of metabolites present in the kauri leaf apoplast during infection. Of particular interest were changes in carbohydrates which may be targeted by *P. agathidicida* as a source of nutrition. This in turn could allow the identification of *P. agathidicida* CAZymes which may be involved in this process, thus providing a link to the earlier chapter investigating the role of *P. agathidicida* CAZymes in virulence and pathogenicity.

Proton **n**uclear **m**agnetic **r**esonance (^{1}H NMR) is a highly reproducible, quantitative, and non-destructive method that can be used to detect proton-containing chemical compounds in complex biological samples (Deflorio et al., 2012, Markley et al., 2017). Briefly, this method exposes the sample to an external magnetic field and then, on applying a radio frequency which serves to excite the protons, flips them into a higher spin state. Upon returning to the lower spin state, the energy released by the protons is transformed and interpreted as a signal. Each molecule gives a unique spectrum of signals, and the intensity of this spectrum, read as the height of the peak, is proportional to the molar concentration. In this way, molecules can be identified, and changes in the molar concentration of these molecules can be monitored.

Such a method is highly applicable to plant–microbe interactions, where metabolites produced by the plant or microbe can be identified and quantitatively monitored over an infection time-course to assess whether changes occur in response to the stress/treatment being tested. For example, ^{1}H NMR has been used to investigate metabolomic differences between clones of Sitka spruce (*Picea sitchensis*) showing different levels of susceptibility to the white rot fungus *Heterobasidion annosum* sensu stricto (Deflorio et al., 2012). While no conclusive differences were identified between clones, metabolomic differences were observed in response to the inoculation of *P. sitchensis* with *H. annosum* in sapwood (lower levels of all metabolites) compared to bark (higher peaks observed in the aromatic region (6–9 ppm)) (Deflorio et al., 2012). ^{1}H NMR has also been used to investigate plant resistance to insect pests. By comparing

the metabolome of chrysanthemums (*Dendranthema grandiflora*) which were resistant or susceptible to thrips (*Frankliniella occidentalis*), higher concentrations of two phenylpropanoids (chlorogenic acid and feruloyl acid) were found in the resistant chrysanthemums (Leiss et al., 2009b). Subsequent thrip feeding assays further confirmed that chlorogenic acid is involved in chrysanthemum resistance to thrips (Leiss et al., 2009b).

Due to the cultural agreements in place at the time, this experiment could not be performed on infected kauri roots or leaves and was instead conducted *in vitro*, by inoculating *P. agathidicida* into kauri **a**poplastic **w**ash **f**luid (AWF) harvested from leaf tissue, with subsequent analysis by ^{1}H NMR. More specifically, this study used an exploratory metabolic fingerprinting approach which, rather than focusing on particular peaks, simplified the entire spectrum into 'buckets' to both reduce the complexity of the data and generate a smaller set of variables (Sousa et al., 2013). Multivariate analysis was then used to find buckets that were significantly different to help identify which metabolites may be relevant to the molecular interaction between kauri and *P. agathidicida* (Deborde et al., 2017).

4.2 Methods

4.2.1 Biological materials

Oomycete and plant material used in this chapter are listed in **Table 4.1**.

Table 4.1. Oomycete and plant material.

Organism	Characteristics	Native location	Reference
Oomycete			
Phytophthora agathidicida	NZFS 3770	Great Barrier Island (Ngati Rehua), New Zealand	Guo et al. (2020a)
Plant material			
Agathis australis[a]	MW8-E[b]	Waipoua Forest, New Zealand	This study
A. australis	MW8-G	Waipoua Forest, New Zealand	This study
A. australis	MW8-H	Waipoua Forest, New Zealand	This study
A. australis	MW8-M	Waipoua Forest, New Zealand	This study
A. australis	MW8-N	Waipoua Forest, New Zealand	This study

[a]Special thanks to Taoho Patuawa and Te Roroa for allowing access to kauri saplings from the Scion Healthy Trees Healthy Future programme.

[b]Each letter refers to the seed cones collected from a single tree.

4.2.2 Media

All media used in this chapter are described in **Appendix 3.3**.

4.2.3 Growth conditions

4.2.3.1 *Agathis australis* (kauri)

Agathis australis (kauri) saplings (approximately two years old) were obtained from Scion, having been germinated from seed and exposed to sheltered but otherwise natural conditions in Rotorua, New Zealand, with regular access to water. Seed was obtained from Waipoua Forest as part of the Healthy Trees, Healthy Futures research programme in partnership with Te Roroa, who have cultural authority over this germplasm. Kauri saplings from five different family lines were obtained, each family line representing seed collected from a single mature kauri tree. In Palmerston North, New Zealand, kauri were initially housed in a plant growth room, with a 12 h:12 h light:dark setting and watered regularly on an as-needed basis. Due to the COVID-19 pandemic, they were temporarily moved to an outside

location in Pahiatua, New Zealand, exposed to natural conditions and watered as required. As soon as possible, the kauri were moved back to Palmerston North, where they were kept in a covered greenhouse. As such, the light source and temperatures were natural. Although temperature fluctuated less than outside conditions, there was little exposure to wind, and regular watering.

4.2.3.2 *Phytophthora agathidicida*

P. agathidicida NZFS 3770 (hereafter referred to as *P. agathidicida* 3770), previously purified from a single zoospore in our lab, was initially sub-cultured onto cornmeal selective agar (containing 250 µg/mL (w/v) ampicillin, 10 µg/mL (w/v) rifampicin, 10 µg/mL (w/v) pimaricin, and 100 µg/mL (w/v) pentachloronitrobenzene). Subculturing for active growth was carried out on clarified V8 agar. Sub-culturing for subsequent inoculation into liquid media was carried out on clarified V8 agar with cellophane membranes, where small agar pieces containing *P. agathidicida* were placed in the middle of cellophane membrane discs (~1 cm diameter). Cellophane membranes that had been completely covered in *P. agathidicida* mycelia were used to inoculate liquid media. All *P. agathidicida* growth was conducted at 22°C in the dark, with growth on solid media over 3–5 days, while growth in liquid media was over 10 days. For long-term storage*, P. agathidicida* 3770 grown on V8 agar as above was diced into small pieces and inoculated into 1.5 mL tubes containing sterile water; these water stocks were maintained at 22°C in the dark for several months.

4.2.4 Harvesting kauri leaf apoplastic wash fluid

Kauri, grown as previously described (**section 4.2.3.1**), were watered approximately 24 h prior to AWF extraction from leaves. Kauri leaves were removed from the plant at the petiole and injected just below the abaxial or adaxial surface with sterile water using an 0.5 ml syringe with needle (0.33 x 13 mm) (Terumo, Tokyo, Japan) until a dark colour change was observed, indicating the leaf apoplast was saturated. Leaves were then blotted dry and placed in a 50 mL Falcon tube (Fisher Scientific, Waltham, Massachusetts, USA) lined with a nappy liner, so that they were not sitting in the bottom of the tube. The Falcon tubes containing the kauri leaves were centrifuged at 1,000 x *g* for 20 min at 4°C to collect AWF.

4.2.5 Carbohydrate usage analysis

4.2.5.1 Growth of *P. agathidicida* in kauri leaf apoplastic wash fluid

To obtain enough volume of leaf AWF for the experiment, AWF from several kauri trees belonging to the same family group was pooled to create one biological replicate (2–3 mL kauri leaf AWF). A total of four biological replicates were generated from each of the five family groups of kauri (MW8-E,

MW8-G, MW8-H, MW8-M, MW8-N). Each pooled AWF sample was filtered through a 0.2 µm filter (Ahlstrom-Munksjö, Helsinki, Finland), and a 300 µl aliquot (time zero (T0) sample) taken and mixed with an equal volume of NMR buffer (0.1 mol/L phosphate buffer (supplied by Laura Raymond, Scion; L.R.), pH 7, containing 10% (w/v) DMSO, 0.2% (w/v) NaN_3, and 0.05% (w/v) sodium 3-trimethylsilylpropanoate (TSP)), then stored at –80°C. The remaining filtered AWF from each sample was split between two 15 mL Falcon tubes, one of which was inoculated with a cellophane membrane disc covered in *P. agathidicida* 3770 mycelia taken from clarified V8 agar, while the other was mock-inoculated with a sterile cellophane membrane disc which had also been in contact with clarified V8 agar. Both inoculated and mock-inoculated samples were incubated at 22°C, 180 rpm (C10 platform shaker, New Brunswick Scientific, Enfield, Connecticut, USA), in the dark. At 24 h and 10 days post-inoculation, 300 µL samples of AWF (inoculated and mock-inoculated) were taken, mixed with an equal volume of NMR buffer, and stored at –80°C. Once samples had been acquired for all five of the available kauri family groups, they were sent to L.R. at Scion (Rotorua, New Zealand) on dry ice for further analysis.

4.2.5.2 NMR data acquisition from samples

Carried out by L.R.

- The frozen samples were warmed to room temperature and transferred to 5 mm borosilicate NMR tubes for analysis. One dimensional ^{1}H NMR spectra of the kauri leaf AWF in buffer were acquired on a Bruker Avance III 400 NMR fitted with a 5 mm Prodigy BBO cryoprobe (Bruker, Switzerland) operating at a ^{1}H frequency of 400.13 MHz. A standard Bruker "noesygppr1d" pulse sequence with water suppression achieved by application of a 25 Hz presaturation field at a transmitter frequency offset (o1) of 1881.10 Hz was used. The internal probe temperature was set to 300 K with a 5-min temperature stability delay. The spectral data were obtained in 65 K data points, a relaxation delay of 8 sec and 512 scans. The spectra were then Fourier transformed, phased and baseline corrected, and all spectra were calibrated relative to TSP resonance at 0.00 ppm.

4.2.5.3 Multivariate and statistical analysis

Carried out by L.R.

- The resulting spectra were used for untargeted secondary metabolite fingerprinting by 'bucketing' the spectra from 0.00 to 10.00 parts per million (ppm), with a bucket size of 0.04 ppm using AMIX software (Bruker, Germany). Bucketed data were normalised to total intensity then evaluated using principal component analysis (PCA) with a pareto scaling

method using SIMCA 16 software (Sartorius Stedim Data Analytics AB, Sweden) to obtain the maximum variation between the samples and to reduce complexity of the NMR spectra. A two-tailed Mann–Whitney U test ($P < 0.05$) was carried out on key buckets identified by PCA using Microsoft Excel for Office 365.

Carried out by E.B.

- A two-tailed Mann-Whitney U test ($P < 0.05$) was carried out on all normalised spectral buckets. Buckets with statistically significant differences between *P. agathidicida*-inoculated or mock-inoculated (control) samples at either 24 h or 10 days post-inoculation in three or more kauri family lines were selected for further analysis. The values of replicate samples were averaged, and these were graphed for each selected bucket using Microsoft Excel version 2018.

4.3 Results

Disclosure: Initial analysis of the NMR data presented in this section (**Section 4.3**) was carried out by Laura Raymond (L.R.) (Scion), and subsequently re-analysed by Ellie Bradley (E.B., author). As such, all PCAs and the associated loading plots (**Figure 4.1–4.6**) were performed, and figures provided, by L.R. Where possible, text relating to the aforementioned figures was by E.B. Selection and analysis, including figures, of the statistical relevance of spectral buckets was carried out by E.B. A copy of the report '^{1}H NMR screening of the second trial of kauri apoplastic fluid inoculated with *P. agathidicida*' provided by L.R. is available upon request.

During analysis of the ^{1}H NMR data, L.R. used an in-house database to identify a few key metabolites which included sucrose and glucose as well as shikimic and quinic acid, compounds which are associated with plant defence (Santos-Sánchez et al., 2019, Volpi e Silva et al., 2019). As the carbohydrate region (3–5 ppm) was considerably overlapped, identifying other carbohydrates proved difficult.

4.3.1 Time zero

Kauri leaf AWF passed through a 0.2 µm filter, but uninoculated, was the time zero (T0) sample. A PCA score plot of the T0 sample (**Figure 4.1**) showed that 77.0% of the variance was explained by four principal components (PCs), with 37.7% of the variance explained by PC1 and a further 16.3% of the variance explained by PC2. However, this prediction was not particularly reliable as it had a Q^2 (cum) value of only 0.234. Q^2 values provide an estimate of how reasonable the prediction is, but in metabolomics, only a $Q^2 > 0.5$ is considered acceptable (Triba et al., 2015). **Figure 4.1** shows considerable variation in the metabolite profile of kauri leaf AWF, even within family groups. The loadings plot (**Figure 4.2**) helped to describe how much each characteristic (in this case 'bucket') affected a PC, such that characteristics clustered near the origin of PC1 and PC2 had little effect on the PCs, while those further away (e.g. 3.7 ppm or 3.94 ppm) had a stronger effect. Consequently, the loadings plot showed that many of the key spectral buckets which may be responsible for driving the differences between kauri family lines were from the carbohydrate range (3–5 ppm), including sucrose at 5.42 ppm, as well as plant defence pathway compounds shikimic acid (6.46 ppm) and quinic acid (2.06 ppm). Ultimately, no clear differences were observed between the different family lines in the T0 samples.

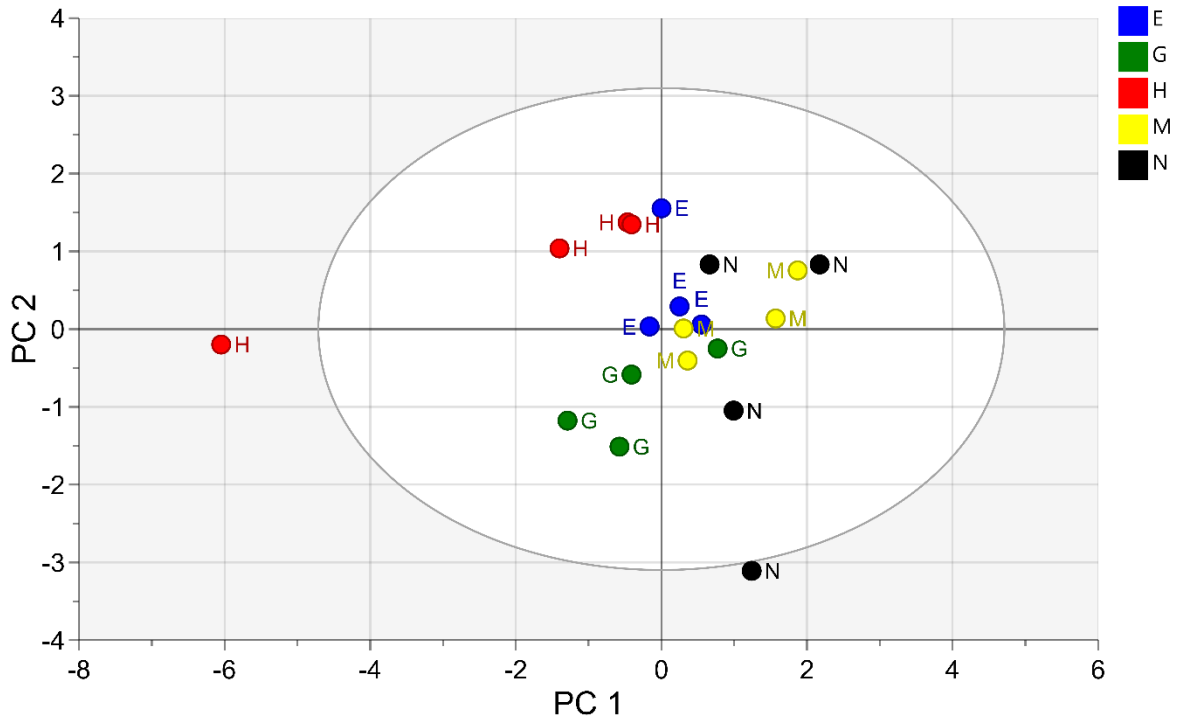

Figure 4.1. Principal component analysis (PCA) score plot (PC1 vs. PC2) of the time zero (T0) kauri leaf apoplastic wash fluid (AWF) proton nuclear magnetic resonance (1H NMR) dataset.

Kauri leaf AWF was harvested from five different family lines (E, blue; G, green; H, red; M, yellow; and N, black) using the infiltration-centrifugation method. To generate enough volume, several trees belonging to the same family line were pooled to give one biological replicate. A total of four biological replicates were used for each of the five family lines. Four components explained 77.0% of the variance (Q2 (cum) 0.234). The Hotelling's T2 ellipse is shown with a 95% confidence interval.

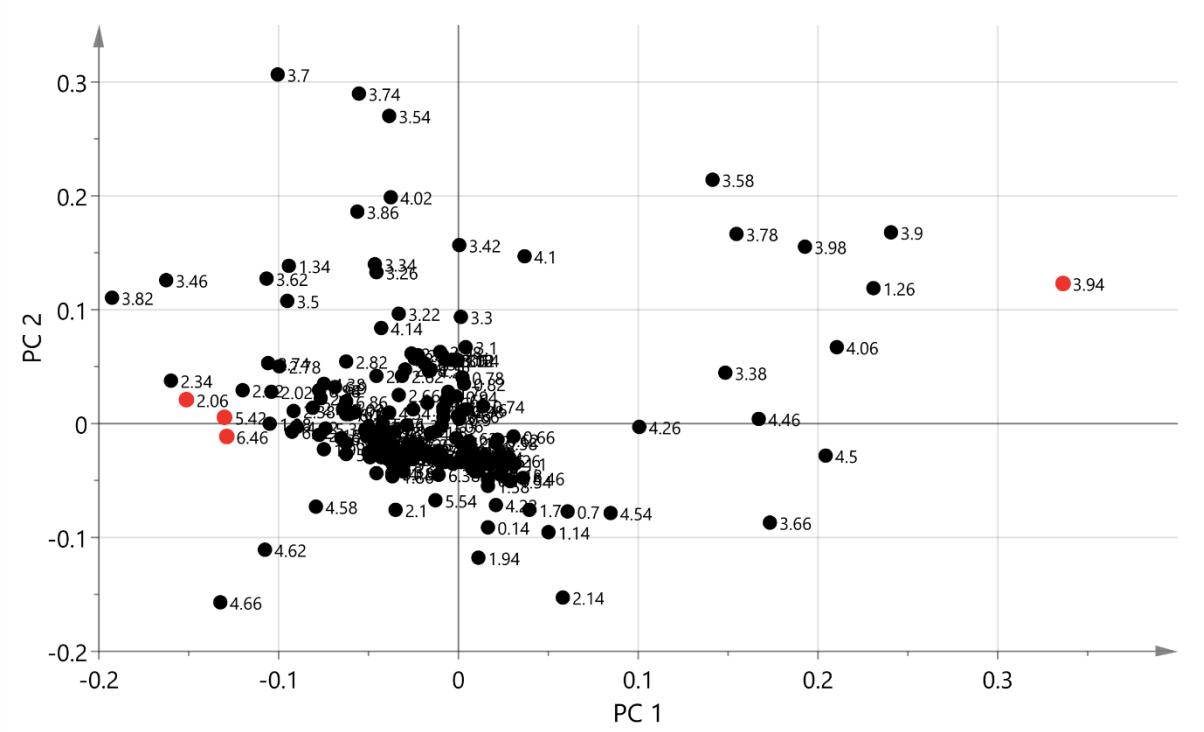

Figure 4.2. Principal component analysis (PCA) loadings plot of the time zero (T0) kauri leaf apoplastic wash fluid (AWF) proton nuclear magnetic resonance (^{1}H NMR) dataset.

Spectral buckets which may explain the variation observed in the T0 PCA score plot include many from the carbohydrate region 3–5 ppm, including sucrose (5.42 ppm). Other buckets which may be driving variation include shikimic (6.46 ppm) and quinic (2.06 ppm) acid, as well as many others which have not been identified (e.g., 3.94). Buckets mentioned in this legend are highlighted in red.

4.3.2 24 h post-inoculation

Filtered kauri leaf AWF was inoculated with either cellophane membranes (mock-inoculated control) or *P. agathidicida* mycelia grown on cellophane membranes. Samples were taken for NMR analysis 24 h post-inoculation (T24h). A PCA of the T24h dataset (**Figure 4.3**) found 92.5% of the variance (Q^2 (cum) 0.629) was explained by nine components, with PC1 describing 25.1% and PC2 describing 19.6% of the variance. The loadings plot (**Figure 4.4**) was similar to the T0 loadings plot, in that the key drivers of the variation appear to be buckets which included the two identified plant defence pathway components, shikimic (6.46 ppm) and quinic (2.06 ppm) acid, as well as buckets from the overlapped carbohydrate region including both glucose (5.22 ppm) and sucrose (5.42 ppm). Interestingly, while the untreated kauri leaf AWF from family G was clustered with other inoculated and non-inoculated samples, the *P. agathidicida*-inoculated samples of this same family clustered away from the other samples. This suggests that a difference in metabolite profile has occurred in this family. However, there were no clear differences observed between the remaining kauri families, or between different treatments, at T24h.

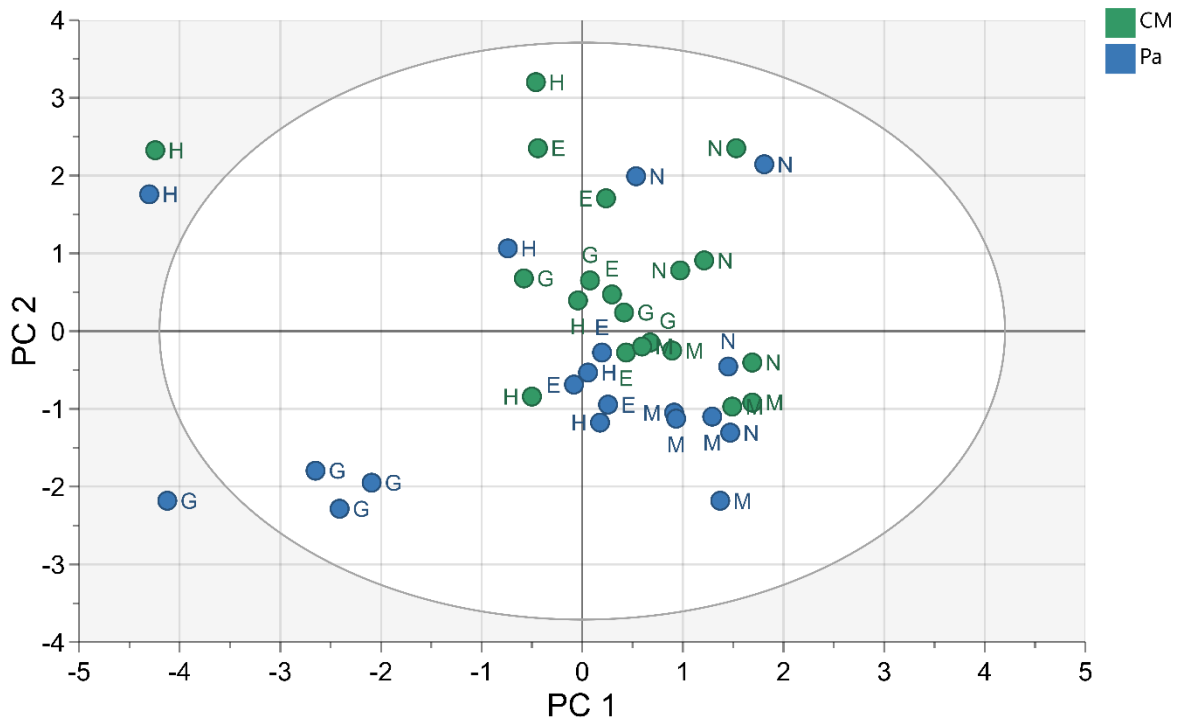

Figure 4.3. Principal component analysis (PCA) score plot (PC1 vs. PC2) of the time 24 h (T24h) kauri leaf apoplastic wash fluid (AWF) proton nuclear magnetic resonance (1H NMR) dataset.

Kauri leaf AWF was harvested from five different family lines (E, G, H, M, and N) using the infiltration-centrifugation method, with several trees belonging to the same family line pooled to give one biological replicate. A total of four biological replicates were used for each of the five family lines. AWF was filtered through a 0.2 µm filter and inoculated with either cellophane membranes (negative control; CM, green) or *Phytophthora agathidicida* mycelia grown on cellophane membranes (Pa, blue). Samples were taken for 1H NMR analysis 24 h post-inoculation (hpi). A PCA was performed on the T24h dataset using SIMCA 16 software. Nine components explained 92.5% of the variance (Q2 (cum) 0.629). The Hotelling's T2 ellipse is shown with a 95% confidence interval. One of the replicates of *P. agathidicida* inoculated into kauri leaf AWF extracted from family 'E' has not been included as the acquired data were not satisfactory.

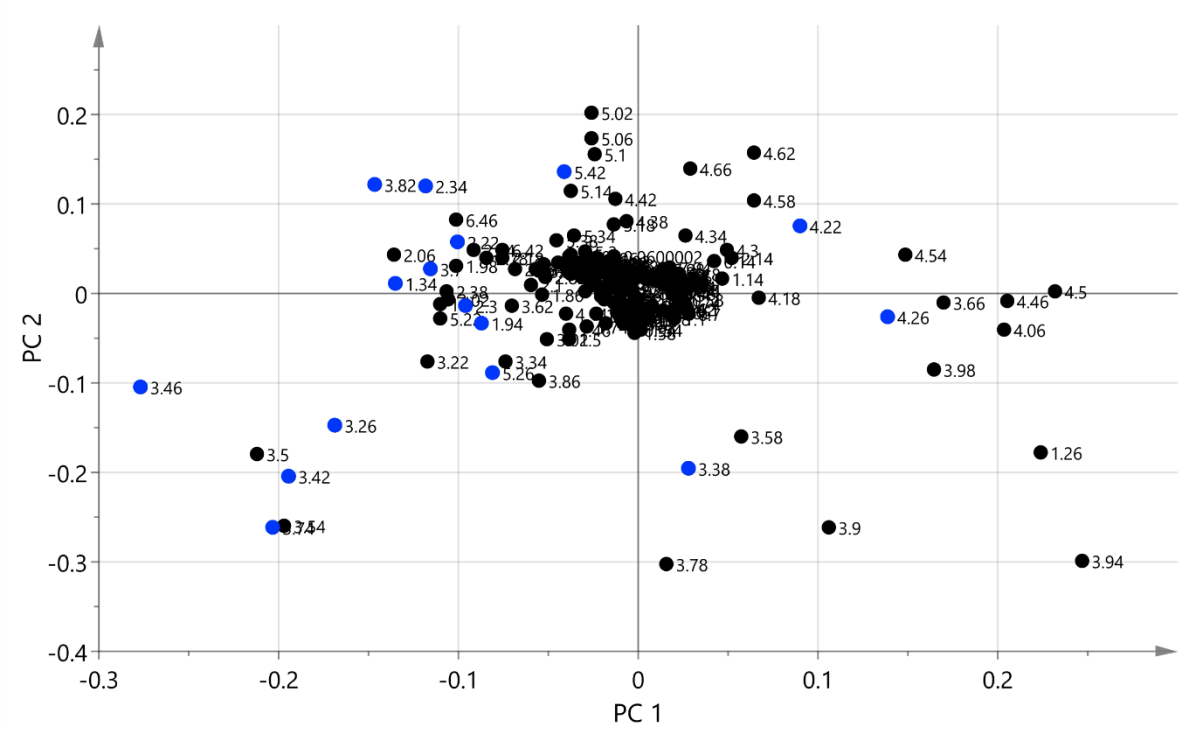

Figure 4.4. Principal component analysis (PCA) loadings plot of the *Phytophthora agathidicida* time 24 h (T24h) kauri leaf apoplastic wash fluid (AWF) proton nuclear magnetic resonance (^{1}H NMR) dataset.

Spectral buckets which drive the variation observed in the T24h PCA score plot include many from the carbohydrate region 3–5 ppm, including both sucrose (5.42 ppm) and glucose (5.22 ppm). Other buckets which may be driving variation include shikimic (6.46 ppm) and quinic (2.06 ppm) acid. Samples were taken for ^{1}H NMR analysis at 24 h post-inoculation (hpi). Points highlighted in blue are discussed in **section 4.3.4**.

4.3.3 Ten days post-inoculation

A final sample of kauri leaf AWF inoculated with *P. agathidicida* or cellophane membranes (negative control) was taken 10 days post-inoculation (T10d). A PCA of the T10d dataset (**Figure 4.5**) showed a subtle but clear distinction between *P. agathidicida*-inoculated samples and controls. Seven components explained 85.7% of the variance (Q^2 (cum) 0.534), with 28.3% described by PC1 and a further 16.6% described by PC2. The corresponding loadings plot (**Figure 4.6**), similar to both the T24h and T0 datasets, illustrated that the key drivers of the variation detected in the T10d dataset were spectral buckets from shikimic and quinic acid as well as the overlapped carbohydrate region. However, as sucrose (5.42 ppm) was not identified, it is likely it is with the mass of spectral buckets that are clustered around the origin, suggesting it is not responsible for driving the variation observed between *P. agathidicida*-inoculated samples and controls at this time point.

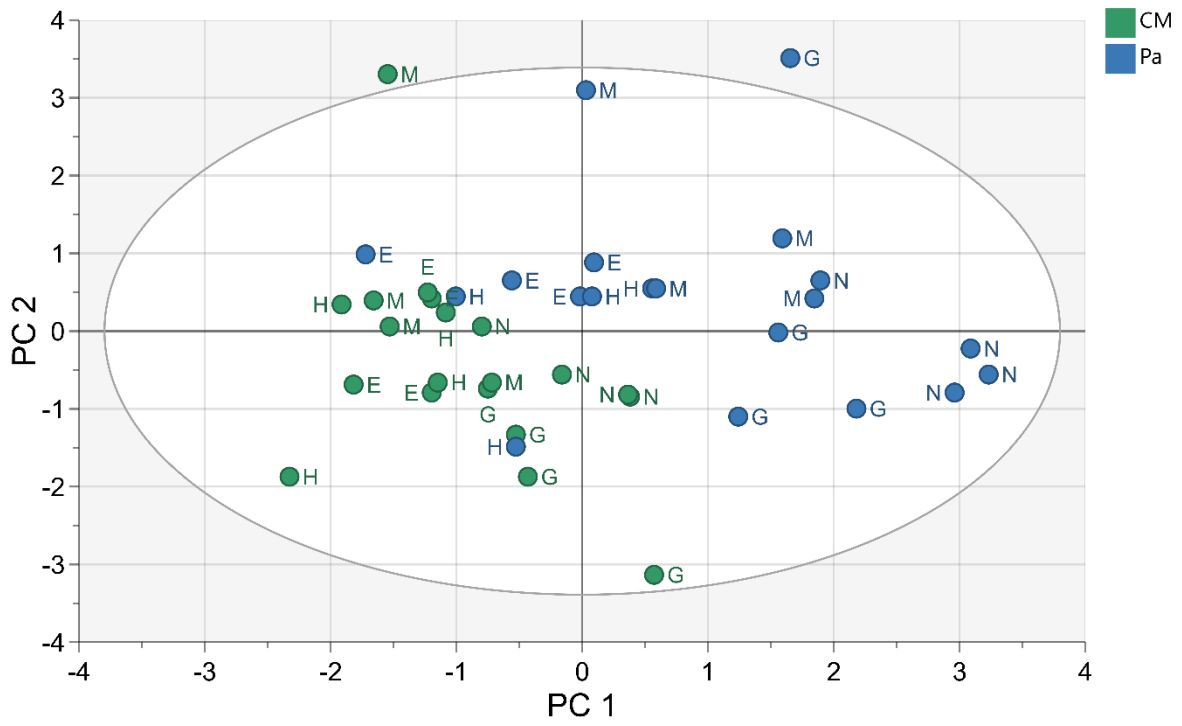

Figure 4.5. Principal component analysis (PCA) score plot (PC1 vs. PC2) of the *Phytophthora agathidicida* (Pa) time 10-day (T10d) kauri leaf apoplastic wash fluid (AWF) proton nuclear magnetic resonance (^{1}H NMR) dataset.

Kauri leaf AWF was harvested from five different family lines (E, G, H, M, and N) using the infiltration-centrifugation method, with several trees belonging to the same family line pooled to give one biological replicate. A total of four biological replicates were used for each of the five family lines. AWF was filtered through a 0.2 µm filter and inoculated with either cellophane membranes (negative control, CM, green) or *P. agathidicida* (Pa) mycelia grown on cellophane membranes (Pa, blue). Samples were taken for ^{1}H NMR analysis at 10 d post-inoculation (dpi). A PCA was performed on the T10d dataset using SIMCA 16 software. Seven components explained 85.7% of the variance (Q^2 (cum) 0.534). The Hotelling's T2 ellipse is shown with a 95% confidence interval.

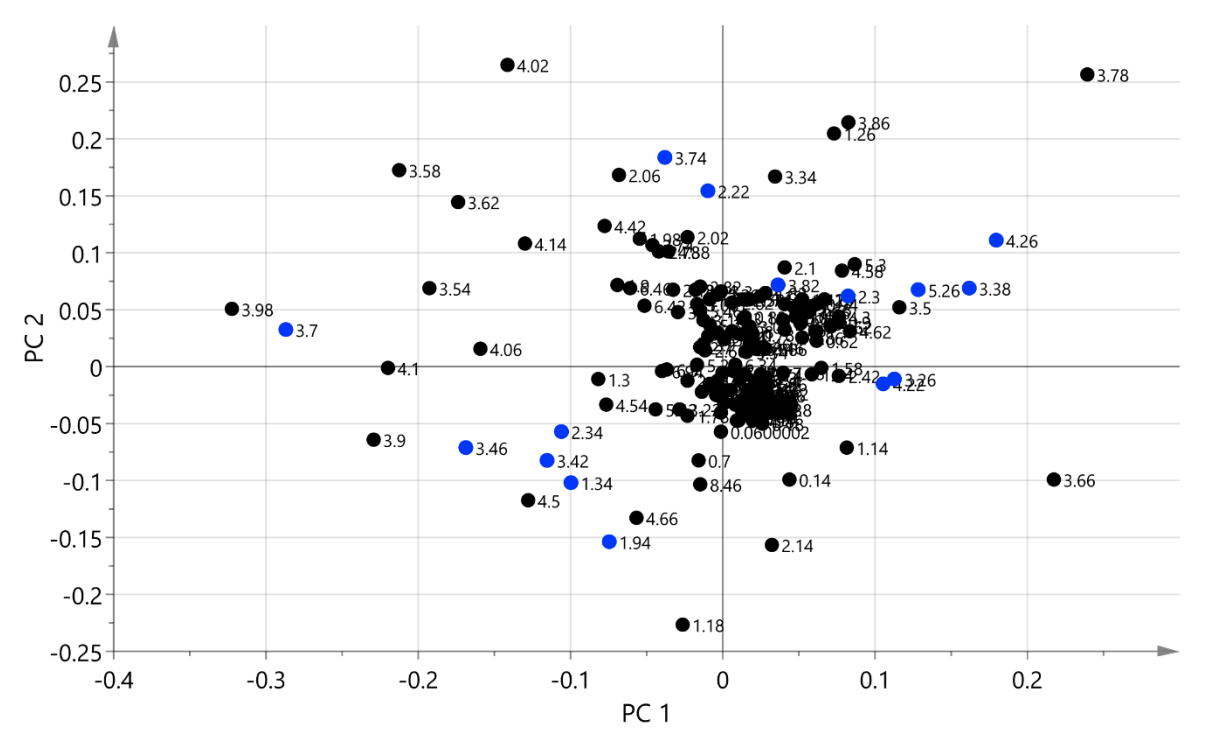

Figure 4.6. Principal component analysis (PCA) loadings plot of the *Phytophthora agathidicida* time 10-day (T10d) kauri leaf apoplastic wash fluid (AWF) proton nuclear magnetic resonance (^{1}H NMR) dataset.

Spectral buckets driving the variation observed in the T10d PCA score plot include many from the carbohydrate region (3–5 ppm), as well as shikimic (6.46 ppm) and quinic (2.06 ppm) acid. Samples were taken for ^{1}H NMR analysis at 10 days post-inoculation (dpi). Points highlighted in blue are discussed in **section 4.3.4**.

4.3.4 Selected key spectral buckets

Overall, there were very few changes detected in kauri leaf AWF inoculated with *P. agathidicida* 3770 compared to the negative controls which were inoculated with cellophane membrane discs. In fact, only 22 of the 199 spectral buckets which covered 0.06–7.98 ppm were identified as having considerable or substantial differences between controls and *P. agathidicida*-inoculated samples at either 24 hpi or 10 dpi in three or more of the kauri family lines. Considerable or substantial differences are defined as differences which were significant when performing a two-tailed Mann–Whitney U test ($P < 0.05$), though the threshold for significance was lost when adjusting for the false discovery rate. Furthermore, upon manual investigation, only 17 of the 22 identified significant spectral buckets appeared to present consistent results (**Table 4.2**). Unsurprisingly, many of the 17 selected spectral buckets were identified as drivers of the differences observed in the PCA models, as shown by their corresponding loadings plot. In the loadings plot for the T24h dataset (**Figure 4.4**), it was only the bucket at 1.38 ppm, which was not detectable and thus must be clustered around the origin, that did not appear to be a driver, and in the T10d dataset (**Figure 4.6**), neither buckets at 5.42 ppm nor at 1.38 ppm appeared to be drivers of the differences that were observed. Four main observations summarise these results:

- In buckets 3.70 ppm, 3.46 ppm, 3.42 ppm, 1.94 ppm, and 1.34 ppm, little to no change in signal was observed in the controls; however, a decrease in signal was observed in *P. agathidicida*-inoculated samples (**Table 4.2**, **Figure 4.7**).

- In buckets 4.26 ppm, 2.30 ppm, 2.22 ppm, and 1.38 ppm, little to no change was observed in the controls, but an increase in signal was observed in *P. agathidicida*-inoculated samples (**Table 4.2**, **Figure 4.7**).

- In buckets 5.42 ppm, 4.22 ppm, 3.82 ppm, and 2.34 ppm, an overall decrease in signal was observed by 10 dpi in both controls and *P. agathidicida*-inoculated samples. However, this decrease was observed earlier, at 24 hpi, in *P. agathidicida*-inoculated samples (**Table 4.2**, **Figure 4.7**).

- In buckets 3.74 ppm, 3.38 ppm, and 3.26 ppm, an overall increase in signal was observed by 10 dpi in both controls and *P. agathidicida*-inoculated samples. However, in *P. agathidicida*-inoculated samples, this increase was observed earlier, at 24 hpi (**Table 4.2**, **Figure 4.7**).

A possible exception to these observations was bucket 5.26 ppm, where the initial increase in signal at 24 hpi was followed by a decline in signal at 10 dpi in *P. agathidicida*-inoculated samples. However,

despite the secondary decline, both control and *P. agathidicida*-inoculated samples had an increased signal at 10 dpi compared to T0 (**Table 4.2**, **Figure 4.7**).

General observations for each of the 17 selected buckets are below.

Table 4.2. Results of a two-tailed Mann-Whitney U test (P < 0.05) in selected spectral buckets from the kauri leaf apoplastic wash fluid (AWF) proton nuclear magnetic resonance (^{1}H NMR) dataset.

Kauri family	5.42 ppm[f]	5.26 ppm	4.26 ppm	4.22 ppm	3.82 ppm	3.74 ppm	3.70 ppm	3.46 ppm	3.42 ppm	3.38 ppm	3.26 ppm	2.34 ppm	2.30 ppm	2.22 ppm	1.94 ppm	1.38 ppm	1.34 ppm
T0[a] vs. T24h Pa[b]																	
E	0.001	0.115	0.657	0.000	0.001	0.112	0.263	0.032	0.007	0.233	0.010	0.034	0.544	0.234	0.569	0.310	0.790
G	0.000	0.000	0.007	0.000	0.001	0.000	0.186	0.001	0.001	0.000	0.001	0.004	0.001	0.599	0.010	0.559	0.411
H	0.064	0.016	0.527	0.020	0.047	0.122	0.168	0.854	0.393	0.428	0.017	0.478	0.959	0.500	0.816	0.117	0.933
M	0.000	0.001	0.303	0.041	0.001	0.008	0.076	0.645	0.328	0.051	0.002	0.003	0.562	0.169	0.565	0.798	0.716
N	0.000	0.386	0.078	0.003	0.003	0.999	0.016	0.035	0.056	0.210	0.176	0.001	0.268	0.017	0.006	0.097	0.561
T0 vs. T24h CM[c]																	
E	0.147	0.048	0.292	0.022	0.020	0.212	0.182	0.015	0.233	0.452	0.292	0.108	0.198	0.995	0.841	0.175	0.739
G	0.078	0.597	0.784	0.219	0.848	0.873	0.749	0.187	0.203	0.974	0.649	0.493	0.793	0.932	0.768	0.535	0.975
H	0.635	0.058	0.558	0.608	0.428	0.795	0.233	0.889	0.886	0.752	0.233	0.812	0.869	1.000	0.847	0.790	0.834
M	0.187	0.998	0.893	0.462	0.519	0.682	0.736	0.170	0.607	0.429	0.206	0.524	0.969	0.943	0.724	0.961	0.603
N	0.331	0.051	0.732	0.285	0.156	0.382	0.203	0.111	0.397	0.143	0.771	0.624	0.437	0.423	0.705	0.435	0.766
T0 vs. T10d Pa[d]																	
E	0.000	0.030	0.010	0.003	0.000	0.552	0.082	0.000	0.005	0.008	0.054	0.000	0.007	0.059	0.006	0.031	0.000
G	0.001	0.888	0.004	0.002	0.000	0.001	0.013	0.001	0.001	0.017	0.030	0.001	0.103	0.018	0.000	0.085	0.024
H	0.022	0.006	0.029	0.033	0.014	0.368	0.006	0.002	0.001	0.079	0.511	0.016	0.939	0.135	0.343	0.013	0.013
M	0.000	0.495	0.004	0.226	0.026	0.188	0.001	0.003	0.003	0.059	0.097	0.005	0.011	0.033	0.000	0.059	0.001
N	0.000	0.003	0.001	0.013	0.030	0.102	0.008	0.001	0.036	0.003	0.019	0.001	0.005	0.011	0.001	0.008	0.006
T0 vs. T10d CM[e]																	
E	0.001	0.053	0.459	0.002	0.000	0.181	0.614	0.301	0.494	0.125	0.454	0.001	0.404	0.402	0.520	0.449	0.204
G	0.000	0.018	0.889	0.008	0.003	0.252	0.498	0.674	0.060	0.194	0.000	0.008	0.340	0.973	0.019	0.256	0.951
H	0.025	0.923	0.169	0.009	0.011	0.211	0.136	0.083	0.364	0.607	0.613	0.115	0.690	0.656	0.367	0.533	0.139
M	0.007	0.718	0.309	0.033	0.004	0.108	0.747	0.128	0.001	0.032	0.024	0.019	0.752	0.921	0.020	0.866	0.653
N	0.001	0.934	0.794	0.002	0.014	0.818	0.206	0.123	0.631	0.606	0.033	0.006	0.559	0.506	0.067	0.313	0.796

Kauri family	5.42 ppm[f]	5.26 ppm	4.26 ppm	4.22 ppm	3.82 ppm	3.74 ppm	3.70 ppm	3.46 ppm	3.42 ppm	3.38 ppm	3.26 ppm	2.34 ppm	2.30 ppm	2.22 ppm	1.94 ppm	1.38 ppm	1.34 ppm
T24h Pa vs. T10d Pa																	
E	0.792	0.404	0.016	0.008	0.087	0.359	0.399	0.000	0.000	0.001	0.006	0.023	0.014	0.320	0.002	0.176	0.000
G	0.757	0.271	0.001	0.002	0.116	0.000	0.031	0.000	0.000	0.957	0.001	0.001	0.336	0.015	0.000	0.054	0.019
H	0.314	0.234	0.102	0.776	0.393	0.733	0.429	0.040	0.007	0.241	0.073	0.104	0.989	0.215	0.425	0.390	0.013
M	0.138	0.318	0.005	0.153	0.277	0.256	0.136	0.005	0.019	0.896	0.932	0.345	0.008	0.164	0.178	0.054	0.054
N	0.651	0.053	0.002	0.160	0.041	0.201	0.937	0.179	0.717	0.211	0.126	0.927	0.012	0.058	0.046	0.052	0.349
T24h CM vs. T10d CM																	
E	0.012	0.714	0.933	0.009	0.001	0.047	0.274	0.734	0.198	0.082	0.713	0.044	0.795	0.329	0.474	0.677	0.223
G	0.000	0.009	0.645	0.013	0.003	0.293	0.336	0.369	0.036	0.190	0.000	0.003	0.489	0.962	0.015	0.665	0.924
H	0.046	0.265	0.463	0.012	0.032	0.295	0.956	0.143	0.453	0.877	0.291	0.231	0.788	0.662	0.336	0.278	0.162
M	0.014	0.718	0.329	0.064	0.001	0.145	0.960	0.397	0.001	0.104	0.034	0.005	0.756	0.973	0.016	0.785	0.968
N	0.005	0.197	0.977	0.002	0.005	0.259	0.925	0.867	0.184	0.100	0.039	0.010	0.847	0.898	0.101	0.768	0.958
T24h Pa vs. T24h CM																	
E	0.007	0.207	0.767	0.001	0.000	0.021	0.957	0.003	0.013	0.162	0.016	0.293	0.286	0.214	0.822	0.890	0.562
G	0.000	0.000	0.003	0.000	0.001	0.000	0.036	0.001	0.001	0.000	0.001	0.001	0.002	0.636	0.008	0.220	0.423
H	0.135	0.361	0.916	0.027	0.148	0.252	0.606	0.943	0.395	0.602	0.060	0.630	0.902	0.517	0.734	0.133	0.895
M	0.000	0.002	0.323	0.083	0.000	0.003	0.058	0.382	0.424	0.091	0.002	0.001	0.621	0.148	0.634	0.804	0.906
N	0.002	0.152	0.023	0.003	0.003	0.506	0.061	0.151	0.147	0.096	0.211	0.001	0.866	0.132	0.003	0.334	0.580
T10d Pa vs. T10d CM																	
E	0.046	0.265	0.025	0.061	0.097	0.456	0.121	0.041	0.049	0.151	0.195	0.014	0.018	0.125	0.054	0.124	0.562
G	0.027	0.640	0.005	0.440	0.723	0.054	0.093	0.002	0.004	0.043	0.697	0.001	0.160	0.017	0.000	0.209	0.013
H	0.158	0.053	0.145	0.295	0.993	0.836	0.047	0.065	0.077	0.046	0.808	0.055	0.667	0.241	0.829	0.003	0.801
M	0.261	0.720	0.005	0.121	0.882	0.726	0.002	0.000	0.000	0.268	0.777	0.003	0.006	0.033	0.000	0.011	0.001
N	0.036	0.001	0.001	0.108	0.258	0.121	0.021	0.000	0.012	0.004	0.124	0.004	0.007	0.015	0.001	0.036	0.003

[a]T0 = Kauri leaf apoplastic wash fluid (AWF) at time 0 (T0). Sample taken after filtration through 0.2 µm filter, but prior to inoculation.

[b]T24h Pa = Samples taken of kauri leaf AWF 24 hours after inoculation with *P. agathidicida* mycelia grown on a cellophane membrane.

[c]T24h CM = Samples taken of kauri leaf AWF 24 hours after inoculation with cellophane membranes (control).

[d]T10d Pa = Samples taken of kauri leaf AWF 10 days after inoculation with *P. agathidicida* mycelia grown on a cellophane membrane.

[e]T10d CM = Samples taken of kauri leaf AWF 10 days after inoculation with cellophane membranes (control).

[f]ppm = Parts per million.

Green = Substantial increase (from the earlier to the later time point, or from *P. agathidicida*-inoculated to mock-inoculated); Blue = Substantial decrease (from the earlier to the later time point, or from *P. agathidicida*-inoculated to mock-inoculated).

Table 4.3. Average percentage change in signal intensity observed in selected spectral buckets from the kauri leaf apoplastic wash fluid (AWF) proton nuclear magnetic resonance (^{1}H NMR) dataset.

	5.42 ppm[f]	**5.26 ppm**	**4.26 ppm**	**4.22 ppm**	**3.82 ppm**	**3.74 ppm**	**3.7 ppm**	**3.46 ppm**	**3.42 ppm**	**3.38 ppm**	**3.26 ppm**	**2.34 ppm**	**2.3 ppm**	**2.22 ppm**	**1.94 ppm**	**1.38 ppm**	**1.34 ppm**
T0[a] vs. T24h Pa[b]	-69.4	24.3	1.6	-13.6	-15.7	7.7	-6.1	4.1	6.9	7.7	88.1	-50.0	16.0	8.5	-3.6	7.7	15.9
T0 vs. T24h CM[c]	-11.5	1.3	1.2	-2.6	-4.1	-1.3	-2.2	-1.5	-1.7	-0.2	6.5	-9.0	6.8	0.7	0.7	4.5	-1.3
T0 vs. T10d Pa[d]	-78.4	9.0	20.8	-8.3	-15.2	4.8	-9.0	-18.3	-9.0	11.3	34.8	-76.7	63.7	29.7	-33.2	23.4	-54.2
T0 vs. T10d CM[e]	-62.7	3.9	2.6	-12.6	-15.5	3.3	-2.2	-4.0	2.9	3.4	30.2	-42.2	7.2	2.9	6.6	3.8	-18.2
T24h Pa vs. T10d Pa	-25.4	-10.6	19.3	6.3	0.7	-2.2	-3.1	-20.1	-13.5	3.5	-20.1	-42.7	44.6	19.7	-28.7	14.6	-59.3
T24h CM vs. T10d CM	-57.9	3.1	1.4	-10.2	-11.8	4.6	0.0	-2.5	4.7	3.6	22.8	-36.4	0.5	2.2	6.0	-0.7	-17.4
T24h Pa vs. T24h CM	204.0	-17.3	0.0	13.0	13.8	-8.0	4.3	-3.7	-6.4	-7.2	-35.7	117.7	-4.9	-6.9	8.4	-2.5	-11.6
T10d Pa vs. T10d CM	77.8	-0.9	-15.0	-4.6	-0.2	-1.4	7.5	17.4	13.1	-7.1	3.1	156.3	-27.6	-20.2	63.6	-15.6	79.2

[a]T0 = Kauri leaf apoplastic wash fluid (AWF) at time 0 (T0). Sample taken after filtration through 0.2 µm filter, but prior to inoculation.

[b]T24Pa = Samples taken of kauri leaf AWF 24 hours after inoculation with *P. agathidicida* mycelia grown on a cellophane membrane.

[c]T24CM = Samples taken of kauri leaf AWF 24 hours after inoculation with cellophane membranes (control).

[d]T10Pa = Samples taken of kauri leaf AWF 10 days after inoculation with *P. agathidicida* mycelia grown on a cellophane membrane.

[e]T10CM = Samples taken of kauri leaf AWF 10 days after inoculation with cellophane membranes (control).

[f]ppm = Parts per million.

Bucket 5.42 ppm (sucrose)

An average 69% decrease (**Table 4.3**) was observed in the signal of bucket 5.42 ppm (sucrose) in *P. agathidicida*-inoculated 24 hpi samples compared to controls at T0 (**Figure 4.7 A**). This difference was substantial (**Table 4.2**) in all families except H, although H still followed the same downwards trend. No such trend was observed in the T24h control samples. A substantial decrease was observed in all families in both *P. agathidicida*-inoculated and control samples at 10 dpi. Thus, while the signal of the 5.42 ppm bucket decreases over time, the decrease was observed earlier (24 hpi) in *P. agathidicida*-inoculated samples.

Bucket 5.26 ppm (glucose and unknown carbohydrate)

A slight (average 24% (**Table 4.3**)) but substantial increase in signal was observed in bucket 5.26 ppm in *P. agathidicida*-inoculated T24h samples for three (G, H, M) of the five families (**Figure 4.7 B**). The remaining two families (E and N) followed the same increasing trend, while no such trend was observed for the controls over the same period. However, the signal of the 5.26 ppm bucket decreased slightly in the *P. agathidicida*-inoculated samples at 10 dpi compared to those at 24 hpi. The overall increase in signal from T0 to T10d in *P. agathidicida*-inoculated samples was substantial in three families (E, H and N) (**Table 4.2**). No increase in signal was observed in the T24h control samples, though an increase in signal was observed in all families in the T10d control samples (**Appendix 4.1**). Kauri family 'M' was an anomaly in that an overall decrease in signal of the 5.26 ppm bucket was observed in both control and *P. agathidicida*-inoculated samples at 10 dpi compared to T0.

4.26 ppm (unknown carbohydrate)

A substantial increase (with an average of 21% (**Table 4.3**)) in signal (**Table 4.2**) was observed in all five families at the 4.26 ppm bucket in *P. agathidicida*-inoculated samples at 10 dpi (**Figure 4.7 C**). Similar findings were not observed in the mock-inoculated controls, suggesting this increase was due to the presence of *P. agathidicida* in the kauri leaf AWF.

4.22 ppm (unknown carbohydrate)

A substantial decrease in signal (**Table 4.2**) of the 4.22 ppm bucket was observed in all families at 10 dpi regardless of the treatment (*P. agathidicida* or cellophane membrane control) (**Figure 4.7 D**). However, the decrease in signal occurred earlier in the *P. agathidicida*-inoculated samples, with a substantial decrease in signal at 24 hpi (**Table 4.3, Appendix 4.1**). Accordingly, comparison of *P. agathidicida* and control samples at 24 hpi demonstrated that the control samples had a substantially

higher signal in this bucket compared to *P. agathidicida*-inoculated samples, whereas by 10 dpi no meaningful differences were detected. Thus, while the signal of the 4.22 ppm bucket in kauri leaf AWF decreased overtime, inoculation of kauri leaf AWF with *P. agathidicida* quickened this process.

3.82 ppm (unknown carbohydrate)

A substantial decrease in signal (**Table 4.2**) was observed in the 3.82 ppm bucket 24 hpi with *P. agathidicida* by all families (**Figure 4.7 E**). No such observation was made in the cellophane membrane-inoculated controls. However, both control and *P. agathidicida*-inoculated samples demonstrated a meaningful reduction in signal between T0 and 10 dpi. Thus, while the signal for the 3.82 ppm bucket decreased substantially over time, inoculation with *P. agathidicida* appeared to speed up this process.

3.74 ppm (unknown carbohydrate)

Overall, the signal for the 3.74 ppm bucket increased over time, regardless of treatment (**Figure 4.7 F**). However, treatment with *P. agathidicida* appeared to speed up this process, with a higher signal observed in *P. agathidicida*-inoculated samples at 24 hpi compared to T0 controls, a difference that was substantial in three (E, G, and M) of the five families (**Table 4.2**). No meaningful difference in signal of the 3.74 ppm bucket was observed between treatments at 10 dpi in any of the families.

3.70 ppm (unknown carbohydrate)

A decrease in signal was observed in the 3.70 ppm bucket for all families inoculated with *P. agathidicida* between T0 and 10 dpi (**Figure 4.7 G**). This decrease was substantial for all families except 'E' (**Table 4.2**). No such difference was observed in cellophane membrane-inoculated controls over the same period. As a result, *P. agathidicida*-inoculated kauri leaf AWF samples had less signal in the 3.70 ppm bucket compared to cellophane membrane-inoculated controls at 10 dpi.

3.46 ppm (unknown carbohydrate)

At 10 dpi, a substantial decrease (**Table 4.2**), compared to the T0 controls, in the signal of the 3.46 ppm bucket was observed in the kauri leaf AWF inoculated with *P. agathidicida*, but not the T10d cellophane membrane controls (**Figure 4.7 H**). Accordingly, a higher signal was observed in control samples at 10 dpi compared to *P. agathidicida* samples at the same time point.

3.42 ppm (unknown carbohydrate)

A substantial decrease in the signal of the 3.42 ppm bucket (**Table 4.2**) was observed in all *P. agathidicida*-inoculated samples at 10 dpi (**Figure 4.7 I**) compared to T0. In contrast, the signal of the 3.42 ppm bucket remained consistent over time in the cellophane membrane-inoculated controls. Thus, it is likely the presence of *P. agathidicida* in the kauri leaf AWF was responsible for signal decrease in the 3.42 ppm bucket.

3.38 ppm (unknown carbohydrate)

The signal of the 3.38 ppm bucket had increased 24 hpi with *P. agathidicida* compared to the T24h cellophane membrane controls which remained constant (**Figure 4.7 J**). By 10 dpi, the signal had increased in both control and *P. agathidicida*-inoculated samples relative to T0 (**Appendix 4.1**). However, despite the increased signal in cellophane membrane controls, the signal was still higher in kauri leaf AWF samples inoculated with *P. agathidicida*. A difference which was substantial in three (G, H, and N) of the five families (**Table 4.2**).

3.26 ppm (unknown carbohydrate)

An average increase of 88% (**Table 4.3**) in signal of the 3.26 ppm bucket was observed in all *P. agathidicida*-inoculated samples by 24 hpi, and this increase was considerable (**Table 4.2**) in four of the five families (except N) (**Figure 4.7 K**). However, by 10 dpi, the signal of the 3.26 ppm bucket had increased in both the *P. agathidicida*-inoculated samples and the cellophane membrane controls, such that there were no substantial differences observed between the treatments at this time point. Thus, while an increase in signal of the 3.26 ppm bucket occurred over time in kauri leaf AWF, inoculation with *P. agathidicida* appeared to speed up this process initially.

2.34 ppm

An average 50% (**Table 4.3**) decrease in the signal of the 2.34 ppm bucket was observed in *P. agathidicida*-inoculated, but not cellophane membrane-inoculated, kauri leaf AWF samples by 24 hpi (**Figure 4.7 L**). This decrease in signal was considerable in four (E, G, M, and N) of the five families analysed (**Table 4.2**). By 10 dpi, the signal of the 2.34 ppm bucket had also substantially decreased in most (E, G, M, and N) of the control samples. However, the signal of the *P. agathidicida*-inoculated samples had continued to decrease, and by 10 dpi was still considerably lower than the signal observed in the T10d cellophane membrane controls. Ultimately, the signal in the 2.34 ppm bucket was found to decrease over time; however, inoculation with *P. agathidicida* appeared to speed up this process considerably.

2.30 ppm

The signal of the 2.30 ppm bucket increased over time in the *P. agathidicida*-inoculated samples (**Table 4.3, Appendix 4.1**), with a substantial increase (**Table 4.2**) in signal between T0 and 10 dpi for three (E, M, and N) of the five families analysed (**Figure 4.7 M**). No such differences were observed in the cellophane membrane control inoculated samples, suggesting that inoculation of kauri leaf AWF with *P. agathidicida* was responsible for the signal increase in the 2.30 ppm bucket.

2.22 ppm

The signal of the 2.22 ppm bucket had increased at 10 dpi compared to T0 in the *P. agathidicida*-inoculated samples (**Table 4.3, Appendix 4.1**), an increase which was statistically meaningful (**Table 4.2**) in three (G, M, and N) of the five families analysed (**Figure 4.7 N**). In contrast, signal levels in the control samples remained constant at both 24 hpi and 10 dpi.

1.94 ppm

The signal of the 1.94 ppm bucket was particularly variable in the *P. agathidicida*-inoculated samples at 24 hpi (**Figure 4.7 O**). However, by 10 dpi, the signal of this bucket was consistently lower in *P. agathidicida*-inoculated samples than it was at T0 (an average 33% decrease) (**Table 4.3**)), or in the control samples at 10 dpi. Thus, inoculating kauri leaf AWF with *P. agathidicida* appeared to result in decreased signal of the 1.94 ppm bucket.

1.38 ppm

An increase in the signal of the 1.38 ppm bucket was observed in *P. agathidicida*-inoculated samples 10 dpi compared to T0 (**Table 4.3, Appendix 4.1**), and this increase was considerable (**Table 4.2**) in three (E, H, and N) of the five families analysed (**Figure 4.7 P**). No such increase in signal was observed in the control samples at the same time point.

1.34 ppm

A considerable amount of variation in signal of the 1.34 ppm bucket between families in both the initial T0 sample and the subsequent 24 hpi sample was detected, regardless of treatment (**Figure 4.7 Q**). However, a consistent and substantial (**Table 4.2**) decrease in signal was observed in all *P. agathidicida*-inoculated samples 10 dpi, while no meaningful differences were observed in the control samples over the same period.

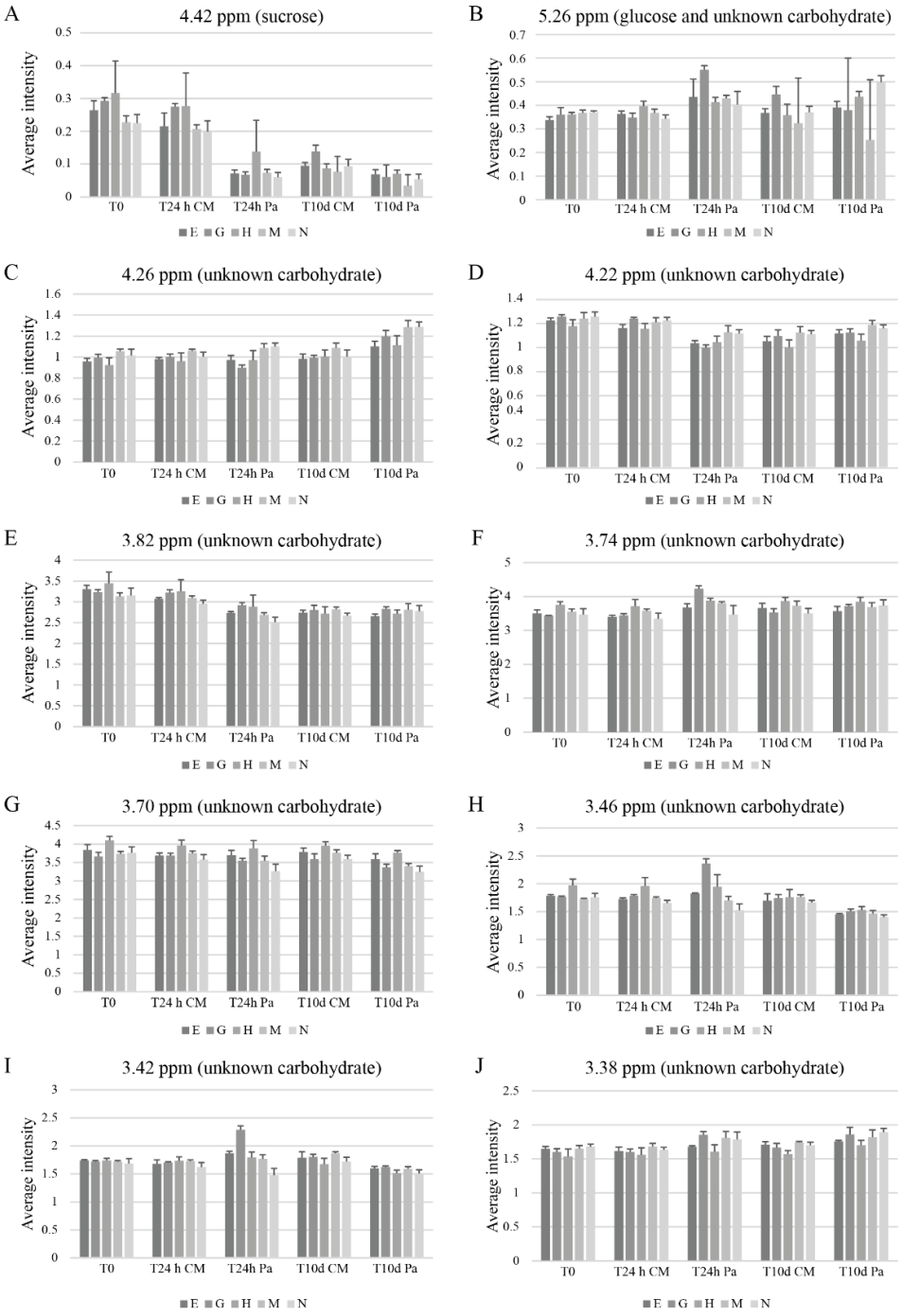

Figure 4.7 A–J. Average signal intensities of selected spectral buckets identifies *Phytophthora agathidicida*-induced changes in kauri leaf apoplastic wash fluid (AWF).

Clustered column chart describing the changes observed in kauri AWF inoculated with *P. agathidicida* compared to mock-inoculated controls at selected spectral buckets over time. Kauri leaf AWF was harvested and inoculated with cellophane membranes with, or without, *P. agathidicida*. Samples were taken for analysis at: Time 0 (prior to inoculation), 24 hours post-inoculation (hpi), and 10 days post-inoculation (dpi). Spectral buckets graphed were selected because consistent significant differences (two-tailed Mann-Whitney U test ($P < 0.05$)) between *P. agathidicida*-inoculated and controls were observed in a least three of the five kauri families. Four biological replicates were included. Spectral buckets are as follows: **(A)** 5.42 ppm (sucrose); **(B)** 5.26 ppm (unknown carbohydrate); **(C)** 4.26 ppm (unknown carbohydrate); **(D)** 4.22 ppm (unknown carbohydrate); **(E)** 3.82 ppm; **(F)** 3.74 ppm (unknown carbohydrate); **(G)** 3.70 ppm; H, 3.46 ppm (unknown carbohydrate); **(I)** 3.42 ppm; **(J)** 3.38 ppm.

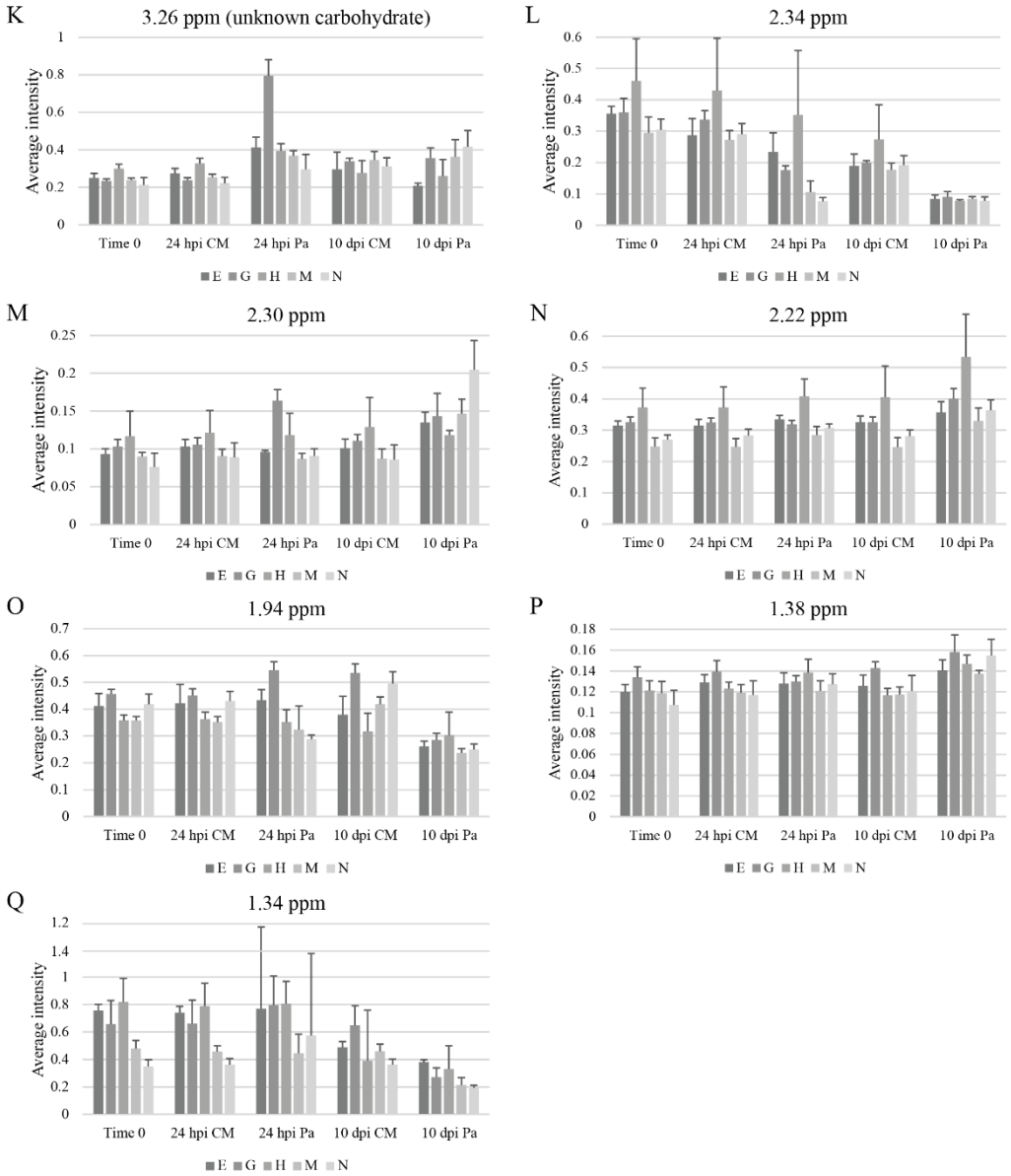

Figure 4.7 K–Q: Average signal intensities of selected spectral buckets identifies *Phytophthora agathidicida*-induced changes in kauri leaf apoplastic wash fluid (AWF).

Clustered column chart describing the changes observed in kauri leaf AWF inoculated with *P. agathidicida* compared to controls at selected spectral buckets over time. Kauri leaf AWF was harvested and inoculated with cellophane membranes with, or without, *P. agathidicida*. Samples were taken for analysis at: Time 0 (prior to inoculation), 24 hours post-inoculation (hpi), and 10 days post-inoculation (dpi). Spectral buckets graphed were selected because consistent significant differences (two-tailed Mann-Whitney U test ($P < 0.05$) between *P. agathidicida*-inoculated and controls were observed in a least three of the five kauri families. Four biological replicates were performed. Spectral buckets are as follows: **(K)** 3.26 ppm; **(L)** 2.34 ppm; **(M)** 2.30 ppm; **(N)** 2.22 ppm; **(O)** 1.94 ppm; **(P)** 1.38 ppm; **(Q)** 1.34 ppm.

4.5 Discussion

The purpose of this chapter was to identify whether inoculation with *P. agathidicida* altered the composition of metabolites in the kauri apoplast. To this end, AWF was harvested from kauri leaves and inoculated with either *P. agathidicida* or mock-inoculated with cellophane membranes. Samples were taken at T0 (uninfected), T24h (24 h after inoculation/mock-inoculation), and T10d (10 days after inoculation/mock-inoculation) and analysed by ^{1}H NMR.

The T0 sample clearly demonstrated that there is a lot of variation within kauri families, and as such that they did not segregate according to the family identifier. Each 'family line' in this study represented cones that were harvested from an individual tree. While kauri trees have both male and female cones, the pollen responsible for fertilising the female cones is wind dispersed, and thus may have originated from any number of kauri trees (Hill et al., 2018). Thus, variation within kauri families would be expected.

^{1}H NMR detected distinguishable differences in 17 spectral buckets between kauri leaf AWF inoculated with *P. agathidicida* and control samples. However, only two of the key spectral buckets were positively identified, one of which was sucrose at 5.42 ppm. The remaining identified spectral bucket contained glucose and an unknown carbohydrate. Glucose should be found at 5.24 ppm, but due to bucketing is instead found at 5.22 and 5.26 ppm, which can make it difficult to determine the changes observed.

Of the 17 spectral buckets, 11 were from the carbohydrate region of the spectrum (3–5 ppm), while the remaining six were at the aliphatic end of the spectrum (0.9–3 ppm) and may represent amino acids (Ali et al., 2009). One of the observations made during analysis of the NMR data was that a decrease was observed in spectral buckets following inoculation with *P. agathidicida* in comparison to the cellophane-inoculated controls, suggesting the presence of proteases and invertases in the AWF.

Compared to the T0 control, *P. agathidicida*-inoculated kauri leaf AWF showed an almost 73% decrease at 24 hpi in the sucrose spectral bucket (5.42 ppm). This is in line with findings that apoplastic sucrose levels decline dramatically during infection of tomato and potato leaflets with *P. infestans* (Kagda et al., 2020). Sucrose is one of the many plant-produced metabolites able to be utilised by oomycetes, including *Phytophthora* species (Judelson & Ah-Fong, 2018, Rodenburg et al., 2018). The increased speed by which the sucrose spectrum decreased in inoculated samples compared to cellophane membrane controls suggested that *P. agathidicida* may indeed be degrading and assimilating sucrose, likely for nutrition. Oomycetes are known osmotrophs, using enzymes to digest large molecules into smaller ones which are subsequently imported into the cell (Richards & Talbot, 2013), and *P. agathidicida* zoospores have been shown to be strongly attracted towards sucrose (Armstrong, 2018).

Sucrose is hydrolysed by enzymes known as invertases (enzyme commission (EC) number 3.2.1.26), enzymes which play important roles in the transport and release of sucrose in the apoplast (Roitsch et al., 2003), into glucose and fructose. EC 3.2.1.26 enzymes are found in the GH32, GH68 and GH100 CAZyme families. While no GH68 or GH100-encoding genes were found in the *P. agathidicida* genome, four GH32-encoding genes (Pag002401, Pag002402, Pag002403, Pag002404) were identified which shared at least 75% identity with a *P. infestans* invertase (PITG_14237) (Kagda et al., 2020). All four GH32-encoding genes were predicted to be secreted, suggesting they could indeed function extracellularly to break down sucrose for import into the cell. Indeed, one of these proteins (Pag002401) was identified in *P. agathidicida* culture filtrate (including kauri leaf AWF) (**Chapter 5, Appendix 5.1**). While none of these GH32 enzymes met the arbitrary expression cut-off (50 FPKM) for selection in **Chapter 3** based on the original mapping of the transcriptome (Guo & Panda, Unpublished), re-mapping to the newest version of the genome (Guo & Shiller, Unpublished) demonstrates that three of these genes are expressed above 50 FPKM during peak expression in kauri roots and leaves 48 hpi. This suggests they should have been selected under the original criteria and may represent an interesting avenue for further study.

In contrast to sucrose, an average 24% increase was observed in the 5.26 spectral bucket (glucose plus unknown) in *P. agathidicida*-inoculated samples 24 hpi compared to the T0 control. However, by 10 dpi only a 9% increase was observed. Glucose and fructose are produced in a 1:1 ratio upon hydrolysis of sucrose, thus it makes sense that glucose levels increase while sucrose levels decrease. An increase in glucose levels upon infection has also been reported in grapevines (*Vitis vinifera* ssp. *vinifera*) susceptible to downy mildew (caused by members of Peronosporaceae family which include *Phytophthora* species) (Ali et al., 2009), and in *Brassica rapa* cultivars infected with hemibiotrophic fungal pathogen *Fusarium oxysporum* (Abdel-Farid et al., 2009). Interestingly however, a similar increase was not observed in kauri leaf AWF inoculated with cellophane membranes, even at 10 dpi, despite an average decrease of over 60% in the 5.42 ppm bucket representing sucrose.

Of the 17 spectral buckets identified as 'of interest', an overall reduction or a faster reduction compared to cellophane controls was observed in nine of them (5.42 ppm (sucrose), 4.22 ppm, 3.82 ppm, 3.70 ppm, 3.46 ppm, 3.42 ppm, 2.34 ppm, 1.94 ppm and 1.34 ppm). As above, this is likely due to degradation and/or assimilation by *P. agathidicida.* For the six buckets which were identified in the carbohydrate region (3–5 ppm), it is possible that the decrease in signal was due to hydrolysis by a *P. agathidicida* CAZyme. However, without knowing the identity of the metabolite, no hypotheses can be formed as to which CAZyme family these enzymes may belong.

That the signal of the remaining eight selected buckets increased over time was also of interest. During an *in vivo* experiment, this increase could be a result of the host's response to infection. However, using

kauri leaf AWF, this is less likely to be the case. An advantage to using kauri leaf AWF is that it provides a clear picture regarding the changes in response to *P. agathidicida* infection, without being affected by host responses. Consequently, the increasing signal of one bucket is likely due to the decreasing signal of another, as one metabolite is hydrolysed to form subsequent products.

One of the few metabolites that could be confidently identified was quinic acid (2.06 ppm). Quinic acid is a known precursor to lignin synthesis (Volpi e Silva et al., 2019) and commonly used as a biomarker of plant defence. Both Chin et al. (2014) and Girelli et al. (2019) found levels of quinic acid were higher in *Candidatus* Liberibacter asiaticus-infected and symptomatic oranges and *Xylella fastidiosa* subsp. *pauca*-infected olives respectively, compared to controls. However, no such changes were observed in the spectral bucket identified as quinic acid (2.06 ppm) in this study. This is not surprising as kauri leaf AWF would not contain the required host cellular machinery to produce a defence response.

While this study was designed as a preliminary exploration into the changes of kauri leaf AWF, there are limitations, the most obvious being that the experiment was not carried out *in planta*. While using kauri leaf AWF has allowed targeted investigation of metabolite changes caused by *P. agathidicida*, changes in metabolite composition occurring as a consequence of plant-pathogen interactions have not been captured. Furthermore, *P. agathidicida* is a root pathogen, and the AWF was harvested from kauri leaves. Future experiments could exploit *N. benthamiana* as an alternative host (Guo, Unpublished-b), investigating metabolome differences in *P. agathidicida*-infected *N. benthamiana* roots.

The lack of identification of the key spectral buckets was another limitation of this study, which made it difficult to put the results into perspective and make comparisons to other organisms and/or pathosystems. In particular, the high overlap in the carbohydrate region (3–5 ppm) meant that while the in-house database contained a wide range of identified carbohydrates, they were not able to be conclusively identified. Key metabolites could be identified in future experiments using ion chromatography or liquid chromatography-mass spectrometry to identify basic sugars and other metabolites respectively. Once identified, these metabolites could be run as external standards to the NMR analysis. Unfortunately, these analyses could not be performed in this study as the cost of this was prohibitive.

If research was to proceed with the identification of key spectral buckets, an additional study should also be performed with a more hypothesis-driven approach. It has been shown that the metabolite profiles of kauri leaf AWF do not cluster together, thus future experiments would not need to consider the family lines. Instead, all the family lines could be grouped together, thus increasing the number of

replicates. An increased number of replicates and a focus only on key spectral buckets, such as those highlighted in this chapter, would considerably improve the statistical power of the experiment.

Chapter five: Analysis of the extracellular secretome of *Phytophthora agathidicida* grown in liquid media.

5.1 Introduction

The secretome is a term used to describe both the cell secretory machinery and all proteins secreted by a cell, whether they are classically secreted through the endoplasmic reticulum (ER)-Golgi pathway or are non-classically secreted proteins which generally lack an amino (N)-terminal signal peptide and may be secreted via extracellular vesicles or an as yet unknown mechanism (Poschmann et al., 2022, Wolf & Casadevall, 2014, Tjalsma et al., 2000).

For eukaryotic microorganisms, the extracellular secretome (i.e. the sum of all proteins secreted by the cell into the extracellular environment) is essential to niche colonization (Brown et al., 2012, Klosterman et al., 2011, González-Fernández et al., 2015, Rovenich et al., 2014). This is no truer than for phytopathogenic eukaryotic microorganisms, such as fungi and oomycetes, where the extracellular secretome has been shown to play a vital role in both pathogenicity (i.e. the ability to cause disease) and virulence (i.e. the degree of pathogenicity) (Li et al., 2020). Indeed, such pathogenicity and virulence factors, collectively referred to as effectors, play essential roles in everything from adhesion to the host surface, to host penetration, nutrient acquisition, warding off competing microbes and suppression of the plant immune system (Girard et al., 2013, Gonzalez-Fernandez & Jorrin-Novo, 2012). While gene expression data can be used to determine which effector genes are expressed during host colonisation (as evidenced in **Chapter 3**) or, for that matter, during growth outside of the host in the surrounding environment, these data do not always correlate to protein presence or abundance. Thus, to identify which effector proteins are likely to be involved in these processes, proteomic data are often needed.

While a subset of eukaryotic pathogen-produced effector proteins are translocated into the host cell to perform their functions (e.g. RxLRs/Crinklers) (Wawra et al., 2012), many of the interactions between pathogen- and plant-secreted proteins occur in the apoplast, the extracellular space between plant cells. Over the years, proteomics has been shown to be a valuable tool for studying the extracellular secretome of eukaryotic phytopathogenic organisms *in planta* (Kim et al., 2013, Kondratev et al., 2022, Mesarich et al., 2018, Nogueira-Lopez et al., 2018). For example, 75 **s**mall, **s**ecreted **p**roteins (SSPs) of the tomato leaf mould fungus, *Cladosporium fulvum*, were identified through **l**iquid **c**hromatography–**m**ass **s**pectrometry (LC–MS) analysis of apoplastic wash fluid from infected tomato leaves, of which nine were found to be likely recognised by immune receptors in at least one of 14 wild tomato accessions tested (Mesarich et al., 2018).

Proteomic analyses have also been successfully used to study the extracellular secretome of eukaryotic phytopathogens *in vitro* (Cooke et al., 2014, Do Vale et al., 2012, Li et al., 2019, Meijer et al., 2014, Sinha et al., 2022). Such analyses have been undertaken because, in some cases, certain effector proteins have been found to be produced in culture. For example, more than 30 effector candidates were identified from the fungal pear pathogen *Venturia pirina*, where the authors grew *V. pirina* inside cellophane membranes in an attempt to mimic *in planta* growth conditions under the pear cuticle (Cooke et al., 2014). In another proteomics study, 40 *Fusarium proliferatum* proteins were identified and an additional 65 increased in abundance in the culture filtrate of Czapek's liquid medium containing banana peel, compared to culture filtrate of Czapek's liquid medium without banana peel (Li et al., 2019), thereby suggesting involvement of the identified proteins in colonisation of banana.

To date, no study has investigated the extracellular secretome of *Phytophthora agathidicida* using proteomics. Such knowledge is vital, as it may provide insights into the pathogenicity and virulence mechanisms of this devastating plant pathogen and, in this way, provide information that can inform disease control programs. Unfortunately, a cultural agreement to investigate the extracellular proteome of *P. agathidicida* during infection of kauri (*Agathis australis*) tissue (i.e. during colonization of kauri roots or leaves) could not be established in time for this PhD project. Thus, with this in mind, and based on proteomic information gained from other eukaryotic microbial phytopathogens (see above), the extracellular secretome of *P. agathidicida* was investigated during growth in nutrient-rich and nutrient-poor axenic culture conditions, as well as during growth in apoplastic wash fluid (AWF) isolated from kauri leaves, using a proteomics approach.

5.2 Methods

5.2.1 Biological materials

The oomycete and plant material used in this chapter are listed in **Table 5.1**.

Table 5.1. Oomycete and plant material.

Organism	Strain or line	Origin	Reference
Oomycete			
Phytophthora agathidicida	NZFS 3770	Great Barrier Island (Ngati Rehua), New Zealand	Guo et al. (2020a)
Plant material			
Agathis australis[a]	MW8-E[b]	Waipoua Forest, New Zealand	This study
A. australis	MW8-G	Waipoua Forest, New Zealand	This study
A. australis	MW8-H	Waipoua Forest, New Zealand	This study
A. australis	MW8-M	Waipoua Forest, New Zealand	This study
A. australis	MW8-N	Waipoua Forest, New Zealand	This study

[a]Special thanks to Taoho Patuawa and Te Roroa for allowing access to kauri saplings from the Scion Healthy Trees Healthy Future programme.

[b]Each letter refers to the seed cones collected from a single tree.

5.2.2 Media

All media used in this study are described in **Appendix 3.3**.

5.2.3 Growth conditions

Growth conditions of kauri (*A. australis*) and *P. agathidicida* are as described in **Chapter 4, section 4.2.3.**

5.2.4 Harvesting kauri leaf apoplastic wash fluid (AWF)

Harvesting of kauri leaf AWF was carried out as described in **Chapter 4, section 4.2.4.**

5.2.5 Analysis of the extracellular *P. agathidicida* secretome

5.2.5.1 Inoculation of liquid broth media

A single cellophane membrane disc covered in actively growing *P. agathidicida* mycelia (**section 4.2.3**) was inoculated into 15 mL of liquid broth medium (either Henniger, Plich, PD, V8, or clarified V8 (**Appendix 3.3**)) in a Petri dish (Labserv, Fisher Scientific). For each medium, four biological replicates were carried out. AWF from leaves of kauri saplings was also used as a liquid growth medium (**section 4.2.4**); however, due to the small volumes obtained, AWF from several different trees was pooled together, filtered through a 0.2 µm filter (Ahlstrom-Munksjö, Helsinki, Finland), and split into four replicates of approximately 3 mL each. Furthermore, due to small volumes, *P. agathidicida* was inoculated into a 15 mL Falcon tube, rather than a Petri dish, containing kauri AWF.

5.2.5.2 Harvesting of culture filtrates for secreted proteins

At 10 days post-inoculation, culture filtrate was harvested by first straining the culture through a nappy liner to remove the large mycelial mats, and then filtering through a 0.2 µm filter (Ahlstrom-Munksjö) to remove any remaining mycelial fragments. Filtered culture filtrate was incubated at –20°C until frozen, then freeze-dried, and stored at –20°C until required.

5.2.5.3 Sample preparation for proteomics analysis by gel digestion

Running and staining of the gel

Freeze-dried culture filtrate was resuspended in 200 µL milliQ water. A 20 µL aliquot was mixed with 5 µL of protein loading dye (containing 2.1% (v/v) Tris-HCl (Invitrogen) from a 15.8% (w/v) pH 6.8 stock solution, 52% (v/v) glycerol (Sigma-Aldrich), 4.2% (v/v) SDS (Invitrogen) from a 20% (w/v) stock solution, and 0.02% (v/v) bromophenol blue (Bio-Rad Laboratories, Hercules, California, USA) from a 1% (w/v) stock solution) and simmered at 80°C for 5 min before it was loaded onto a 4–20% Mini-Protean® Tgx™ Precast Protein Gel (Bio-Rad) alongside the precision plus protein TM dual xtra pre-stained protein standards (Bio-Rad) and bovine serum albumin (BSA) (Thermo Scientific), which was used as a processing positive control. Proteins were resolved by sodium dodecyl sulfate (SDS) polyacrylamide gel electrophoresis in running buffer (7.2% (w/v) glycine, 1.5% (w/v) Tris, 0.5% (w/v) SDS) at 100 V for 10 min, followed by 200 V for 30 min. Proteins in the gel were stained overnight in colloidal Coomassie (0.1% (w/v) brilliant blue G250 Coomassie (Sigma, USA), 10% (w/v) ammonium sulphate $(NH_4)_2SO_4$, 1% (v/v) phosphoric acid (Ajax FineChem)).

De-staining of the gel

Colloidal Coomassie was decanted, and the gel was rinsed several times in water. Each gel lane was cut out and split into six equal-sized fragments which were finely diced and placed in a protein LoBind tube (Eppendorf, Hamburg, Germany). Each tube was incubated at 45°C for 20 min with 300 µL of 1 x ABC (0.4% (v/v) ammonium bicarbonate (Fisher Scientific, Merelbeke, Belgium)) from a 4 x ABC (1.6% (w/v) ammonium bicarbonate) stock solution in 50% (v/v) methanol (Fisher Scientific) to de-stain. Any liquid was removed from the tube and 500 µL of MeCN (Fisher Scientific) was added. Tubes were vortexed until the gel pieces inside had dehydrated and turned white. Excess liquid was pipetted off and the samples were dried in a SpeedVac (Savant SPD131DDA SpeedVac Concentrator, Thermo Scientific, USA) for 10 min.

Reduction and alkylation of proteins

To the dried gel fragments, 150 µL of reducing solution (0.15% (v/v) dithiothreitol (DTT, Sigma, Missouri, USA) from a 1 M (15.4% (w/v)) stock solution in 1 x ABC) was added and incubated at 45°C for 1 h. The supernatant was removed, and gel pieces were rinsed with 200 µL of LC–MS-grade water (Fisher Scientific, Merelbeke, Belgium). Any remaining water was removed, and gel pieces were dehydrated with 500 µL of MeCN. Once excess liquid had been removed, the gel pieces were dried in a SpeedVac for an additional 10 min. The gel pieces were incubated in the dark with 200 µL of alkylation solution (0.37% (w/v) iodoacetamide (Sigma-Aldrich) in 1 x ABC) for 30 min. The supernatant was removed, and gel pieces were rinsed in LC–MS-grade water and dehydrated with MeCN twice more. Finally, the gel pieces were dried thoroughly in the SpeedVac for approximately 10 min.

Gel digestion and protein extraction

Dried gel pieces were rehydrated in 130 µL digestion solution (0.1% (v/v) $CaCl_2$ from a 10% stock solution was added to trypsin (Sigma Aldrich)) and rested on ice for 2 min. The resulting Trypsin solution was added to 1 x ABC, resulting in a digestion solution containing 2% (v/v) trypsin, with excess solution removed and replaced by 1 x ABC for incubation at 37°C overnight. The next day, gel pieces were sonicated (Elmasonic, Elma, Wetzikon, Switzerland) for 2 min and supernatant was collected in a fresh LoBind tube. Tubes were sonicated for a further 2 min after addition of 110 µL of 5% (v/v) formic acid (Ajax Finechem) in 40% (v/v) MeCN. The supernatant was added to the previous supernatant in a LoBind tube. A final 2-min sonication was carried out after the addition of 110 µL 0.1% (v/v) formic acid in 80% (v/v) MeCN, and the supernatant added to the previous two collections. The volume of the combined supernatants was reduced to 30 µL in a SpeedVac. Samples were then transferred to glass vials (ThermoFisher Scientific) for storage at –80°C prior to LC–MS analysis.

5.2.5.4 LC–MS analysis of peptide samples (carried out by Trevor Loo (T.L.), Massey University)

Peptides in each sample were separated by their affinity for water on a reverse-phase C18 column and analysed by mass spectrometry (MS) using the Top10 method (Michalski et al., 2011). Details for the chromatographic and mass spectrometric settings are listed in **Table 5.2** and **Table 5.3**, respectively.

Full MS1 scans were acquired over a mass range of 375–1,600 m/z, with detection in the Orbitrap mass analyser at a resolution setting of 70,000. Fragment ion spectra produced via higher energy collisional dissociation (HCD) were acquired with a resolution setting of 17,500. For data-dependent acquisition of HCD spectra, the 10 most intense ions were selected for fragmentation in each scan cycle. Full MS as well as fragment ion spectra were detected in the Orbitrap mass analyser. Exclusion conditions were optimized according to observed chromatographic peak width (typically 10–15 sec).

Table 5.2. Liquid Chromatography–Mass Spectrometry (LC–MS) instrument configuration.

nanoLC system	Dionex UltiMate™ 3000 RSLCnano System (ThermoFisher Scientific, Waltham, MA, USA)
Mass spectrometer	QExactive Plus (ThermoFisher Scientific)
Ionization source	Nano Flex™ (ThermoFisher Scientific)
Trapping column	PepMap100 C18, 3µm particle size, 75 µm inner diameter, 2 cm length (ThermoFisher Scientific)
Analytical column	PepMap C18, 2 µm particle size, 75 µm inner diameter, 50 cm length (ThermoFisher Scientific)
Flow rates	Trap: 15 µL/min Analytical: 300 nL/min
Column oven temperature	50°C
Gradient	3–30% acetonitrile in 0.1% formic acid/water over 60 min
Mobile phase	Trap loading: 0.1% TFA/2% MeCN/water Analytical A: 0.1% formic acid/2% MeCN/water Analytical B: 0.1% formic acid/98% MeCN/water

Table 5.3. Liquid chromatography–mass spectrometry mass spectrometer settings.

Capillary temperature	**250°C**
S-Lens RF level	**50%**
Polarity	**Positive**
Source voltage	**1.5 kV**
AGC target	**Full MS: 3e6, MS*2*: 1e5**
Max. injection times	**Full MS: 150 ms, MS*2*: 110 ms**
Full MS scan range	**375–1600 m/z**
Resolution settings	**Full MS: 70,000, MS*2*: 17,500**
Number of microscans	**1**
Isolation width	**1.4 m/z**
Loop count (TopN)	**10**
MSX count	**1**
Normalised collision energies	**25, 30, 35**
Charge exclusion	**Unassigned, 1, >7**
Peptide match	**Preferred**
Exclude isotopes	**On**
Dynamic exclusion	**15 sec**
Spectrum data type	**Full MS: Profile, MS2: Centroid**

5.2.5.5 *In silica* analysis of LC–MS raw data

Database search (carried out by T.L. and Ellie Bradley (E.B.))

The raw data spectra files were searched against the in-house *P. agathidicida* 3770 database of predicted proteins, generated from the latest PacBio chromosome-level genome sequence (Cox et al., Unpublished), using the Proteome Discoverer™ search engine (ThermoFisher Scientific). The search parameters used matched the specifications of the Q Exactive instrument, and variables resulting from chemical treatment and suspected natural modifications of proteins are listed in **Table 5.4**. The reverse database search option was enabled by default, and all protein hits were filtered to satisfy a false

discovery rate (FDR) of 1% or better and have at least two unique peptides across at least two biological replicates of at least one sample type (**Table 5.4**).

Table 5.4. Liquid chromatography–mass spectrometry data analysis parameters.

Search engine	Proteome Discoverer v2.4.1.15
Databases	*Phytophthora agathidicida* NZFS 3770 predicted proteins
Taxonomy	*Phytophthora agathidicida*
Enzyme	Trypsin
Max number of missed cleavages	2
Min peptide length	6
Precursor mass tolerance	10 ppm
Fragment mass tolerance	0.02 Da
Decoy database search	Enabled (default)
Static modifications	Carbamidomethyl (C)
Variable modifications	Oxidation (M), Protein N-terminal acetylation,
False Discovery Rate (FDR)	1%
Display filter	Number of unique peptides ≥ 2

Annotation of identified *P. agathidicida* proteins

The presence of an amino (N)-terminal signal peptide was predicted using SignalP v3.0 (Bendtsen et al., 2004), which is the preferred version of SignalP for annotating signal peptides in oomycetes (Sperschneider et al., 2015). Transmembrane domains were predicted with TMHMM v2.0 (Krogh et al., 2001, Sonnhammer et al., 1998). Only proteins containing an N-terminal signal peptide and lacking transmembrane helices (unless they were predicted over the region encoding a signal peptide), were considered as classically secreted. Protein functional annotations were predicted with InterProScan (Finn et al., 2017) via Geneious v9.1.8 using the Pfam and SMART databases. CAZymes were predicted using dbCAN2 in conjunction with the HMMER, DIAMOND, and eCAMI tools (Yin et al., 2012, Zhang et al., 2018). Only CAZymes predicted by at least two of the tools were annotated as CAZymes. EffectorP v3.0, capable of distinguishing between putatively apoplastic and cytoplasmic effectors, was used to predict candidate effectors (Sperschneider & Dodds, 2022). Comparison to an in-house database was used to identify RxLR and CRN proteins and to provide support for the InterProScan annotation of elicitins and NPP1 proteins. To determine similarity to other proteins, a BLASTp analysis with an e-value threshold of 0.05 was performed against the **N**ational **C**enter for **B**iotechnology **I**nformation (NCBI) **n**on-**r**edundant (nr) protein database (Pruitt et al., 2005). The top 10 BLASTp hits were retained for further analysis. Analysis and extraction of the BLASTp hits was performed by Mercedes Rocafort (Massey University) using the **N**ew Zealand **eS**cience **I**nfrastructure (NESI) platform.

Manipulation and illustration of data

Microsoft Excel v2203 was used to view, sort, and graph data. RStudio v1.4.1717 was used to merge files and generate heatmaps and Venn diagrams. Figures were embellished using Adobe Illustrator v25.2.

5.3 Results

5.3.1 *P. agathidicida* displays distinct protein profiles when grown in different media

As a starting point for the characterization of the 'in culture' extracellular secretome of *P. agathidicida*, the oomycete was first grown in nutrient-rich (clarified V8, V8, PD) and nutrient-poor (Henniger, Plich) liquid broth media. At the same time, *P. agathidicida* was also grown in apoplastic wash fluid (AWF) harvested from the leaves of kauri saplings which, like the Henniger and Plich liquid broth media, is also considered to be a nutrient-poor medium. In any case, it was hoped that the nutrient-poor media would stimulate the production of secreted effector proteins associated with host colonization. Through freeze-drying and subsequent resuspension, culture filtrates were concentrated to approximately 75 times the original concentration, except kauri AWF which was concentrated approximately 15 times the original concentration. Interestingly, the protein profile of the corresponding culture filtrates varied between the different liquid growth media used (**Figure 5.1**), with a clear banding pattern observed in the culture filtrates of all nutrient-poor media and nutrient-rich PD, but not in the culture filtrate of nutrient-rich V8 or clarified V8, which were visible as more of a continuous smear, likely due to the presence of plant proteins in the V8 juice itself. Furthermore, there appeared to be a collection of lower molecular weight proteins in the kauri AWF culture filtrate, compared to those from any of the other culture filtrates examined.

To further assess the differences in the protein profile between culture filtrate types, as well as to assess the level of reproducibility between biological or technical replicates, a **p**rincipal **c**omponent **a**nalysis (PCA) was performed on the proteins identified from the LC–MS peptide data (**Figure 5.2 A**), where **p**rincipal **c**omponent 1 (PC1) explained 46.0% of the variance, while PC2 explained 22.5% of the variance. Based on this analysis, it was determined that, for the most part, the biological replicates clustered robustly. The only exception was one of the V8 culture filtrate biological replicates, which was an outlier. Notably, the culture filtrates of all nutrient-poor media (Plich, Henniger, and kauri AWF) clustered together, though interestingly all biological replicates of clarified V8 and the V8 culture filtrate outlier also clustered along with them. Culture filtrate samples from PD liquid medium clustered separately from other culture filtrate types (**Figure 5.2 A**).

The PCA loadings plot (**Figure 5.2 B**) describes how much each protein (represented by a dot) affects a principal component. The proteins which cluster around the origin of PC1 and PC2 have the least effect, while those further away have a larger effect. A large cluster of proteins in the top left of the plot

(**Figure 5.2 B**) have a strong effect on PC1, while those which cluster between -0.01 and 0 on the PC1 axis have a larger effect on PC2.

In total, 986 *P. agathidicida* proteins were identified across all culture filtrate samples of the different liquid growth media by LC–MS, which accounts for 5.9% of *P. agathidicida* proteins predicted from the genome. A heatmap illustrating the presence/absence of the 986 identified *P. agathidicida* proteins in the different culture filtrates (**Figure 5.3**) further supports the PCA plot. The heatmap (**Figure 5.3**) clearly demonstrates that considerably more *P. agathidicida* proteins were identified in the biological replicates of PD culture filtrate, while growth in kauri leaf AWF resulted in the least number of *P. agathidicida* proteins (although, this is likely in part due to the AWF culture filtrate samples being 5x less concentrated that the other culture filtrate samples). As expected, based on the PCA plot, kauri leaf AWF and Henniger culture filtrates group together, while clarified V8 and most biological replicates of V8 culture filtrate shared a node with Plich culture filtrate (**Figure 5.3**).

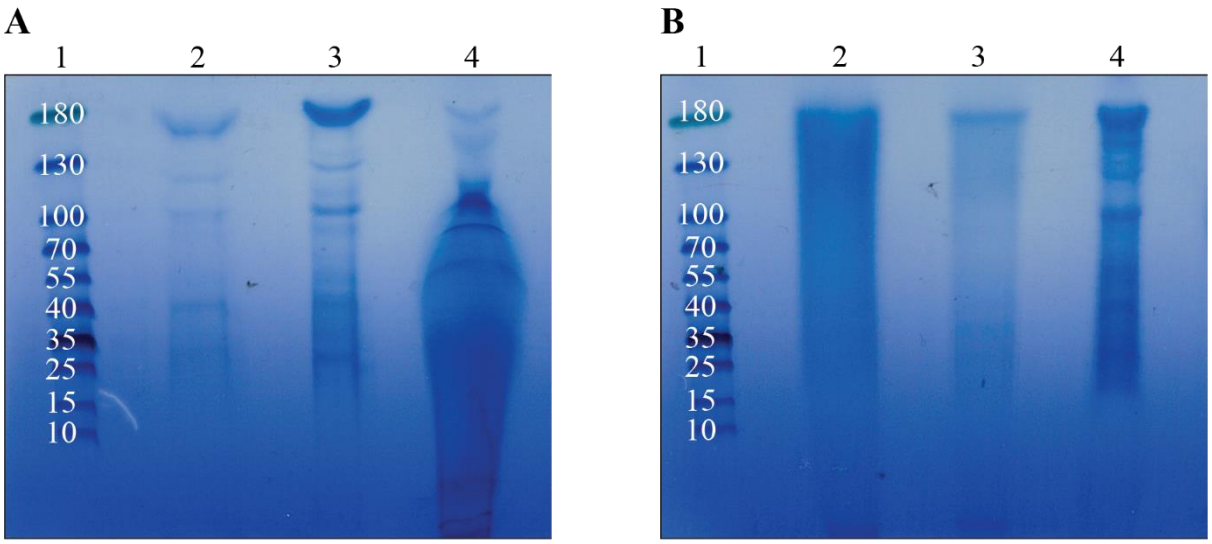

Figure 5.1. Protein profiles of *Phytophthora agathidicida* culture filtrates involving different liquid broth media or apoplastic wash fluid (AWF) from kauri sapling leaves.

P. agathidicida was grown in 10 mL of either Henniger, Plich, V8, clarified V8, or potato dextrose liquid broth medium, or 3 mL of AWF from kauri sapling leaves for 10 days. The resulting culture filtrate was freeze-dried, resuspended in 200 µL milliQ water, mixed with protein loading dye, and resolved on a 4–20% SDS gel by SDS-PAGE, before staining overnight with colloidal Coomassie. Lane 1 in both A and B contains the PageRuler™ pre-stained protein ladder. Gel **(A)** contains nutrient-poor culture filtrate; lane 2 = Henniger liquid broth medium, 3 = Plich liquid broth medium, 4 = kauri leaf AWF. Gel **(B)** contains nutrient-rich culture filtrate; lane 2 = V8 liquid broth medium, 3 = clarified V8 liquid broth medium, 4 = potato dextrose liquid broth medium. Protein profiles are representative of four biological replicates. All culture filtrates were 75 times the original concentration, except that of kauri AWF, which was only 15 times the original concentration.

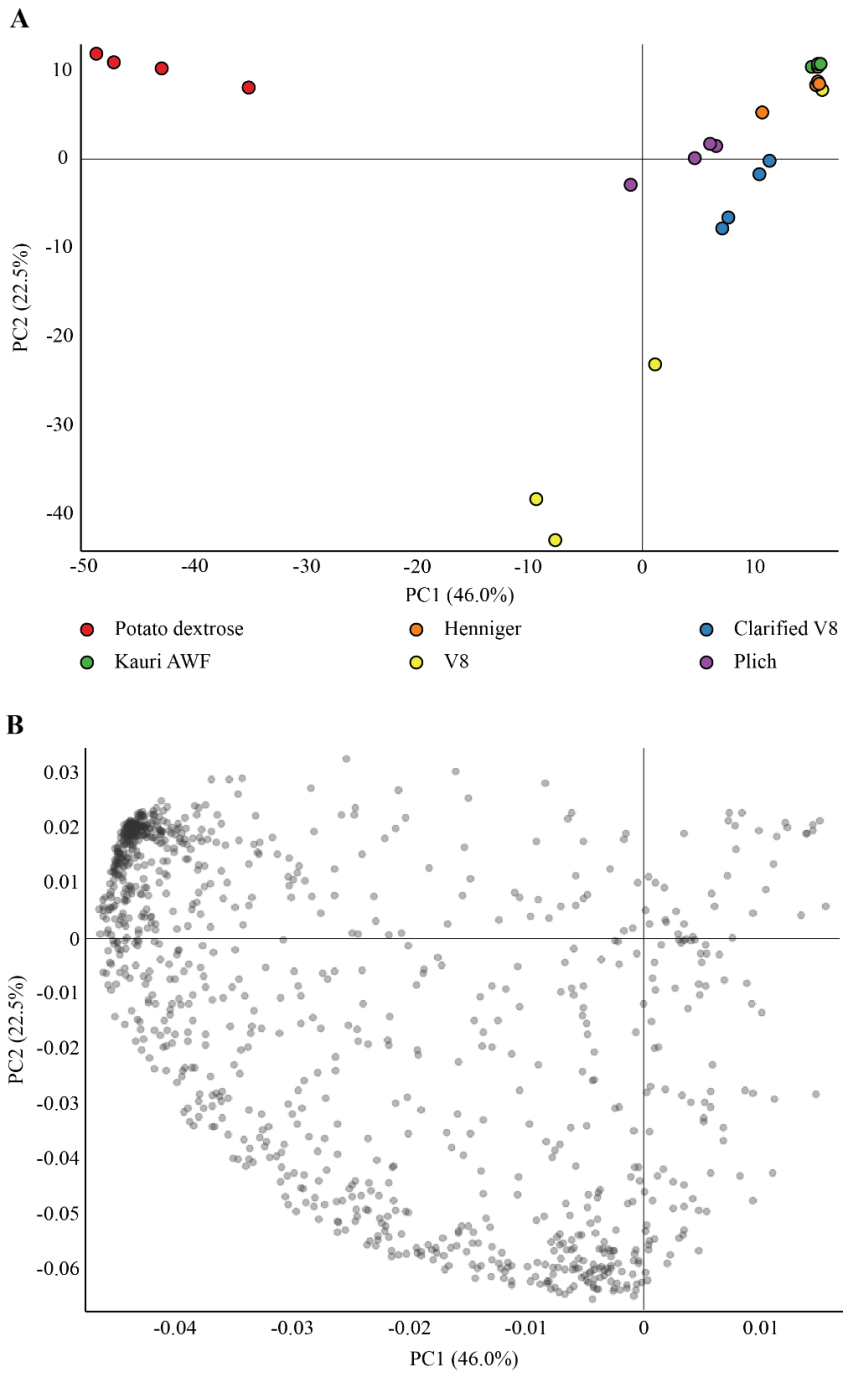

Figure 5.2. Principal component analysis (PCA) score plot of *Phytophthora agathidicida* culture filtrates after liquid chromatography–mass spectrometry (LC–MS) analysis.

P. agathidicida culture filtrates from nutrient-poor (Plich, Henniger, and kauri apoplastic wash fluid (AWF)) and nutrient rich (V8, clarified V8, and potato dextrose) liquid media were analysed by LC–MS analysis 10 days post-inoculation. A total of four biological replicates were analysed for each medium. The resulting peptide data were mapped to *P. agathidicida* predicted proteins. **(A)** A PCA plot was performed on the identified proteins using Proteome Discoverer v2.4.1.15 software. Two components explained 68.5% of the variance. **(B)** A PCA loadings plot suggests many proteins are responsible for the variance observed in the PCA plot.

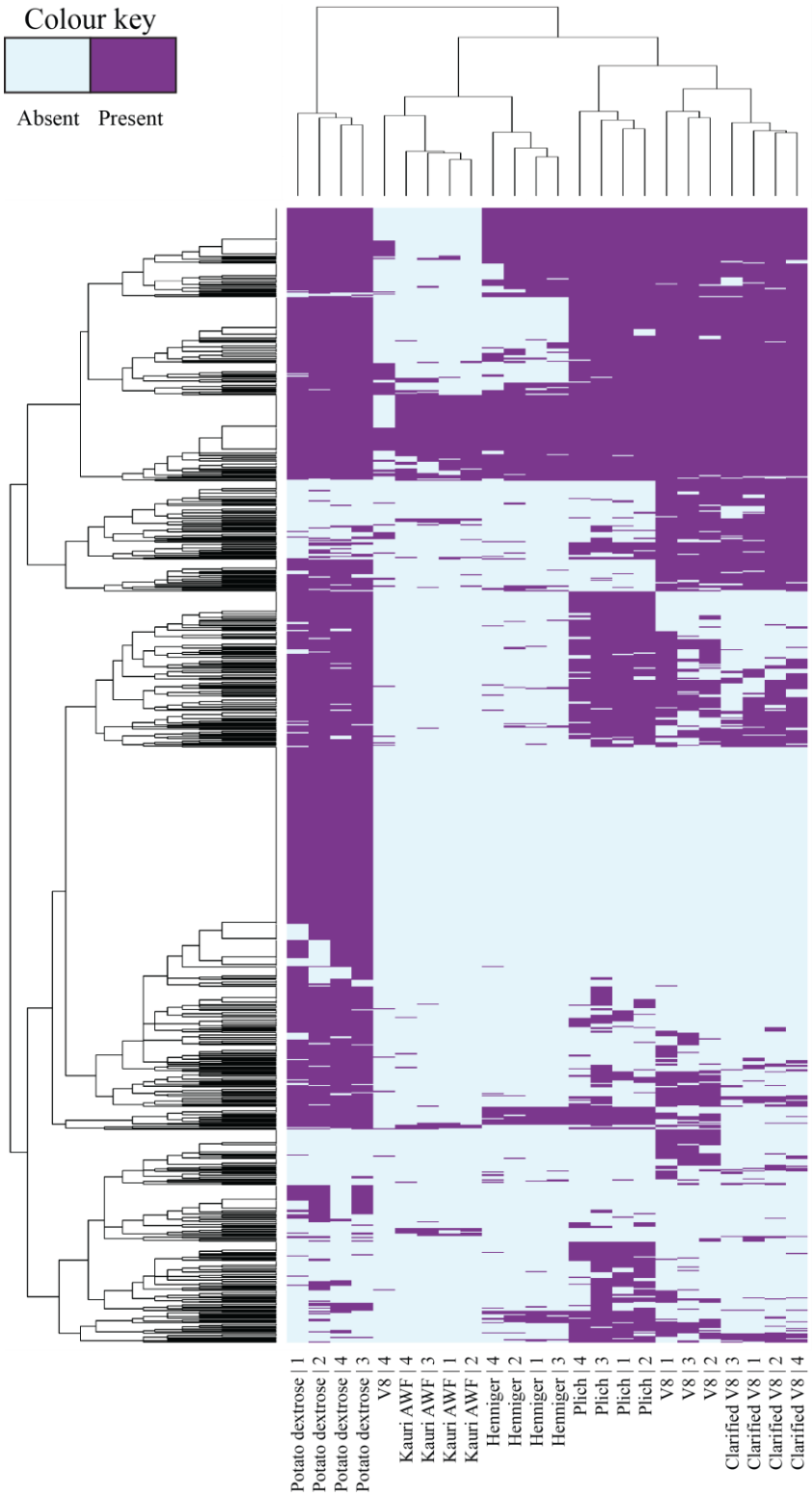

Figure 5.3. Heatmap demonstrating the presence and absence of *Phytophthora agathidicida* proteins identified by liquid chromatography-mass spectrometry in different culture filtrates.

P. agathidicida was grown in 10 mL of either Henniger, Plich, V8, clarified V8, or potato dextrose broth liquid medium, or 3 mL of apoplastic wash fluid (AWF) harvested from leaves of kauri saplings, for 10 days and the resulting culture filtrate analysed by liquid chromatography–mass spectrometry (LC–MS). Proteins were considered as present in a particular culture filtrate type if they were identified in at least two biological replicates (labelled 1–4) with high confidence. Column dendrograms indicate similarity of the biological replicates of the various culture filtrates based on presence/absence of the identified *P. agathidicida* proteins. Branch length is proportional to the degree of dissimilarity.

5.3.2 The number of classically secreted proteins produced by *P. agathidicida* differs between culture filtrates of different liquid growth media

Of the 986 proteins that were identified across all culture filtrate samples, 355 classically secreted proteins of *P. agathidicida* (i.e. that were predicted to have an N-terminal signal peptide, but no transmembrane domain), representing 16.1% of all 2,204 classically secreted proteins (SignalP v3.0) predicted from the *P. agathidicida* genome which did not contain a transmembrane domain (TMHMM v2.0), were confidently detected (**Appendix 5.1**). Thus, a large proportion (578) of the proteins identified have no obvious secretion signal. While a subset of these proteins were predicted to contain one or more transmembrane domains (56), and were therefore likely membrane-associated, the remaining proteins were not predicted to contain either a transmembrane domain or a signal peptide. These proteins may be the result of cytoplasmic contamination, released upon the natural turnover of the cell, or could be due to cell damage during the culture filtrate harvesting process. Alternatively, they may have been secreted from the cell via a non-classical secretion pathway.

Consistent with the PCA plot in **Figure 5.2 A**, the profile of secreted proteins in the different culture filtrates showed that, in most cases, the biological replicates grouped together (**Figure 5.4**). However, as observed in **Figure 5.2**, this was not the case for the fourth biological replicate of the V8 culture filtrate type (**Figure 5.4**). As illustrated in **Figure 5.4**, many of the classically secreted proteins from *P. agathidicida* were identified across all media types, with kauri leaf AWF culture filtrate being the most protein-poor of all the media tested (**Table 5.5**). This paucity of proteins in the kauri leaf AWF culture filtrate is in contrast to the amount of protein observed on the gel in **Figure 5.1**; however, it is anticipated that many of the proteins present in this sample type were of kauri origin. Perhaps not surprisingly, the secreted protein profile of the kauri leaf AWF culture filtrate was unlike any of the other culture filtrate types analysed, with the exception of the single V8 culture filtrate sample which did not group with the other three V8 culture filtrate biological replicates (**Figure 5.4**). As expected, both V8 and clarified V8 culture filtrates possessed similar protein profiles, though the V8 culture filtrate produced a larger number of proteins than clarified V8 culture filtrate (**Table 5.5**). Both nutrient-poor culture filtrates (Henniger and Plich) also produced similar profiles (**Figure 5.4**). Unexpectedly, potato dextrose (a nutrient-rich liquid broth medium) led to the production of a *P. agathidicida* secreted protein profile more like the culture filtrates in nutrient-poor liquid broth media than the other nutrient-rich liquid broth media (**Figure 5.4**).

Venn diagrams (**Figure 5.5 A**) demonstrated that 43% of the classically secreted *P. agathidicida* proteins detected in culture filtrate of nutrient-rich media types were common to all three nutrient-rich media. In contrast, only 27% of secreted proteins present in culture filtrate were common to all three

nutrient-poor media, including kauri leaf AWF (**Figure 5.5 B**). Of interest, only one classically secreted protein was found to be unique to culture filtrate of kauri leaf AWF (**Figure 5.5 C**, **Table 5.5**). This was Pag005016, which was anticipated to be a carbohydrate-binding elicitor lectin (CBEL) protein based on the three of the top 10 BLASTp hits (**Appendix 5.2**). In support of this, Pag005016 is predicted to contain a PAN (Interpro: IPR003609)/APPLE (Interpro: IPR000177) domain, and cellulose-binding domain (Interpro: IPR000254) (**Appendix 5.1**) and shares 83.8% identity with the characterised *Phytophthora parasitica* CBEL (Gaulin et al., 2006, Khatib et al., 2004) (**Figure 5.6**).

Interestingly, only two proteins were found to be unique to the culture filtrate of Henniger liquid medium, and this was also the case in the culture filtrate of the nutrient-rich clarified V8 liquid medium (**Table 5.5**). Higher numbers of unique proteins were identified in the culture filtrate of the nutrient-poor Plich liquid medium and both nutrient-rich V8 and PD liquid media, likely because higher numbers of classically secreted *P. agathidicida* proteins were identified in the culture filtrates of these media overall (**Table 5.5**)

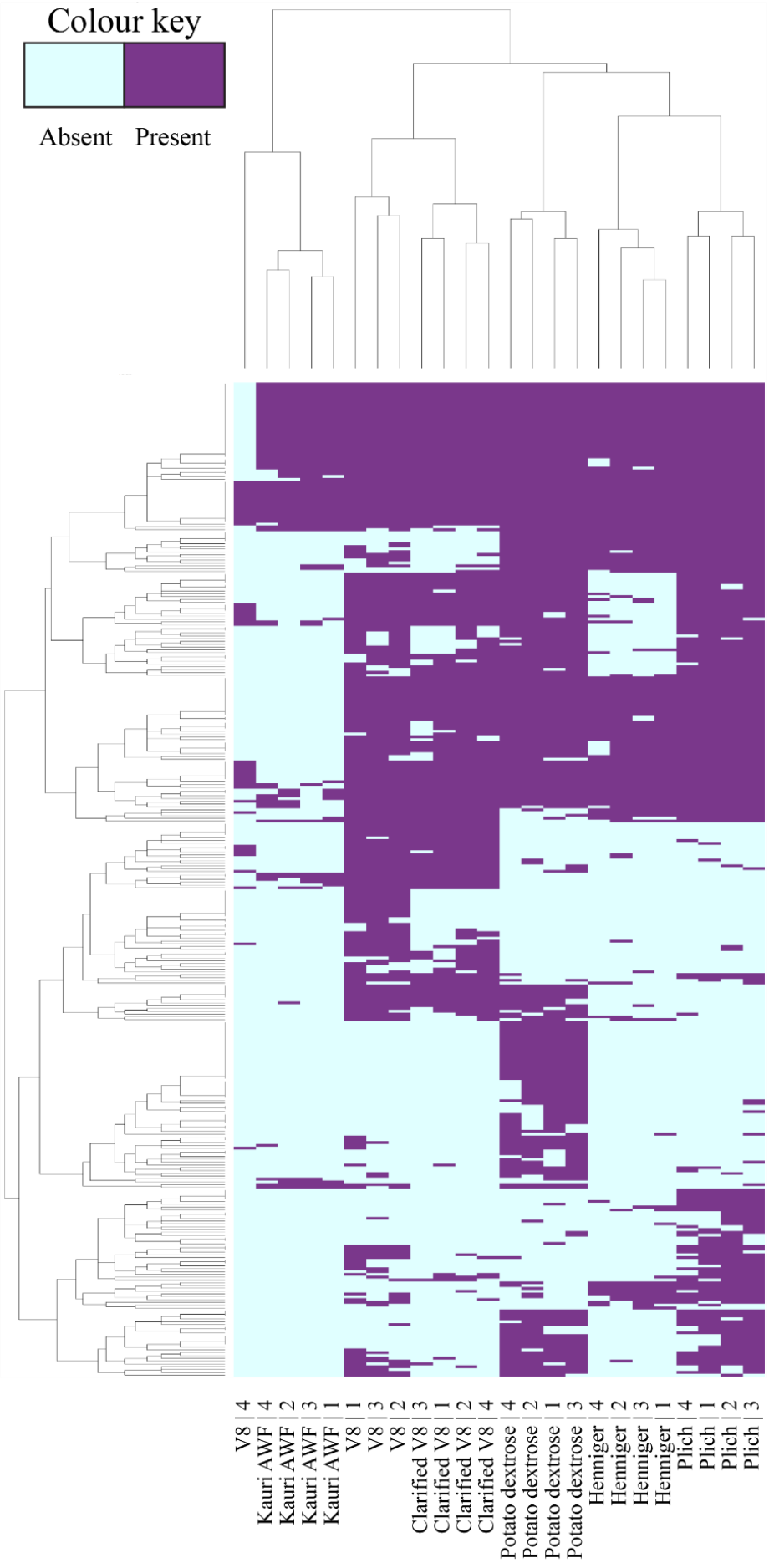

Figure 5.4. Heatmap demonstrating the presence and absence of classically secreted *Phytophthora agathidicida* proteins identified by liquid chromatography-mass spectrometry in different culture filtrates.

P. agathidicida was grown in 10 mL of either Henniger, Plich, V8, clarified V8, or potato dextrose broth liquid medium, or 3 mL of apoplastic wash fluid (AWF) harvested from leaves of kauri saplings, for 10 days and the resulting culture filtrate analysed by liquid chromatography–mass spectrometry (LC–MS). Proteins were considered as present in a particular culture filtrate type if they were identified in at least two biological replicates with high confidence. Proteins were considered as secreted if they were predicted to harbor an N-terminal signal peptide (SignalP v3.0) but not a transmembrane domain (TMHMM v.2.0). Row dendrograms indicate the similarity of each identified *P. agathidicida* classically secreted protein based on presence/absence across the different culture filtrates. Column dendrograms indicate similarity of the biological replicates (labelled 1–4) of the various culture filtrates based on presence/absence of the identified *P. agathidicida* proteins. Branch length is proportional to the degree of dissimilarity.

Table 5.5. Number of unique classically secreted proteins identified in *Phytophthora agathidicida* culture filtrates by liquid chromatography–mass spectrometry (LC–MS).

Liquid broth medium from which the culture filtrate was derived	Number of classically secreted *P. agathidicida* proteins identified	Number of classically secreted *P. agathidicida* proteins unique to each culture filtrate type
Potato dextrose	250	53
V8	231	18
Plich	224	22
Clarified V8	187	3
Henniger	137	2
Kauri leaf apoplastic wash fluid (AWF)	74	1

Classically secreted proteins were considered as present in a particular culture filtrate if they were identified in at least two of the four biological replicates with high confidence by LC–MS.

Nutrient-rich media are shaded in light grey. No shading is used for nutrient-poor media.

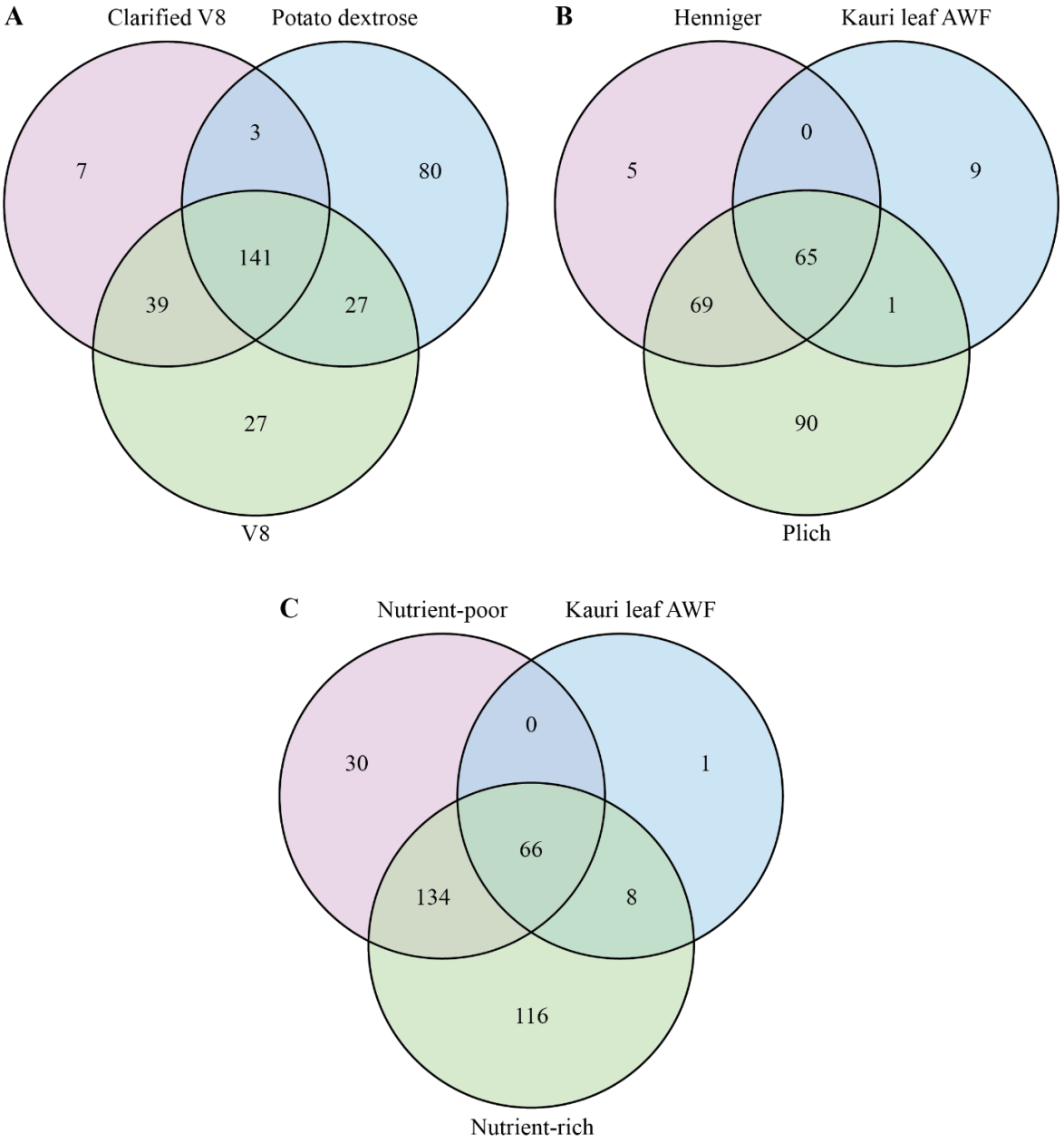

Figure 5.5. Venn diagrams of classically secreted *Phytophthora agathidicida* proteins identified by liquid chromatography–mass spectrometry (LC–MS) in different culture filtrates.

P. agathidicida was grown in 10 mL of either Henniger, Plich, V8, clarified V8, or potato dextrose liquid broth medium, or in 3 mL of apoplastic wash fluid (AWF) harvested from leaves of kauri saplings, for 10 days and the resulting culture filtrate analysed by LC–MS. Venn diagrams demonstrate the numbers of classically secreted *P. agathidicida* proteins unique and/or common to two or more different culture filtrates. **(A)** is a Venn diagram comparing the culture filtrates of different nutrient-rich media, **(B)** investigates the culture filtrates of different nutrient-poor media, **(C)** compares all culture filtrates of the nutrient-rich media (V8, clarified V8, potato dextrose) to all the nutrient-poor media (Plich and Henniger) and includes the culture filtrate of kauri AWF as a separate variable.

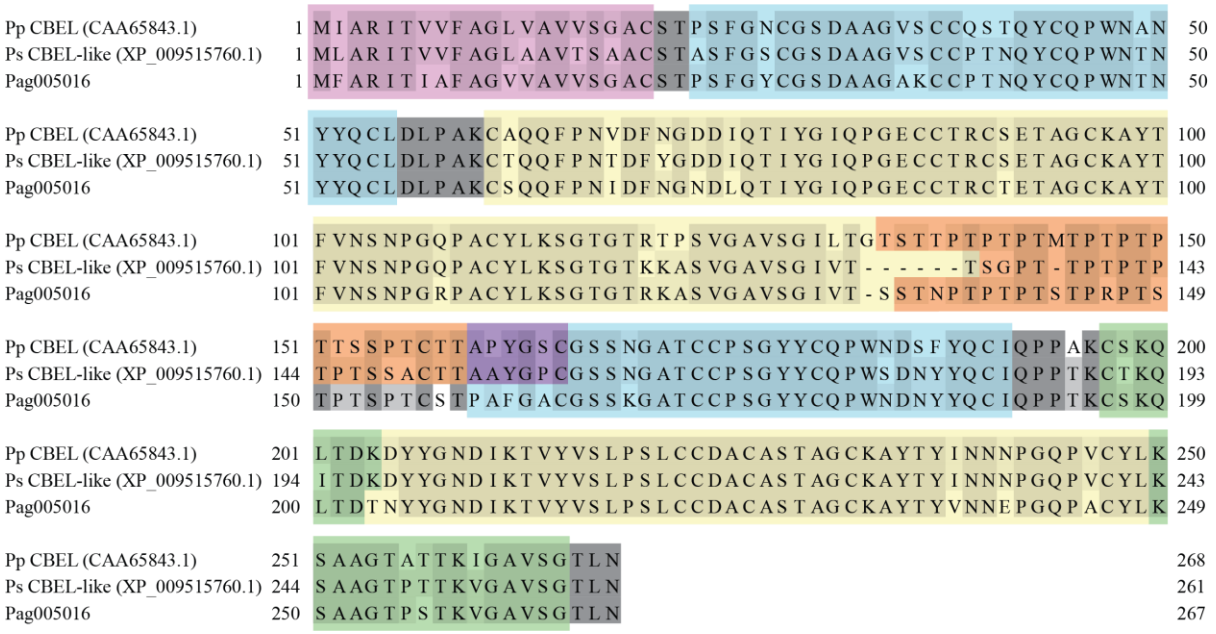

Figure 5.6. Alignment of *Phytophthora parasitica* cellulose binding elicitor lectin (CBEL) with homologs from *Phytophthora sojae* and *Phytophthora agathidicida*.

P. agathidicida Pag005016 was uniquely identified as a classically secreted protein in kauri leaf apoplastic wash fluid (AWF) culture filtrate. BLASTp analysis identified *P. sojae* CBEL-like protein (XP_009515760.1) as the top hit sharing 83.1% identity with Pag005016. The CBEL protein was first characterised in *P. parasitica* (Gaulin et al., 2006, Khatib et al., 2004) and shares 83.2% identity with Pag005016. The N-terminal signal peptide is highlighted in pink, cellulose-binding domain in blue, the PAN domains in orange and the APPLE domains in green. Overlap between the PAN and APPLE domains are highlighted in yellow, while overlap between the PAN and cellulose-binding domain is highlighted purple. Shading is indicative of sequence conservation. The GenBank accession number is in brackets. Pp = *P. parasitica,* Ps = *P. sojae*, Pag = *P. agathidicida*.

5.3.3 Many of the classically secreted proteins produced by *P. agathidicida* in culture filtrate of different liquid media are predicted to be effectors

EffectorP v3.0 (Sperschneider & Dodds, 2022), which is suitable for both fungi and oomycetes and distinguishes apoplastic and cytoplasmic effectors, was used to predict whether the classically secreted *P. agathidicida* proteins are candidate effectors. Based on this analysis, just over one third of the classically secreted *P. agathidicida* proteins were predicted to be effectors (**Figure 5.7 A**), with approximately half of these expected to act in the apoplastic environment between plant cells, and the other half expected to be translocated into the host cell cytoplasm, where they perform their virulence function. Of the putatively apoplastic effectors, over 40% were predicted to belong to the carbohydrate-active enzyme (CAZyme) family (27), though CBELs (3), elicitins (2), necrosis-inducing *Phytophthora* proteins (NPP1s) (2), and an RxLR (1) were also predicted (**Figure 5.7 B**). RxLRs were the largest class of predicted cytoplasmic effectors identified (10), though NPP1 (3) and Crinkler (2) proteins were also identified, along with an elicitin. As RxLRs are cytoplasmic proteins (Liu et al., 2018, Kamoun, 2006), it is likely that the RxLR predicted to be an apoplastic effector by EffectorP is instead a false-positive result. The presence/absence profile (**Appendix 5.3**) of these predicted effector proteins was slightly different from the presence/absence profile of collective classically secreted *P. agathidicida* proteins (**Figure 5.4**). As previously identified in **Figure 5.4**, culture filtrates from both clarified V8 and V8 liquid media grouped together (**Appendix 5.3**), though more proteins were identified in V8 culture filtrate. In line with this, biological replicates from PD culture filtrate clustered on the same branch (**Appendix 5.3**). Interestingly, while culture filtrates from kauri AWF and Henniger liquid media were shown to be very different during analysis of all classically secreted *P. agathidicida* proteins, they both group together when analysing just those proteins that are predicted to be effectors (**Appendix 5.3**).

An RNA-sequencing time-course experiment was performed by other members of our lab in collaboration with Scion, where kauri was infected with *P. agathidicida* type strain 3813 and samples were harvested from kauri root and leaf tissue at 6, 24, 48, and 72 h post-inoculation (hpi) (Guo & Shiller, Unpublished). These data demonstrated that genes encoding apoplastic and cytoplasmic effectors were some of the most highly expressed *in planta* among the set of classically secreted *P. agathidicida* proteins identified during this experiment (**Appendix 5.1**). The predicted elicitin and candidate apoplastic effector Pag014379, which is one of at least four *P. agathidicida* proteins identified in the predicted proteome that share identity with *Phytophthora infestans* INF1 (**Figure 5.8**) (Kamoun et al., 1997), showed the highest level of expression of all the genes encoding for classically secreted *P. agathidicida* proteins. The Pag014379 protein was identified in all culture filtrates analysed in this study and, perhaps unsurprisingly, expression of *Pag014379* was high when grown in clarified V8 broth

(**Appendix 5.1**). While *Pag014379* expression decreased dramatically in kauri leaves 24 hpi, in kauri roots an increase in expression was observed 6 hpi, which subsequently decreased from 24 hpi before increasing again 72 hpi (**Appendix 5.1**). Another highly expressed candidate apoplastic effector was *Pag011407*. The Pag011407 protein, like the candidate elicitin Pag014379, was identified in all culture filtrates used in this study. BLASTp analysis identified homology with a *Phytophthora palmivora* var. *palmivora* OPEL, a protein first characterised in *P. parasitica* (**Figure 5.9**) (Chang et al., 2015). The RNA-sequencing data showed that *Pag011407* was expressed well *in vitro*, and that expression increased in kauri leaves 6 hpi, however the most dramatic change was observed in kauri roots, with a considerable increase at 6 hpi which slowly decreased over time (**Appendix 5.1**).

BLASTp analysis of the 11 RxLRs identified among the classically secreted *P. agathidicida* proteins showed that three were homologs of characterised RxLRs from other *Phytophthora* species. Two RxLRs, Pag017304 and Pag002190, were homologs of *Phytophthora ramorum* PSR2 (*Phytophthora* suppressor of RNAi silencing 2), an RxLR which was first identified in *P. sojae* (Qiao et al., 2013). An alignment of Pag017304 and Pag002190 with *P. sojae* PsPSR2 proteins (KAH7495962.1 (51.9% identity) and KAH7464933.1 (48.4% identity) respectively) illustrates that both the RxLR and EER motif are conserved between PsPSR2 and Pag017304, however this conservation has not been maintained in Pag002190 (**Figure 5.10**). Peak expression of the *PsPSR2* gene in *P. sojae* was between 20–24 hpi of soybean roots, which the authors suggest may indicate a role in regulating the necrotrophic switch (Qiao et al., 2013). Similarly, peak expression of *Pag002190* and *Pag017304* in *P. agathidicida*-infected kauri roots was at 24 hpi and 48 hpi respectively (**Appendix 5.1**). The third RxLR, Pag016631 was identified as a homolog of Avr1b-1 from *P. palmivora* var. *palmivora* (sharing 66.2% identity), another RxLR virulence factor originally identified in *P. sojae* (**Figure 5.11**) (Shan et al., 2004). *Pag016631* was one of the most highly expressed of the candidate RxLR effectors identified, with expression peaking in kauri roots and leaves at 48 hpi (**Appendix 5.1**).

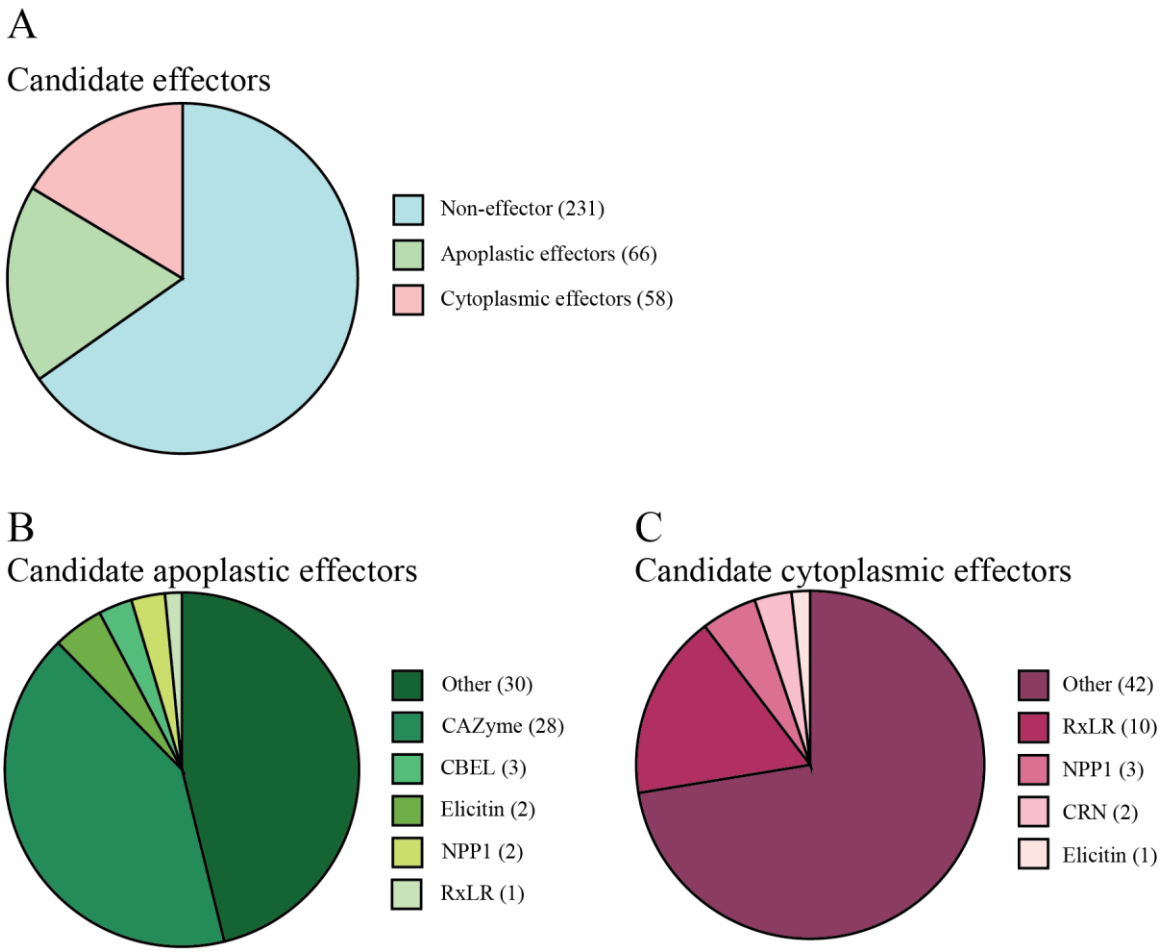

Figure 5.7. Pie graphs detailing the proportion of classically secreted *Phytophthora agathidicida* proteins detected in different culture filtrates that are predicted to be effectors.

P. agathidicida was grown in 10 mL of either Henniger, Plich, V8, clarified V8, or potato dextrose liquid broth medium, or 3 mL of apoplastic wash fluid (AWF) from leaves of kauri saplings for 10 days and the resulting culture filtrate analysed by liquid chromatography–mass spectrometry (LC–MS). **(A)** Proportion of classically secreted *P. agathidicida* proteins identified from LC–MS analysis that are predicted to be effectors. **(B)** Selected classes of classically secreted proteins from (A) that are predicted to be apoplastic effectors. **(C)** Selected classes of classically secreted proteins from (A) that are predicted to be cytoplasmic effectors. Numbers in brackets indicate the number of proteins belonging to that class. Carbohydrate-active enzyme (CAZyme), carbohydrate-binding elicitor lectin (CBEL), necrosis-inducing *Phytophthora* protein (NPP1), crinkling and necrosis protein (CRN).

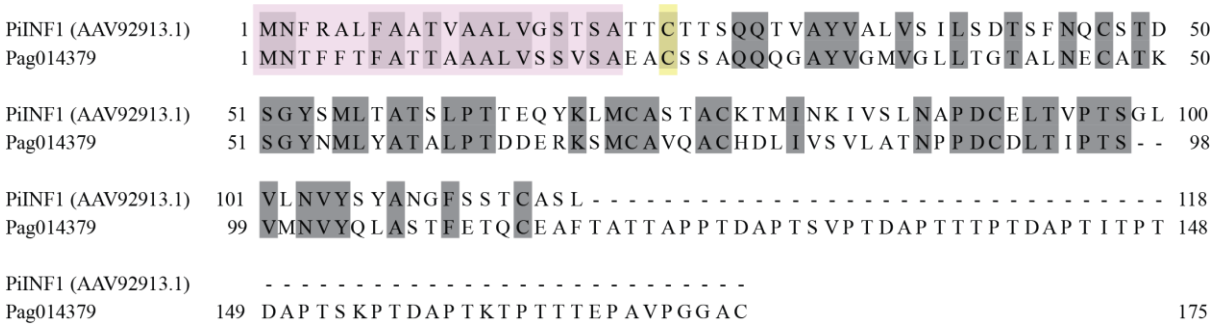

Figure 5.8. Alignment of *Phytophthora infestans* elicitin INF1 with a highly expressed homolog identified among the classically secreted *Phytophthora agathidicida* proteins detected in different culture filtrates.

P. agathidicida Pag014379 was identified as a classically secreted candidate apoplastic effector in culture filtrates with and shares 48.3% identity with the known *P. infestans* INF1 elicitin (Kamoun et al., 1997). The N-terminal signal peptide is highlighted in pink. Conserved cysteine residues which are critical to cell death elicitor activity (Kamoun et al., 1997) are highlighted in yellow. The GenBank accession number is in brackets. Shading indicates conservation. Pi = *P. infestans*, Pag = *P. agathidicida*.

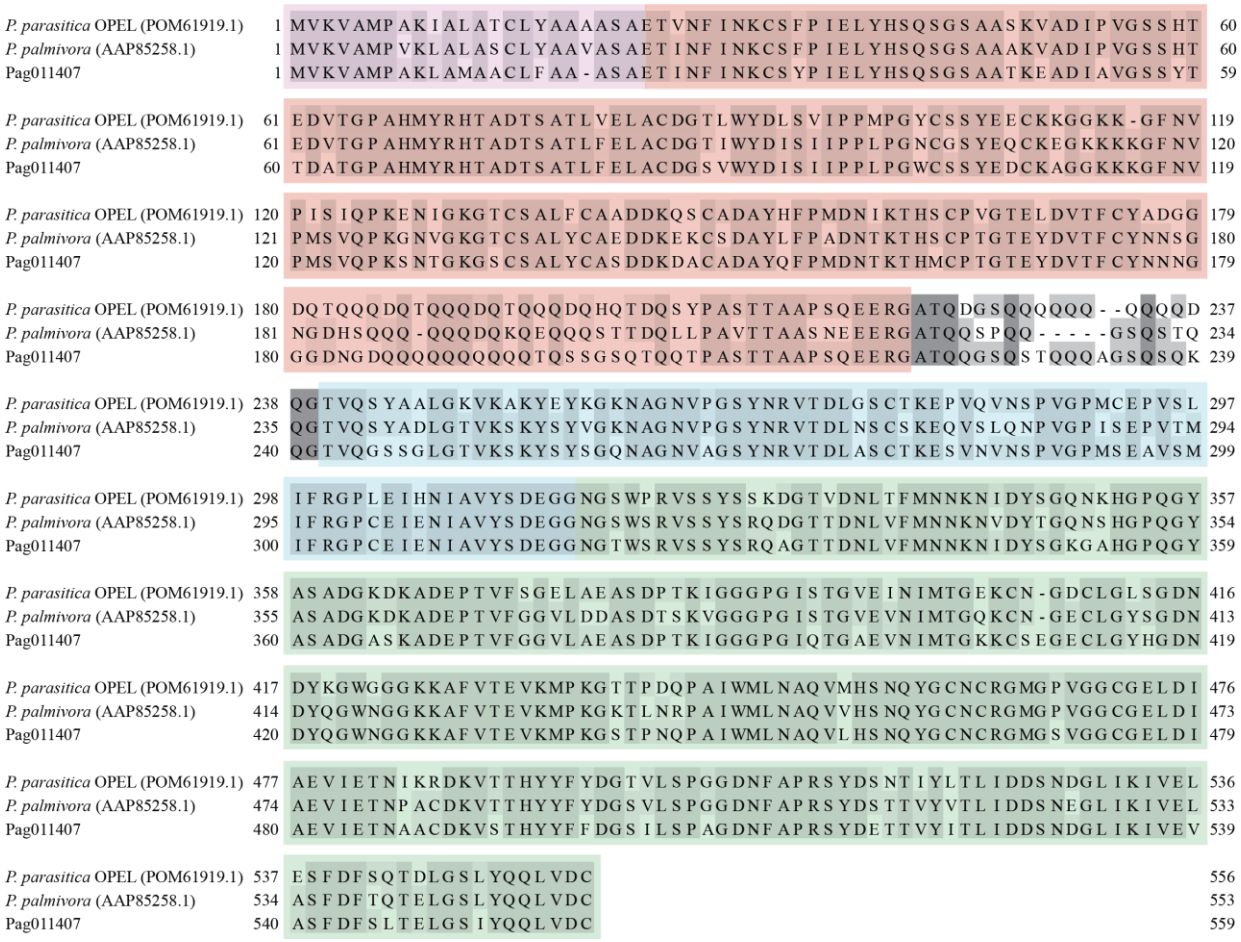

Figure 5.9. Alignment of *Phytophthora parasitica, Phytophthora palmivora* var. *palmivora* OPEL with a highly expressed homolog identified among the classically secreted *Phytophthora agathidicida* proteins detected in different culture filtrates.

P. agathidicida Pag011407 was identified as a classically secreted candidate apoplastic effector in culture filtrates with homology to the *P. palmivora* var. *palmivora* OPEL which was characterised in *P. parasitica* (Chang et al., 2015), sharing 77.4% and 80.2% identity respectively. The N-terminal signal peptide is highlighted in pink, the thaumatin domain in orange, the glycine-rich domain in blue, and the glycoside hydrolase domain in green (Chang et al., 2015). GenBank accession numbers are in brackets. Shading is indicative of sequence conservation. Pag = *P. agathidicida*

Figure 5.10. Alignment of *Phytophthora sojae* RxLR effector PSR2 with homologs in *Phytophthora ramorum* and two candidate RxLR effectors identified among the classically secreted *Phytophthora agathidicida* proteins detected in different culture filtrates.

P. agathidicida Pag017304 and Pag002190 were identified as classically secreted candidate RxLR effectors in culture filtrates with homology to two uncharacterised predicted PSR2 proteins from *P. ramorum*. The PSR2 RxLR effector was first characterised in *P. sojae*. The N-terminal signal peptide is highlighted in pink. Conserved RxLR and EER motifs are highlighted in blue. GenBank accession numbers are in brackets. Shading is indicative of sequence conservation. Ps = *P. sojae*, Pr = *P. ramorum*, Pag = *P. agathidicida*.

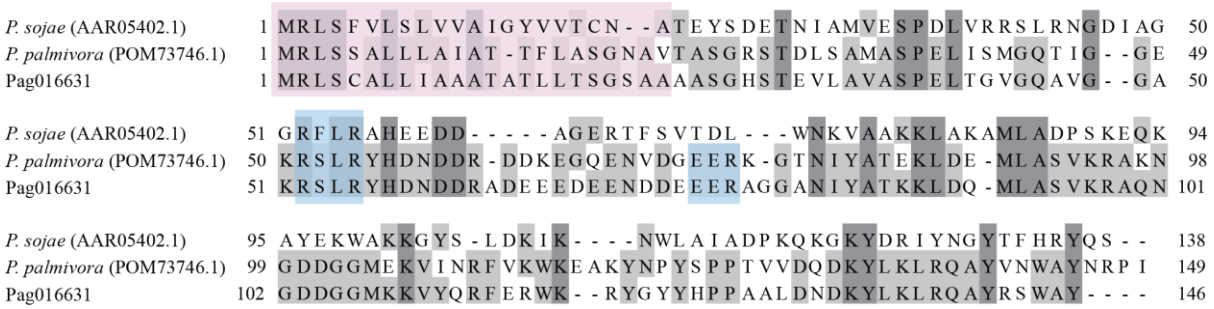

Figure 5.11. Alignment of *Phytophthora sojae* RxLR effector Avr1b-1 with a homolog from *Phytophthora palmivora* and a candidate RxLR effector identified among the classically secreted *Phytophthora agathidicida* proteins detected in different culture filtrates.

P. agathidicida Pag016631 was identified as a classically secreted candidate RxLR effector in culture filtrates with homology to the *P. palmivora* var. *palmivora* Avr1b-1 RxLR effector characterised in *P. sojae*. The amino (N)-terminal signal peptide is highlighted in pink. Conserved RxLR and EER motifs are highlighted in blue. GenBank accession numbers are in brackets. Shading is indicative of conservation. Pag = *P. agathidicida*.

5.3.3 Analysis of the classically secreted proteins produced by *P. agathidicida* in culture filtrate of different media suggests carbohydrate-active enzymes (CAZymes) are over-represented

A considerable portion of the classically secreted *P. agathidicida* proteins identified by LC–MS analysis after growth in various liquid broth media were CAZymes (**Figure 5.12 A**) and of these, the majority were glycoside hydrolase (GH) proteins (**Figure 5.12 B**). Enzymes predicted to be CAZymes (dbCAN2) make up approximately 2% of the proteins predicted from the *P. agathidicida* genome. However, of the classically secreted *P. agathidicida* proteins identified in the culture filtrate of the various liquid media samples, more than 26% were predicted to encode CAZymes (dbCAN2 and BLASTp analysis). A heatmap (**Figure 5.13**) of the classically secreted *P. agathidicida* GH proteins shows a profile like that of the complete set *P. agathidicida* secreted proteins (**Figure 5.4**). Once again, the profile of proteins found in clarified V8 and V8 culture filtrates was very similar, except for one of the V8 replicates. A total of 20 of the 74 identified GHs were found to be present in all media, and this included four belonging to the GH30 and four belonging to the GH12 family. BLASTp analysis revealed that one of these, Pag017848, was the orthologue of the well-known effector, *Phytophthora sojae* PsXEG1. All four GH12 proteins were among those found to trigger a cell death response during *Agrobacterium tumefaciens*-mediated transient transformation assays in *Nicotiana benthamiana* and *Nicotiana tabacum* (**Chapter 3, Figure 3.8**, protein name conversion found in **Appendix 3.5**). RNA-sequencing data showed that of the four GH12 proteins found in all culture filtrates, the genes encoding Pag000709 and Pag017830 exhibited the highest levels of expression, peaking at 48 hpi in both kauri leaves (*Pag000709*, 900 FPKM average; *Pag017830* 721 FPKM average) and roots (*Pag000709*, 752 FPKM average; *Pag017830* 812 FPKM average). The gene encoding the PsXEG1 orthologue, Pag017848, peaked even earlier at 6 hpi and this peak in expression was considerably higher in roots (502 FPKM average) than in leaves (142 FPKM average). While the gene encoding Pag017829 showed little change overall, peaks at 48 hpi in leaves (57 FPKM average) and 72 hpi in roots (63 FPKM average) were observed. Unlike *Pag000709* (162 FPKM), *Pag017830*, *Pag017848*, and *Pag017829,* all showed relatively low levels of expression (≤18 FPKM) in clarified V8 liquid medium.

No *P. agathidicida* GH proteins were identified as uniquely produced in the culture filtrate of kauri AWF. Seven GH proteins were uniquely identified in the culture filtrate of PD liquid medium, many of which were GH28 enzymes. Only one GH28 was found to be uniquely produced by *P. agathidicida* in the culture filtrate of Henniger liquid medium, although five different GH proteins from several different GH families were uniquely identified in the culture filtrate of Plich liquid medium.

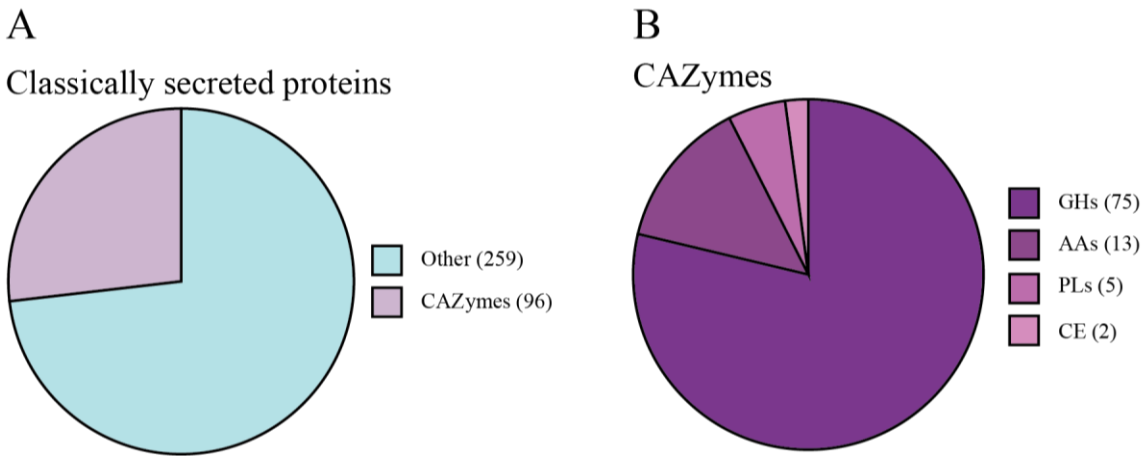

Figure 5.12. Pie graphs showing the proportion of classically secreted *Phytophthora agathidicida* proteins identified in different culture filtrates by liquid chromatography–mass spectrometry that are predicted to be carbohydrate-active enzymes (CAZymes).

P. agathidicida was grown in 10 mL of either Henniger, Plich, V8, clarified V8, or potato dextrose liquid broth medium, or 3 mL of apoplastic wash fluid (AWF) from leaves of kauri saplings for 10 days and the resulting culture filtrate analysed by liquid chromatography–mass spectrometry (LC–MS). **(A)** Pie graph showing the proportion of classically secreted *P. agathidicida* proteins identified from LC–MS analysis that are predicted to be CAZymes. **(B)** *P. agathidicida* CAZymes from A. are predicted to belong to the following families: Glycoside hydrolase (GH), Auxiliary activity (AA), Polysaccharide lyase (PL), Carbohydrate esterase (CE). Numbers in brackets indicate the number of proteins belonging to that class.

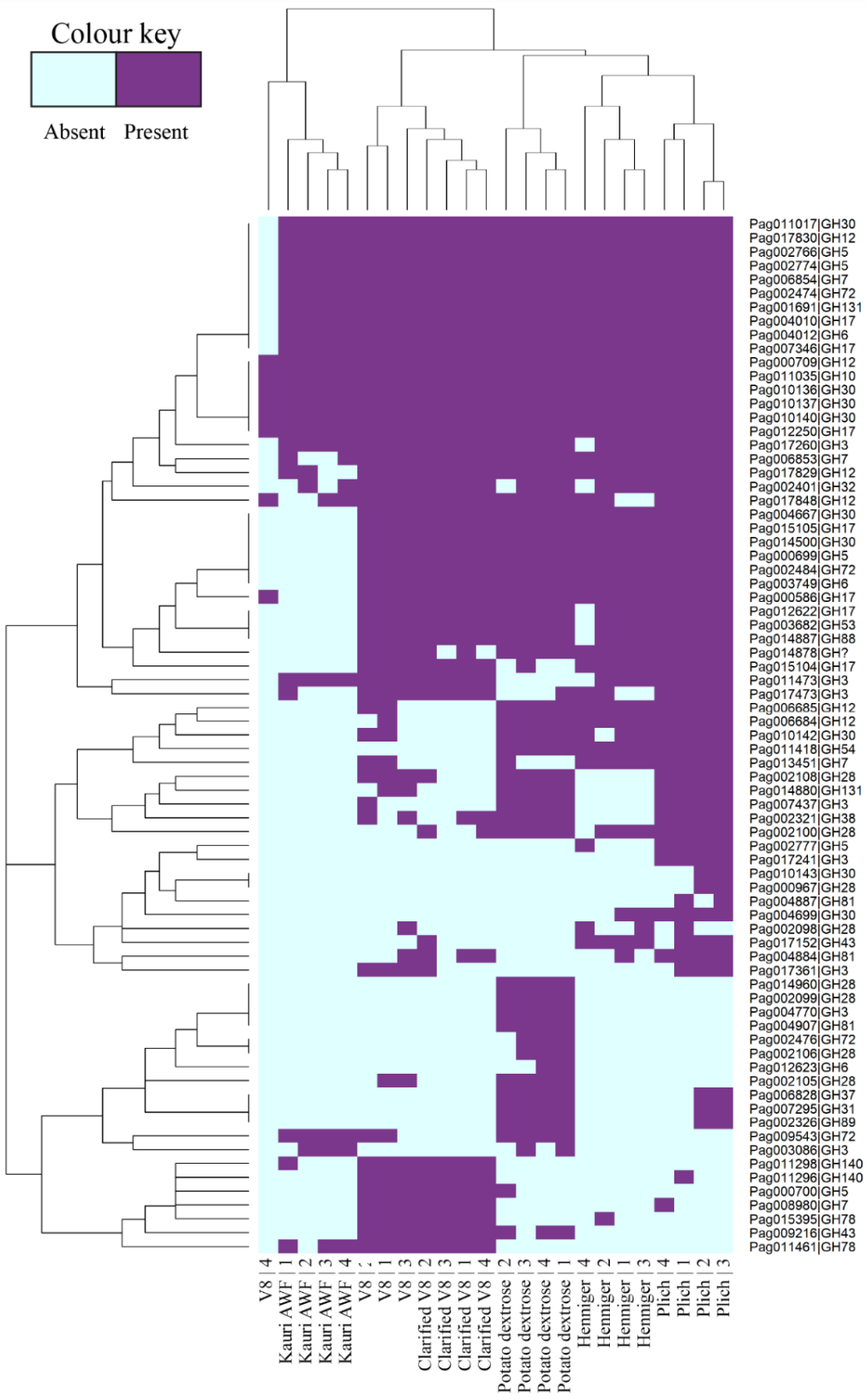

Figure 5.13. Heatmap demonstrating the presence and absence of classically secreted *Phytophthora agathidicida* glycoside hydrolase (GH) proteins identified by liquid chromatography-mass spectrometry in different culture filtrates.

P. agathidicida was grown in 10 mL of either Henniger, Plich, V8, clarified V8, or potato dextrose liquid broth medium, or 3 mL of apoplastic wash fluid (AWF) from leaves of kauri saplings for 10 days and the resulting culture filtrate analysed by LC–MS. Proteins were marked as present in a particular culture filtrate type if they were identified in at least two biological replicates with high confidence. CAZyme annotation was performed using dbCAN2. Row dendrograms indicate the similarity of each identified *P. agathidicida* classically secreted predicted GH protein based on presence/absence across the different culture filtrates. Column dendrograms indicate similarity of the biological replicates (labelled 1–4) of the various culture filtrates based on presence/absence of the identified *P. agathidicida* proteins. Branch length is proportional to the degree of dissimilarity.

5.3.4 Analysis of non-secreted *P. agathidicida* proteins may provide valuable insights into non-classically secreted effectors

An important, but often neglected, part of the data are proteins which are predicted to be present in culture filtrate but lack an N-terminal signal peptide. Indeed, in this study, only proteins identified in *P. agathidicida* culture filtrate which were predicted to contain an N-terminal signal peptide were analysed in detail. One explanation for the presence of proteins with no signal peptide in the *P. agathidicida* secretome is intracellular contamination. The top hit of a BLASTp analysis of proteins lacking both an N-terminal signal peptide and a transmembrane domain, identified seven proteins that are predicted to be associated with mitochondria, suggesting that their presence is the result of cytoplasmic contamination.

Another explanation is that these proteins undergo non-classical secretion, such as the *P. sojae* isochorismatase, PsIsc1 (Liu et al., 2014). A BLASTp analysis of the PsIsc1 protein sequence (G4YEI5.1) against proteins predicted in the *P. agathidicida* genome identified one protein, Pag004037, with homology to PsIsc1 (91.7% identity) (**Figure 5.14**). Conserved catalytic residues present in both PsIsc1 and the corresponding homolog from the phytopathogenic fungus *Verticillium dahliae*, VdIsc1, were also found to be conserved in Pag004037 (**Figure 5.14**) (Liu et al., 2014). Furthermore, Pag004037 was predicted to lack both a transmembrane domain and signal peptide and was identified only in the culture filtrate of PD liquid medium (**Appendix 5.4**). Thus it was surprising that RNA sequencing data (Guo & Shiller, Unpublished), showed that *Pag004037* was expressed (83 FPKM average) *in vitro* (**Appendix 5.4**). Expression of *Pag004037* was found to decrease slightly upon kauri infection of leaves but increased again to peak at 72 hpi (**Appendix 5.4**). Despite an initial slight decrease at 6 hpi in *P. agathidicida*-infected kauri roots, expression of *Pag004037* steadily increased to peak at 72 hpi (**Appendix 5.4**).

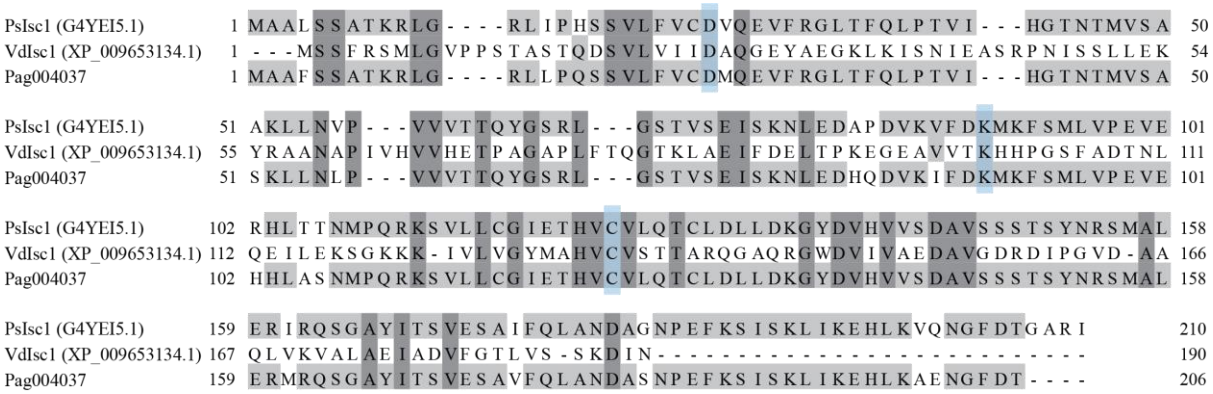

Figure 5.14. Alignment of *Phytophthora sojae* and *Verticillium dahliae* non-classically secreted isochorismatase 1 protein (Isc1) with a homolog identified among *Phytophthora agathidicida* proteins detected in different culture filtrates.

P. agathidicida Pag004037 was identified as a homolog of both *P. sojae* and *V. dahliae* Isc1 during a BLASTp analysis against proteins predicted from the *P. agathidicida* genome. Conserved residues, which form the catalytic triad and are critical for isochorismatase activity, are highlighted in blue (Liu et al., 2014). GenBank accession numbers are in brackets. Shading indicates sequence conservation. Ps = *P. sojae*, Vd = *V. dahliae*, Pag = *P. agathidicida*

5.4 Discussion

This chapter focused on the use of LC–MS to identify proteins from the *P. agathidicida* extracellular secretome during growth in liquid culture. Like in the study by Meijer et al. (2014), *P. agathidicida* was inoculated into liquid media which covered a range of different nutritive values. While LC–MS is a useful technique to study plant pathogens, it is not infallible. In this study, trypsin was used to digest proteins into shorter 700–1,500 kDa peptides for MS analysis. Trypsin cuts at the carboxyl end of arginine (R) and lysine (K) residues, leaving a charged end which is easily detectable by MS. However, some proteins may have too many or too few (or no) R/K residues, and thus are not detected by MS analysis. Additional proteins may not be detected simply by chance due to their low abundance. Despite these limitations, many studies have shown that LC–MS is an invaluable technique for studying the presence (and abundance) of proteins under different conditions (Meijer et al., 2014), or during different life stages (Andronis et al., 2022, Savidor et al., 2008). The aim of this chapter was to investigate the extracellular secretome of *P. agathidicida* grown in different liquid media. Of particular interest was whether growth of *P. agathidicida* in kauri leaf AWF, or even nutrient-poor liquid media, would be sufficient to stimulate production of proteins, termed effectors, involved in host colonisation.

In agreement with earlier studies investigating the secretome of *Phytophthora* species (Andronis et al., 2022, Meijer et al., 2014, Severino et al., 2014), several proteins belonging to well-known effector families were identified. Of the 43 elicitins predicted in the *P. agathidicida* genome, only six were identified among the classically secreted *P. agathidicida* proteins, fewer than the 11 identified in the secretome of *P. infestans* (Meijer et al., 2014) or the 14 identified in the *P. cinnamomi* secretome (Andronis et al., 2022). Elicitins are thought to act as extracellular sterol carriers in *Phytophthora* species (Mikes et al., 1998, Vauthrin et al., 1999), as *Phytophthora* are sterol auxotrophs (Steel & Drysdale, 1988, Latijnhouwers et al., 2003) unable to make sterols themselves, but must instead harvest them from their environment (including from plant plasma membranes) (Vauthrin et al., 1999). At least four of the 43 predicted *P. agathidicida* elicitins were found to be homologs of *P. infestans* INF1, one of which, Pag014379, was the most highly expressed of all classically secreted *P. agathidicida* proteins and was identified in all culture filtrates as a candidate apoplastic effector. This is not surprising, as many *Phytophthora* species are predicted to have more than one *PiINF1*-like gene, including *P. infestans* (Liu et al., 2015). *P. infestans* PiINF1 is a well-known elicitin expressed in *P. infestans* mycelia and in the later stages of infection during sporulation and leaf necrosis (Kamoun et al., 1997). Interestingly, while PiINF1 triggers a cell death response upon infiltration into *N. benthamiana* following its recognition by a plasma membrane-associated lectin-like receptor kinase (Kamoun et al., 1997, Kanzaki et al., 2008), no cell death response is observed in tomato, despite activation of the jasmonic acid and ethylene biosynthesis plant defence pathways (Kawamura et al., 2009). *P.*

agathidicida INF1 has previously been shown to elicit a cell death response in *N. benthamiana* (Guo et al., 2020a), and has been used as a positive control in **Chapter 3**. PaINF1 was not detected in culture filtrate as it was had not been annotated in the version of the genome that was used for analysis. Nevertheless, it would be of interest to determine whether the Pag014379 elicitin was also able to elicit a cell death response in *N. benthamiana*.

Another candidate apoplastic effector of interest identified among the classically secreted *P. agathidicida* proteins was Pag011407 which appears to encode an OPEL. OPELs are thought to be oomycete-specific effectors (Araújo et al., 2019). Characterised in *P. parasitica*, *PpOPEL* was expressed during all life stages, though expression increased during infection of *N. benthamiana* (Chang et al., 2015). Though PpOPEL is thought to produce a DAMP, the substrate and products are unknown, as despite containing active site residues for laminarase, and despite mutation of these residues abolishing cell death activity, no enzymatic activity has yet been detected on either laminarin or 1,3-β-glucan (Chang et al., 2015).

Eleven RxLR proteins were identified across the complete set of culture filtrates, all of which were predicted to be candidate effectors. Three of these RxLRs were homologs of previously characterised RxLR proteins, PsPSR2 and Avr1b-1. The *P. sojae* RxLR PSR2 is thought to suppress the RNA-interference silencing mechanism by targeting the accumulation of specific trans-acting short interfering RNAs (ta-siRNAs) and has been shown to have an important role in virulence (Qiao et al., 2013). Furthermore, PSR2 proteins are apparently abundant in *Phytophthora* species, with up to 84 PSR2-like proteins identified in *P. ramorum* (He et al., 2019). The RxLR Avr1b-1 was also identified in *P. sojae*, where it is recognised and triggers cell death in soybean carrying the *Rps1b* resistance gene (Shan et al., 2004). Consequently, knock-out of the *Avr1b-1* gene in *P. sojae* was found to increase virulence of the pathogen in soybean carrying *Rps1b* (Gu et al., 2021).

In addition to the above effectors, six NPP1 and four CRNs were identified in the classically secreted *P. agathidicida* proteins. Similarly, eight and four NPP1 proteins were identified in the *P. cinnamomi* and *P. plurivora* culture filtrate secretomes respectively (Andronis et al., 2022, Severino et al., 2014). The NPP1 protein from *P. parasitica* has been shown to elicit plant defence responses in both parsley and *Arabidopsis thaliana*, including cell death and the production of reactive oxygen species (ROS), in an interaction that is dependent on two conserved cysteine residues (C56 and C82) (Fellbrich et al., 2002). CRNs, named for the crinkling and necrosis phenotype observed upon infiltration are abundant in the genomes of plant-pathogenic oomycetes, and share an N-terminal conserved LXLFLAK motif (Stam et al., 2013, Torto et al., 2003). The number of CRNs are thought to have expanded in species which include a necrotrophic phase, and are targeted to the host nucleus, though the temporal distribution of expression suggests CRN may serve a diverse range of roles, with one class of CRNs

expressed early during infection and again during the later stages of infection, while the other class is only expressed during the later stages of colonisation (Stam et al., 2013). Interestingly, no CRNs were identified in the *P. cinnamomi* secretome (Andronis et al., 2022), while 13 were identified in the secretome of *P. infestans* (Meijer et al., 2014).

Approximately 39% of secreted proteins in the *P. agathidicida* predicted protein list are predicted to be effectors (27.7% cytoplasmic, 11.2% apoplastic). Analysis of the classically secreted *P. agathidicida* proteins in this study shows that 34.7% are predicted to be effectors. However, 18.4% of the classically secreted *P. agathidicida* proteins identified in this study were predicted to be apoplastic effectors, which equates to just over 27% of the total predicted apoplastic effector repertoire of *P. agathidicida*. The opposite is true of cytoplasmic effectors, with only 16.4% (accounting for less than 10% of the predicted *P. agathidicida* cytoplasmic effector repertoire) predicted from those classically secreted into the various culture filtrates. Thus, it could be said that culture filtrate of *P. agathidicida*, following growth in liquid media, appears to be enriched for candidate apoplastic effectors but depleted for candidate cytoplasmic effectors. As cytoplasmic effectors are destined to be secreted into the host cell cytoplasm, it could be that they simply are not produced in the absence of a specific host-derived signal, or are quickly degraded in culture. In contrast, apoplastic effectors are found in the apoplastic space between cells, and as such may be more likely to be consistently produced, even if at a lower level, in the absence of a host signal.

Strikingly, over 40% of *P. agathidicida* candidate apoplastic effectors identified in this study belonged to the CAZyme family. In total, this study identified over 25% of the entire predicted *P. agathidicida* CAZyme repertoire from culture filtrate. However, this apparent enrichment of CAZymes is not unique to *P. agathidicida.* LC–MS analysis of the secretome of a necrotrophic soil-borne fungal pathogen, *Macrophomina phaseolina*, also identified a large number of CAZymes, particularly GH proteins, in culture filtrate (Sinha et al., 2022). Furthermore, over 56% of the *P. plurivora* culture filtrate secretome was identified to have hydrolase activity (Severino et al., 2014). Surprisingly, hydrolase activity only accounted for less than 14% of the GO terms enriched in the culture filtrate secretome of *P. cinnamomi* (Andronis et al., 2022); however, this could be due to the different *in silica* analyses used.

A key focus of this thesis has been characterising GH12 proteins. While **Chapter 2** discussed the role of GH12 proteins in the virulence and pathogenicity of other phytopathogens (both fungal and oomycete), **Chapter 3** identified that of the eight *P. agathidicida* GH12 proteins predicted in the genome, six consistently elicited a cell death response in *N. benthamiana* and *N. tabacum*. The same six *P. agathidicida* GH12 cell death elicitors were identified in *P. agathidicida* culture filtrate in this study. Interestingly, only four were identified as candidate apoplastic effectors, specifically Pag017848 (the PsXEG1 homolog), and three GH12s which were both similar in sequence and encoded by genes

that were clustered together in the genome (Pag000709, Pag017829 and Pag017830) which suggests they have likely arisen from a gene duplication event. Furthermore, all four GH12 proteins that were identified as candidate apoplastic effectors were found to be present in the culture filtrate of all liquid media used during this study. Interestingly, gene expression data suggested that expression of the *PsXEG1* homolog, *Pag017848*, peaks first at 6 hpi with considerably higher expression in roots than leaves, while expression of *Pag000709* and *Pag017830* peaks at 48 hpi, followed by *Pag017829* which peaks at 72 hpi in roots (see **Figure 3.11 A, Appendix 3.5**) These temporal differences may suggest that these proteins serve different roles during infection and subsequent colonisation of host tissues. Interestingly, analysis of *PsXEG1* expression during infection of soybean suggests that expression increases as soon as 10 minutes post-inoculation and peaks 1 hpi (Ma et al., 2015b), time points which were not captured during the *P. agathidicida* RNA sequencing analysis (Guo & Shiller, Unpublished). The two remaining *P. agathidicida* cell death-eliciting GH12 proteins from **Chapter 3** (Pag006684 and Pag006685) were not predicted to be effectors and were only found in the culture filtrates of PD, Plich, and Henninger liquid media, though Pag006685 was also identified in V8 culture filtrate. Neither of the two *P. agathidicida* GH12 proteins that failed to trigger a cell death response in **Chapter 3** were observed in any of the culture filtrates analysed during this study. This is not surprising as the RNA sequencing data suggested that these proteins were only expressed during *P. agathidicida* infection of kauri and, even then, expression levels were very low and were primarily in kauri roots (**Figure 3.11 A, Appendix 3.5**). This suggests that a specific plant-derived signal is required to induce expression.

Other studies have also highlighted the presence of pectinesterases in the culture filtrate secretomes of both *P. plurivora* and *P. cinnamomi*; these enzymes play an important role in plant cell wall degradation (Andronis et al., 2022, Severino et al., 2014). However, only two pectinesterases (CE8) were predicted in *P. agathidicida*, one of which (Pag017846) was identified among the classically secreted *P. agathidicida* proteins produced in culture filtrate, though it was not predicted to be a candidate effector. Furthermore, the Pag017846 protein was among those investigated in **Chapter 3** but was found not to trigger a cell death response in *N. benthamiana* or *N. tabacum*, suggesting it is not recognised as a MAMP, or acting as a DAMP, at least in those plant species (**Figure 3.10**).

Of particular interest was the CBEL protein, Pag005016, which was uniquely produced in the culture filtrate of kauri leaf AWF. Surprisingly, despite only being identified in culture filtrate of kauri leaf AWF, data from the RNA-sequencing experiment (Guo & Shiller, Unpublished) suggested that *Pag005016* was in fact highly expressed *in vitro*, but that expression levels decreased during infection of kauri (both leaves and roots), the opposite of what would be expected based on the LC–MS protein findings. It has already been mentioned that transcription does not always correspond to translation and appropriate post-translational modifications, thus it could be that the high transcription rate *in vitro* does not result in high protein production, or that the protein has a high turnover rate. The observed decrease

in expression in response to plant inoculation may indicate that this protein is downregulated to avoid detection by the plant immune system, similar to what is observed with enzymes involved in synthesis of β-1,6-glucan from the hemibiotrophic fungal pathogen *Colletotrichum graminicola* during biotrophic infection of maize (Oliveira-Garcia & Deising, 2013, Oliveira-Garcia & Deising, 2016). That Pag005016 was only detected in kauri leaf AWF culture filtrate is therefore surprising but may indicate that the appropriate plant-derived signal is not present to cause the apparent downregulation observed in the RNA-sequencing data. It is also possible that the different conditions in kauri leaf AWF aid in stability of the Pag005016 protein. A BLASTp analysis of the known *P. parasitica* CBEL (CAA65843.1) (Gaulin et al., 2006, Khatib et al., 2004) against the list of *P. agathidicida* proteins predicted from the genome identified five homologous proteins, three of which were identified as classically secreted candidate apoplastic effectors from culture filtrate. Similarly, two CBEL proteins were predicted in the secretome of *P. plurivora*, one of which was a homolog of the *P. parasitica* CBEL (Severino et al., 2014). A CBEL was also identified in the secretome of *P. cinnamomi* (Andronis et al., 2022). The cellulose-binding domain of the *P. parasitica* var. *nicotianae* CBEL is a potent elicitor of plant cell death in a number of plant species, including *A. thaliana* and *N. tabacum*, where it is recognised as a PAMP (Gaulin et al., 2006, Gaulin et al., 2002, Khatib et al., 2004). While the exact role of the CBEL remains unknown, it has no apparent role in pathogenicity or virulence, but is thought to be involved in deposition of the *Phytophthora* cell wall (Gaulin et al., 2002). Surprisingly, when Pag005016 and another CBEL detected as a classically secreted *P. agathidicida* protein in the culture filtrate of PD liquid medium were both screened for their ability to act as MAMPs or DAMPs in *N. benthamiana* and *N. tabacum* (**Chapter 3, Figure 3.10**), they were not found to trigger any consistent cell death response.

While both the PCA score plot (**Figure 5.2A**) and heatmap (**Figure 5.3**) demonstrated that culture filtrate from the nutrient-rich PD liquid medium is different to all the other culture filtrates analysed, this changed when only the secreted proteins were analysed. Analysis of *P. agathidicida* classically secreted proteins suggested that the culture filtrate of kauri leaf AWF was the most different to the other culture filtrates. Indeed, the heatmap of classically secreted proteins suggested that the culture filtrate of nutrient-rich PD liquid medium was more like the culture filtrates of the nutrient-poor Plich and Henniger media. At odds with this, the PCA plot of all identified *P. agathidicida* proteins suggested the culture filtrate of kauri leaf AWF clustered close to the other nutrient-poor liquid media, Plich and Henniger. Taken together, this shows that the growth medium plays an important part in the proteins that are produced by *P. agathidicida*.

In many cases, the observations regarding the number of proteins produced in the different culture filtrates were as expected. The highest number of proteins were identified in the nutrient-rich PD liquid medium. More proteins were identified in the culture filtrate of V8 agar than clarified V8. Given that

clarified V8 liquid medium is a filtered form of V8 liquid medium this is not surprising, as clarified V8 is likely missing some of the sugars present in V8. However, it was slightly surprising that the nutrient-poor Plich liquid medium produced such a high number of proteins, though a personal observation at the time of harvest 10 days post-*P. agathidicida* inoculation was that the oomycete grew very well in this medium. Given that an apparent abundance of proteins was observed in the kauri leaf AWF culture filtrate in the SDS gel, it was perhaps unexpected that this would give the smallest number of individual proteins. Thus, it is likely that many of the small molecular weight proteins observed on the SDS gel were of plant origin. Furthermore, that the overlap between classically secreted *P. agathidicida* proteins identified in Plich and Henniger culture filtrate was so high (over 96% of the proteins identified in Henniger culture filtrate were also found in Plich culture filtrate), suggests that Henniger medium does not stimulate the production of any unique classes of protein. A similar situation was observed in kauri leaf AWF culture filtrate, with more than 87% of the classically secreted *P. agathidicida* proteins found in the culture filtrate of kauri leaf AWF also present in Plich culture filtrate. Taken together, this is evidence that kauri leaf AWF is not required to stimulate the production of all proteins associated with host colonisation, at least, no more so than some of the other liquid media investigated. Interestingly, while other studies have investigated the *in vitro* secretome of *Phytophthora* species using a selection of nutrient-rich (V8) or nutrient-poor (Plich, Henninger or Ribeiros) liquid media (Andronis et al., 2022, Meijer et al., 2014, Severino et al., 2014), the highest number of *P. agathidicida* proteins were produced in nutrient-rich PD liquid medium. Thus, it would be of interest to use this medium in future studies, in the hope that it would aid in identification of an increased number of proteins.

While the focus of this chapter has primarily been on the production of classically secreted proteins, it should be acknowledged that more than half of the proteins identified with high confidence during this study did not contain a signal peptide or a transmembrane domain. There are two possible explanations for this, the first being intracellular contamination. A small amount of intracellular contamination is likely to have occurred during normal cellular turnover. In addition, despite the careful way in which the *P. agathidicida* mycelia was harvested, a low level of intracellular contamination was expected. A proteomics study on the plant-pathogenic oomycete *Albugo candida* used the presence of proteins predicted to localise to the mitochondrial inner membrane to evaluate whether cytoplasmic contamination had occurred (Gómez-Pérez et al., 2022). Of all the *P. agathidicida* proteins lacking a signal peptide and transmembrane domain, the top BLASTp hit of seven proteins suggest they are associated with the mitochondria and subsequently that their presence is the result of cytoplasmic contamination (**Appendix 5.2**).

The second explanation is that these proteins have been secreted in a non-classical manner. An example of non-classical secretion has also been observed in *P. sojae* with the identification of the isochorismatase, PsIsc1, which suppresses salicylate-mediated immunity *in planta* dependent on

catalytic activity (Liu et al., 2014). Despite the lack of an N-terminal signal peptide, the PsIsc1 protein was still identified in culture supernatant by Western blot and through localisation of PsIsc1-mRFP fusions (Liu et al., 2014), suggesting secretion by a non-classical, but as yet unknown mechanism. More recently, using Brefeldin A to inhibit the classical ER-to-Golgi secretion pathway, Wang et al. (2017) demonstrated that some effectors, in particular the cytoplasmic *P. infestans* RxLR effector, Pi04314, are secreted via an alternative, non-classical pathway. Similarly, the *P. infestans* Pi22926 RxLR was also found to be secreted from the haustorium in a non-classical manner (Wang et al. 2018b). In line with this, evidence suggests that *Magnaporthe oryzae,* a hemibiotrophic fungal pathogen of rice, also uses more than one secretory mechanism, whereby apoplastic effectors tend to be classically secreted, while cytoplasmic effectors are non-classically secreted (Giraldo et al., 2013). Interestingly, while PiIsc underwent non-classical secretion in the absence of a signal peptide (Liu et al., 2014), the Pi04314 RxLR effector was predicted to be non-classically secreted despite the presence of an N-terminal signal peptide (Wang et al., 2017). Importantly, a homolog to PsIsc1 was identified in *P. agathidicida* as Pag004037, which also lacked an N-terminal secretion signal and transmembrane domain yet was still identified in the culture filtrate of liquid PD medium. That Pag004037 was only identified in liquid PD medium despite expression of the *Pag004037* gene in liquid clarified V8 could suggest that the protein was not stable in clarified V8 medium, or that by chance it was not detected. Regardless, the presence of Pag004037 is validation that a homolog of PsIsc1 is present and produced by *P. agathidicida*, and thus it is likely that other non-classically secreted *P. agathidicida* proteins exist. The identification of these proteins and the role they play during infection and subsequent colonisation of host tissues is an area for future investigation.

It is apparent from this study that while some effector proteins are produced in culture, many others are not, likely due to the need for a specific host-derived signal. Thus, it would be beneficial to conduct a proteomic analysis of *P. agathidicida* during infection of kauri roots, or at the very least during infection of *N. benthamiana*, a model plant species in which the leaves have been shown to be susceptible to *P. agathidicida* infection (Guo, Unpublished-b). Alternatively, there has been some success in supplementing liquid medium with banana peel to stimulate protein production in *F. proliferatum*, a pathogen of banana (Li et al., 2019). Similarly, proteomic differences were observed when the oomycete root pathogen *P. plurivora*, which infects a number of tree species including European beech (*Fagus sylvatica* L.) (Jung et al., 2000), was grown in Henninger liquid medium with/without root extract from European beech (Severino et al., 2014). Consequently, it could be of interest to attempt supplementing liquid medium with kauri root material or extract to determine if that stimulates production of host colonisation-associated proteins.

Ultimately, results from this chapter serve to validate a subset of the *P. agathidicida* proteins predicted from the genome. Importantly, included in those validated proteins are a majority of the GH12 proteins

highlighted in previous chapters, as well as a number of other candidate effectors, both apoplastic and cytoplasmic. Furthermore, it demonstrates that liquid media, while sufficient to stimulate production of a considerable proportion of apoplastic effector proteins, does not adequately stimulate production of cytoplasmic effector proteins, thereby suggesting that specific, plant-derived signals are necessary for the production of such effectors.

Chapter 6.0 Discussion and future directions

6.1 Introduction

Phytophthora species are well-known as plant pathogens and their destructive capabilities have been well-recorded (Birch & Cooke, 2013, Dorrance et al., 2009). In native systems, a natural balance is often observed between hosts and their pathogens, a result of co-evolution, which suggests severe disease is rarely observed. However, disease outbreaks develop when a pathogen is introduced into a foreign environment which lacks natural biotic (e.g. predators) and abiotic (e.g. temperature) mechanisms of control and contains abundant non-resistant hosts (Santini et al., 2013). Consequently, the international plant trade is thought to be the primary source of introduced exotic plant pathogens, including *Phytophthora* species (Santini et al., 2013, Brasier, 2008). For example, *Phytophthora kernoviae*, thought to be native to New Zealand (Gardner et al., 2015, Studholme et al., 2019), has been introduced into the United Kingdom (UK), presumably through infected nursery stock in the 1990s (Brasier, 2007, Brasier, 2008). In the UK, *P. kernoviae* is known to cause dieback of beech trees and rhododendrons but has also been found on the native bilberry (*Vaccinium myrtillus*) (Beales et al., 2009, Brasier, 2008), and the repercussions of this introduction are still not fully understood. In addition to foreign introduction of pathogens, climate change, which is predicted to be an important factor affecting both host physiology and the aggressiveness of plant pathogens, is anticipated to result in a tipping point for some pathogen-plant interactions (Burdon & Zhan, 2020, Hunjan & Lore, 2020). Under this scenario, the changing climate tips an interaction in favor of the pathogen, leading to disease.

Soil-borne *Phytophthora* species commonly infect plants through the roots and have been shown to target a broad range of hosts, including both food crops and forests. For example, *P. cinnamomi*, has a worldwide distribution and infects over 5,000 plant species, more than 4,000 of which are native to Australia (Hardham & Blackman, 2018). *Phytophthora* species also harbor extremely large families of effector proteins, molecules that facilitate host infection and colonization, which likely contribute to their success as plant pathogens. Both the RxLR and CRN families are well-known examples of cytoplasmic effectors that serve a variety of different functions and have undergone huge expansions in *Phytophthora* species (Haas et al., 2009, Stam et al., 2013, Armitage et al., 2018, Rojas-Estevez et al., 2020, Jiang et al., 2008, Wang et al., 2011a). Meanwhile, necrosis- and ethylene-inducing peptide 1-like proteins (NLPs), and some glycoside hydrolase (GH) proteins are examples that have been shown to act as apoplastic effectors, operating in the intercellular spaces between plant cells (reviewed in Li et al. (2020b) and **Chapter 2** (Bradley et al. (2022)). The study of these two classes of effector proteins is crucial to understanding the molecular mechanisms underpinning infection and for developing novel disease control strategies against these pathogens.

Some of the commonly studied *Phytophthora* species include the infamous *Phytophthora infestans*, causal agent of potato late blight, *Phytophthora sojae*, a pathogen of soybean, and *Phytophthora parasitica*, a broad host range pathogen which significantly impacts citrus (Wang et al., 2011b, Meng et al., 2014, Sandhu et al., 2019). These pathogens are all of great economic importance, as they affect key crops and agricultural exports (Guenthner et al., 2001, Panabieres et al., 2016, Tyler, 2007). Furthermore, their genomic sequences are readily available (Haas et al., 2009, Liu et al., 2016, Tyler et al., 2006), and they have all been shown to be amenable to genetic transformation (Cao et al., 2022, Bailey et al., 1991, Fang & Tyler, 2016, Judelson et al., 1991). Together this provides incentive to better understand these pathogens and how they cause disease in an effort to manage their impacts. In contrast, *Phytophthora agathidicida* is a relatively recently discovered pathogen which interacts with a coniferous host that requires more time and space to grow than crop species such as potato and soybean, and whose economic value cannot be compared to that of soybean, potato or citrus (Bradshaw et al., 2020). Furthermore, the cultural importance of kauri places certain restrictions on the types of experiments that can be performed with this tree species in conjunction with *P. agathidicida* or the molecules this pathogen produces. For this reason, all *Agrobacterium tumefaciens*-mediated transient transformation assays (ATTAs) performed in this thesis were done in either *Nicotiana benthamiana* or *Nicotiana tabacum*. Despite this, considerable resources have been directed towards better understanding how *P. agathidicida* causes disease, with the goal of mitigating its devastating effects on kauri forests. Indeed, a chromosome-level genome and transcriptomic data based on a time-course experiment during *P. agathidicida* infection of kauri are soon to be available, and will be invaluable assets, providing a glimpse of the inner molecular workings of *P. agathidicida* (Cox et al., Unpublished, Guo & Shiller, Unpublished). Of note, *P. agathidicida* has been shown to infect other plant species, both native (*Knightia excelsa* (rewarewa)) and exotic (e.g. *Lolium perenne* and *Pinus radiata*), as well as *N. benthamiana* (Guo, Unpublished-b, Lewis, 2018, Ryder, 2016). While one study has provided some preliminary information of the function of selected RxLR effectors in the model host species *N. benthamiana* (and *N. tabacum*) (Guo et al., 2020a), very little is known about how *P. agathidicida* interacts with its host at a molecular level. Furthermore, it is not yet known whether *P. agathidicida* is amenable to genetic manipulation.

This thesis attempted to better understand the molecular interaction between *P. agathidicida* and its plant hosts, utilizing and contributing to further development of existing resources, and working within the limitations that come with understanding the cultural importance of kauri, a native host of *P. agathidicida*. The focus of this thesis was to identify and characterize proteinaceous effectors and invasion patterns, with a particular focus on GHs from *P. agathidicida* that may have a role in the ability of this pathogen to infect and colonize its host. This chapter puts into context the discoveries made and highlights future experiments that would further progress this avenue of study.

6.2 Chapter 2: A review into the role of secreted GH proteins as invasion patterns and effectors of plant-associated fungi and oomycetes.

This review was intended to be a comprehensive analysis regarding what is currently understood about the role of pathogen-produced GH proteins in the virulence and pathogenicity of fungal and oomycete plant pathogens. It uncovered a large number of proteins representing 17 different GH families, with various predicted functions, including some that induce defence responses in host plants. However, for many of these proteins, the mechanism of action is still unknown. Indeed, many of the issues brought to light in the review are the same issues that have been brought to light by results in other chapters of this thesis. Some of these include:

- Overlooking potential virulence factors because of their inability to elicit a strong and consistent cell death response.
- Deciphering the molecular difference between members of the same family which trigger a response compared to those which do not.
- Further understanding the function these proteins play *in planta*, beyond their ability to elicit a plant cell death response, including how they interact with other proteins.
- Identifying proteins which may be secreted by un-conventional/non-classical means; and the importance of studying the interaction between a pathogen and its natural host.

However, the results of this thesis also further cement another point made in the review, that the role of secreted GH proteins in plant-pathogen interactions should not be overlooked. In fact, it is likely that GH proteins as a whole are representative of a largely understudied class of effector proteins with important roles in host infection and colonization. As discussed below, *P. agathidicida* GH12 proteins clearly have a role to play in pathogen virulence, though the exact nature of that role is yet to be understood. Furthermore, it is likely that GH proteins are involved in the hydrolysis of plant-derived carbohydrate metabolites during *P. agathidicida* infection of kauri. Identification of these metabolites may in turn aid identification of the enzymes responsible.

6.3 Chapter 3: Progress in characterizing *P. agathidicida* CAZymes and their role in the molecular interaction with the plant host.

To the best of my knowledge, **Chapter 3** represents the first comprehensive analysis of the GH repertoire of a plant-pathogen. Of the 242 GHs that were identified in *P. agathidicida*, 48, representing 18 different families, were initially selected for *in planta* analysis as they were predicted to be secreted into the apoplastic space between plant cells and were expressed during *P. agathidicida* infection of kauri. Expression of these proteins in model species *N. benthamiana* and *N. tabacum* determined that only six proteins belonging to the GH12 family were capable of inducing a strong, consistent cell death response. This is consistent with previous research (Ma et al., 2015b), which showed variation in both the number of GH12-encoding genes in the genomes of *Phytophthora* species, and the number that elicited a cell death response in *N. benthamiana*; *P. sojae* (4/11), *P. parasitica* (6/11), *Phytophthora capsica (*8/12), *P. infestans* (1/6). Further analysis revealed that the cell death responses observed in response to *P. agathidicida* GH12 proteins (**Chapter 3, section 3.3.4**) appeared to be dependent on secretion to the apoplast but was independent of xyloglucanase activity. Furthermore, the cell death induced by at least one of the six GH12 proteins was able to be suppressed by *P. agathidicida* RxLR40, which has previously been shown capable of suppressing cell death induced by a *P. agathidicida* RxLR protein, RxLR24 (Guo et al., 2020a). Finally, production of these proteins in *N. benthamiana* prior to inoculation with *P. agathidicida* resulted in decreased lesion size. This could suggest that activation of the plant immune response acts to slow infection by the invading pathogen, or alternatively, that *P. agathidicida* is unable to infect dead or dying tissue during early host infection.

This chapter supports previous findings regarding the role of GH12 proteins in *Phytophthora* virulence. That so many GH12 proteins from different pathogens trigger cell death suggests that many of those pathogens likely have effectors capable of suppressing GH12-induced cell death, at least until such time as it is required (e.g. during the switch to necrotrophy in hemibiotrophic pathogens). In line with previous findings, it appears that RxLRs are one of the key classes of effectors deployed by *Phytophthora* pathogens to carry out this suppression role.

The identification of *P. agathidicida* GH12 proteins that induce plant cell death in *N. benthamiana* and *N. tabacum* also represents the first identification of GH12 cell death-inducing proteins from both *P. agathidicida* and a clade 5 *Phytophthora* species. Other GH12 cell death-inducing proteins have previously been identified in clades 1 (*Phytophthora nicotianae*/*P. parasitica*), 1c (*P. infestans*), 2b (*P. capsici*), and 7b (*P. sojae*), as well as several fungal plant pathogens (*Botrytis cinerea*, *Magnaporthe oryzae*, *Verticillium dahliae*, *Fusiarium graminearum* and *Fusarium oxysporum*) (Yang et al., 2017, Zhu et al., 2017, Zhang et al., 2021c, Ma et al., 2015b, Yang et al., 2021), while several RxLR proteins

as well as homologs of the *P. infestans* INF1 elicitin from *P. agathidicida* have previously been found to induce cell death in *Nicotiana* species (Guo et al., 2020a). Very little research has been done on other known members of clade 5 which include *Phytophthora castaneae*, *Phytophthora cocois*, and *Phytophthora heveae* (Weir et al., 2015).

A map of the *P. agathidicida* genome demonstrated that the GH12 proteins are found in clusters. Two of these clusters were found on chromosome 1 (Pag|009588|009589|009590 and Pag|009574|009575), another cluster on chromosome 3 (Pag|004637|004638) and a single gene, the PsXEG1 homolog Pa009244, on chromosome 9. These clusters suggest that the GH12-encoding genes are undergoing gene duplication followed by sequence diversification. The effects of this could result in the modification of recognition epitopes or functional diversification (analogous to the apparent evolution of *P. sojae* PsXLP1 as a decoy to block PsXEG1 inhibition by plant-derived inhibitors (Ma et al., 2017)), possibly driven by selective pressure to escape recognition as MAMPs. Similar observations of gene clustering were also observed for other GH protein-encoding genes, including those encoding members of the GH17 and GH28 families (**section 3.3.2**).

Of all the GH proteins with a role in pathogen-plant interactions identified in **Chapter 2** (Bradley et al., 2022), only three other GH families from *Phytophthora* species have been identified. The *P. sojae* GH7a cellobiohydrolase triggers cell death in both *N. benthamiana* and soybean and is important for *P. sojae* virulence; functions which are dependent on the cellobiohydrolase enzyme activity (Tan et al., 2020). However, none of the two *P. agathidicida* GH7 proteins were observed to induce a plant cell death response when expressed in *N. benthamiana* or *N. tabacum*. The silencing of genes encoding two *P. parasitica* GH10 xylanases (PpXyn1 and PpXyn2) demonstrated their importance in *P. parasitica* virulence on *N. benthamiana* (Lai & Liou, 2018), although it was not investigated whether either of these proteins elicit a plant cell death response. In relation to this, expression of two *P. agathidicida* GH10 proteins in *N. benthamiana* or *N. tabacum* did not result in a plant cell death response, though it is not known if these proteins are required for *P. agathidicida* virulence. Finally, infiltration of the *P. parasitica* OPEL, which contained a GH16 domain, was found to induce plant immune responses including plant cell death, callose deposition, and accumulation of reactive oxygen species (ROS) in *N. tabacum* (Chang et al., 2015). Interestingly, while the GH domain was capable of inducing ROS accumulation and callose deposition, it was not sufficient to elicit a plant cell death response; instead, the laminarinase active site motif was found to be required for induction of cell death (Chang et al., 2015). While a homolog of the *P. parasitica* OPEL was identified in *P. agathidicida*, cloning of this gene was unsuccessful, and investigation was not pursued further. An OPEL was also identified in the proteomics study in **Chapter 5** (Pag011407) which was different from that predicted in **Chapter 3** (Pa005543 or Pag013080). This may be a good candidate for future investigation.

Given that a cellulose-binding domain, demonstrated to elicit a cell death response in *N. tabacum* (Gaulin et al., 2006), was conserved between *P. agathidicida* and *P. parasitica* CBELs, it was surprising that neither of the two *P. agathidicida* CBEL proteins investigated triggered a cell death response in *N. tabacum* or *N. benthamiana*. This may suggest that the amount of protein did not reach the threshold required for detection, that abiotic conditions were not optimal for recognition, or that other unknown factors were required to contribute to recognition and subsequent induction of plant defence responses.

Future work required to fill knowledge gaps

Assess the role of *P. agathidicida* GH12 cell death elicitors in virulence and pathogenicity.

Studies in both oomycetes and fungi have used gene silencing or deletion to determine the potential role of protein-encoding genes in the pathogenicity or virulence of plant pathogens (Lai & Liou, 2018, Ma et al., 2015b, Shanmugam et al., 2017, Wei et al., 2022). Despite ATTAs with GH12 proteins showing an effect on *P. agathidicida* lesion size, it is not yet clear whether the cell death response induced by GH12 proteins affects the virulence or pathogenicity of *P. agathidicida*. Gene silencing or CRISPR may help to answer this question. Despite not eliciting a cell death response in *N. benthamiana* or *N. tabacum*, it may also be of interest to determine whether Pa|009574 and/or Pa|009575 contribute to *P. agathidicida* virulence, as it is not yet clear what impact cell death has on virulence or pathogenicity and cell death is not a requirement for a role in virulence or pathogenicity. Silencing an individual gene in *P. agathidicida* would allow the analysis of the contribution of that particular gene to *P. agathidicida* virulence during infection assays carried out on kauri (native host) or *N. benthamiana* (model host), while silencing a cluster or clusters of GH12 genes would help identify any functional redundancy that exists. This goal could be achieved using CRISPR gene editing technology, a useful tool capable of knocking out or disrupting both single genes and gene clusters, which has recently been established in several *Phytophthora* species (Fang & Tyler, 2016, Gumtow et al., 2018, Tian et al., 2020). Alternatively, CRISPR could instead be used to replace *P. agathidicida* GH12 protein-encoding genes with enzymatic-inactive versions to determine whether the enzymatic functions carried out by these GH12 proteins is required for virulence or pathogenicity during host infection. Inoculation of the resulting *P. agathidicida* mutants on *N. benthamiana* or kauri, whereupon the ensuing lesion can be measured, and the biomass quantified, would allow investigation of the contribution of this gene family to *P. agathidicida* pathogenicity or virulence in both native host (kauri) and model host (*N. benthamiana*) species.

Identify the plant receptor responsible for recognition of *P. agathidicida* cell-death eliciting GH12 proteins

Given that several *P. sojae* GH12 proteins trigger plant cell death in *Nicotiana* species, and that it has been demonstrated that they, along with other GH12 proteins from *P. infestans*, *P. parasitica* and the fungal plant pathogen *V. dahliae*, are recognized by the *N. benthamiana* NbRXEG1 leucine-rich repeat receptor (Wang et al., 2018), it is likely that this receptor is also responsible for recognising *P. agathidicida* cell death-triggering GH12 proteins. However, this has not been tested. If the *P. agathidicida* GH12 cell death elicitors were no longer able to elicit such a cell death response upon co-infiltration with a virus-induced gene silencing (VIGS) construct designed to suppress NbRXEG1 (Wang et al., 2018), this would suggest that NbRXEG1 is indeed responsible for recognition of these proteins in *N. benthamiana.*

It is important to mention that, as it stands, it is still unknown whether the cell death response elicited by *P. agathidicida* GH12 proteins in *N. benthamiana* and *N. tabacum*, is also elicited in kauri or, indeed, whether any of the other GH proteins induce a cell death response in kauri. To my knowledge, the ability of GH proteins to elicit a cell death response has not yet been tested in gymnosperms, so it is unknown whether they have the capacity to respond. If cell death is indeed triggered by these *P. agathidicida* enzymes, the logical next step would be to determine whether enzyme activity is required for this interaction and whether the kauri genome encodes a receptor homologous to NbRXGE1 (provided it has been demonstrated that this is indeed the receptor responsible for recognition of the *P. agathidicida* GH12 proteins). Given RNA-sequencing data has shown that *P. agathidicida* genes encoding GH12 proteins are highly expressed during infection of kauri, if infiltration with purified *P. agathidicida* GH12 proteins did not elicit a plant cell death response in kauri, it would suggest that the kauri genome does not encode a homologous receptor, or that receptor had sufficient sequence differences that it was unable to recognize the *P. agathidicida* GH12 proteins. Alternatively, it could be that *P. agathidicida* GH12 proteins are recognized by an immune receptor in kauri, but that the response induced upon recognition does not result in plant cell death.

Should *P. agathidicida* GH proteins elicit a cell death response in kauri, it would be of interest, if permitted by cultural license, to identify the receptor responsible for recognition. It has previously been shown that the cell death and plant immune responses induced upon recognition of PsXEG1 by RXEG1 in *N. benthamiana* are dependent on the leucine-rich repeat (LRR) receptor-like kinases (RLK) BRI1-associated kinase-1 (BAK1) and suppressor of BIR1 (SOBIR), which are known to be involved in signal transduction of extracellular LRR receptors (Wang et al., 2018, Liebrand et al., 2014). Similarly, Zhang et al. (2021) and Gui et al. (2017) found that *N. benthamiana* cell death triggered by the *F. oxysporum* and *V. dahliae* GH12 proteins FoEG1 and VdEG1 respectively also required both BAK1 and SOBIR1,

while the GH12 protein VdEG3 required only BAK1 (Gui et al., 2017). Given the similarities between *Phytophthora* GH12 proteins, it is likely that the recognition of GH12 proteins from *P. agathidicida* also involves interaction with BAK1 and SOBIR1. Thus, VIGS of the BAK1 and SOBIR1-encoding genes in kauri prior to expression of the *P. agathidicida* GH12 cell death-inducing proteins, could help identify whether the receptor responsible for recognition is an extracellular LRR receptor (Wang et al., 2018).

Investigate the properties of a GH12 protein required for recognition and subsequent cell death.

The phylogenetic tree in **Chapter 3** illustrated that only a subset of the GH12 proteins produced by fungal and oomycete plant pathogens are able to elicit a plant cell death response. Why or how the remaining GH12 proteins (Pa|009574 and Pa|009575) escape detection is not yet understood.

While Pa|009575 contains an N-terminal signal peptide, a large portion of the N-terminus is missing, and it is only the C-terminal half of the protein that aligns with the other GH12 proteins, resulting in a considerably shorter GH12 domain and a loss of one of the predicted catalytic sites. In contrast, Pa|009574 is a similar length to four of the other *P. agathidicida* GH12 proteins and both predicted catalytic sites are conserved (discussed in **Chapter 3**, **section 3.4**). It was demonstrated that recognition of *P. sojae* PsXEG1 by the NbRXEG1 receptor of *N. benthamiana*, and subsequent cell death, was independent of enzyme activity (Ma et al., 2015b, Wang et al., 2018). The independence of enzymatic activity for cell death induction was also observed for GH12 proteins of *P. agathidicida* (**Chapter 3**, **section 3.3.6**), and *V. dahliae* (Gui et al., 2017), suggesting that the GH12 proteins from these organisms are recognized as microbe-associated molecular patterns (MAMPs). However, the cell death response in rice elicited by the *M. oryzae* GH12 proteins MoCel12A and MoCel12B was dependent on endo-glucanase activity, suggesting the products of enzymatic activity (3^1-β-D-Cellobiosyl-glucose and 3^1-β-D-Cellotriosyl-glucose) released from rice cell walls are recognized as damage-associated molecular patterns (DAMPs), rather than direct recognition of the GH12 proteins themselves (Yang et al., 2021). Together, this supports a role for GH12 proteins as both MAMPs and DAMPs.

It is important to note that neither Pa|009574 nor Pa|009575 were highly expressed *in vitro*, or *in planta* during *P. agathidicida* infection of kauri, nor were they produced in any of the liquid media analysed in **Chapter 5**. The lack of expression may indicate that they are functionally redundant or unimportant during the life-stages analyzed. Investigating the expression of these two genes during differing life stages of *P. agathidicida*, or during infection of different host plants may provide further insight. While most literature concerning *P. agathidicida* focuses on kauri as a host, *P. agathidicida* has been shown to infect other plant species (both native and exotic) in lab settings (Ryder, 2016, Lewis et al., 2019, Bradshaw et al., 2020, Lewis, 2018). Therefore, it is reasonable to expect that *P. agathidicida* may

infect other plant species in a natural system. Consequently, it could be that expression of Pa|009574 and Pa|009575 requires a specific host-derived signal not found in culture or in kauri.

Interestingly, while the known cell death elicitor PiINF1 was found to trigger strong cell death in *N. benthamiana* and *N. tabacum*, no such response was observed in tomato (Kawamura et al., 2009). However, despite the lack of visual response, it was shown that expression of PiINF1 in tomato resulted in activation of plant defence response pathways, resulting in resistance to the bacterial pathogen *Ralstonia solanacearum* (Kawamura et al., 2009). That expression of Pa|009574 or Pa|009575 in *N. benthamiana* did not appear to affect *P. agathidicida* lesion size likely suggests that these proteins do not induce expression of plant defence pathways. However, this is something that could be confirmed by reverse-transcriptase quantitative polymerase chain reaction (RTqPCR) of *N. benthamiana* defence response genes, such as those that encode pathogenesis-related proteins (Abbas et al., 2018), following expression of the GH12 proteins of interest in *N. benthamiana* via ATTAs.

Explore suppressors of *P. agathidicida* GH12-triggered cell death

While the characterization of *P. agathidicida* GH12 proteins has been in isolation thus far, this is not representative of the natural system. As previously discussed, the cell death response triggered by GH12 proteins limited *P. agathidicida* growth in *N. benthamiana* (**section 3.4**). However, under natural infection of this host, colonization by the pathogen can proceed freely, likely because *P. agathidicida* produces effector proteins capable of suppressing the plant cell death response in order for infection to occur. In line with the ability of *Phytophthora* pathogens to suppress cell death mediated by other proteins, 23 RxLR effectors from *P. sojae* that had previously been identified to suppress cell death triggered by INF1 were also shown to suppress the cell death response triggered by PsXEG1 in soybean (Ma et al., 2015b). Interestingly, three *P. sojae* RxLR effectors that suppressed cell death induced *by P. sojae* RxLR effectors, but not INF1, were also unable to suppress cell death induced by PsXEG1 (Ma et al., 2015b, Wang et al., 2011a), suggesting that RxLRs involved in suppression target different branches of the plant immune response and that plant cell death induced by INF1 and GH12 was a part of the same cell-signaling pathway. However, despite demonstration that PaRxLR40 could suppress PaRxLR24-induced cell death, but not INF1-induced cell death in *N. benthamiana* (Guo et al., 2020a), PaRxLR40 was shown to consistently suppress cell death induced by the GH12 protein Pa|009244 (**Chapter 3, section 3.3.7,** discussed in **section 3.4**).

It could be of interest to use known suppressors of the plant immune system from other *Phytophthora* species to help elucidate the signalling pathway(s) associated with the recognition of *P. agathidicida* GH12 proteins. For example, *P. infestans* RxLR effectors PexRD2 and Pi22926 were shown to interact specifically with the kinase domain of a mitogen-activated protein kinase kinase kinase (MAPKKK)

from *N. benthamiana* (MAPKKKε) and potato (MAPKKKβ2) respectively, which are involved in the regulation of plant cell death mechanisms (Melech-Bonfil & Sessa, 2010, Ren et al., 2019, King et al., 2014). Expression of PiPexRD2 or Pi22926 suppressed cell death induced by effector/receptor pairs that were dependent on MAPKKKε, such as Avr4/Cf4 (effectors of *Cladosporium fulvum*), but not cell death induced by PiINF1, demonstrating they manipulate the same signalling pathway (King et al., 2014, Ren et al., 2019). Meanwhile, several effectors can suppress the cell death response triggered by INF1, suggesting they function as part of a different signalling pathway. Pi7316 interacts with a MAPKKK in *N. benthamiana* (NbVIK) and to suppress INF1-induced cell death, but not Cf4/Avr4-induced cell death (Murphy et al., 2018), while Avr3a is known to suppress both INF1 and Cf4/Avr4 by binding to, and stabilizing CMPG1, an E3 ubiquitin ligase from potato (Bos et al., 2010, Gilroy et al., 2011).

Nevertheless, it is likely that other suppressors of *P. agathidicida* GH12-induced cell death exist. While protein pull-down experiments would help to identify whether any *P. agathidicida* effector proteins directly interact with the cell death-eliciting GH12 proteins, they are not suitable for identifying proteins which indirectly inhibit plant cell death (e.g. RxLRs). Identifying proteins that have a similar expression pattern to GH12 protein-encoding genes may help to select top candidates. Cloning and subsequent analysis via suppression assays (ATTAs) *in planta* would help to elucidate their role. VIGS assays of plant proteins such as kinases thought to be involved in transduction of the immune system signal as a result of GH12 recognition, would further contribute to identifying the molecular pathway involved.

Analysis of the localisation of *P. agathidicida* GH12 proteins.

The ambiguous results of the screening assay investigating expression of GH12 cell death elicitors without a signal peptide in *N. benthamiana* via ATTAs calls into question localization of these proteins, particularly Pa|009244, Pa|009588, Pa|009589, and Pa|009590. Previous studies have indicated that GH12 proteins are likely localized to the apoplastic space between plant cells, the so-called battlefield of plant-pathogen interactions (Gui et al., 2017, Ma et al., 2015b, Yang et al., 2021). However, to my knowledge, this has not yet been directly observed. Cloning the GH12 protein of interest with a fluorophore fusion and analysing localisation using confocal microscopy following expression in *N. benthamiana* via ATTAs would provide evidence of GH12 localisation *in planta* (Liu et al., 2018, Ren et al., 2019, Wang et al., 2018).

Identify proteins important in the interaction between *P. agathidicida* and *N. benthamiana*.

It is important to recognize that *P. agathidicida* effectors that are important for infection of kauri, may not be important for infection and colonization of *N. benthamiana*. Much of the identification of *P.*

agathidicida proteins with potential roles in infection and colonization during this study has relied on the transcriptome resulting from the infection of kauri by *P. agathidicida*. A transcriptome *of P. agathidicida* infection of *N. benthamiana* would go a long way towards identifying proteins which may be important in this interaction. Furthermore, given the large phylogenetic distance between kauri and *N. benthamiana*, comparison of the two transcriptomes may allow identification of proteins likely to be important to host colonization in general, as well as identification of proteins with species-specific relevance.

6.4 Chapter 4: Identifying metabolite changes in kauri leaf apoplastic wash fluid in response to inoculation with *Phytophthora agathidicida*.

This chapter sought to identify whether there were changes in the metabolites found in kauri leaf apoplastic wash fluid (AWF) as a consequence of *P. agathidicida* inoculation. Kauri leaf AWF was harvested from kauri trees belonging to five different families and inoculated with either cellophane membranes (CMs; negative control) or CMs covered with *P. agathidicida* mycelia. Samples were taken prior to inoculation (T0), 24 hours post-inoculation (T24h Pa and T24h CM), and 10 days post-inoculation (T10d Pa and T10d CM) and sent for NMR analysis. NMR spectra were bucketed, with a bucket size of 0.04 ppm, and of the 250 buckets considerable differences between *P. agathidicida*-inoculated samples and CM controls were observed in 17. An overall decrease in metabolites for *P. agathidicida*-inoculated samples was observed in five buckets, while an overall increase was observed in four buckets. Of the remaining eight buckets, changes were observed in *P. agathidicida*-inoculated samples by 24 hpi, while these differences were only observed in CM controls 10 dpi. Despite using an in-house database to try and identify the metabolites represented by these spectral buckets, only sucrose, at 5.42 ppm, and glucose (together with an unknown carbohydrate) at 5.26 ppm, were able to be positively identified due to the high overlap in the carbohydrate region. Thus, while many of the metabolites identified to change are predicted to be carbohydrates, their exact identity remains unknown.

Many studies have used ^{1}H NMR to study the plant-induced metabolomic changes in response to pathogen invasion, with a particular focus on resistant cultivars, in an attempt to identify metabolites responsible for plant resistance (Bednarek et al., 2005, Mirnezhad et al., 2010, Figueiredo et al., 2008, Leiss et al., 2009a, Leiss et al., 2009b, Abdel-Farid et al., 2009). While this may be an avenue that can be pursued in future, this study aimed to identify which plant (kauri)-produced metabolites were being utilized by the *P. agathidicida* pathogen in a bid to better understand the molecular mechanism behind *P. agathidicida* infection. That this study was carried out *in vitro* provided the unique opportunity to study the changes in the apoplast in absence of the plants ability to manipulate the presence or absence of metabolites.

This study was the first of its kind investigating the interaction between kauri leaf AWF and *P. agathidicida* infection and demonstrated the *P. agathidicida* appears to metabolise sucrose as a source of nutrition in the apoplast, likely an important energy source during early colonisation. Despite not being able to identify many of the metabolites, convincing changes were observed in the other 16 spectral buckets, encouraging results which suggest this is a viable way of studying the impact of *P. agathidicida* infection *in vitro*.

Future work required to fill knowledge gaps

Investigate whether the same metabolites are modified in non-host species

The 17 spectral buckets identified in this chapter which underwent changes in response to *P. agathidicida* infection were found in the AWF of kauri leaves. To understand whether or not these metabolites are specific to the *P. agathidicida*-kauri interaction, a similar experiment could also be carried out in a different host species, such as *N. benthamiana*. *N. benthamiana* plants require less time and space to grow and harvesting AWF from *N. benthamiana* leaves is faster and provides greater yield compared to kauri, which would allow a greater number of replicates to be performed. In addition, focusing only on the 17 spectral buckets which were previously shown to exhibit changes in response to *P. agathidicida* infection would greatly improve the statistical power of the analysis.

If similar changes were observed in the AWF of *N. benthamiana* leaves it would be of further interest to determine whether these changes were specific to *P. agathidicida* or were common across *Phytophthora* species. Inoculation of *N. benthamiana* leaf AWF with a broad host-range *Phytophthora* pathogen like *P. cinnamomi* which has previously been shown to be capable of infecting *N. benthamiana* (Belisle et al., 2019), and analysing the spectral buckets of interest via NMR, would help to answer these questions.

Identify metabolites involved in plant resistance to *P. agathidicida*

As mentioned above, many NMR studies have been used to identify metabolites which are uniquely present or abundant in plants that are resistant to a pathogen of interest. While it is unclear whether there is substantial variation in susceptibility to *P. agathidicida* within the *A. australis* (kauri) species, glasshouse trails suggest that *Agathis robusta* (Queensland kauri) is not susceptible to *P. agathidicida* infection (Bradshaw et al., 2020). Thus, it could be of interest to compare the metabolome profiles of *A. australis* and *A. robusta* AWF inoculated with *P. agathidicida*. Identification of key metabolites involved in resistance to *P. agathidicida* may help inform future control strategies for this pathogen.

6.5 Chapter 5: Identification and validation of proteins in the *P. agathidicida* extracellular secretome.

The aim of **Chapter 5** was to understand what *P. agathidicida* proteins were secreted into media, and to determine if any of the media used in this experiment were able to replicate *in planta* conditions, thus resulting in the secretion of effector candidates traditionally secreted *in planta*. While similar studies have been carried out on the culture filtrate of other *Phytophthora* species, including *P. infestans* (Meijer et al., 2014), *P. cinnamomi* (Andronis et al., 2022) and *Phytophthora plurivora* (Severino et al., 2014), this was the first for *P. agathidicida*.

P. agathidicida was grown in liquid media (potato dextrose, V8, clarified V8, Plich, Henninger, and kauri leaf AWF) for 10 days, and the culture filtrate harvested for analysis via liquid chromatography-mass spectrometry (LC-MS). The resulting data showed that of the 986 *P. agathidicida* proteins predicted to be present in at least two samples of culture filtrate from the same media, 355 were predicted to be secreted. Furthermore, of the 96 classically secreted CAZyme-encoding proteins identified in *P. agathidicida* culture filtrate, 75 of them were predicted to be GH proteins. This represents approximately 35% of the secreted GH protein-encoding genes predicted from the *P. agathidicida* genome

Ultimately, none of the media tested in this study was able to replicate *in planta* conditions. The most similar medium to *in planta* conditions, based on the fact that it utilized a growing substrate isolated from the plant, was kauri leaf AWF, which was observed to have the lowest number of proteins identified in the culture filtrate. However, given that perception of specific host-derived signals is likely an important trigger for expression of genes involved in host-colonisation, it is not surprising this environment was not replicated among the media used. Despite this, the culture filtrate of plant-pathogens grown in liquid media has been shown to have an important role in the search for cell death elicitors, with many, including PsXEG1 (Ma et al., 2015b) and PpOPEL (Chang et al., 2015), identified from culture filtrates (Pettongkhao & Churngchow, 2019, Ricci et al., 1989, Billard et al., 1988, Ben M'Barek et al., 2015, Bailey, 1995). In fact, if *P. agathidicida* culture filtrate had been used as the starting point for investigation of cell death elicitors, GH12 proteins would have undoubtably been identified, given that four of the six cell death-eliciting GH12 proteins were identified in all six types of culture filtrates analysed. This may reflect that many of the proteins secreted into media are highly conserved and participate in core functions required for pathogen growth. From a host perspective, these are ideal targets for recognition and may convey broad protection against a wide range of pathogens. Thus, growth in liquid media appears to be an effective way to identify to GH proteins and other cell death elicitors which may have implications in pathogen-plant interactions. The identification of these

cell death elicitors and their cognate plant immune receptors has important implications for disease control.

Future work required to fill knowledge gaps

Identification of further *P. agathidicida* effectors of interest.

Phytophthora plant pathogens are predicted to host a swathe of effector proteins, with different roles in pathogenicity and virulence (Naveed et al., 2020, Wang & Jiao, 2019). However, to date only the GH12 proteins (**Chapter 3**), RxLRs and several homologs to *P. infestans* INF1 (Guo et al., 2020a) have been identified which elicit a plant cell death response in *N. benthamiana* and are predicted to have a role in *P. agathidicida* virulence and/or pathogenicity, suggesting there are many yet to be discovered. Using existing resources in combination with the proteins identified during *P. agathidicida* growth in liquid media may enable some of these discoveries.

The availability of a complete, chromosome-level, *P. agathidicida* genome, together with the RNA-sequencing time course experiment carried out during *P. agathidicida* infection of kauri leaves and roots are invaluable tools in the identification of new effector candidates. Given *P. agathidicida* is a root pathogen, top candidates are going to be those which are highly expressed during early infection of kauri roots, suggesting they are required to aid pathogen infection and colonization. Although it has been shown that N-terminal signal peptides are not always required for secretion into the plant apoplast, the presence of a signal peptide and absence of transmembrane domains are still useful predictions to refine the list of potential candidates. Homology to other known effectors in other pathosystems may also highlight candidate effectors with the most promise.

Elicitins are oomycete-specific proteins, found only in *Phytophthora* and some *Pythium* species, which are generally suspected to have a role in sterol recruitment (Midgley et al., 2022, Wang et al., 2021, Jiang et al., 2005), a critical task given that *Phytophthora* species are sterol auxotrophs (Wang et al., 2021). Identified for their ability to elicit a cell death response in tabacco, elicitins have been identified in many *Phytophthora* species, including *P. infestans* (INF1) (Kamoun et al., 1997), *P. cinnamomi* (Cinnamomin) (Huet & Pernollet, 1989), *P. palmivora* (Palmivorein) (Churngchow & Rattarasarn, 2000), and *P. parasitica* (Parasiticein) (Nespoulous et al., 1992). Interestingly, of the 355 *P. agathidicida* proteins identified across all culture filtrates that were predicted to be secreted, an elicitin (Pag014379) found in all culture filtrates was also found to be the most highly expressed (based on the RNA-sequencing data). Discussed in **section 5.4**, this candidate effector is an excellent target for future analysis.

The genomes of *Phytophthora* species also harbor large numbers of genes encoding NLPs, apoplastic effectors with a 'necrosis-inducing *Phytophthora* protein 1' (NPP1) domain (Gijzen & Nurnberger, 2006). Given that *P. sojae* PsNPP1 (Qutob et al., 2002) and *P. infestans* PiNPP1 (Kanneganti et al., 2006) are highly expressed during later infection, it has been suggested that NLPs may be involved in the switch to necrotrophic growth (Dong et al., 2012, Qutob et al., 2002, Midgley et al., 2022). To date, 25 NPP1-encoding genes have been predicted in the *P. agathidicida* genome (Cox et al., Unpublished), six of which encoded proteins that were identified in *P. agathidicida* culture filtrate via LC–MS analysis. An increase in expression during mid-late infection of kauri roots was observed in five of those identified in *P. agathidicida* culture filtrate (Guo & Shiller, Unpublished), consistent with findings in other *Phytophthora* species (Kanneganti et al., 2006, Qutob et al., 2002). Taken together, this suggests that *P. agathidicida NLP* genes that are highly expressed during infection would be valid candidates for further analysis.

Crinklers (CRN) are another class of cytoplasmic effectors in plant-pathogenic oomycetes (Torto et al., 2003, Stam et al., 2013). They consist of a conserved N-terminal domain (with a LXLFLAK motif) and a variable C-terminal domain (Stam et al., 2013), similar to RxLRs. In *Phytophthora* species they have been shown to be involved in the regulation of plant defence responses (Liu et al., 2011, Midgley et al., 2022, Maximo et al., 2019, Zhang et al., 2014b). For example, the cell death response induced by *P. sojae* CRN63 during the necrotrophic stage of infection is initially suppressed by PsCRN115 during early infection (Liu et al., 2011, Zhang et al., 2014b). Both PsCRN63 and PsCRN115 were found to interact directly with *N. benthamiana* catalase NbCAT1, thought to be involved in maintaining ROS homeostasis (Zhang et al., 2014b). NbCAT1 is recruited to the nucleus, whereupon PsCRN63 promotes accumulation of H_2O_2, resulting in plant cell death (Zhang et al., 2014b). PsCRN115 inhibits PsCRN63 accumulation of H_2O_2, thereby suppressing PsCRN63-induced plant cell death (Zhang et al., 2014b). While only two CRN proteins were identified in *P. agathidicida* culture filtrate, 145 genes encoding these proteins have been predicted so far in the *P. agathidicida* genome (Cox et al., Unpublished). Highly expressed *P. agathidicida* CRNs would therefore be worthwhile candidates for further investigation.

Once selected, cloning of these genes and subsequent expression *in planta* would identify those recognized by plant immune receptors which induce a plant defence response. Additional experiments could include evaluating changes in expression of plant defence-related genes (RT-qPCR), ROS or NO levels and measuring *P. agathidicida* biomass by RT-qPCR. Deletion or disruption of these genes in *P. agathidicida*, for example using CRISPR gene editing technology, and subsequent analysis of the resultant *P. agathidicida* mutants and their capacity for pathogenicity or virulence on host plants would further contribute to understanding whether these proteins have a role in host infection or colonization. Transient expression of these proteins with fluorophore fusions *in planta* would aid in localization

analysis, while protein pull-downs complemented with yeast-two-hybrid or bimolecular fluorescence complementation assays could identify interacting partners.

7.0 Conclusion

We live in a world where the effects of climate change are already being felt and where changing environmental conditions have already led to range expansion of some plant pathogens (e.g. fungal coffee rust pathogen *Hemileia vastatrix* (Avelino et al., 2015)). However, most research and policy in the field of plant pathogens is focused on the surveillance and control of pathogens which impact food and economic security, primarily agricultural crops (Ristaino et al., 2021). Despite this, an argument can also be made for the increasing importance of healthy forests. Reforestation/afforestation is instrumental in providing an economically viable way of mitigating climate change through sequestration of carbon from the atmosphere (Austin et al., 2020). Therefore, it stands to reason that healthy forests are essential for the health and well-being of society and the economy, not to mention ecological biodiversity. Consequently, a better understanding of pathogen distribution and interactions at a macro, micro and molecular level are required to allow development of management and control strategies against plant pathogens (Ristaino et al., 2021).

One such control strategy for the management of *Phytophthora agathidicida* is the use of phosphite, which acts to inhibit oomycete growth while stimulating plant defence responses (Smillie et al., 1989), to treat infected kauri (reviewed in Bradshaw et al. (2020)). So far, results have been promising, and research has shown that *P. agathidicida* is highly sensitive to phosphite (Hunter et al., 2022). In addition, the oomycide oxathiapiprolin has shown to be effective against *P. agathidicida* in a laboratory setting, though its use under natural environmental conditions is still to be determined (Lacey et al., 2021a). Together, this research, along with the closure of forest tracks and research into improved methods of *P. agathidicida* detection, contributes to the containment of this organism until a long-term solution can be established (Bradshaw et al., 2020, Lacey et al., 2021b, Winkworth et al., 2020). One such solution is the identification of resistance within the kauri population and consequent development of a durable breeding strategy, an integral part of which is understanding the pathogen–plant interaction at a molecular level and identifying pathogen-derived invasion patterns that may be recognized by the host plant.

In this thesis, six GH12 proteins were identified from *P. agathidicida* that elicited a cell death response in the model host *Nicotiana benthamiana* independent of their enzymatic activity, suggesting they are recognized as MAMPs by a cognate immune receptor, likely NbRXEG1. In addition, glycoside hydrolase (GH) proteins were implicated in the growth of *P. agathidicida* in kauri leaf apoplastic wash fluid (AWF), not only due to changes in sucrose and other unknown metabolites, expected to represent carbohydrates, in the metabolite profile of kauri leaf AWF inoculated with *P. agathidicida*; but also because approximately 20 GH proteins were identified in the culture filtrate of *P. agathidicida* grown

in kauri leaf AWF. Taken together, this is compelling evidence which suggests *P. agathidicida* GH proteins play an important role during interaction with the host plant. The exact nature of that role, its contribution to *P. agathidicida* virulence and pathogenicity, and whether it can be exploited as a control strategy is yet to be established.

Furthermore, this thesis has shown that growth of *P. agathidicida* in liquid medium, particularly potato dextrose, stimulates the production of a considerable proportion of secreted candidate apoplastic effector proteins encoded in the *P. agathidicida* genome. Many of which (elicitins, necrosis-like proteins, OPELs, and CAZymes which have not yet been studied such as GH32 proteins) represent excellent targets for further investigation in regard to their role as potential invasion patterns. Further research, including the identification of new *P. agathidicida* invasion patterns and, importantly, their cognate immune receptors, will only serve to enhance understanding of the molecular interaction between *P. agathidicida* and its host plant. This knowledge may then inform the development of resistance programmes.

Appendices

Appendix 2.1. Selected secreted glycoside hydrolase (GH) proteins from plant-associated fungi and oomycetes with roles in promoting plant colonization and/or activating plant immune responses.

Protein name	GH family classification	Plant-associated fungus or oomycete (and lifestyle)	Characterized role in promoting host colonization and/or activating the plant immune system*	Corresponding PRR if known (and plant)	References
Avenacinase	GH3	*Gaeumannomyces graminis* var. avenae (necrotrophic pathogen)	Avenacinase. Detoxifies the antifungal saponin avenacin in oat [7]. Pathogenicity factor in oat.		Turner (1961); Osbourn et al. (1991); Bowyer et al. (1995)
Tomatinase	GH3	*Septoria lycopersici* (necrotrophic pathogen)	Tomatinase. Detoxifies the antifungal saponin α-tomatine to β2-tomatine in tomato [7]. Pathogenicity factor in tomato.		Sandrock et al. (1995); Bouarab et al. (2002)
GH7.188	GH5	*Lasiodiplodia theobromae* (necrotrophic pathogen)	Putative cellulase. Over-expression increases pathogen virulence in grape.		Yan et al. (2018)

LbGH5-CBM1	GH5	*Laccaria bicolor* (ectomycorrhizal fungus)	Involved in the establishment of symbiosis in poplar.		Zhang et al. (2018), Zhang et al. (2021b)
PsGH7a	GH7	*Phytophthora sojae* (hemibiotrophic pathogen)	Cellobiohydrolase. Triggers cell death in diverse plant species. Virulence factor. Requires enzymatic activity to trigger cell death and for virulence function (*Nicotiana benthamiana*).		Tan et al. (2020)
FoTom1	GH10	*Fusarium oxysporum* f. sp. *lycopersici* (hemibiotrophic pathogen)	Tomatinase. Detoxifies the antifungal saponin α-tomatine to tomatidine in tomato [7]. Virulence factor in tomato.		Roldan-Arjona et al. (1999), Pareja-Jaime et al. (2008)
CfTom1	GH10	*Cladosporium fulvum* (biotrophic pathogen)	Tomatinase. Detoxifies the antifungal saponin α-tomatine to tomatidine in tomato [7]. Virulence factor in tomato.		Ökmen et al. (2013)
FGSG_11487 FGSG_11304	GH10	*Fusarium graminearum* (hemibiotrophic pathogen)	Xylanases. FGSG_11304: Enzymatic activity inhibited by wheat xylanase inhibitor XIP1. FGSG_11487: Triggers cell death in wheat independently of enzymatic		Tundo et al. (2015)

			activity. Cell death, but not enzymatic activity, inhibited by XIP1.		
RSAG8_07159	GH10	*Rhizoctonia solani* (necrotrophic pathogen)	Triggers cell death in *N. benthamiana*.		Anderson et al. (2017)
FgXyr1 and FgPg1	GH10 and GH28	*F. graminearum* (hemibiotrophic pathogen)	Xylanase and polygalacturonase, respectively. Function synergistically to promote virulence in soybean and wheat. Individually not important for virulence.		Paccanaro et al. (2017)
VmXyl1	GH10	*Valsa mali* (necrotrophic pathogen)	Xylanase. Virulence factor in apple.		Yu et al. (2018)
PpXyn1 and PpXyn2	GH10	*Phytophthora parasitica* (hemibiotrophic pathogen)	Xylanases. Virulence factors in *Nicotiana benthamiana* and tomato.		Lai & Liou (2018)
RcXYN1	GH10	*Rhizoctonia cerealis* (necrotrophic pathogen)	Xylanase. Triggers cell death in wheat and *N. benthamiana*. Virulence factor in wheat.		Lu et al. (2020)

Xyn1 and Xyn2	GH10	*Ustilago maydis*	Xylanases. Virulence factors in maize.		Moreno-Sánchez et al. (2021)
TvEIX	GH11	*Trichoderma viride* (root symbiont and biocontrol agent)	β-1-4-endoglucanase (xylanase). Recognised as a MAMP in *N. benthamiana* cv. Xanthi and tomato, triggering cell death and other immune responses.	LRR-RLPs SlEIX1 and SlEIX2 (tomato). Unknown (*N. benthamiana* cv. Xanthi)	Bailey et al. (1990); Furman Matarasso et al. (1999); Ron and Avni (2004)
Xylanase 11	GH11	*Trichoderma reesei* (root symbiont and biocontrol agent)	Xylanase. Triggers cell death and other immune responses in *Nicotiana tabacum* and tomato independent of enzymatic activity.		Enkerli et al. (1999)
BcXyn11A	GH11	*Botrytis cinerea* (necrotrophic pathogen)	β-1,4-endoxylanase. Recognized as a MAMP in tomato and *N. tabacum*, triggering cell death and other immune responses [2]. Virulence factor in tomato.		Brito et al. (2006), Frías et al. (2019), Noda et al. (2010)
FG_03624 FGSG_10999	GH11	*F. graminearum* (hemibiotrophic pathogen)	Xylanases. Triggers cell death in wheat. Enzymatic and cell death activity inhibited by *Triticum aestivum* xylanase inhibitor TAXI III. Cell death activity independent of enzymatic activity.		Sella et al. (2013), Tundo et al. (2015), Moscetti et al. (2015), Tundo et al. (2021)

VdEIX3	GH11	*Verticillium dahliae* (hemibiotrophic pathogen)	Recognised as a MAMP in *N. benthamiana*, triggering cell death and other immune responses [2].	LRR-RLP NbEIX2 (*N. benthamiana*)	Yin et al. (2021)
Vd424Y	GH11	*V. dahliae* (hemibiotrophic pathogen)	Virulence factor. Possibly localises to plant nucleus [8]. Triggers cell death in several plant species. Cell death dependent on BAK1 and SOBIR1 in *N. benthamiana*.		Liu et al. (2021)
Xyn11A	GH11	*U. maydis*	Xylanase. Virulence factor in maize.		Moreno-Sánchez et al. (2021)
PsXEG1	GH12	*P. sojae* (hemibiotrophic pathogen)	Xyloglucanase. Recognized as a MAMP in *N. benthamiana* [2] . Triggers cell death in other solanaceous plants, including *N. benthamiana*. Virulence factor in soybean. Interacts with soybean glucanase inhibitor protein GmGIP1.	LRR-RLP XEG1 (*N. benthamiana*)	Ma et al. (2015b); Ma et al. (2017); Wang et al. (2018)
PsXLP1	GH12	*P. sojae* (hemibiotrophic pathogen)	Decoy protein for soybean glucanase inhibitor protein GmGIP1 [6]. Virulence factor in the presence of PsXEG1.		Ma et al. (2015b); Ma et al. (2017)

PpXEG1	GH12	*P. parasitica* (hemibiotrophic pathogen)	Xyloglucanase. Interacts with glucanase inhibitor protein NbGIP1 in *N. benthamiana*.		Ma et al. (2015b); Ma et al. (2017)
PpXLP1	GH12	*P. parasitica* (hemibiotrophic pathogen)	Lacks enzyme activity. Triggers cell death in *N. benthamiana*. Interacts with NbGIP1 in *N. benthamiana*.		Ma et al. (2015b); Ma et al. (2017)
Ps119627 Ps138787 Ps109280	GH12	*P. sojae* (hemibiotrophic pathogen)	Trigger cell death in *N. benthamiana.*		Ma et al. (2015b)
PPTG_16567 PPTG_16566 PPTG_19220 PPTG_16273 PPTG_16272 PPTG_16267 PPTG_16271	GH12	*P. parasitica* (hemibiotrophic pathogen)	Trigger cell death in *N. benthamiana.*		Ma et al. (2015b)

Pc111741 Pc99469 Pc106898 Pc107122 Pc15454 Pc15453	GH12	*Phytophthora capsici* (hemibiotrophic pathogen)	Trigger cell death in *N. benthamiana.*		Ma et al. (2015b)
PITG_06962	GH12	*Phytophthora infestans* (hemibiotrophic pathogen)	Triggers cell death in *N. benthamiana*.		Ma et al. (2015b)
FGSG_05851	GH12	*F. graminearum* (hemibiotrophic pathogen)	Triggers cell death in *N. benthamiana.*		Ma et al. (2015b)
VdEG1 VdEG3	GH12	*V. dahliae* (hemibiotrophic pathogen)	Triggers cell death independent of enzyme activity in *N. benthamiana*. Virulence factor in cotton. Enzymatic activity required for virulence.		Gui et al. (2017)

BcXyg1	GH12	*B. cinerea* (necrotrophic pathogen)	Triggers cell death in dicot plants independent of enzyme activity.		Zhu et al. (2017)
FoEG1	GH12	*F. oxysporum* (hemibiotrophic pathogen)	Recognized as a MAMP in *N. tabacum*, *N. benthamiana*, tomato and cotton, triggering cell death and other immune responses [2]. Virulence factor in cotton.		Zhang et al. (2021d)
MoCel12A and MoCel12B	GH12	*Magnaporthe oryzae* (hemibiotrophic pathogen)	β-glucanase (endoglucanase). Releases oligosaccharides from hemicellulose in rice cell walls; predicted to support nutrition for fungal growth [3].	OsCERK1-OsCEBiP complex (rice)	Yang et al. (2021)
BcGs1	GH15	*B. cinerea* (necrotrophic pathogen)	Triggers cell death in tomato, cucumber, pea and *N. tabacum*. Induces expression of plant defence response genes and lignin accumulation in tomato.		Zhang et al. (2015); Yang et al. (2018a)
OPEL	GH16	*P. parasitica* (hemibiotrophic pathogen)	Cell death elicitor, possibly due to DAMP release [4]. Induces expression of plant defence genes.		Chang et al. (2015)

BcCrh1	GH16	*B. cinerea* (necrotrophic pathogen)	Transglycosylase. Cytoplasmic effector involved in fungal cell wall biosynthesis. Triggers cell death and other defence responses in *N. benthamiana* and tomato.		Bi et al. (2021)
CfGH17-1 CfGH17-5	GH17	*Cladosporium fulvum* (biotrophic pathogen)	CfGH17-1: 1,3-β-glucanase Releases (oligo)saccharides from tomato cell wall (predicted to support fungal growth and reproduction through nutrition) [3]. Released (oligo)saccharides trigger cell death upon recognition as DAMPs in tomato [4]. CfGH17-5: Predicted 1,3-β-glucanase.Triggers cell death in tomato.		Ökmen et al. (2019)
DsGH17-1	GH17	*Dothistroma septosporum* (hemibiotrophic pathogen)	Predicted 1,3-β-glucanase. Triggers cell death in tomato.		Ökmen et al. (2019)
MfGH17-1	GH17	*Pseudocercospora fijiensis* (hemibiotrophic pathogen)	Predicted 1,3-β-glucanase. Triggers cell death in specific cultivars of tomato.		Ökmen et al. (2019)

VDECH	GH18	*V. dahliae* (hemibiotrophic pathogen)	Triggers cell death and induction of defence genes in *Arabidopsis* and cotton.		Cheng et al. (2017)
MpChi	GH18	*Moniliophthora pernicosa* (hemibiotrophic pathogen)	Inactive chitinase. Sequesters chitin fragments to prevent chitin-triggered immunity [5A].		Fiorin et al. (2018)
MrChi	GH18	*Moniliophthora rorei* (hemibiotrophic pathogen)	Inactive chitinase. Sequesters chitin fragments to prevent chitin-triggered immunity [5A].		Fiorin et al. (2018)
MoChia1/MoChi1	GH18	*M. oryzae* (hemibiotrophic pathogen)	Chitinase. Triggers cell death independently of enzymatic activity in rice. Virulence factor. Sequesters chitin fragments to prevent chitin-triggered immunity in rice [5A]. Interacts with OsMBL1 in rice.	Tetratricopeptide-repeat protein OsTPR1 (rice)	Han et al. (2019); Yang et al. (2019)

UvCBP1	GH18	*Ustilaginoidea virens* (biotrophic pathogen)	Virulence factor. Competes with rice OsCEBiP for the binding of chitin (i.e. may sequester chitin fragments to suppress chitin-triggered immunity [5A]).		Li et al. (2021b)
MbA_GH25	GH25	*Moesziomyces bullatus* ex Albugo (epiphytic yeast)	Lysozyme. Reduces infection by the oomycete *Albugo laibachii* (white rust disease pathogen) in *Arabidopsis thaliana* at the phyllosphere.		Eitzen et al. (2021)
BcPG1 BcPG2 BcPG3 BcPG4 BcPG5 BcPG6	GH28	*B. cinerea* (necrotrophic pathogen)	Endopolygalacturonases. Trigger cell death or chlorosis on a number of plant species independently (BcPG1, BcPG3) or dependently (BcPG2) of enzymatic activity. Virulence factors. BcPG2 is inhibited by polygalacturonase inhibitor protein VvPGIP1 of grape.	LRR-RLP AtRBPG1/RBPG1 (*A. thaliana*)	ten Have et al. (1998); Wubben et al. (1999); Kars et al. (2005); Joubert et al. (2007); Zhang et al. (2014)
AcPG1	GH28	*Alternaria citri* (necrotrophic pathogen)	Endopolygalacturonase. Virulence factor on citrus fruit.		Isshiki et al. (2001)

CLPG1	GH28	*Colletotrichum lindemuthianum* (hemibiotrophic pathogen)	Endopolygalacturonase. Triggers plant cell death and induces plant defence response in *N. tabacum* dependent on enzyme activity.		Boudart et al. (2003)
LbGH28A	GH28	*L. bicolor* (ectomycorrhizal fungus)	Endopolygalacturonase. Involved in the establishment of symbiosis.		Zhang et al. (2021b)
BcAra1	GH43	*B. cinerea* (necrotrophic pathogen)	Endoarabinanase. Host-specific contribution to virulence.		Nafisi et al. (2014)
MoAbfB	GH43	*M. oryzae* (hemibiotrophic pathogen)	α-L-arabinofuranosidase. Required for full virulence in rice. Degrades the rice cell wall, releasing oligosaccharides that are recognized as DAMPs [4].		Wu et al. (2016)
EG1	GH45	*R. solani* (necrotrophic pathogen)	Endoglucanohydrolase (cellulase). Recognized as a MAMP in maize, *N. tabacum* and *A. thaliana* [2], triggering cell death and other immune responses.		Guo et al. (2021); Ma et al. (2015a)
Um01829/UmAfg1/UmErc1	GH51	*U. maydis* (biotrophic pathogen)	Exo-1,3-β-glucanase. Organ-specific virulence factor. Sequesters 1,3-β-glucan to prevent ROS burst [5A].		Lanver et al. (2014); Schilling et al. (2014);

			Involved in fungal cell-to-cell movement in maize bundle sheath cells.		Ökmen et al. (in preparation)
UhErc1	GH51	*U. hordei*	Exo-1,3-β-glucanase. Organ-specific virulence factor. Sequesters 1,3-β-glucan to prevent ROS burst [5A]. Involved in fungal cell-to-cell movement in maize bundle sheath cells.		Ökmen et al. (in preparation)
Ssaxp	GH54	*S. sclerotiorum* (necrotrophic pathogen)	Putative arabinofuranosidase/β-xylosidase. Virulence factor in Canola.		Yajima et al. (2009)
Arb93B	GH93	*F. graminearum* (hemibiotrophic pathogen)	Predicted arabinanase. Virulence factor in wheat. Suppresses plant immune responses.		Hao et al. (2019)

DAMP, damage-associated molecular pattern; MAMP, microbe-associated molecular pattern; GH, glycoside hydrolase; LRR, leucine-rich repeat; PRR, pattern recognition receptor; RLP, receptor-like protein; ROS, reactive oxygen species. *Corresponding panel number in Figure 1, where known, is shown in square brackets.

Appendix 3.1. Complete list of biological materials used in chapter three.

Organism/strain	Characteristics	Reference
***Agrobacterium tumefaciens* (Strain/transformant)**		
GV3101::pMP90	pMP90 (pTiC58); C58C1; Rif^R, $Gent^R$	Hellens et al. (2000)
EB 027 (Pb002159)	GV3101/pEB40; Rif^R, $Gent^R$, Kan^R	This study
EB 030 (Pb009590E137D)	GV3101/pEB62; Rif^R, $Gent^R$, Kan^R	This study
EB 031 (Pb009589E134D)	GV3101/pEB63; Rif^R, $Gent^R$, Kan^R	This study
EB 032 (Pb009588E135D)	GV3101/pEB64; Rif^R, $Gent^R$, Kan^R	This study
EB 033 (Pb009244E136D)	GV3101/pEB65; Rif^R, $Gent^R$, Kan^R	This study
EB 034 (Pb004638E134D)	GV3101/pEB66; Rif^R, $Gent^R$, Kan^R	This study
EB 035 (Pb009588-NoSP)	GV3101/pEB68; Rif^R, $Gent^R$, Kan^R	This study
EB 036 (Pb009589-NoSP)	GV3101/pEB69; Rif^R, $Gent^R$, Kan^R	This study
EB 037 (Pb009590-NoSP)	GV3101/pEB70; Rif^R, $Gent^R$, Kan^R	This study
EB 038 (Pb009244-NoSP)	GV3101/pEB71; Rif^R, $Gent^R$, Kan^R	This study
EB 039 (Pb004637-NoSP)	GV3101/pEB72; Rif^R, $Gent^R$, Kan^R	This study
EB 040 (Pb004638-NoSP)	GV3101/pEB73; Rif^R, $Gent^R$, Kan^R	This study
EB 081 (PHAG|07462)	GV3101/pEB55; Rif^R, $Gent^R$, Kan^R	This study
EB 082 (Pb003260)	GV3101/pEB56; Rif^R, $Gent^R$, Kan^R	This study
EB 083 (Pb003493)	GV3101/pEB57; Rif^R, $Gent^R$, Kan^R	This study
EB 084 (Pb004370)	GV3101/pEB58; Rif^R, $Gent^R$, Kan^R	This study
EB 085 (Pb005342)	GV3101/pEB59; Rif^R, $Gent^R$, Kan^R	This study
EB 086 (Pb010936)	GV3101/pEB60; Rif^R, $Gent^R$, Kan^R	This study
EB 091 (Pb001110)	GV3101/pEB35; Rif^R, $Gent^R$, Kan^R	This study
EB 092 (Pb009575#2)	GV3101/pEB31; Rif^R, $Gent^R$, Kan^R	This study
EB 093 (Pb009575#3)	GV3101/pEB32; Rif^R, $Gent^R$, Kan^R	This study
EB 094 (Pb009575#4)	GV3101/pEB33; Rif^R, $Gent^R$, Kan^R	This study
EB 095 (Pb008620)	GV3101/pEB43; Rif^R, $Gent^R$, Kan^R	This study
EB 096 (Pb010674)	GV3101/pEB51; Rif^R, $Gent^R$, Kan^R	This study
EB 097 (PHAG|10819)	GV3101/pEB44; Rif^R, $Gent^R$, Kan^R	This study
EB 098 (Pb010672)	GV3101/pEB52; Rif^R, $Gent^R$, Kan^R	This study
EB 099 (PHAG|01058)	GV3101/pEB45; Rif^R, $Gent^R$, Kan^R	This study
EB 100 (Pb008512)	GV3101/pEB36; Rif^R, $Gent^R$, Kan^R	This study
EB 101 (Pb009529)	GV3101/pEB46; Rif^R, $Gent^R$, Kan^R	This study
EB 102 (Pb004319)	GV3101/pEB38; Rif^R, $Gent^R$, Kan^R	This study
EB 103 (Pb011130)	GV3101/pEB47; Rif^R, $Gent^R$, Kan^R	This study
EB 104 (Pb006336)	GV3101/pEB39; Rif^R, $Gent^R$, Kan^R	This study

EB 105 (Pb001510)	GV3101/pEB48; Rif^R, $Gent^R$, Kan^R	This study
EB 106 (Pb002158)	GV3101/pEB49; Rif^R, $Gent^R$, Kan^R	This study
EB 107 (Pb002164)	GV3101/pEB50; Rif^R, $Gent^R$, Kan^R	This study
EB 122 (Pb002171)	GV3101/pEB30; Rif^R, $Gent^R$, Kan^R	This study
EB 131 (Pa010456)	GV3101/pEB53; Rif^R, $Gent^R$, Kan^R	This study
EB 132 (Pb000646)	GV3101/pEB54; Rif^R, $Gent^R$, Kan^R	This study
EB 133 (Pb000646)	GV3101/pEB61; Rif^R, $Gent^R$, Kan^R	This study
EB 134 (Pb009575#1)	GV3101/pEB15; Rif^R, $Gent^R$, Kan^R	This study
EB 182 (Pb009637E135D)	GV3101/pEB67; Rif^R, $Gent^R$, Kan^R	This study
RBG 110 (PaRxLR53)	GV3101/pPaRxLR53; Rif^R, $Gent^R$, Kan^R	This study
RBG 28 (R3a)	GV3101/pR3a Rif^R, $Gent^R$, Kan^R	This study
RBG 29 (Avr3a)	GV3101/pAvr3a; Rif^R, $Gent^R$, Kan^R	This study
RBG 336 (Pb004638)	GV3101/pEB11; Rif^R, $Gent^R$, Kan^R	This study
RBG 337 (Pb009590)	GV3101/pEB12; Rif^R, $Gent^R$, Kan^R	This study
RBG 338 (Pb009589)	GV3101/pEB13; Rif^R, $Gent^R$, Kan^R	This study
RBG 339 (Pb009588)	GV3101/pEB14; Rif^R, $Gent^R$, Kan^R	This study
RBG 341 (Pb009574)	GV3101/pEB16; Rif^R, $Gent^R$, Kan^R	This study
RBG 342 (Pb004637)	GV3101/pEB17; Rif^R, $Gent^R$, Kan^R	This study
RBG 382 (Pb005713)	GV3101/pEB18; Rif^R, $Gent^R$, Kan^R	This study
RBG 383 (Pb003416)	GV3101/pEB19; Rif^R, $Gent^R$, Kan^R	This study
RBG 384 (Pb003420)	GV3101/pEB20; Rif^R, $Gent^R$, Kan^R	This study
RBG 385 (Pb010041)	GV3101/pEB21; Rif^R, $Gent^R$, Kan^R	This study
RBG 386 (Pb005790)	GV3101/pEB22; Rif^R, $Gent^R$, Kan^R	This study
RBG 391 (Pb008554)	GV3101/pEB23; Rif^R, $Gent^R$, Kan^R	This study
RBG 392 (Pb006337)	GV3101/pEB24; Rif^R, $Gent^R$, Kan^R	This study
RBG 393 (Pb002157)	GV3101/pEB25; Rif^R, $Gent^R$, Kan^R	This study
RBG 394 (Pb006097)	GV3101/pEB26; Rif^R, $Gent^R$, Kan^R	This study
RBG 395 (Pb000587)	GV3101/pEB27; Rif^R, $Gent^R$, Kan^R	This study
RBG 396 (Pb004761)	GV3101/pEB28; Rif^R, $Gent^R$, Kan^R	This study
RBG 397 (Pb010669)	GV3101/pEB29; Rif^R, $Gent^R$, Kan^R	This study
RBG 404 (PaRxLR83)	GV3101/pPaRxLR83; Rif^R, $Gent^R$, Kan^R	This study
RBG 420 (PaRxLR99)	GV3101/pPaRxLR99; Rif^R, $Gent^R$, Kan^R	This study
RBG 427 (PaRxLR106)	GV3101/pPaRxLR106; Rif^R, $Gent^R$, Kan^R	This study
RBG 428 (PaRxLR107)	GV3101/pPaRxLR107; Rif^R, $Gent^R$, Kan^R	This study
RBG 437 (Pb001110-like)	GV3101/pEB34; Rif^R, $Gent^R$, Kan^R	This study
RBG 438 (Pb004285)	GV3101/pEB37; Rif^R, $Gent^R$, Kan^R	This study
RBG 46 (GFP)	GV3101/pGFP; Rif^R, $Gent^R$, Kan^R	This study
RBG 480 (Pb010670)	GV3101/pEB41; Rif^R, $Gent^R$, Kan^R	This study

RBG 481 (Pb010677)	GV3101/pEB42; Rif^R, $Gent^R$, Kan^R	This study
RBG 49 (PaINF1)	GV3101/pPaINF1; Rif^R, $Gent^R$, Kan^R	This study
RBG 56 (PaRxLR1)	GV3101/pPaRxLR1; Rif^R, $Gent^R$, Kan^R	This study
RBG 61 (PaRxLR6)	GV3101/pPaRxLR6; Rif^R, $Gent^R$, Kan^R	This study
RBG 81 (PaRxLR26)	GV3101/pPaRxLR26; Rif^R, $Gent^R$, Kan^R	This study
RBG 93 (PaRxLR38)	GV3101/pPaRxLR38; Rif^R, $Gent^R$, Kan^R	This study
RBG 94 (PaRxLR39)	GV3101/pPaRxLR39; Rif^R, $Gent^R$, Kan^R	This study
RBG 95 (PaRxLR40)	GV3101/pPaRxLR40; Rif^R, $Gent^R$, Kan^R	This study
RBG301 (Pb009244)	GV3101/pEB10; Rif^R, $Gent^R$, Kan^R	This study
Escherichia coli		
DH5α	F^-, φ80*lac*ZΔM15, Δ(*lac*ZYA-*argF*), U169, *rec*A1, *end*A1, *hsd*R17 (r_k^-, m_k^-), *pho*A , *sup*E44, λ^-, *thi*-1, *gyr*A96, *rel*A1	Hanahan (1985)
EB 043 (Pb009588-NoSP)	DH5α/pEB68; Kan^R	This study
EB 044 (Pb009589-NoSP)	DH5α/pEB69; Kan^R	This study
EB 045 (Pb009590-NoSP)	DH5α/pEB70; Kan^R	This study
EB 046 (Pb009244-NoSP)	DH5α/pEB71; Kan^R	This study
EB 047 (Pb004637-NoSP)	DH5α/pEB72; Kan^R	This study
EB 048 (Pb004638-NoSP)	DH5α/pEB73; Kan^R	This study
EB 054 (Pb001110)	DH5α/pEB35; Kan^R	This study
EB 056 (Pb009575#1)	DH5α/pEB15; Kan^R	This study
EB 069 (PHAG|07462)	DH5α/pEB55; Kan^R	This study
EB 071 (Pb003260)	DH5α/pEB56; Kan^R	This study
EB 073 (Pb003493)	DH5α/pEB57; Kan^R	This study
EB 075 (Pb004370)	DH5α/pEB58; Kan^R	This study
EB 077 (Pb005342)	DH5α/pEB59; Kan^R	This study
EB 079 (Pb010936)	DH5α/pEB60; Kan^R	This study
EB 087 (Pb009575#2)	DH5α/pEB31; Kan^R	This study
EB 088 (Pb009575#3)	DH5α/pEB32; Kan^R	This study
EB 089 (Pb009575#4)	DH5α/pEB33; Kan^R	This study
EB 090 (Pb002171)	DH5α/pEB30; Kan^R	This study
EB 108 (Pb008620)	DH5α/pEB43; Kan^R	This study
EB 109 (Pb010674)	DH5α/pEB51; Kan^R	This study
EB 110 (PHAG|10819)	DH5α/pEB44; Kan^R	This study
EB 111 (Pb010672)	DH5α/pEB52; Kan^R	This study
EB 112 (PHAG|01058)	DH5α/pEB45; Kan^R	This study
EB 113 (Pb008512)	DH5α/pEB36; Kan^R	This study
EB 114 (Pb009529)	DH5α/pEB46; Kan^R	This study
EB 115 (Pb004319)	DH5α/pEB38; Kan^R	This study

EB 116 (Pb011130)	DH5α/pEB47; Kan^R	This study
EB 117 (Pb002159)	DH5α/pEB40; Kan^R	This study
EB 118 (Pb001510)	DH5α/pEB48; Kan^R	This study
EB 119 (Pb002158)	DH5α/pEB49; Kan^R	This study
EB 120 (Pb002164)	DH5α/pEB50; Kan^R	This study
EB 123 (Pa010456)	DH5α/pEB53; Kan^R	This study
EB 124 (Pb000646)	DH5α/pEB54; Kan^R	This study
EB 125 (Pb000646-like)	DH5α/pEB61; Kan^R	This study
EB 135 (Pb004637)	DH5α/pEB80; Kan^R	This study
EB 144 (Pb009244cm)	DH5α/pEB81; Kan^R	This study
EB 145 (Pb009589cm)	DH5α/pEB82; Kan^R	This study
EB 146 (Pb009590cm)	DH5α/pEB83; Kan^R	This study
EB 155 (Pb010677)	DH5α/pEB42; Kan^R	This study
EB 156 (Pb004637-1st *Bsa*I mutation)	DH5α/pEB84; Kan^R	This study
EB 159 (Pb009588)	DH5α/pEB85; Kan^R	This study
EB 160 (Pb004637-1st and 2nd *Bsa*I mutation)	DH5α/pEB86; Kan^R	This study
EB 180 (Pb004637E135D)	DH5α/pEB67; Kan^R	This study
Phytophthora agathidicida		
Pa3770	*P. agathidicida* type strain 3770	Studholme et al. (2016)
Pichia pastoris		
GS115	His4, Mut+, His-, Aox1, Aox2	Invitrogen; Schutter et al. (2009)
Pp004637	GS115; pEB78	This study
Pp004637-E116D	GS115; pEB79	This study
Pp009244	GS115; pEB74	This study
Pp009244-E117D	GS115; pEB75	This study
Pp009588	GS115; pEB76	This study
Pp009588-E113D	GS115; pEB77	This study
Plants		
Nicotiana benthamiana	LAB variant, NbRdr1	John Cleland (Wylie & Li, 2022)
Nicotiana tabacum	Wisconsin 38	Murashige & Nakano (1967)

Appendix 3.2. Complete list of plasmids used in chapter three.

Plasmid	Characteristics	Reference
pICH86988	**Binary vector; 35S promoter; OCS terminator; lacZ; Kan^R**	**Weber et al. (2011)**
pEB10	pICH86988 containing 5′PR1α-3xFLAG-Mature Pb009244; Kan^R	This study
pEB11	pICH86988 containing 5′PR1α-3xFLAG-Mature Pb004638; Kan^R	This study
pEB12	pICH86988 containing 5′PR1α-3xFLAG-Mature Pb009590; Kan^R	This study
pEB13	pICH86988 containing 5′PR1α-3xFLAG-Mature Pb009589; Kan^R	This study
pEB14	pICH86988 containing 5′PR1α-3xFLAG-Mature Pb009588; Kan^R	This study
pEB15	pICH86988 containing 5′PR1α-3xFLAG-Mature Pb009575; Kan^R	This study
pEB16	pICH86988 containing 5′PR1α-3xFLAG-Mature Pb009574; Kan^R	This study
pEB17	pICH86988 containing 5′PR1α-3xFLAG-Mature Pb004637; Kan^R	This study
pEB18	pICH86988 containing 5′PR1α-3xFLAG-Mature Pb005713; Kan^R	This study
pEB19	pICH86988 containing 5′PR1α-3xFLAG-Mature Pb003416; Kan^R	This study
pEB20	pICH86988 containing 5′PR1α-3xFLAG-Mature Pb003420; Kan^R	This study
pEB21	pICH86988 containing 5′PR1α-3xFLAG-Mature Pb010041; Kan^R	This study
pEB22	pICH86988 containing 5′PR1α-3xFLAG-Mature Pb005790; Kan^R	This study
pEB23	pICH86988 containing 5′PR1α-3xFLAG-Mature Pb008554; Kan^R	This study
pEB24	pICH86988 containing 5′PR1α-3xFLAG-Mature Pb006337; Kan^R	This study
pEB25	pICH86988 containing 5′PR1α-3xFLAG-Mature Pb002157; Kan^R	This study
pEB26	pICH86988 containing 5′PR1α-3xFLAG-Mature Pb006097; Kan^R	This study
pEB27	pICH86988 containing 5′PR1α-3xFLAG-Mature Pb000587; Kan^R	This study
pEB28	pICH86988 containing 5′PR1α-3xFLAG-Mature Pb004761; Kan^R	This study
pEB29	pICH86988 containing 5′PR1α-3xFLAG-Mature Pb010669; Kan^R	This study
pEB30	pICH86988 containing 5′PR1α-3xFLAG-Mature Pb002171; Kan^R	This study
pEB31	pICH86988 containing 5′PR1α-3xFLAG-Mature Pb009575#2; Kan^R	This study
pEB32	pICH86988 containing 5′PR1α-3xFLAG-Mature Pb009575#3; Kan^R	This study
pEB33	pICH86988 containing 5′PR1α-3xFLAG-Mature Pb009575#4; Kan^R	This study
pEB34	pICH86988 containing 5′PR1α-3xFLAG-Mature Pb001110-like; Kan^R	This study
pEB35	pICH86988 containing 5′PR1α-3xFLAG-Mature Pb001110; Kan^R	This study
pEB36	pICH86988 containing 5′PR1α-3xFLAG-Mature Pb008512; Kan^R	This study
pEB37	pICH86988 containing 5′PR1α-3xFLAG-Mature Pb004385; Kan^R	This study
pEB38	pICH86988 containing 5′PR1α-3xFLAG-Mature Pb004319; Kan^R	This study
pEB39	pICH86988 containing 5′PR1α-3xFLAG-Mature Pb006336; Kan^R	This study
pEB40	pICH86988 containing 5′PR1α-3xFLAG-Mature Pb002159; Kan^R	This study
pEB41	pICH86988 containing 5′PR1α-3xFLAG-Mature Pb010670; Kan^R	This study
pEB42	pICH86988 containing 5′PR1α-3xFLAG-Mature Pb010677; Kan^R	This study

pEB43	pICH86988 containing 5′PR1α-3xFLAG-Mature Pb008620; Kan^R	This study
pEB44	pICH86988 containing 5′PR1α-3xFLAG-Mature PHAG|10819; Kan^R	This study
pEB45	pICH86988 containing 5′PR1α-3xFLAG-Mature PHAG|01058; Kan^R	This study
pEB46	pICH86988 containing 5′PR1α-3xFLAG-Mature Pb009529; Kan^R	This study
pEB47	pICH86988 containing 5′PR1α-3xFLAG-Mature Pb011130; Kan^R	This study
pEB48	pICH86988 containing 5′PR1α-3xFLAG-Mature Pb001510; Kan^R	This study
pEB49	pICH86988 containing 5′PR1α-3xFLAG-Mature Pb002158; Kan^R	This study
pEB50	pICH86988 containing 5′PR1α-3xFLAG-Mature Pb002164; Kan^R	This study
pEB51	pICH86988 containing 5′PR1α-3xFLAG-Mature Pb010674; Kan^R	This study
pEB52	pICH86988 containing 5′PR1α-3xFLAG-Mature Pb010672; Kan^R	This study
pEB53	pICH86988 containing 5′PR1α-3xFLAG-Mature Pa010456; Kan^R	This study
pEB54	pICH86988 containing 5′PR1α-3xFLAG-Mature Pb000646; Kan^R	This study
pEB55	pICH86988 containing 5′PR1α-3xFLAG-Mature PHAG|07462; Kan^R	This study
pEB56	pICH86988 containing 5′PR1α-3xFLAG-Mature Pb003260; Kan^R	This study
pEB57	pICH86988 containing 5′PR1α-3xFLAG-Mature Pb003493; Kan^R	This study
pEB58	pICH86988 containing 5′PR1α-3xFLAG-Mature Pb004370; Kan^R	This study
pEB59	pICH86988 containing 5′PR1α-3xFLAG-Mature Pb005342; Kan^R	This study
pEB60	pICH86988 containing 5′PR1α-3xFLAG-Mature Pb010936; Kan^R	This study
pEB61	pICH86988 containing 5′PR1α-3xFLAG-Mature Pb000646-like; Kan^R	This study
pEB62	pICH86988 containing 5′PR1α-3xFLAG-Mature Pb009590E137D; Kan^R	This study
pEB63	pICH86988 containing 5′PR1α-3xFLAG-Mature Pb009589E134D; Kan^R	This study
pEB64	pICH86988 containing 5′PR1α-3xFLAG-Mature Pb009588E135D; Kan^R	This study
pEB65	pICH86988 containing 5′PR1α-3xFLAG-Mature Pb009244E136D; Kan^R	This study
pEB66	pICH86988 containing 5′PR1α-3xFLAG-Mature Pb004638E134D; Kan^R	This study
pEB67	pICH86988 containing 5′PR1α-3xFLAG-Mature Pb004637E135D; Kan^R	This study
pEB68	pICH86988 containing 5′3xFLAG-Mature Pb009588; Kan^R	This study
pEB69	pICH86988 containing 5′3xFLAG-Mature Pb009589; Kan^R	This study
pEB70	pICH86988 containing 5′3xFLAG-Mature Pb009590; Kan^R	This study
pEB71	pICH86988 containing 5′3xFLAG-Mature Pb009244; Kan^R	This study
pEB72	pICH86988 containing 5′3xFLAG-Mature Pb004637; Kan^R	This study
pEB73	pICH86988 containing 5′3xFLAG-Mature Pb004638; Kan^R	This study
pPIC9-6xHis	**AOS promoter; AOS terminator; Amp^R**	**In house vector modified from Invitrogen supplier**
pEB74	pPIC9 containing 5’FLAG-Mature Pb009244	This study
pEB75	pPIC9 containing 5’FLAG-Mature Pb009244E117D	This study
pEB76	pPIC9 containing 5’FLAG-Mature Pb009588	This study
pEB77	pPIC9 containing 5’FLAG-Mature Pb009588E113D	This study

pEB78	pPIC9 containing 5’FLAG-Mature Pb004637	This study
pEB79	pPIC9 containing 5’FLAG-Mature Pb004637E116D	This study
pUC19	**Cloning vector; High copy number; Lac promoter; Amp^{R}**	**Norrander et al. (1983)**
pEB80	pUC19 containing 5'Mature Pb004637	This study
pEB81	pUC19 containing 5'Mature Pb009244E136D	This study
pEB82	pUC19 containing 5'Mature Pb009589E134D	This study
pEB83	pUC19 containing 5'Mature Pb009590E137D	This study
pEB84	pUC19 containing 5'Mature Pb004637-1st *Bsa*I mutation	This study
pEB85	pUC19 containing 5'Mature Pb009588	This study
pEB86	pUC19 containing 5'Mature Pb004637-1st and 2nd *Bsa*I mutation	This study

Appendix 3.3. Media used in this thesis.

Buffered glycerol-complex medium (BMGY) and buffered methanol-complex medium (BMMY)

BMGY broth was made with 1% (w/v) yeast extract (Merck) and 2% (w/v) peptone (Invitrogen). The resulting solution was autoclaved to sterilise and once cooled 10% (v/v) of a 13.4% (w/v) stock solution of YNB (Invitrogen), 10% potassium phosphate buffer (8.4% (v/v) of 174.2 g/L K_2HPO_4 (Ajax lab chemicals, New South Wales, Australia), 91.6% (v/v) of 136.1 g/L KH_2PO_4 (Ajax lab chemicals, New South Wales, Australia), pH 6.0), 0.02% (v/v) of an already 0.02% (w/v) stock solution of biotin (Sigma-Aldrich) and either 10% (v/v) of an already 10% (w/v) stock solution of glycerol (Ajax lab chemicals, New South Wales, Australia) for BMGY or 10% (v/v) of a 5% (v/v) methanol (Emsure®) stock solution for BMMY.

Clarified V8 liquid broth and agar medium

For a 5x-clarified V8 liquid broth medium stock solution, 0.1% (w/v) $CaCO_3$ (BDH Chemicals Ltd, New Zealand) was added to original V8 vegetable juice (Campbell's, Camden, New Jersey, USA)) and centrifuged at 4,000 rpm (Heraeus Megafuge 16R Centrifuge (ThermoFisher Scientific, Waltham, Massachusetts, USA)) for 20 min. The resulting supernatant was then filtered through two layers of 3MM Whatmann® filter paper (Sigma-Aldrich) and stored at –20°C until required. When required, 20% (v/v) of the 5x stock solution was used to make a 1x-clarified V8 broth. To make clarified V8 agar medium, 1.5% (w/v) bacteriological agar (Acumedia ®, Michigan, USA) was added. Both clarified V8 broth and agar media were sterilised by autoclaving prior to use.

Cornmeal agar

Cornmeal agar was made with 1.75% (w/v) cornmeal agar (Sigma-Aldrich, St. Louis, Missouri, USA). After the medium was autoclaved for sterilisation, the following selective agents were added: ampicillin (ACTGene, New Jersey, USA) 250 µg/mL, rifampicin (Duchefa Biochemie, Haarlem, The Netherlands) 10 µg/mL, pimaricin (Sigma-Aldrich) 10 µg/mL, pentachloronitrobenzene (Sigma-Aldrich) 100 µg/mL. Pentachloronitrobenzene was first made as a 5 mg/ml stock in 95% (v/v) ethanol and heated at 70°C until dissolved.

Henniger liquid broth medium

To make Henniger liquid broth medium, the following stock solutions were made: (10% (w/v) $KH_2PO_4.3H_2O$ (J.T.Baker®, Phillipsburg, New Jersey, USA), 50% (w/v) $NaNO_3$ (Ajax FineChem,

NSW, Australia), 26% (w/v) $CaCl_2.2H_2O$ (Ajax FineChem), 5% (w/v) $(NH_4)_2SO_4$ (Ajax FineChem), 20% (w/v) tartaric acid (Sigma-Aldrich), 4% (w/v) succinic acid (Sigma-Aldrich), 40% (w/v) α-ketoglutaric acid (Sigma-Aldrich), 6% (w/v) L-alanine (Sigma-Aldrich), 1% (w/v) L-leucine (Sigma-Aldrich), 10% (w/v) D-amino-butyric acid (Sigma-Aldrich), 0.4% (w/v) L-tryptophane (Sigma-Aldrich), 10% (w/v) cysteine hydrochloride (Sigma-Aldrich), 5% (w/v) arginine hydrochloride (Sigma-Aldrich), 0.02% (w/v) thiamine (Sigma-Aldrich)). These stock solutions were diluted to a final concentration of 0.02% (v/v) $KH_2PO_4.3H_2O$, 0.05% (v/v) $NaNO_3$, 0.026% (v/v) $CaCl_2.2H_2O$, 0.005% (v/v) $(NH_4)_2SO_4$, 0.02% (v/v) tartaric acid, 0.02% (v/v) succinic acid, 0.04% (v/v) α-ketoglutaric acid, 0.036% (v/v) L-alanine, 0.02% (v/v) L-leucine, 0.02% (v/v), D-amino-butyric acid, 0.008% (v/v) L-tryptophane, 0.02% (v/v) cysteine hydrochloride, 0.001% (v/v) arginine hydrochloride, 0.02% (v/v) thiamine. Also added was 0.015% (w/v) $MgCO_3$, 0.001% (w/v) $FeSO_4.7H_2O$, 0.03% (w/v) L-glutamic acid, 0.02% (w/v) L-asparagine, and 1% (w/v) glucose. The resulting solution was adjusted to pH 5.5 and autoclaved to sterilise.

Lysogeny broth (LB) medium

LB medium was made with 2% LB (Duchefa Biochemie, Haarlem, The Netherlands) (w/v) (low salt) and 0.1% glucose (Labserv, Auckland, New Zealand) (w/v). LB agar was made with the addition of 1.5% (w/v) bacteriological agar (Acumedia®, Michigan, United States of America (USA)). Where chemical selection was required, selective agents were added at the appropriate concentration after the medium was autoclaved (ampicillin (ACTGene, New Jersey, USA) 100 µg/mL, kanamycin (ACTGene) 50 µg/mL, gentamycin (ACTGene) 30 µg/mL, rifamycin (Duchefa Biochemie) 10 µg/mL, Isopropyl β-D-1-thiogalactopyranoside (IPTG) (Gold Biotechnology, Missouri, USA) 100 µg/mL, or 5-bromo-4-chloro-3-indolyl-β-D-galactopyranoside (X-gal) (Progenz Industries Ltd., Queensland, Australia) 20 µg/mL).

MD agar

Minimal dextrose (MD) agar was made with addition of 1.5% (w/v) bacteriological agar (Acumedia®) to water, which was subsequently autoclaved. Once the agar solution had cooled the following was added before pouring: dextrose (Sigma-Aldrich) to a final concentration of 2% (v/v) from a filter-sterilised 20% (w/v) stock; yeast nitrogen base (YNB) with ammonium sulphate and without amino acids (Invitrogen) to a final concentration of 1.3% (v/v) from a filter-sterilised stock solution of 13.4% (w/v); biotin (Sigma-Aldrich) to a final concentration of 0.008% (v/v) from a filter-sterilised stock solution of 0.02% (w/v).

MMA medium

MMA medium was made by dissolving 2% sucrose, 0.5% Murashige and Skoog salts (without vitamins) (Sigma-Aldrich), 0.19% MES (Sigma-Aldrich) in milliQ water and adjusting the pH to 5.6. The medium was sterilised by autoclaving.

Plich liquid broth medium

Plich liquid broth medium was made with 0.05% (w/v) KH_2PO_4 (J.T.Baker®, Phillipsburg, New Jersey, USA), 0.025% (w/v) $MgSO_4.7H_2O$ (Scharlau, Barcelona, Spain), 0.01% (w/v) asparagine (Sigma-Aldrich), 0.0001% (w/v) thiamine (Sigma-Aldrich), 0.05% (w/v) yeast extract (Sigma-Aldrich), 0.001% (w/v) β–sitosterol (Sigma-Aldrich), and 2.5% (w/v) glucose (Sigma-Aldrich). Plich liquid broth medium was sterilised by autoclaving.

Potato dextrose (PD) liquid broth medium

PD liquid broth medium was made with 2.4% (w/v) potato dextrose (BD, Franklin Lakes, New Jersey, USA). PD liquid broth medium was sterilised by autoclaving.

Preparation of cellophane membranes

Cellophane membranes (Waugh Rubber Bands, Wellington, New Zealand) were cut into circles approximately 10 mm in diameter. The cellophane membrane circles were rinsed three times in water, and autoclaved (suspended in water). The rinsing and autoclaving process was repeated three times, to remove any agents that may inhibit *P. agathidicida* growth, before the cellophane membrane circles were used. Sterile cellophane membrane circles were placed on clarified V8 agar medium.

V8 medium

For a 5x V8 stock solution, 0.1% (w/v) $CaCO_3$ was added to original V8 vegetable juice (Campbell's, Camden, New Jersey, USA). From there, 20% of the stock solution was used to make 1x V8 broth, which was autoclaved for sterilisation prior to use.

YEB medium

YEB medium was made with 0.5% (w/v) beef extract (Sigma-Aldrich), 0.5% bacteriological peptone (Invitrogen), 0.5% (w/v) sucrose, 0.1% (w/v) yeast extract (Merck, New Jersey, USA), 0.2% (v/v) 1M $MgSO_4$ (Sigma-Aldrich). The medium was sterilised by autoclaving, after which the appropriate

antibiotics could be added (kanamycin (ACTGene) 50 μg/mL, gentamycin (ACTGene) 30 μg/mL, rifamycin (Duchefa Biochemie) 10 μg/mL).

YPD medium

Yeast-extract, peptone, dextrose (YPD) broth was made with 0.5% (w/v) yeast extract (Merck, New Jersey, USA), 1% (w/v) peptone (Invitrogen, California, USA), and if agar was required, 1.5% (w/v) bacteriological agar (Acumedia®) was added prior to autoclaving. Once cooled, dextrose (Sigma-Aldrich) was added from a filter-sterilised 20% (w/v) stock solution to a final concentration of 2% (v/v).

Appendix 3.4. Complete list of primers used in chapter three.

Primer name	Sequence 5'-3'	Purpose
EB56	GGTCTCGCAAGGGCGAGTACTGCGGTCAATGGG	GG Pb009244
EB57	GGTCTCGAAGCCTAGTTGACAGCAGCCGAGTACGAC	GG Pb009244
EB60	GGTCTCGCAAGGCGGACTTTTGCGACCAGTGG	GG Pb004637
EB61	GGTCTCGAAGCCTAATCACGGCGGACGCGACGAAG	GG Pb004637
EB62	GGTCTCGCAAGGAGAAGGAATTCTGTGGCAAACAGAACAAGAC	GG Pa3770_0011427
EB63	GGTCTCGAAGCCTACTTCTTCAAGTGCACTGCGGTCGAAT	GG Pa3770_0011427
EB64	GGTCTCGCAAGGCGGACTTCTGCGACCAGTGG	GG Pb004638
EB65	GGTCTCGAAGCTTACTCACGACGAACACGGCGGC	GG Pb004638
EB66	GGTCTCGCAAGGAGAAGGAGTTCTGTGGCCAATGGAACTC	GG Pb009590
EB67	GGTCTCGAAGCCTACGCCGTGTTGACTGCAGCC	GG Pb009590
EB68	GGTCTCGCAAGGCGGAGTTCTGCGGCCGC	GG Pb009589
EB69	GGTCTCGAAGCTTACACCGTGTGTACAGCCGCCG	GG Pb009589
EB70	GGTCTCGCAAGCAAGAGTACTGCCTCCGCAACGACC	GG Pb009588
EB71	GGTCTCGAAGCCTACAGCACCTTCACCGAGTAGGTCGAC	GG Pb009588
EB72	GGTCTCGCAAGGAGAAAGAAATGTGTGGCGACTGGGACAC	GG Pb009574
EB73	GGTCTCGAAGCTTACTTCTGCGAGAAACCAACATCTCCCTG	GG Pb009574
EB74	GGTCTCGCAAGGACTCCATCATGAAGTCCACTTACACGGG	GG Pb011130
EB75	GGTCTCGAAGCCTAGTTTTGCTGGATGTTAGGCACCACTGT	GG Pb011130
EB76	GGTCTCGCAAGGACCCGCGAGTGATGATCGAGTCTAC	GG Pb009529
EB77	GGTCTCGAAGCTTACAAAATCCAGCCCGCCGTGATG	GG Pb009529
EB78	GGTCTCGCAAGGCTCTCTTAACTTCCACCTACACTGGCAC	GG PHAG_12062
EB79	GGTCTCGAAGCCTATTTGCGAATTCGACGAGTGCAAGCG	GG PHAG_12062
EB84	GGTCTCGCAAGAGCGATGCCCCGTACTCGAC	GG Pb008554
EB85	GGTCTCGAAGCTTACGCAAGCTGCTCAACCTCCAG	GG Pb008554
EB86	GGTCTCGCAAGGAGAAGGAATTCTGTGGCAAACAGAACAAG	GG Pb009575
EB87	GGTCTCGAAGCCTACTTCTTCAAGTGCACTGCGGTCG	GG Pb009575
EB88	GGTCTCGCAAGGCGGACGACCAGCCTTTGC	GG Pb006337
EB89	GGTCTCGAAGCCTAGTTACGGCGACGAACCTTGCAG	GG Pb006337
EB90	GGTCTCGCAAGCTATCGACCGGTGTGTGCTACGC	GG Pb002157
EB91	GGTCTCGAAGCTTAGTTTGAAGCCACTCTGCATCCTCG	GG Pb002157
EB92	GGTCTCGCAAGACCAAGCTCAAAACGGGTGTCTGC	GG Pb002171
EB93	GGTCTCGAAGCTTAGTCGCGACGGAGACGGC	GG Pb002171
EB94	GGTCTCGCAAGAATGGAGTTTGCTACGATCCCAACCAC	GG Pb005713
EB95	GGTCTCGAAGCTCACTGACGCAGGCGCTGAG	GG Pb005713
EB96	GGTCTCGCAAGAACGGTGTCTGCTACGACCCG	GG Pb006097
EB97	GGTCTCGAAGCGAAGCTTACAGCGAGCAGATATTCTCCACAGG	GG Pb006097
EB98	GGTCTCGCAAGGGCTCGGATGACGTTTACCAGTCC	GG Pb001110
EB99	GGTCTCGAAGCCTAAGCGTTGCAGGAGCTGTTGC	GG Pb001110
EB100	GGTCTCGCAAGAAAGACTACACGGTCAAGACCGATGC	GG Pb000923
EB101	GGTCTCGAAGCTTACACGGCAACGCCCTTGATCTC	GG Pb000923
EB102	GGTCTCGCAAGATCGACTGCAACAATTGGTCCATGC	GG Pb003416
EB103	GGTCTCGAAGCTTACTTGTTGAAGACGACAGTCTGAATGGAG	GG Pb003416
EB104	GGTCTCGCAAGTGTTCCAGTTGGTCGTCGCTCTAC	GG Pb003420
EB105	GGTCTCGAAGCCTACACGATTTTGGTGTCCTCGGATGC	GG Pb003420

EB106	GGTCTCGCAAGGTGGACCGCAGCAAGTTCCG	GG Pb008512
EB107	GGTCTCGAAGCCTACTCGAGCGCCTGATCGTACAC	GG Pb008512
EB108	GGTCTCGCAAGGCGTACGTCAACCCCGGCG	GG Pb010041
EB109	GGTCTCGAAGCTCATTCTTGAGCCTGAGCACTTGAGC	GG Pb010041
EB110	GGTCTCGCAAGGGGATCACGTTCTCGGCGTTGC	GG Pb000587
EB111	GGTCTCGAAGCTTAGCTAGATCCAGACGATGAGTCCTCCA	GG Pb000587
EB112	GGTCTCGCAAGGGCCCTTGCGATATCTACAATGACGC	GG Pb004285
EB113	GGTCTCGAAGCCTAAGCTACGGATCCGCTCGAGC	GG Pb004285
EB114	GGTCTCGCAAGCAGCAGGTTGGTGACAACACCG	GG Pb004761
EB115	GGTCTCGAAGCTTAGTTGCGGCGCTTGCATGC	GG Pb004761
EB116	GGTCTCGCAAGGTTCACGAGGACCAGACGATGTCTC	GG Pb005788
EB117	GGTCTCGAAGCCTAATCGCAACGCTCTAGCCACG	GG Pb005788
EB118	GTGTGGCTTTGAACGTCGAGGAGC	Pb005788 overlapping F
EB119	GCTCCTCGACGTTCAAAGCCACAC	Pb005788 overlapping R
EB120	GGTCTCGCAAGCAACAGCCAGGAACCAACACCC	GG Pb005790
EB121	GGTCTCGAAGCCTAGTACGTTGAACCGAAATCGCCTG	GG Pb005790
EB122	GGTCTCGCAAGGCACCCTGGGAGCAGTACATCC	GG Pb004319
EB123	GGTCTCGAAGCTTACGCGTCCTTGGCGACGAC	GG Pb004319
EB124	GGTCTCGCAAGGCAACCACCGACCCCGC	GG Pb000751
EB125	GGTCTCGAAGCTTACACCTTCACCGTCAGCTGGG	GG Pb000751
EB126	GGTCTCGCAAGGAGAAGGAATTCTGTGGCAAACAGAACAAG	GG Pb009650
EB127	GGTCTCGAAGCTTACTTCTGCGAGAAACCAACATCTCCC	GG Pb009650
EB128	GGTCTCGCAAGGCGGACCAGCCGCTTCC	GG Pb006336
EB129	GGTCTCGAAGCTTACTTGCGACGAGCGCAGC	GG Pb006336
EB130	GGTCTCGCAAGACGCTGCCTGGTGTGTGCTAC	GG Pb002159
EB131	GGTCTCGAAGCTTACATGGCGCAGTTGGCAGTC	GG Pb002159
EB132	GGTCTCGCAAGGCCGACGCGGGCAGCG	GG Pb002064
EB133	GGTCTCGAAGCTTAGCACTGGACGGTGTCAGGTTCAC	GG Pb002064
EB134	CCTTTGGACAAATGCTGTGGGATGG	Pb002064 overlapping F
EB135	CCATCCCACAGCATTTGTCCAAAGG	Pb002064 overlapping R
EB136	GGTCTCGCAAGTCGCCCATGATGCGTCAAGAGG	GG Pb010663
EB137	GGTCTCGAAGCTTAGCAGGAGATGCTGCTCGGTTC	GG Pb010663
EB138	ACCTTCGGTGAAAAAAAATGGTCGGGTCC	Pb010663 overlap F
EB139	GGACCCGACCATTTTTTTTCACCGAAGGT	Pb010663 overlap R
EB140	GGTCTCGCAAGTCTCCCATGCTGCGTCAAGCG	GG Pb010669
EB141	GGTCTCGAAGCCTAAACACTGAGGCTGCTGGGCAG	GG Pb010669
EB142	GGTCTCGCAAGTCAACGATGCTGCGTCAAGAAGC	GG Pb010670
EB143	GGTCTCGAAGCTTAAACGACAACACCACTGGGGGC	GG Pb010670
EB144	GGTCTCGCAAGTTCGACGTGGTCACTCAAGACGATG	GG Pb010677
EB145	GGTCTCGAAGCTCAGCACTGCACGTTGCTCG	GG Pb010677
EB146	AACGTTCAGCCCAAAGCTTTGGGAC	Pb010677 overlap F
EB147	GTCCCAAAGCTTTGGGCTGAACGTT	Pb010677 overlap R
EB148	GGTCTCGCAAGGACGATGTGACCCAGAACGAAGTCAC	GG Pb010678
EB149	GGTCTCGAAGCTTAGCACTGCATGGTGTCGGGG	GG Pb010678
EB150	GGTCTCGCAAGGCCTCCATCCCTCGTGCGTG	GG Pb008620
EB151	GGTCTCGAAGCTCAGTATATCTTGTTCACGATCAAGTGGATAGC	GG Pb008620
EB152	GGTCTCGCAAGGATGAATGGGACGCTCAAACTGATGTG	PHAG|10819

EB153	GGTCTCGAAGCTTACTCAAAGGATCCGTACGGGTGC	PHAG|10819
EB154	CTGGACAGCGCGCTGGCCCCATC	Pb009575 overlapping PCR
EB155	GATGGGGCCAGCGCGCTGTCCAG	Pb009575 overlapping PCR
EB156	GGTCTCCGTACTGGTCGCAAGATGGTGACG	Pb008512 split primers with BsaI site
EB157	GGTCTCAGTACGCGCCACCAACTCCTG	Pb008512 split primers with BsaI site
EB158	GGTCTCCGTGCAGGACCTTGTACAGGAAC	Pb005788 split primers with BsaI site
EB159	GGTCTCTGCACGATGTCCTTCAGTAGCTC	Pb005788 split primers with BsaI site
EB160	GGTCTCTCGATGAGGTGGATCCTGTCG	Pb004319 split primers with BsaI site
EB161	GGTCTCCATCGAGAATGAACTCGAAGCCG	Pb004319 split primers with BsaI site
EB162	GGTCTCGACAACGAACCCGACGTGG	Pb000751 split primers with BsaI site
EB163	GGTCTCGTTGTCACTTGACCCACCATCC	Pb000751 split primers with BsaI site
EB164	GGTCTCGAACACGGCCGAGTCCAAG	Pb008620 split primers with BsaI site
EB165	GGTCTCGTGTTCACCTCACTAGGGGAAAC	Pb008620 split primers with BsaI site
EB166	GGTCTCGCTGGGTCTGTACGACAACG	PHAG|10819 split primers with BsaI site
EB167	GGTCTCCCCAGCTGTAGTTTGAGCTTGAC	PHAG|10819 split primers with BsaI site
EB168	GAATTTCTCGGGTGACCTCACGG	Pb009650 overlapping primer to mutate BsaI site
EB169	CCGTGAGGTCACCCGAGAAATTC	Pb009650 overlapping primer to mutate BsaI site
EB170	GATGAGCGGCTCTCCCACGAC	Pb000751 overlapping primer to mutate BsaI site
EB171	GTCGTGGGAGAGCCGCTCATC	Pb000751 overlapping primer to mutate BsaI site
EB172	CCACATCGGACTCCTCACGC	Pb006336 overlapping primer to mutate BsaI site
EB173	GCGTGAGGAGTCCGATGTGG	Pb006336 overlapping primer to mutate BsaI site
EB174	GCTTGAGACGCAATGGGCGC	Pb002159 overlapping primer to mutate BsaI site
EB175	GCGCCCATTGCGTCTCAAGC	Pb002159 overlapping primer to mutate BsaI site
EB176	GTGACAACGGACTCCGTATC	Pb010670 overlapping primer to mutate BsaI site

EB177	GATACGGAGTCCGTTGTCAC	Pb010670 overlapping primer to mutate BsaI site
EB178	GATCACGGGACTCACGCTG	Pb010677 overlapping primer to mutate BsaI site
EB179	CAGCGTGAGTCCCGTGATC	Pb010677 overlapping primer to mutate BsaI site
EB180	GATCTCCGGACTCACGATCG	Pb010678 overlapping primer to mutate BsaI site
EB181	CGATCGTGAGTCCGGAGATC	Pb010678 overlapping primer to mutate BsaI site
EB182	GCTGGTCACCCAACATTAACATCAACCGTGACCCCC	Pb008620 overlapping primer to mutate BsaI site
EB183	GGGGGTCACGGTTGATGTTAATGTTGGGTGACCAGC	Pb008620 overlapping primer to mutate BsaI site
EB184	GCCAATGAGACGGTGACGTAC	PHAG|10819 overlapping primer to mutate BsaI site
EB185	GTACGTCACCGTCTCATTGGC	PHAG|10819 overlapping primer to mutate BsaI site
EB186	CGTCGAATACGACCTCATGGTGTGG	Mutate first catalytic site of Pb009590
EB187	CCACACCATGAGGTCGTATTCGACG	Mutate first catalytic site of Pb009590
EB188	CGGCGTACGACCTGATGGTGTG	Mutate first catalytic site of Pb009589
EB189	CACACCATCAGGTCGTACGCCG	Mutate first catalytic site of Pb009589
EB190	GATCGAGTACGACTTGATGGTGTGG	Mutate first catalytic site of Pb009588
EB191	CCACACCATCAAGTCGTACTCGATC	Mutate first catalytic site of Pb009588
EB192	GCAACGAGTACGACATCATGATCTGGC	Mutate first catalytic site of Pb009244
EB193	GCCAGATCATGATGTCGTACTCGTTGC	Mutate first catalytic site of Pb009244
EB194	CTAACGAGTTCGACATCATGATCTGG	Mutate first catalytic site of Pb004638
EB195	CCAGATCATGATGTCGAACTCGTTAG	Mutate first catalytic site of Pb004638
EB196	GAGAAGGAGTTCGACATCATGATCTGG	Mutate first catalytic site of Pb004637
EB197	CCAGATCATGATGTCGAACTCCTTCTC	Mutate first catalytic site of Pb004637
EB198	CCCGGGCCCGACTACAAGGACGACGATGACAAGGGCGAGTACTGCGGTCAATGGG	Pb009244 into *P. pastoris*
EB199	GAATTCCTAGTTGACAGCAGCCGAGTACGAC	Pb009244 into *P. pastoris*
EB200	CCCGGGCCCGACTACAAGGACGACGATGACAAGGCGGAGTTCTGCGGCCGC	Pb009589 into *P. pastoris*

EB201	GAATTCTTACACCGTGTGTACAGCCGCCG	Pb009589 into *P. pastoris*
EB202	CCCGGGCCCGACTACAAGGACGACGATGACAAGGAGAAGGAGTTCTGTGGCCAATGGAACTC	Pb009590 into *P. pastoris*
EB203	GAATTCCTACGCCGTGTTGACTGCAGCC	Pb009590 into *P. pastoris*
EB204	CCCGGGCCCGACTACAAGGACGACGATGACAAGCAAGAGTACTGCCTCCGCAACGACC	Pb009588 into *P. pastoris*
EB205	GAATTCCTACAGCACCTTCACCGAGTAGGTCGAC	Pb009588 into *P. pastoris*
EB206	CCCGGGCCCGACTACAAGGACGACGATGACAAGGCGGACTTTTGCGACCAGTGG	Pb004637 into *P. pastoris*
EB207	GAATTCCTAATCACGGCGGACGCGACGAAG	Pb004637 into *P. pastoris*
EB208	CCCGGGCCCGACTACAAGGACGACGATGACAAGGCGGACTTCTGCGACCAGTGG	Pb004638 into *P. pastoris*
EB209	GAATTCTTACTCACGACGAACACGGCGGC	Pb004638 into *P. pastoris*
EB210	GACTGGAAAGCGGGCAGTG	pUC19 screening primer
EB211	GCAGACAAGCCCGTCAGG	pUC19 screening primer
EB212	GGTCTCGCAAGGACGGCGCATGCAGCG	GG Pa010456
EB213	GGTCTCGAAGCTTACAGGTACGTGGTGTCCACCC	GG Pa010456
EB214	GGTCTCGCAAGGCCTGCTCCACTCCTTCCTTCG	GG Pa000646
EB215	GGTCTCGAAGCTTAGTTGAGCGTTCCCGACACAGC	GG Pa000646
EB216	GGTCTCGCAAGTCCGTGTCCGTGAGCTTTGTCAAC	GG Pa005543
EB217	GGTCTCGAAGCTTAGCTGATCAGGTTCGAAACCGAGG	GG Pa005543
EB218	GGTCTCGCAAGCAGGACTGCTCCACCCCTTCC	PHAG 07462
EB219	GGTCTCGAAGCTTAGTTGAGGGTACCCGATACAGCACC	PHAG 07462
EB220	GGTCTCGCAAGGACCTGCCAATGATGAGATCCG	GG Pa003260, Pa003268, Pa003269
EB221	GGTCTCGAAGCCTACGCCGAGGTGTTCGG	GG Pa003260, Pa003268, Pa003269
EB222	GGTCTCGCAAGGAGGACCAAGCCGTTGTTCAC	GG Pa003493
EB223	GGTCTCGAAGCTTAGGCGTACACGCACTTGC	GG Pa003493
EB224	GGTCTCGCAAGCACCCAGAATTCATCTACCGGT	GG Pa004370
EB225	GGTCTCGAAGCTCACGCTTTTTCTTCAACAGCG	GG Pa004370
EB226	GGTCTCGCAAGCTGGAAGACCTGCCCGTG	GG Pa004433
EB227	GGTCTCGCAAGCTGGAAGACCTGCCCGTG	GG Pa004433
EB228	GGTCTCGCAAGGACGAACCGACTACTCTGGAC	GG Pa005342
EB229	GGTCTCGAAGCTTACGACGAACCCTCAGTGGTC	GG Pa005342
EB230	GGTCTCGCAAGGGTGATGCGACCCCCAG	GG Pa008135
EB231	GGTCTCGAAGCTTAGCAGTAGAAGAAACCACCGA	GG Pa008135
EB232	GGTCTCGCAAGGAGACCGCCGCCCAC	GG Pa008898
EB233	GGTCTCGAAGCTTAATGCTTCGAGCTGGCCAC	GG Pa008898
EB234	GGTCTCGCAAGGCCGATGGCGTGACCC	GG Pa010936
EB235	GGTCTCGAAGCTTAGCAGTAGAAGAAGCCGCC	GG Pa010936
EB236	GGTCTCGCAAGGCCTGCTCCACTCCTTCCTTCGGCT	GG Pa000646
EB237	GGTCTCGAAGCTTAGTTGAGCGTTCCCGACACAGCG	GG Pa000646
EB238	GGTCTCGCAAGCAGGACTGCTCCACCCCTTCCTTCGGTA	GG Unannotated Pb000646-like
EB239	GGTCTCGAAGCTTAGTTGAGGGTACCCGATACAGCACCG	GG Unannotated Pb000646-like

EB242	GAATTCCATCACCATCACCATCACCATCACGGCGAGTACTGCGGTCAATG	Pb009244 into *P. pastoris* EcoRI-8xHIS F
EB243	GAATTCCATCACCATCACCATCACCATCACCAAGAGTACTGCCTCCGCAAC	Pb009588 into *P. pastoris* EcoRI-8xHIS F
EB244	GAATTCCATCACCATCACCATCACCATCACGCGGAGTTCTGCGGCC	Pb009589 into *P. pastoris* EcoRI-8xHIS F
EB245	GAATTCCATCACCATCACCATCACCATCACGAGAAGGAGTTCTGTGGCCAATG	Pb009590 into *P. pastoris* EcoRI-8xHIS F
EB246	GAATTCCATCACCATCACCATCACCATCACGAGAAAGAAATGTGTGGCGACTG	Pb009574 into *P. pastoris* EcoRI-8xHIS F
EB247	GCGGCCGCCTAGTTGACAGCAGCCGAGTAC	Pb009244 into *P. pastoris* NotI R
EB248	GCGGCCGCCTACAGCACCTTCACCGAGTAG	Pb009588 into *P. pastoris* NotI R
EB249	GCGGCCGCTTACACCGTGTGTACAGCCG	Pb009589 into *P. pastoris* NotI R
EB250	GCGGCCGCCTACGCCGTGTTGACTGCAG	Pb009590 into *P. pastoris* NotI R
EB251	GCGGCCGCTTACTTCTGCGAGAAACCAACATCTC	Pb009574 into *P. pastoris* NotI R
EB252	GAATTCGGCGAGTACTGCGGTCAATG	Pb009244 into *P. pastoris* EcoRI F
EB253	GAATTCCAAGAGTACTGCCTCCGCAAC	Pb009588 into *P. pastoris* EcoRI F
EB254	GAATTCGCGGAGTTCTGCGGCC	Pb009589 into *P. pastoris* EcoRI F
EB255	GAATTCGAGAAGGAGTTCTGTGGCCAATG	Pb009590 into *P. pastoris* EcoRI F
EB256	GAATTCGAGAAAGAAATGTGTGGCGACTG	Pb009574 into *P. pastoris* EcoRI F
EB257	GCGGCCGCCTAGTGATGGTGATGGTGATGGTGATGGTTGACAGCAGCCGAGTACG	Pb009244 into *P. pastoris* NotI-STOP-8xHIS R
EB258	GCGGCCGCCTAGTGATGGTGATGGTGATGGTGATGCAGCACCTTCACCGAGTAGGTCGAC	Pb009588 into *P. pastoris* NotI-STOP-8xHIS R
EB259	GCGGCCGCCTAGTGATGGTGATGGTGATGGTGATGCACCGTGTGTACAGCCGC	Pb009589 into *P. pastoris* NotI-STOP-8xHIS R
EB260	GCGGCCGCCTAGTGATGGTGATGGTGATGGTGATGCGCCGTGTTGACTGCAG	Pb009590 into *P. pastoris* NotI-STOP-8xHIS R
EB261	GCGGCCGCCTAGTGATGGTGATGGTGATGGTGATGCTTCTGCGAGAAACCAACATCTC	Pb009574 into *P. pastoris* NotI-STOP-8xHIS R
EB262	GGGCGACGACACCACTACTC	Mutate BsaI site in Pb004637 F
EB263	GAGTAGTGGTGTCGTCGCCC	Mutate BsaI site in Pb004637 R
EB264	GAAGCTGTCATCGGTTACTCAG	pPic9 screening F
EB265	CGTAAGTGCCCAACTTGAAC	pPic9 screening R
EB266	GAATTCGAGAAAGAAATGTGTGGCGACTGGG	Redesign of primer EB256

EB268	CGAGTACGACATCATGATCTGG	Pb009244 catalytic mutant
EB269	CATGATGTCGTACTCGTTGCTG	Pb009244 catalytic mutant
EB270	CGTACGACCTGATGGTGTGG	Pb009589 catalytic mutant
EB271	CATCAGGTCGTACGCCGTCTC	Pb009589 catalytic mutant
EB272	CGAATACGACCTCATGGTGTG	Pb009590 catalytic mutant
EB273	CATGAGGTCGTATTCGACGTTG	Pb009590 catalytic mutant
EB274	GAGTACGACTTGATGGTGTGG	Pb009588 catalytic mutant
EB275	CATCAAGTCGTACTCGATCTCG	Pb009588 catalytic mutant
EB276	GAATTCTTCGACGTGGTCACTCAAGACG	Pb010677 into *P. pastoris* EcoRI F
EB277	GCGGCCGCCTAGTGATGGTGATGGTGATGGTGATGGCACTG CACGTTGCTCG	Pb010677 into *P. pastoris* NotI-STOP-8xHIS R
EB278	GAATTCGACCTGCCAATGATGAGATCCG	Pb003260 into *P. pastoris* EcoRI F
EB279	GCGGCCGCCTAGTGATGGTGATGGTGATGGTGATGCGCCGA GGTGTTCGGCATAG	Pb003260 into *P. pastoris* NotI-STOP-8xHIS R
EB280	GAATTCGACGAACCGACTACTCTGGAC	Pb005342 into *P. pastoris* EcoRI F
EB281	GCGGCCGCCTAGTGATGGTGATGGTGATGGTGATGCGACGA ACCCTCAGTGGTC	Pb005342 into *P. pastoris* NotI-STOP-8xHIS R
EB282	CGAGACGACTACTCAGGGC	Mutate first BsaI site in Pb004637 F
EB283	GTAGTCGTCTCGTCGCCC	Mutate first BsaI site in Pb004637 R
EB284	GGAGACGACCCCTCCTCC	Mutate second BsaI site in Pb004637 F
EB285	GGGGTCGTCTCCAGTTGG	Mutate second BsaI site in Pb004637 R
EB286	GTTCGACATCATGATCTGGCTGG	Mutate catalytic site in Pb004637 F
EB287	CATGATGTCGAACTCCTTCTCGC	Mutate catalytic site in Pb004637 R
EB288	GGCACGCAGACTACGACC	Mutate T back to C in Pb004637 (bsaI-mt x 2 cm)
EB289	GTCTGCGTGCCCGTCG	Mutate T back to C in Pb004637 (bsaI-mt x 2 cm)

Appendix 3.5. Cross-referenced protein identities.

Cross-referenced *Phytophthora agathidicida* protein identities from the Pa3770 PacBio predicted proteome (Pa), Pa3772 Illumina predicted proteome (Pa3772), and the recently acquired Pag3770 PacBio predicted proteome (Pag).

Pag3770 ID	Pa3770 ID	Pa3772 ID	Protein type
Glycoside hydrolases (GH)			
Pag007437	Pa008620	Pa3772|12459	GH3
Pag017473	-	Pa3772|10819	GH3
Pag017835	-	Pa3772|01058	GH3
Pag005100	Pa000587	Pa3772|05440	GH5
Pag002774	Pa007147	Pa3772|13973	GH5
Pag014880	Pa006408	-	GH6
Pag014881	Pa006408	-	GH6
Pag006854	Pa004761	Pa3772|09270	GH7
Pag013524	Pa005788	Pa3772|13959	GH7
Pag013451	Pa005790	-	GH7
Pag000800	Pa009529	Pa3772|11202	GH10
Pag011035	Pa011130	Pa3772|10261	GH10
Pag006684	Pa004637	Pa3772|02502	GH12
Pag006685	Pa004638	Pa3772|02503	GH12
Pag017848	Pa009244	Pa3772|09148	GH12
Pag000731	Pa009574	-	GH12
Pag017831	Pa009575	-	GH12
Pag000709	Pa009588	Pa3772|09073	GH12
Pag017830	Pa009589	Pa3772|09072	GH12
Pag017829	Pa009590	Pa3772|09071	GH12
Pag001691	Pa001510	Pa3772|02546	GH17
Pag012622	Pa002157	Pa3772|08235	GH17
Pag012621	Pa002158	Pa3772|08236	GH17
Pag012620	Pa002159	Pa3772|08237	GH17
Pag012614	Pa002164	Pa3772|08545	GH17
Pag012606	Pa002171	Pa3772|06548	GH17
Pag013309	Pa005713	Pa3772|11227	GH17
Pag003682	Pa006097	Pa3772|03703	GH17
Pag004426	Pa001110	Pa3772|04013	GH19
Pag006227	Pa001110-like	-	GH19
Pag000967	Pa002064	Pa3772|08005	GH28
Pag002114	Pa010663	Pa3772|11552	GH28
Pag002113	Pa010664	Pa3772|11553	GH28
Pag002108	Pa010669	Pa3772|09413	GH28
Pag002107	Pa010670	Pa3772|09412	GH28
Pag002105	Pa010672	Pa3772|13875	GH28

Pag002102	Pa010674 and Pa010675	Pa3772|12892	GH28
Pag002099	Pa010677	Pa3772|13283	GH28
Pag002098	Pa010678	Pa3772|12772	GH28
Pag004667	Pa000923	Pa3772|10344	GH30
Pag010136	Pa003416	Pa3772|11623	GH30
Pag010137	Pa003417	Pa3772|11624	GH30
Pag010142	Pa003420	Pa3772|11269	GH30
Pag007295	Pa008512	Pa3772|00722	GH31
Pag017152	Pa010041	Pa3772|01768	GH43
Pag011418	Pa004285	Pa3772|10526	GH54
Pag011461	Pa004319	Pa3772|11040	GH78
Pag004884	Pa000751	Pa3772|09856	GH81
Pag007346	Pa008554	Pa3772|11435	GH105
Pag004010	Pa006336	Pa3772|11298	GH131
Pag004012	Pa006337	Pa3772|04128	GH131
Pag011298	Pa004184	Pa3772|12992 and Pa3772|14066	GH140
Carbohydrate related proteins			
Pag005016	Pa000646	-	CBEL-like
Pag005019	Pa000646	-	CBEL-like
Pag005021	-	Pa3772|07462	CBEL
Pag013080	Pa005543	Pa3772|07202	OPEL
Pag017846	PaI010456	-	Pectinesterase (CE)
Hypothetical proteins			
Pag009905	Pa003260	-	Hypothetical
Pag009916	Pa003268	-	Hypothetical
Pag009916	Pa003269	-	Hypothetical
Pag009917	Pa003269	-	Hypothetical
Pag009917	Pa003268	-	Hypothetical
Pag015886	Pa003493	-	Hypothetical
Pag015887	Pa003493	-	Hypothetical
Pag011543	Pa004370	Pa3772|04268	Hypothetical
Pag011633	Pa004433	-	Hypothetical
Pag010805	Pa005342	Pa3772|13895	Hypothetical
Pag010804	Pa005342	Pa3772|13895	Hypothetical
Pag013683	Pa008135	Pa3772|07952	Hypothetical
Pag003218	Pa008898	Pa3772|03786	Hypothetical
Pag009100	Pa010936	-	Hypothetical

CBEL = Carbohydrate-binding elicitor lectin (Gaulin et al., 2006, Gaulin et al., 2002, Khatib et al., 2004).

OPEL (Chang et al., 2015).

CE = Carbohydrate esterase

Appendix 3.6. Schematic of the pICH86988 expression vector.

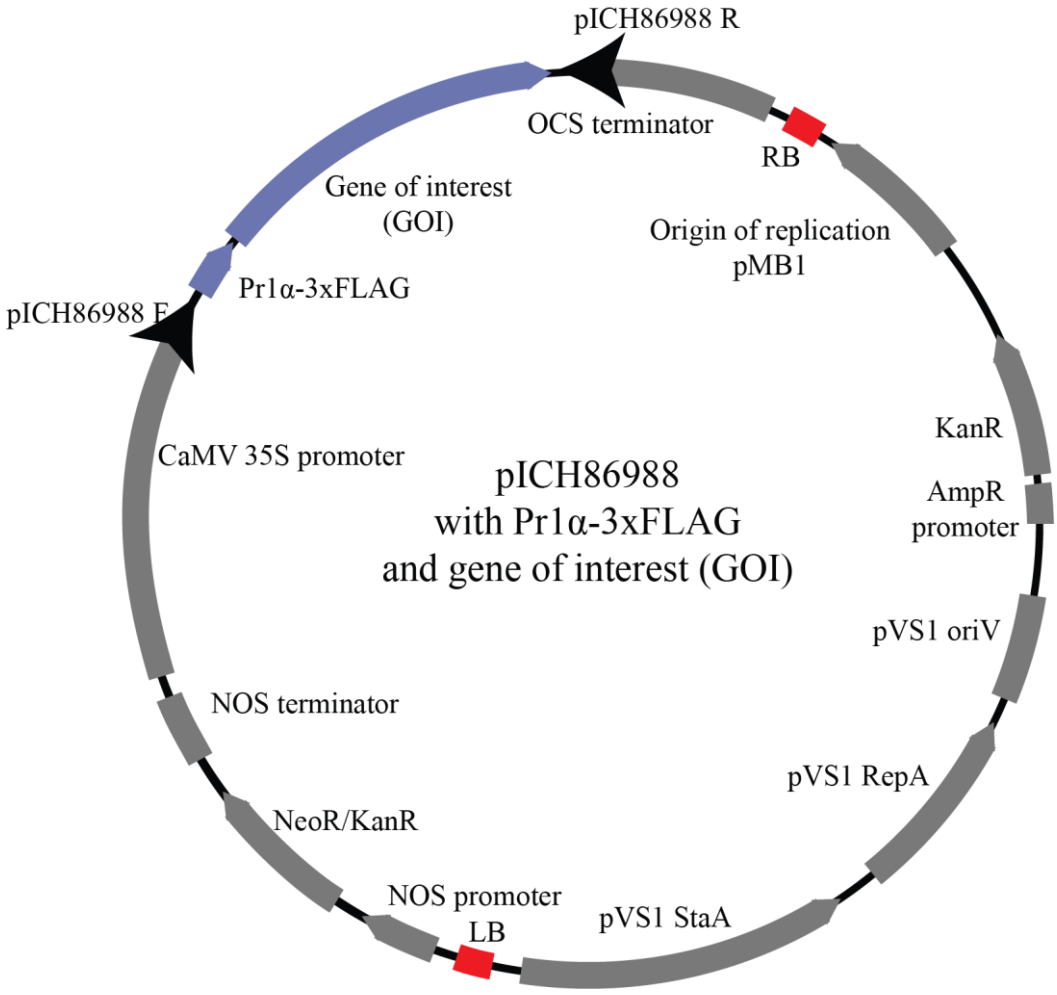

Map of pICH86988 containing the PR1α-3xFLAG tag and gene of interest.

Expression is driven by the constitutive Cauliflower mosaic virus promoter. The multiple cloning site (MCS) within which the PR1α-3xFLAG tag and gene of interest are inserted is also within the *lacZα* gene from *Escherichia coli* which acts as a selectable marker. Bacterial colonies which harbor a plasmid with a disruption of *lacZα*, such as a gene insertion, are white, whereas a complete *lacZα* gene would result in blue colonies. The gene for kanamycin, neomycin, and geneticin® resistance is driven by the nopaline synthase (NOS) promoter from *Agrobacteria tumefaciens*. Only the regions between the left and right borders (red) are transferred into the plant genome. Additional regions of note are the stability and replication proteins from the *Pseudomonas* plasmid pVS1, a second kanamycin resistance gene, and the origin of replication from the high copy number pMB1. The pICH86988 F and R PCR screening primers used in this study are indicated by black arrows.

Appendix 3.7. Western blots.

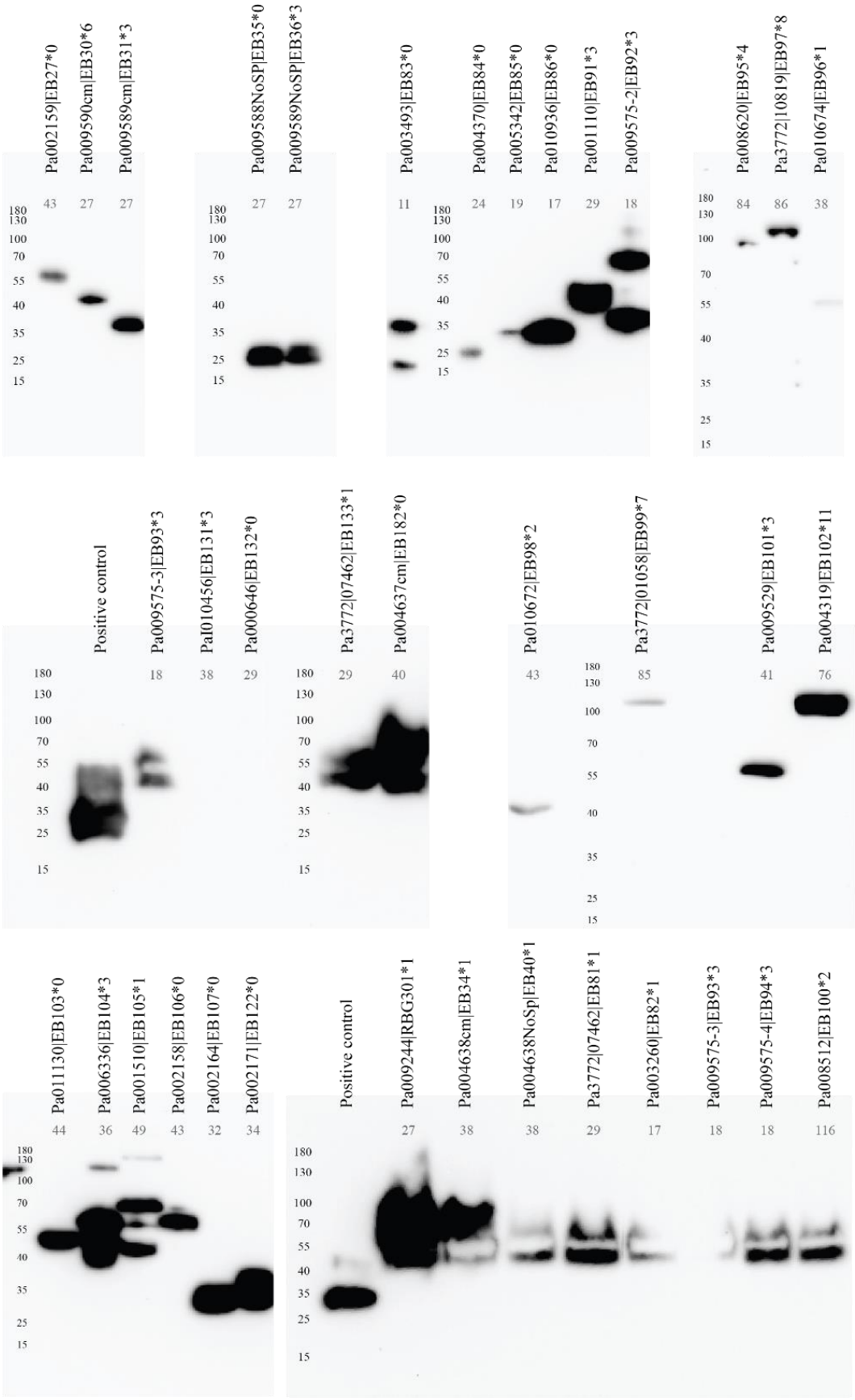

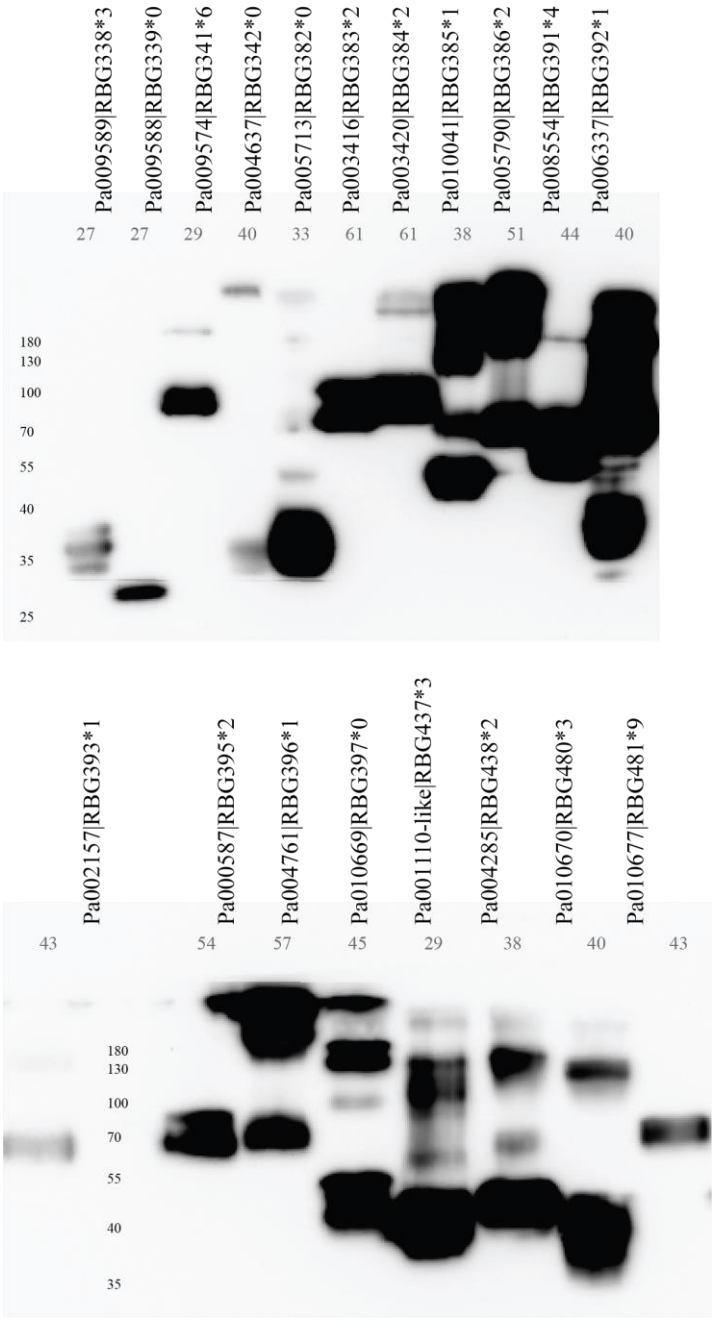

Western blots demonstrate *Phytophthora agathidicida* proteins of interest were produced by *Agrobacterium tumefaciens* transient transformation assays in *Nicotiana benthamiana*.

A. tumefaciens-mediated transient transformation assays were performed in *N. benthamiana.* Leaves were harvested 48 hours post-inoculation and frozen in liquid nitrogen. Western blots were performed with total protein extracted from the harvested leaves and using an anti-FLAG antibody. Protein identification (ID) corresponding to the Pa3770 PacBio genome (where possible) is given, followed by the biological material ID number. The number after the asterisk corresponds to the number of glycosylation sites predicted using NetNGlyc version 1.0 (Gupta & Brunak, 2002). Grey number below protein ID is the predicted size of the mature peptide.

Appendix 3.8. RNA sequencing information for selected *Phytophthora agathidicida* genes.

Results of a time-course RNA sequencing experiment during infection of kauri roots and leaves with *P. agathidicida* (Guo & Shiller, Unpublished).

Pag3770 ID[a]	Pa3770 ID[b]	Protein type encoded	*In vitro*[c]	Kauri leaf 6 hpi[d]	Kauri leaf 24 hpi	Kauri leaf 48 hpi	Kauri leaf 72 hpi	Kauri root 6 hpi	Kauri root 24 hpi	Kauri root 48 hpi	Kauri root 72 hpi
Pag007437	*Pa008620*	GH3[e]	16.0	11.7	9.4	12.6	18.5	10.2	9.7	20.5	27.6
Pag017473	*Pa3772|10819*	GH3	14.4	5.2	0.0	19.4	13.4	1.9	9.0	196.1	176.2
Pag017835	*Pa3772|01058*	GH3	0.0	0.0	0.0	4.3	1.2	0.0	0.0	59.8	56.8
Pag005100	*Pa000587*	GH5	18.9	59.0	25.8	13.3	10.5	17.4	78.3	7.1	12.8
Pag002774	*Pa007147*	GH5	17.3	78.1	10.0	120.1	138.8	74.5	93.8	88.5	75.2
Pag014880	*Pa006408*	GH6	4.3	71.9	5.7	18.8	68.0	179.6	35.8	5.4	15.7
Pag014881	*Pa006408*	GH6	1.1	7.6	5.6	0.8	0.5	7.5	7.4	0.4	0.9
Pag006854	*Pa004761*	GH7	29.6	487.5	68.9	430.5	393.0	272.1	285.0	325.6	285.6
Pag013524	*Pa005788*	GH7	2.2	1.6	3.5	2.9	2.8	1.4	7.3	5.5	3.6
Pag013451	*Pa005790*	GH7	24.1	412.0	338.5	2480.4	2081.2	127.3	1855.5	1849.4	1087.0
Pag000800	*Pa009529*	GH10	0.1	0.0	4.9	39.0	40.6	0.0	14.5	54.3	37.4
Pag011035	*Pa011130*	GH10	73.2	103.0	21.8	450.8	432.1	73.8	250.0	478.6	419.1
Pag006684	*Pa004637*	GH12	5.2	152.7	13.6	135.3	146.2	13.3	226.3	202.5	118.4
Pag006685	*Pa004638*	GH12	23.6	79.4	12.4	8.5	120.2	43.6	10.6	1.7	6.1
Pag017848	*Pa009244*	GH12	15.0	142.1	1.0	15.7	33.0	502.7	126.9	61.1	147.5
Pag000731	*Pa009574*	GH12	0.0	0.0	0.0	6.9	4.1	0.0	10.3	4.6	3.5
Pag017831	*Pa009575*	GH12	0.0	6.9	0.0	0.0	19.8	45.0	11.3	0.9	4.3
Pag000709	*Pa009588*	GH12	162.4	242.6	174.1	899.8	626.6	42.3	412.8	752.5	569.4
Pag017830	*Pa009589*	GH12	18.3	204.7	34.7	721.1	425.9	13.9	603.5	812.3	491.7

Pag3770 ID[a]	Pa3770 ID[b]	Protein type encoded	*In vitro*[c]	Kauri leaf 6 hpi[d]	Kauri leaf 24 hpi	Kauri leaf 48 hpi	Kauri leaf 72 hpi	Kauri root 6 hpi	Kauri root 24 hpi	Kauri root 48 hpi	Kauri root 72 hpi
Pag017829	*Pa009590*	GH12	11.1	50.1	4.0	57.2	50.4	3.4	21.7	49.1	63.4
Pag001691	*Pa001510*	GH17	10.8	3.7	1.0	6.8	23.0	21.2	6.7	24.0	90.6
Pag012622	*Pa002157*	GH17	1.1	30.2	7.0	0.6	3.1	142.5	42.7	10.5	39.8
Pag012621	*Pa002158*	GH17	270.9	917.1	96.9	419.0	354.3	1207.1	972.0	1117.3	1026.9
Pag012620	*Pa002159*	GH17	24.2	95.1	19.4	53.5	333.6	325.3	97.1	76.6	130.5
Pag012614	*Pa002164*	GH17	1.2	57.1	3.4	145.6	224.2	0.0	69.0	155.9	83.6
Pag012606	*Pa002171*	GH17	10.5	69.2	41.3	133.6	86.9	42.5	54.8	100.5	104.6
Pag013309	*Pa005713*	GH17	1.0	21.5	0.0	0.6	0.6	79.3	21.1	1.7	7.2
Pag003682	*Pa006097*	GH17	18.0	123.4	8.5	52.6	39.5	108.3	58.7	60.8	49.4
Pag004426	*Pa001110*	GH19	1.8	9.0	2.9	55.1	86.2	15.8	62.3	20.6	10.2
Pag006227	*Pa001110-like*	GH19	0.1	2.9	3.8	1.1	1.0	0.0	1.9	2.3	0.6
Pag000967	*Pa002064*	GH28	0.6	20.8	9.5	34.7	16.1	0.0	12.9	27.8	24.1
Pag002114	*Pa010663*	GH28	0.0	0.0	0.0	1.3	52.3	0.0	1.5	0.0	0.2
Pag002113	*Pa010664*	GH28	0.0	0.0	0.0	1.3	84.4	0.0	0.0	0.1	0.3
Pag002108	*Pa010669*	GH28	3.7	378.6	2.6	30.7	47.5	60.5	126.6	117.8	69.5
Pag002107	*Pa010670*	GH28	0.2	189.3	3.6	70.6	29.6	0.0	90.8	169.8	84.2
Pag002105	*Pa010672*	GH28	4.1	738.1	0.0	43.7	58.5	628.9	174.4	128.2	67.4
Pag002102	*Pa010674* and *Pa010675*	GH28	0.0	40.1	0.0	0.5	2.7	162.9	64.3	3.7	3.2
Pag002099	*Pa010677*	GH28	0.1	71.1	1.8	57.6	112.9	14.4	7.5	9.2	1.0
Pag002098	*Pa010678*	GH28	0.0	9.1	1.9	22.0	8.0	9.3	74.3	92.1	83.2
Pag004667	*Pa000923*	GH30	4.5	0.0	9.0	62.7	34.3	0.0	30.2	17.9	11.5
Pag010136	*Pa003416*	GH30	7.8	4.6	0.2	0.3	2.5	2.7	1.1	11.5	59.9
Pag010137	*Pa003417*	GH30	246.8	64.3	27.5	33.5	40.6	154.1	146.8	70.3	95.2
Pag010142	*Pa003420*	GH30	0.8	5.4	2.3	54.9	23.5	13.7	16.5	54.8	36.1
Pag007295	*Pa008512*	GH31	103.9	94.1	57.0	77.2	85.1	89.6	99.8	86.3	95.6
Pag017152	*Pa010041*	GH43	0.1	1.1	0.0	7.2	18.0	0.0	57.4	68.8	49.1

Pag3770 ID[a]	Pa3770 ID[b]	Protein type encoded	*In vitro*[c]	Kauri leaf 6 hpi[d]	Kauri leaf 24 hpi	Kauri leaf 48 hpi	Kauri leaf 72 hpi	Kauri root 6 hpi	Kauri root 24 hpi	Kauri root 48 hpi	Kauri root 72 hpi
Pag011418	*Pa004285*	GH54	3.4	11.8	24.0	213.9	224.0	2.9	44.9	36.7	16.3
Pag011461	*Pa004319*	GH78	1.4	0.5	0.0	3.8	4.0	0.0	6.4	85.0	100.9
Pag004884	*Pa000751*	GH81	3.2	29.7	5.3	28.5	55.1	32.6	15.0	19.7	17.8
Pag007346	*Pa008554*	GH105	0.0	0.0	0.0	0.0	0.0	0.0	0.0	0.0	0.0
Pag004010	*Pa006336*	GH131	19.8	940.8	102.5	785.5	573.6	574.0	925.3	697.6	508.8
Pag004012	*Pa006337*	GH131	0.0	0.0	0.0	0.0	0.0	0.0	0.0	0.0	0.0
Pag011298	*Pa004184*	GH140	0.2	0.0	0.0	10.1	13.9	0.0	10.5	97.5	72.9
Pag005016	*Pa000646*	CBEL-like[f]	169.3	44.1	5.4	1.4	19.4	76.3	64.4	92.8	198.7
Pag005019	*Pa000646*	CBEL-like	179.5	54.9	5.6	2.5	20.4	77.1	62.2	93.3	203.8
Pag005021	*Pa3772|07462*	CBEL	0.0	0.0	0.0	0.0	0.0	0.0	0.0	0.0	0.0
Pag013080	*Pa005543*	OPEL[g]	12.9	71.5	23.3	24.1	111.8	193.8	34.9	21.3	58.4
Pag017846	*PaI010456*	Pectinesterase (CE)[h]	0.1	39.4	4.3	19.6	5.9	34.1	65.6	122.7	75.3
Pag009905	*Pa003260*	Hypothetical[i]	0.1	4425.7	2748.0	236.9	451.1	7855.7	1921.4	372.5	136.0
Pag009916	*Pa003268*	Hypothetical	0.1	6637.4	3703.8	322.8	483.6	12142.3	2869.7	514.9	193.0
Pag009916	*Pa003269*	Hypothetical	0.1	6637.4	3703.8	322.8	483.6	12142.3	2869.7	514.9	193.0
Pag009917	*Pa003269*	Hypothetical	0.1	6601.9	3641.9	321.7	454.1	12131.0	2839.2	506.2	190.1
Pag009917	*Pa003268*	Hypothetical	0.1	6601.9	3641.9	321.7	454.1	12131.0	2839.2	506.2	190.1
Pag015886	*Pa003493*	Hypothetical	795.6	55.9	109.6	7334.6	9616.7	188.8	205.0	6442.5	4273.2
Pag015887	*Pa003493*	Hypothetical	794.3	55.9	109.6	7280.8	9598.3	188.8	205.0	6428.4	4258.2
Pag011543	*Pa004370*	Hypothetical	0.0	323.0	467.2	19.1	25.1	1004.6	187.5	26.2	21.8

Pag3770 ID[a]	Pa3770 ID[b]	Protein type encoded	*In vitro*[c]	Kauri leaf 6 hpi[d]	Kauri leaf 24 hpi	Kauri leaf 48 hpi	Kauri leaf 72 hpi	Kauri root 6 hpi	Kauri root 24 hpi	Kauri root 48 hpi	Kauri root 72 hpi
Pag011633	*Pa004433*	Hypothetical	302.9	134.8	31.2	120.6	218.6	229.2	206.8	610.8	1017.6
Pag010805	*Pa005342*	Hypothetical	4.1	1620.4	963.4	108.4	108.4	3281.3	1408.4	131.7	85.4
Pag010804	*Pa005342*	Hypothetical	4.9	1639.3	964.8	108.4	108.2	3254.2	1405.2	134.1	85.3
Pag013683	*Pa008135*	Hypothetical	0.0	2816.6	3044.8	218.7	296.4	5045.2	1447.9	146.5	128.2
Pag003218	*Pa008898*	Hypothetical	894.2	339.4	135.8	657.9	955.5	313.0	322.4	1254.5	1224.3
Pag009100	*Pa010936*	Hypothetical	0.0	676.4	1260.9	35.2	79.9	1076.0	964.8	72.4	146.5

FoRNA sequences have been re-mapped to the latest *P. agathidicida* PacBio genome, and are not representative of the data that were available at the time of selection of the *P. agathidicida* genes of interest.

Values represent average fragments per kilobase million (FPKM)

[a] Identification number based on annotation of the most recent *P. agathidicida* 3770 PacBio genome.

[b] Identification number of the *P. agathidicida* 3770 PacBio (Pa), *P. agathidicida* 3770 Illumina (PaI), or *P. agathidicida* 3772 Illumina genome (Pa3772).

[c] *In vitro* expression data was obtained from *P. agathidicida* grown in clarified V8 medium.

[d] Hours post-inoculation.

[e] These genes are predicted to encode proteins which belong to the glycoside hydrolase (GH) superfamily (Zhang et al., 2018).

[f] These genes are predicted to encode proteins with homology to the identified *Phytophthora parasitica* cellulose binding elicitor lectin (CBEL) (Gaulin et al., 2006, Khatib et al., 2004).

[g] This gene is predicted to encode a protein homologous to the *P. parasitica* OPEL (Chang et al., 2015).

[h] This gene encodes a protein belonging to the carbohydrate esterase (CE) superfamily (Zhang et al., 2018).

[i] These genes are predicted to be highly expressed in *P. agathidicida* and encode secreted hypothetical proteins of unknown function.

Appendix 3.9. Photographs of *Phytophthora agathidicida* lesions on *Nicotiana benthamiana*.

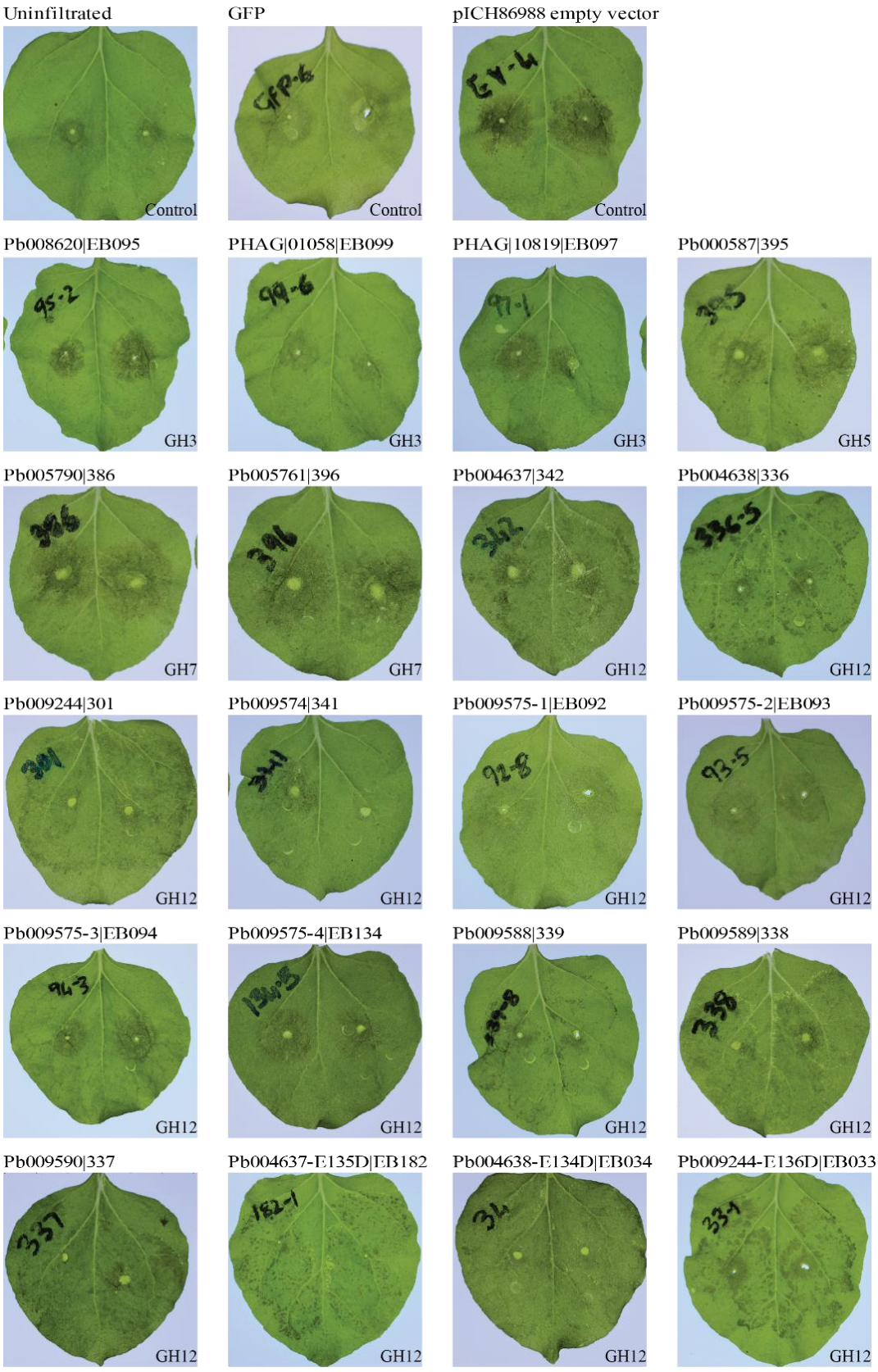

Pb009588-E135D|EB032

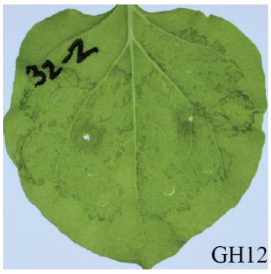

Pb009589-E134D|EB031

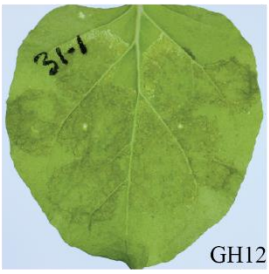

Pb009590-E137D|EB030

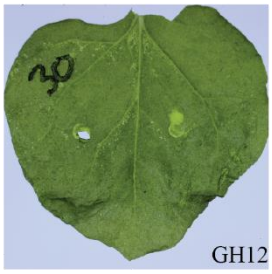

Pb004637-NoSP|EB039

Pb004638-NoSP|EB040

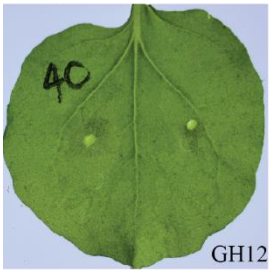

Pb009244-NoSP|EB038

Pb009588-NoSP|EB035

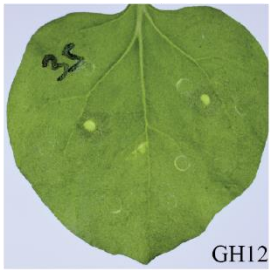

Pb009589-NoSP|EB036

Pb009590-NoSP|EB037

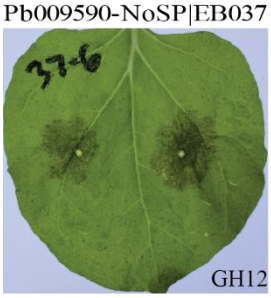

Pb001510|EB105

Pb002157|393

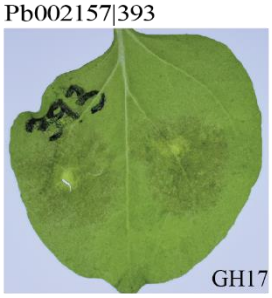

Pb002158|EB106

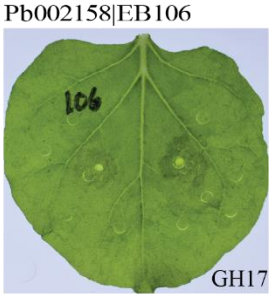

Pb002159|EB27

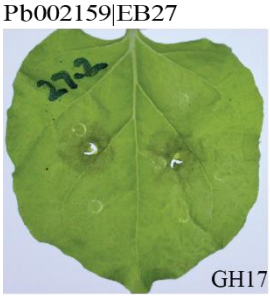

Pb002164|EB107

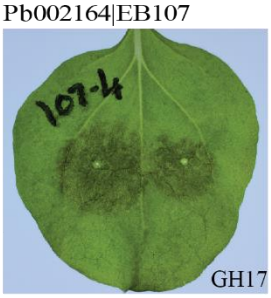

Pb002171|EB122

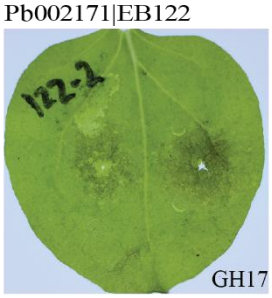

Pb005713|382

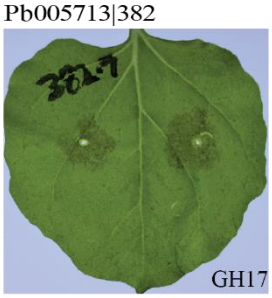

Pb006097|394

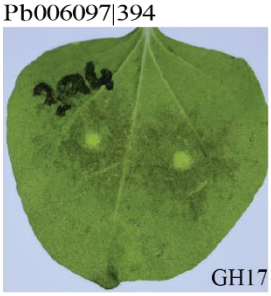

Pb001110|EB091

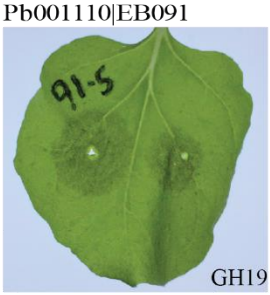

Pb001110-like|437

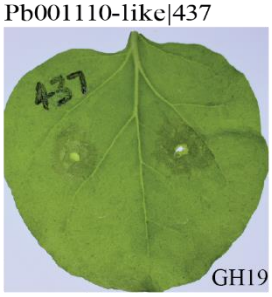

Pb010669|397

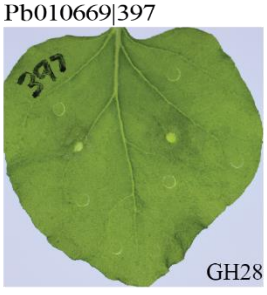

Pb010670|480

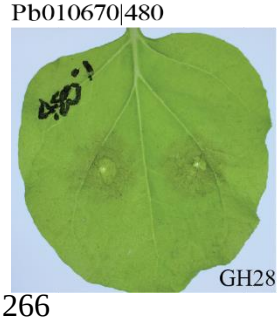

Pb010672|EB098

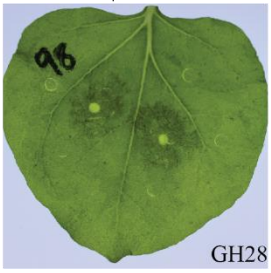

Pb010674|EB096

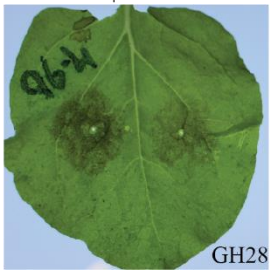

Pb010677|481

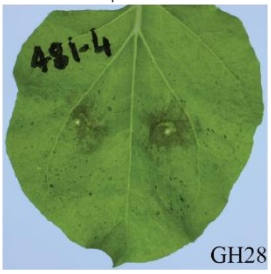

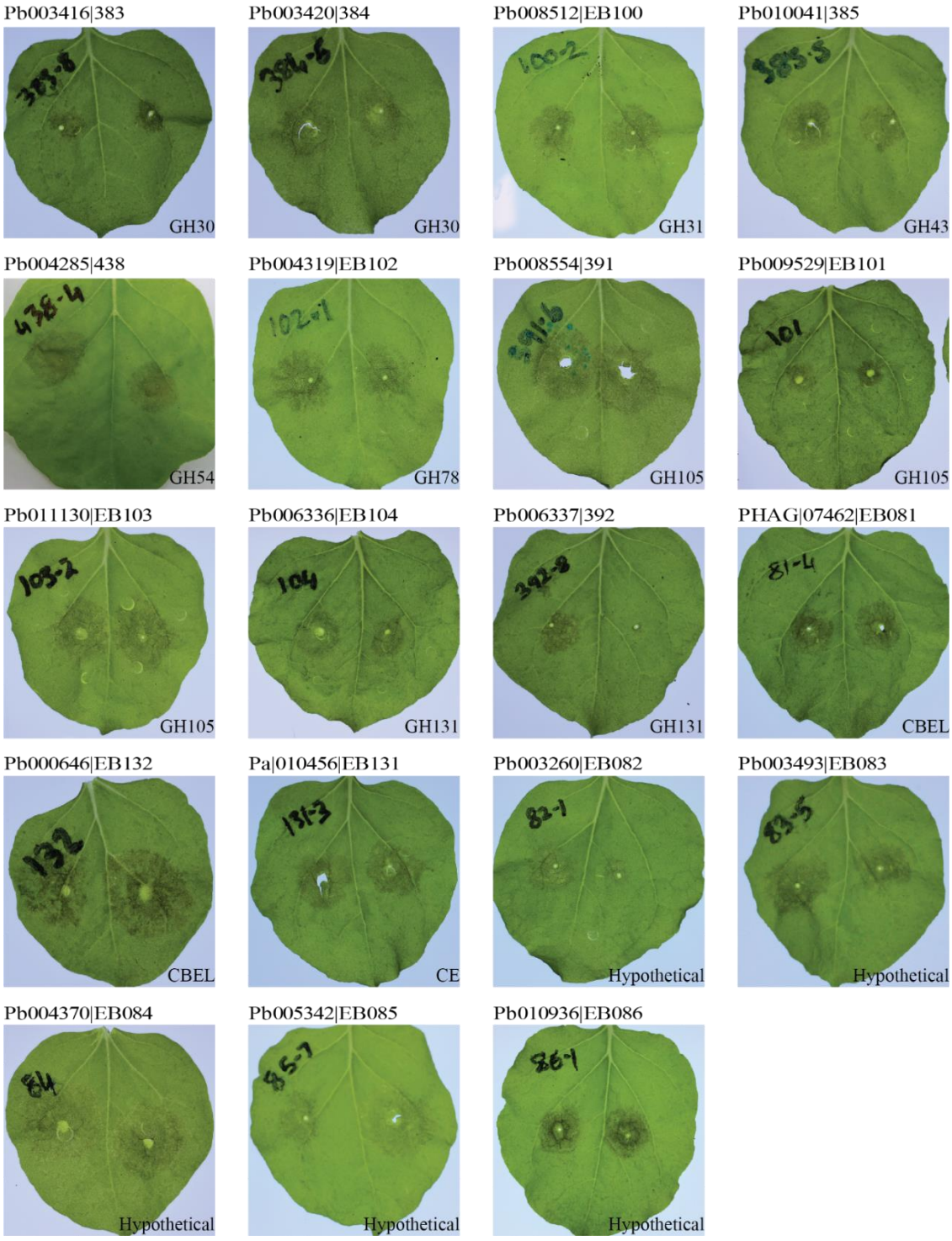

Photographs of *Nicotiana benthamiana* leaves infiltrated with *Agrobacterium tumefaciens* carrying a gene of interest and subsequently inoculated with *Phytophthora agathidicida*.

A. tumefaciens transient transformation assays were performed in *N. benthamiana* to produce the *P. agathidicida* protein of interest. The infiltrated leaves were harvested 24 hours post inoculation and actively growing *P. agathidicida* mycelia on V8 agar was inoculated at the site of infiltration 24 hours later. After 48 hours of incubation, lesions were photographed and measured. Photos are representative of observations made across at least three independent experiments.

Appendix 4.1. Percentage change observed in selected spectral buckets.

Kauri family	5.42 ppm[f]	5.26 ppm	4.26 ppm	4.22 ppm	3.82 ppm	3.74 ppm	3.7 ppm	3.46 ppm	3.42 ppm	3.38 ppm	3.26 ppm	2.34 ppm	2.3 ppm	2.22 ppm	1.94 ppm	1.38 ppm	1.34 ppm
T0[a] vs. T24h Pa[b]																	
E	-72.8	28.6	1.5	-15.7	-17.4	4.9	-3.7	2.4	7.3	1.9	66.3	-34.6	3.2	6.6	5.2	6.6	1.6
G	-76.8	52.8	-9.7	-20.7	-9.8	23.2	-3.1	34.2	33.2	15.9	246.5	-51.6	59.4	-2.1	19.5	-3.1	21.6
H	-56.5	14.3	4.9	-11.5	-16.4	3.4	-5.4	-1.4	3.2	4.8	32.3	-23.7	1.2	9.3	-2.0	14.3	-1.5
M	-67.7	16.9	3.0	-9.2	-14.3	7.1	-5.0	-1.3	3.0	9.7	55.7	-64.5	-3.7	14.4	-9.3	1.9	-7.1
N	-73.5	8.7	8.2	-11.0	-20.5	0.0	-13.3	-13.3	-12.4	6.2	39.9	-75.6	19.7	14.0	-31.5	18.7	65.1
T0 vs. T24h CM[c]																	
E	-18.6	7.6	2.3	-5.1	-7.0	-2.8	-3.9	-3.5	-3.6	-2.1	9.9	-19.3	10.8	0.0	2.5	7.5	-1.9
G	-5.9	-3.2	0.7	-1.3	-0.3	0.2	0.7	1.2	-1.0	0.1	2.0	-6.3	2.1	-0.4	-1.2	4.1	0.7
H	-12.8	9.6	4.0	-1.8	-5.5	-0.9	-3.4	-0.8	-0.4	1.9	9.6	-6.7	3.8	0.0	1.1	1.5	-3.7
M	-9.0	0.0	0.2	-2.4	-1.3	0.7	0.5	1.3	0.6	1.9	6.8	-7.9	0.3	-0.7	-1.6	0.3	-4.9
N	-11.4	-7.6	-1.4	-2.5	-6.4	-3.7	-4.7	-5.7	-3.9	-2.9	4.2	-4.7	16.8	4.7	2.9	8.9	3.3
T0 vs. T10d Pa[d]																	
E	-73.9	15.6	14.9	-8.7	-19.9	1.9	-6.5	-18.8	-8.3	6.8	-17.2	-76.9	45.0	13.5	-36.9	17.3	-50.1
G	-79.3	5.4	20.2	-10.6	-12.6	8.3	-8.0	-14.6	-5.9	16.1	53.0	-75.5	39.0	23.3	-38.0	18.1	-59.2
H	-77.6	20.7	20.6	-10.4	-21.2	2.5	-8.2	-22.5	-13.0	10.9	-13.2	-83.5	1.4	43.3	-16.0	21.3	-60.2
M	-85.0	-31.0	21.9	-4.0	-10.4	4.0	-8.9	-15.2	-7.4	10.4	53.6	-72.4	63.1	33.3	-34.3	15.8	-56.2
N	-76.1	34.1	26.6	-7.9	-12.0	7.5	-13.6	-20.1	-10.6	12.5	97.7	-75.2	170.1	35.0	-40.8	44.3	-45.2

T0 vs. T10d CM[e]																
E	-64.0	9.0	2.6	-14.2	-17.2	4.5	-1.5	-5.1	2.9	3.7	19.0	-47.2	8.2	3.3	-8.0	4.9	-35.6
G	-52.6	23.8	-0.4	-12.9	-13.4	2.7	-2.2	-1.0	4.7	4.1	46.9	-44.7	7.4	-0.1	17.3	6.5	-1.3
H	-72.4	-0.8	8.9	-14.9	-21.3	3.1	-3.6	-11.2	-3.9	2.6	-7.6	-40.9	10.7	8.6	-12.0	-3.7	-52.4
M	-66.5	-12.1	3.2	-9.3	-9.9	5.1	0.6	2.6	8.8	5.4	46.0	-40.6	-3.0	-1.0	17.2	-1.2	-4.5
N	-58.1	-0.4	-1.3	-11.5	-15.5	0.9	-4.4	-5.3	2.1	1.1	46.9	-37.5	12.6	3.9	18.5	12.3	2.8
T24h Pa vs. T10d Pa																
E	-4.0	-10.1	13.2	8.2	-3.0	-2.9	-2.9	-20.7	-14.6	4.7	-50.2	-64.7	40.5	6.4	-40.0	10.0	-50.9
G	-10.9	-31.0	33.2	12.7	-3.1	-12.1	-5.0	-36.4	-29.4	0.2	-55.8	-49.4	-12.8	26.0	-48.1	21.9	-66.4
H	-48.5	5.6	14.9	1.2	-5.8	-0.8	-2.9	-21.4	-15.7	5.8	-34.4	-78.4	0.2	31.1	-14.3	6.1	-59.6
M	-53.7	-41.0	18.4	5.7	4.5	-2.9	-4.1	-14.1	-10.1	0.6	-1.4	-22.2	69.3	16.5	-27.6	13.6	-52.9
N	-9.9	23.3	17.0	3.5	10.7	7.5	-0.4	-7.9	2.0	6.0	41.4	1.3	125.6	18.4	-13.6	21.6	-66.8
T24h CM vs. T10d CM																
E	-55.7	1.3	0.3	-9.7	-10.9	7.6	2.5	-1.6	6.7	5.9	8.2	-34.6	-2.4	3.3	-10.3	-2.5	-34.4
G	-49.7	27.8	-1.0	-11.8	-13.1	2.5	-2.8	-2.2	5.8	4.0	44.0	-40.9	5.2	0.2	18.7	2.3	-2.0
H	-68.4	-9.5	4.7	-13.3	-16.7	4.1	-0.2	-10.4	-3.5	0.7	-15.7	-36.6	6.6	8.6	-12.9	-5.2	-50.6
M	-63.2	-12.1	3.0	-7.1	-8.7	4.3	0.1	1.3	8.1	3.5	36.7	-35.5	-3.2	-0.3	19.1	-1.5	0.4
N	-52.7	7.8	0.1	-9.3	-9.7	4.7	0.3	0.4	6.2	4.1	40.9	-34.4	-3.6	-0.8	15.2	3.2	-0.5
T24h Pa vs. T24h CM																
E	199.2	-16.3	0.9	12.6	12.6	-7.4	-0.1	-5.8	-10.2	-3.9	-3.3	-33.9	-24.9	-2.8	23.5	7.4	-6.2
G	305.0	-36.6	11.5	24.5	10.5	-18.7	3.9	-24.6	-25.7	-13.7	-20.6	-70.6	-62.6	-12.5	93.4	-35.9	1.8
H	100.7	-4.1	-0.8	10.9	13.1	-4.2	2.1	0.6	-3.5	-2.8	0.0	-17.2	1.1	-5.3	22.2	2.6	-8.5
M	181.6	-14.4	-2.7	7.4	15.1	-5.9	5.7	2.6	-2.4	-7.1	-11.0	-31.4	-4.5	-16.2	159.8	4.1	-13.2
N	233.7	-15.0	-8.9	9.6	17.7	-3.6	9.9	8.7	9.7	-8.6	-13.3	-25.5	9.6	-28.3	289.6	-2.4	-8.2

T10d Pa vs. T10d CM																	
E	37.9	-5.7	-10.7	-6.0	3.4	2.6	5.4	16.9	12.2	-2.9	-0.8	43.7	56.3	-5.8	128.6	-25.4	-8.9
G	128.7	17.4	-17.1	-2.6	-1.0	-5.2	6.3	16.0	11.3	-10.4	-17.8	-4.0	54.7	-4.9	125.9	-22.7	-19.1
H	23.2	-17.8	-9.6	-5.1	0.0	0.6	5.0	14.7	10.5	-7.5	-4.8	6.4	44.1	-3.3	259.1	9.1	-24.2
M	124.1	27.5	-15.4	-5.5	0.5	1.1	10.4	21.0	17.5	-4.5	-11.1	-4.9	26.5	-29.2	115.3	-40.5	-25.8
N	75.0	-25.7	-22.0	-3.9	-4.0	-6.2	10.6	18.5	14.2	-10.2	-21.9	-25.7	26.3	-35.9	152.5	-58.3	-23.1

[a]T0 = Kauri leaf apoplastic wash fluid (AWF) at time 0 (T0). Sample taken after filtration through 0.2 µm filter, but prior to inoculation.

[b]T24h Pa = Samples taken of kauri leaf AWF 24 hours after inoculation with *P. agathidicida* mycelia grown on a cellophane membrane.

[c]T24h CM = Samples taken of kauri leaf AWF 24 hours after inoculation with cellophane membranes (control).

[d]T10d Pa = Samples taken of kauri leaf AWF 10 days after inoculation with *P. agathidicida* mycelia grown on a cellophane membrane.

[e]T10d CM = Samples taken of kauri leaf AWF 10 days after inoculation with cellophane membranes (control).

[f]ppm = Parts per million.

Appendices 5.1-5.4

Appendices for Chapter 5 (5.1-5.4) can be accessed online at https://masseyuni-my.sharepoint.com/:f:/g/personal/ebradley_massey_ac_nz/Ek_XH_Npz5xBnEXu93kkbUwBFda-BmpV2K9gBwesM719ew?e=emOU7j.

References

Abbas HMK, Xiang J, Ahmad Z, Wang L, Dong W, 2018. Enhanced *Nicotiana benthamiana* immune responses caused by heterologous plant genes from *Pinellia ternata*. *BMC Plant Biology* **18**, 357.

Abdel-Farid IB, Jahangir M, Van Den Hondel CaMJJ, Kim HK, Choi YH, Verpoorte R, 2009. Fungal infection-induced metabolites in *Brassica rapa*. *Plant Science* **176**, 608-15.

Abramovitch RB, Martin GB, 2004. Strategies used by bacterial pathogens to suppress plant defenses. *Current Opinion in Plant Biology* **7**, 356-64.

Accessscience E, 2015. Fungus-like microorganisms of the Oomycota.

Agler MT, Ruhe J, Kroll S, *et al.*, 2016. Microbial hub taxa link host and abiotic factors to plant microbiome variation. *Plos Biology* **14**, e1002352.

Aguilera-Galvez C, Champoret N, Rietman H, *et al.*, 2018. Two different R gene loci co-evolved with *Avr*2 of *Phytophthora infestans* and confer distinct resistance specificities in potato. *Studies in Mycology* **89**, 105-15.

Alberts B, Johnson R, Lewis J, 2002. Chapter 24 The adaptive immune system. In. *Molecular Biology of the cell.* New York: Garland Science.

Ali K, Maltese F, Zyprian E, Rex M, Choi YH, Verpoorte R, 2009. NMR metabolic fingerprinting based identification of grapevine metabolites associated with downy mildew resistance. *Journal of Agricultural and Food Chemistry* **57**, 9599-606.

Ali S, Ganai BA, Kamili AN, *et al.*, 2018. Pathogenesis-related proteins and peptides as promising tools for engineering plants with multiple stress tolerance. *Microbiological Research* **212-213**, 29-37.

Altschul SF, Madden TL, Schaffer AA, *et al.*, 1997. Gapped BLAST and PSI-BLAST: a new generation of protein database search programs. *Nucleic Acids Research* **25**, 3389-402.

Amaro TMMM, Thilliez GJA, Motion GB, Huitema E, 2017. A perspective on CRN proteins in the genomics age: Evolution, classification, delivery and function revisited. *Frontiers in Plant Science* **8**.

Anderson RG, Deb D, Fedkenheuer K, Mcdowell JM, 2015. Recent progress in RXLR effector research. *Molecular Plant-Microbe Interactions* **28**, 1063-72.

Andronis CE, Jacques S, Lipscombe R, Tan K-C, 2022. Comparative sub-cellular proteome analyses reveals metabolic differentiation and production of effector-like molecules in the dieback phytopathogen *Phytophthora cinnamomi*. *bioRxiv*, 2022.02.15.480627.

Aoki Y, Haga S, Suzuki S, 2020. Direct antagonistic activity of chitinase produced by *Trichoderma* sp. SANA20 as biological control agent for grey mould caused by *Botrytis cinerea*. *Cogent Biology* **6**, 1747903.

Araújo ACD, Fonseca FCDA, Cotta MG, Alves GSC, Miller RNG, 2019. Plant NLR receptor proteins and their potential in the development of durable genetic resistance to biotic stresses. *Biotechnology Research and Innovation* **3**, 80-94.

Arentz F, 2017. *Phytophthora cinnamomi* A1: An ancient resident of New Guinea and Australia of Gondwanan origin? *Forest Pathology* **47**, e12342.

Armitage AD, Lysøe E, Nellist CF, *et al.*, 2018. Bioinformatic characterisation of the effector repertoire of the strawberry pathogen *Phytophthora cactorum*. *Plos One* **13**, e0202305.

Armstrong C, 2018. *Chemotaxis and inhibition of the kauri killer, Phytophthora agathidicida*: University of Otago, Master of Science.

Ashby E, Tolich L, Froud K, 2022. Waitākere Ranges long-term kauri health monitoring survey. In: Stanley M, ed.

Auckland-Council, 2017. Kauri dieback report: An investigation into the distribution of kauri dieback, and implications for its future management, within the Waitakere ranges regional park.

Austin KG, Baker JS, Sohngen BL, *et al.*, 2020. The economic costs of planting, preserving, and managing the world's forests to mitigate climate change. *Nature Communications* **11**, 5946.

Avelino J, Cristancho M, Georgiou S, *et al.*, 2015. The coffee rust crises in Colombia and Central America (2008–2013): impacts, plausible causes and proposed solutions. *Food Security* **7**, 303-21.

Avni A, Bailey BA, Mattoo AK, Anderson JD, 1994. Induction of ethylene biosynthesis in *Nicotiana tabacum* by a *Trichoderma viride* xylanase is correlated to the accumulation of 1-aminocyclopropane-1-carboxylic acid (ACC) synthase and ACC oxidase transcripts. *Plant Physiology* **106**, 1049-55.

Aziz A, Gauthier A, Bézier A, *et al.*, 2007. Elicitor and resistance-inducing activities of beta-1,4 cellodextrins in grapevine, comparison with beta-1,3 glucans and alpha-1,4 oligogalacturonides. *Journal of Experimental Botany* **58**, 1463-72.

Bailey AM, Mena GL, Herrera-Estrella L, 1991. Genetic transformation of the plant pathogens *Phytophthora capsici* and *Phytophthora parasitica*. *Nucleic Acids Research* **19**, 4273-8.

Bailey BA, 1995. Purification of a protein from culture filtrates of *Fusarium oxysporum* that induces ethylene and necrosis in leaves of *Erythroxylum coca*. *Phytopathology* **85**, 1250-5.

Bailey BA, Dean JF, Anderson JD, 1990. An ethylene biosynthesis-inducing endoxylanase elicits electrolyte leakage and necrosis in *Nicotiana tabacum* cv Xanthi leaves. *Plant Physiology* **94**, 1849-54.

Bailey BA, Korcak RF, Anderson JD, 1992. Alterations in *Nicotiana tabacum* L. cv Xanthi cell membrane function following treatment with an ethylene biosynthesis-inducing endoxylanase. *Plant Physiology* **100**, 749-55.

Bailey BA, Korcak RF, Anderson JD, 1993. Sensitivity to an ethylene biosynthesis-inducing endoxylanase in *Nicotiana tabacum* L. cv Xanthi is controlled by a single dominant gene. *Plant Physiology* **101**, 1081-8.

Bangham AD, Horne RW, Glauert AM, Dingle JT, Lucy JA, 1962. Action of saponin on biological cell membranes. *Nature* **196**, 952-5.

Bar M, Avni A, 2009. EHD2 inhibits ligand-induced endocytosis and signaling of the leucine-rich repeat receptor-like protein LeEix2. *Plant Journal* **59**, 600-11.

Bar M, Sharfman M, Avni A, 2011. LeEix1 functions as a decoy receptor to attenuate LeEix2 signaling. *Plant Signaling & Behavior* **6**, 455-7.

Bar M, Sharfman M, Ron M, Avni A, 2010. BAK1 is required for the attenuation of ethylene-inducing xylanase (Eix)-induced defense responses by the decoy receptor LeEix1. *Plant Journal* **63**, 791-800.

Barrangou R, Fremaux C, Deveau H, *et al.*, 2007. CRISPR provides acquired resistance against viruses in prokaryotes. *Science* **315**, 1709-12.

Bassett C, 1972. The *Dothistroma* situation 1972. *Farm forestry* **14**, 47-52.

Bassett IE, Horner IJ, Hough EG, *et al.*, 2017. Ingestion of infected roots by feral pigs provides a minor vector pathway for kauri dieback disease *Phytophthora agathidicida*. *Forestry* **90**, 640-8.

Beales PA, Giltrap PG, Payne A, Ingram N, 2009. A new threat to UK heathland from *Phytophthora kernoviae* on *Vaccinium myrtillus* in the wild. *Plant Pathology* **58**, 393-.

Becker M, Becker Y, Green K, Scott B, 2016. The endophytic symbiont *Epichloë festucae* establishes an epiphyllous net on the surface of *Lolium perenne* leaves by development of an expressorium, an appressorium-like leaf exit structure. *New Phytologist* **211**, 240-54.

Becquer A, Guerrero-Galán C, Eibensteiner JL, *et al.*, 2019. Chapter Three - The ectomycorrhizal contribution to tree nutrition. . In: Cánovas FM, ed. *Advances in Botanical Research.* Academic Press, 77-126. (89.)

Bednarek P, Schneider B, Svatoš A, Oldham NJ, Hahlbrock K, 2005. Structural complexity, differential response to infection, and tissue specificity of indolic and phenylpropanoid secondary metabolism in *Arabidopsis* roots. *Plant Physiology* **138**, 1058-70.

Beever RE, Bellgard SE, Waipara N, 2010. *Phytophthora* taxon "*Agathis*" and management of kauri dieback. *Forest Health News* **208**, 1-4.

Beever RE, Waipara NW, Ramsfield TD, Dick MA, Horner IJ, 2009. Kauri (*Agathis australis*) under threat from *Phytophthora*? In. *Proceedings of the Fourth Meeting of IUFRO Working Party S07.02.09.*

Belisle RJ, Mckee B, Hao W, *et al.*, 2019. Phenotypic characterization of genetically distinct *Phytophthora cinnamomi* isolates from Avocado. *Phytopathology* **109**, 384-94.

Bellgard SE, Padamsee M, Probst CM, Lebel T, Williams SE, 2016a. Visualizing the early infection of *Agathis australis* by *Phytophthora agathidicida*, using microscopy and fluorescent in situ hybridization. *Forest Pathology* **46**, 622-31.

Bellgard SE, Pennycook SR, Weir BS, Ho W, Waipara N, 2016b. *Phytophthora agathidicida*. *Forest Phytophthoras* **6**, 1-8.

Bellgard SE, Probst CH, 2018. Oospore deactivation of *Phytophthora agathidicida*: alkaline based solutions. In.: Landcare Research.

Bellgard SE, Weir BS, Pennycook SR, *et al.*, 2013. Specialist *Phytophthora* research: Biology, pathology, ecology and detection of PA. Unpublished: Landcare Research.

Bellincampi D, Cervone F, Lionetti V, 2014. Plant cell wall dynamics and wall-related susceptibility in plant–pathogen interactions. *Frontiers in Plant Science* **5**.

Ben M'barek S, Cordewener JHG, Tabib Ghaffary SM, *et al.*, 2015. FPLC and liquid-chromatography mass spectrometry identify candidate necrosis-inducing proteins from culture filtrates of the fungal wheat pathogen *Zymoseptoria tritici*. *Fungal Genetics and Biology* **79**, 54-62.

Bendtsen JD, Nielsen H, Von Heijne G, Brunak S, 2004. Improved prediction of signal peptides: SignalP 3.0. *Journal of Molecular Biology* **340**, 783-95.

Benedetti M, Pontiggia D, Raggi S, *et al.*, 2015. Plant immunity triggered by engineered in vivo release of oligogalacturonides, damage-associated molecular patterns. *Proceedings of the National Academy of Sciences* **112**, 5533-8.

Bergin D, Steward G, 2004. Kauri ecology, establishment, growth, and management. *New Zealand Indigenous Tree Bulletin* **2**, 1-50.

Bhuiyan NH, Selvaraj G, Wei Y, King J, 2009. Role of lignification in plant defense. *Plant Signaling & Behavior* **4**, 158-9.

Bi K, Scalschi L, Jaiswal N, *et al.*, 2021. The *Botrytis cinerea* Crh1 transglycosylase is a cytoplasmic effector triggering plant cell death and defense response. *Nature Communications* **12**, 2166.

Billard V, Bruneteau M, Bonnet P, *et al.*, 1988. Chromatographic purification and characterization of elicitors of necrosis on tobacco produced by incompatible *Phytophthora* species. *Journal of Chromatography A* **440**, 87-94.

Birch PR, Cooke DE, 2013. The early days of late blight. *Elife* **2**, e00954.

Birch PRJ, Boevink PC, Gilroy EM, Hein I, Pritchard L, Whisson SC, 2008. Oomycete RXLR effectors: delivery, functional redundancy and durable disease resistance. *Current Opinion in Plant Biology* **11**, 373-9.

Blair JE, Coffey MD, Park SY, Geiser DM, Kang S, 2008. A multi-locus phylogeny for *Phytophthora* utilizing markers derived from complete genome sequences. *Fungal Genetics and Biology* **45**, 266-77.

Bohm H, Albert I, Oome S, Raaymakers TM, Van Den Ackerveken G, Nurnberger T, 2014. A conserved peptide pattern from a widespread microbial virulence factor triggers pattern-induced immunity in *Arabidopsis*. *Plos Pathogens* **10**, e1004491.

Boller T, Felix G, 2009. A renaissance of elicitors: Perception of microbe-associated molecular patterns and danger signals by pattern-recognition receptors. *Annual Review of Plant Biology* **60**, 379-406.

Bos JIB, Armstrong MR, Gilroy EM, *et al.*, 2010. *Phytophthora infestans* effector AVR3a is essential for virulence and manipulates plant immunity by stabilizing host E3 ligase CMPG1. *Proceedings of the National Academy of Sciences of the United States of America* **107**, 9909-14.

Bos JIB, Kanneganti TD, Young C, *et al.*, 2006. The C-terminal half of *Phytophthora infestans* RXLR effector AVR3a is sufficient to trigger R3a-mediated hypersensitivity and suppress INF1-induced cell death in *Nicotiana benthamiana*. *Plant Journal* **48**, 165-76.

Bouarab K, Melton R, Peart J, Baulcombe D, Osbourn A, 2002. A saponin-detoxifying enzyme mediates suppression of plant defences. *Nature* **418**, 889-92.

Bowyer P, Clarke BR, Lunness P, Daniels MJ, Osbourn AE, 1995. Host-range of a plant-pathogenic fungus determined by a saponin detoxifying enzyme. *Science* **267**, 371-4.

Bradley EL, Ökmen B, Doehlemann G, Henrissat B, Bradshaw RE, Mesarich CH, 2022. Secreted glycoside hydrolase proteins as effectors and invasion patterns of plant-associated fungi and oomycetes. *Frontiers in Plant Science* **13**.

Bradshaw RE, Bellgard SE, Black A, *et al.*, 2020. *Phytophthora agathidicida*: research progress, cultural perspectives and knowledge gaps in the control and management of kauri dieback in New Zealand. *Plant Pathology* **69**, 3-16.

Brar S, Tabima JF, Mcdougal RL, *et al.*, 2018. Genetic diversity of *Phytophthora pluvialis*, a pathogen of conifers, in New Zealand and the west coast of the United States of America. *Plant Pathology* **67**, 1131-9.

Brasier C. *Pytophthora ramorum* + *P. kernoviae* = International biosecurity failure. *Proceedings of the Sudden Oak Death Third Science Symposium, 2007*. Santa Rosa, CA 133-9.

Brasier CM, 2008. The biosecurity threat to the UK and global environment from international trade in plants. *Plant Pathology* **57**, 792-808.

Brasier CM, Beales PA, Kirk SA, Denman S, Rose J, 2005. *Phytophthora kernoviae* sp nov., an invasive pathogen causing bleeding stem lesions on forest trees and foliar necrosis of ornamentals in the UK. *Mycological Research* **109**, 853-9.

Brito N, Espino J, González C, 2006. The endo-beta-1,4-xylanase xyn11A is required for virulence in *Botrytis cinerea*. *Molecular Plant Microbe Interactions* **19**, 25-32.

Bronkhorst J, Kasteel M, Van Veen S, *et al.*, 2021. A slicing mechanism facilitates host entry by plant-pathogenic *Phytophthora*. *Nature Microbiology* **6**, 1000-6.

Brown I, Trethowan J, Kerry M, Mansfield J, Bolwell GP, 1998. Localization of components of the oxidative cross-linking of glycoproteins and of callose synthesis in papillae formed during the interaction between non-pathogenic strains of *Xanthomonas campestris* and French bean mesophyll cells. *The plant Journal* **15**, 333-43.

Brown NA, Antoniw J, Hammond-Kosack KE, 2012. The predicted secretome of the plant pathogenic fungus *Fusarium graminearum*: A refined comparative analysis. *Plos One* **7**, e33731.

Brutus A, Reca IB, Herga S, *et al.*, 2005. A family 11 xylanase from the pathogen *Botrytis cinerea* is inhibited by plant endoxylanase inhibitors XIP-I and TAXI-I. *Biochemical and Biophysical Research Communications* **337**, 160-6.

Brutus A, Sicilia F, Macone A, Cervone F, Lorenzo GD, 2010. A domain swap approach reveals a role of the plant wall-associated kinase 1 (WAK1) as a receptor of oligogalacturonides. *Proceedings of the National Academy of Sciences* **107**, 9452-7.

Buchfink B, Reuter K, Drost H-G, 2021. Sensitive protein alignments at tree-of-life scale using DIAMOND. *Nature Methods* **18**, 366-8.

Bulman LS, Gadgil PD, Kershaw DJ, Ray JW, 2004. Assessment and control of *Dothistroma* needle-blight. In.: Forest research.

Burdon JJ, Zhan J, 2020. Climate change and disease in plant communities. *Plos Biology* **18**, e3000949.

Busk PK, Pilgaard B, Lezyk MJ, Meyer AS, Lange L, 2017. Homology to peptide pattern for annotation of carbohydrate-active enzymes and prediction of function. *Bmc Bioinformatics* **18**, 214.

Byers A-K, Condron L, O'callaghan M, Waipara N, Black A, 2020. Soil microbial community restructuring and functional changes in ancient kauri (*Agathis australis*) forests impacted by the invasive pathogen *Phytophthora agathidicida*. *Soil Biology and Biochemistry* **150**, 108016.

C P Vance, T K Kirk A, Sherwood RT, 1980. Lignification as a mechanism of disease resistance. *Annual Review of Phytopathology* **18**, 259-88.

Cai RM, Lewis J, Yan SC, *et al.*, 2011. The plant pathogen *Pseudomonas syringae* pv. tomato is genetically monomorphic and under strong selection to evade tomato immunity. *Plos Pathogens* **7**, e1002130.

Cao J, Qiu M, Ye W, Wang Y, 2022. *Phytophthora sojae* transformation based on the CRISPR/Cas9 system. *Biological Protocol* **12**, e4352.

Cao Y, Liang Y, Tanaka K, *et al.*, 2014. The kinase LYK5 is a major chitin receptor in *Arabidopsis* and forms a chitin-induced complex with related kinase CERK1. *Elife* **3**, e03766.

Carrión VJ, Perez-Jaramillo J, Cordovez V, *et al.*, 2019. Pathogen-induced activation of disease-suppressive functions in the endophytic root microbiome. *Science* **366**, 606-12.

Cesari S, 2018. Multiple strategies for pathogen perception by plant immune receptors. *New Phytologist* **219**, 17-24.

Cesari S, Bernoux M, Moncuquet P, Kroj T, Dodds PN, 2014. A novel conserved mechanism for plant NLR protein pairs: the "integrated decoy" hypothesis. *Frontiers in Plant Science* **5**, e00606.

Chang YH, Yan HZ, Liou RF, 2015. A novel elicitor protein from *Phytophthora parasitica* induces basal plant immunity and systemic acquired resistance. *Molecular Plant Pathology* **16**, 123-36.

Chen J, Zhou L, Din IU, *et al.*, 2021. Antagonistic activity of *Trichoderma* spp. against *Fusarium oxysporum* in rhizosphere of radix pseudostellariae triggers the expression of host defense genes and improves its growth under long-term monoculture system. *Frontiers in Microbiology* **12**.

Chin EL, Mishchuk DO, Breksa AP, Slupsky CM, 2014. Metabolite signature of *Candidatus* Liberibacter asiaticus infection in two citrus varieties. *Journal of Agricultural and Food Chemistry* **62**, 6585-91.

Churngchow N, Rattarasarn M, 2000. The elicitin secreted by *Phytophthora palmivora*, a rubber tree pathogen. *Phytochemistry* **54**, 33-8.

Clarke CR, Chinchilla D, Hind SR, *et al.*, 2013. Allelic variation in two distinct *Pseudomonas syringae* flagellin epitopes modulates the strength of plant immune responses but not bacterial motility. *New Phytologist* **200**, 847-60.

Claverie J, Balacey S, Lemaître-Guillier C, *et al.*, 2018. The cell wall-derived xyloglucan is a new DAMP triggering plant immunity in *Vitis vinifera* and *Arabidopsis thaliana*. *Frontiers in Plant Science* **9**, 1725.

Collemare J, Lebrun M-H. Fungal secondary metabolites: Ancient toxins and novel effectors in plant–microbe interactions. In. *Effectors in Plant–Microbe Interactions.* 377-400.

Cook DE, Mesarich CH, Thomma BPHJ, 2015. Understanding plant immunity as a surveillance system to detect invasion. *Annual Review of Phytopathology* **53**, 541-63.

Cooke IR, Jones D, Bowen JK, *et al.*, 2014. Proteogenomic analysis of the *Venturia pirina* (Pear scab fungus) secretome reveals potential effectors. *Journal of Proteome Research.* **13**, 3635-44.

Cord-Landwehr S, Melcher RL, Kolkenbrock S, Moerschbacher BM, 2016. A chitin deacetylase from the endophytic fungus *Pestalotiopsis* sp. efficiently inactivates the elicitor activity of chitin oligomers in rice cells. *Scientific Reports* **6**, 38018.

Couturier M, Navarro D, Olivé C, *et al.*, 2012. Post-genomic analyses of fungal lignocellulosic biomass degradation reveal the unexpected potential of the plant pathogen *Ustilago maydis*. *Bmc Genomics* **13**, 57.

Cox MP, Bradshaw RE, Shiller J, Guo Y, Unpublished. A new chromosome level genome for the kauri dieback pathogen, *Phytophthora agathidicida*. In. In preparation.

Crombie WML, Crombie L, Green JB, Lucas JA, 1986. Pathogenicity of 'take-all' fungus to oats: Its relationship to the concentration and detoxification of the four avenacins. *Phytochemistry* **25**, 2075-83.

Dangl JL, Jones JDG, 2001. Plant pathogens and integrated defence responses to infection. *Nature* **411**, 826-33.

Dawson JW, 1986. The vines, epiphytes and parasites of New Zealand forests. *Tuatara* **28**, 43-70.

De Jonge R, Van Esse HP, Kombrink A, *et al.*, 2010. Conserved fungal LysM effector Ecp6 prevents chitin-triggered immunity in plants. *Science* **329**, 953-5.

De Lange PJ, Rolfe JR, Barkla JW, *et al.*, 2018. Conservation status of New Zealand indigenous vascular plants, 2017. In. *New Zealand threat classification series 22*. Department of Conservation, Te Papa Atawhai, 86. (Publishing Team DOC, Te Papa Atawhai, ed.)

Dean J, Gamble H, Anderson J, 1989. The ethylene biosynthesis-inducing xylanase: its induction in *Trichoderma viride* and certain plant pathogens. *Phytopathology* **79**, 1071-8.

Dean JF, Anderson JD, 1991. Ethylene biosynthesis-inducing xylanase : II. Purification and physical characterization of the enzyme produced by *Trichoderma viride*. *Plant Physiology* **95**, 316-23.

Dean R, Van Kan JaL, Pretorius ZA, *et al.*, 2012. The Top 10 fungal pathogens in molecular plant pathology (vol 13, pg 414, 2012). *Molecular Plant Pathology* **13**, 804-.

Deborde C, Moing A, Roch L, Jacob D, Rolin D, Giraudeau P, 2017. Plant metabolism as studied by NMR spectroscopy. *Progress in Nuclear Magnetic Resonance Spectroscopy* **102-103**, 61-97.

Deflorio G, Horgan G, Jaspars M, Woodward S, 2012. Defence response of sitka spruce before and after inoculation with *Heterobasidion annosum*: 1H NMR fingerprinting of bark and sapwood metabolites. *Analytical and Bioanalytical Chemistry* **402**, 3333-44.

Deyoung BJ, Innes RW, 2006. Plant NBS-LRR proteins in pathogen sensing and host defense. *Nature Immunology* **7**, 1243-9.

Dick MA, Williams NM, Bader MKF, Gardner JF, Bulman LS, 2014. Pathogenicity of *Phytophthora pluvialis* to *Pinus radiata* and its relation with red needle cast disease in New Zealand. *New Zealand Journal of Forestry Science* **44**, 1-12.

Dickman MB, Fluhr R, 2013. Centrality of host cell death in plant-microbe interactions. *Annual Review of Phytopathology* **51**, 543-70.

Diéguez-Uribeondo J, García MA, Cerenius L, *et al.*, 2009. Phylogenetic relationships among plant and animal parasites, and saprotrophs in Aphanomyces (Oomycetes). *Fungal Genetics and Biology* **46**, 365-76.

Do Vale LH, Gómez-Mendoza DP, Kim MS, *et al.*, 2012. Secretome analysis of the fungus *Trichoderma harzianum* grown on cellulose. *Proteomics* **12**, 2716-28.

Dodds PN, Lawrence GJ, Catanzariti AM, *et al.*, 2006. Direct protein interaction underlies gene-for-gene specificity and coevolution of the flax resistance genes and flax rust avirulence genes. *Proceedings of the National Academy of Sciences of the United States of America* **103**, 8888-93.

Doehlemann G, Hemetsberger C, 2013. Apoplastic immunity and its suppression by filamentous plant pathogens. *New Phytologist* **198**, 1001-16.

Dong S, Kong G, Qutob D, *et al.*, 2012. The NLP toxin family in *Phytophthora sojae* includes rapidly evolving groups that lack necrosis-inducing activity. *Molecular Plant-Microbe Interactions* **25**, 896-909.

Dorrance AE, Mills D, Robertson AE, Draper MA, Giesler L, Tenuta A, 2009. *Phytophthora* root and stem rot of soybean. *The Plant Health Instructor*

Drula E, Garron ML, Dogan S, Lombard V, Henrissat B, Terrapon N, 2022. The carbohydrate-active enzyme database: functions and literature. *Nucleic Acids Research* **50**, D571-d7.

Du J, Vleeshouwers VGaA, 2014. The do's and don'ts of effectoromics. In: Birch P, Jones JT, Bos JIB, eds. *Plant-pathogen interactions: Methods and protocols.* Totowa, NJ: Humana Press, 257-68.

Durrant WE, Dong X, 2004. Systemic acquired resistance. *Annual Review of Phytopathology* **42**, 185-209.

Ecroyd CE, 1982. Biological flora of New Zealand 8. *Agathis australis* (D. Don) Lindl. (Araucariaceae) kauri. *New Zealand Journal of Botany* **20**, 17-36.

Eddy SR, 2011. Accelerated profile HMM searches. *PLoS Computational Biology* **7**, e1002195.

Edgar RC, 2004. MUSCLE: multiple sequence alignment with high accuracy and high throughput. *Nucleic Acids Research* **32**, 1792-7.

Eisenhaber B, Schneider G, Wildpaner M, Eisenhaber F, 2004. A sensitive predictor for potential GPI lipid modification sites in fungal protein sequences and its application to genome-wide studies for *Aspergillus nidulans, Candida albicans Neurospora crassa, Saccharomyces cerevisiae* and *Schizosaccharomyces pombe*. *Journal of Molecular Biology* **337**, 243-53.

Eitzen K, Sengupta P, Kroll S, Kemen E, Doehlemann G, 2021. A fungal member of the *Arabidopsis thaliana* phyllosphere antagonizes *Albugo laibachii* via a GH25 lysozyme. *Elife* **10**, e65306.

El Gueddari NE, Rauchhaus U, Moerschbacher BM, Deising HB, 2002. Developmentally regulated conversion of surface-exposed chitin to chitosan in cell walls of plant pathogenic fungi. *New Phytologist* **156**, 103-12.

Engler C, Kandzia R, Marillonnet S, 2008. A one pot, one step, precision cloning method with high throughput capability. *Plos One* **3**, e3647.

Environment DF, Affaris FaR, Commission F, Research F, 2021. Forestry commission acts on new tree disease in Devon & Cornwall. In. GOV.UK. (2022.)

Erb M, Kliebenstein DJ, 2020. Plant secondary metabolites as defenses, regulators, and primary metabolites: The blurred functional trichotomy. *Plant Physiology* **184**, 39-52.

Fang YF, Tyler BM, 2016. Efficient disruption and replacement of an effector gene in the oomycete *Phytophthora sojae* using CRISPR/Cas9. *Molecular Plant Pathology* **17**, 127-39.

Farvardin A, González-Hernández AI, Llorens E, García-Agustín P, Scalschi L, Vicedo B, 2020. The Apoplast: A Key Player in Plant Survival. *Antioxidants (Basel, Switzerland)* **9**, 604.

Fatima U, Senthil-Kumar M, 2015. Plant and pathogen nutrient acquisition strategies. *Frontiers in Plant Science* **6**.

Fawke S, Doumane M, Schornack S, 2015. Oomycete interactions with plants: Infection strategies and resistance principles. *Microbiology and Molecular Biology Reviews* **79**, 263-80.

Fellbrich G, Romanski A, Varet A, *et al.*, 2002. NPP1, a *Phytophthora*-associated trigger of plant defense in parsley and *Arabidopsis*. *Plant Journal* **32**, 375-90.

Ferrari S, Savatin D, Sicilia F, Gramegna G, Cervone F, De Lorenzo G, 2013. Oligogalacturonides: plant damage-associated molecular patterns and regulators of growth and development. *Frontiers in Plant Science* **4**.

Fesel PH, Zuccaro A, 2016. β-glucan: Crucial component of the fungal cell wall and elusive MAMP in plants. *Fungal Genetics and Biology* **90**, 53-60.

Figueiredo A, Fortes AM, Ferreira S, *et al.*, 2008. Transcriptional and metabolic profiling of grape (*Vitis vinifera* L.) leaves unravel possible innate resistance against pathogenic fungi. *Journal of Experimental Botany* **59**, 3371-81.

Finn RD, Attwood TK, Babbitt PC, *et al.*, 2017. InterPro in 2017-beyond protein family and domain annotations. *Nucleic Acids Research* **45**, D190-D9.

Fiorin GL, Sanchéz-Vallet A, Thomazella DPT, *et al.*, 2018. Suppression of plant immunity by fungal chitinase-like effectors. *Current Biology* **28**, 3023-30.e5.

Flor HH, 1942. Inheritance of pathogenicity in *Melampsora lini*. *Phytopathology* **32**, 653-69.

Fluhr R, Sessa G, Sharon A, Ori N, Lotan T, 1991. Pathogenesis-related proteins exhibit both pathogen-induced and developmental regulation. In: Hennecke H, Verma DPS, eds. *Advances in Molecular Genetics of Plant-Microbe Interactions Vol. 1: Proceedings of the 5th International Symposium on the Molecular Genetics of Plant-Microbe Interactions, Interlaken, Switzerland, September 9–14, 1990.* Dordrecht: Springer Netherlands, 387-94.

Franich RA, Wells LG, Barnett JR, 1977. Variation with tree age of needle cuticle topography and stomatal structure in *Pinus radiate* D. Don. *Annals of Botany* **41**, 621-6.

Fraser EDG, 2003. Social vulnerability and ecological fragility: Building bridges between social and natural sciences using the Irish potato famine as a case study. *Conservation Ecology* **7**, 9.

Fraser S, Martin-Garcia J, Perry A, *et al.*, 2016. A review of Pinaceae resistance mechanisms against needle and shoot pathogens with a focus on the *Dothistroma-Pinus* interaction. *Forest Pathology* **46**, 453-71.

Frías M, González M, González C, Brito N, 2019. A 25-residue peptide from *Botrytis cinerea* xylanase BcXyn11A elicits plant defenses. *Frontiers in Plant Science* **10**, 474.

Fu L, Zhu C, Ding X, *et al.*, 2015. Characterization of cell-death-inducing members of the pectate lyase gene family in *Phytophthora capsici* and their contributions to infection of pepper. *Molecular Plant Microbe Interactions* **28**, 766-75.

Fuchs Y, Anderson JD, 1987. Purification and characterization of ethylene inducing proteins from cellulysin. *Plant Physiology* **84**, 732-6.

Fuchs Y, Saxena A, Gamble HR, Anderson JD, 1989. Ethylene biosynthesis-inducing protein from cellulysin is an endoxylanase. *Plant Physiology* **89**, 138-43.

Fujikawa T, Kuga Y, Yano S, *et al.*, 2009. Dynamics of cell wall components of *Magnaporthe grisea* during infectious structure development. *Molecular Microbiology* **73**, 553-70.

Fujikawa T, Sakaguchi A, Nishizawa Y, *et al.*, 2012. Surface α-1,3-glucan facilitates fungal stealth infection by interfering with innate immunity in plants. *Plos Pathogens* **8**, e1002882.

Furman-Matarasso N, Cohen E, Du Q, Chejanovsky N, Hanania U, Avni A, 1999. A point mutation in the ethylene-inducing xylanase elicitor inhibits the β-1-4-endoxylanase activity but not the elicitation activity. *Plant Physiology* **121**, 345-52.

Futuyma DJ, 2009. Evolution. In. *Evolution.* Sunderland, MA: Sinauer Associates Inc. (2.)

Gadgil PD, 1973. *Phytophthora heveae*, a pathogen of kauri. *New Zealand Journal of Forestry Science* **4**, 59-63.

Ganley RJ, Sniezko RA, Newcombe G, 2008. Endophyte-mediated resistance against white pine blister rust in *Pinus monticola*. *Forest Ecology and Management* **255**, 2751-60.

Gao F, Zhang B-S, Zhao J-H, *et al.*, 2019. Deacetylation of chitin oligomers increases virulence in soil-borne fungal pathogens. *Nature Plants* **5**, 1167-76.

Garcia-Ceron D, Lowe RGT, Mckenna JA, *et al.*, 2021. Extracellular vesicles from *Fusarium graminearum* contain protein effectors expressed during infection of corn. *J Fungi (Basel)* **7**.

Gardner JF, Dick MA, Bader MKF, 2015. Susceptibility of New Zealand flora to *Phytophthora kernoviae* and its seasonal variability in the field. *New Zealand Journal of Forestry Science* **45**, 1-12.

Gassmann W, Hinsch ME, Staskawicz BJ, 1999. The *Arabidopsis RPS*4 bacterial-resistance gene is a member of the TIR-NBS-LRR family of disease-resistance genes. *The plant Journal* **20**, 265-77.

Gaulin E, Drame N, Lafitte C, *et al.*, 2006. Cellulose binding domains of a *Phytophthora* cell wall protein are novel pathogen-associated molecular patterns. *Plant Cell* **18**, 1766-77.

Gaulin E, Jauneau A, Villalba F, Rickauer M, Esquerré-Tugayé MT, Bottin A, 2002. The CBEL glycoprotein of *Phytophthora parasitica* var-*nicotianae* is involved in cell wall deposition and adhesion to cellulosic substrates. *Journal of Cell Science* **115**, 4565-75.

Gijzen M, Nurnberger T, 2006. Nep1-like proteins from plant pathogens: Recruitment and diversification of the NPP1 domain across taxa. *Phytochemistry* **67**, 1800-7.

Gilroy EM, Taylor RM, Hein I, Boevink P, Sadanandom A, Birch PRJ, 2011. CMPG1-dependent cell death follows perception of diverse pathogen elicitors at the host plasma membrane and is suppressed by *Phytophthora* infestans RXLR effector AVR3a. *New Phytologist* **190**, 653-66.

Giraldo MC, Dagdas YF, Gupta YK, *et al.*, 2013. Two distinct secretion systems facilitate tissue invasion by the rice blast fungus *Magnaporthe oryzae*. *Nature Communications* **4**, 1996-.

Girard V, Dieryckx C, Job C, Job D, 2013. Secretomes: the fungal strike force. *Proteomics* **13**, 597-608.

Girelli CR, Angilè F, Del Coco L, *et al.*, 2019. (1)H-NMR metabolite fingerprinting analysis reveals a disease biomarker and a field treatment response in *Xylella fastidiosa* subsp. pauca-infected olive trees. *Plants-Basel* **8**, 115.

Gomez-Gomez L, Boller T, 2000. FLS2: An LRR receptor-like kinase involved in the perception of the bacterial elicitor flagellin in *Arabidopsis*. *Molecular Cell* **5**, 1003-11.

Gómez-Pérez D, Schmid M, Chaudhry V, *et al.*, 2022. Proteins released into the plant apoplast by the obligate parasitic protist *Albugo* selectively repress phyllosphere-associated bacteria. *bioRxiv*, 2022.05.16.492175.

Gonzalez-Fernandez R, Jorrin-Novo JV, 2012. Contribution of proteomics to the study of plant pathogenic fungi. *Journal of Proteome Research* **11**, 3-16.

González-Fernández R, Valero-Galván J, Gómez-Gálvez FJ, Jorrín-Novo JV, 2015. Unraveling the *in vitro* secretome of the phytopathogen *Botrytis cinerea* to understand the interaction with its hosts. *Frontiers in Plant Science* **6**.

Gopal J, Oyama K, 2005. Genetic base of Indian potato selections as revealed by pedigree analysis. *Euphytica* **142**, 23-31.

Gow NaR, Latge JP, Munro CA, 2017. The fungal cell wall: Structure, biosynthesis, and function. *Microbiology Spectrum Journal* **5**.

Gu B, Shao G, Gao W, *et al.*, 2021. Transcriptional variability associated with CRISPR-mediated gene replacements at the *Phytophthora sojae* Avr1b-1 locus. *Frontiers in Microbiology* **12**.

Guenthner JF, Michael KC, Nolte P, 2001. The economic impact of potato late blight on US growers. *Potato Research* **44**, 121-5.

Gui YJ, Chen JY, Zhang DD, *et al.*, 2017. *Verticillium dahliae* manipulates plant immunity by glycoside hydrolase 12 proteins in conjunction with carbohydrate-binding module 1. *Environmental Microbiology* **19**, 1914-32.

Gui YJ, Zhang WQ, Zhang DD, *et al.*, 2018. A *Verticillium dahliae* extracellular cutinase modulates plant immune responses. *Molecular Plant-Microbe Interactions* **31**, 260-73.

Guindon S, Dufayard JF, Lefort V, Anisimova M, Hordijk W, Gascuel O, 2010. New algorithms and methods to estimate maximum-likelihood phylogenies: Assessing the performance of PhyML 3.0. *Systematic Biology* **59**, 307-21.

Gumtow R, Wu D, Uchida J, Tian M, 2018. A *Phytophthora palmivora* extracellular cystatin-like protease inhibitor targets papain to contribute to virulence on Papaya. *Molecular Plant-Microbe Interactions* **31**, 363-73.

Guo X, Liu N, Zhang Y, Chen J, 2022. Pathogen-associated molecular pattern active sites of GH45 endoglucanohydrolase from *Rhizoctonia solani*. *Phytopathology* **112**, 355-63.

Guo X, Zhong D, Xie W, *et al.*, 2019. Functional identification of novel cell death-inducing effector proteins from *Magnaporthe oryzae*. *Rice (New York, N.Y.)* **12**, 59-.

Guo Y, Unpublished-a. An additional 32 RxLRs were identified in the *Phytophthora agathidicida* NZFS 3770 genome.

Guo Y, Unpublished-b. *Nicotiana benthamiana* as an alternative host for *Phytophthora agathidicida*.

Guo Y, Dupont P-Y, Mesarich CH, *et al.*, 2020a. Functional analysis of RXLR effectors from the New Zealand kauri dieback pathogen *Phytophthora agathidicida*. *Molecular Plant Pathology* **21**, 1131-48.

Guo Y, Panda P, Unpublished. RNA-sequencing time-course experiment during *Phytophthora agathidicida* infection of kauri (*Agathis australis*).

Guo Y, Shiller J, Unpublished. A time course RNA-sequencing analysis of *Phytophthora agathidicida* during infection of kauri.

Guo YN, Dupont PY, Mesarich CH, *et al.*, 2020b. Functional analysis of RXLR effectors from the New Zealand kauri dieback pathogen *Phytophthora agathidicida*. *Molecular Plant Pathology* **21**, 1131-48.

Gupta R, Brunak S, 2002. Prediction of glycosylation across the human proteome and the correlation to protein function. *Pacific Symposium on Biocomputing*, 310-22.

Gust AA, Felix G, 2014. Receptor like proteins associate with SOBIR1-type of adaptors to form bimolecular receptor kinases. *Current Opinion in Plant Biology* **21**, 104-11.

Gust AA, Pruitt R, Nürnberger T, 2017. Sensing danger: Key to activating plant immunity. *Trends in Plant Science* **22**, 779-91.

Haas BJ, Kamoun S, Zody MC, *et al.*, 2009. Genome sequence and analysis of the Irish potato famine pathogen *Phytophthora infestans*. *Nature* **461**, 393-8.

Han Y, Song L, Peng C, *et al.*, 2019. A *Magnaporthe* chitinase interacts with a rice jacalin-related lectin to promote host colonization. *Plant Physiology* **179**, 1416-30.

Hanahan D, 1985. Techniques for transformation of *E. coli*. *DNA cloning: A practical approach* **1**, 109-135.

Hane JK, Paxman J, Jones DaB, Oliver RP, De Wit P, 2020. "CATAStrophy," a genome-informed trophic classification of filamentous plant pathogens – How many different types of filamentous plant pathogens are there? *Frontiers in Microbiology* **10**.

Hansen EM, 2015. *Phytophthora* species emerging as pathogens of forest trees. *Current Forestry Reports* **1**, 16-24.

Hao G, Mccormick S, Vaughan MM, *et al.*, 2019. *Fusarium graminearum* arabinanase (Arb93B) enhances wheat head blight susceptibility by suppressing plant immunity. *Molecular Plant-Microbe Interactions®* **32**, 888-98.

Hardham AR, 2005. *Phytophthora cinnamomi*. *Molecular Plant Pathology* **6**, 589-604.

Hardham AR, Blackman LM, 2018. *Phytophthora cinnamomi*. *Molecular Plant Pathology* **19**, 260-85.

He J, Ye W, Choi DS, *et al.*, 2019. Structural analysis of *Phytophthora* suppressor of RNA silencing 2 (PSR2) reveals a conserved modular fold contributing to virulence. *Proceedings of the National Academy of Sciences* **116**, 8054-9.

He Q, Mclellan H, Boevink PC, Birch PRJ, 2020. All roads lead to susceptibility: The many modes of action of fungal and oomycete intracellular effectors. *Plant Communications* **1**, 100050.

Hellens R, Mullineaux P, Klee H, 2000. A guide to *Agrobacterium* binary Ti vectors. *Trends in Plant Science* **5**, 446-51.

Henrissat B, 1991. A classification of glycosyl hydrolases based on amino acid sequence similarities. *Biochemical Journal* **280**, 309-16.

Henrissat B, Davies G, 1997. Structural and sequence-based classification of glycoside hydrolases. *Current Opinion in Structural Biology* **7**, 637-44.

Hill L, Ashby E, Waipara N, *et al.*, 2021. Cross-cultural leadership enables collaborative approaches to management of kauri dieback in Aotearoa New Zealand. *Forests* **12**, 1671.

Hill L, Waipara N, 2017. Kauri dieback report 2017: An investigation into the distribution of kauri dieback, and implications for its future management, within the Waitakere Ranges Regional Park. Version 2. In.: Auckland Council.

Hill S, Waipara N, Peart A, Mackie B, Keen D, 2018. Kauri care guide. Auckland Council.

Hirst P, Richardson TE, Carson SD, Bradshaw RE, 1999. *Dothistroma pini* genetic diversity is low in New Zealand. *New Zealand Journal of Forestry Science* **29**, 459-72.

Hobbs E, Gloster T, Chapman S, Pritchard L. Comprehensive evaluation of CAZyme prediction tools in fungal and bacterial species. *Proceedings of the Microbiology Society Annual Conference 2021, 2021*: Figshare.

Hoffmann AA, Hercus MJ, 2000. Environmental stress as an evolutionary force. *Bioscience* **50**, 217-26.

Horner IJ, Arnet MJ, 2020. Phosphite large tree treatment trials: brief report April 2020. Plant and Food Research.

Horner IJ, Hough EG, 2013. Phosphorous acid for controlling *Phytophthora* taxon *Agathis* in kauri: glasshouse trials. *New Zealand Plant Protection* **66**, 242-8.

Horner IJ, Hough EG, 2014. Pathogenicity of four *Phytophthora* species on kauri: in vitro and glasshouse trails. *New Zealand Plant Protection* **67**, 54-9.

Horner IJ, Hough EG, Horner M, 2015. Forest efficacy trials on phosphite for control of kauri dieback. *New Zealand Plant Protection* **68**, 7-12.

Horner NR, Grenville-Briggs LJ, Van West P, 2012. The oomycete *Pythium oligandrum* expresses putative effectors during mycoparasitism of *Phytophthora infestans* and is amenable to transformation. *Fungal Biology* **116**, 24-41.

Hou S, Liu Z, Shen H, Wu D, 2019. Damage-associated molecular pattern-triggered immunity in plants. *Frontiers in Plant Science* **10**.

Huang J, Yang M, Lu L, Zhang X, 2016. Diverse functions of small RNAs in different plant–pathogen communications. *Frontiers in Microbiology* **7**.

Huet J-C, Pernollet J-C, 1989. Amino acid sequence of cinnamomin, a new member of the elicitin family, and its comparison to cryptogein and capsicein. *FEBS Letters* **257**, 302-6.

Huet JC, Sallé-Tourne M, Pernollet JC, 1994. Amino acid sequence and toxicity of the alpha elicitin secreted with ubiquitin by *Phytophthora infestans*. *Molecular Plant Microbe Interactions* **7**, 302-4.

Hunjan MS, Lore JS, 2020. Climate change: Impact on plant pathogens, diseases, and their management. In: Jabran K, Florentine S, Chauhan BS, eds. *Crop Protection Under Changing Climate.* Cham: Springer International Publishing, 85-100.

Hunter S, Mcdougal R, Williams N, Scott P, 2022. Variability in phosphite sensitivity observed within and between seven *Phytophthora* species. *Australasian Plant Pathology* **51**, 273-9.

Hyde KD, Xu J, Rapior S, *et al.*, 2019. The amazing potential of fungi: 50 ways we can exploit fungi industrially. *Fungal Diversity* **97**, 1-136.

IPPC, FAO, 2017. Plant health and food security. In: International Plant Protection Convention, Food and Agriculture Organization of the United Nations.

Jacoby RP, Koprivova A, Kopriva S, 2020. Pinpointing secondary metabolites that shape the composition and function of the plant microbiome. *Journal of Experimental Botany* **72**, 57-69.

Jeong S, Trotochaud AE, Clark SE, 1999. The *Arabidopsis* CLAVATA2 gene encodes a receptor-like protein required for the stability of the CLAVATA1 receptor-like kinase. *The Plant Cell* **11**, 1925-33.

Jia Y, Mcadams SA, Bryan GT, Hershey HP, Valent B, 2000. Direct interaction of resistance gene and avirulence gene products confers rice blast resistance. *Embo Journal* **19**, 4004-14.

Jiang H, Zhang L, Zhang J-Z, Ojaghian MR, Hyde KD, 2016. Antagonistic interaction between *Trichoderma asperellum* and *Phytophthora capsici in vitro*. *Journal of Zhejiang University-SCIENCE B* **17**, 271-81.

Jiang RH, Tripathy S, Govers F, Tyler BM, 2008. RXLR effector reservoir in two *Phytophthora* species is dominated by a single rapidly evolving superfamily with more than 700 members. *Proceedings of the National Academy of Sciences of the United States of America* **105**, 4874-9.

Jiang RHY, De Bruijn I, Haas BJ, *et al.*, 2013. Distinctive expansion of potential virulence genes in the genome of the oomycete fish pathogen *Saprolegnia parasitica*. *PLOS Genetics* **9**, e1003272.

Jiang RHY, Tyler BM, 2012. Mechanisms and evolution of virulence in oomycetes. *Annual Review of Phytopathology, Vol 50* **50**, 295-318.

Jiang RHY, Tyler BM, Whisson SC, Hardham AR, Govers F, 2005. Ancient origin of elicitin gene clusters in *Phytophthora* genomes. *Molecular Biology and Evolution* **23**, 338-51.

Johnson R, 2000. Classical plant breeding for durable resistance to diseases. *Journal of Plant Pathology* **82**, 3-7.

Johnston PR, Horner IJ, Beever RE. *Phytophthora cinnamomi* in New Zealand's indigenous forests. In: Mccomb JA, Hardy GES, Tommerup IC, eds. *Proceedings of the Phytophthora in Forests and Natural Ecosystems', 2001*. Albany, Western Australia: Murdoch University Print, 41-8.

Jones JDG, Dangl JL, 2006. The plant immune system. *Nature* **444**, 323-9.

Joubert DA, Kars I, Wagemakers L, *et al.*, 2007. A polygalacturonase-inhibiting protein from grapevine reduces the symptoms of the endopolygalacturonase BcPG2 from *Botrytis cinerea* in *Nicotiana benthamiana* leaves without any evidence for in vitro interaction. *Molecular Plant Microbe Interactions* **20**, 392-402.

Judelson HS, Ah-Fong AMV, 2018. Exchanges at the plant-oomycete interface that influence disease. *Plant Physiology* **179**, 1198-211.

Judelson HS, Tyler BM, Michelmore RW, 1991. Transformation of the oomycete pathogen, *Phytophthora infestans*. *Molecular Plant Microbe Interactions* **4**, 602-7.

Jung T, Blaschke H, Oßwald W, 2000. Involvement of soilborne *Phytophthora* species in central European oak decline and the effect of site factors on the disease. *Plant Pathology* **49**, 706-18.

Jung T, Colquhoun IJ, Hardy GES, 2013. New insights into the survival strategy of the invasive soilborne pathogen *Phytophthora cinnamomi* in different natural ecosystems in Western Australia. *Forest Pathology* **43**, 266-88.

Jung T, Jung MH, Cacciola SO, *et al.*, 2017. Multiple new cryptic pathogenic *Phytophthora* species from Fagaceae forests in Austria, Italy and Portugal. *Ima Fungus* **8**, 219-44.

Kagda MS, Martínez-Soto D, Ah-Fong AMV, Judelson HS, Kahmann R, 2020. Invertases in *Phytophthora infestans* localize to haustoria and are programmed for infection-specific expression. *Mbio* **11**, e01251-20.

Kaku H, Nishizawa Y, Ishii-Minami N, *et al.*, 2006. Plant cells recognize chitin fragments for defense signaling through a plasma membrane receptor. *Proceedings of the National Academy of Sciences of the United States of America* **103**, 11086-91.

Kamoun S, 2006. A catalogue of the effector secretome of plant pathogenic oomycetes. *Annual Review of Phytopathology* **44**, 41-60.

Kamoun S, Furzer O, Jones JDG, *et al.*, 2015. The top 10 oomycete pathogens in molecular plant pathology. *Molecular Plant Pathology* **16**, 413-34.

Kamoun S, Van West P, Vleeshouwers VGaA, De Groot KE, Govers F, 1998. Resistance of *Nicotiana benthamiana* to *Phytophthora infestans* Is mediated by the recognition of the elicitor protein INF1. *The Plant Cell* **10**, 1413-25.

Kamoun S, Vanwest P, Dejong AJ, Degroot KE, Vleeshouwers VGaA, Govers F, 1997. A gene encoding a protein elicitor of *Phytophthora infestans* is down-regulated during infection of potato. *Molecular Plant-Microbe Interactions* **10**, 13-20.

Kanneganti TD, Huitema E, Cakir C, Kamoun S, 2006. Synergistic interactions of the plant cell death pathways induced by *Phytophthora infestans* Nepl-like protein PiNPP1.1 and INF1 elicitin. *Molecular Plant Microbe Interactions* **19**, 854-63.

Kanyuka K, Rudd JJ, 2019. Cell surface immune receptors: the guardians of the plant's extracellular spaces. *Current Opinion in Plant Biology* **50**, 1-8.

Kanzaki H, Saitoh H, Takahashi Y, *et al.*, 2008. NbLRK1, a lectin-like receptor kinase protein of *Nicotiana benthamiana*, interacts with *Phytophthora infestans* INF1 elicitin and mediates INF1-induced cell death. *Planta* **228**, 977-87.

Kariyawasam GK, Richards JK, Wyatt NA, *et al.*, 2022. The *Parastagonospora nodorum* necrotrophic effector SnTox5 targets the wheat gene Snn5 and facilitates entry into the leaf mesophyll. *New Phytologist* **233**, 409-26.

Kars I, Mccalman M, Wagemakers L, Van Kan JaL, 2005. Functional analysis of *Botrytis cinerea* pectin methylesterase genes by PCR-based targeted mutagenesis: Bcpme1 and Bcpme2 are dispensable for virulence of strain B05.10. *Molecular Plant Pathology* **6**, 641-52.

Kawamura Y, Hase S, Takenaka S, *et al.*, 2009. INF1 elicitin activates jasmonic acid- and ethylene-mediated signalling pathways and induces resistance to bacterial wilt disease in tomato. *Journal of Phytopathology* **157**, 287-97.

Keegstra K, 2010. Plant cell walls. *Plant Physiology* **154**, 483-6.

Kettles GJ, Bayon C, Canning G, Rudd JJ, Kanyuka K, 2017. Apoplastic recognition of multiple candidate effectors from the wheat pathogen *Zymoseptoria tritici* in the nonhost plant *Nicotiana benthamiana*. *New Phytologist* **213**, 338-50.

Khatib M, Lafitte C, Esquerré-Tugayé M-T, Bottin A, Rickauer M, 2004. The CBEL elicitor of *Phytophthora parasitica* var. *nicotianae* activates defence in *Arabidopsis thaliana* via three different signalling pathways. *New Phytologist* **162**, 501-10.

Kim SG, Wang Y, Lee KH, *et al.*, 2013. In-depth insight into *in vivo* apoplastic secretome of rice-*Magnaporthe oryzae* interaction. *Journal of Proteomics* **78**, 58-71.

Kimberley M, Bergin D, Beets P, 2014. Carbon sequestration by planted native trees and shrubs. In. *Tane's Tree Trust.* Rotorua: Scion digital print centre. (10.5.)

King SR, Mclellan H, Boevink PC, *et al.*, 2014. *Phytophthora infestans* RXLR effector PexRD2 interacts with host MAPKKK ε to suppress plant immune signaling. *Plant Cell* **26**, 1345-59.

Kinloch BB, Dupper GE, 2002. Genetic specificity in the white pine-blister rust pathosystem. *Phytopathology* **92**, 278-80.

Klosterman SJ, Subbarao KV, Kang S, *et al.*, 2011. Comparative genomics yields insights into niche adaptation of plant vascular wilt pathogens. *Plos Pathogens* **7**, e1002137.

Kombrink E, Schmelzer E, 2001. The hypersensitive response and its role in local and systemic disease resistance. *European Journal of Plant Pathology* **107**, 69-78.

Kondratev N, Middleditch MJ, Denton-Giles M, Bradshaw RE, Cox MP, Dijkwel PP, 2022. The secreted proteome of necrotrophic *Ciborinia camelliae* causes nonhost-specific virulence. *Plant Pathology* **71**, 437-45.

Krogh A, Larsson B, Von Heijne G, Sonnhammer EL, 2001. Predicting transmembrane protein topology with a hidden Markov model: application to complete genomes. *Journal of Molecular Biology* **305**, 567-80.

Krol E, Mentzel T, Chinchilla D, *et al.*, 2010. Perception of the *Arabidopsis* danger signal peptide 1 involves the pattern recognition receptor AtPEPR1 and its close homologue AtPEPR2. *Journal of Biological Chemistry* **285**, 13471-9.

Kroon LPNM, Brouwer H, De Cock AWaM, Govers F, 2012. The genus *Phytophthora* anno 2012. *Phytopathology* **102**, 348-64.

Kubicek CP, Starr TL, Glass NL, 2014. Plant cell wall-degrading enzymes and their secretion in plant-pathogenic fungi. *Annual Review of Phytopathology, Vol 52* **52**, 427-51.

Kuć J, 1997. Molecular aspects of plant responses to pathogens. *Acta Physiologiae Plantarum* **19**, 551-9.

Kulye M, Liu H, Zhang Y, Zeng H, Yang X, Qiu D, 2012. Hrip1, a novel protein elicitor from necrotrophic fungus, *Alternaria tenuissima,* elicits cell death, expression of defence-related genes and systemic acquired resistance in tobacco. *Plant, Cell & Environment* **35**, 2104-20.

Kumar M, Turner S, 2015. Cell wall biosynthesis. In. *eLS.* 1-11.

La Spada F, Stracquadanio C, Riolo M, Pane A, Cacciola SO, 2020. *Trichoderma* counteracts the challenge of *Phytophthora nicotianae* infections on tomato by modulating plant defense mechanisms and the expression of crinkler, necrosis-inducing *Phytophthora* protein 1, and cellulose-binding elicitor lectin pathogenic effectors. *Frontiers in Plant Science* **11**.

Lacey RF, Fairhurst MJ, Daley KJ, *et al.*, 2021a. Assessing the effectiveness of oxathiapiprolin toward *Phytophthora agathidicida*, the causal agent of kauri dieback disease. *FEMS Microbes* **2**.

Lacey RF, Sullivan-Hill BA, Deslippe JR, Keyzers RA, Gerth ML, 2021b. The fatty acid methyl ester (FAME) profile of *Phytophthora agathidicida* and its potential use as diagnostic tool. *FEMS Microbiology Letters* **368**.

Lai MW, Liou RF, 2018. Two genes encoding GH10 xylanases are essential for the virulence of the oomycete plant pathogen *Phytophthora parasitica*. *Current Genetics* **64**, 931-43.

Lairini K, Ruiz-Rubio M, 1997. Detection of tomatinase from Fusarium oxysporum f. sp. lycopersici in infected tomato plants. *Phytochemistry* **45**, 1371-6.

Lamb C, Dixon RA, 1997. The oxidative burst in plant disease resistance. *Annual Review of Plant Physiology and Plant Molecular Biology* **48**, 251-75.

Langner T, Göhre V, 2016. Fungal chitinases: function, regulation, and potential roles in plant/pathogen interactions. *Current Genetics* **62**, 243-54.

Latijnhouwers M, De Wit PJGM, Govers F, 2003. Oomycetes and fungi: similar weaponry to attack plants. *Trends in Microbiology* **11**, 462-9.

Lawrence SA, Armstrong CB, Patrick WM, Gerth ML, 2017. High-throughput chemical screening identifies compounds that inhibit different stages of the *Phytophthora agathidicida* and *Phytophthora cinnamomi* life cycles. *Frontiers in Microbiology* **8**.

Lawrence SA, Burgess EJ, Pairama C, *et al.*, 2019. Mātauranga-guided screening of New Zealand native plants reveals flavonoids from kānuka (*Kunzea robusta*) with anti-*Phytophthora* activity. *Journal of the Royal Society of New Zealand* **49**, 137-54.

Laxalt AM, Raho N, Have AT, Lamattina L, 2007. Nitric oxide is critical for inducing phosphatidic acid accumulation in xylanase-elicited tomato cells. *Journal of Biological Chemistry* **282**, 21160-8.

Le Roux C, Huet G, Jauneau A, *et al.*, 2015. A receptor pair with an integrated decoy converts pathogen disabling of transcription factors to immunity. *Cell* **161**, 1074-88.

Leiss KA, Choi YH, Abdel-Farid IB, Verpoorte R, Klinkhamer PG, 2009a. NMR metabolomics of thrips (*Frankliniella occidentalis*) resistance in *Senecio* hybrids. *Journal of chemical ecology* **35**, 219-29.

Leiss KA, Maltese F, Choi YH, Verpoorte R, Klinkhamer PG, 2009b. Identification of chlorogenic acid as a resistance factor for thrips in *Chrysanthemum*. *Plant Physiology* **150**, 1567-75.

Lewis K, 2018. *Characterising the growth response and pathogenicity of Phytophthora agathidicida in soils from contrasting land-uses*: Lincoln University, Master of Science.

Lewis KSJ, Black A, Condron LM, *et al.*, 2019. Land-use changes influence the sporulation and survival of *Phytophthora agathidicida*, a lethal pathogen of New Zealand kauri (*Agathis australis*). *Forest Pathology* **49**, e12502.

Li J, Wen JQ, Lease KA, Doke JT, Tax FE, Walker JC, 2002. BAK1, an *Arabidopsis* LRR receptor-like protein kinase, interacts with BRI1 and modulates brassinosteroid signaling. *Cell* **110**, 213-22.

Li Q, Zhang M, Shen D, *et al.*, 2016. A *Phytophthora sojae* effector PsCRN63 forms homo-/hetero-dimers to suppress plant immunity via an inverted association manner. *Scientific Reports* **6**, 26951.

Li T, Wu Y, Wang Y, *et al.*, 2019. Secretome profiling reveals virulence-associated proteins of *Fusarium proliferatum* during interaction with banana fruit. *Biomolecules* **9**.

Li Y, Han Y, Qu M, *et al.*, 2020. Apoplastic cell death-inducing proteins of filamentous plant pathogens: Roles in plant-pathogen interactions. *Frontiers in Genetics* **11**.

Li Z-X, Chen M, Miao Y-X, *et al.*, 2021. The role of AcPGIP in the kiwifruit (*Actinidia chinensis*) response to *Botrytis cinerea*. *Functional Plant Biology* **48**, 1254-63.

Liebrand TWH, Van Den Berg GCM, Zhang Z, *et al.*, 2013a. Receptor-like kinase SOBIR1/EVR interacts with receptor-like proteins in plant immunity against fungal infection. *Proceedings of the National Academy of Sciences of the United States of America* **110**, 10010-5.

Liebrand TWH, Van Den Berg GCM, Zhang Z, *et al.*, 2013b. Receptor-like kinase SOBIR1/EVR interacts with receptor-like proteins in plant immunity against fungal infection (vol 110, pg 10010, 2013). *Proceedings of the National Academy of Sciences of the United States of America* **110**, 13228-.

Liebrand TWH, Van Den Burg HA, Joosten MHaJ, 2014. Two for all: receptor-associated kinases SOBIR1 and BAK1. *Trends in Plant Science* **19**, 123-32.

Liu B, Gu W, Lu B, Wang F, Zhang B, Bi J, 2021a. Promoting potato as staple food can reduce the carbon-land-water impacts of crops in China. *Nature Food* **2**, 570-7.

Liu H, Ma X, Yu H, *et al.*, 2016. Genomes and virulence difference between two physiological races of *Phytophthora nicotianae*. *Gigascience* **5**, 3.

Liu J-J, Zamany A, Sniezko RA, 2013. Anti-microbial peptide AMP: nucleotide variation, gene expression, and host resistance in the white pine blister rust (WPBR) pathosystem. *Planta* **237**, 43-54.

Liu L, Wang Z, Li J, *et al.*, 2021b. *Verticillium dahliae* secreted protein Vd424Y is required for full virulence, targets the nucleus of plant cells, and induces cell death. *Molecular Plant Pathology* **22**, 1109-20.

Liu N, Zhang X, Sun Y, *et al.*, 2017. Molecular evidence for the involvement of a polygalacturonase-inhibiting protein, GhPGIP1, in enhanced resistance to *Verticillium* and *Fusarium* wilts in cotton. *Scientific Reports* **7**, 39840.

Liu T, Song T, Zhang X, *et al.*, 2014. Unconventionally secreted effectors of two filamentous pathogens target plant salicylate biosynthesis. *Nature Communications* **5**, 4686.

Liu T, Ye W, Ru Y, *et al.*, 2011. Two host cytoplasmic effectors are required for pathogenesis of *Phytophthora sojae* by suppression of host defenses. *Plant Physiology* **155**, 490-501.

Liu Y, Lan X, Song S, *et al.*, 2018. *In planta* functional analysis and subcellular localization of the oomycete pathogen *Plasmopara viticola* candidate RXLR effector repertoire. *Frontiers in Plant Science* **9**.

Liu Z-Q, Qiu A-L, Shi L-P, *et al.*, 2015. SRC2-1 is required in PcINF1-induced pepper immunity by acting as an interacting partner of PcINF1. *Journal of Experimental Botany* **66**, 3683-98.

Lo Presti L, Lanver D, Schweizer G, *et al.*, 2015. Fungal effectors and plant susceptibility. *Annual Review of Plant Biology* **66**, 513-45.

Loc NH, Huy ND, Quang HT, Lan TT, Thu Ha TT, 2020. Characterisation and antifungal activity of extracellular chitinase from a biocontrol fungus, *Trichoderma asperellum* PQ34. *Mycology* **11**, 38-48.

Lohr VI, 2013. Diversity in landscape plantings: Broader understanding and more teaching needed. *Horttechnology* **23**, 126-9.

Lombard V, Ramulu HG, Drula E, Coutinho PM, Henrissat B, 2014. The carbohydrate-active enzymes database (CAZy) in 2013. *Nucleic Acids Research* **42**, 490-5.

Lotan T, Fluhr R, 1990. Xylanase, a novel elicitor of pathogenesis-related proteins in tobacco, uses a non-ethylene pathway for induction. *Plant Physiology* **93**, 811-7.

Lowe S, Browne M, Boudjelas S, De Poorter M, 2000. *100 of the world's worst invasive alien species: A selection from the global invasive species database*. The Invasive Species Specialist Group (ISSG) a specialist group of the Species Survival Commission (SSC) of the World Conservation Union (IUCN).

Ma XY, Xu GY, He P, Shan LB, 2016. SERKing coreceptors for receptors. *Trends in Plant Science* **21**, 1017-33.

Ma Y, Chang Z-Z, Zhao J-T, Zhou M-G, 2008. Antifungal activity of *Penicillium striatisporum* Pst10 and its biocontrol effect on *Phytophthora* root rot of chilli pepper. *Biological Control* **44**, 24-31.

Ma Y, Han C, Chen J, *et al.*, 2015a. Fungal cellulase is an elicitor but its enzymatic activity is not required for its elicitor activity. *Molecular Plant Pathology* **16**, 14-26.

Ma ZC, Song TQ, Zhu L, *et al.*, 2015b. A *Phytophthora sojae* glycoside hydrolase 12 protein is a major virulence factor during soybean infection and is recognized as a PAMP. *Plant Cell* **27**, 2057-72.

Ma ZC, Zhu L, Song TQ, *et al.*, 2017. A paralogous decoy protects *Phytophthora sojae* apoplastic effector PsXEG1 from a host inhibitor. *Science* **355**, 710-4.

Mamarabadi M, Jensen B, Lübeck M, 2008. Three endochitinase-encoding genes identified in the biocontrol fungus *Clonostachys rosea* are differentially expressed. *Current Genetics* **54**, 57-70.

Manfredini C, Sicilia F, Ferrari S, *et al.*, 2005. Polygalacturonase-inhibiting protein 2 of *Phaseolus vulgaris* inhibits BcPG1, a polygalacturonase of *Botrytis cinerea* important for pathogenicity, and protects transgenic plants from infection. *Physiological and Molecular Plant Pathology* **67**, 108-15.

Mansfield J, Genin S, Magori S, *et al.*, 2012. Top 10 plant pathogenic bacteria in molecular plant pathology. *Molecular Plant Pathology* **13**, 614-29.

Markley JL, Brüschweiler R, Edison AS, *et al.*, 2017. The future of NMR-based metabolomics. *Current Opinion in Biotechnology* **43**, 34-40.

Martin-Hernandez AM, Dufresne M, Hugouvieux V, Melton R, Osbourn A, 2000. Effects of targeted replacement of the tomatinase gene on the interaction of *Septoria lycopersici* with tomato plants. *Molecular Plant-Microbe Interactions* **13**, 1301-11.

Martin F, Kohler A, Murat C, *et al.*, 2010. Périgord black truffle genome uncovers evolutionary origins and mechanisms of symbiosis. *Nature* **464**, 1033-8.

Martin FN, Blair JE, Coffey MD, 2014. A combined mitochondrial and nuclear multilocus phylogeny of the genus *Phytophthora*. *Fungal Genetics and Biology* **66**, 19-32.

Martínez-Cruz J, Romero D, Hierrezuelo J, Thon M, De Vicente A, Pérez-García A, 2021. Effectors with chitinase activity (EWCAs), a family of conserved, secreted fungal chitinases that suppress chitin-triggered immunity. *The Plant Cell* **33**, 1319-40.

Matthiesen RL, Abeysekara NS, Ruiz-Rojas JJ, Biyashev RM, Maroof MaS, Robertson AE, 2016. A method for combining isolates of *Phytophthora sojae* to screen for novel sources of resistance to *Phytophthora* stem and root rot in Soybean. *Plant Disease* **100**, 1424-8.

Maximo HJ, Dalio RJD, Dias RO, Litholdo CG, Felizatti HL, Machado MA, 2019. PpCRN7 and PpCRN20 of *Phythophthora parasitica* regulate plant cell death leading to enhancement of host susceptibility. *BMC Plant Biology* **19**, 544.

McCarthy CGP, Fitzpatrick DA, 2017. Phylogenomic reconstruction of the oomycete phylogeny derived from 37 genomes. *mSphere* **2**, e00095-17.

McCarthy HM, Tarallo M, Mesarich CH, Mcdougal RL, Bradshaw RE, 2022. Targeted gene mutations in the forest pathogen *Dothistroma septosporum* using CRISPR/Cas9. *Plants (Basel, Switzerland)* **11**.

McGowan J, Fitzpatrick DA, 2017. Genomic, network, and phylogenetic analysis of the oomycete effector arsenal. *mSphere* **2**, e00408-17.

Meijer HJG, Mancuso FM, Espadas G, *et al.*, 2014. Profiling the secretome and extracellular proteome of the potato late blight pathogen *Phytophthora infestans*. *Molecular & cellular proteomics : MCP* **13**, 2101-13.

Melech-Bonfil S, Sessa G, 2010. Tomato MAPKKKε is a positive regulator of cell-death signaling networks associated with plant immunity. *The plant Journal* **64**, 379-91.

Mélida H, Bacete L, Ruprecht C, *et al.*, 2020. Arabinoxylan-oligosaccharides act as damage associated molecular patterns in plants regulating disease resistance. *Frontiers in Plant Science* **11**.

Mélida H, Sopeña-Torres S, Bacete L, *et al.*, 2018. Non-branched β-1,3-glucan oligosaccharides trigger immune responses in *Arabidopsis*. *Plant Journal* **93**, 34-49.

Meng Y, Zhang Q, Ding W, Shan W, 2014. *Phytophthora parasitica*: a model oomycete plant pathogen. *Mycology* **5**, 43-51.

Mesarich CH, Okmen B, Rovenich H, *et al.*, 2018. Specific hypersensitive response-associated recognition of new apoplastic effectors from *Cladosporium fulvum* in wild tomato. *Molecular Plant-Microbe Interactions* **31**, 145-62.

Meyers BC, Dickerman AW, Michelmore RW, Sivaramakrishnan S, Sobral BW, Young ND, 1999. Plant disease resistance genes encode members of an ancient and diverse protein family within the nucleotide-binding superfamily. *Plant Journal* **20**, 317-32.

Michalski A, Damoc E, Hauschild JP, *et al.*, 2011. Mass spectrometry-based proteomics using Q Exactive, a high-performance benchtop quadrupole Orbitrap mass spectrometer. *Molecular and Cellular Proteomics* **10**, M111.011015.

Michelmore RW, Christopoulou M, Caldwell KS, 2013. Impacts of resistance gene genetics, function, and evolution on a durable future. *Annual Review of Phytopathology, Vol 51* **51**, 291-319.

Midgley KA, Van Den Berg N, Swart V, 2022. Unraveling plant cell death during *Phytophthora* infection. *Microorganisms* **10**, 1139.

Mikes V, Milat ML, Ponchet M, Panabières F, Ricci P, Blein JP, 1998. Elicitins, proteinaceous elicitors of plant defense, are a new class of sterol carrier proteins. *Biochemical and Biophysical Research Communications* **245**, 133-9.

Mirnezhad M, Romero-González RR, Leiss KA, Choi YH, Verpoorte R, Klinkhamer PGL, 2010. Metabolomic analysis of host plant resistance to thrips in wild and cultivated tomatoes. *Phytochemical Analysis* **21**, 110-7.

Mittler R, Vanderauwera S, Gollery M, Van Breusegem F, 2004. Reactive oxygen gene network of plants. *Trends in Plant Science* **9**, 490-8.

Miya A, Albert P, Shinya T, *et al.*, 2007. CERK1, a LysM receptor kinase, is essential for chitin elicitor signaling in *Arabidopsis*. *Proceedings of the National Academy of Sciences of the United States of America* **104**, 19613-8.

Moller EM, Bahnweg G, Sandermann H, Geiger HH, 1992. A simple and efficient protocol for isolation of high-molecular-weight DNA from filamentous fungi, fruit bodies, and infected-plant tissues. *Nucleic Acids Research* **20**, 6115-6.

Moroz N, Fritch KR, Marcec MJ, Tripathi D, Smertenko A, Tanaka K, 2017. Extracellular alkalinization as a defense response in potato cells. *Frontiers in Plant Science* **8**.

Moscetti I, Faoro F, Moro S, *et al.*, 2015. The xylanase inhibitor TAXI-III counteracts the necrotic activity of a *Fusarium graminearum* xylanase in vitro and in durum wheat transgenic plants. *Molecular Plant Pathology* **16**, 583-92.

MPI, 2014. New Zealand's strategy for managing kauri dieback disease. In. *Kia toitū he kauri, Keep kauri standing.* Ministry for Primary Industries.

MPI, 2016. Keep kauri standing. In. Keep kauri standing: Kia toitu he kauri. Ministry for Primary Industries.

Murashige T, Nakano R, 1967. Chromosome complement as a determinant of the morphogenic potential of tobacco cells. *American Journal of Botany* **54**, 963-970.

Murphy F, He Q, Armstrong M, *et al.*, 2018. The potato MAP3K StVIK is required for the *Phytophthora infestans* RXLR effector Pi17316 to promote disease. *Plant Physiology* **177**, 398-410.

Nalley L, Tsiboe F, Durand-Morat A, Shew A, Thoma G, 2016. Economic and Environmental Impact of Rice Blast Pathogen (Magnaporthe oryzae) Alleviation in the United States. *Plos One* **11**.

Naveed ZA, Wei X, Chen J, Mubeen H, Ali GS, 2020. The PTI to ETI continuum in *Phytophthora*-plant interactions. *Frontiers in Plant Science* **11**.

Nespoulous C, Huet J-C, Pernollet J-C, 1992. Structure-function relationships of α and β elicitins, signal proteins involved in the plant-*Phytophthora* interaction. *Planta* **186**, 551-7.

Newman MA, Sundelin T, Nielsen JT, Erbs G, 2013. MAMP (microbe-associated molecular pattern) triggered immunity in plants. *Frontiers in Plant Science* **4**, 1-14.

Ngou BPM, Jones JDG, Ding P, 2021. Plant immune networks. *Trends in Plant Science*.

Nicoletti R, De Stefano M, De Stefano S, Trincone A, Marziano F, 2004. Antagonism against *Rhizoctonia solani* and fungitoxic metabolite production by some *Penicillium* isolates. *Mycopathologia* **158**, 465-74.

Noda J, Brito N, González, 2010. The *Botrytis cinerea* xylanase Xyn11A contributes to virulence with its necrotizing activity, not with its catalytic activity. *BMC Plant Biology* **10**, 1-15.

Nogueira-Lopez G, Greenwood DR, Middleditch M, *et al.*, 2018. The apoplastic secretome of *Trichoderma virens* during interaction with maize roots shows an inhibition of plant defence and scavenging oxidative stress secreted proteins. *Frontiers in Plant Science* **9**.

Noorifar N, Savoian MS, Ram A, *et al.*, 2021. Chitin deacetylases are required for *Epichloë festucae* endophytic cell wall remodeling during establishment of a mutualistic symbiotic interaction with *Lolium perenne*. *Molecular Plant Microbe Interactions* **34**, 1181-92.

Norrander J, Kempe T, Messing J, 1983. Construction of improved M13 vectors using oligodeoxynucleotide-directed mutagenesis. *Gene* **26**, 101-6.

Nürnberger T, Lipka V, 2005. Non-host resistance in plants: new insights into an old phenomenon. *Molecular Plant Pathology* **6**, 335-45.

Oh SK, Young C, Lee M, *et al.*, 2009. *In planta* expression screens of *Phytophthora infestans* RXLR effectors reveal diverse phenotypes, including activation of the *Solanum bulbocastanum* disease resistance protein Rpi-blb2. *Plant Cell* **21**, 2928-47.

Ökmen B, Bachmann D, De Wit P, 2019. A conserved GH17 glycosyl hydrolase from plant pathogenic Dothideomycetes releases a DAMP causing cell death in tomato. *Molecular Plant Pathology* **20**, 1710-21.

Okmen B, Doehlemann G, 2014. Inside plant: biotrophic strategies to modulate host immunity and metabolism. *Current Opinion in Plant Biology* **20**, 19-25.

Ökmen B, Etalo DW, Joosten MHaJ, *et al.*, 2013. Detoxification of α-tomatine by *Cladosporium fulvum* is required for full virulence on tomato. *New Phytologist* **198**, 1203-14.

Oldroyd GED, Staskawicz BJ, 1998. Genetically engineered broad-spectrum disease resistance in tomato. *Proceedings of the National Academy of Sciences of the United States of America* **95**, 10300-5.

Oliveira-Garcia E, Deising HB, 2013. Infection structure-specific expression of β-1,3-glucan synthase is essential for pathogenicity of *Colletotrichum graminicola* and evasion of β-glucan-triggered immunity in maize. *Plant Cell* **25**, 2356-78.

Oliveira-Garcia E, Deising HB, 2016. Attenuation of PAMP-triggered immunity in maize requires down-regulation of the key β-1,6-glucan synthesis genes KRE5 and KRE6 in biotrophic hyphae of *Colletotrichum graminicola*. *The plant Journal* **87**, 355-75.

Orwin J, 2007a. Kauri forest - Protecting Kauri. In. *Te Ara - The encyclopedia of New Zealand.* https://teara.govt.nz/en/kauri-forest/page-4. (2018.)

Orwin J, 2007b. Kauri forest -Kauri forest ecology. In. *Te Ara -The encyclopedia of New Zealand.*

Osbourn A, 1996. Saponins and plant defence - A soap story. *Trends in Plant Science* **1**, 4-9.

Osswald W, Fleischmann F, Rigling D, *et al.*, 2014. Strategies of attack and defence in woody plant-*Phytophthora* interactions. *Forest Pathology* **44**, 169-90.

Paccanaro MC, Sella L, Castiglioni C, *et al.*, 2017. Synergistic effect of different plant cell wall-degrading enzymes is important for virulence of *Fusarium graminearum*. *Molecular Plant Microbe Interactions* **30**, 886-95.

Padamsee M, Johansen RB, Stuckey SA, *et al.*, 2016. The arbuscular mycorrhizal fungi colonising roots and root nodules of New Zealand kauri *Agathis australis*. *Fungal Biology* **120**, 807-17.

Padamsee M, Probst CM, Anand N, Lebel T, Williams SE, Bellgard SE, 2015. An inside look at *Phytophthora agathidicida*: Early infection in the roots of kauri seedlings. In. Scion News.

Pan QL, Wendel J, Fluhr R, 2000. Divergent evolution of plant NBS-LRR resistance gene homologues in dicot and cereal genomes. *Journal of Molecular Evolution* **50**, 203-13.

Panabieres F, Ali GS, Allagui MB, *et al.*, 2016. *Phytophthora nicotianae* diseases worldwide: new knowledge of a long-recognised pathogen. *Phytopathologia Mediterranea* **55**, 20-40.

Pareja-Jaime Y, Roncero MIG, Ruiz-Roldan MC, 2008. Tomatinase from *Fusarium oxysporum* f. sp lycopersici is required for full virulence on tomato plants. *Molecular Plant-Microbe Interactions* **21**, 728-36.

Patil RS, Ghormade V, Deshpande MV, 2000. Chitinolytic enzymes: an exploration. *Enzyme and Microbial Technology* **26**, 473-83.

Petersen TN, Brunak S, Von Heijne G, Nielsen H, 2011. SignalP 4.0: discriminating signal peptides from transmembrane regions. *Nature Methods* **8**, 785-6.

Petit-Houdenot Y, Fudal I, 2017. Complex interactions between fungal avirulence genes and their corresponding plant resistance genes and consequences for disease resistance management. *Frontiers in Plant Science* **8**, e01072.

Pettongkhao S, Churngchow N, 2019. Novel cell death-inducing elicitors from *Phytophthora palmivora* promote infection on *Hevea brasiliensis*. *Phytopathology* **109**, 1769-78.

Pierleoni A, Martelli PL, Casadio R, 2008. PredGPI: a GPI-anchor predictor. *Bmc Bioinformatics* **9**.

Podger FD, Newhook FJ, 1971. *Phytophthora cinnamomi* in indigenous plant communities in New Zealand. *New Zealand Journal of Botany* **9**, 625-38.

Poinssot B, Vandelle E, Bentéjac M, *et al.*, 2003. The endopolygalacturonase 1 from *Botrytis cinerea* activates grapevine defense reactions unrelated to its enzymatic activity. *Molecular Plant Microbe Interactions* **16**, 553-64.

Popper ZA, Michel G, Hervé C, *et al.*, 2011. Evolution and diversity of plant cell walls: from algae to flowering plants. *Annual Review of Plant Biology* **62**, 567-90.

Poschmann G, Bahr J, Schrader J, Stejerean-Todoran I, Bogeski I, Stühler K, 2022. Secretomics—A key to a comprehensive picture of unconventional protein secretion. *Frontiers in Cell and Developmental Biology* **10**.

Pritchard L, Birch PRJ, 2014. The zigzag model of plant–microbe interactions: is it time to move on? *Molecular Plant Pathology* **15**, 865-70.

Pruitt KD, Tatusova T, Maglott DR, 2005. NCBI reference sequence (RefSeq): a curated non-redundant sequence database of genomes, transcripts and proteins. *Nucleic Acids Research* **33**, D501-4.

Pusztahelyi T, Holb I, Pócsi I, 2015. Secondary metabolites in fungus-plant interactions. *Frontiers in Plant Science* **6**.

Qiao Y, Liu L, Xiong Q, *et al.*, 2013. Oomycete pathogens encode RNA silencing suppressors. *Nature genetics* **45**, 330-3.

Quidde T, Osbourn AE, Tudzynski P, 1998. Detoxification of alpha-tomatine by *Botrytis cinerea*. *Physiological and Molecular Plant Pathology* **52**, 151-65.

Qutob D, Kamoun S, Gijzen M, 2002. Expression of a *Phytophthora sojae* necrosis-inducing protein occurs during transition from biotrophy to necrotrophy. *The plant Journal* **32**, 361-73.

Qutob D, Kemmerling B, Brunner F, *et al.*, 2006. Phytotoxicity and innate immune responses induced by Nep1-like proteins. *Plant Cell* **18**, 3721-44.

Raaymakers TM, Van Den Ackerveken G, 2016. Extracellular recognition of oomycetes during biotrophic infection of plants. *Frontiers in Plant Science* **7**.

Rafiei V, Vélëz H, Tzelepis G, 2021. The role of glycoside hydrolases in phytopathogenic fungi and oomycetes virulence. *International Journal of Molecular Sciences* **22**.

Rahman MZ, Uematsu S, Kimishima E, *et al.*, 2015. Two plant pathogenic species of *Phytophthora* associated with stem blight of Easter lily and crown rot of lettuce in Japan. *Mycoscience* **56**, 419-33.

Ramsfield TD, Dick MA, Beever RE, Horner IJ, Mcalonan MJ, Hill CF. *Phytophthora kernoviae* in New Zealand. *Proceedings of the Phytophthoras in Forests and Natural Ecosystems, 2007*. Monterey, California, USA.

Rebaque D, Del Hierro I, López G, *et al.*, 2021. Cell wall-derived mixed-linked β-1,3/1,4-glucans trigger immune responses and disease resistance in plants. *The plant Journal* **106**, 601-15.

Reeser P, Sutton W, Hansen E, 2013. *Phytophthora pluvialis*, a new species from mixed tanoak-Douglas-fir forests of western Oregon, U.S.A. *North American Fungi* **8**, 1-8.

Ren Y, Armstrong M, Qi Y, *et al.*, 2019. *Phytophthora infestans* RXLR effectors target parallel steps in an immune signal transduction pathway. *Plant Physiology* **180**, 2227-39.

Ricci P, Bonnet P, Huet JC, *et al.*, 1989. Structure and activity of proteins from pathogenic fungi *Phytophthora* eliciting necrosis and acquired resistance in tobacco. *European Journal of Biochemistry* **183**, 555-63.

Richards TA, Talbot NJ, 2013. Horizontal gene transfer in osmotrophs: playing with public goods. *Nature Reviews Microbiology* **11**, 720-7.

Rietman H, Bijsterbosch G, Liliana CM, *et al.*, 2012. Qualitative and quantitative late blight resistance in the potato cultivar Sarpo Mira is determined by the perception of five distinct RXLR effectors. *The American Phytopathological Society* **25**, 910-9.

Ristaino JB, Anderson PK, Bebber DP, *et al.*, 2021. The persistent threat of emerging plant disease pandemics to global food security. *Proceedings of the National Academy of Sciences* **118**, e2022239118.

Rizzi YS, Happel P, Lenz S, *et al.*, 2021. Chitosan and chitin deacetylase activity are necessary for development and virulence of *Ustilago maydis*. *Mbio* **12**, e03419-20.

Robin C, Smith I, Hansen EM, 2012. *Phytophthora cinnamomi*. *Forest Phytophthoras* **2**, e3041.

Rocafort M, Arshed S, Hudson D, *et al.*, 2022. CRISPR-Cas9 gene editing and rapid detection of gene-edited mutants using high-resolution melting in the apple scab fungus, *Venturia inaequalis*. *Fungal Biology* **126**, 35-46.

Rocafort M, Fudal I, Mesarich CH, 2020. Apoplastic effector proteins of plant-associated fungi and oomycetes. *Current Opinion in Plant Biology* **56**, 9-19.

Rodenburg SYA, Seidl MF, De Ridder D, Govers F, 2018. Genome-wide characterization of *Phytophthora infestans* metabolism: a systems biology approach. *Molecular Plant Pathology* **19**, 1403-13.

Rodriguez RJ, White JF, Arnold AE, Redman RS, 2009. Fungal endophytes: diversity and functional roles. *New Phytologist* **182**, 314-30.

Roitsch T, Balibrea ME, Hofmann M, Proels R, Sinha AK, 2003. Extracellular invertase: Key metabolic enzyme and PR protein. *Journal of Experimental Botany* **54**, 513-24.

Rojas-Estevez P, Urbina-Gómez DA, Ayala-Usma DA, *et al.*, 2020. Effector repertoire of *Phytophthora betacei*: In search of possible virulence factors responsible for its host specificity. *Frontiers in Genetics* **11**.

Roldan-Arjona T, Perez-Espinosa A, Ruiz-Rubio M, 1999. Tomatinase from *Fusarium oxysporum* f. sp *lycopersici* defines a new class of saponinases. *Molecular Plant-Microbe Interactions* **12**, 852-61.

Ron M, Avni A, 2004. The receptor for the fungal elicitor ethylene-inducing xylanase is a member of a resistance-like gene family in tomato. *Plant Cell* **16**, 1604-15.

Ron M, Kantety R, Martin GB, *et al.*, 2000. High-resolution linkage analysis and physical characterization of the EIX-responding locus in tomato. *Theoretical and Applied Genetics* **100**, 184-9.

Rooney HC, Van't Klooster JW, Van Der Hoorn RA, Joosten MH, Jones JD, De Wit PJ, 2005. *Cladosporium* Avr2 inhibits tomato Rcr3 protease required for Cf-2-dependent disease resistance. *Science* **308**, 1783-6.

Rosa-Fernandes L, Rocha VB, Carregari VC, Urbani A, Palmisano G, 2017. A perspective on extracellular vesicles proteomics. *Frontiers in Chemistry* **5**.

Rossman AY, Palm ME, 2006. Why are *Phytophthora* and other oomycota not true fungi? In. https://www.apsnet.org/edcenter/intropp/PathogenGroups/Pages/Oomycetes.aspx: The American Phytopathological Society. (2018.)

Rotblat B, Enshell-Seijffers D, Gershoni JM, Schuster S, Avni A, 2002. Identification of an essential component of the elicitation active site of the EIX protein elicitor. *Plant Journal* **32**, 1049-55.

Rovenich H, Boshoven JC, Thomma BP, 2014. Filamentous pathogen effector functions: of pathogens, hosts and microbiomes. *Current Opinion in Plant Biology* **20**, 96-103.

Rovenich H, Zuccaro A, Thomma BPHJ, 2016. Convergent evolution of filamentous microbes towards evasion of glycan-triggered immunity. *New Phytologist* **212**, 896-901.

Rui Y, Dinneny JR, 2020. A wall with integrity: surveillance and maintenance of the plant cell wall under stress. *New Phytologist* **225**, 1428-39.

Ryals JA, Neuenschwander UH, Willits MG, Molina A, Steiner HY, Hunt MD, 1996. Systemic acquired resistance. *Plant Cell* **8**, 1809-19.

Ryder JM, 2016. *What is the host range of P. agathidicida (causal agent of kauri dieback disease) in New Zealand?*: University of Auckland, Master of Science.

Sabbadin F, Urresti S, Henrissat B, *et al.*, 2021. Secreted pectin monooxygenases drive plant infection by pathogenic oomycetes. *Science* **373**, 774-9.

Sánchez-Vallet A, Mesters JR, Thomma BPHJ, 2015. The battle for chitin recognition in plant-microbe interactions. *FEMS Microbiology Reviews* **39**, 171-83.

Sánchez-Vallet A, Saleem-Batcha R, Kombrink A, *et al.*, 2013. Fungal effector Ecp6 outcompetes host immune receptor for chitin binding through intrachain LysM dimerization. *eLife* **2**, e00790-e.

Sander JD, Joung JK, 2014. CRISPR-Cas systems for editing, regulating and targeting genomes. *Nature Biotechnology* **32**, 347-55.

Sandhu JS, Nayyar S, Kaur A, *et al.*, 2019. Foot rot tolerant transgenic rough lemon rootstock developed through expression of β-1,3-glucanase from *Trichoderma* spp. *Plant Biotechnology Journal* **17**, 2023-5.

Santini A, Ghelardini L, De Pace C, *et al.*, 2013. Biogeographical patterns and determinants of invasion by forest pathogens in Europe. *New Phytologist* **197**, 238-50.

Santos-Sánchez NC, Salas-Coronado R, Hernández-Carlos B, Villanueva-Cañongo C, 2019. *Shikimic acid pathway in biosynthesis of phenolic compounds*. London: IntechOpen.

Sarris PF, Duxbury Z, Huh SU, *et al.*, 2015. A plant immune receptor detects pathogen effectors that target WRKY transcription factors. *Cell* **161**, 1089-100.

Sattelmacher B, 2001. The apoplast and its significance for plant mineral nutrition. *New Phytologist* **149**, 167-92.

Savidor A, Donahoo RS, Hurtado-Gonzales O, *et al.*, 2008. Cross-species global proteomics reveals conserved and unique processes in *Phytophthora sojae* and *Phytophthora ramorum*. *Molecular & cellular proteomics : MCP* **7**, 1501-16.

Scholthof K-BG, 2007. The disease triangle: pathogens, the environment and society. *Nature Reviews Microbiology* **5**, 152-6.

Schornack S, Van Damme M, Bozkurt TO, *et al.*, 2010. Ancient class of translocated oomycete effectors targets the host nucleus. *Proceedings of the National Academy of Science U S A* **107**, 17421-6.

Schulze B, Mentzel T, Jehle AK, *et al.*, 2010. Rapid heteromerization and phosphorylation of ligand-activated plant transmembrane receptors and their associated kinase BAK1. *Journal of Biological Chemistry* **285**, 9444-51.

Schutter KD, Lin Y-C, Tiels P, *et al.*, 2009. Genome sequence of the recombinant protein production host *Pichia pastoris*. *Nature Biotechnology* **27**, 561-566.

Scott P, Williams N, 2014. *Phytophthora* diseases in New Zealand forests. *New Zealand Journal of Forestry Science* **59**, 14-21.

Sella L, Gazzetti K, Faoro F, *et al.*, 2013. A *Fusarium graminearum* xylanase expressed during wheat infection is a necrotizing factor but is not essential for virulence. *Plant Physiology and Biochemistry* **64**, 1-10.

Severino V, Farina A, Fleischmann F, *et al.*, 2014. Molecular profiling of the *Phytophthora plurivora* secretome: A step towards understanding the cross-talk between plant pathogenic oomycetes and their hosts. *Plos One* **9**, e112317.

Shabab M, Shindo T, Gu C, *et al.*, 2008. Fungal Effector Protein AVR2 Targets Diversifying Defense-Related Cys Proteases of Tomato. *The Plant Cell* **20**, 1169-83.

Shan WX, Cao M, Dan LU, Tyler BM, 2004. The Avr1b locus of *Phytophthora sojae* encodes an elicitor and a regulator required for avirulence on soybean plants carrying resistance gene Rps1b. *Molecular Plant-Microbe Interactions* **17**, 394-403.

Shanmugam V, Sharma V, Bharti P, *et al.*, 2017. RNAi induced silencing of pathogenicity genes of *Fusarium* spp. for vascular wilt management in tomato. *Annals of Microbiology* **67**, 359-69.

Sharon A, Fuchs Y, Anderson JD, 1993. The elicitation of ethylene biosynthesis by a *Trichoderma* xylanase is not related to the cell wall degradation activity of the enzyme. *Plant Physiology* **102**, 1325-9.

Shen D, Liu T, Ye W, *et al.*, 2013. Gene duplication and fragment recombination drive functional diversification of a superfamily of cytoplasmic effectors in Phytophthora sojae. *Plos One* **8**, e70036-e.

Shimizu T, Nakano T, Takamizawa D, *et al.*, 2010. Two LysM receptor molecules, CEBiP and OsCERK1, cooperatively regulate chitin elicitor signaling in rice. *Plant Journal* **64**, 204-14.

Shiu SH, Bleecker AB, 2003. Expansion of the receptor-like kinase/Pelle gene family and receptor-like proteins in *Arabidopsis*. *Plant Physiology* **132**, 530-43.

Sinha N, Patra SK, Ghosh S, 2022. Secretome analysis of *Macrophomina phaseolina* identifies an array of putative virulence factors responsible for charcoal rot disease in plants. *Frontiers in Microbiology* **13**, 847832-.

Smillie R, Grant BR, Guest DI, 1989. The mode of action of phosphite: evidence for both direct and indirect modes of action on three *Phytophthora* spp. in plants. *Phytopathology* **79**, 921-6.

Smith HM, 2017. Risk posed by different vector types for the spread of Kauri dieback - A risk analysis on interactions that are suspected to threaten kauri. In. *Kauri Dieback Programme.* Ministry for Primary Industries.

Smith JA, Blanchette RA, Burnes TA, Gillman JH, David AJ, 2006. Epicuticular wax and white pine blister resut resistance in resistant and susceptible selections of eastern white pine (*Pinus strobus*). *Phytopathology* **96**, 171-7.

Snelders NC, Kettles GJ, Rudd JJ, Thomma B, 2018. Plant pathogen effector proteins as manipulators of host microbiomes? *Molecular Plant Pathology* **19**, 257-9.

Snelders NC, Petti GC, Berg GCMVD, Seidl MF, Thomma BPHJ, 2021. An ancient antimicrobial protein co-opted by a fungal plant pathogen for *in planta* mycobiome manipulation. *Proceedings of the National Academy of Sciences* **118**, e2110968118.

Snelders NC, Rovenich H, Petti GC, *et al.*, 2020. Microbiome manipulation by a soil-borne fungal plant pathogen using effector proteins. *Nature Plants* **6**, 1365-74.

Sonnhammer EL, Von Heijne G, Krogh A, 1998. A hidden Markov model for predicting transmembrane helices in protein sequences. *Proceedings - International Conference on Intelligent Systems for Molecular Biology* **6**, 175-82.

Sousa SaA, Magalhães A, Ferreira MMC, 2013. Optimized bucketing for NMR spectra: Three case studies. *Chemometrics and Intelligent Laboratory Systems* **122**, 93-102.

Souza CA, Li S, Lin AZ, *et al.*, 2017. Cellulose-derived oligomers act as damage-associated molecular patterns and trigger defense-like responses. *Plant Physiology* **173**, 2383-98.

Sperschneider J, Dodds PN, 2022. EffectorP 3.0: Prediction of apoplastic and cytoplasmic effectors in fungi and oomycetes. *Molecular Plant-Microbe Interactions* **35**, 146-56.

Sperschneider J, Williams AH, Hane JK, Singh KB, Taylor JM, 2015. Evaluation of secretion prediction highlights differing approaches needed for oomycete and fungal effectors. *Frontiers in Plant Science* **6**, 1168.

St Clair DA, 2010. Quantitative disease resistance and quantitative resistance loci in breeding. *Annual Review of Phytopathology, Vol 48* **48**, 247-68.

Stam R, Jupe J, Howden AJM, *et al.*, 2013. Identification and characterisation CRN effectors in *Phytophthora capsici* shows modularity and functional diversity. *Plos One* **8**, e59517.

Staskawicz BJ, Ausubel FM, Baker BJ, Ellis JG, Jones JDG, 1995. Molecular-genetics of plant-disease resistance. *Science* **268**, 661-7.

Steel CC, Drysdale RB, 1988. Electrolyte leakage from plant and fungal tissues and disruption of liposome membranes by α-tomatine. *Phytochemistry* **27**, 1025-30.

Steward GA, Beveridge AE, 2010. A review of New Zealand kauri (*Agathis australis* (D.Don) Lindl.): its ecology, history, growth and potential for management for timber. *New Zealand Journal of Forestry Science* **40**, 33-59.

Steward GA, Hansen L, Dungey HS, 2014a. Economics of New Zealand plants kauri forestry -a model exercise. *New Zealand Journal of Forestry* **59**, 31-6.

Steward GA, Kimberley MO, Mason EG, Dungey HS, 2014b. Growth and productivity of New Zealand kauri (*Agathis australis* (D.Don) Lindl.) in planted forests. *New Zealand Journal of Forestry Science* **44**.

Sticher L, Mauchmani B, Metraux JP, 1997. Systemic acquired resistance. *Annual Review of Phytopathology* **35**, 235-70.

Studholme DJ, Mcdougal RL, Sambles C, *et al.*, 2016. Genome sequences of six *Phytophthora* species associated with forests in New Zealand. *Genomics Data* **7**, 54-6.

Studholme DJ, Panda P, Sanfuentes Von Stowasser E, *et al.*, 2019. Genome sequencing of oomycete isolates from Chile supports the New Zealand origin of *Phytophthora kernoviae* and makes available the first *Nothophytophthora* sp. genome. *Molecular Plant Pathology* **20**, 423-31.

Takeda T, Takahashi M, Nakanishi-Masuno T, *et al.*, 2010. Characterization of endo-1,3-1,4-β-glucanases in GH family 12 from *Magnaporthe oryzae*. *Applied Microbiology and Biotechnology* **88**, 1113-23.

Takeda T, Takahashi M, Shimizu M, *et al.*, 2022. Apoplastic CBM1-interacting proteins bind conserved carbohydrate binding module 1 motifs in fungal hydrolases to counter pathogen invasion. *bioRxiv*, 2021.12.31.474618.

Takken FLW, Goverse A, 2012. How to build a pathogen detector: structural basis of NB-LRR function. *Current Opinion in Plant Biology* **15**, 375-84.

Tan X, Hu Y, Jia Y, *et al.*, 2020. A conserved glycoside hydrolase family 7 cellobiohydrolase PsGH7a of P*hytophthora sojae* is required for full virulence on soybean. *Frontiers in Microbiology* **11**, 1285.

Tanaka K, Heil M, 2021. Damage-associated molecular patterns (DAMPs) in plant innate immunity: Applying the danger model and evolutionary perspectives. *Annual Review of Phytopathology* **59**, 53-75.

Tasset C, Bernoux M, Jauneau A, *et al.*, 2010. Autoacetylation of the *Ralstonia solanacearum* effector PopP2 targets a lysine residue essential for RRS1-R mediated immunity in *Arabidopsis*. *Plos Pathogens* **6**.

Ten Have A, Breuil WO, Wubben JP, Visser J, Van Kan JA, 2001. *Botrytis cinerea* endopolygalacturonase genes are differentially expressed in various plant tissues. *Fungal Genetics and Biology* **33**, 97-105.

Ten Have A, Mulder W, Visser J, Van Kan JaL, 1998. The endopolygalacturonase gene Bcpg1 is required for full virulence of *Botrytis cinerea*. *The American Phytopathological Society* **11**, 1009-16.

Thines M, 2014. Phylogeny and evolution of plant pathogenic oomycetes—a global overview. *European Journal of Plant Pathology* **138**, 431-47.

Thomma BPHJ, Nurnberger T, Joosten MHaJ, 2011. Of PAMPs and effectors: The blurred PTI-ETI dichotomy. *Plant Cell* **23**, 4-15.

Tian M, Benedetti B, Kamoun S, 2005. A second kazal-like protease inhibitor from *Phytophthora infestans* inhibits and interacts with the apoplastic pathogenesis-related protease P69B of tomato. *Plant Physiology* **138**, 1785-93.

Tian M, Huitema E, Da Cunha L, Torto-Alalibo T, Kamoun S, 2004. A kazal-like extracellular serine protease inhibitor from *Phytophthora infestans* targets the tomato pathogenesis-related protease P69B. *Journal of Biological Chemistry* **279**, 26370-7.

Tian M, Navet N, Wu D, 2020. CRISPR-Cas9-mediated gene editing of the plant pathogenic oomycete *Phytophthora palmivora*. In: Islam MT, Bhowmik PK, Molla KA, eds. *CRISPR-Cas Methods*. New York, NY: Springer US, 87-98.

Tian M, Win J, Song J, Van Der Hoorn R, Van Der Knaap E, Kamoun S, 2007. A *Phytophthora infestans* cystatin-like protein targets a novel tomato papain-like apoplastic protease. *Plant Physiology* **143**, 364-77.

Tjalsma H, Bolhuis A, Jongbloed JD, Bron S, Van Dijl JM, 2000. Signal peptide-dependent protein transport in *Bacillus subtilis*: a genome-based survey of the secretome. *Microbiology and Molecular Biology Reviews* **64**, 515-47.

Tor M, Lotze MT, Holton N, 2009. Receptor-mediated signalling in plants: molecular patterns and programmes. *Journal of Experimental Botany* **60**, 3645-54.

Torres MA, Dangl JL, Jones JDG, 2002. *Arabidopsis* gp91phox homologues AtrbohD and AtrbohF are required for accumulation of reactive oxygen intermediates in the plant defense response. *Proceedings of the National Academy of Sciences* **99**, 517-22.

Torto TA, Li S, Styer A, *et al.*, 2003. EST mining and functional expression assays identify extracellular effector proteins from the plant pathogen *Phytophthora*. *Genome research* **13**, 1675-85.

Triba MN, Le Moyec L, Amathieu R, *et al.*, 2015. PLS/OPLS models in metabolomics: the impact of permutation of dataset rows on the K-fold cross-validation quality parameters. *Molecular BioSystems* **11**, 13-9.

Tundo S, Moscetti I, Faoro F, *et al.*, 2015. *Fusarium graminearum* produces different xylanases causing host cell death that is prevented by the xylanase inhibitors XIP-I and TAXI-III in wheat. *Plant Science* **240**, 161-9.

Tundo S, Paccanaro MC, Bigini V, *et al.*, 2021. The *Fusarium graminearum* FGSG_03624 xylanase enhances plant immunity and increases resistance against bacterial and fungal pathogens. *International Journal of Molecular Sciences* **22**, 10811.

Tundo S, Paccanaro MC, Elmaghraby I, *et al.*, 2020. The xylanase inhibitor TAXI-I increases plant resistance to *Botrytis cinerea* by inhibiting the BcXyn11a xylanase necrotizing activity. *Plants* **9**, 601.

Turner EMC, 1961. An enzymic basis for pathogenic specificity in *Ophiobolus graminis*. *Journal of Experimental Botany* **12**, 169-75.

Tyler BM, 2007. *Phytophthora sojae*: Root rot pathogen of soybean and model oomycete. *Molecular Plant Pathology* **8**, 1-8.

Tyler BM, 2009. Entering and breaking: virulence effector proteins of oomycete plant pathogens. *Cellular Microbiology* **11**, 13-20.

Tyler BM, Tripathy S, Zhang XM, *et al.*, 2006. *Phytophthora* genome sequences uncover evolutionary origins and mechanisms of pathogenesis. *Science* **313**, 1261-6.

Tzelepis G, Dubey M, Jensen DF, Karlsson M, 2015. Identifying glycoside hydrolase family 18 genes in the mycoparasitic fungal species *Clonostachys rosea*. *Microbiology* **161**, 1407-19.

Vaahtera L, Schulz J, Hamann T, 2019. Cell wall integrity maintenance during plant development and interaction with the environment. *Nature Plants* **5**, 924-32.

Van Den Burg HA, Harrison SJ, Joosten MH, Vervoort J, De Wit PJ, 2006. *Cladosporium fulvum* Avr4 protects fungal cell walls against hydrolysis by plant chitinases accumulating during infection. *Molecular Plant Microbe Interactions* **19**, 1420-30.

Van Der Biezen EA, Jones JDG, 1998. Plant disease-resistance proteins and the gene-for-gene concept. *Trends in Biochemical Sciences* **23**, 454-6.

Van Der Burgh AM, Joosten MHaJ, 2019. Plant immunity: Thinking outside and inside the box. *Trends in Plant Science* **24**, 587-601.

Van Der Hoorn RaL, Kamoun S, 2008. From guard to decoy: A new model for perception of plant pathogen effectors. *Plant Cell* **20**, 2009-17.

Van Esse HP, Van't Klooster JW, Bolton MD, *et al.*, 2008. The *Cladosporium fulvum* virulence protein Avr2 inhibits host proteases required for basal defense. *Plant Cell* **20**, 1948-63.

Vauthrin S, Mikes V, Milat M-L, *et al.*, 1999. Elicitins trap and transfer sterols from micelles, liposomes and plant plasma membranes. *Biochimica et Biophysica Acta (BBA) - Biomembranes* **1419**, 335-42.

Veneault-Fourrey C, Commun C, Kohler A, *et al.*, 2014. Genomic and transcriptomic analysis of *Laccaria bicolor* CAZome reveals insights into polysaccharides remodelling during symbiosis establishment. *Fungal Genetics and Biology* **72**, 168-81.

Verkaik E, Braakhekke WG, 2007. Kauri trees (*Agathis australis*) affect nutrient, water and light availability for their seedlings. *New Zealand Journal of Ecology* **31**, 39-46.

Vleeshouwers VGaA, Oliver RP, 2014. Effectors as tools in disease resistance breeding against biotrophic, hemibiotrophic, and necrotrophic plant pathogens. *Molecular Plant-Microbe Interactions* **27**, 196-206.

Volpi E Silva N, Mazzafera P, Cesarino I, 2019. Should I stay or should I go: are chlorogenic acids mobilized towards lignin biosynthesis? *Phytochemistry* **166**, 112063.

Wallis CM, Reich RW, Lewis KJ, Huber DPW, 2010. Lodgepole pine provenances differ in chemical defense capacities against foliage and stem diseases. *Canadian Journal of Forest Research* **40**, 2333-44.

Wan JR, Zhang XC, Neece D, *et al.*, 2008. A LysM receptor-like kinase plays a critical role in chitin signaling and fungal resistance in *Arabidopsis*. *Plant Cell* **20**, 471-81.

Wang QQ, Han CZ, Ferreira AO, *et al.*, 2011a. Transcriptional programming and functional interactions within the *Phytophthora sojae* RXLR effector repertoire. *Plant Cell* **23**, 2064-86.

Wang S, Boevink PC, Welsh L, Zhang R, Whisson SC, Birch PRJ, 2017. Delivery of cytoplasmic and apoplastic effectors from *Phytophthora infestans* haustoria by distinct secretion pathways. *New Phytologist* **216**, 205-15.

Wang W, Jiao F, 2019. Effectors of *Phytophthora* pathogens are powerful weapons for manipulating host immunity. *Planta* **250**, 413-25.

Wang W, Liu X, Govers F, 2021. The mysterious route of sterols in oomycetes. *Plos Pathogens* **17**, e1009591.

Wang Y, Meng Y, Zhang M, *et al.*, 2011b. Infection of *Arabidopsis thaliana* by *Phytophthora parasitica* and identification of variation in host specificity. *Molecular Plant Pathology* **12**, 187-201.

Wang Y, Xu YP, Sun YJ, *et al.*, 2018. Leucine-rich repeat receptor-like gene screen reveals that *Nicotiana* RXEG1 regulates glycoside hydrolase 12 MAMP detection. *Nature Communications* **9**, 1-12.

Wang S, Welsh L, Thorpe P, *et al.*, 2018b. The *Phytophthora infestans* haustorium is a site for secretion of diverse classes of infection-associated proteins. *mBio* **9**, e01216-18

Wanke A, Malisic M, Wawra S, Zuccaro A, 2020a. Unraveling the sugar code: the role of microbial extracellular glycans in plant–microbe interactions. *Journal of Experimental Botany* **72**, 15-35.

Wanke A, Rovenich H, Schwanke F, *et al.*, 2020b. Plant species-specific recognition of long and short β-1,3-linked glucans is mediated by different receptor systems. *The plant Journal* **102**, 1142-56.

Waterhouse GM, 1963. Key to the species of *Phytophthora* de Bary. *Mycological Papers* **92**, 1-22.

Wawra S, Belmonte R, Löbach L, Saraiva M, Willems A, Van West P, 2012. Secretion, delivery and function of oomycete effector proteins. *Current Opinion in Microbiology* **15**, 685-91.

Weber E, Engler C, Gruetzner R, Werner S, Marillonnet S, 2011. A modular cloning system for standardized assembly of multigene constructs. *Plos One* **6**, e16765.

Wei W, Xu L, Peng H, *et al.*, 2022. A fungal extracellular effector inactivates plant polygalacturonase-inhibiting protein. *Nature Communications* **13**, 2213.

Weiberg A, Jin H, 2015. Small RNAs—the secret agents in the plant–pathogen interactions. *Current Opinion in Plant Biology* **26**, 87-94.

Weir BS, Paderes EP, Anand N, *et al.*, 2015. A taxonomic revision of *Phytophthora* Clade 5 including two new species, *Phytophthora agathidicida* and *P. cocois*. *Phytotaxa* **205**, 21-38.

Whisson SC, Boevink PC, Moleleki L, *et al.*, 2007. A translocation signal for delivery of oomycete effector proteins into host plant cells. *Nature* **450**, 115-9.

Whitmore TC, 1980. Utilization, potential, and conservation of *Agathis*, a genus of tropical asian conifers. *Economic Botany* **34**, 1-12.

Williams N, Faulds C, 2018. Hunt for kauri that are resistant to Kauri dieback disease. In: Ballance A, ed. *Radio New Zealand.*

http://www.radionz.co.nz/national/programmes/ourchangingworld/audio/2018651966/hunt-for-kauri-that-are-resistant-to-kauri-dieback-disease: Radio New Zealand.

Win J, Chaparro-Garcia A, Belhaj K, *et al.*, 2012. Effector biology of plant-associated organisms: Concepts and perspectives. *Cold Spring Harbor Symposia on Quantitative Biology* **77**, 235-47.

Winkworth RC, Bellgard SE, Mclenachan PA, Lockhart PJ, 2021. The mitogenome of *Phytophthora agathidicida*: Evidence for a not so recent arrival of the "kauri killing" *Phytophthora* in New Zealand. *Plos One* **16**, e0250422.

Winkworth RC, Nelson BCW, Bellgard SE, Probst CM, Mclenachan PA, Lockhart PJ, 2020. A LAMP at the end of the tunnel: A rapid, field deployable assay for the kauri dieback pathogen, *Phytophthora agathidicida*. *Plos One* **15**, e0224007.

Wolf JM, Casadevall A, 2014. Challenges posed by extracellular vesicles from eukaryotic microbes. *Current Opinion in Microbiology* **22**, 73-8.

Wu CH, Derevnina L, Kamoun S, 2018. Receptor networks underpin plant immunity. *Science* **360**, 1300-1.

Wubben JP, Mulder W, Ten Have A, Van Kan JA, Visser J, 1999. Cloning and partial characterization of endopolygalacturonase genes from *Botrytis cinerea*. *Applied and Environmental Microbiology* **65**, 1596-602.

Wylie S, Li H, 2022. Historical and scientific evidence for the origin and cultural importance to Australia's First-Nations Peoples of the laboratory accession of *Nicotiana benthamiana*, a model for plant virology. *Viruses* **14**, 771.

Wyse SV, Burns BR, 2013. Effects of *Agathis australis* (New Zealand kauri) leaf litter on germination and seedling growth differs among plant species. *New Zealand Journal of Ecology* **37**, 178-83.

Xia Y, Ma Z, Qiu M, *et al.*, 2020. N-glycosylation shields *Phytophthora sojae* apoplastic effector PsXEG1 from a specific host aspartic protease. *Proceedings of the National Academy of Sciences* **117**, 27685-93.

Xu J, Zhang H, Zheng J, Dovoedo P, Yin Y, 2019. eCAMI: simultaneous classification and motif identification for enzyme annotation. *Bioinformatics* **36**, 2068-75.

Yamaguchi Y, Huffaker A, Bryan AC, Tax FE, Ryan CA, 2010. PEPR2 is a second receptor for the Pep1 and Pep2 peptides and contributes to defense responses in *Arabidopsis*. *Plant Cell* **22**, 508-22.

Yamaguchi Y, Pearce G, Ryan CA, 2006. The cell surface leucine-rich repeat receptor for AtPep1, an endogenous peptide elicitor in *Arabidopsis*, is functional in transgenic tobacco cells. *Proceedings of the National Academy of Sciences of the United States of America* **103**, 10104-9.

Yang C, Liu R, Pang J, *et al.*, 2021. Poaceae-specific cell wall-derived oligosaccharides activate plant immunity via OsCERK1 during *Magnaporthe oryzae* infection in rice. *Nature Communications* **12**, 2178.

Yang C, Yu Y, Huang J, *et al.*, 2019. Binding of the *Magnaporthe oryzae* chitinase MoChia1 by a rice tetratricopeptide repeat protein allows free chitin to trigger immune responses. *The Plant Cell* **31**, 172-88.

Yang M, Duan SC, Mei XY, *et al.*, 2018a. The *Phytophthora cactorum* genome provides insights into the adaptation to host defense compounds and fungicides. *Scientific Reports* **8**, 6534.

Yang X, Tyler BM, Hong CX, 2017. An expanded phylogeny for the genus *Phytophthora*. *Ima Fungus* **8**, 355-84.

Yang Y, Zhang Y, Li B, Yang X, Dong Y, Qiu D, 2018b. A *Verticillium dahliae* pectate lyase induces plant immune responses and contributes to virulence. *Frontiers in Plant Science* **9**.

Yano A, Suzuki K, Uchimiya H, Shinshi H, 1998. Induction of hypersensitive cell death by a fungal protein in cultures of tobacco cells. *Molecular Plant-Microbe Interactions*® **11**, 115-23.

Yao Z, Rashid KY, Adam LR, Daayf F, 2011. *Verticillium dahliae*'s VdNEP acts both as a plant defence elicitor and a pathogenicity factor in the interaction with *Helianthus annuus*. *Canadian Journal of Plant Pathology* **33**, 375-88.

Yin YB, Mao XZ, Yang JC, Chen X, Mao FL, Xu Y, 2012. dbCAN: a web resource for automated carbohydrate-active enzyme annotation. *Nucleic Acids Research* **40**, W445-W51.

Yin Z, Wang N, Pi L, *et al.*, 2021. *Nicotiana benthamiana* LRR-RLP NbEIX2 mediates the perception of an EIX-like protein from *Verticillium dahliae*. *Journal of Integrative Plant Biology* **63**, 949-60.

Zadoks JC, 2008. The potato murrain on the european continent and the revolutions of 1848. *Potato Research* **51**, 5-45.

Zerillo MM, Adhikari BN, Hamilton JP, Buell CR, Levesque CA, Tisserat N, 2013. Carbohydrate-active enzymes in *Pythium* and their role in plant cell wall and storage polysaccharide degradation. *Plos One* **8**, e72572.

Zhang B, Gao Y, Zhang L, Zhou Y, 2021a. The plant cell wall: Biosynthesis, construction, and functions. *Journal of Integrative Plant Biology* **63**, 251-72.

Zhang D, Burroughs AM, Vidal ND, Iyer LM, Aravind L, 2016. Transposons to toxins: the provenance, architecture and diversification of a widespread class of eukaryotic effectors. *Nucleic acids research* **44**, 3513-33.

Zhang F, Labourel A, Haon M, *et al.*, 2022. The ectomycorrhizal basidiomycete *Laccaria bicolor* releases a GH28 polygalacturonase that plays a key role in symbiosis establishment. *New Phytologist* **233**, 2534-47.

Zhang H, Xu F, Wu Y, Hu HH, Dai XF, 2017a. Progress of potato staple food research and industry development in China. *Journal of Integrative Agriculture* **16**, 2924-32.

Zhang H, Yohe T, Huang L, *et al.*, 2018. dbCAN2: a meta server for automated carbohydrate-active enzyme annotation. *Nucleic Acids Research* **46**, 95-101.

Zhang L, Hua C, Pruitt RN, *et al.*, 2021b. Distinct immune sensor systems for fungal endopolygalacturonases in closely related Brassicaceae. *Nature Plants* **7**, 1254-63.

Zhang L, Yan J, Fu Z, *et al.*, 2021c. FoEG1, a secreted glycoside hydrolase family 12 protein from *Fusarium oxysporum*, triggers cell death and modulates plant immunity. *Molecular Plant Pathology* **22**, 522-38.

Zhang LS, Kars I, Essenstam B, *et al.*, 2014a. Fungal endopolygalacturonases are recognized as microbe-associated molecular patterns by the *Arabidopsis* receptor-like protein Responsiveness to *Botrytis* polygalacturonases1. *Plant Physiology* **164**, 352-64.

Zhang M, Ahmed Rajput N, Shen D, *et al.*, 2015. A *Phytophthora sojae* cytoplasmic effector mediates disease resistance and abiotic stress tolerance in *Nicotiana benthamiana*. *Scientific Reports* **5**, 10837.

Zhang M, Li Q, Liu T, *et al.*, 2014b. Two cytoplasmic effectors of *Phytophthora sojae* regulate plant cell death via interactions with plant catalases. *Plant Physiology* **167**, 164-75.

Zhang XX, Dodds PN, Bernoux M, 2017b. What do we know about NOD-like receptors in plant immunity? *Annual Review of Phytopathology, Vol 55* **55**, 205-29.

Zhao Z, Liu H, Wang C, Xu J-R, 2013. Comparative analysis of fungal genomes reveals different plant cell wall degrading capacity in fungi. *Bmc Genomics* **14**, 274.

Zhu WJ, Ronen M, Gur Y, *et al.*, 2017. BcXYG1, a secreted xyloglucanase from *Botrytis cinerea*, triggers both cell death and plant immune responses. *Plant Physiology* **175**, 438-56.

Zipfel C, 2014. Plant pattern-recognition receptors. *Trends in Immunology* **35**, 345-51.